6th International Conference on Thermal Equipment, Renewable Energy and Rural Development

TE-RE-RD 2017

Moieciu de Sus
8-10 Iunie 2017

6th International Conference on Thermal Equipment, Renewable Energy and Rural Development
TE-RE-RD 2017

ORGANIZERS:

University "POLITEHNICA" of Bucharest
Faculty of Mechanical Engineering and Mechatronics -
Faculty of Biotechnical Systems Engineering -

National Institute of Research – Development for Machines and Installations Designed to Agriculture and Food Industry – INMA

Society of Romanian Agricultural Mechanical Engineers – SIMAR

PROCEEDINGS

Editors:

Assoc. Prof.dr.ing.Gabriel-Paul NEGREANU
Senior Lecturer dr.ing.Iulian-Claudiu DUȚU

Moieciu de Sus – Romania
8-10 June 2017

ISSN 2359 – 7941

Editura POLITEHNICA PRESS

COVER: **Gabriel-Paul Negreanu**

SCIENTIFIC COMMITTEE

Dr. Atanas ATANASOV	BULGARIA
Prof. Viorel BĂDESCU	ROMANIA
Prof. Hristo BELOEV	BULGARIA
Prof. Alexandru DOBROVICESCU	ROMANIA
Dr. Cătălin DUMITRESCU	ROMANIA
Prof. Iliya ILIEV	BULGARIA
Prof. Ion V. ION	ROMANIA
Prof. Krzysztof JESIONEK	POLAND
Prof. Önder KABAŞ	TURKEY
Prof. Imre KISS	ROMANIA
Prof. Silvio KOSUTIC	CROATIA
Prof. Gheorghe LĂZĂROIU	ROMANIA
Prof. Edmond MAICAN	ROMANIA
Prof. Milan MARTINOV	SERBIA
Prof. Nicolay MIHAILOV	BULGARIA
Prof. Jaroslaw MILESKI	POLAND
Prof. Alfonso NASTRO	ITALY
Prof. Vlastimir NIKOLIC	SERBIA
Prof. Simeon OKA	SERBIA
Prof. Constantin PANĂ	ROMANIA
Prof. Gigel PARASCHIV	ROMANIA
Prof. Ionel PÎŞĂ	ROMANIA
Dr. Ion PIRNĂ	ROMANIA
Prof. Tudor PRISECARU	ROMANIA
Prof. Violeta RASHEVA	BULGARIA
Prof. Kemal Çağatay SELVİ	TURKEY
Prof. Mariana-Florentina ŞTEFĂNESCU	ROMANIA
Prof. Marija TODOROVIC	SERBIA
Dr. Cristina-Elena RADA	ITALY
Prof. Rosen VASILEV	BULGARIA
Georgi VALTCHEV	BULGARIA
Prof. Gheorghe VOICU	ROMANIA
Dr. Nikolai ZLATOV	UK

ORGANIZING COMMITTEE

Chairman	Prof. Lucian MIHĂESCU	ROMANIA
Co-chairmen	Prof. Sorin-Ştefan BIRIŞ	ROMANIA
	Dr. Gabriel-Paul NEGREANU	ROMANIA
	Dr. Valentin VLĂDUŢ	ROMANIA
	Dr. Iulian-Claudiu DUŢU	ROMANIA

Members	Dr. Cristian-Gabriel ALIONTE	ROMANIA
	Dr. Valentin APOSTOL	ROMANIA
	Prof. Mircea BĂDESCU	ROMANIA
	Dipl.Eng. Viorel BERBECE	ROMANIA
	Dr. Cristina COVALIU	ROMANIA
	Dr. Mihaela-Florentina DUȚU	ROMANIA
	Dr. Irina Aura ISTRATE	ROMANIA
	Dipl.Eng. Mihai MATACHE	ROMANIA
	Dr. Elena POP	ROMANIA
	Dipl. Eng. Elena SORICĂ	ROMANIA
Secretary	Dipl. Eng. Iuliana GĂGEANU	ROMANIA
	Dipl. Eng. Mariana MUNTEANU	ROMANIA

CONFERENCE SPONSORS

CONFERENCE PROGRAMME

Thursday, June 08	Friday, June 09	Saturday, June 10
	Breakfast	Breakfast
15.00 - 16.00 Registration of participants	08.30 - 09.30 Registration of participants	09.00 - 12.00 Networking
16.00 - 16.30 Opening ceremony	09.30 - 11.00 Oral presentations “Sections 1 & 2”	12.00 Participants’ departure
16.30 - 18.30 Plenary session	11.00 - 11.30 Coffee break	
18.30 – 22.00 Welcome Cocktail	11.30 - 13.00 Oral presentations “Sections 1 & 2”	
	13.00 - 14.30 Lunch	
	14.30 - 16.30 Oral presentations “Sections 1 & 2”	
	16.30 - 17.00 Coffee break	
	17.00 - 18.30 Workshop	
	19.30 - 22.00 Conference Dinner	

CONTENTS

SECTION 1: THERMAL EQUIPMENT

SECTION 2: RENEWABLE ENERGY

SECTION 3: RURAL DEVELOPMENT

BIOMASS STORAGE APPROACH IMPACT OF A POWER PLANT

Lecturer I. BITIR-ISTRATE Ph.D[1], Associate Prof. M. SCRIPCARIU Ph.D.
Politehnica University of Bucharest, Energy Faculty

Abstract- The aim of the paper is to reveal the impact of biomass storage on the economic efficiency for a power plant. It is about a technic to buy the green fuel for 2-3 month in advance both for a better price and for a natural or industrial reduction of wood residues humidity. An extra space would be necessary, but the advantages in term of biomass consumption are clearly calculated. A buffer amount of cash is needed to cover the drying period for the power plant. The economic efficiency of biomass storage approach is positive in certain conditions to be discussed. Conclusions and recommendations are drawn by comparing results for different sizes of biomass plants.

Keywords-Biomass, Economic efficiency.

1. INTRODUCTION

The use of biomass to generate electricity is one of the most desirable method to cover the energy demand. Usually the wood residue humidity is a problem to manage for power plant engineers. The higher the level of water in biomass, the more necessary fuel for combustion. Figure 1 presents a typically biomass power plant diagram where all processes are represented. Biomass storage is necessary for many reasons. Firstly, a buffer in fuel supply is indicated for avoiding the situations when plant could be affected by biomass lack.

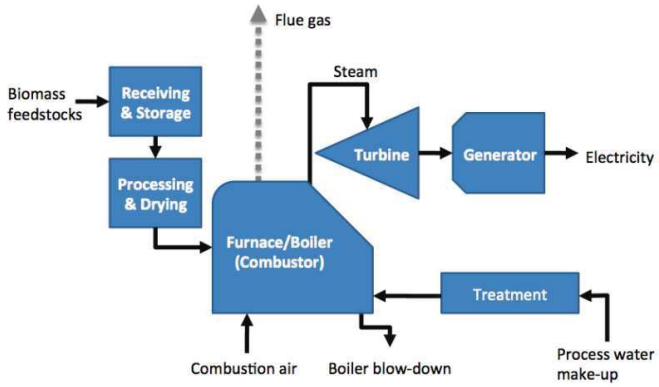

Figure 1 Biomass power process flow diagram [1]

Secondly, a natural humidity reduction of the biomass is obtained when fuel is stored for few weeks at least. This technic is named passive drying. In order to avoid internal heat generation in stored biomass an uncommitted form of wood residues is recommended. The natural drying process is depending on the fuel moisture content, the storage area, the ambient conditions such as air temperature, air circulation and relative humidity. If the drying period is too extended there are some risks related to the process: microbial activity and potential biomass self-ignition [3]. Optimal way to manage a biomass storage is LIFO principle (Last In First Out). The best storage geometry is elongated strings with a width of double the height for increasing the cooling effect from the surroundings [3].

1 Splaiul Independentei 202 A, Bucharest, Romania
Tel. 0040214029846 Email ioanistrate2005@yahoo.com

2. OPTIMAL TIME OF BIOMASS STORAGE

As previously discussed, the storage period for passive drying has to be a subject of optimization. If it is too short, not enough moisture content is extracted. If it is too extended, microbial problem and self-ignition risk are possible.

Ambient air temperature has a big impact on natural drying performances. When high levels of air temperature are recorded, the moisture evaporation is accelerated. Contrarily, when the air temperatures are low and rainfall period is in place a rewetting process could be installed.

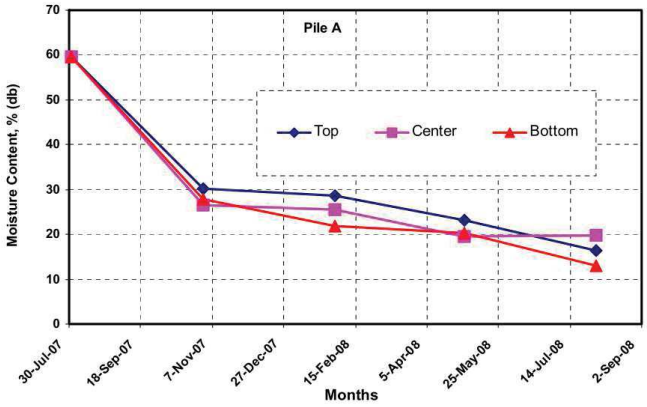

Figure 2 Change in moisture content of wood chips pile covered with tarp [4]

Afzal & al. [4] experienced the passive drying technic in different weather conditions. Moisture content reduction has been accelerated when storage started in July. No significant changes was recorded when air humidity increased at lower temperature, starting with November. The least moisture content drop of the biomass bundles was observed between February and April during one year storage period.

Codina and Lopez [5] presented very interesting results on moisture content evolution during 9 month storage of biomass. Important humidity reduction have been obtained during the first 3 months, even if the starting water content was about 40%. Rewetting is recorded when storage is extended over 3 months.

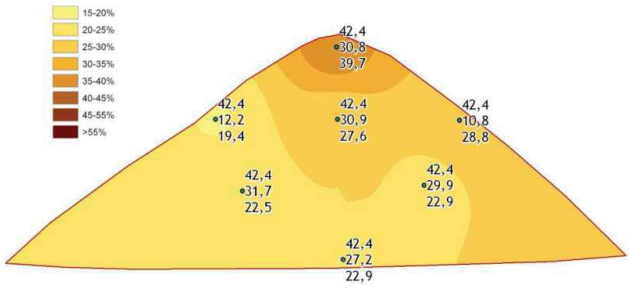

Figure 3 Moisture profile of a wood chip pile stored under a textile,
May – top, Aug –middle, Jan -bottom [5]

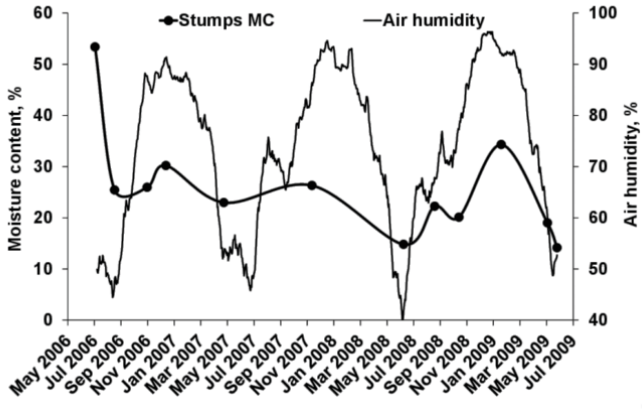

Figure 4 Average moisture content of Norway spruce wood and relative air humidity in time [6]

According to Laurila's [6] experiment in Finland, the initial moisture content right after harvesting was 53%. The humidity decreased fairy quickly at the storage site in one month to 31%. No significant variations outside the range 20-30% water content have been recorded.

Considering all these examples, we can conclude that a period of 3 months biomass storage could be considered for a real case. Over this limit, no significant moisture reduction can be obtained. At the same time, microbial problem and self-ignition risk are possible. Depending on the moment position in the year, over 3 months of storage, the humidity level could rise because of the rainy season. No advantages are calculated if this period of time is exceeded.

3. RELATION PRICE – HUMIDITY IN BIOMASS PROCUREMENT

Obviously, more moisture content, bigger price for energy unit is paid. It is because the biomass supplier has to carry more water to bring a fixed energy content in fuel. For example, at 60% moisture, a level of 60 USD/tonne leads to a net energy price at 10 USD/GJ. The same biomass weight price, at 40% moisture, leads to 6 USD/GJ.

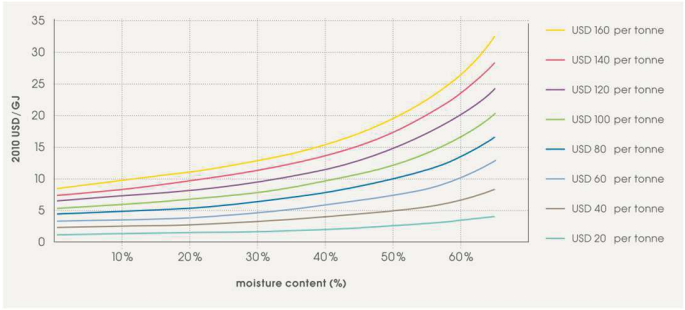

Figure 5 Impact of moisture content on the price of feedstock cost on a net energy basis [2]

Another interesting approach is to pay for the energy content of the biomass. Considering 10 USD/GJ as a target in procurement process, if the moisture content is 40%, the biomass price is 100 USD/tonne, but if 60% humidity level can be accepted, the price could decrease to 60 USD/tonne. A storage facility is built for naturally drying biomass from 60% to 40% in less than 3 months. It is an optimization on how much the storage will cost and money savings in procurement. Additionally, an important amount of cash will be stored in biomass until the evaporation process is over and electricity is produced and sold. Is it a business to follow for the power plant? A case study is presented for answering to this dilemma.

4. CASE STUDY – 9 MWe STEAM TURBINE BIOMASS PLANT

A 9 MWe steam turbine power plant has been selected for calculation. The reference situation is to use 60% moisture biomass to fuel the boiler. HHV for the biomass is calculated at 5,940 kJ/tonne. For these data, hourly fuel consumption is 20.28 t/h biomass for 9 MWe electricity generation.

Table 1 Biomass yield considering moisture content with HHV and LHV indication

Moisture [%]	HHV [kJ/tonne]	LHV [kJ/tonne]	Biomass yield [tonne/h]
40	10,120	8,349	11.90
50	8,030	6,624	15.00
60	5,940	4,900	20.28

Considering 40% moisture in fuel, with HHV = 10,12 kJ/tonne, the real biomass yield for boiler supply is about 11.9 tonne/h. Less water in introduced in boiler, less energy is consumed for engines, more efficient the burning process becomes.

For 8,000 hours/year running period for the power plant, the fuel consumption at 60% moisture is calculated at 162,240 tonne/year. At 60 USD/tonne, the annual fuel cost could be 9.73 mil. USD/year.

For the same period, is biomass at 40% is used the annual consumption is 95,200 tonne/year. At 100 USD/tonne, the biomass cost 9.52 mil USD/year.

A simple calculation shows that 17.94 tonnes biomass at 60% humidity is necessary to obtain 11.9 tonnes dried biomass at 40% after 3 month of storage in natural conditions. A biomass amount reduction of 2.34 tonne/h could be obtained. For 8,000 hours/year, the fuel save could be 18,720 tonne/year. In term of money, the saving could be about 1.12 mil USD/year. The additional benefits (internal power plants consumption reduction) have not been considered for the economic analysis.

It is important to evaluate the financial effort to make for the plant owner in order to pay the stored drying biomass. Considering 2,200 hours/year the period when the fuel is in the storage facility, about 40,000 tonnes have to be extra-paid. At 60 USD/tonne, an amount of 2.4 mil. USD is necessary to block for storage and drying processes. Usually a credit line has to be open for running this business. The interest rate could be considered 1%/year, so the credit line cost will be 0,024 mil USD/year.

For storage purposes, a facility has to be built. An important free space has to be identified very close to the boiler house. A designer will draw optimal configuration for the storage area, optimising the way to supply fuel for burning process. Biomass density could be assumed at 0.300 tonne/m^3. Necessary volume for storage could reach 133,333 m^3. Supposing 3 m height for the biomass stack, a minimum 44,444 m^2 area is necessary for the facility.

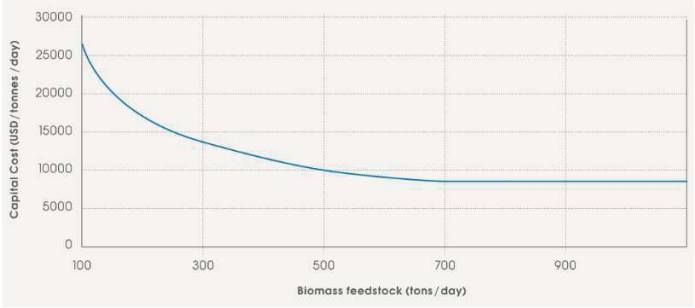

Figure 6 Capital cost of natural drying facilities for different size of biomass feedstock [2]

According to Figure 6, for the presented case study the capital cost can reach 4 mil. USD if a natural biomass drying process is installed. These calculation proves that biomass storage for the power plant is not an easy business. Important investments are demanded for preparing the storage facility, huge free areas demanded, a credit line has to be available for paying biomass to be dried and no exceptional fuel cost reduction is obtained.

First important conclusion is that if high quality biomass is available on the market, no natural drying technology is suitable for improvements to the power plant economic efficiency.

The question to answer is what will be the results for an industrial drying process for the biomass? Would the drying become more efficient if the process period is reduced from 3 months to few hours?

5. INDUSTRIAL DRYING USE FOR BIOMASS PLANT OPTIMIZATION

Once the economic analysis for the natural drying made, the next question is how an industrial drying equipment could improve the business. A residual heat is available from the steam turbine and a warm water recovery circuit could be installed. Exhausted gases for the boiler is an important heat source to use for drying too.

The necessary area will reduce at maximum 10,000 m^2, the credit line cost will decrease accordingly. Important investment in drying facility has to be made. Several technologies are available for industrial drying as following: rotary drum, belt/conveyor, cascade/fluidized bed, flash/ pneumatic, superheated steam, bed/grate.

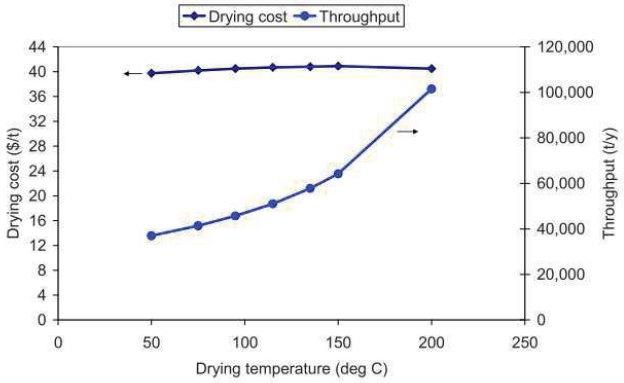

Figure 7 Economical aspects of industrial biomass drying process [7]

Haque and Somerville [7] presents the average drying cost for the biomass in relation with the process temperature. As shown in the Figure 7, the real cost of eliminating the moisture tends to be constant at 40 USD/tonne, which is exactly the difference between the biomass cost at 40% and 60% moisture.

Second important conclusion is that if high quality biomass is available on the market, no industrial drying technology is suitable for improvements to the power plant economical efficiency.

6. FINAL CONCLUSIONS ON DRYING IMPACT ON POWER PLANT ECONOMIC EFFICIENCY

As previously calculated in the article, no drying process is suitable when less of 40% moisture biomass is available on the market.

Natural facilities for drying are huge areas consumers, with positive impact on the power plant when strong negotiations on fuel price for high quantities can be realized. High capital costs are demanded but 4 years payback period can be obtained, if land is available.

Industrial facilities for biomass drying ask for less capital cost, but energy consumption could be expensive. Use of exhausted heat is essential for improving the economy efficiency of the project. It is suitable for small or medium daily quantities of fuel and some optimization in term of biomass storage in relation with external temperature and available storage space to reduce heat consumption is possible.

7. REFERENCES

[1] National Renewable Energy Laboratory: Technical Manual for the SAM Biomass Power Generation. Technical Report NREL/TP-6A20-52688 September 2011.

[2] International Renewable Energy Agency: Renewable Energy Technologies: Cost analysis series, Biomass for Power Generation. Volume 1 Power Sector, June 2012.

[3] Anders Eriksson: Energy efficient storage of biomass at Vattenfall heat and power plants. Swedish University of Agricultural Sciences Department of Energy and Technology. ISSN 1654-9392 Uppsala 2011

[4] M.T.Afzal, A.H.Bedane, S.Sokhansanj and W.Mahmood: Storage of comminuted and uncomminuted forest biomass and its effect on fuel quality. BioResources 5(1) 55-69.

[5] M.Codina, I.Lopez: Drying of wood-forest chips. Chapter XI, *www.biomasstradecentre2.eu*

[6] J. Laurila: Moisture content, weight loss and potential of energy wood in South and Central Ostrobothnia regions in western Finland. Department of Science, Faculty of Agriculture and Forestry, University of Helsinky,
http://dx.doi.org/10.14214/df.167

[7] N.Haque, M.Somerville: Techno-economic and environmental evaluation of biomass dryer. 5th BSME International Conference on Thermal Engineering, Procedia Engineering 56 (2013) 650-655

REVIEW ON EXISTING BROWN'S GAS (HHO) PRODUCTION'S SYSTEMS AND ANALYSIS OF CAPABILITIES FOR ITS USE IN PRACTICE

Deyan Deltchev[1], Angel Terziev, Iliya Iliev

ABSTRACT

A literature review of existing Brown's gas generators is presented in this work. Factory parameters for leading electrolyzers' manufacturers are compared and analysed. The article provides an applicability overview of Brown's gas electrolyzers in practice and their significance. An extensive review Brown's gas effects has been done when used as an additive to liquid fossil fuel, as well as the results.

1. INTRODUCTION

As the fossil fuels era ends, the world is trying more intensively to find a sustainable substitute. Fluctuations in fossil fuel prices make the world look for a cheaper source of energy. The continuous growth in the consumption of primary energy sources is also of great significance. Fig. 1 shows information about the consumption and production of liquid fossil fuels, and their projection into the future is also presented [1]. The figure shows that the production/consumption of fossil fuels, in that five-year period increased by approximately 9%. The estimated increase is even higher.

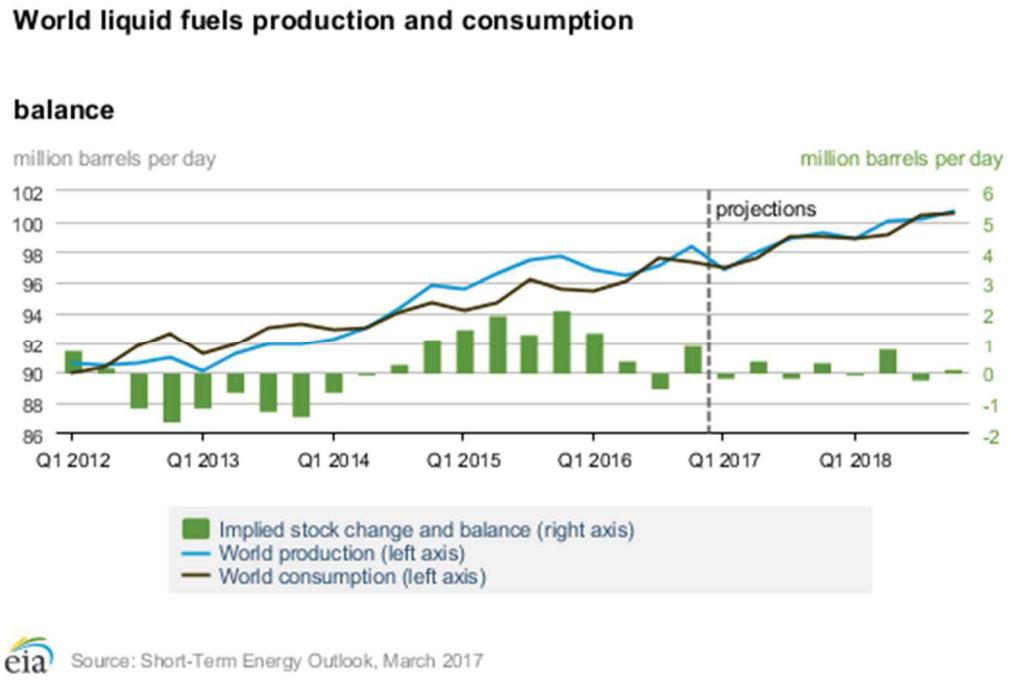

Figure 1 World liquid fuels production and consumption [1]

[1]Sofia, Bulgaria,+359 887918028, deyan.deltchev@gmail.com

Along with the development of technologies related to the renewable energy sources use such as wind, sun and water, intensive worked is also put on technology improvement for thermo fusion and production and storage of hydrogen. The so-called Brown gas or oxy-hydrogen gas, can also be referred to the sources listed above (inscribed as HHO). In 1977 Yull Brown patented electrolyzer technology for producing gas, named later on its discoverer – Brown's Gas [2].
Practically, the Brown's gas (HHO) production represents electrolysis of distilled water and a certain amount of potassium hydroxide solution. There are various theories, conducted experiments and studies, what actually constitutes Brown's gas from scientists like George Wiseman, Stanley Meyer and in recent days - by Chris Eckman. Most of them are agree with George Wiseman definition about the Brown gas. He defined this gas, as "it is entire mixture of gasses evolving from an electrolyzer specifically designed to electrolyze water and not separate the resulting gasses". Each Brown's Gas generator is composed of the following elements shown in Fig. 2:

- Cell – the vessel, where electrolysis happens;
- Bubbler – secure from backfire;
- Reservoir – electrolyte storing;
- Battery – supplying the needed electricity;
- Connections between each vessel.

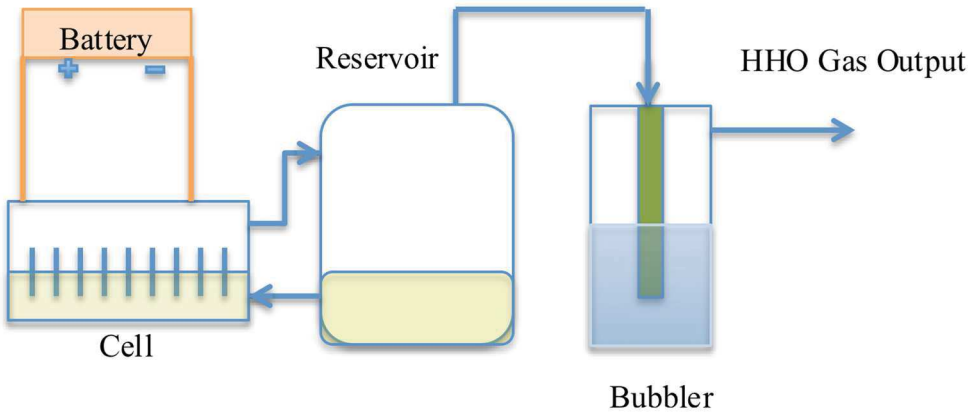

Figure 2 HHO electrolyzer block diagram

One characteristics of Brown's gas is its flame temperature. By isolated combustion the flame reaches a temperature around 137^0 C [3], which can be measured quite accurately and easily using the modern tools such as a thermal imaging camera system. When, however, the flame comes in contact with another material different from the air, significantly higher temperatures are achieved. Brown's gas has the property to sublimate the tungsten [4] (tungsten has a melting point of 3422^0 C).

The purpose of this work is a critical analysis of existing technologies for the Brown's gas production and their implication.

2. EXISTING BROWN'S GAS TECHNOLOGIES. TECHNICAL DATA

Electrolyzers for the Brown's gas production can be categorized on several counts:

- Cell construction type;
- Maximal Brown's gas production measured in *l/h* or m^3/h;
- The necessary electricity amount for *1l* Brown's gas production, resp. Brown's gas amount produced from 1 *kWh*

Given that, the most established manufacturers do not disclose detailed technical performance of their electrolyzers, a comparison has been made only between officially specified data, namely the electrolyzers parameters such as machines performance and power consumption. Tab. 1 presents the electrolyzers' data manufactured by leading companies in the sector. The indicated features are maximum power consumption, maximum amount of HHO, which can be produced by the generator and the ratio "amount - produced gas" for 1 *kWh*. The data are taken from the manufacturers official websites [5] [6] [7].

		EPOCH Energy Technology Co.*	Okay Energy Equipment Co. Ltd.	B.E.S.T. KOREA CO., LTD.
Modell		*EP- 500*	*CCS3000*	*WE-3000*
Voltage	*V*	380	380	380
Maximum power consumption	*kWh*	11,5	9	11,25
Max. Gas output	*(L/h)*	3000	3000	3000
Gross Weight	*(kg)*	315	330	950
Ratio	*L/kWh*	261	333	267

Table 1 HHO generator models data

It should be noted that B.E.S.T. KOREA CO. Ltd electrolyzers production is in the range 3,000 - 24,000, while the product portfolio of EPOCH Energy Technology CO. and Okay Energy Equipment CO. Ltd includes Brown's gas generators with a small capacity in the range 200. Generators of different manufacturers are chosen and shown in Tab. 1 with a similar Brown's gas (*l/h*) performance. The information given in Tab. 1 shows that Okay Energy Equipment Co. Ltd generator has the highest performance of Brown gas production per 1 *kWh* input power. It should be noted that the manufacturers official websites data are from 2001, only EPOCH Energy Technology CO. and Okay Energy Equipment CO. announced innovations in theirs generators. For the B.E.S.T. KOREA CO. Ltd Brown's Gas generators no information concerning the technology's improvement is presented. According to the same table the B.E.S.T. KOREA CO. Ltd. model WE-3000 has greatest weight reaching 950 kg. Although the other two Brown's gas generator models have up to three times less weight, their weight remains significant. There is another class Brown's gas generators, which have much smaller dimensions and weight, which can be hand-held. Fig. 3 shows a Spirflame® model 250HP [9] of the company SPIRIG based in Switzerland. This is their generator with the highest Brown's gas productivity. The electrolyszer is able to produce up to 250 *l/h* of gas. This is 12 times lower output compared to machines presented above. On the other hand, the weight of 250HP without electrolytic liquid is 52 kg. This makes it easily portable, unlike the B.E.S.T. KOREA CO. Ltd., EPOCH Energy Technology CO. and Okay Energy Equipment CO. Ltd. Models.

** Max Gas output for EP-500 was estimated by the max. water consumption given by the manufacturer multiplied by 1,866[8]*

Figure 3 Spirflame® 250HP

3. APPLICATION IN THE PRACTICE

Small Brown's gas generators with an approximate capacity of around 500 *l/h* are successfully used as welding machinery in goldsmith and jewellery industry [10]. In addition to its small Brown's gas productivity, they are characterized by small dimensions and weight. Generators with greater Brown's gas productivity, as the Italian company OWELD [11] find application in the industry. These Brown's gas generators are used for the welding of copper wires in electric motors and transformers.

Brown's gas finds intensive applications in recent years as addition to fuel for heaters, boilers, engines, etc. The information published by B.E.S.T. KOREA CO. Ltd [12] showed that their Brown's gas generator can be installed to existing combustion plants (operating on diesel, oil fuel, LPG and LNG). The results of such combination reflects in two aspects:

1. Fuel consumption savings;
2. CO_2 emissions decrease.

Similar results are achieved in households using a mixture between the HHO and diesel fuel in boilers. Results for the effects of the mixing HHO gas and diesel fuel in boiler system are presented below. Experiment scheme is presented on Fig. 4.

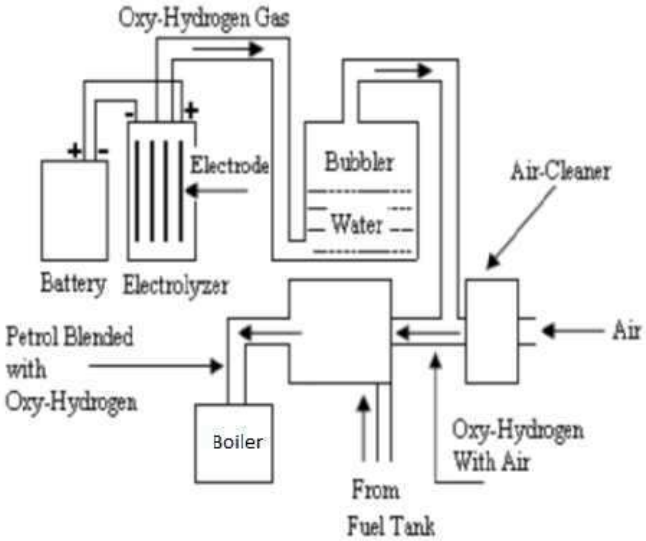

Figure 4. Experiment Setup [13]

The conducted experimental study shows that by feeding Brown's gas through the air tract to the combustion chamber, the boiler thermal efficiency increases from 79% to 82%, and the

combustion efficiency increased from 89.5% to 92.2%. The following is established as the technological solution proposed by B.E.S.T. KOREA CO. Ltd and in the conducted:

1. Positive environmental effect due to decrease emissions of NOx, CO2 (by 20%), SO2 (a decrease from 260 PPM to 160 PPM);
2. Boiler efficiency increasing at reduced diesel fuel consumption, as a result of Brown's gas addition in the fuel mixture. "Thermal efficiency of the boiler increases due to the reduction of diesel flow rates occurring at same energy out (temperature of water was set fixed at 80 ^{0}C to achieve constant boiler operating condition)".[13]

A number of papers are available describing the work of an internal combustion engine on Brown's gas mixture with petrol/diesel fuel. The measurements show significant improvements in the engine performance – reduction of unburned hydrocarbons with 5%, reduction in CO emissions with 13.5% and reduction of the specific fuel consumption by 14% [14]. The conclusions are that the addition of HHO to the fossil fuel, significantly improves hydrocarbons combustion in the combustion chamber, resulting in primary fuel (petrol/diesel) savings. The analysis of exhaust gases is also impressive, as emissions of CO, CO_2, NOx and HC, and smoke are drastically reduced.

Similar results are declared by Automotive students from Anna University, India. They conducted bench tests of petrol single cylinder engine working ones only on petrol and after that on Brown's gas and petrol fuel mixture. The tests results show 6% reduction in absolute fuel consumption and 11% reduction in specific fuel consumption at full load, in the case where gasoline was mixed with Browns gas. The reached savings are small, but still they are some. Environmental effects are also significant, there was significantly emissions reducing measured - unburned HC reduced by 88%, CO by 94%, NOx by 58%, and smoke emissions is reduced by 18%. A disadvantage must be pointed out that the tests were conducted on 100cc single-cylinder engine, and that the supplied amount of Brown's gas to the combustion chamber was not mentioned. [15]

To achieve positive economic and environmental effects in a mixed mode (liquid fossil fuel and Brown's gas) the amount of Brown's gas supplied to the system is essential.

In December 2016, a test was conducted jointly with NIS at the Technical University Sofia, Bulgaria. For the test needs diesel engine of 1,900 cc was used. During the test, the engine was fed with Brown's gas from 10 *l/min* to 100 *l/min*. The following parameters were monitored - fuel consumption, exhaust gas analysis, and smoke emissions. The test has shown that by adding less then 30 *l/min* Brown's gas to the engine, did not account for any changes compared to the standard engine parameters when working only on diesel fuel. At the maximum of 100 *l/min* Brown's gas following values were recorded:

- 1,4 times smoke emissions decrease;
- 2,7 times NOx emissions decrease;
- 6 times CO emissions decrease;
- Up to 15,7 % specific fuel consumption saving.

The exact amount of Brown's gas is not indicated in the most studies. There have not been tests with different Brown's gas amounts fed into the systems. The author's opinion is that this may be due in part to the inability to adjust the generator to supply different amounts of Brown's gas.

When determining the economic effects the cost for the energy input of the Brown's gas

production is of significant importance. That is the only way to calculate the real effect of fossil fuels saving. If it is necessary to identify savings in monetary aspect, it is necessary to compare the costs for the primary system's energy carriers with the cost for energy carriers in co-combustion system, as the costs for Brown's gas production are added.

4. CONCLUSIONS

At the present moment, it can be concluded that the Brown's gas generators have rather low productivity per unit of input energy. However, there are positive results from the use of Brown's gas. Economic effects of the fuel savings are small, but they are a sign of Brown's gas capabilities to increase the performance of generators. Undisputed is the Brown's gas environmental impact in mixed fuel systems (engines, boilers, incinerators, boilers) or welding machines. This is a very important aspect, making it one the main reasons it is worth to use and develop this type of technology.

References

[1] https://www.eia.gov/outlooks/steo/report/global_oil.cfm

[2] Yull Brown. *US patent number 4,014,777 issued on March 29, 1977, and US patent number 4,081,656 issued on March 28, 1978.*

[3] George Wiseman, Eagle Research, Brown's Gas Book 1, Version March 2002, P17

[4] George Wiseman, Eagle Research, Brown's Gas Book 1, Version March 2002, P5

[5] http://www.oxy-hydrogen.com/s/2/product-51676/Standard-Oxy-hydrogen-Generator-EP-500.html

[6] http://www.browngas.com/eng_bestkorea/product_1.htm.

[7] http://www.okayenergy.com/oxyhydrogen/ccs3000.html

[8] THE HISTORY AND FUTURE THE HISTORY AND FUTURE OF BROWN'S GAS by J. J. Hurtak, PhD, PhD and Desiree Hurtak, PhD www.nexusmagazin.com june-july 2014 page 51

[9] http://www.spirig.com/index.php?id=162&L=1

[10] https://www.eagle-research.com/Links/BG/bglink2.html

[11] http://oweld.com/applications/

[12] http://www.browngas.com/eng_bestkorea/mixed_1.htm

[13] T. Tabazah a, M. A. Hamdana,*, O. Abo Deyab b and E. Abdelhafeza „Utilization of Water Produced Hydrogen for Domestic Heating Purposes", Tabaza et al. / Int. J. of Thermal & Environmental Engineering, 7 (2014) 95-99

[14] Ali Can Yilmaz, Erinc¸ Uludamar, Kadir Aydin, Department of Mechanical Engineering, C¸ukurova University: "Effect of hydroxy (HHO) gas addition on performance and exhaust emissions in compression ignition engines

[15] E. Leelakrishnan, N. Lokesh, H.Suriyan "PERFORMANCE AND EMISSION CHARACTERISTICS OF BROWN'S GAS ENRICHED AIR IN SPARK IGNITION ENGINE ", student of Automobile Engineering, Sri Ram Engineering College, Anna University, Chennai, India, International Journal of Innovative Research in Science, Engineering and Technology Vol. 2, Issue 2, February 2013, ISSN: 2319-8753

THERMAL ANALYSIS OF LIGHT WEIGHT WALL MADE FROM SANDWICH PANELS IN THE ASPECT OF THERMAL INSULATION DESIGN FOR SUSTAINABLE BUILT ENVIRONMENT

Dhafer Manea Hachim[1], Qahtan A. Abed[2],

[1,2] *Asst. Prof. Dr. Eng. Al-Furat Al-Awsat Technical University, Enginnering Technical College- Najaf, Iraq.*

ABSTRACT

Based on the energy saving design in cold winter and hot summer zone like Iraq weather conditions, a prototype of sandwich wall panel (SWP) is analyzed by COMSOL Multiphysics ver. 5.0 programe. A new design of sandwich wall panel that enhances thermal insulation of Iraqi buildings by adding an insulating multilayer inside the wall is presented. The thermophilically properties of the insulating multilayer SWP, the external environment impact (solar irradiation, temperature, wind speed, etc.) and durability are taken into account. The major influence of solar irradiation is highlighted as it can increase heat transfer crossing the insulation wall. The result showed, the proposed sandwich wall panel can effectively save a significant amount of energy consumption in terms of electricity spent on heating and cooling. The thermal conductivity, convective heat transfer coefficient, specific heat, density, capacity, and surface emissivity of materials are necessary to evaluate the temperature distribution and the performance of the suggested sandwich wall panel.

Keywords: thermal performance, sandwich wall panel, light weight wall.

1. INTRODUCTION

The majority of brick walls are continually exposed to environment, which makes the walls focused to the solar radiation unavoidably. As a result, higher temperature in Summer and lower temperature in winter is one of the most important factors affecting living in the buildings.

The thermal energy of the building is priority areas of development. In the near zero energy building consumption, the energy consumption from the external walls ranging betwen 60% ~ 70% [1]. Therefore, more demand is put on the materials and formation design in external panel of building. On my point of view, the more functions are confirmed on the material used in walls of the building, such as the environmental effect (warm weather and cold weather), waterproof property, fireproof property and wall durability. Sandwich wall panel (SWP) is one of the best options to overcome the warm and cool in summer and winter seasons respectively. The Sandwich wall panel consists of a lightweight core and two rigid faces[2]. The importance of the thermal energy flux through a sandwich wall panel has been presented by [3]. The thermal performance of concrete three-wythe sandwich wall panels with two-wythe sandwich wall panels have been compared by [4]. Some analytical models proposed for a dynamic non-linear by using

[2] Corresponding author, email qahtan77@yahoo.com

finite element method (FEM) to analyse three-dimensional concrete wall [5]. The use of a sandwich wall panel could help increase insulate and hardness, whilst at the same time weight reduction[6]. The thermal insulation configurations of the brick walls have been studied analytically by [7]. The authors were focused on cooling and the heating requirements. A number of research studies relevant to energy efficiency and thermal performance of walls buildings have focused on the behaviour of heat transfer of wall for three rooms with a different combination of building elements were compared experimentally and theoretically [8].

Previous studies have been limited primarily to increase the temperature in side of the bulding in cold weathers. In the present study, a theoretical mathematical time-dependent model is developed for estimation of the heat transfer in the brick wall and sandwich panel wall in different boundary condition (ambint temperature and solar irradaince). The simulation investigation is established on measure weather data from Alternate and Renewable Energy Research Unit- Technical Engineering College Najaf.

2. NUMERICAL MODELLING

Weather conditions are the main factors that affects on the building materials in general of Iraq and special of south Iraq. In this work we propose a simulation which uses to show how the thermal capacity of the wall in iraq building. The two separate cases for wall have been simulated throu using the numerical model summarized down. The first one is brick wall and the second one is sandwich wall panel. The walls have the same solar radiation collection surface area but different wall materials. The length, hight and width of the brick wall and SWP are 5m, 3m and 0.3m and 5m, 3m and 0.05m respectively. The assumptions are made in this analysis: The heat flux through the two types of wall is under quise- study state conditions three dimensionals. The constant thermal conductivity (do not change with temperature) for solid materials of wall.

Take into consideration a three dimensional body in heat transfer conditions. In order to analyze heat transfer through the wall, we assume that the conductive heat transfer of wall materials can be expressed with Fourier's Law. The energy equation of the heat conduction in the wall is [9]:

$$K\left(\frac{\partial^2 T}{\partial x^2}+\frac{\partial^2 T}{\partial y^2}\frac{\partial^2 T}{\partial z^2}\right)=\rho C_p\frac{\partial T}{\partial t} \tag{1}$$

Where K is the thermal conductivity of wall [W/(m.K)], T is the temperature in any position of the wall [K], Q is the rate of heat generated within wall [W/m^3], ρ is the density of wall used [kg/m^3] and C_p is the wall specific heat [J/(kg.K)].

The thermal loads on the surfaces of wall (inside and outside) are described in the following boundary conditions equation as it is shown in figure 1.

$$K\frac{\partial T}{\partial n}l+q=0 \tag{2}$$

where l is the direction cosine of an outward vector perpendicular to the boundary and q is the sum of all heat fluxes normal to the outside wall surfaces [W/m^2].

$$q = \alpha G_{sol} + \varepsilon\sigma(T_{w,out}^4 - T_{sky}^4) + q_{con} \quad (3)$$

For outside wall surface convection heat transfer equation

$$q_{con,out} = h_{\infty}(T_{amb} - T_{w,out}) \quad (4)$$

For inside wall surface convection heat transfer equation

$$q_{con,in} = h_{c,in}(T_{in} - T_{w,in}) \quad (5)$$

where G_{sol} Total solar radiation on a horizontal surface, α, ϵ and σ Absorption and emissivity coefficient of wall and Stefan- Boltzman constant respectively, h_{∞} and $h_{c,in}$ Convective heat transfer coefficient for outside and for insid respectively [W/m^2.K], $T_{w,in}$, $T_{w,out}$ and T_{amb} Inside, outside wall surfaces and ambient temperatures respectively [K], $q_{con,in}$ and $q_{con,out}$ Heat transfer by cnvection between inside and outside wall surface respectively [W/m^2].

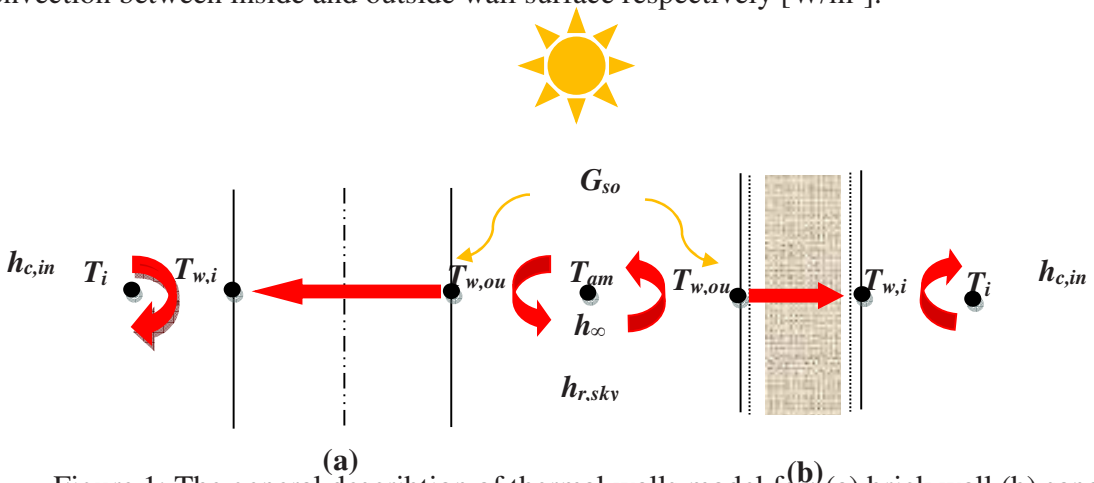

Figure 1: The general describtion of thermal walls model for: (a) brick wall (b) sandwich wall panel.

The traditional brick walls account for about 80% of the Iraq's housing. The proposed brirk wall constructed with brick, plaster and cement. The parameters of brick wall and SWP are presented in Table 1. The table tabulats the apparent thermal conductivity for brick and lightweight core with two rigid faces of SWP.

Table 1: Parameters of brick wall and sandwich wall panel used in this study

Parameters	Value		Units
	Brick wall	Sandwich wall panel	
Inside Room Temperature	298.15	298.15	K
Inside heat transfer coefficent	8.33	8.33	W/(m²·K)
Outside heat transfer coefficent for summer	22.666	22.666	W/(m²·K)
Emissivity of brick	0.9	0.9	------
Absorption of brick	0.6	0.2	------
Density of brick	1970	40	kg/m³
Thermal conductivity	0.7	0.026	W/(m·K)
Thermal capacity	800	750	J/(kg·K)

3. MODEL VALIDATION

The mathematical model proposed here refers to the thermal performance of two different types of wall (brick wall and SWP). In order to check the accuracy of this simulation, the results of this simulation were compared with those of other researchers[8]. Table 2. shows that simulated and measured U- value, for two different walls materal (Foam concrete and Fiber glass). There is good agreement between simulated result and measured (average erro for Foam concrete and Fiber glass are 10.9% and 8.5% respectively). Therefore, the model can be used to perform enough accurate simulations.

Table 2: Comparison between experimental results of [9] with theoretical results of present work.

Insulating material	Thickness (mm)	U-value (W/m^2 K) Kumar (2013)	U-value (W/m^2 K) Present work	Error (%)
Foam concrete (K= 0.070)	75	0.711	0.799	10.927
	100	0.567	0.621	8.706
	125	0.471	0.508	7.253
	140	0.428	0.458	6.589
Fiber glass (K =0.040)	50	0.631	0.697	9.397
	70	0.479	0.517	7.350
	75	0.452	0.485	6.639
	100	0.353	0.373	5.361

4. RESULTS AND DISCUSSION

The thermal heat transfer analysis is a very important function in the design for many applications of engineering. The conservation of thermal energy of building is dependent on the ability of a walls and windows in reducing the amount of heat transferring into or from the outside of the building to the inside. Therefore, the importance work to do a comparison of the thermal performance between the traditional housing wall and the SWP.

Heat flux and inside room temperatures, were obtained from the numerical simulation (by using the COMSOL Multiphysics), using as input data weather conditions of Najaf, Iraq (32° 1' N / 44° 19' E). The thermal performance of the house walls are affected by the level of solar irradiance and ambient temperature. Figure 2 shows the variation of ambient temperature and solar irradiance on a sunny day (21/July/2015). The solar irradiance and ambient temperature were measured at time intrevel 30 minutes by Alternate and Renewable Energy Research Unit-Technical Engineering College Najaf. The maximum value 32.4 °C and the maximum solar irradiance was 878 W/m^2.

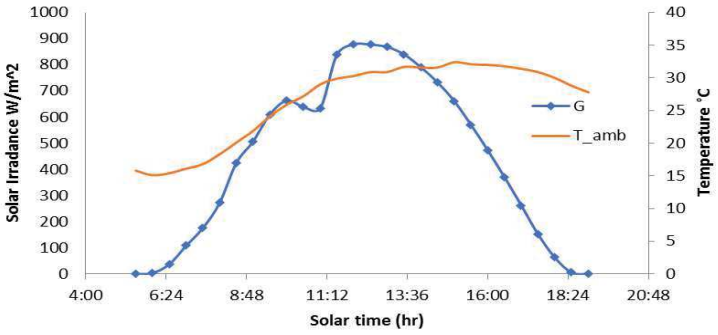

Figure 2: Variation of ambient temperature and solar irradiance on (21/July/2015)

Figure 3 below shows the distributed brick wall and sandwich wall temperature during a suny day 21/July/ 2015 in the midle of the ady at 12:00 pm. That is, the solar irradiance, out sid air temperature and avarege wind speed are 878 W/m^2, 20 °C and 2.5m/s respectively. In figure 3, it can be observed that the higher temperatures accumulated in brick wall compering with SWP. A larger value of thermal resistance of wall R_t indicate a lower heat flow rate from outside to inside (good insulator). The result showed that the avarege thermal resistance duringe simulation day for the bick wall and SWP are 1.56 and 1.956 [K.m^2/W] respectively.

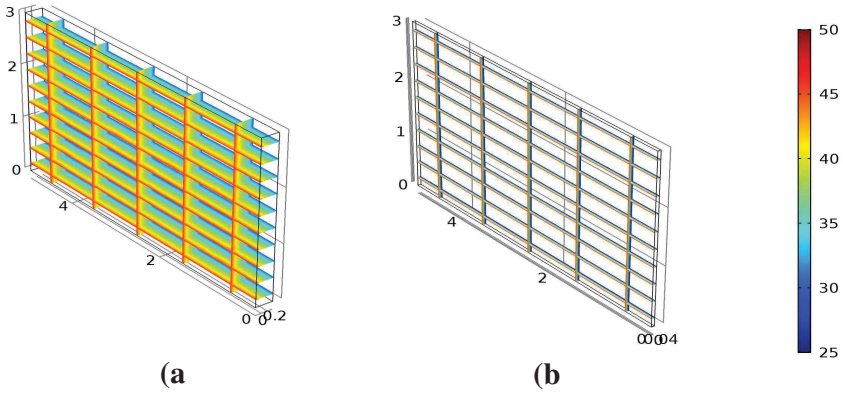

Figure 3: Temperature distribution intow types of wall: (a) Brick wall, (b) Sandwich wall panel.

The quasi- study thermal analysis determines temperatures and heat flux that vary with time because the input buadary conditions change with time such as ambient temperature and solar irradiance. The three dimensional (3D) simulation model was used to simulate the performance of two types of wall houses typical in Iraq.

Actually, the main problem in Iraq is hot weather conditions especially in summer season. For the reason that, it is important to provide a good comparison for the heat capacity of the walls at night-time. Lengthily, the time independent heat flux during continuity 21h through same service area of the brick wall and sandwich wall pane is shown in figure 4. Its shows the variation of heat flow from outside to inside during the day and night on summertime data (21/July/ 2015).

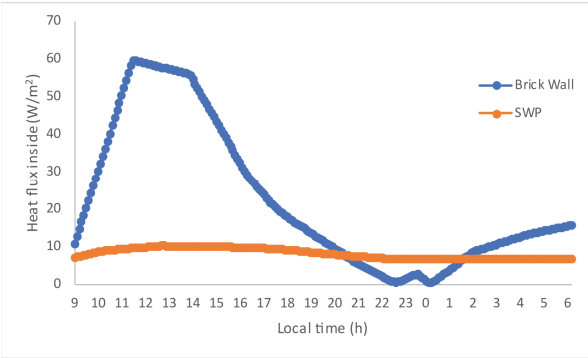

Figure 4: comparison of heat flux of brick wall and SWP during the day and night time

The simulation results show the higher temperature storage in the brick wall during the day-time and relest to inside at night- time. Take into consideration, this parameter is discomfort conditions due to overheating according to the adjustment approach. On the opposite in the sandwich wall panel the heat flux nearly is constant during the day and night time.

5. CONCLUSIONS

In our work, we simulate the effect of global solar radiation on two types of walls with different materials. One is made of brick (R_t = 1.56 K.m^2/W) and the other wall is made of SWP (R_t = 1.956 K.m^2/W) and the outside surfaces of both walls are subjected to global solar radiation from the south in Najaf city-Iraq. The inner walls surfaces are subjected to convection in room temperature of 25 °C (inside the room). The simulation is assumed to be for 24 hours (day and night). The results show that total heat transfer in brick wall is greater becuase of the lower thermal resistance. Moreover, during night the brick wall behaves like a heat source that releases its stored heat to the inside of the room, wheras this is not ture for the SWP.

6. REFRENCES

[1] M. Dunn, “Book review,” *J. Exp. Mar. Bio. Ecol.*, vol. 336, p. 263, 2006.

[2] D. Bushnell, “Optimum design via PANDA2 of composite sandwich panels with honeycomb or foam cores,” *AIAA J.*, 1997.

[3] A. Joudi, H. Svedung, and M. Rönnelid, “Energy efficient surfaces on building sandwich panels—A dynamic simulation model,” *Energy Build.*, vol. 43, no. 9, pp. 2462–2467, 2011.

[4] B. J. Lee and S. Pessiki, “Thermal performance evaluation of precast concrete three-wythe sandwich wall panels,” *Energy Build.*, vol. 38, no. 8, pp. 1006–1014, 2006.

[5] N. Inoue, K. J. Yang, and A. Shibata, “Dynamic non-linear analysis of reinforced concrete shear wall by finite element method with explicit analytical procedure,” *Earthq. Eng. Struct. Dyn.*, vol. 26, no. 9, pp. 967–986, 1997.

[6] X. Lü, T. Lu, V. Penttala, and T. Lehtinen, “Study of heat and moisture transport for concrete sandwich panel wall construction,” *Build. Serv. Eng. Res. Technol.*, vol. 25, no. 2, pp. 89–98, 2004.

[7] T. G. Theodosiou and A. M. Papadopoulos, “The impact of thermal bridges on the energy demand of buildings with double brick wall constructions,” *Energy Build.*, vol. 40, no. 11, pp. 2083–2089, 2008.

[8] M. Charde, S. Bhati, A. Kheterpal, and R. Gupta, “Comparative thermal performance of static sunshade and brick cavity wall for energy efficient building envelope in composite climate,” *Therm. Sci.*, vol. 18, no. 3, pp. 925–934, 2014.

[9] A. Kumar and B. M. Suman, “Experimental evaluation of insulation materials for walls and roofs and their impact on indoor thermal comfort under composite climate,” vol. 59, pp. 635–643, 2013.

EXPERIMENTAL ASPECTS OF LASER IGNITION USE AT SPARK IGNITION ENGINE

Bogdan Done
University Politehnica of Bucharest,
Department of Thermotechnics, Engines, Thermal Equipment and Refrigeration Installations,

ABSTRACT

New technologies are represented by laser ignition systems which can be successfully used in classic petrol engines. Laser ignition technology brings many advantages for engine operation control, engine performance improvement and pollutant emissions reduction. The objective of the paper is the experimental research of laser ignition use in the spark ignition engine. The laser plug ignition system was mounted on an experimental spark ignition engine and was tested at the regime of 90% load and 2800 rev/min, at a dosage of λ=0.9. The experimental results present the influence of laser ignition on different engine parameters compared to the reference operating regime of the engine equipped with classic spark ignition systems. The influences on in-cylinder pressure, heat release rate, engine efficiency and pollutant emissions level are analysed. Compared to the conventional spark plug ignition system, the laser ignition system assures the increase of engine operating efficiency at the investigated regime.

1. INTRODUCTION

At present, pollutant emissions and greenhouse gases produced by automotive internal combustion engines as well the need for engines efficiency improvement, have intensified research in the field of in-cylinder combustion processes. One new technology is the laser ignition system which can be successfully used in classic petrol engines. Laser ignition technology has many advantages in terms of engine operation control, the improvement of engine performance and the reduction of pollutant emissions. One main aspect is that laser-induced sparks are as a rule smaller in size, shorter in duration and have higher temperatures, [1], [2]. Laser technology is one of the most recently developed technologies for combustion management to be successfully applied to classic spark ignition engines. Laser technology can be used to develop a new Laser Plug Ignition system (LPI) able to control the ignition and combustion processes which will lead to the improvement of the performance of the engine in terms of pollutant emissions and fuel efficiency, [3]. The phase of spark formation in correlation with breakdown intensity and the subsequent ignition, which depends on minimum ignition energy (MIE) must be established for LPI use, [1]. With reference to the phase of spark formation, mention must be made of the fact that the delivered energy is sufficient for ignition but its intensity is very low, insufficient for the spark to be formed; spark formation may occur but the energy for combustion is insufficient, [1], [3].

There are four main mechanisms which by means of laser radiation can ignite a mixture of air-fuel: thermal initiation (TI), non-resonant breakdown (NRB), resonant breakdown (RB) and photo-chemical ignition (PCI) [3]. During the thermal initiation (TI) phase the in-cylinder mixture uses laser energy to reach threshold ignition temperature. Also, the TI phase can be established [3], [4] by heating a specific target surface inside the combustion chamber. During the non-resonant breakdown (NRB) phase the laser beam creates an electric field of high intensity which leads to dielectric breakdown of the air-fuel mixture , [1]. At one or more specific wavelengths, the resonant absorption at atomic level is specific to the resonant breakdown phase (RB).

Rezonantei 1-3, bl. 15-16, ap. 74, sector 4, Bucharest, 0761405655, bogdan.done@yahoo.fr

Compared to NRB, during the RB the free electrons required for the breakdown process are created. The free electrons are created in two preceeding steps : the stage of non-resonant (NRPD) photo-dissociation of a molecule and the resonant photo-ionization of the atom created during the NRPD stage. The essential stage for the processes of non-resonant breakdown (NRB) and resonant breakdown (RB) is the non-resonant photo-dissociation of a molecule (NRPD) by absorption and ionization. The non-resonant breakdown is a laser ignition mechanism that emits light, heat and a shockwave, [5], [6]. Photo-chemical ignition (PCI) is a process that requires the absorption and dissociation of a single photon in ultraviolet radiation [5], [6]. The method using two-protons or non-resonant photo-dissociation of a molecule absorption in matter can lead to energy release in the form of a single high-energy photon, when the intensity is high. The benefit of this process is that the short wavelengths can be used for resonant absorption based on the action of longer wavelength laser light, [5], [6]. Regarding the mechanism of non-resonant breakdown, Dearden et. al. used laser-induced sparks that offer the advantage of small size design, but are shorter in duration and operate at higher temperatures [5], [7].

Comparative results regarding the operation of an automobile engine that was ignited with classical spark plugs as well as with laser spark plugs were presented recently by research groups from National Institute for Laser, Plasma and Radiation Physics (INFLPR) and Renault Technologie Roumanie (RTR), Bucharest, Romania [8]. Subsequent to the measurements made for the engine K7M 812k, a lower CO and HC emissions level were identified, using the Laser Plug Ignition. At the speed regime of 1500 min-1, due to the improvement of combustion process based on laser ignition use, the CO emissions decreased by 18…25% and the HC emission decreased by 14…17%. For higher engine speeds, over 2000 min-1, the decreases are limited to ~3%. When laser was used the NO_X emission increased by 8% at a speed of 1500 min-1 and by 2% at a speed of 2000 min-1, researchers from INFLPR and RTR explained that the higher flame temperature reached in the first part of combustion leads to the production of significant quantities of NO_X, [8]. As a solution for NO_X emission reduction the INFLPR and RTR proposed the increase of EGR rate (Exhaust Gas Recirculation), [8]. The researchers from INFLPR explained the CO2 emissions increase at laser ignition use by stating that the carbon content entering into combustion and resulting from the combustion process is constant and it is necessary to make a compromise between HC and NOX for the internal combustion engine calibration, [8]. Measurement results show that the power of the engine ignited by laser system increases by ~3% compared to the classical ignition system. For INFLPR the most critical problem of laser ignition (LI) used during the experimental investigation was the risk of destroying the optical element coatings. The optical element is designed to construct the focusing line and damage of the lenses from the pump line can sometimes appear during engine operation, [5], [7], [8]. Usually, the laser lenses are purchased from standard market, being designed with no special coatings. This technical issue is eliminated by a special coating technology applied to the lenses, using high-damage threshold layers, [15]. Also, in order to eliminate this disadvantage, uncoated lenses can be used at critical points in the laser beam (for high intensity laser beam). The second solution, proposed by many researchers has already been used for different engines but has resulted in a deposit of the combustion products on the sapphire window. H. Ranner et. al. [7] investigated the problem and proposed the self-cleaning solution, a method that cleans the window with the laser beam itself, and can be applied in three steps. As for the first method Ranner [7] explains that the initial part from the higher laser pulse energy, Ep= 4 [mJ], was able to clean the laser window, but only partially. The second method proposes the possibility of using two laser pulses due to the increased length duration of the pump puls. To clean the lenses the first laser pulse was used, this cleaning method being the most efficient. The third cleaning method applied by Ranner [7] used a four stroke engine which admits

double triggering per cycle. Thus, in order to clean the window of cylinder no.4 before a new ignition started, the laser pulses were applied into cylinder no. 4 in the exhaust stroke while the ignition was being initiated in cylinder no.1, [7]. The window of laser plugs for cylinder no. 2 and 3 were cleaned in the same way. Due to the fact that Ranner used a water compact cooling system for each laser plug, the engine was able to operate for a few hours without coatings issues for windows or for optical elements, [9], [10]. Mullett and Dearden [5], [11], studied the LI system performance on a Ford Zetec engine at the speed regime of 1500 min-1 and 30° before Top Dead Centre (TDC) and calculated the different Laser energy values between 12...16 [mJ], [5]. Regarding the control of emissions, the reduction of pollutant emissions, especially the NOX emission, can be successfully assured by the use of exhaust gases to dilute the inlet fresh charge. The use of high ratios of exhaust gas recirculation (EGR), especially at partial load operation regimes, can significantly improve the engine efficiency, knowing that in urban traffic, automotives consume 30% of their fuel in idle conditions [12], [13]. R. D. Fruechte et al. reached the conclusion that a reduction in idle speed from 800 min-1 to 650 min-1 could assure fuel savings of up to 24% at idle regime [12], [14]. With no electrodes to quench the flame kernel as in the case of classical spark plugs, the LPI could offer improved cold-start performance. The present paper shows some aspects of the experimental investigation of laser ignition use on an experimental engine equipped with laser plug ignition system. The paper analyses the effects of LI use on in-cylinder pressure, heat release rates and heat release laws versus classic spark plug ignition.

2. EXPERIMENTAL INVESTIGATION

The experimental research was developed on an experimental single cylinder SI engine, equipped with Laser Plug Ignition. The engine operating regime was 2800 rev/min, 90% load. The experimental engine was mounted on the test bed adequately instrumented, as follows: Schönebeck B4 hydraulic dynamometer, coupling, electronic speed transducer, air flow meter, hydraulic dynamometer water pump, AVL DiCom Analyzer 4000, gasoline fuel pump, gravimetric fuel flow meter, gasoline consumption tap, fuel tank, inlet air temperature measurement indicator, exhaust gas temperature measurement indicator, engine oil temperature measurement indicator, engine oil pressure measurement indicator, cooling liquid temperature measurement indicator, PC equipped with AVL acquisition board, crank angle encoder, cooling fan, cooler, engine water pump, Kistler charge amplifier, piezoelectric Kistler pressure transducer and spark plug ignition. The engine is equipped with a laser ignition system that has the following components: laser plug ignition, optical fibre, laser diode, laser power supply, PC with soft laser, the ensemble breaker distributor (cam with one corner). The laser spark used in the experiments was provided by INFLPR, Laboratory of Solid-State Quantum Electronics, Magurele, Romania as shown in figure 1.

Figure 1: A photo of a laser spark plug is shown in comparison with a classical spark plug. The plasma induced in air by optical breakdown is visible.
(Courtesy of INFLPR, Laboratory of Solid-State Quantum Electronics, Magurele, Romania).

The laser medium was a Nd:YAG/Cr4+:YAG ceramic structure (Baikowski Co., Japan) that consisted of a 8.0-mm long, 1.0-at.% Nd:YAG ceramic, optically-bonded to a Cr4+:YAG ceramic with saturable absorption (SA) [8], [15]. The initial transmission of Cr4+:YAG SA was around 40%. The monolithic configuration of the resonator was obtained by coating the high reflectivity mirror at lasing wavelength, λem= 1.06 μm on the Nd:YAG free side and the outcoupling mirror with reflectivity R= 50% at λem on the Cr4+:YAG free surface. The Nd:YAG side was coated for high transmission (T> 0.98) at the pump wavelength, λp= 807 nm. The optical pump was performed with a fiber-coupled diode laser (JOLD-120-QPXF-2P, Jenoptik, Germany) that was operated in quasi continuous-wave mode; the pump pulse duration was 250 μs and repetition rates up to 100 Hz were used. Typically, the laser yielded pulses with energy of 3.8 mJ at 1.06 μm for the pump with pulses of ~35 mJ at 807 nm; the laser pulse duration was around 1 ns.

3. RESULTS

The experimental research was carried out on the SI engine firstly equipped with Spark Plug Ignition system (SPI), defined as reference and secondly on the engine equipped with Laser Plug Ignition system (LPI) . The operating regime was 2800 rev/min, 90 % load and air-fuel ratio λ=0.9. For the investigated regime, the data were measured with a resolution of 1 CAD and recorded with the AVL data acquisition system.

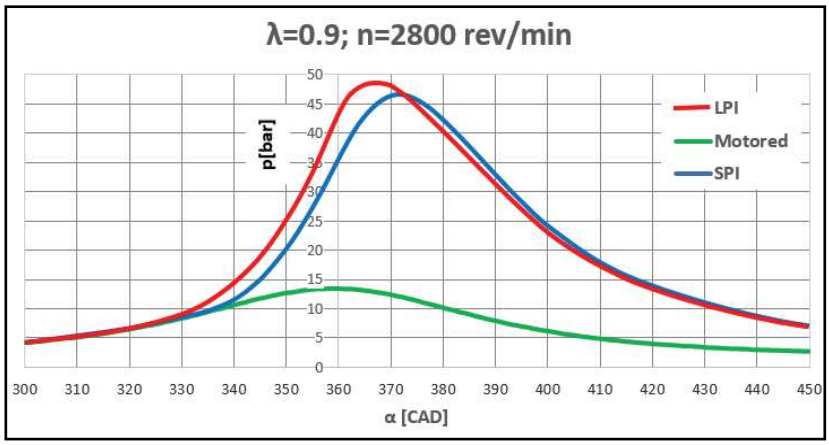

Figure 2: Pressure diagrams registered for Spark Ignition System and Laser

Figure 2 presents the averaged in-cylinder pressure diagrams measured for Spark Ignition System and for Laser Ignition System. The peak pressure rise from 46 bar up to 48 bar. The increase of maximum pressure, was around 5%. Also, the maximum pressure was achived sooner per cycle for laser ignition compared to spark ignition, the angle of maximum pressure reached was 2% closer to TDC for Laser Ignition, figure 2. The initial phase ended ~ 8 degrees sooner for laser ignition compared to the spark ignition system. Heat release rate is presented in figure 3. The peak values registered per cycle heat release rate are comparable for the laser and classic ignition systems, but the maximum admitted is 5 CAD sooner per cycle for laser ignition. Also, the heat release rate for laser ignition starts sooner, i.e. 4 CAD quicker versus spark ignition and decreases faster, in a much more significant manner compared to the tendency registered for classic ignition. These aspects are in corellation with the heat release allure, figure 4. In the case of the laser ignition system the heat release starts with 6 CAD sooner, compared to the classic ignition system. The initial phase of the combustion is reached 6 CAD sooner per cycle and has a shorter duration compared to the classic ignition system, being almost 22% shorter, the value decreasing from 9 CAD down to

7 CAD. The reduction of the duration of the initial phase of combustion is due to a much higher energy developed by the laser ignition system versus the spark ignition system. Also this affects the main phase of the combustion which is registered 6…7 CAD sooner per cycle compared to classic ignition, Figure 3.

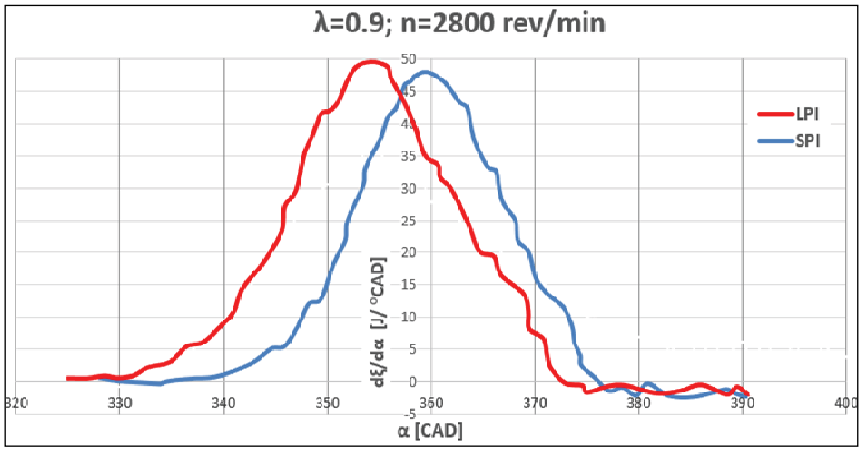

Figure 3: Heat release rate diagrams evaluated for Spark Plug Ignition and Laser Plug Ignition.

The heat release law curve rises faster for LPI comped to SPI and the 10% of conventional mass fraction burned is reached by almost 8 CAD sooner per cycle for the LPI system compared to classic ignition system. The 50% mass fraction burned per cycle is achived before TDC at 354 CAD for laser ignition and at 358 CAD for spark ignition system. The conventional end of the combustion process, reflected by 90% of cycle heat release, appears 5 CAD sooner per cycle for laser ignition system, figure 4. The main influence of laser ignition is reflected on the combustion process which begins sooner and ends earlier compared to the combustion phenomenology registered for the classic ignition system.

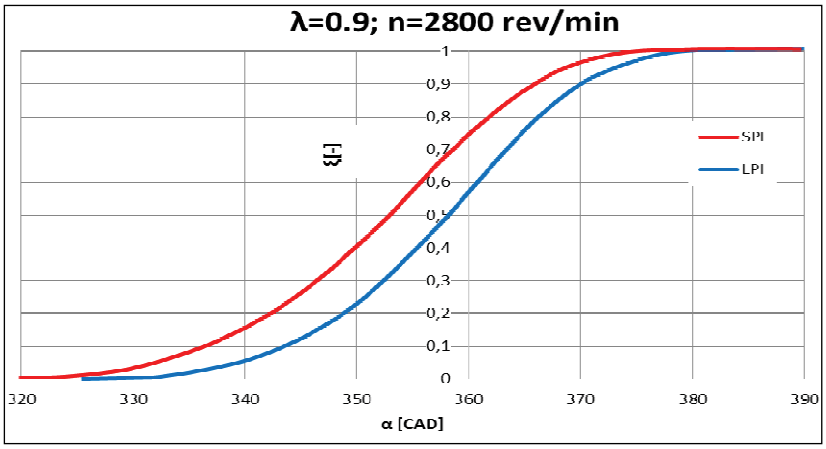

Figure 4: Heat release law diagrams evaluated for Spark Ignition System and Laser Plug Ignition.

4. CONCLUSIONS

The experimental results obtained from the laser ignition use on the spark ignition engine compared to the classic ignition system have led to the following main conclusions:

The in-cylinder maximum pressure increases by almost 2 bar when the laser is used. Also the maximum pressure rise rate registered for classic ignition increases from 1.7 bar/CAD up to 1.9 bar/CAD for laser ignition. The maximum pressure appears ~ 5 CAD sooner per cycle at laser use, the angle of maximum pressure being reached 1.3 % closer to TDC. When the laser ignition system is used the initial phase ends around 8 CAD sooner per cycle compared to the spark ignition system.

The heat release rate and law are accelerated by almost 5 CAD for laser ignition, the maximum values being comparable with the values of SI cycle heat release rate. Reduction of the initial phase of the combustion was 2.4% at laser ignition use versus classic ignition system. The stage of 10% heat release per cycle is reached 7 CAD sooner per cycle with laser ignition system. The reduction of the duration of the initial phase of combustion is due to a much higher energy developed by laser ignition system vesus spark ignition system. Percent of 50% from mass fraction burned per cycle is achived before TDC with 4 CAD sooner for laser ignition.

Acknowledgement

The experiments were performed with a laser spark device developed at National Institute for Laser, Plasma and Radiation Physics, Laboratory of Solid-State Quantum Electronics, Magurele, Ilfov, 077125, Romania. The authors would like to thank Mr. Pavel Nicolaie, Mr. Dinca Mihai and Mrs. Croitoru Gabriela for their help and assistance during the experiments. Also, the authors address special thanks to the AVL GmbH for providing the necessary equipment.

References

[1] P. D. Ronney, *"Laser versus conventional ignition of flames",* Opt. Eng. 33 (2), 510–522 (1994).
[2] N. Negurescu, C. Pana, M.G. Popa, *Internal Combustion Engines. Processes (*Matrixrom Bucharest, 2009).
[3] C. Morgan, "Laser -Induced Breakdown of Gases", Rep. Prog. Phys. 38(5), 621–665 (1975).
[4] S. S. Vorontsov, V. N. Zudov, P. K. Tretyakov, and A. V. Tupikin, *"Peculiarities of the ignition of propane-air premixed flows by CO2 laser radiation, Thermophys. Aeromech"*. 13(4), 615–621 (2006).
[5] G. Dearden and T. Shenton, *Laser ignited engines: progress, challenges and prospects* , Opt. Express 21(S6 Suppl 6), A1113–A1125 (2013).
[6] Y. L. Chen, J. W. L. Lewis, and C. Parigger, *"Spatial & temporal profiles of pulsed laser -induced air plasma emissions, J. Quantitative Spectrosc".* Radiative Transf. 67(2), 91–103 (2000).
[7] H. Ranner, P. K. Tewari, H. Koefler, M. Lackner, E. Wintner, A. K. Agarwal, and F. Wintner*, "Laser cleaning of optical windows in internal combustion engines"*, Opt. Eng. 46(10), 104301 (2007).
[8] N. Pavel, T. Dascalu, G. Salamu, M. Dinca, N. Boicea, and A. Birtas, *Ignition of an automobile engine by high-peak power Nd:YAG/Cr4+:YAG laser -spark devices*, Opt. Express 23(26), 33028-33037 (2015).
[9] S. Lorenz, M. Bärwinkel, R. Stäglich, W. Mühlbauer, and D. Brüggemann, *Pulse train ignition with passively Q-switched laser spark plugs*, Int. J. Engine Res. 17(1), 139–150 (2016).
[10] H. Chen, V. Page, Z. Kuang, E. Lyon, G. Dearden, and T. Shenton, *Multiple Pulse Laser Ignition Control Application in GDI Lean Combustion, presented at the 3rd Laser Ignition Conference (LIC'15),* Argonne National Laboratory, USA, April 27–30, (2015).
[11] J. D. Mullett, Laser-Induced Systemsfor Gasoline Automotivr Engines, PhD Thesis, University of Liverpool (2009).
[12] P. B. Dickinson, A. T. Shenton, J. D. Mullett, G. Dearden, and A. Scarisbrick, "Prospects for LASER ignition in gasoline engine control", 10th Int. Symp. on Advanced Vehicle Control (AVEC10), 22–26 (2010).
[13] R. Jurgen, *Automotive Electronics Handbook* (McGraw-Hill), (1995).
[14] R. D. Fruechte, F. E. Coats, and C. H. Folkerts*, Idle speed control for automobiles*, IEEE Proc. 17th ISECE Conference, 467–472 (1983).
[15] T. Dascalu, G. Salamu, O. Sandu, M. Dinca, and N. Pavel, *Scaling and passively Q-switch operation of a Nd:YAG LASER pumped laterally through a YAG prism*, Opt. & LASER Techn. 67, 164-168 (2015).

EXPERIMENTAL ASPECTS OF THE CYCLE VARIABILITY STUDY OF A SI ENGINE WITH LASER PLUG IGNITION SYSTEM

Bogdan Done
University Politehnica of Bucharest
Department of Thermotechnics, Engines, Thermal and Refrigeration Equipment

The Laser Plug Ignition system could be used to replace the Spark Plug Ignition system of the Spark Ignition Engines with several main advantages related to engine performance and the reduction of pollutant emissions, a topic which has been researched for the last thirty years. The paper presents the preliminary results of the cycle variability study carried out on an SI Engine equipped with a Laser Plug Ignition system. The laser plug ignition system was mounted on an experimental spark ignition engine and was tested at the regime of 90% load and 2800 rev/min, at a dosage of λ=0.9. Compared to the classic ignition system, the Laser Plug Ignition system assures the reduction of the combustion process variability, reflected in the lower values of the coefficient of variability evaluated for the indicated mean effective pressure, maximum pressure, maximum pressure angle and maximum pressure rise rate.

Keywords: laser, cycle variability, spark ignition engine, combustion and performance.

1. INTRODUCTION

In the current global context of severe restrictions regarding the limits of the level of pollutant emissions and greenhouse gases produced by automotive internal combustion engines and in view of efficiency improvement, researchers have been focusing on the use of new technologies regarding combustion process control, [1], [11].

Thus, pollution reduction and fuel efficiency can be controlled at the induction phase in the engine in-cylinder, by direct control of the ignition and combustion processes. Such a new technology may be represented by the Laser Plug Ignition system (LPI), also known as Laser Ignition system (LI), [2]. In order to take place, the process of LI requires two basic steps: spark formation (generally limited by breakdown intensity) and subsequent ignition (generally limited by a 'minimum ignition energy' or MIE), [1]. For example, it is possible either to deliver sufficient energy for ignition but with insufficient intensity (i.e. no spark forms), or to form a spark but with insufficient energy for combustion.There are four well-known main mechanisms in use by which laser radiation can ignite combustible gas mixtures [2] and which are constantly evolving: I. Thermal initiation (TI); II. Non-resonant breakdown (NRB); III. Resonant breakdown (RB); IV. Photo-chemical ignition (PCI).

The most widely studied LI mechanism is NRB. It is similar to conventional electric SI as it produces plasma that emits light, heat and a shockwave, [5], [6], [7]. However, laser-induced sparks are generally smaller in size, shorter in duration and have higher temperatures [5], [13]. Another important issue is the reduction of cycle variability in engine operation, with benefits on efficiency and emissions, [10], [13]. Basically, the phenomena of cycle dispersion are the results of the variations of the combustion process, produced by imperfect mixing of in-cylinder fill in terms of homogeneity, by the phenomena produced in the formation of the plasma channel between the spark plug electrodes, by heat transfer from the flame core to spark plug electrodes, by convective heat transfer from the developed nucleus to the mass of initial mixture and by variation of the engine in-cylinder turbulence, [10], [14], [15], [16]. Cycle variability is strongly influenced by dosage, local air-fuel ratio and by the in-cylinder turbulent velocity field, [10], [12], [13].

Rezonantei 1-3, bl. 15-16, ap. 74, sector 4, Bucharest, 0761405655, bogdan.done@yahoo.fr

Recently, researchers from the National Institute for Laser, Plasma and Radiation Physics (INFLPR) and Renault Technologie Roumanie (RTR), Bucharest, Romania, have presented comparative results regarding the operation of an automobile engine that was ignited with classical spark plugs but also with laser spark, [4]. In the case of the K7M 812k engine, at a speed of 1500 rpm, the coefficient of variation $(COV)_{Pmax}$ decreases by 15% and the $(COV)_{IMEP}$ improvement was in the range of 18.5% (at 920-mbar load) to 22.6% (at 880-mbar load), [4]. The researchers noticed that the cyclic variability of an engine is improved at both high speed and load regimes, showing a lower influence of LPI on the coefficients of variability, expected in these conditions [4]. At 2000 rpm speed regime and high 920-mbar load, small differences between $(COV)_{Pmax}$ and $(COV)_{IMEP}$ for classic and LI ignition systems were noticed, [4]. Also, the results indicate a higher stability of the car engine that was operated at medium speeds by LPI, resulting in reduced noise, vibrations and mechanical stress, [4].
Mullett and Dearden [5], studied the LI system performance and cycle variability on a Ford Zetec engine at the regime of 1500 rpm and 36° before Top Dead Centre (TDC), [5]. Mullett calculated, for different values of laser energy in-cylinder, between 4...92 mJ, the ratio between the COV of IMEP determinant for the LI system and for SI system, [5].
The ratio of COV values for IMEP evaluated for Laser Plug Ignition system and for classic ignition system continuously decreased with the increase of in-cylinder laser energy, [8]. Regarding the combustion stability, for stoichiometric operation, $\lambda = 1$, the LI system was found to outperform the SI system in terms of reduced $(COV)_{IMEP}$ [8]. Dickinson compares the values of $(COV)_{IMEP}$ over a wide range of ignition angles at 1500 rpm, 2.62 bar brake mean effective pressure (BMEP), and analyses the effect of load on $(COV)_{IMEP}$ when operating at 1500 rpm at minimum advance for best torque (MBT), [8].
Shenton, Mullett and Dearden show that LI system improves the combustion stability, explained by measured values of $(COV)_{IMEP}$, [8] and with proper control, these improvements can enable engines to be run under leaner conditions, with higher EGR concentrations, or at lower idle speeds without increasing the noise, vibration and harshness characteristics of a vehicle. LI gives significantly shorter plasma duration compared to SI, [8]. With the recent development of higher average power and higher pulse frequency lasers, it is expected that a multi-strike LI system and associated combustion control can reduce the probability of misfires under high levels of dilution. The prospects for LI are also interesting from a control perspective, from optical sensing of the in-cylinder combustion made possible through self-cleaning (SC) of the laser beam pathway, to the array of possible ignition activation and control mechanisms, [8]. It is anticipated that, combined with the capability to control the ignition location and timing, this will play a significant role in the optimization of future engines by dynamic feedback control, [7]. In case of new ignition system use, like Laser Plug Ignition system, a study of cycle variability for the main parameters that characterize the engine running is imminent.

2. EXPERIMENTAL INVESTIGATION

The experimental research was developed on an experimental single cylinder SI engine, equipped with laser Plug Ignition. The operating regime was 2800 rev/min, 90 % load. This operating regime, defined by the fact that speed is close to the maximum torque speed regime, is often used in exploitation and presents interest for investigation. The load is reduced at 90% in order to assure acceptable mechanical stress of the engine and does not affect the mechanical structure and function of the laser spark plug during this preliminary investigation. The experimental engine was mounted on the test bed adequate instrumented for the experimental investigations carried, its schema being presented in Figure 1.

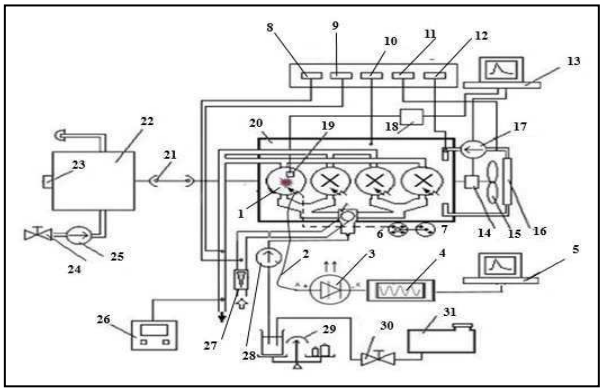

Figure 1: Experimental test bed schema

Figure 2: Compared LPI and SPI

The test bed: 1- laser plug ignition, 2 - optical fibre, 3- laser diode, 4 - laser power supply, 5 - PC with soft laser, 6,7 - the ensemble breaker distributor (cam with one corner), 8 - inlet air temperature measurement indicator, 9 - exhaust gas temperature measurement indicator, 10 - engine oil temperature measurement indicator, 11- engine oil pressure measurement indicator,12 -cooling liquid temperature measurement indicator,13 - PC equipped with AVL acquisition board, 14 - crank angle encoder, 15 - cooling fan, 16 - cooler,17 - engine water pump, 18 - Kistler charge amplifier , 19 - piezoelectric Kistler pressure transducer, 20 - spark plug ignition, 21- coupling, 22 - Schönebeck B4 hydraulic dynamometer, 23 - mechanical snuff speed, 24 - air flow meter, 25 - hydraulic dynamometer water pump, 26 - AVL DiCom Analyzer 4000, 27 - air flow meter, 28 - gasoline fuel pump, 29 - gravimetric fuel flow meter ,30 gasoline consumption tap, 31 - tank.

The laser spark used in the experiments was provided by INFLPR, Laboratory of Solid-State Quantum Electronics, Magurele, Romania. The photo in Figure 2 shows a laser spark plug compared with a classical spark plug. The plasma induced in air by optical breakdown is visible. The laser medium was a Nd:YAG/Cr^{4+}:YAG ceramic structure (Baikowski Co., Japan) that consisted of a 8.0-mm long, 1.0-at.% Nd:YAG ceramic, optically-bonded to a Cr^{4+}:YAG ceramic with saturable absorption (SA) [4], [9]. The initial transmission of Cr^{4+}: YAG SA was around 40%. Monolithic configuration of the resonator was obtained by coating the high reflectivity mirror at lasing wavelength, λ_{em}= 1.06 μm on the Nd:YAG free side and the outcoupling mirror with reflectivity R= 50% at λ_{em} on the Cr^{4+}:YAG free surface. The Nd:YAG side was coated for high transmission (T> 0.98) at the pump wavelength, λ_p= 807 nm. The optical pump was performed with a fiber-coupled diode laser (JOLD-120-QPXF-2P, Jenoptik, Germany) that was operated in quasi continuous-wave mode; the pump pulse duration was 250 μs and repetition rates up to 100 Hz were used. Typically, the laser yielded pulses with energy of 3.8 mJ at 1.06 μm for the pump with pulses of ~35 mJ at 807 nm; the laser pulse duration was around 1 ns. Cyclical variability is evaluated mainly by the variation of pressure differences, which are reflected in the calculated values of coefficients of cyclical variability, [10], [13].The cycle variability can be characterized by coefficients of a cylinder pressure variation. The intensity of the cycle variability phenomena is defined by the coefficient of cycle variability, [10], [13]. For "n" consecutive cycles, if is considered a normal distribution of the deviation probabilities, the squared average deviation can be calculated and the cycle variability coefficient is defined as:

$$(COV)a_i = \frac{\sqrt{\frac{\sum_{i=1}^{n}(a_i - \frac{\sum_{i=1}^{n} a_i}{n})^2}{n-1}}}{\sum_{i=1}^{n} a_i} \cdot 100\% \quad (1)$$

where n is the number of cycles, a is the parameter of which variability is studiedand is defined for indicated mean effective pressure IMEP, maximum pressure pmax, maximum pressure rise rate (dp/dα)max and the angle where maximum pressure occurs, αpmax in the cycle number "i".

The way of cycle variability evaluation for regimes with spark timing closer to the value of spark timing for maximum torque brake (MTB) the coefficient of variation (COV) of maximum pressure is suitable, [10], [13]. When the maximum pressure occurs, the COV of maximum pressure angle is used for characterization of the combustion cycle variability during the initial phase of combustion [10], [13].The variation of the IMEP, appreciated by $(COV)_{IMEP}$, is the most suitable instrument to define the engine respond to the combustion process variability. From this point of view, the limit value of $(COV)_{IMEP}$ defines practically the limit of mixture leaning, [10], [13].This cycle coefficient can also indicate the variability of flame development during the initial phase of combustion [10], [11].A higher combustion velocity reduces the influence of turbulence and reduces the cycle variability [10, 11]. The quality of the in-cylinder mixture influences the combustion process through chemical reaction speed, with a maximum in the area of rich dosage. As a result, the initial and final phases of the combustion process have minimal duration at the dosage for which the chemical reaction speeds are maximum, λ=0.9 [11], [12]. At the mixture leaning, the duration of those two phases increase and the total combustion duration also increases. The normal automotive engine manoeuvrability is assured if the coefficients values are fewer than 10% [10], [13].

3. RESULTS

The experimental research was carried on the SI engine firstly equipped with Spark Plug Ignition system (SPI), defined as reference, and secondly for the engine equipped with laser Plug Ignition system (LPI). The operating regime was 2800 rev/min, 90 % load and air-fuel ratio λ=0.9. For the investigated regime, the data were measured with a resolution of 1 CAD and recorded with the AVL data acquisition system. Analysis of the consecutive pressure diagrams, the cycle variability coefficients were calculated for IMEP, maximum pressure, maximum pressure rise rate and angle of maximum pressure. COV values are presented in the following figures.

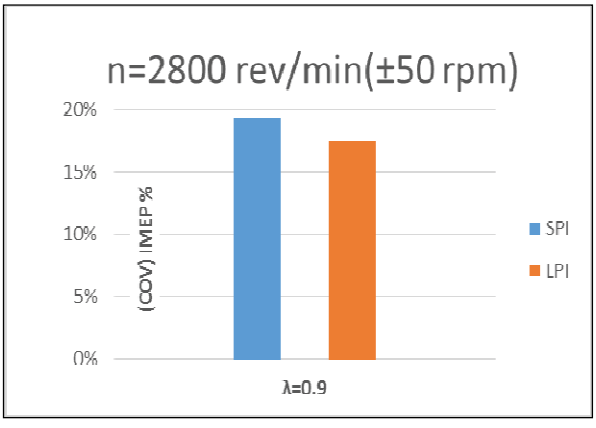

Figure 3: The $(COV)_{IMEP}$ evaluated for SPI and LPI systems

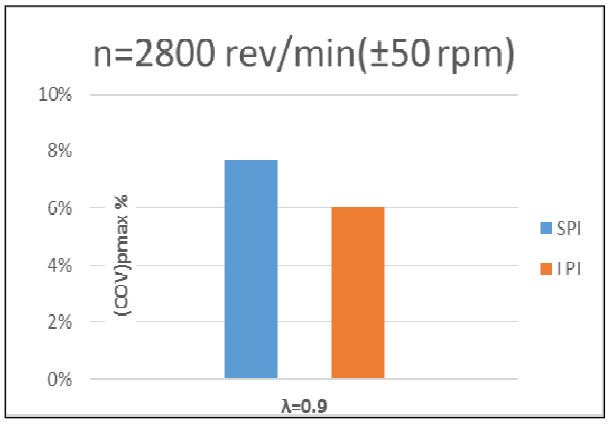

Figure 4: The (COV)pmax evaluated for SPI and LPI

The values of COV calculated for IMEP for Spark Plug Ignition (SPI) and for laser Plug Ignition (LPI) are presented in the Figure 3.

The value of COV of IMEP decreases with 1.9 % at the use of LPI, fact that shows an improvement of the combustion stability at the use of laser Plug Ignition system versus classic ignition system.
A lower value of $(COV)_{IMEP}$, registered at the LPI use, as figure shows, indicates a better engine respond at the variability of the combustion process, at λ=0.9. Also, the reduced value of the COV for indicated mean effective pressure shows a much lower variability of the flame development into the initial phase of the combustion process when the LPI is used comparative to the spark plug system.
The values of COV calculated for maximum pressure for Spark Plague Ignition (SPI) and for laser Plug Ignition (LPI) are presented in Figure 4. The value of COV of maximum pressure decreases from 7.7% down to 6 %. The variability coefficient improves its value with almost 1.7 % when the laser Plug Ignition system is used comparative to the classic spark ignition system. The decrease of COV for maximum pressure is correlated with the variation tendency registered for the COV of IMEP.

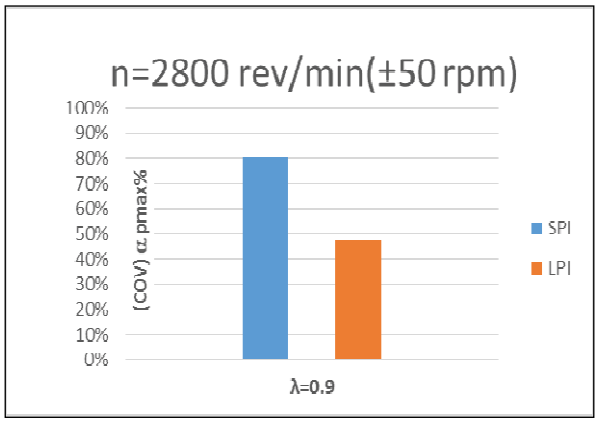

Figure 5: The $(COV)_{\alpha pmax}$ evaluated for SPI and LPI systems

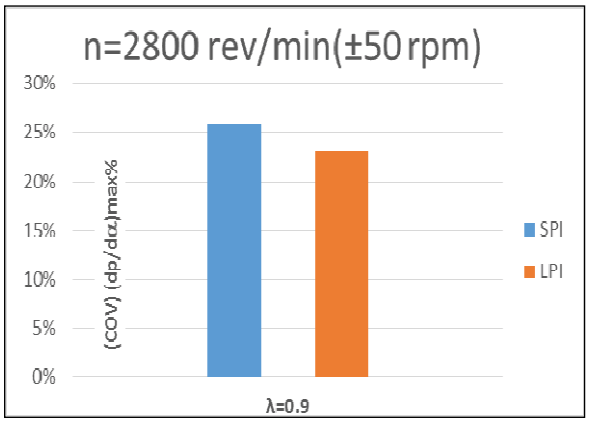

Figure 6: The $(COV)_{(dp/d\alpha)max}$ evaluated for SPI and LPI

The COV of maximum pressure angle, illustrated in Figure 5, defined by the angle when maximum pressure occurs per cycle, decreases from 80.8% value registered for SPI down to 47.5% for LPI. The decrease of the COV of maximum pressure angle, with 33.5% at LASER Plug Ignition system use, reflects a lower cycle variability of the combustion process registered during the initial phase of the combustion; this fact is correlated with the variation tendency registered also for COV of IMEP, Figure 3.
The COV of maximum pressure rise rate is presented in Figure 5. The calculated values for the LPI system of the COV of maximum pressure rise rate decreases with almost 3.5% comparative to the values registered for the classic ignition system with spark plugs. The decrease of the COV for $(dp/d\alpha)_{max}$ appears in correlation with the reduction of the other COV values calculated for IMEP, maximum pressure and angle of maximum pressure.

4. CONCLUSIONS

Regarding the experimental research of a new laser Plug Ignition system used on a SIE, the main conclusions of the cycle variability study can be formulated as it follows:
The values of COV calculated for IMEP for laser Plug Ignition system (LPI) decrease with 1.9%, fact that shows an improvement of the combustion stability at the use of laser Plug Ignition system versus classic ignition system.

Due to a lower value of $(COV)_{IMEP}$, registered when the laser Plug Ignition system is used, indicates a better engine respond at the variability of the combustion process, for λ=0.9. Moreover, a much lower variability of the flame development during the initial phase of the combustion process when the LPI is used comparative to spark plug system.
The values of $(COV)_{pmax}$ for laser Plug Ignition system (LPI) decrease from 7.7% down to 6%, the variability coefficient improves its value with almost 1,7%. The $(COV)_{pmax}$ decrease is in correlation with the variation tendency registered for $(COV)_{IMEP}$.
The decrease of the COV of maximum pressure angle, $(COV)_{\alpha pmax}$ with 39% when using laser Plug Ignition system, reflects a lower cycle variability of the combustion process registered during the initial phase of the combustion; this fact is correlated with the variation tendency registered for $(COV)_{IMEP}$.
The values of COV for maximum pressure rise rate, $(COV)_{(dp/d\alpha)max}$, decreases with almost 3.5% for LPI system use comparative to the values registered for the classic ignition system with spark plugs. The decreases are in correlation with the reduction of COV values calculated for IMEP, maximum pressure and angle of maximum pressure.
The improved values of the cycle variability coefficients registered for laser ignition versus classic ignition system show a good perspective for further experimental investigations carried on other engine operating regimes.

Acknowledgements

The experiments were performed with a laser spark device developed at National Institute for laser, Plasma and Radiation Physics, Laboratory of Solid-State Quantum Electronics, Magurele, Ilfov, 077125, Romania.The authors would like to thank to Mr. Pavel Nicolaie, Mr. Dinca Mihai and Mrs. Croitoru Gabriela for their help and assistance during the experiments.

References

[1]. *P. D. Ronney,* "laser versus conventional ignition of flames," Opt. Eng. 33(2), 510–522 (1994).
[2]. *C. Morgan,* "laser -Induced Breakdown of Gases," Rep. Prog. Phys. 38(5), 621–665 (1975).
[3]. *S. S. Vorontsov, V. N. Zudov, P. K. Tretyakov, and A. V. Tupikin,* "Peculiarities of the ignition of propane-air premixed flows by CO2 laser radiation," Thermophys. Aeromech. 13(4), 615–621 (2006).
[4]. *N. Pavel, T. Dascalu, G. Salamu, M. Dinca, N. Boicea, and A. Birtas*, "Ignition of an automobile engine by high-peak power Nd:YAG/Cr^{4+}:YAG laser -spark devices," Opt. Express 23(26), 33028-33037 (2015).
[5]. *G. Dearden and T. Shenton*, "laser ignited engines: progress, challenges and prospects," Opt. Express 21(S6 Suppl 6), A1113–A1125 (2013).
[6]. *Y. L. Chen, J. W. L. Lewis, and C. Parigger,* "Spatial & temporal profiles of pulsed laser -induced air plasma emissions," J. Quantitative Spectrosc. Radiative Transf. 67(2), 91–103 (2000).
[7]. *J.D.Mullett,*"Laser-Induced Systemsfor Gasoline Automotive Engines," PhD Thesis, University of Liverpool (2009).
[8]. *P. B. Dickinson, A. T. Shenton, J. D. Mullett, G. Dearden, and A. Scarisbrick,* "Prospects for laser ignition in gasoline engine control," 10th Int. Symp. on Advanced Vehicle Control (AVEC10), 22–26 (2010).
[9]. *T. Dascalu, G. Salamu, O. Sandu, M. Dinca, and N. Pavel,* "Scaling and passively Q-switch operation of a Nd:YAG laser pumped laterally through a YAG prism," Opt. & laser Techn. 67, 164-168 (2015).
[10]. *Heywood, B.* Internal Combustion Engine Fundamentals. New York; Mcgraw-Hill Book Company; 1988.
[11]. *Negurescu, N. Pana, C. Popa, M. G.* Internal Combustion Engines. Processes. Bucharest; Matrixrom, 2009.
[12]. *Frank, R. Heywood, J.B.* The Effect of Fuel Caracteristics on Combustion in a Spark-Ignited Direct-Injection Engine. SAE 902063.
[13]. *Gaiginschi, R.* Increasing of Running Cycle Stability of the Four Stroke Spark Ignition Engine Operating with Lean Mixtures. Doctoral Thesis; Institute Politehnic of Bucharest;1976.
[14]. *Sullivan, P., Ancimer, R., and Wallace, J.* (1999), "Turbulence averaging within spark ignition engines", Experiments in Fluids, Vol.27, No.1, pp.92-101.
[15]. Baby X, Dupont A, Ahmed A, Deslandes W, Charnay G and Michard M. A New Methodology to Analyze Cycle-to-Cycle Aerodynamic Variations. SAE 2002-01-2837. 2002.
[16]. *Ghandhi JB, Herold RE, Shakal JS and Strand TE.* Time-Resolved Particle Image Velocimetry Measurements in an Internal Combustion Engine. SAE Paper 2005-01-3868. 2005.

MICRO CHP – CHANCE OF LOW EMISSIONS RESTRICTIONS

Jerzy DUDA
University of Applied Sciences in Nysa
Krzysztof JESIONEK[1]
Wrocław University of Sciences and Technology

ABSTRACT

Observed in the most recent period exceeding the low standards, the result of which in many metropolitan areas in the country there was smog, caused, that the problem of the limitation of the emission of silt and gas has become one of the most important tasks for the local administration. With survey data of pollutant emissions in the country shows that the largest share has low emissions from furnaces and small boiler room housing estates. This is a phenomenon observed in many EU countries, and therefore requires a systemic solution, involving, inter alia, on the participation of States in funding the modernisation of existing heating systems. A decisive influence on the low emission limit has a selection of heating system and the type of fuel used to produce heat for heating purposes and use in households. This article presents one way of production of hot water for heating purposes and utility in which you apply the micro-cogeneration – μCHP (Micro Combined Heat and Power). This is the production of heat and electricity as a typical cogeneration power plants, only in a much smaller scale, limited to the needs of individual farms.

1. INTRODUCTION

The problem of protection of the environment and reduce harmful emissions of dust and gas as energy security in the European Union the main tasks. In the energy industry, heating and energy-intensive industries – chemical, metallurgical and cement – it issues is successfully implemented in the framework of BREFS and energy climate package 3X20, which requires EU countries to achieve in the year 2020:

- 20 % reduction in greenhouse gases emissions compared to 1990
- increasing to 20 % the share of renewable energy sources (RES) in the production of primary energy (Poland was committed to 15 % RES)
- 20 % reduction of primary energy consumption in relation to 2006.

While the much worse it looks like the problem low emission, which besides to the traffic emission, is the result of mostly emissions of particulate matter and noxious gases coming from the combustion of low calorific solid fuels for heating purposes in furnaces and small boilers. Particularly this winter, low emissions due to the favourable weather conditions (no wind) was particularly difficult. In many regions, the result of low emission was the harmful smog. Therefore, the problem of eliminating the low emission is now one of the priorities.
One of the effective ways is to eliminate the low calorie burning coals, mules carbon and waste and rubbish in the heating systems. At the current level of individual installations, fuel combustion techniques, there are many ways to reduce low-emission, low-carbon fuels costs only limited and modern, high-efficiency boilers for central heating. In the urban agglomeration, the cheapest way to elimination of emissions from individual furnaces is joining the holdings to the heating network. On the other hand, if it is not possible to connect to the heating plant you can apply other, also effective solutions that rely on the use of low-

[1] Wybrzeże Wyspiańskiego 27, 50-370 Wrocław, phone +48 603167561, krzysztof.jesionek@pwr.edu.pl

emission fuel boiler-natural gas, fuel oil or biomass (e.g. wood pellets). Type of fuel and its use dependson the price and access. In the countryside where there is virtually no access to the gas network, this may be the most fuel biomass. However, in urban areas where virtually every household has access to the gas network, the best solution is to switch from fuels-coal to natural gas fired.

2. HOUSING ENERGY CONSUMPTION

Eurostat data shows that in households in Poland, total energy consumption per capita is about 12 % lower than in the countries of the former UE-15 and 9 % lower than in the EU-27 as a whole. While the share of the costs for electricity, gas and other fuels in net income in Poland, are among the highest in the EU and is about 120 % higher than in the EU-15 countries and about 105 % higher than the average in EU-27 countries. It follows that the households in Poland are almost 2 times more sensitive to changes in the cost of energy in comparison to the EU as a whole. In Figure 1 is shown the energy consumption of a typical household in Poland.

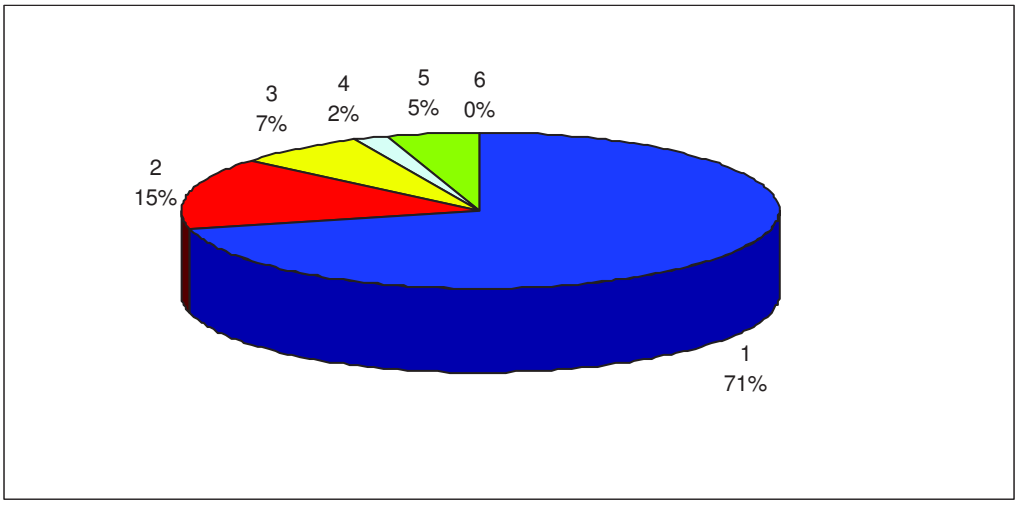

Figure 1: Energy consumption in the household: 1 – heating, 2 – hot water production, 3 – cooking meals, 4 – lighting, 5 – eletrical equipment

Of the data shows that the main part (about 70 %) of energy consumption in the household in Poland is used for heating and the production of hotwater. Compared to the energy consumption for heating purposes in the countries of the former EU-15, where energy consumption for heating purposes is around 50 %, it appears that there are still considerable reserves (possibility to reduce energy for heating), which you can use in order to meet the requirements of the climate package and low emission restrictions. In recent years, housing is observed beneficial changes, among other things, reducing heat losses (improved insulation of buildings) and energy (high efficiency heating systems, ventilation and lighting). In Fig. 2 are shown the changes in the consumption of energy for heating and hot water production targets, which have occurred in recent years in the national housing.

These changes do not, however, have a greater impact on improving the environment, especially in the last period you can conclude after alarming signals about the emission limit is exceeded and the effect of smog in many cities in Poland. High heating costs, especially in older buildings, which is characterised by high heat losses and heating systems with low efficiency of the cause, that is looking for a cheaper, not always eco-friendly solutions. The large dispersion of these small furnaces (detached houses) and their great number causes, that

this is asignificant environmental problem in the country. The solution to this problem requires significant investment. Therefore, the choice of a new individual production system hot water heating purposes and performance requires a deep analysis of both in terms of property and energy efficiency. One increasingly common solution is Association of the production of domestic hot water with electricity generation [1].

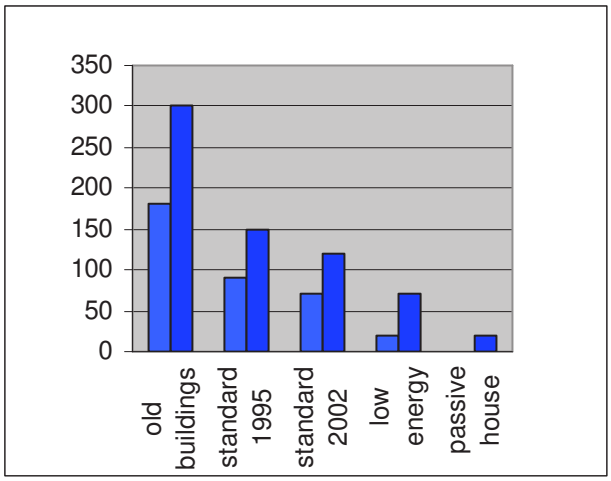

Figure 2: Energy intensity of the housing in Poland, kWh/m^{2}a

3. HOME MICRO-COGENERATION

Micro-cogeneration (μCHP) is the cogeneration process on a smaller scale, which can be applied to an individual household. It consists in the production of hot water for heating purposes and utility and electricity network parameters. Micro-cogeneration in accordance with the provisions of Directive 2004/8/EC means the production associated with the maximum electric power of less than 50 kWel. So far, systems were big application mainly in multi-family residential buildings, public buildings, schools, swimming pools and sports [2]. Such objects are characterized by greater and constant demand for heat and electricity, resulting in a higher energy efficiency. In recent years, it is observed particularly in the countries of the former EU-15, high interest, low heat power μCHP systems below 20 kWth and 0.6÷5.0 kWel. On a chart – Fig. 3 – shows a progressive increase in the applications installation of μCHP.

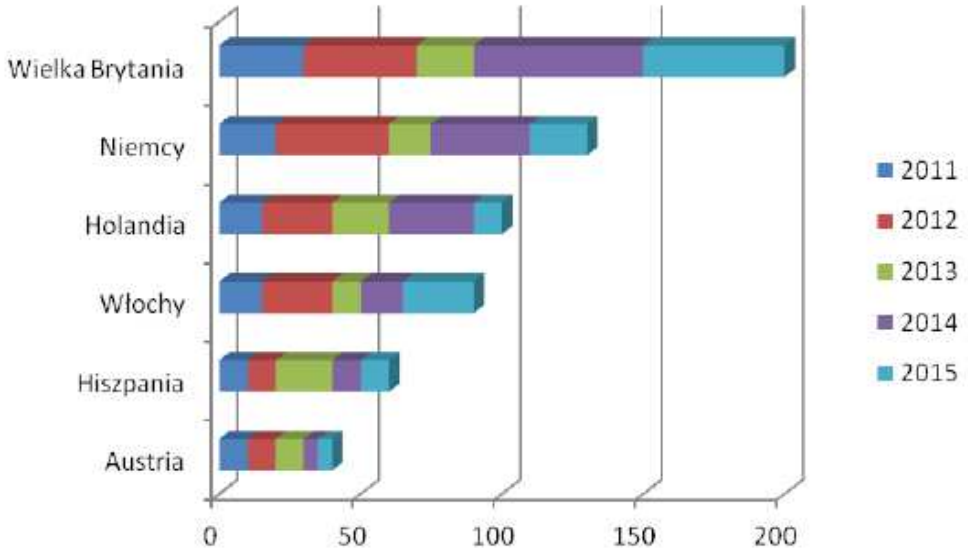

Figure 3: Increase in application of µCHP installation in thousands of units

Such systems have found use mainly in individual households. In Figure 4 is shown a schematic of such system.

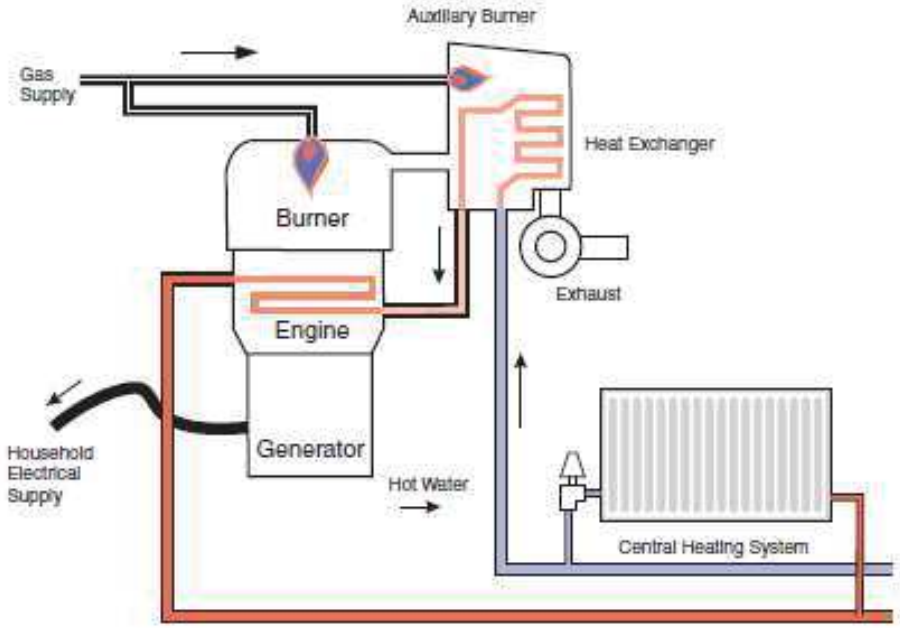

Figure 4: Scheme of µCHP installation

In recent years, it is observed a significant development of installation of µCHP for households with electricity power below 5.0 kWel, which reflects a large demand for such devices. Such devices to generate electricity mostly used: piston engines or Stirling engines. A typical example of the layout of the µCHP with piston engine are the Dachs device of German company SenerTec. For example, one such a device is shown in Fig. 5.

Figure 5: Micro CHP of SenerTec [3]

µCHP device of reciprocating engines are characterized by larger power electric than Stirling engines. Figure 6 shows the device µCHP Hybris Power with Stirling engine production of De Dietrich [4].

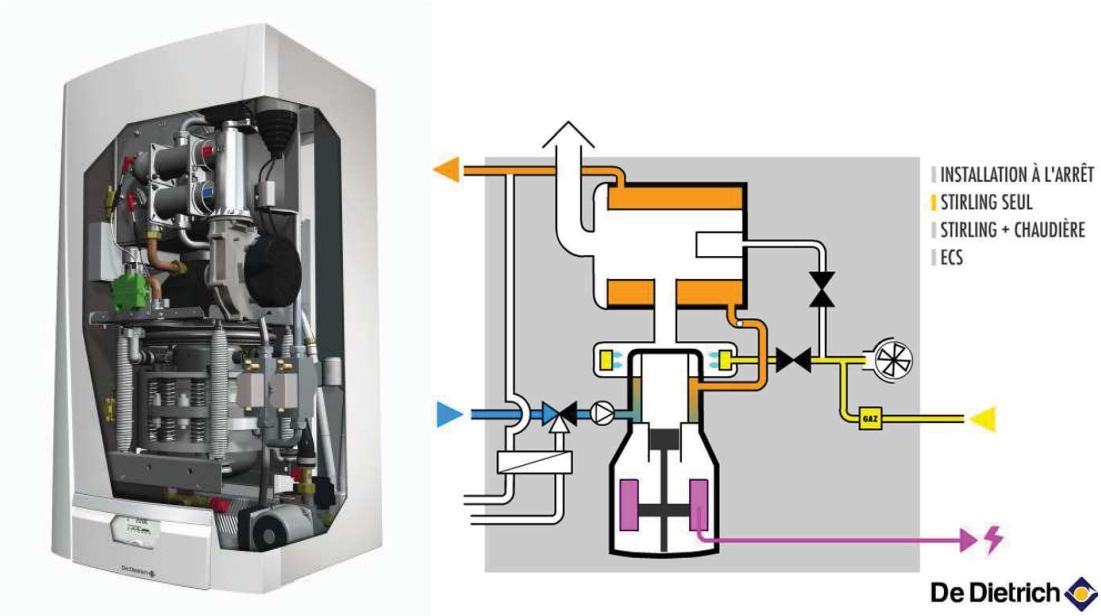

Figure 6: Installation view and technological scheme of HybrisPower

This device is similar to a typical wall gas furnace, condensing. It is equipped with two gas burners and a Stirling engine to produce electricity. The engine is coupled with a generator that produces alternating current with a frequency of 50 Hz and a maximum power of 1.0 kW. Heat output of this device is 5.4÷24.0 kW, consumption of natural gas GZ 50 from 0.5 to the max. 3.7 m^3/h.

4. CONCLUSIONS

Low efficiency of individual heating units and used in them because of the cost, fuel quality, are the main cause of harmful emissions of particulate matter and gases. A significant number of individual heating systems makes these devices belong to the main sources of carbon dioxide emissions in the country. Previous actions to reduce emissions, despite the significant financial incentives not influenced significantly improve an existing State. Presented heating system – home-micro-cogeneration – consisting of the production of heat and electricity in a device installed inside an individual household can be a solution that will reduce harmful emissions. Higher efficiency of μCHP compared to the traditional system of gas heating is an argument for the use of such solutions, [5]. Limitation is the high cost of these installations, especially for individual solutions. μCHP installations should first be applied in multi-family buildings where it is not possible to connect to the heating network and in public buildings. As is clear from the experience of the working installation, depending on the size of the unit and the demand for heat and electricity use μCHP allows in addition to ecological effect, get lower electricity costs by more than 50 % compared to buying this energy from the power plant. Having regard to the profit of the energy produced, the resulting cost of heating is 30÷40 % lower than with traditional heating.

References

[1] Duda J., Kołosowski M., Tomasiak J., „*Mikrokogeneracja szansą rozwoju ekoinnowacyjnych systemów ogrzewania*", „Innowacje w zarządzaniu i inżynierii produkcji" pod redakcją R. Knosali, Oficyna Wydawnicza Polskiego Towarzystw Zarządzania Produkcją, Opole 2016, s. 30-40.

[2] Pisarev V., „*Mikrokogeneracja w projektowaniu systemów energetycznych*", Oficyna Wydawnicza Politechniki Rzeszowskiej.

[3] http://www.e-energy.de

[4] http://www. blog.dedietrich.pl/hybrispower

[5] Dong L., Liu H., Riffat S., *„Development of small-scale and micro-scale biomass-fuelled CHP systems – A literature review*", Applied Thermal Engineering, Vol. 29, Issues 11-12, August 2009, pp. 2119-2126

EQUIPMENT FOR STUDY OF VARIOUS HEAT EXCHANGE CONDITIONS IN CAPILLARY-POROUS STRUCTURES OF POWER EQUIPMENT

Alexander Alexievich Genbach[1], David Iu. Bondartsev[2], Iliya K. Iliev[3]

ABSTRACT

Experimental setup has been developed and studied in order to determine the integral heat-exchange characteristics of the capillary-porous cooling system according to the coolant supply circuit, degree of pressure on the structure, height of the heat exchange surface, design of the tubular arterial structure and micro arteries supplying coolant, orientation of the heating surface and the pressure in the system. A diagram has been shown of the cooling system functionality along with measurements and methodology. Overheated heaters and fuses have been shown at the time of the crisis of heat transfer.

1. INTRODUCTION

We can give a number of experimental equipment that allow us to investigate the integral characteristics of heat transfer: the specific heat fluxes q, the fluid and vapour flow rates m_f, m_{vap}, the pattern of temperature distribution along the height and length of the heat exchange surface.

The studies are carried out in a capillary-porous cooling system which can operate on the principle of a closed evaporative condensation scheme or can be opened. Different heat exchange conditions are studied, i.e. the method of the cooler supply, the degree of clamping of the capillary-porous structure, the ability to feed water along the height of the heat exchange surface, the orientation of the degree relative to the gravitational forces, flat, tubular and curved cooling surfaces, the operation of the system under pressure in advance of the onset of crisis phenomena accompanied by the burning-out of a wall.

To study the mechanism of heat transfer, holography methods [1], generalization of similar [2] and equivalent phenomena [3] are used.

The heat exchange control is carried out due to elliptical systems [1,4,5] by combined action of capillary and mass forces [2,4,6].

The study of heat transfer is of practical nature, it is intended for the creation of various thermal power plants, such as porous casings for pipelines [8], steam coolers of steam boilers [9], porous coatings of poorly heat-conducting material [10], seals in steam turbines [11,12] and a number of other power plants [13,14].

3. Measuring circuit

Fig. 1 depicts the functioning scheme of the porous cooling system, the method for measuring the temperature of the heating surface t_w. The measurement of fluid flow rates m^t_f, m_1, m_2, m_{dr}, m_{con}, $m_{cir.wat}$, m_{air} and vapour flow rates m_{vap}. The accepted indices are “t” - tank, “f”-fluid; “dr” - drain, “con” - condensate, “cir.wat”- circulating water. Control of the temperature of the liquid is represented with t_f^t, t_f^{dr}, t_f^{out}, t_f^{in}, that of the vapor with t_{vap}, and of the electrical insulation $t_{el}^{ins} = t_{diff}$.

Fig. 2 shows the cooling element with a capillary-porous structure. It allows to study the schemes of fluid supply from tubular arteries 3, influence of the height of the heat exchange

[1] Professor DSc, AUES, Almaty, Kasachstan, katerina-1@rambler.ru
[2] PhD Student, AUES, Almaty, Kasachstan, d.bondartsev@saem.kz, cell phone: +77015323661
[3] Professor, PhD, Ruse University, Ruse, Bulgaria, e-mail: iiliev@enconservices.com, cell phone: +359 887306898

surface h, the degree of compression of the structure with the help of a perforated plate 10, and the dispensing intensity of the coolant by micro arteries 11.

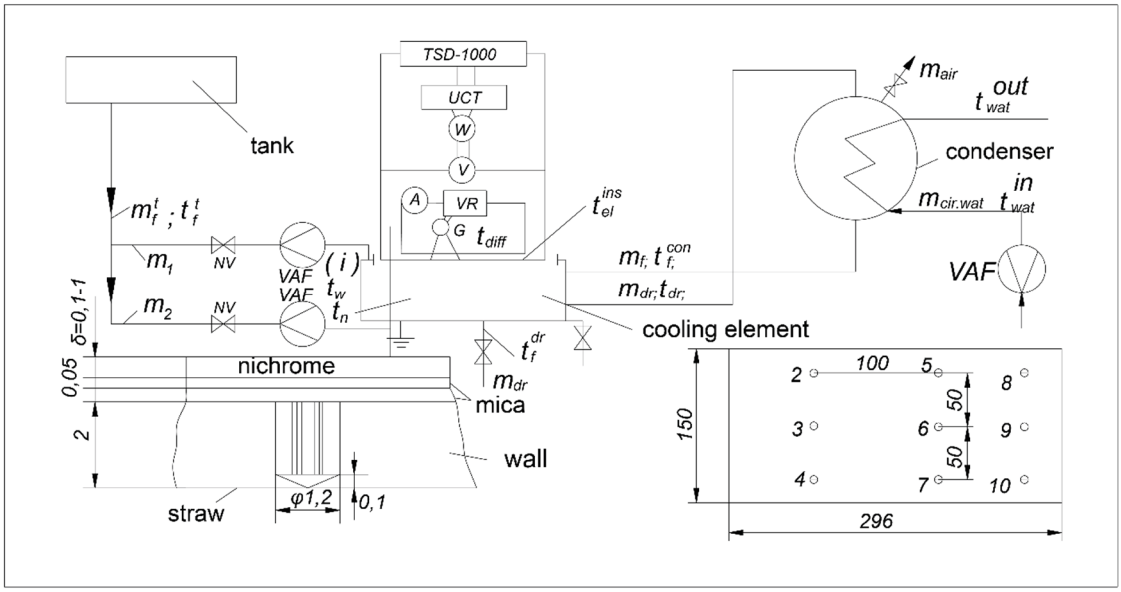

Fig.1. Functioning Scheme fora porous system and the measurement procedure: TSD-1000 – welding transformer; UCT–universal current transformer; W–wattmeter; V–voltmeter; A–ammeter; VR–voltage regulation; G–galvanometer; P–variable-area flowmeter; NV–needle valve.

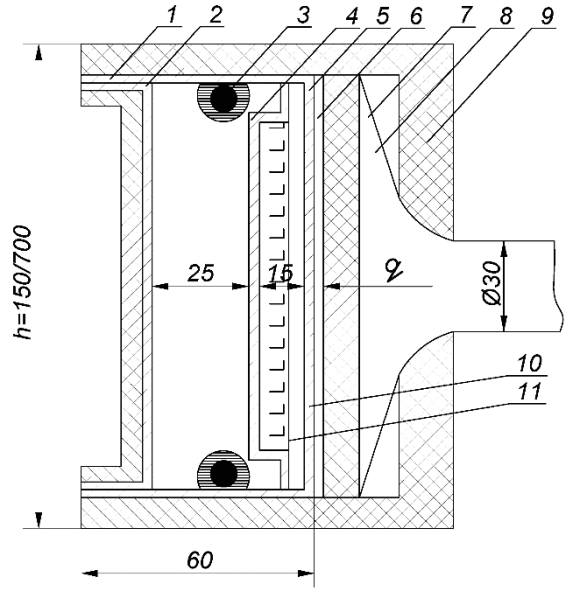

Fig.2. The cooling element with a capillary-porous structure: 1–envelope, 2–cover, 3–tubular arteria, 4–plug, 5–capillary-porous structure, 6–electrical insulation (mica), 7–principal heating unit, 8–guarding heater, 9–heat insulation, 10–perforated clamping plate, 11–micro arteria.

The clamping scheme of a capillary-porous structure is shown in Fig. 3.

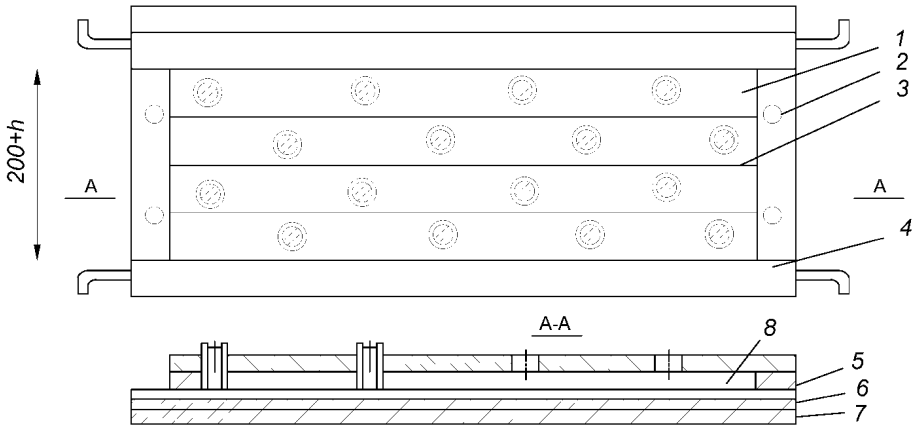

Fig.3. The clamping scheme of a capillary-porous structure: 1 – plates, 2 – clamp screws, 3 – steam slots, 4 – inflow input, 5 – perforated clamping plate, 6 – capillary-porous structure, 7 – heated wall, 8 – micro arteria.

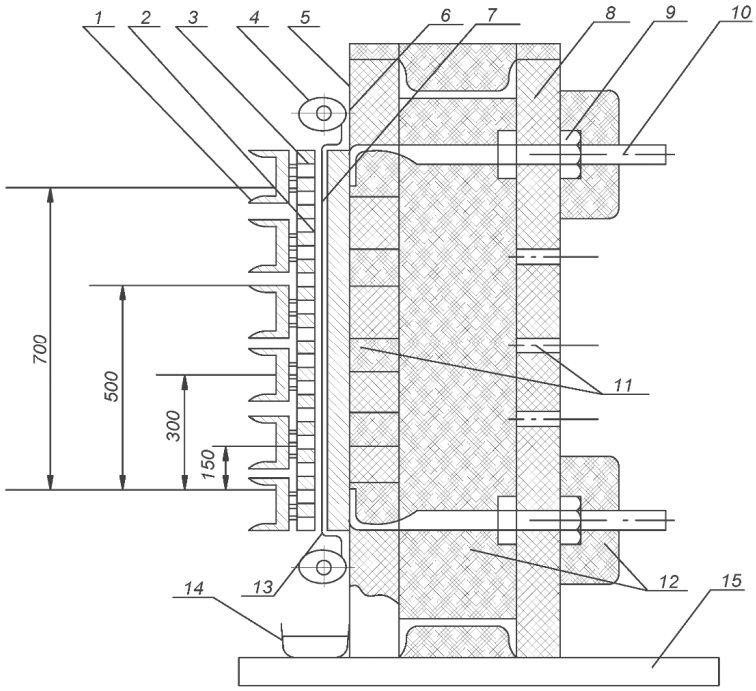

Fig.4. Cross section of flat experimental equipment: 1 – clamping bar, 2 – capillary-porous structure, 3 – perforated clamping plate, 4 – tubular arteria, 5 – asbestos plate, 6 – heating unit, 7 – insulation, 8 – plate, 9 - hold-down nut, 10 – electrode, 11 – windows, 12 – heat insulation, 13 – cooling wall, 14 – chamber collector, 15 – support.

Fig. 4 shows a transverse section of flat experimental equipment with a perforated clamping plate 3, tubular arteries 4 and a capillary-porous structure 2.

Fig. 5 shows the investigation schemes of the influence of the orientation of the heat-release surface.

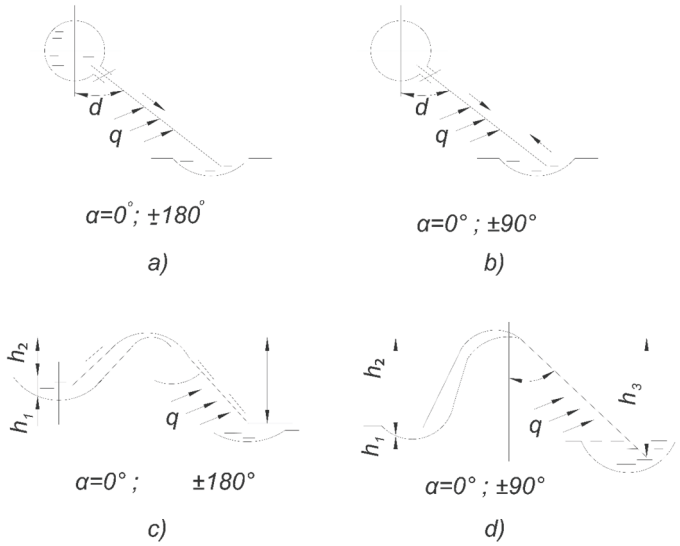

Fig.5 The schemes for investigation of orientation of a heat-release surface: *a,b* – the fluid is supplied by the arteria, *c,d* – "siphon" supply of liquid: α – angle between the cooling surface and the force of gravity.

Fig. 6 shows experimental equipment with a curved surface operating under high pressure.

4. Experimental design

Heat transfer studies were conducted prior to the onset of a boiling crisis with surface overheating and a capillary-porous structure (Fig. 7*a,b*) with the surplus liquid m_f/m_{vap} of (1 ÷ 17.6).

Thus, experimental equipment of integral (average) heat-exchange characteristics of a capillary-porous cooling system is designed and investigated: a scheme of functioning and a measurement procedure, building of a cooling element with tubular arteries, a perforated clamping plate and micro arteries were shown. Various factors were studied: the height of the heat exchange surface, the pressure in the cooling system up to the burning-out of both the wall and the wicks.

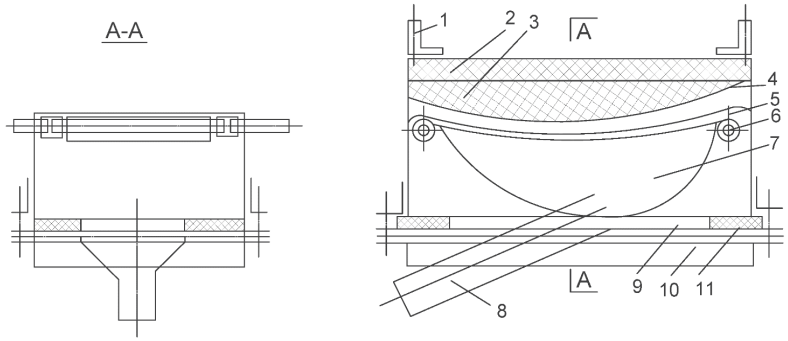

Fig.6 The schemes of experimental equipment with a curved surface operating under high pressure: 1 –electrode, 2 –asbestos plate, 3 – flaked asbestos, 4 –nichrome, 5 –net structure, 6 – liquid supply pipe, 7 –vapor channel, 8 – vapor discharge tube, 9 – envelope, 10 –cover, 11-seal.

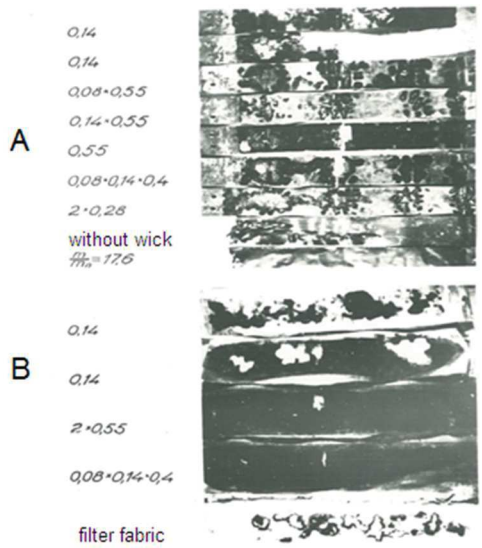

Fig.7. Blown heating units (A) and capillary -porous structures (B) wicks. The surplus of liquid was changed from m_f/m_{vap} = 1 to 17,6.

3. Conditions for experiments

The supply of electrical energy to the main heating unit is carried out from a welding transformer of the TSD-1000 type the output voltage of which compose the following fixed values: 2,5; 5; 7,5 and 10 (see Fig. 1). The electric current feeding the heating unit is measured according to the scheme with a universal transformer of the UCT-6M2 cl.0,2 type. The secondary current is up to 5 A, the primary current is 100 ... 2000 A. The voltage drop on the heating unit is measured by a voltmeter of the D523 cl. 0,5 type.

The greatest possibility of error in current measurement is ± 0,6%, in the voltage drop ± 1%, and in the power it is ± 1,6%. Electric energy is supplied to the guarding heater from a voltage regulation of the VR type.

When studying the onset of liquid boiling and critical loads the current transformer of the TSD-1000 type is used with an output voltage of off-load of 71 V. The electric current intensity is regulated in the ranges of 200 ... 1200 A.

Measurements of liquid and ambient temperatures are performed by mercury thermometers of the TL-4 type with a scale of 0 ... 50^0C and 50 ... 100^0C and a pressure of $0,1^0$C. The temperatures of the liquid and vapour discharge are measured by *chromel-copel* thermocouples made of cable with a diameter of $0.1x10^{-3}$ m. The diameter of the junction head of the thermocouples is $0.4\ x10^{-3}$ m.

The electrodes of thermocouples are isolated by two-channel straws with a diameter of $1.0x10^{-3}$ m fixed with BF-2 glue inside injection needles with a diameter of $1.2x10^{-3}$ m.

In order to measure the wall temperature, the thermocouple electrodes with a diameter of 0.2×10^{-3}m are welded to it by an electric arc formed during the discharge of condensers. For this it is normal to make a borehole to a depth of $1.9x10^{-3}$ m with a diameter of 1.2×10^{-3} with an accuracy of $\pm0.05\times10^{-3}$ m to the surface of the wall with thickness of 2×10^{-3} m. The thermocouple electrodes are insulated with porcelain straws measuring 1.2×10^{-3} m in diameter and they are put along the wall surface between two layers of mica with a thickness of $0.05x10^{-3}$ m glued to the surface of the heating unit. The cold ends of thermocouples are thermostated in melting ice. The electrodes of thermocouples are connected to two twelve-point switches of the PP-63 cl. 0.05 type. To eliminate the effect of induced circulating currents on the thermocouple readings, the equipment and instruments are grounded.

The cooling and circulating fluid flow rates are determined by electric *variable-area flowmeters* of the PED type with a secondary electronic device of the KSDZ-43 cl. 1 type calibrated with a volumetric method. The discharge of the merging liquid and condensate is fixed using a measuring container with a pressure scale of $0.5x10^{-3}$ liters, and the filling time is measured with a stopwatch of the C-P-1b type with a scale interval of 0.1 second.

The greatest possible error in determining of the flow rate of the liquid by variable-area flowmeters does not exceed ± 3%, and by the volumetric method does not exceed ± 2%.

The conditional coefficient of transparency was investigated in the work [2]. The data scattering of the value K_y in the generalization of the experimental data does not exceed ± 16%.

The effective thermal conductivity of the wetted network structure was determined by the formula (1):

$$\lambda_{eff} = \left[1 + \frac{1}{0.5*a*b+C}\right] \quad (1)$$

where a=8x10^3 m^{-1}, C=1.35 for nets 12x18H9T, and a= 1.8x10^3 m^{-1}, C=0.73 for brass nets.

The imbalance of the heat supplied by the current and the heat generated by the circulating and surplus water taking into account Q_{sp} does not exceed ± 12%, and the imbalance of the heat supplied by the vapour in the condenser and the heat generated by the circulating water does not exceed ± 11%.

The material imbalance between the flow rate of the cooling liquid, drainage and condensate flow rates does not exceed ± 10%/

The procedure for measuring and processing of experimental data was published in the works [2-4, 6, 7, 14].

Conclusions

The presented experimental setup is suitable for determination of the integral heat-exchange characteristics of the capillary-porous cooling system and possesses wide possibilities of determining the following: different schemes of filling of the refrigerant, according to the coolant supply circuit; degree of pressure on the structure; height of the heat exchange surface; design of the tubular arterial structure and micro arteries supplying coolant; orientation of the heating surface and the pressure in the system.

References

[1] Polyaev V.M., A.N. Genbach, A.A. Genbach, *Methods of monitoring Energy Processes*//Experimental thermal and fluid science, International of thermodynamics. Experimental Heat Transfer and Fluid Mechanics. Avenue of the Americas – New York, 1995, Vol. 10, April, pp. 273-286.

[2] Polyaev V.M., A.A. Genbach, *Heat Transfer in a Porous System in the Presence of Both Capillary and Gravity Forces*// Thermal Engineering. – 1993, № 7, Volume 40, Moscow, pp. 551-554.

[3] Polyaev V.M., A.N. Genbach, A.A. Genbach, *Limiting states of a surface under thermal action* // Thermophysics of high temperatures. – 1991. Vol.29, № 5. – pp. 923-934.

[4] Polyaev V.M., A.A. Genbach, *Control of heat transfer in a porous cooling system* // Second world conference of experimental heat transfer, fluid mechanics and thermodynamics, Dubrovnik, Yugoslavia, 23 – 28 of June1991, pp. 639 – 644.

[5] Polyaev V.M., A.A. Genbach, D.V. Minashkin, *Processes in a porous electric heat exchanger* // Izvestiya VUZov, Mashinostroenie – 1991. - № 4 – 6. – pp. 73 – 77.

[6] Polyaev V.M., A.A. Genbach, *Analysis of the laws of friction and heat transfer in a porous structure* // Vestnik MSTU, Mashinostroenie, 1991, pp. 86 – 96.

[7] Polyaev V.M., A.A. Genbach, I.N. Bocharova, *Effect of pressure on the intensity of heat transfer in a porous system.* // Proceedings of universities, Mashinostroenie, 1992, № 4 – 6, pp. 68 -72.

[8] Genbach A.A, Bakitivanov I.B., *Protection from earthquakes of TPP foundations by means of porous geo-screens* // Search, MOH PK, № 1 (2), 2012. – pp. 289 – 297.

[9] Genbach A.A, I. Danilchenko, *Porous steam desuperheater of steam boilers* // Industry of Kazakhstan, № 1 (70), 2012. – pp. 72 – 75.

[10] Genbach A.A., K.S. Olzhabayeva, *Visualization of the thermal effect on porous material in the power unit of the power plant* // Bulletin of the National Engineering Academy of the Republic of Kazakhstan, № 3 (45), 2012. – pp. 63 – 67.

[11] Genbach A.A, F.A. Islamov, *Investigation of the sucker fillet in power plants* // Bulletin of KazNTU, № 3 (97), 2013. – pp. 245 – 248.

[12] Genbach A.A., F.A. Islamov. *Modeling of the turbine rotor grinding process* // Bulletin of KazNTU, № 6 (100), 2013. – pp. 235 – 240.

[13] Polyaev V.M., A.A. Genbach, *Areas of application of the porous system* // Izvestiya VUZov. Power engineering. – 1991. № 12. – pp. 97 – 101.

[14] Polyaev V.M., Genbach A.A., *Control of heat exchange in a porous structure*, Transport. – 1992. Vol. 38.

HEAT EXCHANGE IN OIL-COOLER AT POWER STATION

Alexander Alexievich Genbach [1], Karlygash Olzhabayeva [2], Iliya Krastev Iliev [3]

ABSTRACT

Implementation of porous systems in production was preceded by research work on the transfer of energy and matter in the heat exchangers containing capillary-porous coating of different thermal conductivity and porosity. For a heat exchange intensification at evaporation and boiling a capillary cellular coating on the cooled surface is widely used recently. Capillary-porous coatings facilitate the boiling of liquid (the necessary difference is reduced), can significantly intensify the heat exchange at nucleate boiling and increase the critical heat flux.

The need to improve the efficiency of oil coolers of steam turbine installations is increased particularly during the present period which is characterized by constant growth of energy costs, of power supplies as well as increased attention to problems of energy and resource saving.

Offered capillary-porous cooling system eliminates the ingress of oil into the water supply source, and the cooling liquid into the oil supply system. This maintains a high coefficient of heat transfer from the coolant and increases from the heat carrier (oil). The uniformity of the temperature field will stabilize the temperature of the oil. The amount of circulating coolant (by 60-70 times) considerably reduces. The technical solution provides a simple, reliable design, its unification. The described scheme allows us to solve the problem of environmental protection in two aspects: the treatment of wastewater and soil from oil products and the use of low-potential heat.

1. INTRODUCTION

1. Studying of heat exchange processes in a new porous cooling system of power equipment at power plants

When building a physical model of boiling of liquid in a new porous system working under combined action of gravitation and capillary forces [1], for the primary boiling region we consider that the bulk of heat q is transferred by efficient thermal conductivity λ_{ef} in the process of heat exchange

$$q = \lambda_{ef} \Delta T \, \delta_{ef}^{-1}. \quad (1)$$

Assuming that $\delta_{ef} \sim \bar{f}^{-0,5} \, \nu_f^{0,5}$, we will get the correspondence

$$q = C \lambda_{ef} \bar{f}^{0,5} \nu_f^{-0,5} \Delta T \, , \quad (2)$$

$$\bar{f} = 54{,}1 \, \alpha_f \mathrm{J_a} / \bar{R}_o^2 \, ; \, \mathrm{J_a} = \frac{\mathrm{C_p} f \rho_f \Delta \mathrm{T}}{r \rho_{st}};$$

$$\bar{R}_o = 2 \left[\rho_f / g \left(\rho_f - \rho_{st} \right) \right]^{\frac{1}{3}} [0{,}35 (\frac{\sigma^2 \mathrm{T}_s}{r \rho_f \rho_{st} \Delta \mathrm{T}})^{\frac{1}{3}} + (\frac{\lambda_f \Delta \mathrm{T}}{r \rho_{st}})^{\frac{2}{3}}];$$

For the region of developed bubble boiling [2] we consider that extraction of head flux, is realized mainly at the expense of evaporation, i.e. $\approx q_{st} \sim \bar{W} r \rho_{st} \, \bar{\rho}$, where the average volumetric

[1] Professor DSc, AUES, Kasachstan, katerina-1@rambler.ru

[2] PhD Student, AUES, Kasachstan, karla210784@mail.ru

[3] Professor, PhD, Ruse University, Ruse, Bulgaria, e-mail: iiliev@enconservices.com; cell phone: +359 887306898

pulsation speed of a vapour bubble in a cell of a grid-type structure equates to $\bar{W} = dV/d\tau$. Assuming that the volume of a growing bubble is $V \sim R^3$, we will have $\bar{W} = dR^3/d\tau \sim R^2 dR/d\tau$. As the experiment shows, the density of active evaporation centers is $\bar{\rho} \sim R^{-2}$, thus we can write a formula for a heat flux $q \sim \frac{dR}{d\tau} R\bar{\rho}^{0,5} r\rho_{vap}$, where the rate of velocity of the growth of vapor bubbles in the grid-type structures has been determined by empirical data processing

$$\frac{dR}{d\tau} = (13{,}5\ \alpha_f \mathrm{J_a}/\tau)^{0,5}. \qquad (3)$$

Putting the equation (3) to the correspondence (2), and considering the type of the porous structure and heat-accumulating properties of a wall, we have the formula of a heat flux for the developed boiling region (correspondence 1).

Therefore, the formula (1) may be received by considering the fluctuation process of generation of a vapour bubble of critical size with a burst, occurring on the wall or on the carcass of the structure, i.e. $q \sim V_{cr}\ \bar{\rho}\bar{f} r\rho_{st}$,

where V_{cr} - is the volume of a bubble of critical size.

Showing the value V_{cr} through the critical size of a bubble $R_{cr} = 2\sigma/\Delta P$, where $\Delta P = \Delta T r\rho_{st}/T_s$, and using the derived formulas for the values $\bar{\rho}$ и $\bar{f}$, we will have the correspondence $q = const\ f(P)\Delta T^2$. Hence, the initial stage of bubble formation, having the nature of a burst, and being studied by us on an impulse holographic installation [4], is the determining in subsequent regime of active bubble boiling in the studied porous cooling system.

2. Analysis of the derived equations

The analysis of the derived equations demonstrates:

1. To study the porous system there is no such a drastic correspondence of the rate of heat exchange $\alpha = f(b_g, h, L)$, as it takes place in heat pipes, where L – is the length of the surface.
2. The function $q = f(\Delta T)$ is "stronger" than for heat pipes, which is explained by the excess of liquid.
3. The excessive liquid consumption, through which the influence of velocity and under heating of the liquid is reflected, is insignificantly affects the value q, however, its existence is significantly expand the borders of working capacity of the system q_{cr}.
4. Bending the system reduces q.
5. The increased size of cells and larger thickness of structures reduces q.
6. Pressure influences on q more smoothly, than under boiling in a large volume, because the existence of capillary potentiality is a constraining factor.
7. The growth of accumulating capacity of a wall increases q.
8. The density of centres and frequency of generation have larger values, which is connected with larger and more uniform overheating of bordering layer, and departure diameters are smaller than in boiling in a large volume.

3. Model of derived equations

Analysis of holographic interferogram showed that with the value of $q = const$ stable concentration of interferential stripes in the time, characterizing the boiling process as quasi-stationary, were derived. However, some deformation is associated with pulse regime of the boiling process, and availability in the cells of the structure of regularly changing centers of evaporation. At the same time, one can assume that in the near-the-grid area there is an emission of the drops of liquid (figure 1) [2].

With different values q by degree of deformation of forms and density of interferential stripes, heat and hydro dynamical condition of the processes of heat and mass-transfer were assessed.

Therewith we can judge about micro processes and some local processes, for example, about temperature micro topography, on fluctuation phenomena, on emission of drops. The more

intensive the process, the brighter the pictures are expressed. There are some differential pictures, which is impossible to be determined by any other ways.

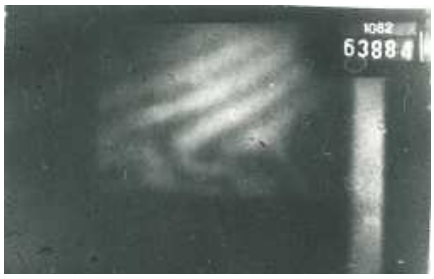

Figure 1 - Holographic interferogram of the process of evaporation in a grid-type porous structure of type 0,4 where $q=1,2.10^5$ W/m^2; $m_f/m_{st}=1,1=opt$

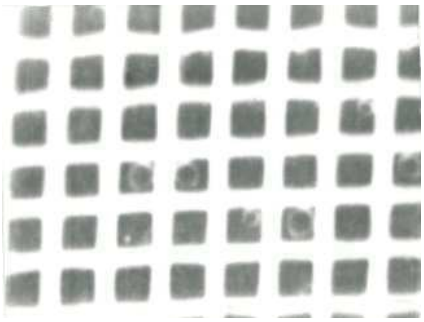

Figure 2 - a fragment of a picture gram of the process of evaporation in a grid-type porous structure of type 0,4 where $q=6,7.10^4$ W/m^2; $m_f/m_{st}=5,2$

For example, in the near-the-grid space, active processes take place within 4.10^{-3} m at $q=40$ kW/m^2 and $q=7.10^{-3}$ kW/m^2 at $q=120$ kW/m^2.

In case of admission of small amounts of the value q, the areas of homogeneity are more enlarged, which notes the stability of the processes in some local area or even on a significant section of surface. At high values q the areas are concentrated right until the sizes of certain cells of the structure. Therefore, one can assume that the nature of liquid boiling shall be determined by the sizes of one or several cells [3].

With the increasing of the value q, the number of evaporation centres increases as well. There are vapour bubbles and their formations, derived due to the junction of separate bubbles. Upon existence of a fine grid in the wall, there is a tendency of filling op and accumulation of vapour bubbles inside it, which creates "dry" areas on the wall.

Such phenomena have not been determined for the grid with large sizes of cells ($0,4.10^{-3}$ m). The sensibility of the structure is higher, as long as it has lesser hydraulic resistance and capacity to derivate, although larger, bubbles (figure 2). In case of smaller values q behaviour with a burst of a double-phase flux is slightly expressed [4].

In case of optimal consumption of liquid, the time of "life" τ_{life} of vapour bubbles has been not more than 1/2500 s, and the holding time (0,006 - 0,014) from the time of "life" for the value q=120 kW/m^2 and twice more for $q=67$ kW/m^2.

The phenomena of growing the bubbles from the film as in thin-film vaporizers did not take place. At the time of destruction, a bubble had the shape of a circle. Phenomenon of the drop carrying away for the structure 0,4 was extremely poor.

The growth of the value q was accompanied by increasing the density of the evaporation centers $\bar{n}$. At q=67 kW/m^2 it was 18/144 bubbles/number of cells, and at $q=120$ kW/m^2– *33/144* bubbles/number of cells.

CONCLUSIONS

Estimated semi empiric correspondences of the described thermos-hydraulic characteristics of the process of evaporation in the grid-type porous structures, such as departure (destroyable) diameter of a vapour bubble, density of the generation centers, the frequency of carrying away and the velocity of the bubble growth ±20%. These values depend on thermal physical properties of the liquid (pressure) and a wall, temperature stress, excess of liquid. Based on internal properties of boiling, simple engineering formulas to calculate the carried away heat flux depending on the type of porous structure and geometry of vapour-generating surface, which generate the empiric data with precision ±20%, were built.

References

[1] Genbach A.A., Olzhabayeva K.S. *Study of heat transfer processes in a porous system new PS* // Industry of Kazakhstan. – 2012. №2, - p.73-75.

[2] Polyaev V.M., Genbach A.A. *The mechanism of evaporation processes in porous cooling system* // Theory workflows nodes and paths of power plants. Proceedings MAI, M., 1991. - p. 81-90.

[3] Polyaev V.M., Genbach A.A. *Control of Heat Transfer in a Porous Cooling System* // Second world conference on experimental heat transfer, fluid mechanics and thermodynamics. – 1991. – p. 639-644.

[4] Polyaev V.M., Genbach A.A., Bocharova I.N. *Local settings steam bubble in the cell of the porous structure* // Bulletin MSTU. Ser. Engineering. - 1993. №2. – p. 47-52.

RESEARCH AND CALCULATION OF HIGH-FORCED CAPILLARY-POROUS HEAT EXCHANGER

Alexander A. Genbach[1], Nellya O. Jamankulova[2]

Almaty University of Power Engineering & Telecommunications,
Heat power engineering faculty, Republic of Kazakhstan, Almaty.

ABSTRACT

A capillary-porous cooling system for caissons of melting units has been studied, developed and calculated. The experimental type of the mesh porous structure $(2\times0.55)\cdot10^{-3}$ m is defined. The heat transfer capacity of the cooling system is increased six times. The hydraulic resistance at boiling of water will be 40.4 times less than in mesh heat pipes, and even more so for the wicks of heat pipes with fibrous, powder and ceramic materials. The caisson allows to carry out cooling of furnaces is explosion-proof due to the maintenance of a trace amount of liquid in the porous structure. The system of caisson of the lining of the unit and the cooling scheme of the caisson by a capillary-porous system is presented. The hydraulic resistance in the capillary-porous structure, the criterial heat transfer equation, taking into account the excess fluid, which determines the speed and underheating of the flux, and the heat-storage capacity of the wall, are obtained by us as a result of experimental studies.

Key words: capillary-porous system; cooling system; caisson; heat flux.

1. INTRODUCTION

The capillary-porous heat exchanger is designed to ensure the explosion-proof operation of melting units in metallurgy. It contains a very small amount of liquid, which eliminates the danger of explosion at the burnout of the cooled element. It is also excludes the ingress of water into the melt, which leads to the explosion of the furnace, as is the case for water and evaporative cooling systems, made in the form of caissons.

The next stage of development of the heat exchanger was the study of a capillary-porous structure.To increase the removal of thermal loads, the management of heat transfer processes is used. For this purpose, the separation of the energy of the boiling stream in the porous structure into energy of the thermal wave and the energy of the vapor flow is investigated [1].

For this purpose also, the process of explosive production of a steam germ is simulated.

The next step in controlling heat exchange is the joint action of mass and capillary forces for coolant transport, creating underheating and forced flow velocity in the structure [2]. Also, the system is capable to increase the critical heat loads by an order of magnitude and can be allocated into a separate class of heat exchangers, characterized by high forcing and intensity of heat transfer. In addition, mass forces make it possible to control the shape and intensity of generation of internal characteristics of a boiling stream in a capillary-porous structure and intensify heat transfer processes [3,4].

2. METHODOLOGY

Physical and mathematical models of processes of boiling in a porous structure are developed for all modes of boiling (initial, transitional, developed and crisis (limiting) [5-8].

[1] Professor Dr.Sc., AUPET, Republic of Kazakhstan, aipet@aipet.kz

[2] PhD Student, AUPET, Republic of Kazakhstan, e-mail: dnellya@mail.ru, cell: +77019303750

Generalization of experimental data on the basis of the theory of similarity and modeling makes it possible to obtain a criterial equation for calculating the heat exchange of boiling and foam flows in porous structures [9] and to create an engineering calculation technique.

We give an example of calculation of such system in relation to the heat exchanger executed in the form of a caisson. The system of caisson of lining (garnissazh lining) of the melting unit is shown in figure 1. The scheme of the caisson with the garnissazh lining consists of: 1 – meling film; 2 – garnissazh; 3 - fireproof packing;; 4 – thermal isolation; 5 – outside metal covering; 6 - temperature variation in the thickness of the lining; 7 – viscosity variation in a garnissazh layer; 8 – caisson wall; 9 – caisson. The following designations are accepted:

q_{pi} , q_u , q_{env}- - the specific heat flux from a melt; the specific heat flux is carried away by a cooling system; the specific heat flux coming to an environment;

t_m , t_{mf} , t_{met} , t_w - temperatures of melting, of melting films, of metal and the protecting wall

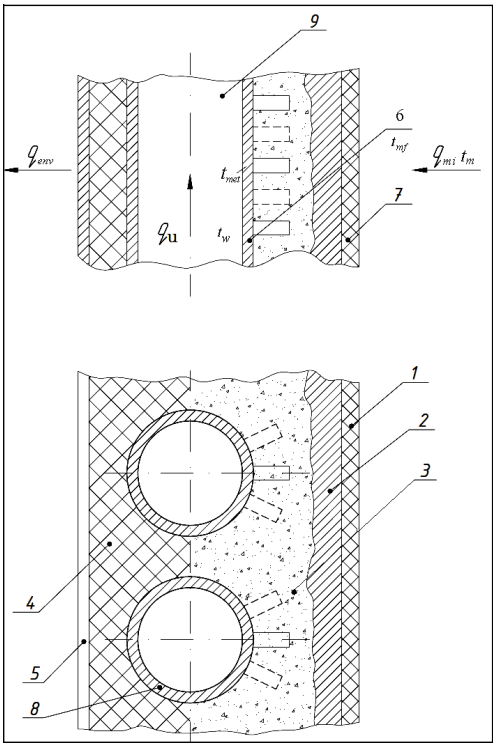

Figure 1: The scheme of the caisson with the garnissazh lining

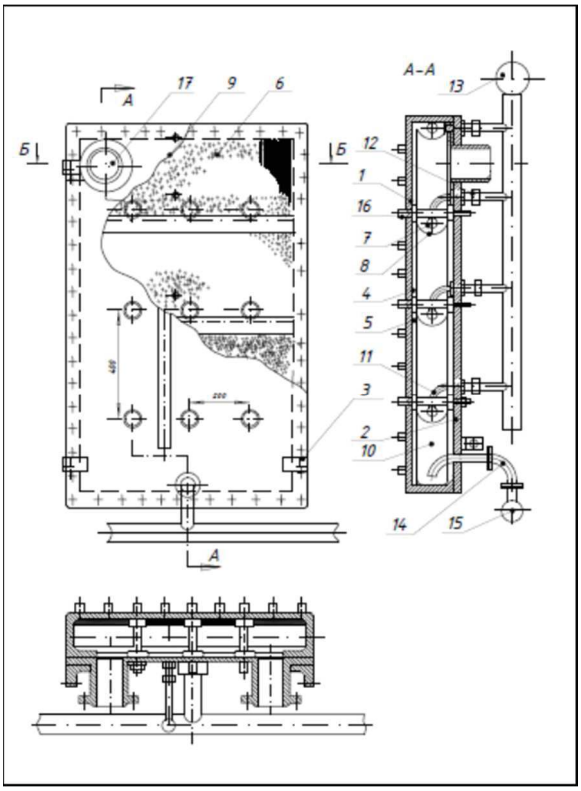

Figure 2: The cooling scheme of the caisson of a capillary-porous system with struts

Figure 2 shows the cooling scheme of the caisson of a capillary-porous system with stiffening ribs made in the form of struts. It consists of: 1 – housing; 2 – cover; 3 – bolt; 4 – wall; 5 - capillary-porous structure; 6 – plate; 7 – artery; 8 – basket; 9 – opening; 10 – channel; 11, 17 – branch pipe; 12 – pipe; 13, 15 – collector; 14 – siphon; 16 – struts.

It can be seen from fig. 2 that a capillary-porous structure has a small thickness (a fraction of millimeters), every second contains a small amount of cooler, which is not dangerous for the formation of an explosive mixture in case of its enter in a melt of a melting furnace.

The design of caissons (fig. 2) represents a box-shaped form. They consist of the housing 1 and a removable cover 2, hermetically bolted on perimeter 3. The internal surface of a wall

4 is covered with the capillary-porous structure 5 pressed by perforated plates 6. Arteries 7 are connected to top ends of structure through the end face of which to the cooled surface liquid is supplied by mass and capillary forces. The lower ends of structure are usually free and immersed in baskets 8 where liquid accumulates due to leaks, droplet entrainment or the excess. On a surface of plates the openings 9 are stamped which provide a steam-out from structure in channel 10 and also serve as catchers of the drops which are thrown out from structure and the flowing-down excess liquid on an external surface of a plate. The artery is connected to a branch pipe 11, with the distributing pipes 12 and a collector 13. The excess of cooling liquid accumulates in the bottom of a caisson and is removed by a siphon 14 in the lower collector 15 and further in the store for return to system. For the purpose of facilitation of a design and preservation of sufficient rigidity, the caissons are provided with struts 16. If the struts made in the form of ribs, they may be located either on the outside or inside the shell and the caisson cover. On a cover, in her upper part, branch pipes 17 with flanges for connection with a steam line are welded. The structure can be extended in the vertical or horizontal direction, the upper or lower ends of which (or both) are connected to an artery. The perforated plates make in a form and the sizes according to structure. The stamped and perforated recesses in them can have the form of the truncated cone, or longitudinal slots with openings facing upwards.

We will calculate the capillary-porous cooling system, made in the form of a box-shaped form (caisson).

The hydraulic resistance is determined by Darcy's law

$$\Delta p = \mu_{liq} \cdot m_{liq} \cdot l /(p_{liq} \cdot F_{ф} \cdot K_y), N/m^2,$$

where K_{cond} is the conditional permeability coefficient, which we determined experimentally [2];

$K_{cond} = 5.5 \cdot 10^{-7} \cdot (b_h/d)^{-1.29} = 5.5 \cdot 10^{-7} \cdot (0.55/0.2)^{-1.29} = 1.49 \cdot 10^{-7}$ m^2;

b_h - hydraulic structure diameter; $b_h = 2 \cdot 5.5 \cdot 10^{-3}/2 = 0.55 \cdot 10^{-3}$ m;

d - average diameter of wire mesh; $d = 0.2 \cdot 10^{-3}$ m;

μ_{liq} - dynamic viscosity of a liquid;

at p = 146 bar, $t_w = 360$ ℃, $\mu_{liq} = 77.5 \cdot 10^{-6}\ Pa \cdot s$;

m_{liq} – flow rate of a liquid;

$m_{liq} = \beta \cdot q \cdot F_u/\text{r} = 1.1 \cdot 6 \cdot 10^5 \cdot 0.942/1027 \cdot 10^3 = 0.605$ kg/s;

β- coefficient of fluid excess; the optimal value is determined experimentally by us, $\beta = 1{,}1$ [5];

$q_{и}$ - heat load, $q_{и} = 6 \cdot 10^5$ W/m^2 (take the maximum value);

r- heat of vaporization, $\text{r} = 1027 \cdot 10^3$ J/kg;

$F_{и}$ – heat exchange surface; take $F_{и} = 1 \cdot 0.942 = 0.942$ m^2;

p_{liq}- density of the liquid; $\text{p}_{liq} = 610$ kg/m^2;

$F_{ф}$- “live” section of the capillary-porous mesh structure

$F_{ф} = l \cdot \delta_{ф} = 1 \cdot 1.04 \cdot 10^{-3} = 1.04 \cdot 10^{-3}$ m^2;

ε - porosity of structure; $\varepsilon = 0.7$;

$\delta_{ф}$- thickness of structure; $\delta_{ф} = 2 \cdot 0.52 \cdot 10^{-3} = 1.04 \cdot 10^{-3}$ m.

Then

$$\Delta P = \frac{77.5 \cdot 10^{-6} \cdot 0.605 \cdot 1}{610 \cdot 1.04 \cdot 10^{-3} \cdot 1.49 \cdot 10^{-7}} = 494 \text{ Pa}.$$

The hydraulic resistance of the mesh structure operating only in the field of capillary forces, as in the case of heat pipes, will be equal to

$$\Delta P = \frac{77.5 \cdot 10^{-6} \cdot (0.605/6) \cdot 1}{610 \cdot 1.04 \cdot 10^{-3} \cdot 7.14 \cdot 10^{-10}} = 2 \cdot 10^4 \text{ Pa},$$

where 0.605/6 is recalculation by the magnitude of the critical heat load, which in heat pipes is six times less; the value of K_{cond} in the field of capillary forces is [2]:

$$K_{cond} = 4.305 \cdot 10^{-10} \cdot (b_h/d)^{0,5} = 4.305 \cdot 10^{-10} \cdot (0.55/0.2)^{0,5} = 7.14 \cdot 10^{-10} \text{ m}^2,$$

i.e. the hydraulic resistance of the offered structure will be in $494/2 \cdot 10^4 = 404$ time less. When comparing the mesh structures with ceramic-metal, felt and powder materials, for which the maximum permeability can be $11 \cdot 10^{-10}$ m^2, i.e. in total, in $\frac{1.1 \cdot 10^{-9}}{7{,}14 \cdot 10^{-10}} = 1{,}54$ times more than for the mesh structures operating in the field of capillary forces, and the hydraulic resistance is less in 1.54 times.

In the proposed capillary-porous structure operating under the combined action of mass and capillary forces, the hydraulic resistance at boiling of water will be 40.4 times less than in heat pipes with fine-cell meshes, and even more so with fibrous and ceramic materials that allows to cool the heating surfaces of the larger sizes in relation to caissons of melting furnaces.

3. CONCLUSION

Thus, in comparison with other existing cooling systems (ceramic-metal, felt or powder) the mesh capillary-porous structure working in the field of mass forces has a number of advantages. The permeability coefficient becomes smaller and the hydraulic resistance of the entire structure decreases. There is no need for additional settings for a delivery or drive of such a system, because the motion of the liquid is due to mass and capillary forces in the capillary-porous structure selected experimentally.

Hydraulic resistance at boiling water will be 40.4 times less than in heat pipes with fine cell meshes, and even more so with fibrous, powder or ceramic materials. This allows to cool caisson surfaces of large dimensions.

References

[1] Polyaev V.M., Genbach A.N., Genbach A.A. Methods of Monitoring Energy Process. *Experimental thermal and fluid science, International of Thermodynamics, Experimental Heat Transfer, and Fluid Mechanics*, avenue of the Americas.-New York, 1995, V.10, april, pp. 273-286.

[2] Genbach A.A., Fedorov V.N., Shelginsky A.Y. The intensity of the boiling heat transfer fluid in the capillary-porous structure in the field of mass forces. *Proceedings of MPEI*: *heat and mass exchange processes and plants,* Issue 448, Moscow, 1980, pp. 27-32.

[3] Polyaev V.M., Genbach A.A. The density of nucleation sites and the release of droplets from the porous structure. Proceedings of the universities. *Mechanical Engineering*. 1990, №9, pp. 50-55.

[4] Polyaev V.M., Genbach A.A. Detachable diameter and frequency separation of vapor bubbles in porous structures. *Bulletin MSTU series Mashinos*troenie, 1990, №1, pp. 69-72.

[5] Polyaev V.M., Genbach A.A. The initial area of evaporation in porous structures, working with excess fluid. *Proceedings of the universities. En*ergy, 1991, № 2, pp. 84-87.

[6] Polyaev V.M., Genbach A.A. The mechanism of evaporation processes in porous cooling system. *Teoriya rabochih processov v uzlah i traktah energeticheskih ustanovok: Sbornik trudov MAI*, M., 1991, pp.81-90.

[7] Polyaev V.M., Genbach A.A., Minashkin D.V. Visualization of processes in porous elliptical coil. Proceedings of the universities. *Mechanical Engin*eering, 1991, № 10-12, pp.75-80.

[8] Polyaev V.M., Genbach A.A. Transpiration cooling of the combustion chambers and supersonic nozzles. *Tyazholoe Mashinostroenie*, 1991, №7, pp. 8-10.

[9] Polyaev V., Genbach A. Heat Transfer in a Porous System in the Presence of Both Capillary and Gravity Forces. *Thermal Engineering,* Moscow, 1993, V.40, number 7. pp. 551-554.

SIMPLIFIED DYNAMIC MODEL OF THE BUILDING ENERGY BALANCE FOR THE ENERGY AUDIT RESULTS INTERPRETATION

M. Ibragimova[1], V. Stoyak[1], V.Kambourova[2], W. Streicher[3]
[1]Almaty University of Power Engineering and Telecommunications, Almaty, Kazakhstan
[2]Rousse University, Ruse, Bulgaria
[3]University of Innsbruck , Innsbruck, Austria

Abstract. The dynamic model of building energy performance as an energy consumer has been developed, which includes calculating of heat gains/losses of buildings depending on combined effect of external and internal climatic parameters and calculating of dynamic energy load to energy supply system. The model also includes functional block of solar radiation falling on the building envelope calculation and thermal processes in the room. The model allows to vary the parameters, to take into account both environmental conditions and properties of building structures. A new approach for dynamic simulation of the energy balance of buildings is proposed, based on the using of standard transfer function units and having a number of advantages. Proposed approaches of dynamic simulation may be used to create an effective energy supply control system, also can be used for the interpretation of the energy researches and energy audits of residential and public buildings.

Key words: dynamic simulation model, energy balance of building, dynamic load of energy supply system, transfer functions

1. INTRODUCTION

The building sector accounts for more than 30% of the total world energy consumption, where the share of residential buildings is 74% and non-residential buildings - 26% of the world's energy consumption [1]. The building sector of Kazakhstan consumes about 11% of electric power and 40% supplied heat energy. According to expert estimates, about 70% of buildings have thermal characteristics that do not meet modern requirements (especially for buildings built in the 1950s and 1980s) [2].

Due to inefficient regulation of the heat supply system or regulation by a simplified method, not taking into account the changing of external and internal climatic parameters of buildings in real time, there are situations that at the heating season people to maintain a comfortable condition are forced to open windows or to connect an additional electric heater.

As is known, there are two main categories of heat flows in different buildings [3]: heat flows from outside (heat gains / losses due to temperature difference, from solar radiation, external penetrating air); heat flows occurring inside of buildings (heat generated by people, lighting devices, electrical appliances, etc.).

Most of the factors affecting the thermal conditions of the building are generally determined by a priori information, but the radiant-convective heat exchange of a building with the environment is a complex physical process and it has a significant influence, especially in such climatic conditions, when the winter and summer temperatures differ significantly from comfortable ones.

In recent years, a number of researchers have paid close attention to the dynamic nature of the heat exchange processes of buildings and structures as a factor that allows us to identify the reserves for reducing the energy costs of the building. So the author of the paper [4] argues that at the present level of development of science, technique and technology, it is necessary to apply a dynamic approach to the phenomenon of heat loss and heat accumulation, which allows using system analysis and simultaneous consideration of the unsteadiness of the thermophysical processes, climatic influences to the building and mathematical methods, to obtain new results for a full and detailed assessment of the energy balance of buildings. In the above given paper, the author pays special attention to the fact that most researchers simplify by default and do not notice the following important parameters: the unsteadiness effects of temperature, as well as wind and radiation to buildings and its envelope.

[1] Almaty, Kazakhstan, +7 702 274 99 45
Madina220790@gmail.com

In the author's opinion of [5, 6], an important role in the energy modeling of buildings and structures is played by the accounting the population of buildings. Additionally, well-known software products such as TRNSYS [7], Energy Plus [8], IES [9] and eQuest [10], which are powerful tools in modeling the technical characteristics and performance of building energy systems, takes into account gains from people by using explicit schedules.

The importance of accounting the energy of solar radiation in the study of building energy balance is noted in [11, 12]. In work [11] the authors developed a mathematical model of insolation income based on Simulink and confirmed that taking into account the insolation heat gains allows reducing the consumption of heat energy to 14.3%.

In work [13] it is noted that dynamic modeling of energy consumption and heat losses of buildings allows for more realistic and accurate studies. Thus, the authors, comparing the results of dynamic modeling with the corresponding indicators of the standards EN ISO 13790, revealed significant differences in the determination of the annual supplied energy by heating systems from the required.

The present work is devoted to the research and development of a dynamic simulation model for the integrated accounting of heat gains/losses from climatic parameters in the overall heat balance of buildings and structures in order to obtain sufficiently reliable information about the changing energy needs of buildings (heat/cold) within 24 hours based on meteorological observations and instrumental measurements of internal energy supplies.

2. METHODOLOGY

As is known, the solar radiation is one of the main factors that affects to the thermal regime of building [3]. To taking into account the radiant heat exchange of a building, it is necessary to have a subprogram for calculating the solar radiation on the building's envelope construction elements, depending on the spatial arrangement of the Sun.

For this, firstly, methods and astronomical algorithms determining the spatial location of the Sun at any time of the day were considered and was chosen an algorithm that allows calculating the trajectory of the Sun's motion during the day with an error not exceeding one angular minute for dates in the range of 1900 to 2100years [14].

Secondly, the existing methods for calculating solar radiation on an inclined surface were considered too. Most of the existing methods for calculating solar radiation on an inclined surface use table values of solar radiation intensity and do not allow calculating instantaneous heat gains to the surface. On the basis of the literary analysis, we chose the most suitable method, suggested by the author in [15], which allows calculating the instantaneous admission of the total energy of solar radiation taking into account the cloudiness on an inclined plane located on the Earth's surface at any angle to the horizon and oriented in any direction, at any day of the year.

Combining the noted methods described above, a subprogram was developed by using MATLAB, which calculates the position of the Sun depending on the geographic characteristics of the area and date, as well as the dynamic gains of the total solar radiation to an arbitrarily oriented surface. As an example of solar insolation calculation, a vertical building envelope was installed in the Almaty city (Figure 1). The time interval is 1 day (July 20, 2015 - in the summer and January 20, 2015 - in the winter).

The developed model of complex accounting of radiant-convective heat transfer to the heat balance of a room includes the following mathematical models:

- accounting for heat gains through an opaque building envelope;
- accounting for heat flows through transparent building envelope;
- accounting for radiant heat flow, penetrating through a building envelope.

The mathematical model of accounting for heat gains as a result of radiant-convective heat transfer through an opaque building envelope includes a linear differential heat equation used to find solution of the heat transfer through the thickness of the building envelope construction with initial conditions and boundary conditions of the third kind on the inner side of the wall and the complex boundary conditions of the 1st and 3rd kind on the outside of the wall.

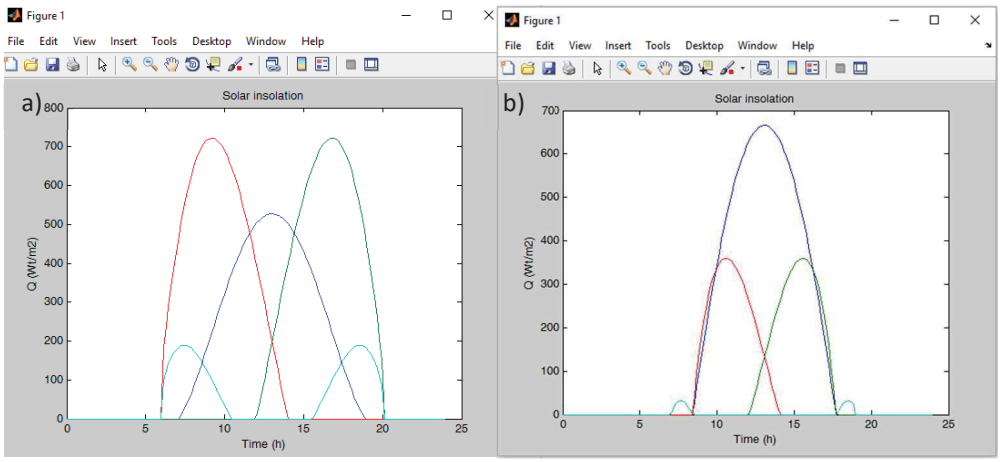

Blue line - heat gains to the south, red line - heat gains to the east, green line - heat gains to the west, blue lines - heat gains to the north wall

Figure 1: Insolation heat gains to the wall in summer (a) and winter (b)

The parameters that were taken into account in the model: heat gains from solar radiation to the building envelope comes depending on the season, date, position of the sun, cloudiness and transparency of the atmosphere, etc .; multi-layered wall; slope and arbitrary orientation of the building envelope.

Accepted assumptions: within each layer of the wall the coefficient of thermal conductivity is constant; the temperature inside the room is assumed constant, which is permissible for the task of maintaining comfortable conditions of premises; the outside air temperature changes according to the harmonic law.

As an example the solution of the problem of non-stationary heat transfer through an opaque building envelope (0.4 m thick brick wall), for the wall in Almaty, which oriented to the south and is located strictly vertically was obtained. Calculations were carried out for the summer day, namely July 20, 2015. To solve the described problem, we use the functions of the MATLAB kernel - the PDEPE function, which is used to solve one-dimensional non-stationary differential equations.

Figure 2 shows the insolation gains on the wall (a), the temperature fluctuations on the outside surface of the wall (blue line) and the outside temperature (green line) (b), the heat gains into the interior through the wall (c). As a result of the complex influence of solar radiation and the temperature of the outside air, temperature variations on the outer surface of the wall are observed, which leads to fluctuations in the heat flux on the inner side of the wall. It should be noted that the internal oscillations of the flow lag about 9 hours.

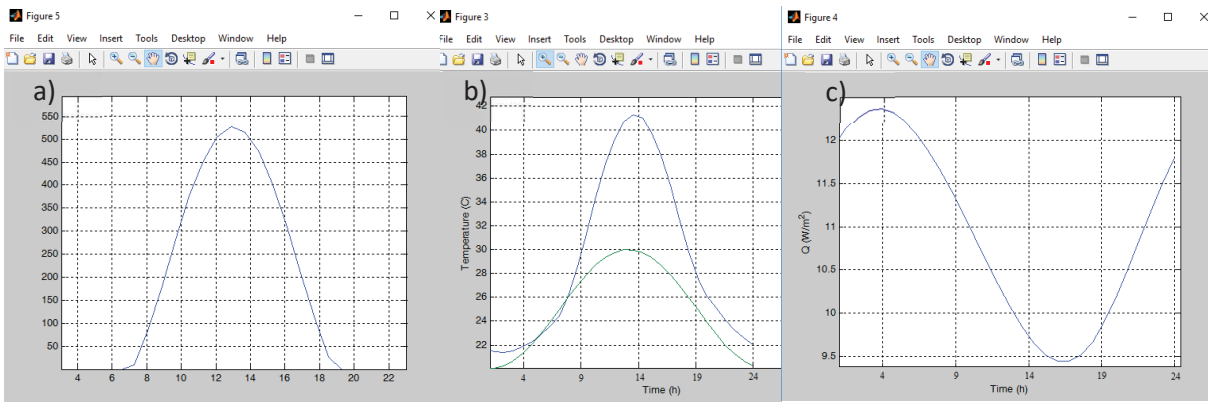

Figure 2: Results of dynamic model calculations

Heat flows through translucent constructions include the convective and radiant component of the heat flux. Convective heat transfer Q_k through translucent constructions is equal to

$$Q_k = \alpha_1 * (T_1 - T(x = 0, \tau)), \quad (1)$$

where α_1 is the heat transfer coefficient of the inner side of the window, W/m^2 * ^{0}C;

T1 - indoor air temperature, ^{0}C;

T (x = 0, τ) - the temperature of the inside surface of the window, ^{0}C.

The radiant (penetrating) component of heat transfer can be represented as:

$$Q_l = Q_{solar} * j * k_l, \quad (2)$$

where j - the factor of accounting for shading by opaque window elements;

k_l - the coefficient of relative penetration of solar radiation through the transparent part of the window.

As an example, a single-compartment glass unit (a plastic window with a coefficient of heat transfer of 0.32 m^2*^{0}C/W) was adopted. The results of the calculation of the subprogram are shown in Figure 3.

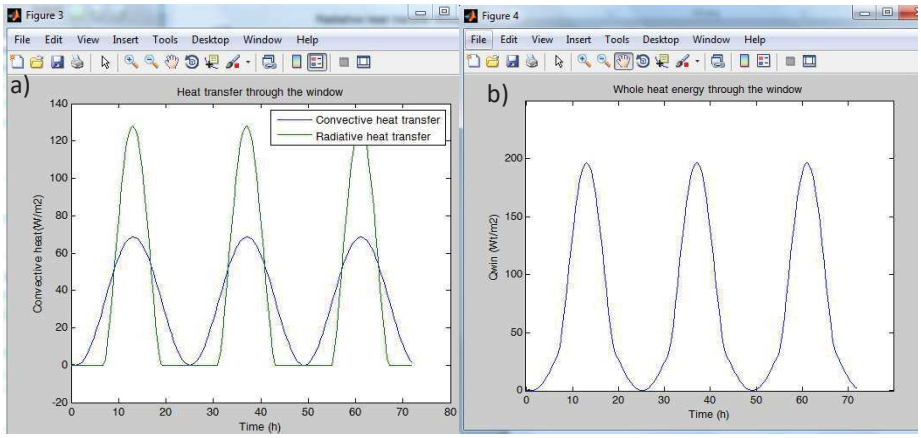

Figure 3: Radiant and convective components of heat input (a) and total heat input (b) through a translucent construction

For an opaque building envelope construction, a transfer function of an aperiodic link with a delay of the first order for a brick wall, described in detail in the previous example, was obtained:

$$W(s) = \frac{k}{Ts+1} e^{-\tau_d s} = \frac{0.051}{112.04 \cdot 10^3 s + 1} e^{-28.2 \cdot 10^3 s}$$

A combination of transfer functions has been developed to simulate the process of heat transfer in a room through an opaque building envelope (Figure 4), the solution of which was obtained by using Simulink. The scheme consists of a subprogram for calculating solar radiation on an inclined surface - 1, an aperiodic link of the first order - 2, a delay link - 3, an external temperature modeling subprogram - 4, transfer functions for calculating convective heat transfer - 5 and a graph for showing the calculation results - 6.

According to the results of the compilation of assembled transfer function scheme in Simulink and the program developed in Matlab, a fairly high coincidence of the results was obtained, which indicates the principle possibility of using the method.

Calculation of energy consumption for the ventilation of indoor air was carried out using standard techniques [16]. For constructing a specialized software of the ventilation influence on the heat balance of a building as part of the dynamic simulation model, in contrast to [16], there was taking into account the dynamics of the effect of diurnal changes of the ambient temperature.

As an example, we consider a room of 15 m^2 and a height of 3 m, in which there is one person. The results of the calculation showed that to provide one person with chilled air in the summer, it is necessary to spend up to 150 W/m^2 of energy on the air-conditioning system.

Let's consider the calculation of total heat gains in the summer and heat losses in winter using the example of a room of 15 m^2, using the subprograms described above. The vertical wall of the room is oriented to the south. The walls, ceiling and floor inside the room have a constant temperature of 20 °C. There is one person in the room who needs to provide comfortable conditions: air temperature - 20 ^{0}C, fresh air volume - 3 m^3/h per 1 m^2 of room. We assume that translucent constructions (window) account for 40% of the external wall and, correspondingly, 60% fall on the non-translucent construction. As initial data for the wall, window, location and climatic parameters in the calculation were adopted in accordance with the conditions described above.

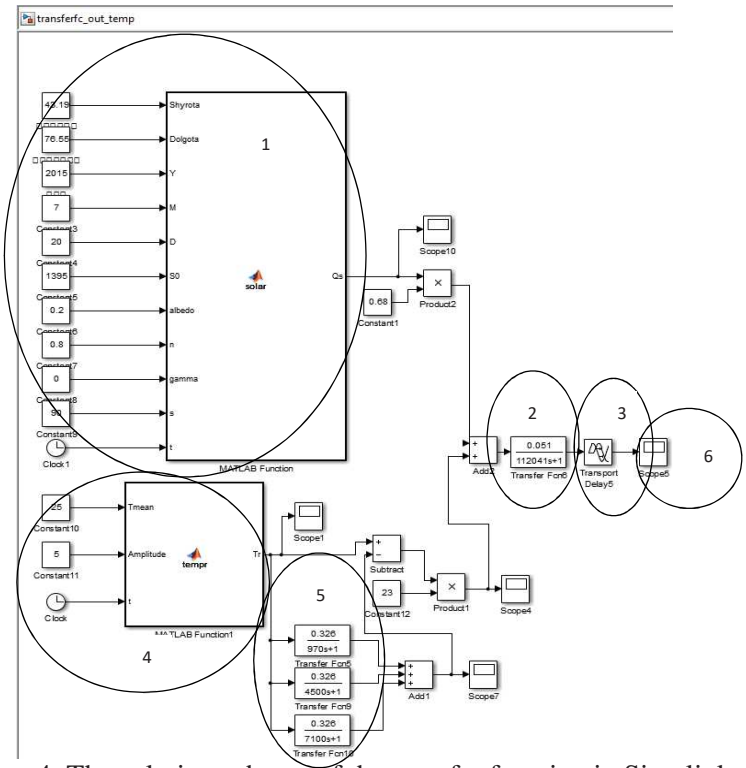

Figure 4: The solution scheme of the transfer function in Simulink

The results of calculating the heat gains to the room in the summer (July 20, 2015) are shown in Figure 5 (a). From the obtained results, it can be concluded that the greatest heat gains occur due to penetrating radiation passing through the window (1150 W). Heat gains through the wall does not exceed 42 W. The maximum total load on the air conditioning system during the day is 1580 W. The daily load profile for the air conditioning system is shown in Figure 5 (b).

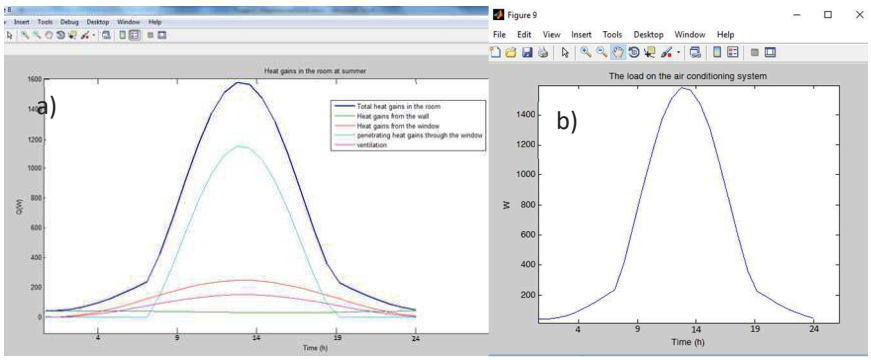

Figure 5: Total heat gain (a) in the room in summer and the required load to the air-conditioning system (b)

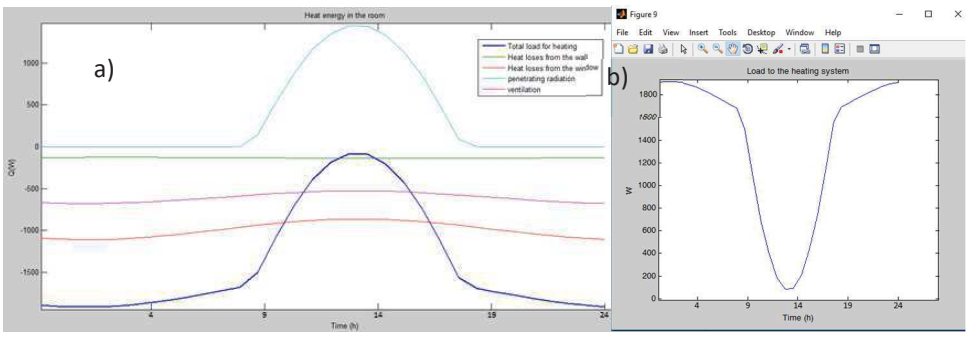

Figure 6: Total heat gains and heat losses (a) in the winter room and the required load to the heating system (b)

Figure 6 (a) shows the heat losses and heat gains in winter (January 20, 2015). According to the obtained results, the maximum heat losses in the room falls through the windows (-870W), the minimum through the wall (-130 W). Heat gains into the room, arising from penetrating radiation, reaches 1400 W.

Thus, in order to maintain comfortable conditions in the room, it is necessary to provide heat supply in accordance with the daily load profile shown in Figure 6 (b).

3. CONCLUSIONS

A refined method for analyzing the energy balance of residential and public buildings is proposed, which takes into account the dynamics of energy flows due to the influence of internal and external climatic parameters. The method allows to calculate the dynamic loads to the heat and cooling supply systems more objectively compared with the existing ones and, accordingly, to coordinate them more effectively with the productivity of the heating and air conditioning devices both at the design stage and during the operation period.

An important result of the work is the creation of a simplified methodology for dynamic modeling of energy balance of buildings, which can be used in the future both in the creation of computer-free embedded control systems of buildings climatic parameters and as a tool for interpreting the results of energy audit and energy research.

References

[1] Stefanovic A., Gordic D. Modeling methodology of the heating energy consumption and the potential reductions due to thermal improvements of staggered block buildings // Elsevier. Energy and buildings. – 2016.– p. 244 – 253

[2] On the approval of "Energy Saving - 2020" Program. Resolution of the Government of the Republic of Kazakhstan from August 29, 2013 № 904.

[3] Ananiev V.A., Balueva L.N., Murashko V.P .Ventilation and air-conditioning. Theory and practice. - M .: Euroclimate, 2008. - 516 p.

[4] Sotnikov A.G. Heat loss and heating load of buildings: a comprehensive physics and mathematics (dynamic) approach. Energy effective technologies.-№ 4 (64).SPb.:2011.-p.18-32

[5] Sokratis P., Elie A. Integrating building performance simulation in agent-based modeling using regression surrogate models: A novel human-in-the-loop energy modeling approach // Elsevier. Energy and buildings. – 2016. – p. 214 - 223

[6] Marshall E., Steinberger J., Dupont V., Foxon T. Combining energy efficiency measure approaches and occupancy patterns in building modelling in the UK residential context // Elsevier. Energy and buildings. – 2016.– p. 98 – 108

[7] URL: http://www.trnsys.com/

[8] URL: https://energyplus.net/

[9] URL: https://www.iesve.com/software

[10] URL: http://www.doe2.com/equest/

[11] Strizhak P.A. Morozov M.N. Mathematical modeling of the thermal regime of the building, taking into account insolyatsonnyh heat gain. Bulletin of the Tomsk Polytechnic University. Engineering georesources. - 2015. - № 8 - p. 36-46

[12] Kim A.A., Smolyaninova T.A. Evaluation insolation classrooms Pacific State University // New ideas of the new century - 2014 Volume 2 - p.119-123

[13] Müller A. Energy demand assessment for space conditioning and domestic hot water: a case study for the Austrian building stock. Dissertation work. – 2015. – p.285

[14] Schlyter P. Computing planetary positions - a tutorial with worked examples. - Sweden. URL: http://stjarnhimlen.se/comp/tutorial.html

[15] Samoilov D. Calculation of heat proceeds from the solar radiation on the Earth's surface: Guidelines//Ed. Y. Pest. - M .: Publishing House of the MSTU. NE Bauman, 2006.- p.20

[16] Livchak V.I. Method for calculating the specific annual consumption of heat energy for heating and ventilation systems of buildings. - Moscow: ABOK - PRESS, 2010. - 6 pages.

INTEGRATION OF BIOMASS RESOURCES INTO EXISTENT DISTRICT HEATING SYSTEM

Ion V. Ion[1],, Florin Popescu, Eugen Dimofte
„Dunarea de Jos" University of Galati

ABSTRACT

District heating is facing a strong technical and economic crisis in Romania. Besides the inheritance of systems with structural deficiencies, the lack of a vision of restructuring / development is the critical factor that can no longer be ignored. The outdated systems - inefficient systems, network losses and high prices of the heat energy resources - led to a massive decrease of dwellings number connected to the system. In this paper the integration of renewable energy source – biomass sources into an existent district heating system is analysed as additional source of heat energy. The case study of a heating system using urban biomass resources (sewage sludge, wood residues) and sunflower husk from oil mill is presented, analysing the efficiency of integration and economic effects.

1. INTRODUCTION

Nowadays, central district heating networks from Romania include a small number of conventional heating plants and cogeneration plants fuelled with fossil fuels. They have become unsustainable as a result of the aging of heat generation systems, abolition or reorganization of enterprises that were served by them, and the loss of heat in networks. The increase of energy cost offered by the systems has led to the massive disconnection of the dwellings. In 1992, approximately 2885000 homes and about 8.5 million people were connected, and today the number of dwellings is less than half. It is obvious that the efficiency of heating systems can only be solved by reorganizing the infrastructure, recalibrating from very large structures to some territorially optimally manageable from an energy and economic point of view [1].

Cogeneration plants demonstrate efficient fuel use and exploit waste heat sourced from power generation. District heating systems must meet the requirements of Directive 2004/8/EC of the European Parliament and of the Council on the promotion of cogeneration based on the useful heat demand in the internal energy market, of Law no. 121/2014 on energy efficiency, which promotes at local and regional level the development and the integrated use of efficient heating systems, especially those using high efficiency cogeneration and to fulfil the criteria and conditions established by GD no. 1215/2009 to qualify for bonus support for high-efficiency cogeneration based on the useful heat demand.

At present, the district heating systems based on cogeneration plant face two markets: a market for electricity, which is a national market and a heat market, which is a local market. A solution as a cogeneration plant heating system to become effective is to get it into local government administration on the basis of local energy planning. This means that cogeneration plants can set their sales prices so they can keep their heat consumers and even to gain new heat users.

Modern district heating systems need to be sustainable, rely on renewable energy and substantially reduced heating demand of buildings. Heating technologies should have reduced network losses and increased efficiency of low temperature heating units. Renewable energy (solar, biomass, geothermal), energy conservation (recovery and use of waste heat) and

[1]Galati, 47 Domneasca St., +40740566214, iion@ugal.ro

combined heat and power generation are key factors in responding to climate change in Europe. The competitiveness of district heating results from the combination of heat supply and distribution conditions. An important condition for heat distribution is that heat demand has to be concentrated in order to minimize distribution costs and heat loss [2].

In order to integrate renewable energy sources into existing district heating systems in a sustainable way, it is necessary to assess the available sources and their potential and to determine the technical and economic suitability. Many renewable energy sources, such as thermal solar energy and geothermal energy, low temperature waste heat in combination with heat pumps can offer at the limit heat at temperature above 100°C. The requirements of these energy sources on the site of generation are also different from those of fossil fuel plants. Reconstruction strategies for large district heating systems must be in line with field conditions. Experience has shown that the use of renewable energy in combination with fossil fuels is the most economically efficient. Biomass and geothermal energy are the most used renewable sources for heat generation. Thermo-solar energy, biogas and biomethane play a secondary role. The success of the integration of renewable energy depends greatly on the specificity of district heating system [3, 4].

The use of biomass requires the appropriate change of the traditional system. When biomass resources are available close to the heat generation site, the cost of biomass transport and storage is low, providing sustainability to the district heating system. Among the biomass resources available in a Romanian city are sewage sludge from wastewater treatment plants, wood from urban tree pruning, grass, wood wastes from municipal wastes, waste streams such as rice husk from rice mills, sunflower husk from oil mills, wood residues (saw dust, pulp wastes, and paper mill).

2. GASIFICATION OF SEWAGE SLUDGE FOR ENERGY VALORIZATION

In the National Sewage Sludge Management Strategy, it is assumed that the utilization of biogas produced by the anaerobic fermentation process is a common process that takes place in new or rehabilitated wastewater treatment plants, where it is cost-effective. Fermented sludge can be valorised by re-use on farmland, co-incineration in cement plants, co-incineration in solid waste incinerators and more recently through gasification. If the energy valorisation of the sludge is chosen, it should be taken into account that more energy is obtained in the case of raw (unfermented) sludge.

Before being used for energy purposes, the sludge is subjected to the following preparatory operations: magnetic separation of ferrous and non-ferrous metals; manual separation of the non-combustible fraction; mechanical sorting; fragmentation; drying and palletisation or briquetting. Fuel produced from sludge is characterized by variable heating value (12-14 MJ/kg), density, moisture content and content of harmful elements and compounds. Sludge from sewage treatment plants has a high water content (97%) which has to be eliminated to reduce transport costs.

By sewage sludge gasification it is generated, on average, 90% gas, 30% charcoal and 5% tar. There are several types of gasifier, but the most commonly used are fixed and fluidized bad. The biomass properties, as shape and size, moisture content, volatile matter and carbon, influence the gasification process [5]. In order to obtain a high calorific gas, the sludge must have a moisture content of (15-20)%. Fixed bed gasifiers produce a gas with lower ash, tar, carbon residue than fluidized bed. The downdraft fluidized bed gasifiers may suffer from the slagging of material layer caused by the high ash content of the biomass. To avoid this phenomenon, the temperature of the layer should be reduced, but this has the effect of increasing losses through the carbon incomplete combustion. Operating conditions greatly influence the performance of the gasification process, such as carbon conversion, synthesis

gas composition, tar formation and reduction. The temperature of the layer influences the composition of the gas, tar concentration, reaction rate, accumulation of ash, etc. A lower temperature leads to a higher tar content and less CO and H_2 in the synthesis gas, and a too high temperature leads to the slagging of the layer. For this reason a temperature is chosen in the range (750-900)°C [6].

As gasifying medium are used air, steam, carbon dioxide and oxygen. The most used medium is air because of the low cost. The generated gas has a reduced calorific value because of the nitrogen content in the air. If steam is used, a higher calorific gas is obtained due to the water-gas shift reaction. The use of steam reduces the efficiency of gasification. The use of oxygen as a gasification medium leads to a higher calorific gas but it is very expensive. The use of steam or carbon dioxide requires heat input for endothermic gasification reactions. Heat can be provided indirectly by circulating a hot material (sand) or using heat exchangers, or directly, by feeding the gasifier with air or oxygen for partial combustion of biomass. The gasification with steam allows the production of a high calorific gas and eliminates the need of using an expensive oxygen production plant when the air and the oxygen are used as a gasification medium. The residence time greatly influences the amount and composition of the tar in the syngas. A high residence time leads to a low content of tar and carbon residue and a higher methane content [6, 7].

In Table 1 are given the composition of three typical syngas generated by different gasifiers of dried sewage sludge [2].

Table 1. Typical composition and calorific value of syngas obtained from sewage sludge [2].

Dry gas composition	Air gasification in a circulating fluid bed system	Circulating fluid bed with 45% oxygen-enriched air	Lurgi-Ruhrgas thermal gasification
H_2	12.2	20.7	29.8
CO	20.9	37.9	24.9
CH_4	1.6	4.6	19.0
C_2+ hydrocarbon	0.6	0.8	12.3
CO_2	0.6	11.4	12.0
N_2	54.8	24.4	1.0
Other	0.2	0.2	1.0
Lower heating value (MJ/Nm^3)	5.2	9.3	22.7

The overall gasification reaction, considering the chemical equation of biomass as $C_nH_mO_pN_q$, can be written as follows:

$$C_nH_mO_pN_q + m_wH_2O + x_g\left(O_2 + 3.76N_2\right) \rightarrow$$
$$\rightarrow x_1CO + x_2H_2 + x_3CO_2 + x_4H_2O + x_5CH_4 + \left(\frac{q}{2} + x_g 3.76\right)N_2 \quad (1)$$

where: $m_w = \frac{M_{biomass} \cdot m}{18(1-m)}$; $M_{biomass}$ – molecular weight of biomass;

The major gasification reactions are [8]:

1. Water–gas reaction
$$C + H_2O \rightarrow H_2 + CO \text{ - } 131.38\text{kJ/mol carbon}$$
2. Boudouard reaction
$$CO_2 + C \rightarrow 2CO \text{ - } 172.58 \text{ kJ/mol carbon}$$
3. Shift conversion
$$CO + H_2O \rightarrow CO_2 + H_2 \text{ -}41.98 \text{ kJ/mol carbon}$$

4. Methanation

$$C + 2H_2 \rightarrow CH_4 \ +74.90 \text{ kJ/mol carbon}$$

5. The cold gas efficiency of biomass gasifier is:

$$\eta_{ceff} = \frac{\dot{V}_{sg} \cdot LHV_{sg}}{\dot{m}_b \cdot LHV_b} \tag{2}$$

where: $\dot{V}_{sg}$ - syngas flow rate (Nm^3/s); $\dot{m}_b$ - biomass flow rate (kg/s);

LHV_{sg} – lower heating value of syngas (kJ/Nm^3):

$$HHV_{sg} = 12760 \cdot H_2 + 12630 \cdot CO + 39760 \cdot CH_4 \ [kJ/Nm^3]$$

$$LHV_{sg} = HHV_{sg} - 2008(H_2 + 2 \cdot CH_4) \ [kJ/Nm^3] \tag{3}$$

H_2, CO and CH_4 represent volume participation of H_2, CO and CH_4 in the produced syngas.

LHV_b – higher heating value of biomass (kJ/kg).

The equivalence ratio, defined as the ratio of actual air fuel ratio to the stoichiometric air fuel ratio, is maintained in practical gasification systems between 0.2 and 0.3 [8].

The syngas composition can be determined by using the thermodynamic equilibrium models, kinetic models, phenomenological models, chemical equilibrium models or Artificial Neural Network (ANN) models. The thermodynamic equilibrium model is the simplest and determines the composition of the syngas for different types of biomass at various gasification temperatures. There are many commercial software packages to simulate numerically the gasification process, such as: UniSim, FactSage, Aspen Plus, Thermo-Calc, Ansys-Fluent, Open Foam.

3. INTEGRATION OF SEWAGE SLUDGE GASIFICATION INTO DISTRICT HEATING SYSTEM

The generated fuel gas by seawater sludge gasification can be burned in boilers, gas turbines or internal combustion engines. Internal combustion engines are more tolerant with regard to the content of contaminants in syngas than gas turbines. Most studies have been conducted on compression-ignition engines. Because syngas has high auto-ignition temperature (above 500°C), it cannot be used alone in the Diesel engines, it can be used in dual-fuel Diesel engines, in which oil is injected in small quantities to initiate the ignition of syngas [9].

A schematic flow chart of the system considered in this study is shown in Fig. 1. It includes the following processes: dewatering, drying, gasification, gas cooling and cleaning, and a combined heat and power plant based on internal combustion engine. The system uses 171 kg/h pellets made from wood from urban tree pruning and wood from municipal waste, 50 kg/h pellets made from sunflower husk and 833 kg/h sewage sludge.

The composition and properties of the biomasses considered as gasification feedstock in this study are given in Table 2.

Table 2. Chemical composition of gasification feedstock.

Analysis	Dry sewage sludge	Sunflower husk pellets	Wood pellets
C	44.6	43.5	48.7
H	5.9	5.9	5.3
O	24.3	37.1	20.9
N	4.9	0.7	0.8
S	1.1	0.2	0.3
W	13.0	9.7	11.6
A	19.2	2.9	12.4

Lower heating value (kJ/kg)	12937	14880	16284

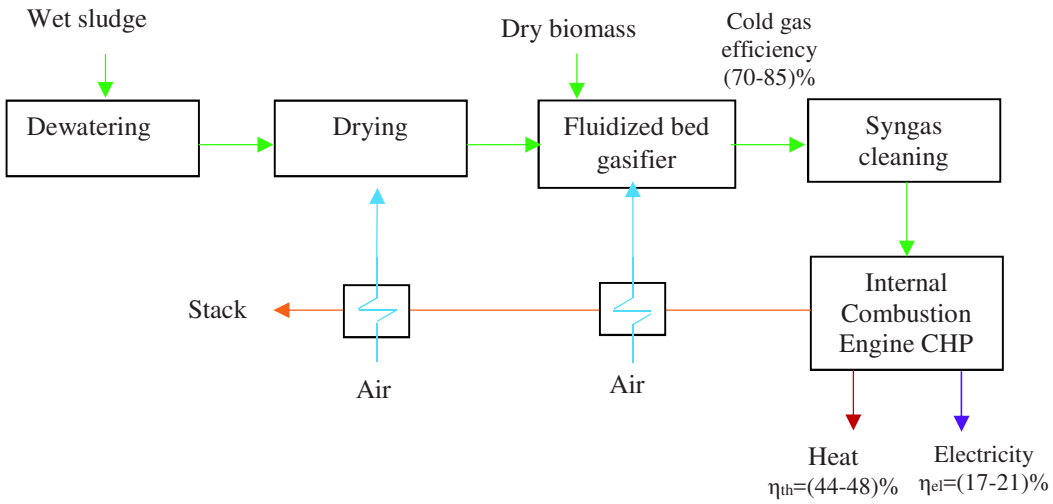

Figure 1: Flow chart of a gasifier CHP plant.

Using data given in Table 2, the chemical formula $C_nH_aO_bN_cS_d$ of biomass resulting by mixing the feedstock is calculated as follow: $a = \frac{H \cdot M_C}{C \cdot M_H}$; $b = \frac{O \cdot M_C}{C \cdot M_O}$; $c = \frac{N \cdot M_C}{C \cdot M_N}$; $d = \frac{S \cdot M_C}{C \cdot M_S}$ where M_C, M_H, M_O, M_N, M_S represents the molecular weight of carbon, hydrogen, oxygen, nitrogen and sulphur respectively.

The composition and lower heating value of syngas and cold gas efficiency were estimated by using the Gasifier program developed by Felicia Fock and Kirstine Thomsen from DTU MEK Denmark (Table 3).

Table 3. Calculated performance of gasifier.

Syngas composition (% vol)	N_2	CO	CO_2	CH_4	H_2	H_2O
	38.1	25.2	6.2	1.9	22.3	6.3
Syngas low heating value (LHV) (kJ/Nm^3)	6676					
Cold gas efficiency (LHV) (%)	85.4					

The electric efficiency of a spark ignition engine based CHP plant with sweater sludge gasification with air in a fluidized bed is 17.5 % and the cold gas efficiency is 72%. The specific plant cost is 18400 $/kWe [12].

In paper [13] is reported an electric efficiency (LHV) of 18.03% for sludge gasification and 20.69% for gasification of mixture 50% sludge and 50% wood. The thermal efficiency (LHV) is 48.55% for sludge gasification and 45.54% for gasification of mixture 50% sludge and 50% wood. The CHP plant uses a gas turbine.

A CHP plant with dual fuel engine fuelled with syngas generated by sweater sludge gasification has the electric efficiency 22% and the thermal efficiency 69% [10].

The energy balance of the system considered in this study is given in Table 4.

Table 4. Technical results.

Thermal input (kWth)	9090.79
Thermal output (kWth)	6272.64
Power output (kWe)	2000
Gross electric efficiency (%)	22

Gross thermal efficiency (%)	69

Taking into account the earned money by selling the extra power energy (83€/MWh plus national support of green certificates 10 €/MWh), by selling the heat (0.1 €/kWh) and by avoiding sludge disposal in landfill (20 €/ton dry mass), the cost of consumed sunflower husk pellets (0.1 €/kg) and the capital cost of 18400 $/kWe results a payback period of about 11 years (for 7000 h/year operation).

4. CONCLUSIONS

There are many ways of biomass resources integration into an existing district heating system. When the district heating system owner has his own resources, this integration is more cost-effective. In the studied case, where a municipality has biomass resources (pellets made from wood from urban tree pruning and wood from municipal wastes, pellets made from sunflower husk and sewage sludge), it was proposed to gasify the available biomass and to use the fuel gas in a CHP plant driven by dual-fuel engine. The power output reaches 2196.9 kW and the thermal output 6890.30 kW. By selling the extra electricity and heat, the system total investment cost of 36799516 € can be recovered after 11 years.

References

[1] Zamfir C. et. al., *Eficiența energetică-prioritate națională pentru reducerea sărăciei energetice, creșterea calității vieții și siguranța consumatorilor de energie*, Academia Română, 2015.

[2] Henrik Lund et al., *4th Generation District Heating (4GDH) Integrating smart thermal grids into future sustainable energy systems*, Energy 68 (2014), pp. 1-11.

[3] Grohnheit P.E., Mortensen B.O.G., *District heating as the infrastructure for competition among fuels and technologies*, Journal of Energy Challenges and Mechanics, Vol. 3, 2016, (2), pp. 64-69.

[4] *** Making district heating renewable, BINE Information Service, www.bine.info

[5] Natalia Kamińska-Pietrzak, Adam Smoliński, *Selected Environmental Aspects of Gasification and Co-Gasification of Various Types of Waste*, Journal of Sustainable Mining, Vol. 12, (4), 2013, pp. 6–13.

[6] Manara P., Zabaniotou A., *Towards sewage sludge based biofuels via thermochemical conversion –A Review*, Renewable and Sustainable Energy Reviews 16 (2012) 2566–2582.

[7] Gramatikov P., Iliev I., Andreev S., Hristoskov I., *Assessment of Opportunities for Landfill Gas Utilization in Bulgaria*, Energy Forum, St. Constantine & Elena, Varna 15 - 19 June 2011, pp. 351-359.

[8] Ftwi Yohaness Hagos, A. Rashid A. Aziz, Shaharin Anwar Sulaiman, *Trends of Syngas as a Fuel in Internal Combustion Engines*, Advances in Mechanical Engineering Volume 2014,

[9] Boehman A.L., Le Corre O., *Combustion of Syngas in Internal Combustion Engines, Combustion Science and Technology*, Vol. 180, Iss. 6, 2008.

[10] Bodo Groß, Christian Eder, Peter Grziwa, Juri Horst, Klaus Kimmerle, *Energy recovery from sewage sludge by means of fluidised bed gasification*, Waste Management 28 (2008), pp. 1819–1826.

[11] Hamilton C.J., *Gasification as an Innovative Method of Sewage-Sludge Disposal*, Water and Environment Journal, Volume 14, Issue 2, 2007, pp. 89-93.

[12] Nicholas P.G. Lumley, et al., *Techno-economic analysis of wastewater sludge gasification: A decentralized urban perspective*, Bioresource Technology, Volume 161, June 2014, pp. 385–394.

[13] Sharon McCahey, *Techno-Economic Evaluation of Sewage Sludge Gasification*, Thermal treatment of sewage sludge for CHP Applications, 15/16 September 2003, Brussels.

[14] Oprea I., Negreanu G., Berbece V., Pîșă I., Mihăescu L., *Efficient use of natural gas for a medium size district heating system,* International Conference on Thermal Equipment, Renewable Energy and Rural Development, TE-RE -RD 2014, Mamaia, 12-14 June 2014, pp. 113-118.

[15] Prabir Basu, *Combustion and Gasification in Fluidized Beds*, CRC Press, 2006.

[16] Vallios I., Tsoutsos Th., Papadakis G., *An applied methodology for assessment of the sustainability of biomass district heating systems*, International Journal of Sustainable Energy, Volume 35-3, 2016.

[17] Karin Ericsson, Sven Werner, *The introduction and expansion of biomass use in Swedish district heating systems*, Biomass and Bioenergy, Volume 94, November 2016, pp. 57–65.

[18] Johannes W. Judex, Michael Gaiffi, H. Christian Burgbache, *Gasification of dried sewage sludge: Status of the demonstration and the pilot plant*, Waste Management, Volume 32, Issue 4, April 2012, pp. 719–723.

NUMERICAL OPTIMISATION OF POLYGONAL BREATHING THERMAL MANIKINS

Ivanov M.[1], Mijorski S.[2]
[1]Senior Assist. Professor, PhD, Technical University of Sofia, FPEPM, Department: "Hydroaerodynamics and Hydraulic Machines", Sofia 1000, Bulgaria
[2]PhD, SoftSim Consult Ltd., Consultant at Technical University of Sofia, FPEPM, Department: "Hydroaerodynamics and Hydraulic Machines", Sofia 1000, Bulgaria

ABSTRACT

The presented paper describes a CFD based optimization approach for improvements in the geometrical shape of a simplified polygonal breathing thermal manikin. A base model of a physiologically identified manikin and two proposed polygonal models were compared. The polygonal models are designed to match the overall 95th percentile of the anthropometric size of a standard person, with and without the addition of proposed flow optimization collars.

The numerical results showed that the optimization with the proposed collars had a positive effect over the resulted flow acceleration at top head and chest zones of the manikin. However, the improvement of the flow characteristics was observed for two of the simulated three breathing phases. A further work for the optimization of the new proposed polygonal manikin is suggested, by introducing additional model modifications, like sharp-edges filleting and closing the mechanical openings.

1. INTRODUCTION

In today's engineering research practice, the real Thermal Manikins (TMs) and Virtual Thermal Manikins (VTMs) are used for overall assessment of the human thermal comfort, as well as for analyses of the indoor air quality in the occupied spaces. They represent modern, complex tools for measurement and analyses of the convective flows around human bodies in different conditions, without excessive risk of human exposure *[Nilsson (2006), Bjørn (1999)]*. However, the main application of the TMs and VTMs is not just in simulating different levels of physical activity (through surface heat losses), but also in simulating other human actions such as breathing, sweating, sneezing, coughing and others.

Performing experimental studies with TMs is sometimes expensive, time consuming, and may require highly skilled labor *[Madsen (1999)]*. Thus, the use of VTMs appears to be an appropriate alternative to the actual manikins' experiments, especially at the design stage of the indoor environment *[Ivanov (2015)]*. But still, a need exists for rather inexpensive and easy to construct and use real TMs, especially when numerical models have to be verified and validated with experimental measurement data. Therefore, the proposed simplified polygonal construction of TM with breathing function, previously modelled by the authors in *Ivanov and Mijorski (2017)*, would present an opportunity for manikin's production cost optimization. However, a numerical optimization at this stage of the design of TMs, by means of CFD (Computational Fluid Dynamics) based analyses, is required.

That is why the global aim of the presented study is to optimize numerically the simplified polygonal shape of the previously proposed thermal manikin, by the implementation of specially designed collars. A comparison analyses is made, between base

[1]Sofia 1000, Bulgaria, "Kliment Ohridski" Blvd. #8, Technical University – Sofia, +359898240221, m_ivanov@tu-sofia.bg

model of a physiologically identified manikin and two proposed polygonal models, one of which is supplied with the additional collars.

2. 3D GEOMETRY MODELLING

The base model (*Humanoid Manikin*) used is multifaceted 3D female manikin, specially remodeled and adapted for the purpose of the study. It represents with high degree of physiological identity a real female human, and has an approximate surface area of 1.8 m^2 and height of 1.65 m. The nasal valve opening was built according to the study of *Lin (2015)* and was initially used by the authors in *Ivanov and Mijorski (2017)*. The nasal opening area is 7.3 x 10^{-5} m^2, as shown on Fig.1. The normal to the nasal opening was specified to 45 degrees from the vertical body axis. Furthermore, exhaust walls from the nasal valve to the nose end were inclined to 15 degrees according to *Nilsson (2006)* and *Lin (2015)*.

The first polygonal model (*Polygonal Manikin*) represents the overall 95th percentile of the anthropometric size of a standard person. It is designed by Georgi Chervendinev (Engineering Design Lab at TU-Sofia, http://design.tu-sofia.bg), in order to meet the basic requirements of the ergonomic design area. It has an approximate surface area of 2 m^2 and height of 1.75 m. The nasal valve opening is constructed in the same way as in the base model, described above.

The second polygonal model (*Polygonal Manikin with Collars*) is in general the same as the first one, but with specially implemented collars in the neck and waist areas. It is supposed that these additional collars will improve the thermal plume characteristics in the free convection zone above the manikin.

Both polygonal manikins are proposed for use in real research applications, as well as for educational purposes, complying with the requirements for: high degree of manufacturability; high degree of mobility; availability in different scales and open design.

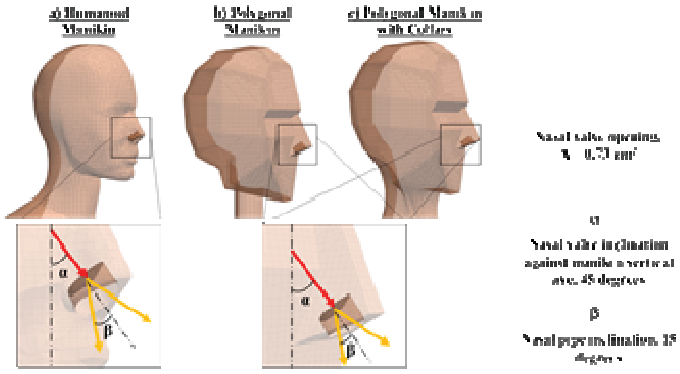

Figure 1: 3D models and nasal valve geometry details

3. CFD MODELLING

The 3D models of the virtual thermal manikins were placed inside rectangular shaped room with dimensions: 3 m height, 4 m width and 4 m depth. The spatial discretization was completed with snappyHexMesh utility, part of an ENGYS® (www.engys.com), which provides an enhanced version of the CFD code OpenFoam® (www.openfoam.com). Details for the generated numerical grids are provided in the Table 1 below.

In all numerical grids was followed one and the same meshing logic, i.e. defining base cell size to 4 10^{-2} m and increasing the refinement level to 6.25 10^{-4} m in the nasal valve zone, in order to capture the detailed geometrical features. Also, the numerical models were well refined at the surfaces of the manikins, with a first layer height of approximately 0.5 10^{-3} m.

These refinements were dictated from the requirement for low y+ values over the manikin surfaces, recommended in the work of *Spalart (2001)*.

Table 1: Poly-mesh details

Type of the elements	Humanoid model	Polygonal model	Polygonal model with collars
hexahedral	94 [%]	92 [%]	92 [%]
polyhedral	3 [%]	6 [%]	6 [%]
prisms	2 [%]	2 [%]	2 [%]
wedges	<1 [%]	<1 [%]	<1 [%]
tetrahedral	<1 [%]	<1 [%]	<1 [%]
Elements	1139195 cells	1417722 cells	1413376 cells

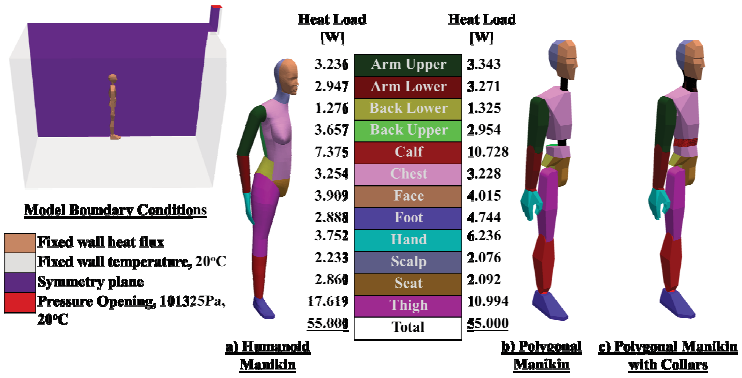

Figure 2: CFD model boundary conditions

In total of nine RANS (Reynolds-averaged Navier–Stokes) CFD simulations were performed, three for each individual virtual manikin. The three phases of the human breathing cycle were simulated, including: inhaling, exhaling and no breathing (the free convection flow case). The implemented solver for all simulations was *buoyantBoussinesqSimpleFoam*. This solver models a buoyant turbulent flow of incompressible fluids with combinations of semi-implicit method for pressure-linked equations (SIMPLE) algorithms. The turbulent features of the resulted buoyant flows were modelled with introduction of the Shear Stress Transport (SST) k-ω turbulence model suggested by *Menter (1993)*. This model is based on a two-equation eddy-viscosity approach, where the SST model formulation combines the use of a k-ω in the inner parts of the boundary layer, but also switches to a k-ε behavior in the free-stream regions of the solutions. In the work of *Menter (2011)* are provided further details of the selected turbulence model. Due to high level of surfaces refinement, the steady state resolving of the buoyant flow close to the manikins would be associated with high nonlinearity of the solutions and some flow fluctuations in the velocity and pressure fields. This effect was overcome with introduction of a flow averaging at the final 1000 iterations for each of the simulations.

The buoyant flows were modeled with the same material properties for the air. These were derived for reference conditions of 101325 Pa for the pressure and 20 ºC for the air temperature. Thus the air density was specified to 1.204kg/m^3, the dynamic viscosity to 1.82 10^{-5} kg/(m.s), kinematic viscosity to 1.51 10^{-5} m^2/s and specific heat to 1006.0 J/(kg·K).

Details regarding the adopted boundary conditions in the CFD simulations are provided in Table 1 and Fig.2. The heat fluxes specified for the manikins' surfaces were derived from the study of *Nilsson (2006)*. These were calculated for total heat load of 110 W from the whole manikin surface.

The velocity inlet for the exhale phase and outlet for the inhale were specified at the nasal valve openings. The approximated flow rates for one nasal valve (6.29 10^{-4} m^3/s for the inlet flow rate and 6.91 10^{-4} m3/s for the outlet flow rate) were calculating based on the study of *Lin (2015).* The formula relates the geometrical characteristic of the nasal valve and the dynamic pressure at the opening:

$$Q = \frac{\left(\Delta P.\pi.r^4\right)}{8.\eta.L} \tag{1}$$

where - Q is total flow rate during inhaling and exhaling, m^3/s;
- ΔP is pressure in the range of 40-80 Pa, selected 60 Pa for the study;
- L is approximated nasal valve length, specified to 0.33 m for the study;
- r is approximated nasal valve radius, specified to 0.11 m for the study;
- η_{20}, kinematic viscosity at 20 ^oC, calculated to 1.51 10^{-5} m^2/s for inhale phase;
- η_{36}, kinematic viscosity at 36 ^oC, calculated to 1.66 10^{-5} m^2/s for exhale phase.

The turbulent intensity for the nasal velocity inlet was approximated to 6.8% by Reynolds number calculation with proposed by *Lin (2015)* eq. 2.

$$\mathrm{Re} = \frac{2.r.Q.\rho}{\eta} \tag{2}$$

Table 2: Implemented boundary conditions

Boundary Name	Boundary Conditions	Inhale	Free convection flow	Exhale
No Slip Walls	Surface temperature, 20 [^oC]	Yes	Yes	Yes
Vent Opening	Air temperature and pressure, 20 [^oC] and 101325 [Pa]	Yes	Yes	Yes
Manikin	Fixed heat flux as per Fig.3	Yes	Yes	Yes
Nasal valve inlet	Inlet flow rate, 6.29 10^{-4} [m^3/s] at 36 [^oC]	No	No	Yes
Nasal valve outlet	Outlet flow rate, 6.91 10^{-4} [m^3/s]	Yes	No	No
Symmetry	Symmetry plane	Yes	Yes	Yes

4. CFD RESULTS

The numerical results are presented at two different sections from the velocity field solutions for the free convection flow (no breathing phase) of the breathing cycle. The first section is perpendicular to the symmetry plane of the CFD domain (see Fig.3) and the second is aligning with the symmetry plane (see Fig. 4). Also, a pointwise data of the numerical solutions for all three phases are presented in graphical format, for a horizontal profile above the manikins' head, again parallel to the symmetry plane at 2.5 m height from the floor.

The monitoring data of the numerical solutions has shown that the maximum air velocity for the free convection flow is reaching the value of 0.6 m/s for the *Humanoid Manikin***,** while the other two models have resulted in lower velocities. For the *Polygonal Manikin* models, it was registered a maximum velocity of 0.54 m/s and 0.57 m/s for the optimized model with the collars.

As it can be seen on Fig. 3 and Fig.4, the thermal plume of the humanoid model is well formed, with higher acceleration in close proximity of the manikin head and as well in the

chest zone. Also, there is a clear flow separation at the manikin's back zone resulted from the increased flow acceleration at the legs (see Fig. 3a).

The polygonal model is associated with increased turbulence of the free convective flow and better mixing of the flow at the manikin's back zone (see Fig. 3b). This effect is in result of the many mechanical openings and the sharp edges of the polygonal elements at the legs and lower back. Also, the effect of the big recess zones at the neck and at the waist is illustrated further in the form of flow recirculation at these areas.

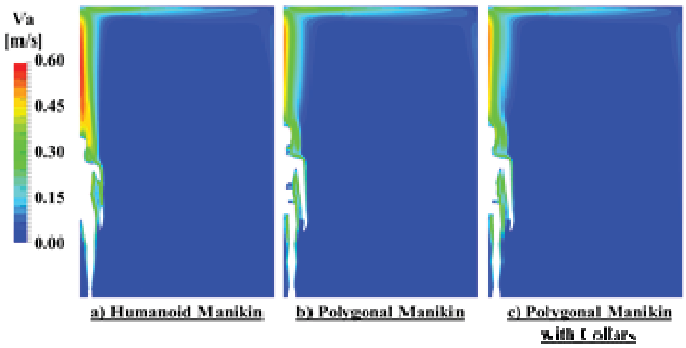

Figure 3: Velocity fields for free convection (no breathing phase) – X section

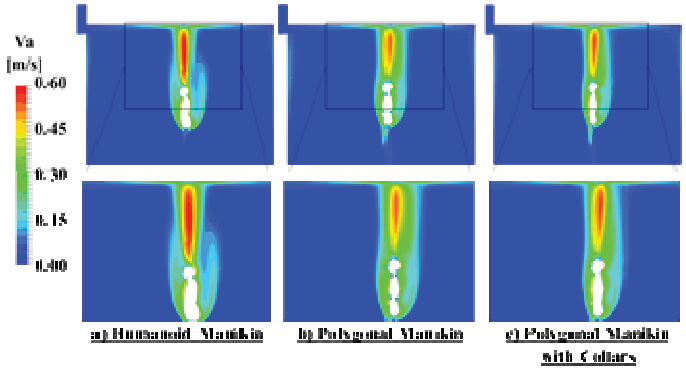

Figure 4: Velocity fields for free convection (no breathing phase) – Y section

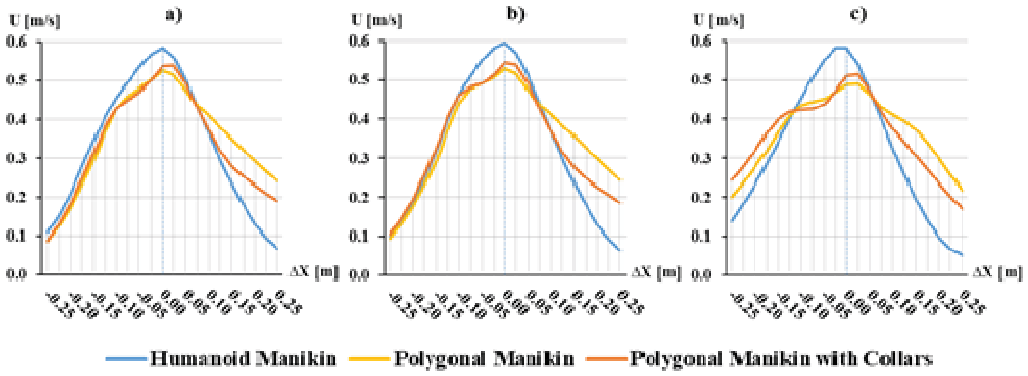

Figure 5: Horizontal air velocity at monitoring points: a) Inhale; b) Free convection; c) Exhale

The polygonal model optimization, with the introduction of the two collars, has resulted in visible flow improvements along the manikin surfaces, but the impact of the increased flow mixing at the legs and lower back zones is still visible, as shown in Fig. 3c. The manikin's back flow is well mixed without distinct flow separation, which was observed in the *Humanoid Manikin*. The big recirculation zones at the neck and the waist do not exist anymore and there is a visible improvement of the flow acceleration near the chest (Fig. 4c).

The pointwise data showed in Fig.5a and b, clearly illustrates the flow characteristics improvement, resulted from the introduction of the two collars. However, for the exhale phase results in Fig. 5c, it was observed worsening of the thermal plume profile. The impact of the exhale flow increases with proposed modifications. Also, from the graphical data is visible the need of further polygonal model modifications in the back and leg zones. Furthermore, the shapes of the velocity profiles are different, especially in the front zone of the manikins.

5. CONCLUSIONS

The numerical optimization study has led to improvement of the free convection flow along the proposed *Polygonal Manikin*. Also, the analyses of the results assisted the understanding of the implications caused by the geometrical characteristic of the model. However, the comparative analyses between smooth surface manikin and polygonal with many sharp edges and openings by itself is a difficult task. The *Humanoid Manikin* model would be characterized with more laminar flow along the surfaces, while the polygonal with more turbulent flow and mixing at the upper zones of the model. In reality, the human body is covered with clothing and accessories (as hat, headphones, glasses and etc,), which would result as well in more turbulent flow and better mixing, which then could have a better match in the thermal plume characteristics of the proposed polygonal manikin.

Further work of the *Polygonal Manikin* optimization should be taken in direction of introduction of the post-manufacture filleting of the sharp edges and additional closing of the mechanical openings with highly flexible material, which will not restrict the movability feature of the model. Furthermore, numerically derived results should be compared with experimental data of clothed thermal manikin. This way, a validation of the proposed virtual thermal manikin would be accomplished and the next design stages for the breathing system could be taken.

Acknowledgements

The presented study is supported by “RDS” at TU-Sofia, as part of the activities under the "Perspective leaders" project, with Contract № 171ПР0016-02, entitled: “Implementation of CFD based intelligent technologies, for design assessment of developed virtual breathing thermal manikin".

References

[1] Bjørn E., *Simulation of human respiration with breathing thermal manikins*, Proceedings of the 3rd international meeting on thermal manikin testing 3IMM, Stockholm, Sweden, 12–13 October, 1999.
[2] Ivanov M., *Compact Breathing Simulation System, Developed as Additional Functionality for Thermal Manikins*, “Romanian Journal of Building Services”, Vol.1, No.3, ISSN: 2393-5154, pp. 1-12, 2015.
[3] Ivanov M., Mijorski S., *CFD modelling of flow interaction in the breathing zone of a virtual thermal manikin*, “Energy Procedia” Journal, Volume 112, pp. 240-251, ISSN: 1876-6102, Elsevier, 2017.
[4] Lin S., *Nasal Aerodynamics*, Chief Editor: Arlen D Meyers, MD, MBA, http://emedicine.medscape.com/article/874822-overview#a1, Updated: May 14, 2015.
[5] Madsen T., *Development of a breathing thermal manikin*, Proceedings of the 3rd international meeting on thermal manikin testing 3IMM, Stockholm, Sweden, 12–13 October, 1999.
[6] Menter F., *Zonal Two Equation k-ω Turbulence Models for Aerodynamic Flows*, AIAA Paper 93, 1993.
[7] Menter F., *Turbulence Modelling for Engineering Flows*, ANSYS Inc., 2011.
[8] Nilsson H., *How to Build and Use a Virtual Thermal Manikin Based on Real Manikin Methods, Sixth International Thermal Manikin and Modelling Meeting*, “Thermal Manikins and Modelling”, ISBN: 962-367-534-8, 2006.
[9] Spalart P., *Young-person’s guide to detached-eddy simulations grids*, NASA/CR-2001-21103, Boeing Commercial Airplanes, Seattle, Washington, 2001.

CARBON FOOTPRINT FROM COAL-FIRED POWER PLANTS IN REPUBLIC OF SERBIA

Mirjana Laković [1], Milica Jović
Faculty of Mechanical Engineering, University of Niš, A. Medvedeva 14, 18000 Niš

ABSTRACT

One of the main sources of carbon dioxide that affect global warming is the energy sector. In this paper, the effects of greenhouse gasses that arise during the production of electricity, with a special analysis of thermal power plants in the Republic of Serbia, were done. Coal-fired power plants represent the largest polluter of the atmosphere because during coal combustion significant amounts of CO2 is released. Carbon footprint is also analyzed in this paper. The carbon footprint from thermal power plants compared to the carbon footprint from other sectors has the highest value. This paper analyzes the changes of the carbon footprint for two years from power plants in the Republic of Serbia.

Keywords: carbon footprint, carbon dioxide, global warming, greenhouse gasses, thermal power plants

1. INTRODUCTION

The Kyoto Protocol defines binding targets for reducing emissions by 37 industrialized countries and the European Union during the first implementation period 2008-2012. year [1]. Since belongs to the group of developing countries (non-Annex I countries), the Republic of Serbia has no quantitative commitments to reduce emissions of greenhouse gasses in the first commitment period. However, Serbia has all the obligations with regard to the establishment and implementation of measures and activities to achieve the objectives of the Convention. The second commitment period under the Protocol was initiated when in December 2012 in Doha, Qatar, signed Amendment Doha. During the second commitment period, the parties have committed themselves to reduce emissions of greenhouse gasses by at least 18% below 1990 levels during the eight-year period 2013 - 2020. Changes from Doha are not yet active.

The tendency of increasing emissions of greenhouse gasses leads to the long-term goal of establishing control of environmental impacts caused by climate change. The carbon footprint has become a widely used concept in emissions assessments [2]. The term carbon footprint is used for greenhouse gas emissions and is generally expressed as CO_2 equivalents (CO_2e), which consists of emissions of CO_2, CH_4 and N_2O. These gasses are translated into the amount of CO_2 (this is called the equivalent amount of CO_2). It is a measure of the total amount of carbon dioxide in the atmosphere in a given time frame which is directly or indirectly transmitted. Carbon footprint helps us to determine the amount of emissions from various sectors, which is useful for quantifying the impact of human activities on the

[1]University of Niš, A. Medvedeva 14, 18000 Niš,
lmirjana@masfak.ni.ac.rs

environment and global warming. In the postindustrial era, the concentration of carbon dioxide in the atmosphere is increasing alarmingly.

The following expression represents the equation to calculate the carbon footprint:

Carbon footprint of a given activity = Activity data (mass/volume/kWh/km) ×Emission factor (CO_2 e per unit)

In the case of thermal power plants [3]:

Carbon footprint (tons CO_2/year) = Yearly electricity consumption of the plant (MWh/year) × Emission factor (tons CO_2/MWh).

2. SERBIAN ENERGY SYSTEM

Thermal power plants in the Republic, Serbia are [4]:

a) Eight power plants with 25 blocks that use lignite as a fuel and the installed capacity of 5.171MW, two of these power plants are located in Kosovo and Metohija
b) Cogeneration plant with a total installed capacity of 425MW of electricity generation, 505MW for the production of thermal energy

Table 1. Thermal power plants in Serbia

Power plant	Location	Number of blocks	Installed power [MW]
Nikola Tesla A	Obrenovac	6	1650
Nikola Tesla B	Obrenovac	2	1290
Kolubara	Veliki Crljeni	5	270
Kostolac A and B	Kostolac	4	1007
Morava	Svilajnac	1	120
Kosovo A and B	Kosovo and Metohija	7	-

From 1 June 1999, the Electric Power Industry of Serbia does not manage its capacity in Kosovo and Metohija.

The energy sector in Serbia has some characteristic weaknesses that contribute to high energy consumption and high emissions of CO_2. These disadvantages are low efficiency due to outdated technology in the sectors of production and consumption, high losses in electricity distribution. In order to reduce CO_2 emissions is necessary to implement a project that will examine what is possible to improve in the thermal power plants to reduce emissions of CO_2 and then put into practice these tests. Any minimal reduction of this gas would bring great benefits to air quality.

3. CARBON FOOTPRINT IN THERMAL POWER PLANT IN SERBIA

In this part of the paper will present the carbon footprint by thermal power plants in the Republic of Serbia for 2008 and 2014. year. The year 2014 has been chosen for comparison because the year had a significant drop in electricity production during that year. The month of May that year in the Republic of Serbia have been flooding and area around the thermal power plant Nikola Tesla A and B was flooded and area of the Obrenovac town. As a result of

the floods in the period from May to September this power plant operated with reduced capacity. The produced quantity of electricity per month for the thermal power plant Nikola Tesla A and B for 2014 is given in Table 2.

Table 2. Produced amount of electricity by month for the 2014 year from the power plants Nikola Tesla A and B [4]

The produced amount of electricity GWh		
Month	Nikola Tesla A	Nikola Tesla B
January	1028	847
February	968	750
March	1005	859
April	931	639
May	368	335
June	440	364
July	537	418
August	459	415
September	510	645
October	549	749
November	504	757
December	550	745
In total	7849	7523

Based on the research that has been shown in [5] values for carbon dioxide emission factor for thermal power plants Nikola Tesla A and Nikola Tesla B were used and that values are shown in Table 3.

Table 3. Carbon dioxide emission factor

Power plant	The mean value of CO_2 emission factor [kg CO_2/kWh]
Nikola Tesla A	1,16
Nikola Tesla B	1,09

Emission factor of the thermal power plant Nikola Tesla A is lower than emission factor of the thermal power plant Nikola Tesla B. The reason for this is that the thermal power plant Nikola Tesla B in recent years modernized and therefore many systems were improved. Based on the known production of electricity and the value of CO_2 emission factor can be calculated Carbon footprint from thermal power plants Nikola Tesla A and B. Table 4 shows the comparative analysis of the carbon footprint for 2008 and 2014.

Table 4. Comparative analysis calculated carbon footprint for the year 2008 compared to the year 2014

	Carbon footprint [t CO_2/year]	
Power plant	Year 2008	Year 2014
Nikola Tesla A	11 482 000	9 104 840
Nikola Tesla B	9 214 000	8 200 070

As can be seen in Table 4 CO_2 emissions are reduced. As the carbon footprint is directly connected to the produced amount of electricity can be noted that this reduction in emissions

is precisely because of that. In fact, based on data from Electric Power Industry of Serbia in 2008 in the considered thermal power plants around were produced the 4GWh more electricity than in the year 2014. On the other hand, the CO_2 emission is the result of constant care for the environment. Same power plants have their own projects related to environmental protection. Thermal power plants are improving their systems for reducing emissions of harmful gasses into the atmosphere. A key project of environmental protection in the thermal power plant Nikola Tesla is associated with the emission of CO_2. That is the reconstruction of electro filters. When adjusting the operation of these power plants to the demands of the law regulations, the priority was given to the reduction of particles from the oldest blocks and adjusting the operation of electro filters to the demands of the European Union (50 mg/m3). The condition of electro filters has a significant impact on air pollution in the surrounding of these blocks situated near settlements. It is, therefore, expected that the reconstruction of these electro filters will have a considerable effect on the improvement of the air quality.

4. CONCLUSIONS

Carbon footprint has appeared as a strong and popular indicator of greenhouse gasses with special emphasis on carbon dioxide. Because of its important role in raising awareness of responsibility to the global warming, many scientists but also politicians try to use it as a tool for management. It is possible to define the carbon footprint for each sector separately and analyze the impact of GHG on the atmosphere. In this paper, special attention was paid to thermal power plants, determining the carbon footprint of power plants. Thermal power plants which used fossil fuel are major polluters, and it is necessary to analyze their impact on the surrounding air. To reduce emissions of greenhouse gasses by technologies which are available, alongside the more intensive level of implementation of energy efficiency and introducing renewable energy sources, it would be necessary to introduce and nuclear energy plants in the Republic of Serbia [6]. However, the period until the middle of this century is long and it can be expected and significant technology intrusions that are now at the experimental plant, or even just a theoretical elaboration (production and use of hydrogen, fuel cells, nuclear fusion, etc.).

References

[1] www.klimatskepromene.rs

[2] Andri et al. “Environmental performance assessment of retrofitting existing coal fired power plants to co-firing with biomass: carbon footprint and emergy approach “, Journal of Cleaner Production 103 (2015) 13-27

[3] Chrysi Laspidou et al., Carbon Footprint Calculation Of Desalination Units In Greece, Fresenius Environmental Bulletin, Volume 21, No. 8b, January 2012

[4] www.eps.rs

[5] Marković et al.,“ Determination of the Specific Carbon Dioxide Emission Factor from Thermal Power Plants Nikola Tesla A and B”, Full Papers Proceeding of International Conference "Power Plants 2014", 28-31.October, 2014, Zlatibor Serbia, ISBN 978-86-7877-024-1

[6] Mihajlo Gavrić et al., The Green Book Of The Electric Power Industry Of Serbia, PE Electric Power Industry of Serbia, 2009

ANALYSIS OF FLAME AERODYNAMICS FOR BURNING TESTS OF ANIMAL FAT MIXED WITH LIQUID HYDROCARBONS

Gh. Lăzăroiu, L.Mihăescu[1], I. Pîşă, G. Negreanu, E. Pop, V. Berbece, A. Bondrea
Politehnica University of Bucharest

ABSTRACT

For the combustion of animal fat mixed with liquid oil has been adopted the solution of using a system with mechanical atomizer and flame swirling. This technology is represented by a wide range of special designed burners, in order to reduce as much as possible, the financial effort for industrial implementation. This paper details the aerodynamics of the flame for the specific case of animal fat burning experiments.

1. GENERAL ASPECTS

Animal fats used in the experimental tests had the following characteristics

- freezing point: 17.4 – 18.8^{0}C
- flash point: 165 – 188^{0}C
- viscosity: 4 E at 45^{0}C; 1.2 E at 75^{0}C
- elemental analysis: C = 68 – 74%; H = 13 – 14%; O = 14.8 – 19%; N = 0.18 – 0.25%
- lower heating value: 35000 – 35500 kJ/kg

2. EXPERIMENTAL DATA

In the experimental tests, mixtures with a maximum fat mass participation of 30% have been done. The fuel analyzed is in cvasi-solid form at ambient temperature. In order to atomize it, the fuel must be preheated to 45^{0}C at least. Figure 1 shows the state of fuel at ambient temperature, in the preheater (dosage 30% fat).

Figure.1. Fuel stat in the preheater at ambient temperature

For a good atomizing, a burner equipped with electric fuel preheater to a temperature of 75^0C, has been chosen.

Swirling air must provide a short jet, suitable for the size of the combustion space.

.For experimental tests a burner GB-Ganz type ANYO 12R-2-1-0, presented in the figure 2, has been selected. This burner has a flame stabilizer which acts based on recirculation of flue gas obtained as a result of the swirl.

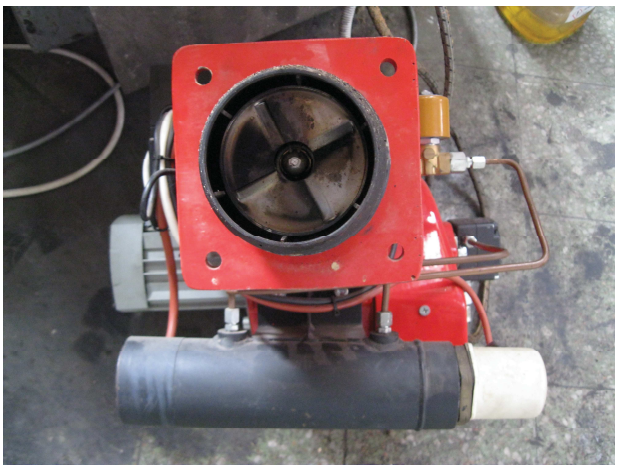

Figure.2. GB GANZ burner

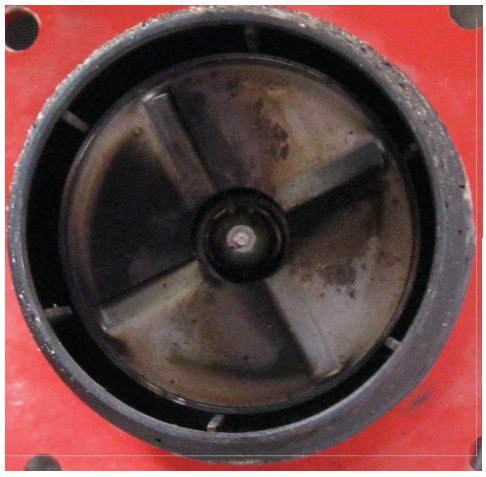

Figure.3 Construction of aerodynamic stabilizer

Figure 3 present the construction of aerodynamic flame stabilizer, characterized by three sections for air flow.

The first section is the central one, in the front of the injection nozzle and has a diameter of 20 mm. The flame will come out through this section being initiated by primary air. The other two sections are intended for the secondary air flow and present the following constructive elements:

- 4 channels with a 60^0 inclination to the axial direction of flow, having the radial length of 25 mm and channel width of 3 mm. These axial channels form a system for generating swirling flow;
- an annular channel located on the periphery of embrasure, with external diameter of 80 mm and an inner diameter of 73 mm. The outdoor air jet achieved by this flow has the purpose to stop the flame bursting under the swirling effect

3. MATHEMATICAL MODEL

The axial air flow velocity through the all three sections is u_x = 20m/s

The swirled jet is characterized by the following parameters:

- the degree of swirl n;
- tangential speed.

The degree of swirl for an axial generating system can be determined by the relationship:

$$n = \frac{8}{3\pi} d \frac{d^3 - d_0^3}{\left(d^2 - d_0^2\right)^2} tg\alpha$$

where: d is the outer diameter of the swirling channel, d_0 - diameter of central zone, and α the positioning angle of geometric elements for swirl

The tested burner is characterized by the following values :

$$d = 70 \text{ mm}; \; d_0 = 20 \text{ mm}; \; \alpha = 60^0$$

By calculus, it results $n = 2.99$.

The amount of swirl generated fall within the limits for liquid fuels.

Tangential velocity is determined by the following relationship:

$$u_\varphi = u_x \frac{d^2}{d^2 - d_0^2} tg\alpha$$

where: u_x – axial velocity (u_x = 20 m/s). By calculus, results:

$$u\varphi = 37.6\, m/s$$

For a set of coaxial swirling jets, the average degree of swirl is determined by the relationship:

$$n_{ech} = \frac{\Sigma n_i \rho_i F_i u_{xi}^2 D_i}{D \Sigma \rho_i F_i u_{xi}^2}$$

where: p is fluid i density, in kg/m^3; F - flow section, m^2; u_{xi} - axial velocity, m/s; D_i - flow channel diameter, m; D - embrasure diameter, m.

The flow is represented by three concentric jets, swirled being only the one from the center. For the diameters and flow sections resulted by interaction of the three jets, the following equivalent degree of swirl has been obtained:

$$n_{ech} = 2.7$$

The internal recirculation formed in the depression zone from the center of the swirl, leads to the increased mass of the swirl jet that can be determined using the relationship:

$$\frac{Dm}{m_0} = (0.32 + 0.4\, n)\frac{x}{D}, \quad kg/kg,$$

where: x is the axial distance, in m; m_0 – initial mass, in kg/s; n – degree of swirl, and D – embrasure diameter, in m.

For equivalent degree, at an average flame temperature of 1100 K, the increasing of the jet mass will become:

$$Dm = m_0 1.4 \rho \frac{x}{D} = 0.259 x \quad kg/s$$

For a flame length of x = 0.4 m results a flame mass intake of 0.1 kg/s.

This entrainment by the swirling flame jet of the ambient air leads to increased combustion and ultimately to burning in a low flame volume.

Figure.4. Aspect of the flame

Figure 4 shows the appearance of the flame length by its ignition into an infinite burning volume, out of the fire.

4. CONCLUSIONS

The flame had a length of 0.45 m. The atomizing of the fuel was achieved with a 0.5 mm nozzle, the size of which was imposed by the need for very fine atomizing.

In conclusion, it is appreciated that the aerodynamic analysis for the burner used has highlighted its ability to be used in the combustion of animal fat mixed with light liquid hydrocarbons. The air jet produced led to a short flame and a significant increase in combustion achieved by internal recycling. These conclusions explain the performance of experimental tests on a 55 kW boiler.

Acknowledgements

This work was supported by a grant of the Romanian National Authority For Scientific Research CNCS – UEFISCDI, project ID PN-II-PT-PCCA-2013-4-1017, "Green Tannery – Methods for Energetic Recovery of Biodegradable Wastes"

References

[1] Mihăescu L., Pănoiu N., Totolo Cr. „Arzătoare turbionare", Ed. Tehnică, Bucureşti, 1986

[2] Mihăescu, L., „Arzătoare pentru hidrocarburi cu NO_x scăzut", Ed. Printech, Bucureşti 2004, ISBN 973-718-039-9

[3] E. Pop, L. Mihaescu, Gh. Lazaroiu, I. Pisa, G. Negreanu, *„Energetic characteristics of animal fats from tannery for energy production"* 4th International Conference on Thermal Equipment Renewable Energy and Rural Development TE-RE-ED 2015, Posada Vidraru 4-6 iunie 2015, Editura Politehnica Press, ISSN 2359-7941, pp 475-478

[4] Nicolici A., Lăzăroiu Gh., Pană C., Negurescu N., Cernat Al., Nuţu C, Mocanu M „*On animal fat use at diesel engine*", 5th International Conference on Thermal Equipment, Renewable Energy and Rural Development, TE-RE-RD 2016 Proceeding, ISSN: 2359-7941, ISSN-L:2457-3302, , Golden Sands, 2-4 June 2016, Bulgaria, pp 483- 488

IMPELLERS SHAPE INFLUENCE ON THE HEAT INDUCED IN LIQUID ENVIRONMENTS

Lucian MÂNDREA[1], Corina Alice BĂBUȚANU[2], Gabriela OPRINA[3]
[1]Politehnica University of Bucharest,
Splaiul Independenței nr.313, sector 6, Bucharest, Romania
[2,3]National Institute for Research and Development in Electrical Engineering ICPE-CA,
Splaiul Unirii nr. 313, sector 3, Bucharest, Romania

ABSTRACT

Mixing reactors are used in a wide variety of industrial processes, starting with the mining industry and up to the cosmetics industry and biotechnology. The movement induced in the liquid by impellers results in obtaining uniform concentration and temperature gradients. It occurs also the temperature increasing due to the heat released by the liquid layers movement. For liquids with a high viscosity, the heat resulted from the movement of the layers can have beneficial effects, or conversely, negative effect for the technological processes. In the present paper the authors studied the influence of the impellers shape on the heat generated by the movement of liquids in mixing reactors. Eight types of impellers (4 turbines with 2 flat blades, 1 turbine with 4 flat blades, 1 turbine with 4 pitched blades, 1 turbine with 6 flat blades and 1 Rushton turbine) were tested in a speed range between 100 and 500 rpm. The moment, the power consumption and the released heat were determined. The experiments have shown that the largest energy consumer was the turbine with 6 flat blades. Under certain conditions the results can be extrapolated to liquids with different densities and viscosities.

1. INTRODUCTION

The exponential growth of the population and the rising living standards from recent decades has led to a substantial increase in needed products of process industries. An important part of the price of these products (up to 50% according to [1]) is represented by the cost of mixing technologies.

The study of mixing processes is done either theoretically by mathematical modeling (analytical or numerical) or experimental by using models that reproduce more or less real plants. Thus, the power consumption by different type of impellers has been studied in several papers, determining the power number or using different correlations between calculated values and experiments [2, 3, 4, 5].

Also, impeller rotation has as effect the increasing of the fluid temperature due to the shear stress that occurs between the fluid layers effect presented in studies like [6,7].

In this paper the authors intend to realize an analytical approach in order to calculate the total amount of energy transformed in heat by rotating a disk with the diameter D in a cylinder full of water.

The disk is placed at the distance h_1 from the superior part of cylinder and at the distance h_2 from the bottom of the cylinder. The water from the cylinder has the density ρ and the dynamic viscosity μ.

The rotating speed of the disk is n, the angular speed is ω and the tangential speed is v as in figure 1 b.

If the flow regime is laminar, then the shear stress is calculated with the Newton law:

[1]Corresponding author: mandrea_lucian@hotmail.com

$$\tau = \mu \frac{v}{h} = \mu \frac{\omega r}{h} \quad (1)$$

The elementary surface where this shear stress acts at the variable radius r is:

$$dS = 2\pi r \cdot dr \quad (2)$$

The elementary force becomes:

$$dF = \tau \cdot dS = 2\pi\mu \frac{\omega}{h} r^2 dr \quad (3)$$

The power lost by friction is:

$$dP = dF \cdot v = 2\pi\mu \frac{\omega^2}{h} r^3 dr \quad (4)$$

As a consequence, the total power lost is:

$$P = \int_0^R dP = \frac{\pi}{2} \mu \frac{\omega^2}{h} R^4 \quad (5)$$

If the power P_1 corresponds with the distance h_1 and P_2 with h_2, because R=D/2, it results the total power lost in the cylinder:

$$P = P_1 + P_2 = \frac{\pi}{32} \frac{h_1 + h_2}{h_1 h_2} \mu \omega^2 D^4 \quad (6)$$

If the flow regime is turbulent, then the shear stress is calculated with the similitude formula:

$$\tau = \varsigma \frac{\rho v^2}{2} = \varsigma \frac{\rho \omega^2 r^2}{2} \quad (7)$$

ζ is the coefficient of the hydraulic local loss.

Following the same reasoning, the total power lost in the cylinder becomes:

$$P = \frac{\pi}{160} (\varsigma_1 + \varsigma_2) \rho \omega^3 D^5 \quad (8)$$

Because h_1 and $h_2$are known in our case, we shall calculate the total amount of heat produced in a certain time taking into consideration the power lost in the laminar regime, which is in fact the minimum power lost:

$$Q = Pt = \frac{\pi}{32} \frac{h_1 + h_2}{h_1 h_2} \mu \omega^2 D^4 t \quad (9)$$

2. METHODOLOGY

In order to calculate the heat generated by liquid motion caused by rotors operation, several set of experimental measurement was made. The purpose of these measurements was to determine the power consumed depending on the type of rotor used.

The experiments were conducted in an experimental setup shown in figure 1 a. It consists of a transparent cylindrical vessel with the ratio D/H of about 1.5 and a capacity of 0.126 m^3.

The experimental setup is equipped with a variable speed motor on whose shaft can be fitted impellers of different types and sizes as in figure 1 c.

Also, the setup is endowed with electronic speed control, and a panel which displays rotational speed and momentum produced by the studied impellers.

The experiments were done with tap water under atmospheric pressure and a temperature of 20°C.

The eight types of impellers (four impellers with two flat blades, an impeller with four flat blades, an impeller with four pitched blades, an impeller with six flat blades and a Rushton turbine were tested in a speed range between 100 and 500 rpm.

All the impellers had a hub diameter of 20 mm and blades size as follows:

- two thin flat blades impeller - 100 mm length and 10 mm width;
- two flat blades impeller - 100 mm length and 20 mm width;
- two wide flat blades impeller - 100 mm length and 40 mm width;
- two short flat blades impeller - 60 mm length and 20 mm width;
- four flat blades impeller - 100 mm length and 20 mm width;
- four pitched blades(45° pitch angle)impeller -100 mm length and 20 mm width;
- six flat blades impeller - 100 mm length and 20 mm width;
- Rushton turbine – 105 mm diameter and 20 mm width.

a

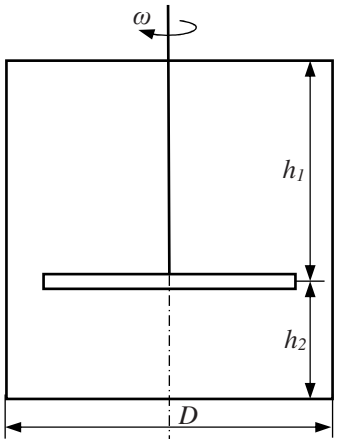

b

c

Figure 1: The experimental setup (a), the rotating disk (b) and the tested impellers (c)

The measurements were done in five different points, vertically located on the center axis of the vessel, at 130, 140, 150, 160 respectively 170 mm from the vessel bottom. The values of resulting temperature variation calculated for 24 hours of functioning are shown in Table 1.

Table 1: The temperature variation for the studied impellers

4 at 45° pitched blades Δt=Q/mc						2 flat wide blades impeller Δt=Q/mc					
n [rot/min]	h = 130mm	h = 140mm	h = 150mm	h = 160mm	h = 170mm	n [rot/min]	h = 130mm	h = 140mm	h = 150mm	h = 160mm	h = 170mm
100	0.05	0.05	0.05	0.05	0.05	100	0.06	0.06	0.06	0.06	0.06
200	0.15	0.16	0.16	0.15	0.16	200	0.25	0.22	0.22	0.23	0.23
300	0.35	0.36	0.34	0.34	0.34	300	0.53	0.48	0.54	0.54	0.55
400	0.69	0.68	0.67	0.67	0.67	400	1.18	0.92	1.12	1.18	1.21
500	1.29	1.21	1.23	1.17	1.16	500					

4 flat blades impeller Δt=Q/mc						2 flat short blades impeller Δt=Q/mc					
n [rot/min]	h = 130mm	h = 140mm	h = 150mm	h = 160mm	h = 170mm	n [rot/min]	h = 130mm	h = 140mm	h = 150mm	h = 160mm	h = 170mm
100	0.06	0.06	0.06	0.05	0.06	100	0.05	0.05	0.05	0.05	0.05
200	0.21	0.19	0.21	0.21	0.18	200	0.12	0.11	0.11	0.11	0.11
300	0.47	0.45	0.47	0.46	0.46	300	0.23	0.21	0.19	0.20	0.20
400	1.04	1.01	1.02	0.94	0.86	400	0.38	0.34	0.33	0.33	0.33
500						500	0.54	0.50	0.50	0.49	0.49
6 flat blades impeller Δt=Q/mc						2 flat thin blades impeller Δt=Q/mc					
n [rot/min]	h = 130mm	h = 140mm	h = 150mm	h = 160mm	h = 170mm	n [rot/min]	h = 130mm	h = 140mm	h = 150mm	h = 160mm	h = 170mm
100	0.06	0.06	0.05	0.06	0.06	100	0.05	0.05	0.05	0.05	0.05
200	0.20	0.22	0.20	0.22	0.21	200	0.14	0.14	0.13	0.13	0.13
300	0.51	0.51	0.53	0.54	0.51	300	0.30	0.29	0.28	0.28	0.27
400	1.12	1.11	1.10	1.05	1.13	400	0.54	0.54	0.50	0.48	0.50
500						500	0.88	0.86	0.82	0.79	0.83
2 flat blades impeller Δt=Q/mc						Rushton turbine Δt=Q/mc					
n [rot/min]	h = 130mm	h = 140mm	h = 150mm	h = 160mm	h = 170mm	n [rot/min]	h = 130mm	h = 140mm	h = 150mm	h = 160mm	h = 170mm
100	0.05	0.05	0.05	0.05	0.05	100	0.06	0.06	0.06	0.06	0.06
200	0.18	0.18	0.18	0.18	0.18	200	0.25	0.25	0.26	0.23	0.23
300	0.42	0.43	0.42	0.42	0.42	300	0.62	0.56	0.64	0.63	0.64
400	0.82	0.83	0.84	0.80	0.80	400	1.18	1.17	1.16	1.14	1.16
500	1.43	1.44	1.48	1.46	1.41						

The diagrams on the temperature change due to the movement of the fluid are shown in figures 2-6.

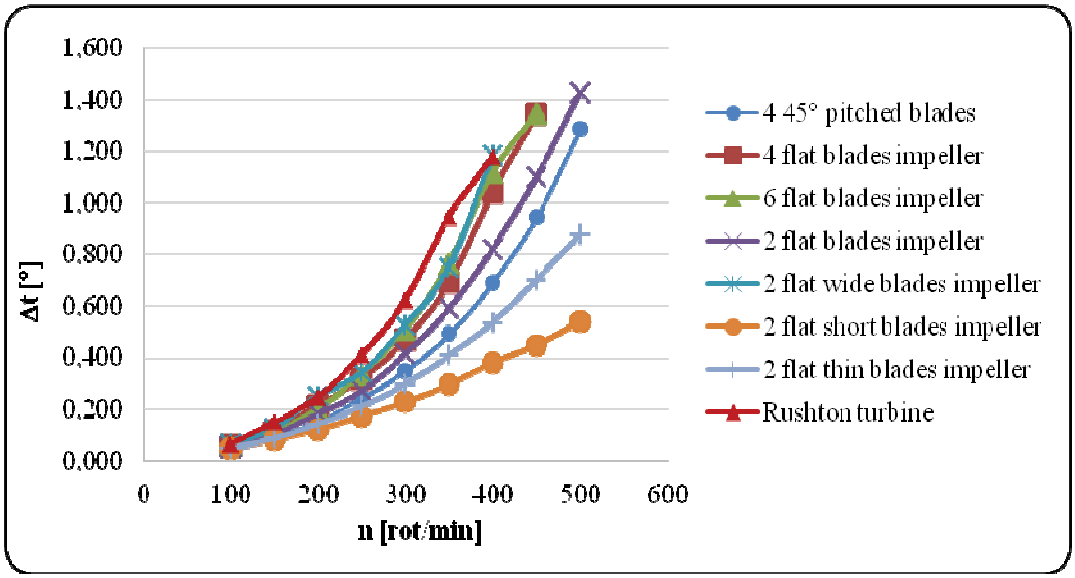

Figure 2: The temperature variation for impellers mounted at 130 mm from the vessel bottom.

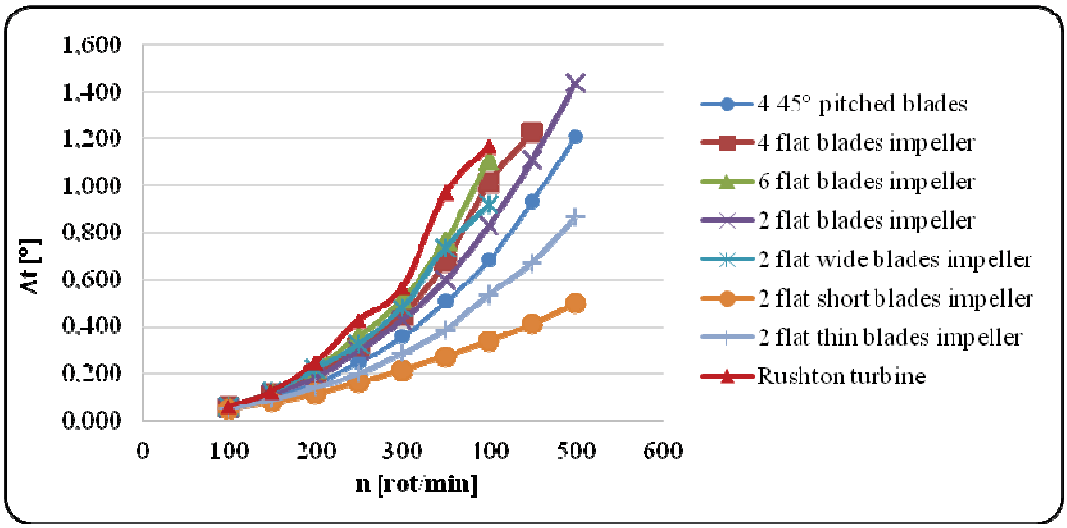

Figure 3: The temperature variation for impellers mounted at 140 mm from the vessel bottom.

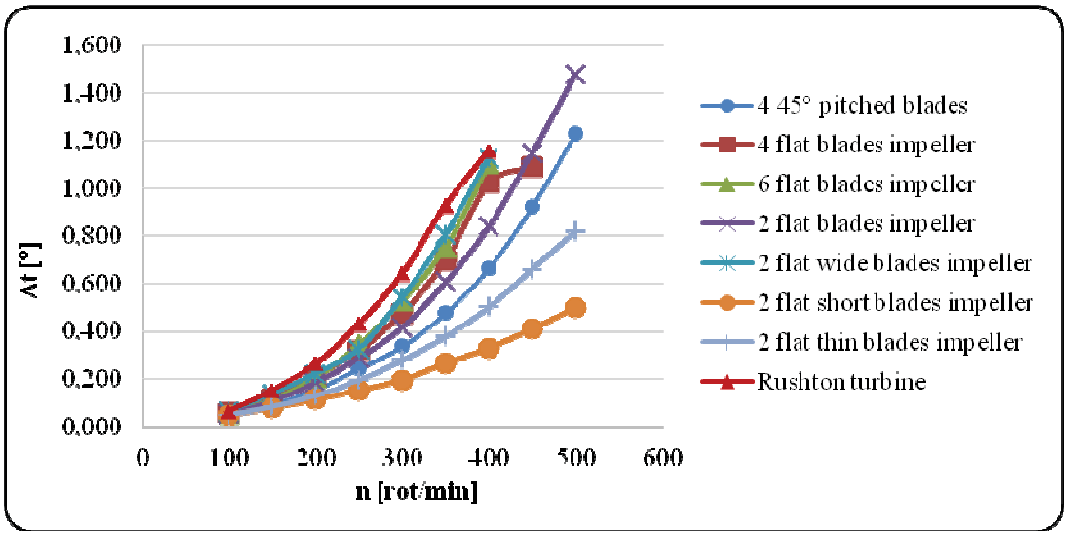

Figure 4: The temperature variation for impellers mounted at 150 mm from the vessel bottom.

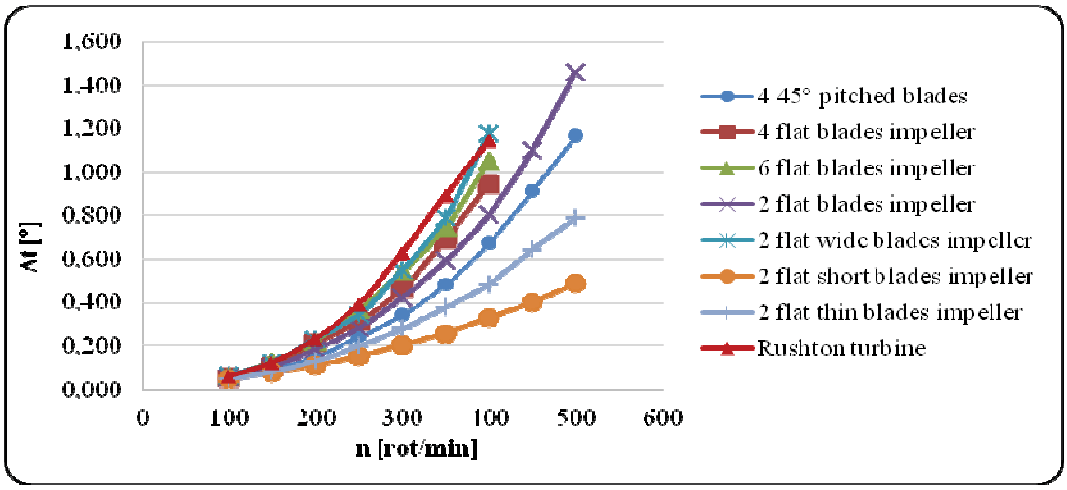

Figure 5: The temperature variation for impellers mounted at 160 mm from the vessel bottom.

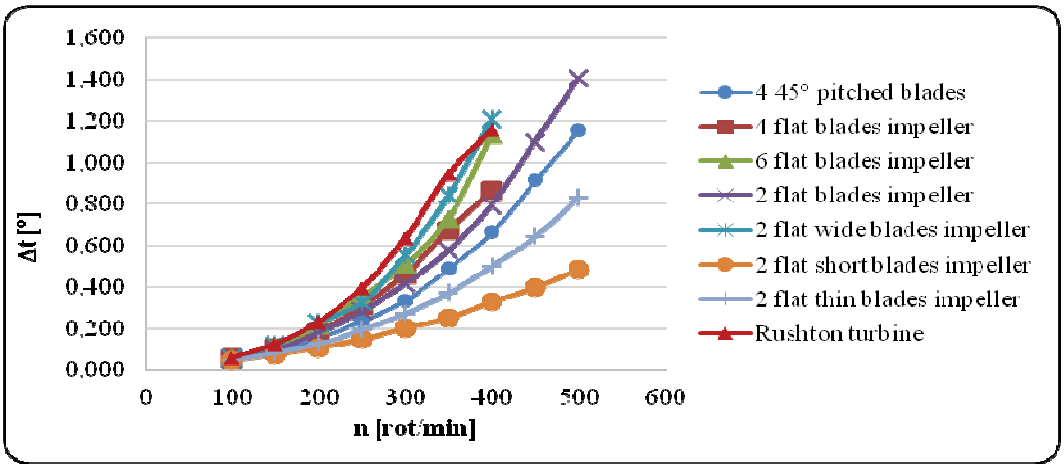

Figure 6: The temperature variation for impellers mounted at 170 mm from the vessel bottom.

3. CONCLUSIONS

A first remark is that the differences of the power consumed with the rotation are less than 1 W if we modify the position of the same impeller in the vessel. This difference could become significant with a more viscous fluid. As we expected, the power lost and transformed into heat is bigger for 6 flat blades than 4 flat blades. The last one is bigger than for 4 pitched blades. The same is with the 2 flat wide blade impellers which create a lost bigger than 2 flat blade impellers, bigger than for 2 flat thin blade impellers, bigger than for 2 flat short blade impellers. The Rushton turbine, which has also a disk, creates the maximum power lost transformed into heat. A significant conclusion is what difference of temperature they create during 24 hours. From (6) we can see that the power lost is proportional with the dynamic viscosity, so if we use oil and if we suppose also that the vessel is an adiabatically system, we can calculate at what temperature the liquid will arrive. These one is a very important result and a very important conclusion for practical use of different liquids.

The research was conducted within NUCLEUS Program, contract no. 14N/2016, financed by the National Authority for Scientific Research and Innovation.

References

[1] Butcher M., Eagles W., 2002, *Fluid mixing re-engineered*, Chemical Technology Journal, https://www.tcetoday.com/~/media/Documents/TCE/Articles/2002/733/733mixing1.pdf
[2] Furukawa H., Kato Y., Inoue Y., Kato T., Tada Y. and Hashimoto S., *Correlation of Power Consumption for Several Kinds of Mixing Impellers*, Hindawi Publishing Corporation International Journal of Chemical Engineering, ISSN: 1687-8078 (Online), Volume 2012, Article ID 106496, 6 pages, doi:10.1155/2012/106496.
[3] Rashid T., Rizvi S.Z.H., Malik S.R, *Study the effect of impeller design on power consumption*, February2013, International Journal of Chemical and Environmental Engineering, Volume 4,No. 1, p. 21-24.
[4] Yoshida M., Ito A., Yamagiwa K.,OhkawaA.,Abe M., TezuraS. and ShimazakiM.,*Effect of impeller clearance on power consumption of unsteadily forward-reverse rotating multiple impellers in an unbaffled agitation vessel*, 2002, Latin American applied research,vol. 32, no, 2, ISSN online 1851-8796 p. 189-194.
[5] Adamiak R., Karcz J., *Effects of type and number of impellers and liquid viscosity on the power characteristics of mechanically agitated gas—liquid systems*, J. Chem. Pap. (2007) 61: p. 16-23, doi:10.2478/s11696-006-0089-6.
[6] Rao D. and Mahey C., *Studies on Impeller Design on Power Consumption from Temperature Rise Data In a Stirred Tank*, AIChE Annual Meeting, Philadelphia PA, November 16-21, 2008, North American Mixing Forum (06), paper #434a, https://aiche.confex.com/aiche/2008/techprogram/S6955.HTM.
[7] *Mixing 101: Flow patterns & Impellers*, http://www.dynamixinc.com/mixing-101-the-basic-principles-of-mixing-and-impellers.

ANALYSIS OF THE POSSIBILITIES OF COMBUSTION OF ANIMAL FAT MIXED WITH LIQUID HYDROCARBONS IN BOILERS WITH SMALL FURNACES

L. Mihăescu[1], Gh. Lăzăroiu, I. Pîşă, E. Pop, G. Negreanu, V. Berbece, A.Bondrea
Politehnica University of Bucharest

ABSTRACT

The paper presents the experimental results of the combustion of animal fat derived from the tanner industry, mixed with liquid hydrocarbons, in boilers with small furnaces. Various mixtures have been studied in which the fat concentration was varied, thus obtaining their limits the addition into liquid hydrocarbons, for a good efficiency. The resulting pollutant emissions were also studied.

1. INTRODUCTION

Combustion of animal fats is a necessity imposed by compliance with environmental requirements. The leather industry, by incinerating this waste, possibly with energy recovery, becomes much more flexible in respect to environmental protection legislation.

The choice of industrial applicability at a low power energy unit, with a small furnace is a consequence of the amount of animal fats resulting from an industrial unit from the tannery industry in Romania.

All the developed research has taken into consideration a mix of animal fats and liquid hydrocarbons, so far to a maximum mixing limit of 30%.

This paper presents the interpretation of a series of experimental test, which included:

- energetic characteristics of fats;
- determination of atomizing possibilities;
- the choice of a technical-economical combustion technology;
- application of the combustion technology as defined in a hot water producing boiler.

The energy characteristics have demonstrated the possibility of spraying animal fats both in a pure state (viscosity at 45^0C being 1.5 - 2E) and mixed with liquid hydrocarbons. The calorific value of animal fats is similar to that of liquid hydrocarbons, having a value of 35000-35500 kJ/kg.

2. EXPERIMENTAL TESTS. RESULTS AND DISCUSSIONS

Combustion tests were conducted using a 50 kW boiler for hot water production, equipped with a mechanical spraying pump burner. The burner includes a fuel preheater, to a level of 75^0C. The installation was completed by a fuel preheater up to a temperature level of 50^0C.

Figure 1 shows the boiler installation with the annexes relating thereto.

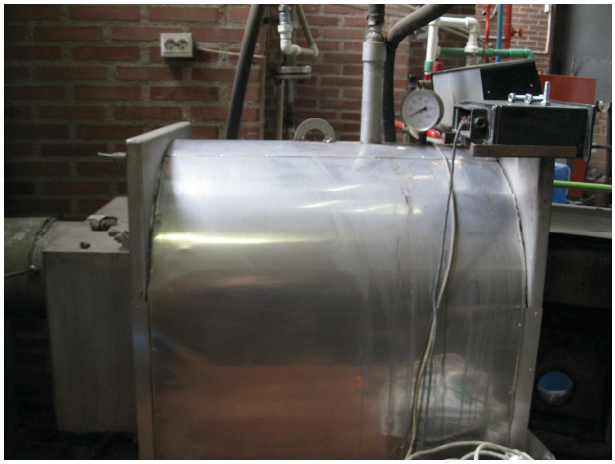

Figure 1. The boiler installation with the related annexes

The burner was equipped with an injector whose spray nozzle diameter was 0.5 mm to achieve as fine droplets as possible. Fuel flow rate during experimental testing was 15 l/h. Flame length L_f at the combustion of sprayed liquid fuels can be determined using relation [5]:

$$L_f = \frac{ut}{(1+A)^2}$$

where: u is the flow velocity at the outlet of the burner, in m/s; t - time, s; A - coefficient characterizing the interaction between the energy characteristics of the fuel and the geometry of the burner.

$$A = 1 + \frac{2.4}{\tau_c}\left(\frac{\rho_a}{\rho_c}\cdot\frac{\nu_a}{\nu_c}\right)^{0.5}\left(\frac{d_j}{d_0}\right)^{1.5}$$

where: τ_c is the surface tension of the fuel, in N/m; ρ_a, ρ_c -air density, i.e. fuel, kg/m^3; ν_a, ν_c -viscosity of air and fuel, respectively m^2/s, d_j, d_o-diameter of the output section, m.

The burner air duct diameter is 80 mm, the output section being 20 mm ($d_j = 8\cdot10^{-2}\,m$; $d_0 = 2\cdot10^{-2}\,m$).

For $\rho_a = 1kg/m^3$; $\rho_c = 948kg/m^3$; $\nu_a = 22\cdot10^{-6}\,m/s$; $\nu_c = 68\cdot10^{-6}\,m/s$; $\tau_c = 32\cdot10^{-3}\,N/m^2$ results: A = 11.3

According to the Spalding burning model for light liquid fuels, the burning time τ for one particle of radius R_0 is determined with the relationship [5]:

$$\tau = \frac{\rho_c c_c R_0^2}{2\lambda\ln(1+B)}$$

$$B = \frac{H_i^i}{\Delta I}\frac{m_{02}}{\beta} + c_c \frac{T_g - T_s}{\Delta I}$$

where: ρ_c is the fuel density in kg/m^3; c_c – specific heat of the fuel, $kJ/(kg \cdot K)$; R_0 – radius of the fuel particle, mm, λ - thermal conductibility, $W/(m \cdot K)$; H_i^i-lower heat value of the fuel; m_{02}- gravimetric concentration of oxygen; β-oxygen required for burning the unit of fuel; ΔI- enthalpy increase when the particle is vaporized, kJ/kg; T_s – particle surface temperature, K; T_g – flue gas temperature, K.

For the used fuel, represented by a 30% mix of animal fat in light hydrocarbon liquids, the calculations were performed for the following physical sizes:

$H_i^i = 35000 - 35500 kJ/kg$; $\rho_c = 948\, kg/m^3$; $c_c = 1{,}8\, kJ/(kg \cdot K)$; $\lambda = 0{,}18\, W/(m \cdot K)$; $m_{02} = 0.23\, kg/kg$; $\beta = 3.3\, m_N^3/kg$; $\Delta I = 500\, kJ/kg$; $T_g - T_s = 800^0\, C$; $T_s = 500\, K$

Testing the burner yielded a flame length of L_f = 0.45 m. The flow rate determined from the burner aerodynamics has indicated a value of u = 20 m/s at 20^{0}C. For a temperature of 900 K, flow velocity reaches the value of u = 66 m/s. The burning time for these values will become:

$$t = \frac{L_f (1+A)^2}{u} = \frac{0.45(1+11.3)^2}{66} = 0.43\, s$$

for this type of burning, the total combustion particle diameter has resulted in:

$$d_p = 2R_0 = 70\, \mu m$$

Within the experimental tests, the burner shown in Figure 2 was mounted on a 55 kW hot water boiler, whose furnace has the dimensions L = 0.76 m, cross-section radius 0.65 m. Figure 3 shows to maximum burning space inside the furnace.

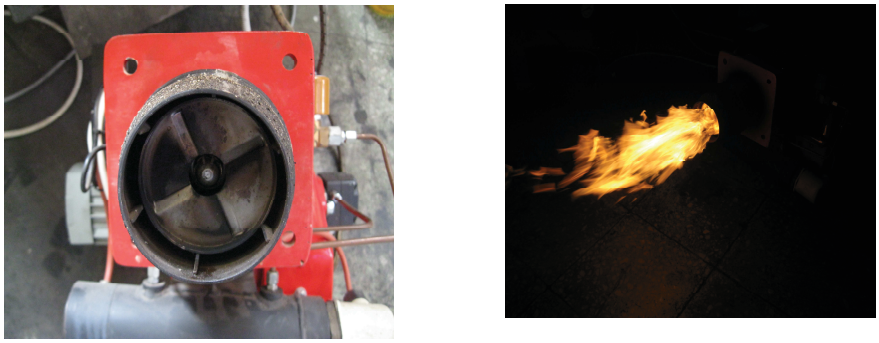

Figure 2. The burner used and the flame obtained during testing, in a free atmosphere

As the flame length during the burner tests in free atmosphere for the animal fat fuel mixed in a proportion of 30% in light liquid hydrocarbons was of 0.45 m, there results full compatibility of the burner with the boiler's furnace.

Figure 3. Maximum burning space inside the furnace

In addition, it also highlights a possible flame size with a maximum of 0.3 m, which allows less fine spraying, with a maximum particle diameter of up to 100 μm in diameter.

3. CONCLUSIONS

The tests carried out have shown a good combustion, characterized by the absence of soot particles and by an acceptable content of carbon monoxide for such fuel. For an excess of air of 2.15-2.43, the emission of CO had values within 900-1200 ppm (animal fats mix 10%, 20%, and 30%), and NOx emissions within the limits of 90-152 mg/m^3_N. As the temperature of the flue gases exhausted at the stack had values of 340-378^{0}C, the efficiency of the boiler was: η=70.4-82%.

In conclusion, as a result of this research, we could prove the limitations of using animal fats mixed in a mass proportion of up to 30% for boilers with low thermal powers. The conclusions drawn lead to the hypothesis of the possibility of the successful use of this fuel in high power thermal plants as well.

Acknowledgements

This work was supported by a grant of the Romanian National Authority For Scientific Research CNCS – UEFISCDI, project ID PN-II-PT-PCCA-2013-4-1017, "Green Tannery – Methods for Energetic Recovery of Biodegradable Wastes"

References

[1] Mihăescu L., Pănoiu N., Totolo Cr. „Arzătoare turbionare", Ed. Tehnică, Bucureşti, 1986

[2] Mihăescu, L., „Arzătoare pentru hidrocarburi cu NO_x scăzut", Ed. Printech, Bucureşti 2004, ISBN 973-718-039-9

[3] E. Pop, L. Mihaescu, Gh. Lazaroiu, I. Pisa, G. Negreanu, *„Energetic characteristics of animal fats from tannery for energy production"* 4th International Conference on Thermal Equipment Renewable Energy and Rural Development TE-RE-ED 2015, Posada Vidraru 4-6 iunie 2015, Editura Politehnica Press, ISSN 2359-7941, pp 475-478

[4] Nicolici A., Lăzăroiu Gh., Pană C., Negurescu N., Cernat Al., Nuţu C, Mocanu M „*On animal fat use at diesel engine*", 5th International Conference on Thermal Equipment, Renewable Energy and Rural Development, TE-RE-RD 2016 Proceeding, ISSN: 2359-7941, ISSN-L:2457-3302, , Golden Sands, 2-4 June 2016, Bulgaria, pp 483- 488

[5] Lemneanu N, Cristea E., Jianu C. *Instalatii de ardere cu combustibili lichizi*, Editura Tehnica, Bucuresti, 1982.

STACK EFFECT IN HIGH-RISE BUILDINGS – IMPORTANCE OF THE CURTAIN WALLING, WINDOWS AND DOORSETS AIRTIGHTNESS FOR THE BUILDING PERFORMANCE

Mijorski S.[1], Ivanov M.[2]
[1] PhD, SoftSim Consult Ltd., Consultant at Technical University of Sofia, FPEPM, Department: "Hydroaerodynamics and Hydraulic Machines", Sofia 1000, Bulgaria
[2] Senior Assist. Professor, PhD, Technical University of Sofia, FPEPM, Department: "Hydroaerodynamics and Hydraulic Machines", Sofia 1000, Bulgaria

ABSTRACT

This paper presents a review of the stack effect phenomenon in high-rise buildings and the associated implications related to the façade curtain walling, windows and doorsets airtightness quality. A 150 m tall office building was numerically modelled with two different classification grades of the construction elements as specified in the European Standards EN 12152 and EN 12207. The analysis was performed under both winter and summer weather conditions (0.4 % of the time exceeded), specified in ASHRAE Handbook - Fundamentals. The numerical results have demonstrated the importance of the construction elements' airtightness properties to the overall building performance. For both winter and summer conditions, the infiltrations in the building have been reduced with 21% by improving the façade airtightness quality from Grade 1 to Grade 2. At the same time, it was observed an up to 35% decrease of the differential pressures at the interior doors.

1. INTRODUCTION

The need for high-rise building development has increased significantly through the recent years. The growing population, the continues globalization – forcing more and more people to flow in the big cities, and the lack of free city centers' land are the main reasons for that. Nevertheless, the high-rise buildings are associated with certain requirements and recommendations to avoid unwanted physical effects as described in *Simmonds P. and Zhu R (2013)*. One of the most common is the stack effect phenomenon, which is a buoyancy-driven and typically occurs in regions with extreme climatic conditions. The main driving force behind the stack effect is the temperature difference between the interior of the buildings and the outside environment, with addition of certain impact of the wind pressure acting on the external envelope. Detailed schematic description of the stack effect process is given in Fig.1.

Thus, for the ***classical stack effect*** under extreme winter conditions, the warmer indoor air rises due to buoyancy forces, creating a pressure difference between bottom and the top of the building. As high the building is, as bigger the total differential pressure is. The process tries to draw air in at the lower building level and pushes air out at the top. To close the cycle, the cold air that has been drawn in, is then heated up by the building services and thermal mass. Additionally, the wind pressure also could have non-negligible impact over the building performance, by increasing or decreasing the differential pressure at the façade construction elements. Depending on the building scheme, height and massing of adjacent developments, the lower and upper levels are subjected to rather different wind pressures, impacting the infiltration and exfiltration through the building envelope. Positive external wind pressures have the ability of enhancing infiltration and counteracting exfiltration, while the negative

[2]Sofia 1000, Bulgaria, "Kliment Ohridski" Blvd. #8, Technical University – Sofia, +359898240221, m_ivanov@tu-sofia.bg

external wind pressures have the ability of enhancing exfiltration and counteracting infiltration (see Fig.1b).

The reversed process could occur in extreme hot regions. In such case, relatively cooler indoor air tends to precipitate due to higher density, creating a pressure build-up at the lower building level. This way, the air is pushed out and drawn at the upper levels. Again, the process is closed by the building services and thermal mass, which cool the introduced warmer air that has been drawn at the top. The process is called ***reverse stack effect***, as shown in Fig.1c.

The design challenges associated with stack effect phenomenon varies from reduced building performance (energy losses), reduction in comfort levels (due to excessive draught and noise levels), health related issues (due to infiltration of no treated air with outdoor pollutants) and to pure mechanical issues related to the elevator and pedestrian doorsets' operation. A detailed review of the stack effect related issue is presented in the work of *Mijorski and Cammelli (2016).*

All these issues could be mitigated with on-time design decisions. By performing numerical simulations, as part of the integrated design process, several mitigation and preventive measures can be proposed. Such as:

- Taking right decision for the façade, windows and doorsets airtightness specifications;
- Adjusting the HVAC systems operation (increasing or decreasing the pressurization levels at different building zones); and
- Introduction of vertical and horizontal building separations.

Other preventive measures are well presented in the work *of Jo et al. (2007)* and *Mijorski and Cammelli (2016).*

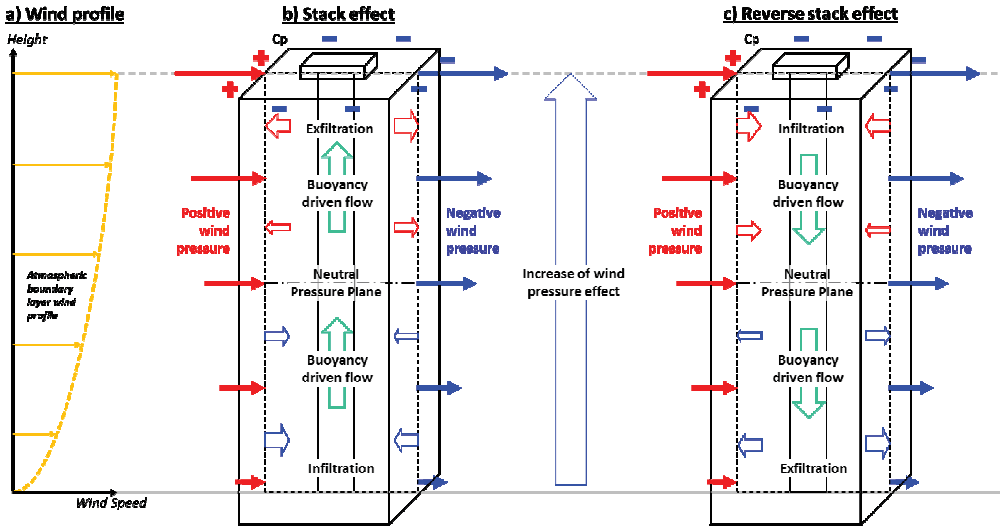

Figure 1: Stack effect diagram: a) Wind profile; b) Stack effect; c) Reverse stack effect.

The aim of the study, described in this paper, is to provide a quantitative numerical assessment over the impact of the façade curtain walling, windows and doorsets airtightness, related with the airflow through a typical office building envelope. In other words, the global purpose is to demonstrate the importance of on-time design decisions and preventing measures, regarding the building construction, partitioning and envelope material quality.

2. BUILDING CONFIGURATION AND SPECIFICATION

For the purposes of the numerical study, a 37-storey / 150 m tall office building of rectangular floor plan was modelled (see Fig.2) in the mild continental climate of Sofia,

Bulgaria. The climate at the site is characterized with relative extreme winter and summer conditions, as specified in *ASHRAE Handbook - Fundamentals (Design Conditions, 2013).* For time exceedance probability of 0.4 %, the winter is characterized with low winds of just 1 m/s (at 10 m height and wind approaching from West) and ambient temperature drops to -12.4 ^{o}C. While for the summer season, the temperature rises to 32.8 ^{o}C and the winds increase to 2.8 m/s, again approaching from West. The approaching winds are demarcated according the typical level layout given in Fig.2.

For accounting the effect of atmospheric boundary layer over the wind profiles, the design wind speed should be recalculated at roof top height. This was completed by assuming an urban terrain for the city of Sofia. Thus, the roof top speed V_H was calculated to 2.4 m/s for winter conditions, and for summer - to 6.7 m/s. Whilst, the magnitude and the distribution of the external mean wind pressures over the building envelope were calculated following *Eurocode EN 1991-1-4 (2005).*

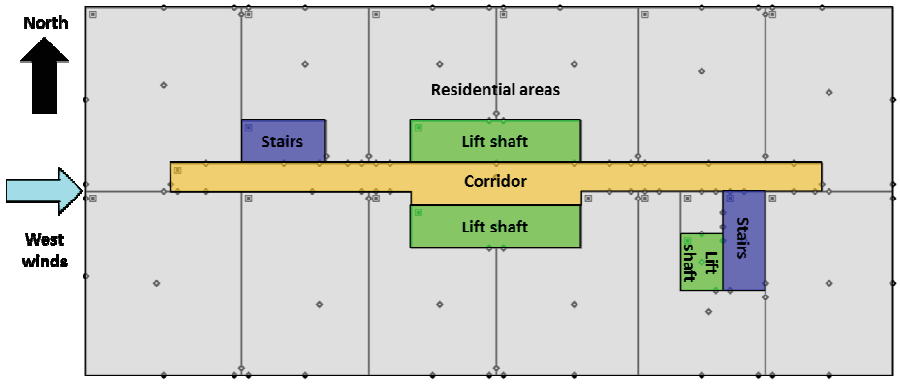

Figure 2: ContamW model – typical level layout and approaching winds.

Two different grades of building envelope elements were selected from *Eurocode EN EN12207 (2014)* for the purposes of the comparative assessment. For all the exterior windows and pedestrian doorsets Grade 1 and Grade 2 were selected. While for all the internal doorsets were defined with fixed grades from A, B and D for all simulated scenarios (see Table 1). At the same time, the lift doors were specified with a uniform door-to-frame gap size of 0.005 m and thickness of 0.05 m. Details for the specified air leakage properties are given in Table 1.

Table 1: Façade, windows and doorsets specifications

Construction element type	Grade	Leakage	Scenarios
Façade curtain walling	A1	1.5 $m^3/m^2 \cdot h$ at 150 Pa	1 and 3
	A2	1.5 $m^3/m^2 \cdot h$ at 300 Pa	2 and 4
Operable exterior windows and doorsets	1	50 $m^3/m^2 \cdot h$ at 100 Pa	1 and 3
	2	27 $m^3/m^2 \cdot h$ at 100 Pa	2 and 4
Interior doorsets - office units	B	6.25 $m^3/m \cdot h$ at 100 Pa	All
Interior doorsets – stairwells	D	0.75 $m^3/m \cdot h$ at 100 Pa	All
Other interior doors	A	12.5 $m^3/m \cdot h$ at 100 Pa	All

The façade curtain walling systems is specified, based on the *Eurocode EN EN12152 (2012),* by selecting Grade A1 and Grade A2 for the comparative analyses (see Table 1). All internal walls and floor areas (shaft and partitioning) were classified as either low, medium or high air flow resistant elements following the specification in Table 2, derived from *ASHRAE Handbook – Fundamentals (2013).*

Heating, Ventilation and Air Conditioning (HVAC) systems were considered in operation at all building's levels by specifying design temperatures for each different type of space, as given in Table 3. The air supplies and extractions were assumed to be in balance at each of the floors. Thus, the stack effect would not be effected by any pressurization and under-pressurization resulted of the HVAC operations, but just of the buoyancy and wind pressure forces. All the operational openings of the building were assumed to be closed with exception of the louvers located at building Mechanical / Electrical / Plumbing (MEP) levels 2, 20 and 30.

Table 2: Porosity levels of the internal walls and partitioning (*ASHRAE Handbook - Fundamentals, Chapter 16, Ventilation and Infiltration, Table 10, 2013*)

Wall type	**Total opening area per square meter**
High air flow resistant walls	0.14×10^{-4} m/m
Medium air flow resistant walls	0.11×10^{-3} m/m
High air flow resistant walls	0.35×10^{-3} m/m
Floors/ceilings	0.52×10^{-4} m/m

Table 3: Design temperatures of the building interior spaces

Space type	**Winter conditions**	**Summer conditions**
Office areas	21ºC	24ºC
Corridors & MEP zones	20ºC	26ºC
Lift and stairwell shafts	5ºC	28ºC

3. NUMERICAL MODELLING AND RESULTS

For the purposes of the study, a computer program ContamW 3.2 was utilized. This is a multi-zone airflow and contaminant transport analysis software developed by the National Institute of Standards and Technology at the United States of America (NIST, https://www.nist.gov/). A detailed review of the ContamW validation is presented in *Emmerich (2001)*. The constructed zone model included all office areas, corridors, vestibules, lift shafts, stairwells and other spaces. It has incorporated detailed representations of the airtightness of the building external envelope, internal partitioning, door and window elements with different types of mathematical models.

The windows, internal/external doorsets and façade curtain walling were modelled through a power law based on a single test data point at specified differential pressure (see Table 1) and a flow exponential of 0.67. The floors, interior walls and partitioning were modelled through a power law based on a given leakage area (given in Table 2) at a differential pressure of 75 Pa, a flow exponential of 0.65 and a discharge coefficient of 0.6. While, the lift doors were represented by quadratic model calculating the volume flow rate at different pressures as given by *Baker et al. (1987)*. Stairwells were modelled through a power law based on flow resistance, fitted to an experimental data provided in the work of *Achakji and Tamura (1988)*. Finally, the lift shafts modelled with power law based on a flow resistance calculation, is performed according to the friction model of Darcy-Weisbach and the friction factors equation of Colebrook given in *ASHRAE Handbook - Fundamentals ("Chapter 21 – Duct Design", 2013)*. Details of theoretical background and all the available mathematical models pertaining to different types of flow paths can be found in *Dols and Polidoro (2015)*.

Table 4: Scenario matrix

Case name	Ambient conditions	Façade curtain walling	Exterior windows and doorsets
Winter – Grade 1	Winter, -12.4 ºC, 1 m/s West winds	Grade A1	Grade 1
Winter – Grade 2	Winter, -12.4 ºC, 1 m/s West winds	Grade A2	Grade 2
Summer –Grade 1	Summer, 32.8 ºC, 2.8 m/s West winds	Grade A1	Grade 1
Summer –Grade 2	Summer, 32.8 ºC, 2.8 m/s West winds	Grade A2	Grade 2

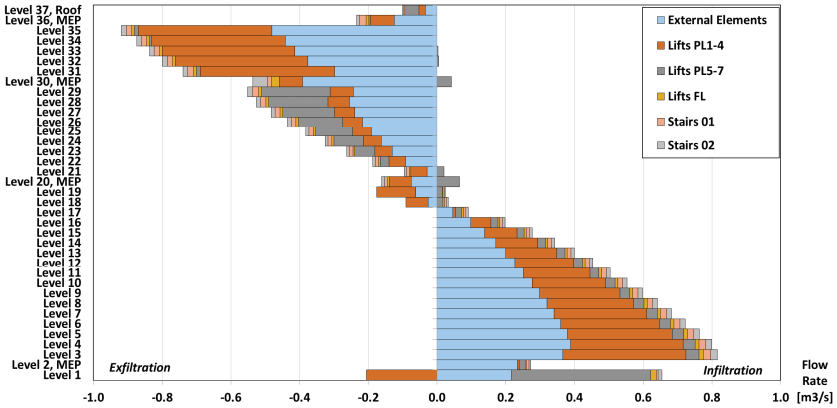

Figure 3: Air flow through different building zones.

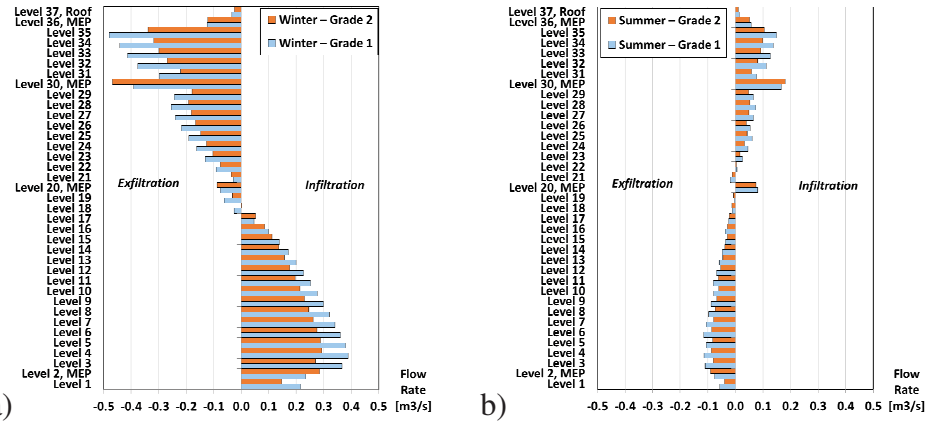

Figure 4: Façade infiltration and exfiltration: a) Winter conditions; b) Summer conditions.

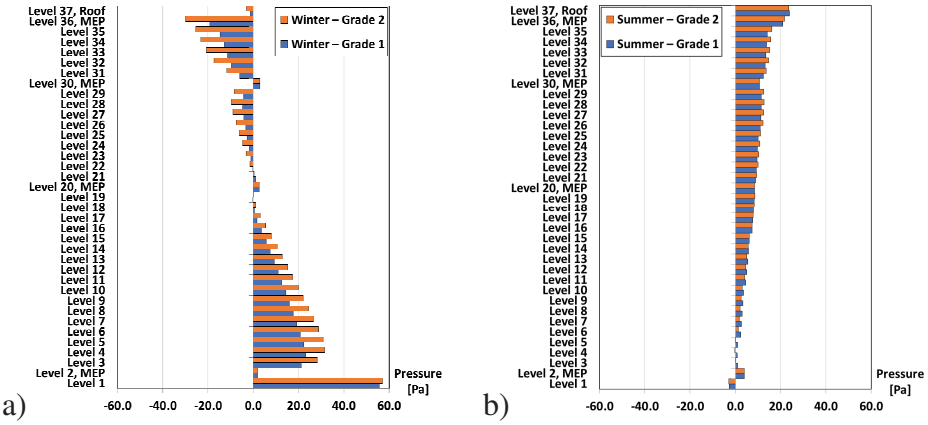

Figure 5: Façade maximum pressure differential: a) Winter conditions; b) Summer conditions.

In the presented study, a total of four cases were modelled, two for winter and two for summer conditions. The comparative analyses were completed for two different façades, external windows and pedestrian doorsets grades, as shown in Table 4.

The numerical results are presented in form of stack charts for the total air flow rates for each of the building levels, describing correspondingly the infiltration and exfiltration through different building zones (whole exterior envelope, individual lift and stairwell shafts). Fig. 3 shows the results of worst case scenario, the Winter – Grade 1, illustrating the resulted air flow through building envelope and core zones. Whilst, in Fig.4 and Fig.5 are given the comparative charts only for the exterior envelope infiltration, correspondingly between Winter – Grade 1 and 2 and between Summer – Grade 1 and 2.

4. ANALYSES AND CONCLUSIONS

The numerical results demonstrate clearly the importance of the construction elements' airtightness properties to the overall building performance. For both winter and summer conditions, the infiltration in the building have been reduced with 21% by changing the façade quality from Grade 1 to Grade 2 (see Fig. 4 and Fig.5). Also, the façade curtain walling, windows and pedestrian doorset improvements resulted in decrease of the interior doors differential pressure, reaching up 35% reduction compared to the derived values in Case 1.

Leakier façade causes more air flow through building interior elements, thus exposing the doors of the cores shafts (lifts and stairwells) to high differential pressure, reaching maximum for internal doors of 33 Pa and 56 Pa for the doors exposed to ambient environment. By increasing the air flow through the building envelope and core zones, the differential pressure can easily exceed the operational threshold of 70 Pa for manually operated doors, thus obstructing the normal access at the lobby areas, premises, stairwells and lift cars. In addition, the excessive infiltration of the exterior air leads to corresponding reduction of the mechanical system performance and effectiveness, together with reduction of indoor air quality. For winter conditions, there is a high risk for suction of polluted outdoor air from road traffic or the sewerage cannels and shafts. Thus, the main benefits of improving building envelope airtightness are in attaining better air quality, higher comfort in the indoor environment and energy savings from MEP systems operation.

References

[1] Achakji G. & Tamura G., *Pressure Drop Characteristics of Typical Stairshafts in High Rise Buildings*. ASHRAE Transactions, 94(1), 1223-1236, 1988;

[2] *ASHRAE Handbook – Fundamentals 2013*, ASHRAE, 2013;

[3] Baker P., Sharples S. & Ward. I., *Air Flow through Cracks*, Building and Environment, 22, 293-304, 1987;

[4] Dols S. & Polidoro B., *CONTAM User Guide and Program Documentation*, NIST Technical Note 1887, Version 3.2n, 2015;

[5] Emmerich S., *Validation of Multizone IAQ Modeling of Residential-Scale Buildings: A Review, National Institute of Standards and Technology*, Gaithersburg, MD. ASHRAE Transactions 2001, V. 107, Pt. 2., 2001;

[6] EN 12152: *Curtain walling-Air permeability-Performance requirements and Classification*, Eurocode, 2012;

[7] EN 12207: *Windows and doors-Air permeability–Classification*, Eurocode, 2014;

[8] EN 1991-1-4: *Action on structures – Part 1-4: General actions wind actions*, Eurocode, 2005;

[9] Jo J., Yeo M. & Kim K., *Effect of Building Design on Pressure-related Problems in High-rise Residential Buildings*, ARCC Spring Research Conference, Eugene, Oregon, USA, 2007;

[10] Mijorski S. & Cammelli S., *Stack Effect in High-Rise Buildings: A Review*, International Journal of High-Rise Buildings, Vol. 5, No 4, 327-338, 2016;

[11] Simmonds P. and Zhu R., *Stack Effect Guidelines for Tall, Mega Tall and Super Tall Buildings*, International Journal of High-Rise Buildings, Vol 2, No 4, 323-330, 2013.

CALCULATING THE EFFICIENCY OF THE ELECTROLYSERS FOR PRODUCTION OF OXYHYDROGEN

Ivaylo Nedelchev, Hristo Zhivomirov, Rosen Vasilev[1], Vyara Vasileva
Technical University of Varna

ABSTRACT

A lot of constructions are known for producing of oxyhydrogen mixture. During the oxy-redox reaction, there are physical factors that interact on this process. Thus the real production of gas is quite different from the theoretical calculated by the well-known Faraday's laws of electrolysis. This mainly depends on the construction of the electrolysers. Two main approaches exist for assessment the efficiency of the electrolysis – by Faradaic losses (Faraday's efficiency) and the overvoltage method (difference between theoretical and real reaction voltage). This paper compares these two approaches for estimating the efficiency in one of the most used construction of electrolysers via variation of its main constructive parameters.

1. DEFINITIONS OF THE EFFICIENCY OF THE ELECTROLITIC CELLS

A lot of constructions are known for producing of oxyhydrogen mixture. During the oxy-redox reaction, there are physical factors that interact the process of the electrolysis. Thus the real production of gas is quite different from the theoretical calculated. According Faraday's law of electrolysis, mass of produced gas mixture of oxyhydrogen can be found as [1,3]:

$$m_T = \frac{Q}{F}.\frac{M}{z} \quad , \tag{1}$$

were: m_T is mass of the materials released over the electrodes, Q is quantity of the electrical charge, used in the electrolysis, M is molar mass of the elements, z is valency number of the ions (electrons transferred per each ion), F is Faraday's constant ($F=96\ 485\ C/mol$). Using the produced mass in reaction m_R, Faraday's efficiency (EF), can be expressed as:

$$EF = \frac{m_R}{m_T}.100\% = \frac{m_R.z.F}{M.I.t}.100\% \quad , \tag{2}$$

were m_R is real mass production, I is current in the cell and t is duration of the reaction. Due to the recombination of the products, involving of some part of the charge-carriers in side reactions and forming by-products, EF is less than 100% [3].

According the Nernst equation [2,5], for pure water, the electrode potential for the reduction producing hydrogen is -0,41V and electrode potential for the oxidation producing oxygen is +0,82V. These potentials are defined according the temperature, number of electrons involved in the reaction and specific concentration of ions. Using direct current supply, the half-reaction of the electrolysis of water is [2,4]:

[1]Varna, Bulgaria Technical Univercity 1 Studentska str., phone number +35952 383 249 email: rsnvasilev@abv.bg

$$2H_2O(l) \rightarrow 2H_2(g) + O_2(g); U_0 = +1{,}229\ V \quad . \tag{3}$$

The real potential for driving reaction is quite different from theoretically calculated and the reaction actually doesn't start on the voltage shown in (1). Therefore the voltage U_r on each single gap between two electrodes, which can drive the reaction, is bigger than U_0. Differences between U_r and U_0 ($\Delta U = U_r - U_0$) is often called "overpotential" and shows, that for the start of the reaction is needed more energy than theoretically calculated, which express the losses in the electrolyser as a heat and side reactions. Calculation the efficiency by overpotential can be expressed as:

$$EV = \frac{E_L}{E_R}.100\% = \frac{\Delta U.I.t.}{U_r.I.t}.100\% = \frac{(U_r - U_0)}{U_r}.100\% \quad , \tag{4}$$

were E_L is energy of the losses, and E_R is the whole energy involved in the reaction.
The overpotetial depends on many complex factors. Most of them are connected with the current density and respectively construction of the electrolytic cell. The main factors, which affect the value of the U_r and therefore the *EV* are:

- activation energy for transferring the charge-carrier from the electrode to the electrolyte.
- reduction of the active surface from the gas bubbles and thus the increase of the current density;
- formation of unequal concentrations of the charge-carriers on the electrodes due to the restriction of the diffusion capabilities of the electrolyte;
- junction resistances in the electrical circuit and opportunities for inducting counter electromotive forces.

2. CONSTRUCTION OF THE TESTED ELECTROLYSER

For calculation efficiency (*EF* and *EV*), it was observed the most used construction of the so called "dry cell", which consists of pack of metal electrodes, electrically insolated with non-conducted separators [1]. Voltage from the direct current source is directly supplied on the lateral and the middle plate of the electrodes as shown on Figure 1.

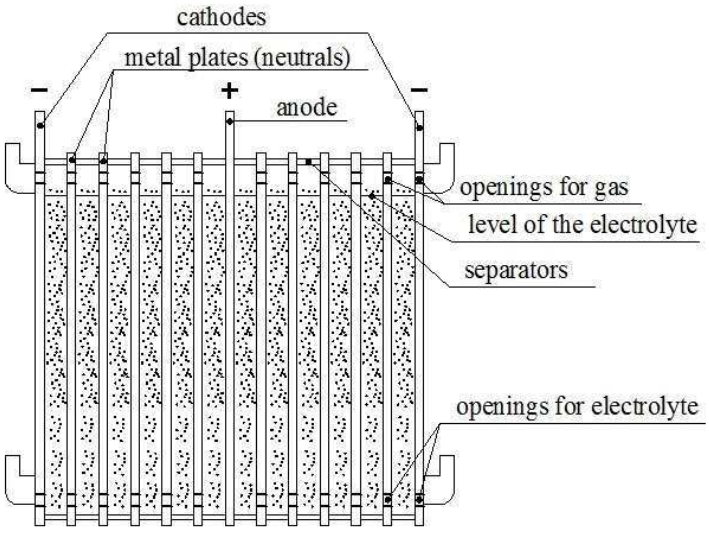

Figure 1: Construction of the tested electrolyser.

This construction forms thin separate cells which are connected in serial and filled with the electrolyte (water and potassium hydroxide). The equal distance between the metal plates and level of the electrolyte in each cell, ensure regular distribution of the potentials over the all plates. The products of the electrolysis are released from the small gap on the top of the electrodes. The main parameters of this type of construction are: number of the metal plates (neutrals) between anode and cathodes – n, distance between each both metal plates – d, material of the electrodes, which is stainless steel type 316L.

3. RESULTS

According to the numbers of the neutrals in the construction n and the applied voltage between anode and cathodes U_{AC}, drop of the voltage over each two metal plates (U_C) will be:

$$U_C = \frac{U_{AC}}{n+1} \quad . \tag{1}$$

It was tested constructions with 4, 5 and 6 numbers of neutrals and distances between them from 0,8 mm to 5 mm as shown in the Table 1.

Table 1: Experiment conditions

Number of neutrals [-]	4	5			6	
Distances between neutrals [mm]	2	0,8	2	5	2	5

Tables 2 - 4 show the efficiency calculated by the Faraday's and overvoltage method obtained by experiments of the electrolyser with 5 neutrals and distances between them from 0.8 mm to 5 mm. The produced oxyhydrogen are expressed as a flow rate (q). Figure 2 - 4 represent the graphic view of the results from Table 2 - 4.

Table 2: EV and EF for experiment conditions: n=5, d=0.8 mm.

I [A]	3.55	4.40	10.50	11.60	16.20
ΔU [V]	0.87	0.87	0.74	0.84	0.82
q [m^3/min].10^{-3}	0.198	0.256	0.269	0.333	0.790
EV [%]	58.57	58.57	62.54	59.52	60.00
EF [%]	47.72	49.77	23.41	24.97	42.69

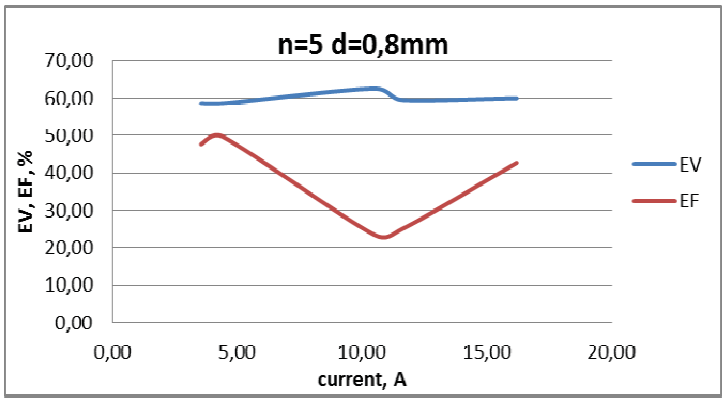

Figure 2: EV and EF vs. the current. For n=5, d=0.8 mm.

Table 3: EV and EF for experiment conditions: n=5, d=2 mm.

I [A]	2.26	5.00	7.40	8.40	10.20
ΔU [V]	0.74	0.84	0.90	0.97	0.99
q [m^3/min].10^{-3}	0.155	0.323	0.525	0.583	0.750
EV [%]	62.44	59.52	57.88	56.21	55.49
EF [%]	62.50	56.14	59.95	56.98	59.56

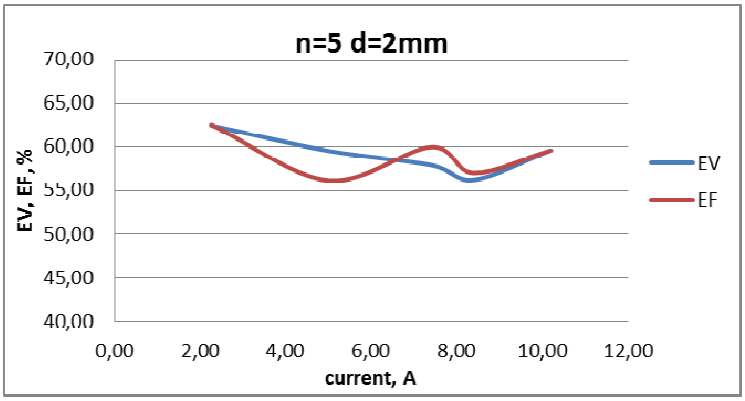

Figure 3: EV and EF vs. the current. For n=5, d=2 mm.

Table 4: EV and EF for experiment conditions: n=5, d=5 mm.

I [A]	1.50	2.34	10.45	11.20	12.44
ΔU [V]	0.75	0.78	1.25	1.15	1.14
q [m^3/min].10^{-3}	0.105	0.153	0.677	0.764	0.808
EV [%]	62.02	61.30	49,56	51.79	51.90
EF [%]	63.69	58.13	46.90	51.55	49.19

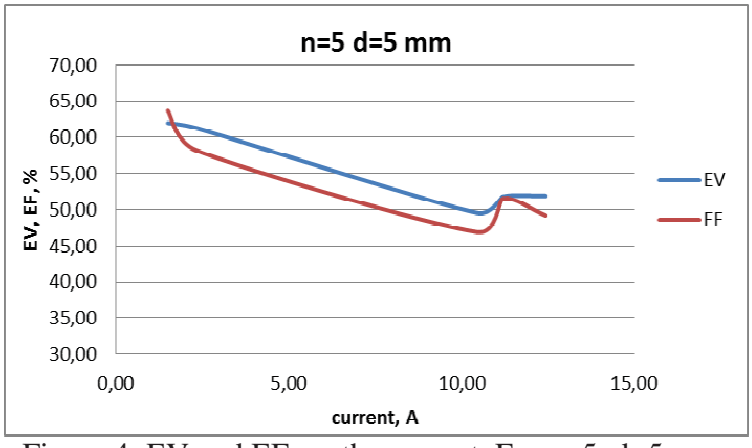

Figure 4: EV and EF vs. the current. For n=5, d=5 mm.

The received data show the main trend of decrease *EV* and *EF* when the current increase. This is in relation with the current density and the factors for affecting the overvoltage, mentioned above. At separation distance d = 0.8 mm, it was found a deep minimum of the EF, which is connected with the massive gas production and bigger influence of the surface tension of the bubbles. The bubbles can't be released easy from electrodes.

The experiment results for test conditions at n=4 and n=6 are shown on the Tables 5 - 7 and Figures 5 - 7.

Table 5: EV and EF for experiment conditions: n=4; d=2 mm.

I [A]	3.40	5.80	6.35	15.80
ΔU [V]	0.82	1.08	1.08	1.62
q [m^3/min].10^{-3}	0.185	0.313	0.356	0.807
EV [%]	60.00	53.25	53.25	43.16
EF [%]	56.95	50.41	52.28	38.65

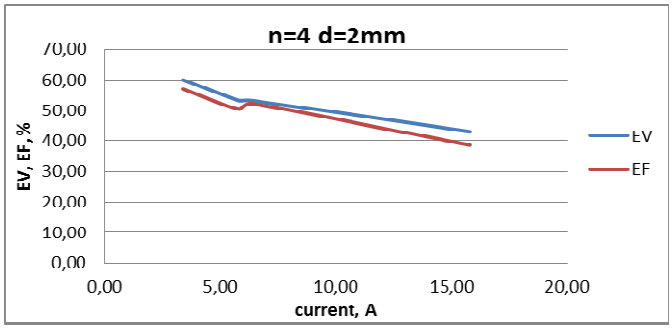

Figure 5: EV and EF vs. the current. For n=4, d=2 mm.

Table 6: EV and EF for experiment conditions: n=6; d=2 mm.

I [A]	1.90	4.90	5.50	7.60	9.78
ΔU [V]	0.54	0.88	1.04	0.93	0.33
q [m^3/min].10^{-3}	0.104	0.382	0.429	0.600	0.447
EV [%]	69.66	58.37	54.15	56.91	78.99
EF [%]	47.69	56.92	52.80	56.22	45.16

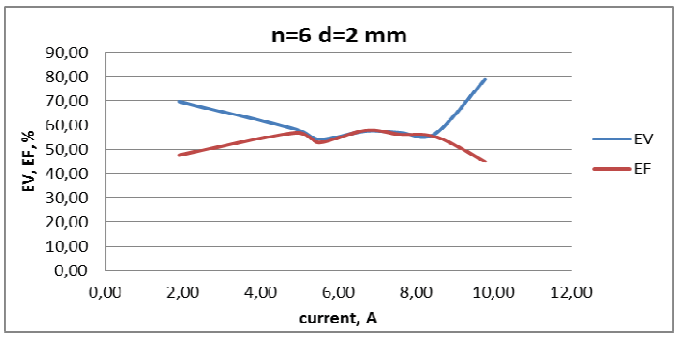

Figure 6: EV and EF vs. the current. For n=6, d=2 mm.

Table 7: EV and EF for experiment conditions: n=6; d=5 mm.

I [A]	1.43	1.73	3.76	5.10
ΔU [V]	0.78	0.73	0.86	1.01
q [m^3/min].10^{-3}	0.110	0.131	0.292	0.412
EV [%]	61.32	62.76	58.97	54.84
EF [%]	59.00	59.57	57.24	55.40

The represented data show dependences of the both efficiency parameters (*EV* and *EF*) on the number of the neutrals. It can be found that the decrease of *n,* makes the electrolyser more sensitive to the current changes. The more is *n* the less is the slope of the main trend of both efficiency diagrams. This is due to the fact that the bigger number of the neutral plates, distributes the current changes over more gaps and therefore its relative influence is smaller.

Usually *EV* is greater than *EF*. The minimums and maximums in the *EV* and *EF* curves show the predomination of the heterogeneous effects at the different current values.

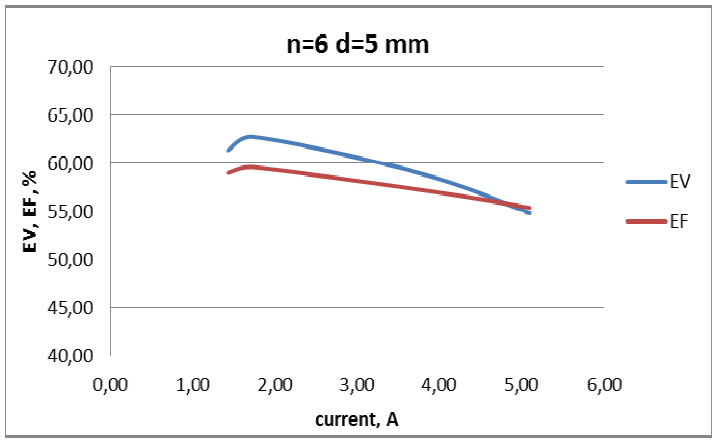

Figure 7: EV and EF vs. the current. For n=6, d=5 mm.

4. CONCLUSIONS

The paper shows comparison between two main approaches for efficiency calculation of the electrolytic cells for oxyhydrogen production. Experimentally was obtained the main dependences of the Faraday's efficiency and overvoltage efficiency of the cells on the main constructive parameters. The influence of some specific effects was shown practically during the electrolysis in the tested constructions.

References

[1] Vasilev R., Nedelchev I., Venkov V., Marinov A., *Examination Parameters of some basic Construction of the Brown gas Generators*, ICEST 2011.
[2] Bard, Allen J., Faulkner, Larry R., *Electrochemical Methods: Fundamentals and Applications*, Wiley 2001.
[3] Strong, F. C., *Faraday's Laws in One Equation,* Journal of Chemical Educatio, 1961.
[4] Wahl, *A Short History of Electrochemistry,* Galvanotechtnik, 2005.
[5] http://calistry.org/calculate/nernstEquation

ON COMBUSTION OF DIESEL FUEL- RAW ANIMAL FATS BLENDS AT DIESEL ENGINE

Adrian Nicolici, Constantin Pana, Niculae Negurescu, Alexandru Cernat[1]
University Politehnica of Bucharest

ABSTRACT

The general objective of the research is analyzes of the preheated gas oil- raw animal fat blends use at the experimental diesel engine, type CFR- IT9-3M. The engine was fuelled firstly with diesel fuel then with diesel fuel-animal fats raw state blends, the raw state animal fats content in blend with diesel fuel being 5%, 10% and 15%. The results of experimental investigations show the animal fats effects on the combustion parameters. At the raw animal fats content increase in mixture with diesel fuel, for same engine adjustments were obtained the follow results: auto ignition delay increases with ~20%; maximum in-cylinder pressure decreases with 10%; heat release rate decreases with ~23%. The animal fats effects on the fuel autoignition and combustion was established. Animal fats can be considered a viable alternative fuel for diesel engine, assuring the replace of the fossil fuels and resolving the major problem of animal wastes.

1. INTRODUCTION

The growing concerns for the depletion of the fossil fuel reserve in accordance with the limitation of emissions [1], [2], [3], greenhouse gases and raw materials availability leading to search for alternative solutions for fossil fuels used in internal combustion engines [3], [4], [5]. The growing concerns for the depletion of the fossil fuel reserve in accordance with the limitation of emissions, greenhouse gases and raw materials availability leading to search for alternative solutions for fossil fuels used in internal combustion engines. For this reason is looking for preferable non fossil origin fuel, renewable, vegetable oil and animal fat can be one of this fuels [1, 2, 3, 4]. The main animal fat advantages - cetane number and calorific value very close to diesel, higher oxygen content it recommend a good alternative fuel for diesel engines. But, the high viscosity and poor vaporization characteristics of animal fats need prior their heating and content limit in blend with diesel fuel. Being in the oxygentaed fuels category [2, 3, 5], animal fats have a composition similar to that of diesel but with a lower quantity of carbon and hydrogen and a higher oxygen content (oxygenated fuel) and biodiesel made it from animal fats is non toxic, sulphur free and lower caloric power slightly lower than diesel [2, 5]. The main problem of animal fats is high viscosity at poor volatility, but there are some methods who can resolve this problem: transesterification, use of blends between diesel fuel and biodiesel fuel, use of blends between biodiesel fuel and alcohol, use of emulsion with alcohol and water, preheating [3, 5]. One problem of biodiesel oils and animal fats is degradation due to oxidation if stored for a period of more then six months. The oxidation reaction is accelerated by exposure to a heat source [4, 5]. Preheating animal fats and blending with diesel is a simple, cheap and does not require engine modification. Animal fats and oils are lipid materials derived from animals products. Physically, oils are liquid at room temperature (20…25^{o}C), and fats are solid. Chemically, both fats and oils are composed of triglycerides [1, 2, 3, 5, 6, 7]. Animal fats are in more parts constituted from tryglicerides of saturated monocarboxylic fat acids with even number or carbon atoms (C12-C18) in which

[1]Blvd. Splaiul Independentei no. 313, +40723470021, cernatalex@yahoo.com

palmitic and stearic acids are predominant [3], [4], [5], [6], [7]. In a test on a agricultural tractor engine (single cylinder, water cooled, 1999 cm^3, power output of 34 kW at 2600 min^{-1}) three different animal fats biodiesel BD BD20, BD 50, BD100) were tested, the performance and the result of next parameters being compared: power output, fuel consumption rate, exhaust gases and particle materials [8]. The test cycle is composed by 3 different engine speeds and 3 different engine loads. As a results of tests at 2600 min^{-1} with a torque of 120 Nm and running time of 72 minutes the BD20 has the maximum power output (34.67 kW) followed by BD50 (34kW) and the last BD100 (32.93 kW). As a consumption rate the BD20 has the smallest consumption followed by the BD50 and BD100 [8]. The quantity of CO_2 is higher in case of BD20 and decreases in case of BD50 and later in case of BD100. The quantity of CO has the same decreasing trend like in case of CO_2 and it has the maximum value in case of BD20 and decreases in case of BD50 and BD100. The NO_x has the same decreasing trend from BD20 to BD100, the difference between BD20 and BD100 being ~15%. The same decreasing trend is registered for PM (Particulate Matter) being more pronounced from previous cases, the decreasing being even over 50% between BD20 and BD100 [8]. At the use of a higher BD (like 100), the emissions of CO, CO_2, NO_x and PM decreases more considerable, the output power is diminished slightly and the consumption increases [8]. Studies carried on an air cooled diesel engine (Lister Petter LS1 model) with direct injection fuelled with diesel fuel and animal fat at ambient temperature, or with the same animal fat preheated to 70°C, and in blending with ethanol and methanol or in emulsions with water show significant influences on combustion process [6, 9]. The in-cylinder maximum pressure recorded the highest values at diesel fuelling, the lowest values being registered for emulsion methanol-animal fats use and for only animal fat use [6, 9]. Animal fats use leads to the increase of the combustion duration comparative to diesel fuelling. This increase appears because large quantities of fuel are injected in order to compensate the lower heating value of animal fats. Because of poor atomization and vaporization of animal fats the physical component of ignition delay increases leading to the increase of ignition delay duration comparative to diesel fuelling [6, 9]. Higher ignition delays are registered also for animal fats-methanol/ethanol emulsions use versus diesel fuel. This influence appears because the value of the latent heat of vaporization of water and methanol/ethanol emulsion is high [6, 9]. Comparative to diesel fuelling the use of animal fats at low temperatures leads to the increase of auto-ignition delay and combustion duration [6, 9]. Due to the fact that is situated in the oxygenated fuels category, [1, 2, 3, 5] animal fats can be a good alternative for diesel engine, in terms of low levels of pollutant emissions (especially for smoke, NO_x and CO_2). The general objective of the research is analyzes of the preheated gas oil-raw animal fat blends use at the CFR- IT9-3M diesel engine. For diesel fuel and gas oil-raw animal fats blends fuelling, the main combustion parameters are analyzed.

2. METHODOLOGY

Preparation of blends between animal fats in raw state and diesel fuel implies the heating of both fuels at over 40°C. At this temperature the raw animal fats are in liquid state and becomes perfect soluble in diesel fuel. The engine is fuelled firstly with gas oil then with different gas oil-raw animal fat blends (x_c=5%, 10% and 15% raw animal fats energetic content in blend with diesel fuel). For each sample were determined/recorded the autoignition delay, pressures and heat release diagrams, for 100 consecutive cycles. The fuel cyclic dose was maintained constant to 28.9 [mm^3/cycle] for all experimental determinations. The experimental investigations results show the raw animal fat effects on autoignition delay, on the combustion parameters (maximum pressure, combustion duration, maximum pressure rise rate, combustion laws and heat release rates characteristics). For same engine adjustments, at

diesel fuel-raw animal fats blends fuelling were obtained the increase of autoignition delay with ~20% and the decrease of maximum pressure with 10%.

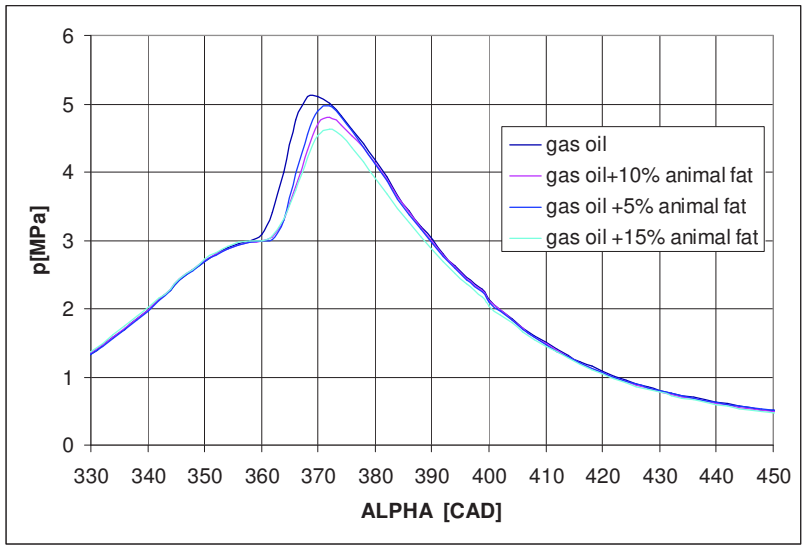

Figure 1: Pressure diagrams

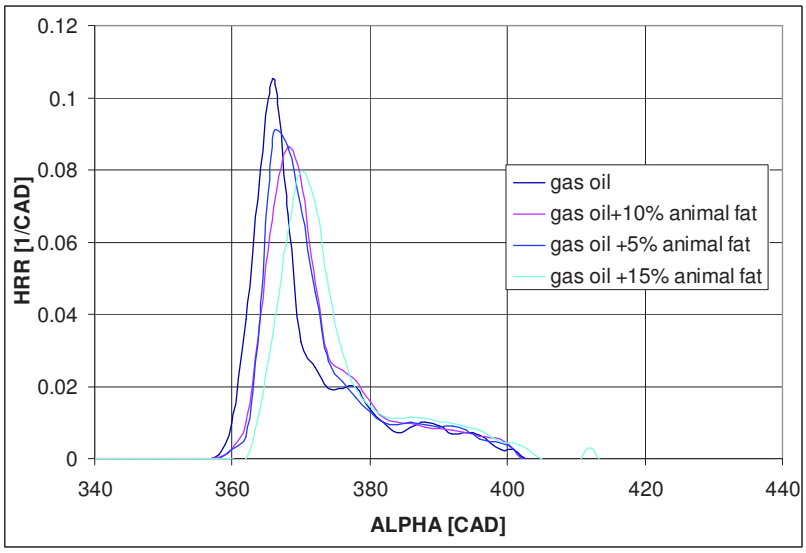

Figure 2: Heat release rate for diesel fuel and diesel fuel-raw animal fats blends

The pressures diagrams registered for the engine fuelled with diesel fuel first and then fuelled with blends of diesel fuel and animal fats in raw state, for the same injection timing value (13 CAD) and for same compression ratio (13.74) are presented in figure 2. The in-cylinder pressure diagrams were obtained by averaging of 100 consecutive cycles. The maximum pressure decreases with the increasing of the fats content, figure 1. At raw animal fats use the maximum heat release rate decreases, figure 2, the autoignition delay duration increases, figure 3, with the increasing of the fats content. The autoignition delay increases from 2.4 [ms] at diesel fuelling to 2.6 [ms] at x_c=5%, 2.7 [ms] at x_c=10% and 2.9 [ms] at x_c=15%. The aggravation of the atomization process because of the animal fats higher viscosity (drops of more large diameter are formed) leads to the reduction of preformed mixture quantity. This issue leads to the increasing of autoignition delay, with 20% at x_c=15%, comparative to classic engine at the rise of animal fats content in blends with diesel fuel. Because the quantity of preformed mixture is lower at engine operating with diesel fuel-

raw state animal fats blends, the diffusive combustion weight increases, fact that leads to the reduction of the maximum heat release rate at the beginning of combustion, figure 2. Because of autoignition delay increasing the combustion is moved into expansion area, at more large volumes, (for constant spark timing), which leads to the slightly decreasing of maximum pressure, figure 1 and to maintaining practically unchanged of the maximum pressure rise rate. This fact is influenced by the reduction of the cycle heat release at the increases of animal fats content, knowing that animal fats have a much lower calorific power comparative to diesel fuel (fuel cyclic dose was constant). The also taking into consideration the calorific power reductions of the used blends and the aggravation of fuel atomization at the increases of animal fats content in blends lead to combustion deterioration and cycle heat release quantity reduction, figure 2.

3. CONCLUSIONS

The paper brings an important contribution in the knowledge field of animal fats use in raw state in blends with diesel fuel at diesel engine fuelling. As a research originality is the establishing of the raw animal fats effects on the fuel auto ignition and combustion. For same engine adjustments, at diesel fuel-animal fats blends fuelling were obtained the increase of auto ignition delay with ~20%, the decrease of maximum heat release rate with 23% and the decrease of maximum pressure with 10%. For this regime, an optimal correlation between animal fats content in blend with gas-oil - injection timing - NO_x emissions level - smoke emission level – in-cylinder maximum pressure was established. Animal fats use can solve the pollution problems in large urban and agriculture areas, the fuelling solution can being easily to implement on all types of diesel engines (including old design models which can be converted to fit the current rules of pollution). Blends of diesel fuel and animal fats in raw state can be considered a viable alternative fuel for diesel engine, assuring the replace of the fossil fuels and resolving the major problem of animal wastes.

Acknowledgements

The authors would like to address special thanks to the AVL GmbH Graz Austria for providing the necessary equipments.

References

[1] Mormino, I., Verhelst, S., Sierens, R., Christian, V., Meulenaer, S., et. al., "*Using Vegetables Oils and Animal Fats in Diesel Engine: Chemical analyses and engine tests",* http://papers.sae.org/2009-01-0493, 2009.
[2] Venkatraman, M., Devaradjane, G., "*Effect of Compression ratio, Injection Timing and Injection Pressure on a DI Diesel engine for better performance and emission fueled with diesel-diesel biodiesel blends*", International Journal of Applied Engineering Research, Dinigul , vol. 1 , no 3 , 2010.
[3] Cernat, A., Pana, C., Negurescu, N., Nutu, C., "*The Animal Fats Use as Fuel at Diesel Engine",* http://www.spms.pub.ro/TanGreen, 2015.
[4]EMA Truck and Engine Manufacturers Association, *Use of Raw Vegetable/Plant Oil or Animal Fats in Compression-Ignition Engines*, 2012, http://www.truckandenginemanufacturers.org.
[5] Popa, M., G., Negurescu, N., Pana, C., *Diesel Engines. Processes*, Vol I ,II, Matrix Rom, Bucharest, 2003.
[6] Senthil Kumar, M., Kerihuel, A., et. al., "*A Comparative Study of Different Methods of Using Animal Fat as a Fuel in a Compression Ignition Engine"*, Journal of Engineering of Gas Turbines and Power, vol. 128, 2006.
[7] International Journal of Emerging Technology and Advanced Engineering Website: www.ijetae.com, ISSN 2250-2459, volume 2, issue 10, 2012.
[8] Youngjung K., Siyoung L., Jonggoo K., Donghyeon K., Honggi C., "*Testing of Agricultural Tractor Engine using Animal-fats Biodiesel as Fuel"*, Energy & Environmental Division, Department of Agricultural Engineering, National Academy of Agricultural Science, Rural Development Administration, Suwon, Republic of Korea, 2013. https://www.e-sciencecentral.org/upload/jbe/pdf/ksam-38-208.pdf.
[9] Kerihuel, A., Kumar, M., S., Bellettre, J., Tazerout, M., *"Investigations on a CI Engine Using Animal Fat and Its Emulsions with Water and Methanol as Fuel",* SAE International, Paper Number 05P-95, 1995.

LIQUEFIED PETROLEUM GAS FUELING OF A TRUCK DIESEL ENGINE – AN EXPERIMENTAL APPROACH

Nikolaos Cristian Nutu[1], Constantin Pana[2], Niculae Negurescu[2], Alexandru Cernat[2]
[1]Rutier Vehicles Department, University Politehnica of Bucharest, Romania
[2]Thermotechnics, Thermal Engines and Equipments, Refrigeration Instalations, University Politehnica of Bucharest, Romania

ABSTRACT

This paper presents experimental investigations of a truck diesel engine fuelled with liquefied petroleum gas. The fuelling method used was the diesel-gas method, which consist in LPG injection (in gaseous aggregation state) in the engine's intake manifold. Fuelling with LPG a diesel engine is a viable solution as far as the price and infrastructure are concerned and because of its good burning properties has a great potential to improve energetically and pollution performances of the engine.

The test bed situated in the Thermotechnics, Engines, Thermal Equipments and Refrigeration Installations Department was adapted to be fuelled with liquefied petroleum gas. The engine used is a turbocharged truck diesel engine with a 10.34 dm^3 displacement. The investigated working regimens were 40% load and 1450 rpm and 55% load and 1450 rpm , and the energetic substitute ratios of the diesel fuel with LPG was situated between [0-24.94%] for 40% load regimen and between [0-30.37%] for 55% load regimen.

1. INTRODUCTION

Liquefied petroleum gas is a fuel which generally consist of a mixture of two hydrocarbons, propane and butane, in different ratios depending on season and producing company. Because of its good burning properties and because of the price liquefied petroleum gas is a very good alternative fuel for the compression ignition engines.

In the table 1 are presented some liquefied petroleum gas properties, compared with the diesel fuel properties.

Table 1. Liquefied petroleum gas properties, comparative with diesel fuel properties [1].

Properties	Diesel fuel	Propane	Butane
Density [kg/m³]	800-840	503	500
Self ignition [ºC]	355	481	544
Stoichiometric A/F ratio [kg/kg]	15	15.71	15.49
Lowe r heating value[MJ/kg]	42.5	46.34	45.55
Cetane number	40-55	-2	-2
Flame temperature	2054	1900	-

[1]phone: 0766911610; e-mail: cristi_cmt@yahoo.com

Because of a lower density of liquid LPG, the mass of the same volume of fuel is lower, 503 kg/m³ for LPG and 800-840 kg/m³ for diesel fuel [1], leading to a lower fuel autonomy for the vehicle fuelled with LPG.

LPG needs a lower quantity of heat to vaporise than diesel fuel 420 kJ/kg to 465 kJ/kg for diesel fuel [1], allowing to consume less local heat in the case of direct injection in the combustion chamber.

The LPG self ignition temperature is higher than the diesel fuel self ignition temperature, 481 ºC – propane, 544 ºC –butane, 355ºC diesel fuel [1] and this combined with a very low cetane number gives LPG very poor self ignition properties. Therefore fuelling a diesel engine with LPG requires the use of specific methods.

The flame temperature of LPG lower than the diesel fuel flame termperature leads to an important reduction in nitrogen oxides emissions level.

The higher LPG lower heating value ensures an increase in the amount of heat released during the combustion of fuel for the same fuel quantity.

Fuelling a diesel engine with LPG involves specific methodes. In this paper the authors chose the Diesel-Gas method, which consists of gaseous LPG injection in the intake manifold of the engine.

This method has been applied also by Tariq Miqdam in [2] with good results regarding the brake specific energetic consumption and pollutant emissions. In the paper [3] the author fuelled with LPG a diesel engine that equip a road vehicle using the diesel-gas method, experiments leading to a reduction in the operating price of the vehicle. Qi et. al. in the work [4] experimented the direct injection of a LPG-diesel fuel mixture with different proportions: 0, 10, 20, 30, 40 %, leading to a decrease in the pollutant emissions of the engine. In the work [5] the authors decreased the level of the nitrogen oxides emission fuelling the diesel engine with LPG but the level of unburned hydrocarbons increased. To reduce this emission a glow plug was used [5]. A decrease of emissions level was achieved by Pali Rosha et al. in [6] , by LPG fuelling a single cylinder diesel engine and using exhaust gas recirculation. The level of nitrogen oxides emissions and carbon dioxide emission decreased compared to standard diesel engine case, while emissions of unburned hydrocarbons and carbon monoxide increased, especially in the partial load regimens. In order to reduce these emissions the authors used a percentage of 16% recycled exhaust gas (for example at 60 % load the level of unburned hydrocarbons and carbon monoxide was reduced with 46.9 %, 27.4 % respectively). Another example of a liquefied petroleum gas diesel engine fuelling is presented in the paper [7] . The authors used liquefied petroleum gas injection into the intake manifold of the engine and rapeseed oil for the pilot injection. The maximum degree of substitution used of rapeseed oil with LPG was 60 %, where the engine cyclic variability was within acceptable limits. The level of unburned hydrocarbons and carbon monoxide emissions decreased but the level of nitrogen oxides emissions increased. To reduce the emission of nitrogen oxides authors used also the exhaust gas recirculation.

This paper presents results of experimental investigations carried out on a truck compression ignition engine fueled with liquefied petroleum gas using the diesel-gas method.

The engine is located in one of the test beds of the Department of Thermotechnics, Engines, Thermal Equipments and Refrigeration instalations .

2. EXPERIMENTAL STUDY

The experimental study was carried out on a compression ignition engine type Roman D2156 MTN 8, with 6 cylinders in line. The main specification and performances of the engine are presented in the table 2 [8].

The test bed consist of: the Roman D2156 MTN 8 diesel engine, Hofman eddy current dyno, AVL data aquisition system, Kistler piezoelectric pressure transducer, AVL Dicom 4000 gas analyser and opacimeter, Optimass masic fuel flow meter, Meriam volumic air flow meter, thermocouples and thermoresistences for temperature measuring, gravimetric system for diesel fuel consumption measuring, gas leak detector. All the equipments were calibrated prior to measurements. The investigated regimens were 40% load and 1450 rpm and 55% load and 1450 rpm. The Diesel-Gas method consists in gaseous LPG injection in the intake manifold of the engine. Therefore the homogeneous mixture of air-LPG is ignited by the flame which appears in the diesel fuel jet.

Table 2. Specifications and performances of the engine D 2156 MTN 8 [8].

Number of cylinders	6
Bore [mm]	121
Stroke [mm]	150
Displacement [L]	10.34
Compression ratio	17
Rated power [kW]	188
Maximum torque [Nm]	900
Admision type	turbocharged

First time was determined the reference, fuelling the engine only with diesel fuel, then the diesel fuel was partially substituted with liquefied petroleum gas, concerning to maintain the same engine power like in the standard case of fuelling with diesel fuel. Therefore, for each substitute ratio investigated, the diesel fuel cycle dose was reduced and the LPG cycle dose was increased. The energetic substitute ratio was calculated with the folowing relation:

$$x_c = \frac{m_{LPG} H_{i_{LPG}}}{m_{LPG} H_{i_{LPG}} + m_{dieselfuel} H_{i_{dieselfuel}}} \quad (1)$$

Where: m_{LPG}- the LPG dose;
$m_{dieselfuel}$-the diesel fuel dose;
H_i- the caloric heating value.

The investigated energetic substitute ratios of the diesel fuel with LPG was situated between [0-24.94]% for 40% load regimen and between [0-30.37] % for 55% load regimen.

In order to reduce the nitrogen oxides emission level for the 55% engine load regimen exhaust gases recirculation was used. The exhaust gas recirculation quantity is defined as a percentage occupied by the gases in the total amount of intake air admitted in the engine. The exhaust gas recirculation quantity was 2.34% form the total amount of air consumed by the engine.

3. RESULTS AND DISCUSIONS

The pressure inside the cylinder increased for all the substitution ratios of diesel with LPG investigated. This can be explained by the intensification of the burning process due to

the presence of LPG-air mixture in the combustion chamber. The figure 1 shows the measured in cylinder pressure for the investigated cases.

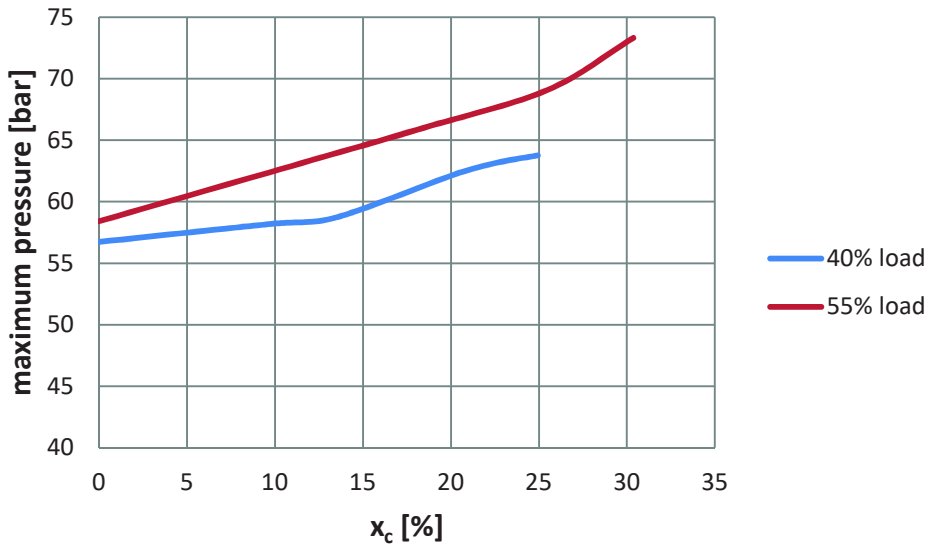

Fig. 1. The maximum pressure inside the cylinder versus the substitute ratio.

The maximum rate or pressure rise increased for all the investigated cases because of a higher flame speed in the homogeneous mixture or air-LPG. The figure 2 presents the maximum rate of pressure rise for the investigated cases.

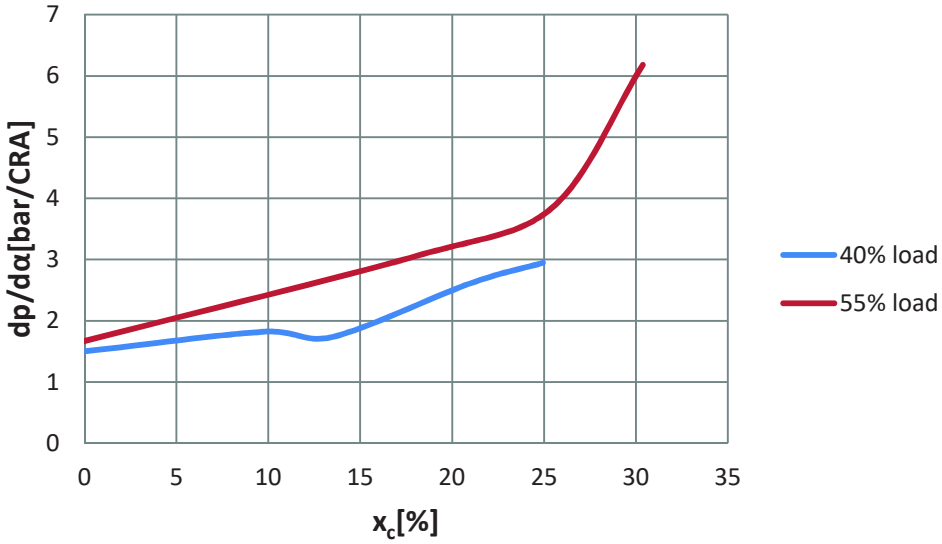

Fig. 2. The maximum rate of pressure rise versus the substitute ratio.

The nitrogen oxides emission level decreased for all the investigated substitute ratios of diesel fuel with LPG because the combustion temperature decreases when exhaust gas recirculation is used and because liquefied petroleum gas has a lower flame temperature than diesel fuel. The nitrogen oxides emission variation is presented in the figure 3.

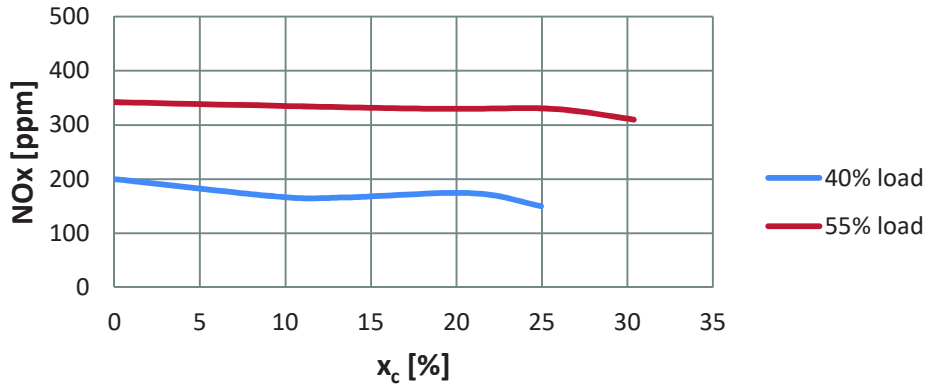

Fig. 3. The nitrogen oxides emission versus the substitute ratio.

The smoke emission level decreased for all the investigated substitute ratios of diesel fuel with LPG in the case of 55% engine load regimen because when LPG is present in the combustion chamber the burning rate of diffusive mixtures decreases and the burning rate of preformed mixtures increase. For the 40% engine load regimen the smoke emission level increased due to the lack of air (the engine load is low and the LPG is injected in the intake manifold and replace a part of air, in order to reduce the smoke emission for the 40% engine load regimen the supercharging pressure must be increased). The figure 4 presents the measured smoke emission level, evaluated by the coefficient of absorbtion k.

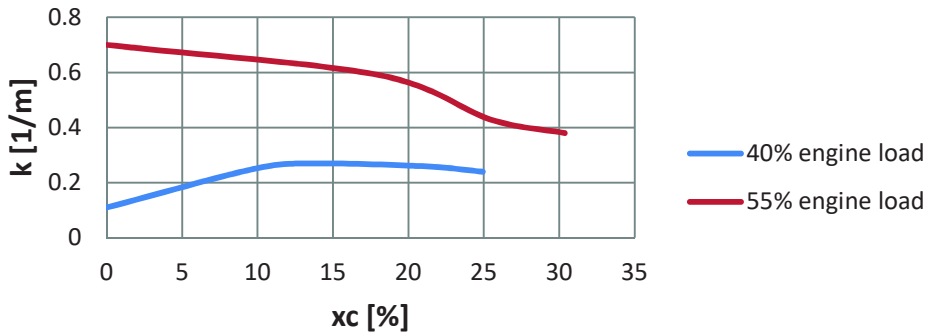

Fig. 4. The smoke emission level versus the substitute ratio.

The brake specific energetic consumption decreased for the substitute ratios of diesel fuel with LPG. Figure 5 presents the brake specific energetic consumption versus the substitute ratio.

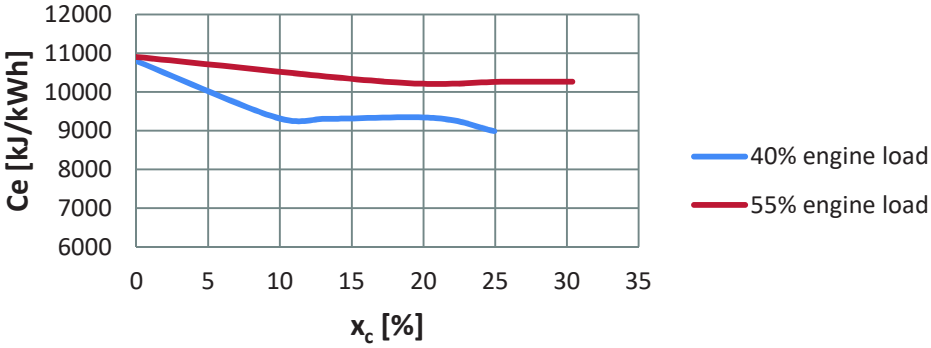

Fig. 5. The energetic specific fuel consumption versus the substitute ratio.

4. CONCLUSIONS

At the LPG engine fuelling were observed the following:

1. The brake specific energetic consumption decreased with ~20% when the substitute ratio was x_c=24.94 in the case of 40% engine load regimen and with ~6% when the substitute ratio was x_c=18.09 in the case of 55% engine load.
2. The nitrogen oxides emission decreased with ~25% for the substitute ratio x_c=24.94 (40% engine load), and ~9% for the substitute ratio x_c=30.37 (55% engine load).
3. The smoke emission level decreased in the case of 55% engine load regimen because when LPG is present in the combustion chamber the burning rate of diffusive mixtures decreases and increased in the case of 40% engine load because of the worsening of intake proces (to decrease this emission the supercharging pressure must be increased) .
4. The maximum pressure and the maximum rate of pressure rise increased in the case of LPG fuelling.

5. ACKNOWLEDGEMENTS

The authors would like to thank to AVL List GmbH Graz, Austria, for providing the possibility to use the research equipments.

6. REFERENCES

[1]. Popa, M. G., Negurescu, N., Pana, C., *Motoare Diesel*, Matrix ROM, Bucuresti 2003.
[2]. Miqdam, T., *Exhaust analysis and performance of a single cylinder diesel engine run on dual fuels mode*, Journal of Engineering, Nr. 4, Vol. 17, 2011.
[3]. Michal, J. et al, *Analysis of engine parameters at using diesel-lpg and diesel-cng mixture in compression-ignition engine*, Acta Universitatis Agriculturae Et Silviculturae Mendelianae Brunensis, vol. 62, nr. 1, 2014.
[4]. Qi, D. H., Bian, Y. Z., Ma, Z.Y., Zhang, C. H., Liu, S. Q., *Combustion and exhaust emission characteristics of a compression ignition engine using liquefied petroleum gas–diesel blended fuel*, Journal of Energy Conversion Management, vol. 48, no. 2, pp 500-509, 2007.
[5]. Vijayabalan, P., Nagarajan, G., Performance, *Emission and Combustion of LPG Diesel Dual Fuel Engine using Glow Plug*, Jordan Journal of Mechanical and Industrial Engineering, Volume 3, Number 2, June. 2009 ISSN 1995-6665 Pages 105 – 110.
[6]. Rosha, P., Bharj, R.S., Gill, K., *Performance and emission characteristics of Diesel+LPG dual fuel engine with exhaust gas recirculation*, International Journal of Science, Engineering and Technology Research (IJSETR), Volume 3, Issue 10, October 2014.
[7]. Tira, H.S, Herreros, J.M., Tsolakis, A., Wyszynski, M.L., *Characteristics of LPG-diesel dual fuelled engine operated with rapeseed methyl ester and gas-to-liquid diesel fuels*, Energy, Volume 47 (2012) 620-629.
[8]. Abăităncei, D., *Motoare pentru autovehicule si tractoare fabricate in Romania*, Alma, Craiova 2011.

SUPPRESSING THE FORMATION OF NITRIC OXIDE BY A SHIFT OF THE COMBUSTION PROCESSES AND ITS DECOMPOSITION BY COAL DUST

B. Ongar[1], V. Kamburova [2], A. Tuymebekova [1].

[1]Almaty University of Power Engineering and Telecommunications, Almaty, Kazakhstan
[2]Rousse University, Ruse, Bulgaria

ABSTRACT

The relevance of the effective organization of expansion-supply and reduction of nitrogen oxides of carbon to molecular nitrogen and gasification to carbon oxides are discussed in the paper. The experimental technique and equipment, calculated and experimental data on the rate and composition of the chemistry-reactions are also presented.
The results of the calculation and the development of the conceptual project for dust supplying Ekibastuz coal of high concentration with a shift of combustion processes Ekibastuz CHP to reduce nitrogen oxides in a reconstruction of the boiler are presented.

1. INTRODUCTION

The tendency to improve the environmental efficiency of the operation of boilers and the fullest use (burning) of fuel with minimum costs for repairs and maintenance of furnace-burner equipment makes it necessary to constantly improve the schemes and methods of burning fuels, and also to utilize various technological procedures (organization of flue gas recirculation, transfer to step-by-step burning, etc.). Specially, the issues of optimization are on pulverized coal boilers because of the gradual quality degradation of the used coals and their alteration into off-design form.

In this case, a twofold decrease in the concentration of nitrogen oxides in flue gases to 500-550 mg / Nm3 by creating a reducing zone of nitric oxide to molecular nitrogen by organizing incomplete combustion in the second tier and in each tier horizontally. It is noted that in order to reduce nitrogen oxides emission from 500-550 to 200 mg / m3, it is expedient to use their selective catalytic reduction with ammonia. After desulfurization at a temperature of 55°C, flue gases flow to an additional steam heater, where their temperature rises to 330-350°C, necessary for the catalytic reduction of nitrogen oxides. Indeed, 3500C is the necessary temperature level, and a sufficient temperature for the catalytic reduction of nitrogen oxides should be 4500C.

This clearly shows the urgency of solving the problem of suppressing the formation of nitrogen oxides. Reducing the temperature of huge flows of hot flue gases to 55°C, and then heating them to 350 / 450°C, catalytic reduction of nitrogen oxides to molecular nitrogen, a repeated reduction in temperature to the temperature of stack gases requires not only a perfect technical solution, but huge capital and operational costs. This is in unrealized theoretical form of solving the problem. From our point of view, what is already realized also considered wrong.

The fact is that during nitrogen oxide reduction to molecular nitrogen in the second stage of combustion with an excess coefficient of air less than one, the resulting carbon

monoxide, hydrogen, methane encourage occurring of 60 times more toxic than oxides of nitrogen and hydrogen sulfide, causing high-temperature corrosion of metals . Therefore, it is necessary to organize the burning of fuel with an excess air coefficient greater than one in order to prevent corrosion and slagging. In addition, in this specially created reduction zones of incomplete combustion, smoking and the formation of carcinogenic agents occur, which, as is known, are related to the first class of toxicity /the nitrogen oxides - to the second class of toxicity/.

Thus, the organization of step-by-step combustion of fuel, in our opinion, does not reduce the amount of harmful emissions to the environment, but complicates and makes less reliable the design and operation of the combustion chamber.

A closer technical solution is a vortex pulverized-coal burner containing annular channels of over-fire air and fuel-air mixtures, positioned into gap between the boilers, designed to reduce the diffusion of oxygen from the over-fire air during displacement with pulverized-coal into fuel-air mixture [1]. This method somewhat prolongs the combustion process and reduces the combustion temperature, which results in a slight suppression of thermal nitrogen oxides at a low level of the furnace burning temperature of pulverized-coal. As for the basic fuel constituents of oxides, their formation is not suppressed in this way, since the oxygen content in the underfire air is quite sufficient for the formation of nitric oxide.

When moisture is supplied to the hot air path by burning fuel oil [2], the suppression of nitrogen oxides is less than the localized phased additions of moisture into the combustion zone of the fuel with intense generation of nitrogen oxides.

The use of high-density pulverized coal (HDC) does not lead to a possible increase in the kinetic temperature of combustion, since the pulverized coal of HDC is diluted in the underfire air before being fed into the burner.

These demerits are characteristic for all existing pulverized-coal burners of various designs.

Therefore, the aim of this work is to increase the fuel combustion efficiency and suppress the nitrogen oxides formation.

On the axis of the burner device, which carries out the burning of solid fuel method, a central channel is installed for additions into the furnace a coal HDC, the gap is placed between the central channel and the channels for additions into the combustion chamber underfire and over-fire air, the gap thickness being equal to 1.5-1.9 equivalent Diameter of the central channel, and the discharge burner is installed above the burner device at a distance of 1.8-2.2 equivalent diameter of the burner device with the direction of its axis down at an angle to the plane of the furnace wall, equal to 65-75 degrees.

Figure 1 shows the vortex version of the proposed burner device, and in Figure 2 - a straight-flow version.

The vortex and straight-flow burner devices, shown in Figures 1 and 2, contain a underfire air channel 1, a over-fire air channel 2, a central channel 3 and a gap 4 between the central channel 3 and air channels 1 and 2.

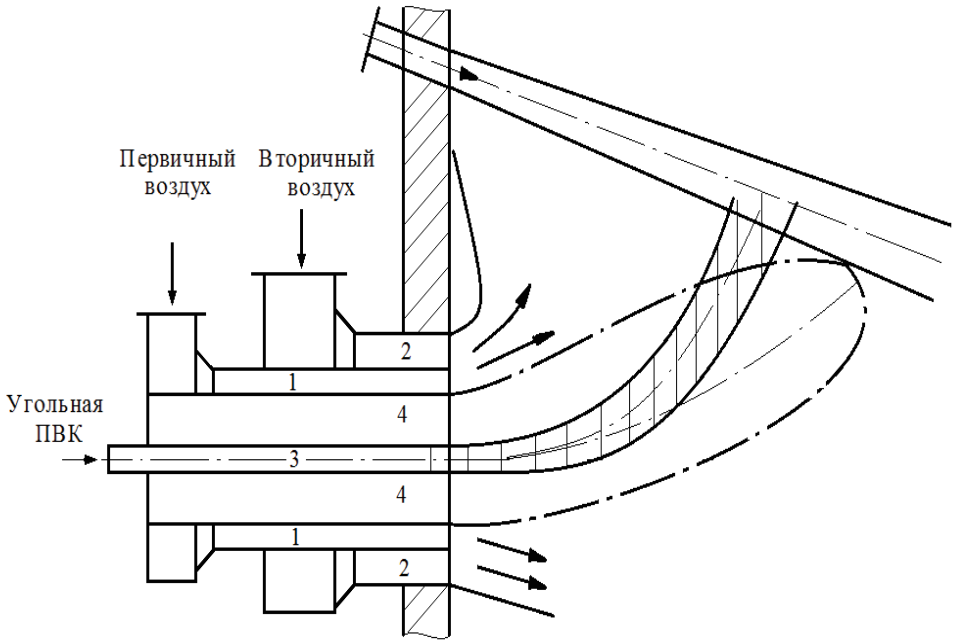

Figure 1- Vortex fuel burner.

Due to the presence of the gap 4, high-density coal dust enters the furnace from the central channel 3 separately and at a distance of the gap 4 from the underfire and over-fire air from channels 1 and 2 into the furnace.

While running mathematical modeling, the following burner geometries were adopted:

- burner screens with a diameter of 70 mm were replaced by flat surfaces.
- for the performed research of the object, it was decided to perform calculations taking into account the estimated volume.

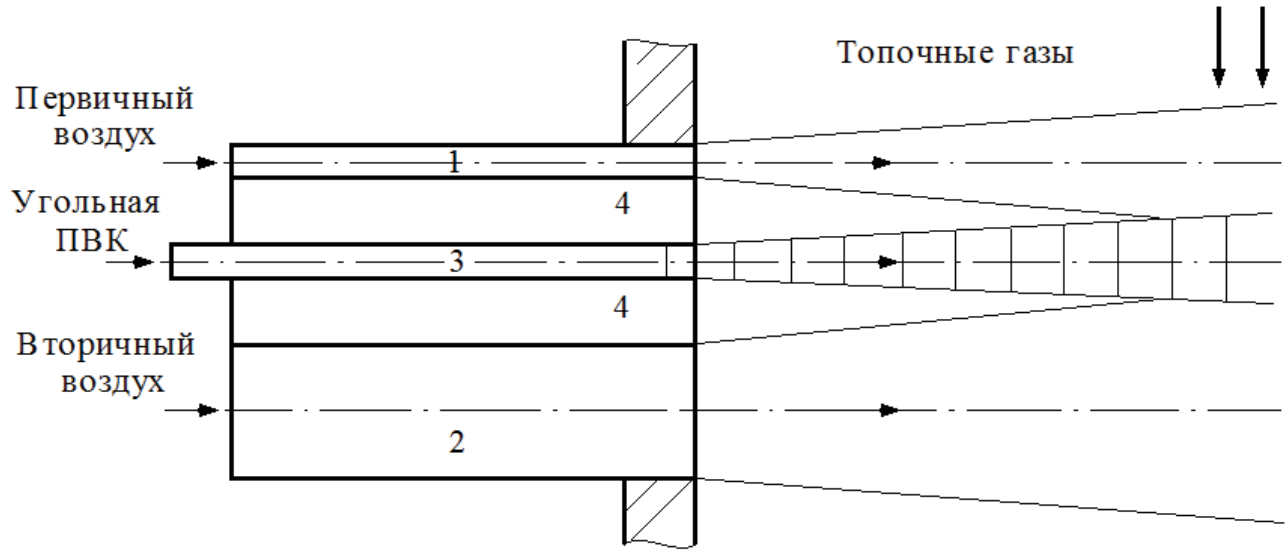

Figure 2 – straight-flow burner.

The basic integral parameters for the aerodynamics of the burner are summarized in Table 1.

Table 1 - Aerodynamic parameters of the vortex burner

Air channel	Inner	Central
Air quantity, r	0,5365	0,0456
Temperature t, ^{0}C	245	245
Sectional area F, m^2	0,1874	0,0246
Average velocity W, m/s	43,3	17,4

Based on the results of mathematical modeling of furnace processes with vortex burners:

- high heat fluxes falling on the elements of the burner are conditioned to the aerodynamics of the flame - the active burning zone starts at 100-120 mm from the tips of the gas pipes and an intense central zone of recirculation of flue gases with a temperature of about 1800 ^{0}C;

- high speed of mixing and intensive recirculation of flue gases ensure rapid burnout of the fuel, which leads to high local maximum temperature and can contribute the formation of nitrogen oxides.

In the vortex burner, over-fire air is supplied through the outer annular channel, underfire air is concentric and contiguous with it, and in the straight-burner, air is supplied through side channels where a underfire air channel is located on the side of the tangential flue gases and the over-fire air duct axis is guided at an angle of 0-10 ^{0} to the axis of the central channel. Gap values of 4, equal to 1.3-1.9 equivalent diameter of the central channel, respectively, larger and smaller volatile yields, conventional exhaust flow rates, underfire and over-fire air twist parameters, thermotechnical characteristics of high-concentration coal dust provide high-speed pyrolysis.

Since burning of volatile substances and coke dust of fuel occurs at an excess ratio of air greater than one, the probability of formation of so-called "fast" nitrogen oxides is excluded.

The degree of formation of nitrogen oxides from the combustion of coal dust contained in waste gases is reduced by organizing the drying of the fuel by flue gases, and not by hot air. The harmful emissions of nitrogen oxides can also be reduced somewhat by the method of supplying the low-dusted drying gas in the present invention through combustion products where partial reduction of nitric oxide occurs due to over-fire combustion reactions.

All these signs allow to reduce the concentration of harmful emissions of nitrogen oxides many times. Thus, for example, the kinetic model of calculation shows that when the oxygen content in pulverized-coal is 1% and its ambient temperature is 1600 K for 0.043, 94% of the released amount of atomic nitrogen recombines into molecular nitrogen and a nine fold suppression of the formation of nitric oxide occurs. This is in ideal conditions. Under real conditions at this temperature, the thermal constituents of the nitrogen oxide formations are ignorable compared to conventional fuel components.

Thus, the proposed invention can give a high result in suppressing the formation of nitrogen oxides and provide the strictest environmental requirements without significant capital and operating costs. It should be noted that pulverized-coal with a high concentration of 20-50 kg / kg of transport gas (air) when fed by a steam ejector and reaching 250 and more kg / kg with a blower under pressure has a mass specific heat for unit mass of 40-500 times less than when transporting in a fuel-air mixture with an ordinary concentration of 0.5 kg / kg air. Therefore the coal HDC in a hot environment is also heated approximately much faster than a conventional fuel-air mixture.

If it is necessary to reduce the concentration of nitrogen oxides further (if the resource of primary environmental protection regime and technological measures is exhausted), a flue gas cleaning method (secondary environmental measures) may be applied, completing in the oxidation and absorption of nitrogen oxides from flue gases [3].

The economic effect is also expected from the exclusion of the "clearing of flame with fuel oil", reaching 6.12 and 30 from capacity of thermal power stations in the USA, the CIS and the RK, respectively.

Conclusions

1. A method for burning solid fuel by heating and addition into a high-density of coal dust furnace / HDC into the combustion chamber // 20-250 kg of dust per kg of gas, underfire and over-fire air through a burner and a low-dust drying gas(LDDG) through a discharge burner, which is distinguished by which the underfire air is preheated to the over-fire air temperature, then the coal HDC is added into the furnace separately from the underfire and over-fire air, separately heated to the flaming temperature of the fuel volatile substances (FVS) and combined with the underfire air , and after burning FVS its coke dust is connected with over-fire air and the LDDG is fed to the intense firing of coke through combustion products.

2. A burner device for carrying out the solid fuel combustion method according to claim 1, comprising channels for additions of the fuel-air mixture and over-fire air and a gap there between, characterized in that the central channel is installed for addition into the coal dust furnace of the HDC along the axis of the burner device, the gap is placed between the central channel and the channel for addition of underfire and over-fire air into the combustion chamber, the gap thickness being equal to 1.3 to 1.9 equivalent to the diameter of central channel, and the discharge burner is installed over the burner device at a distance of 1.8-2.2 equivalent to the diameter of the burner with its direction downward at an angle to the surface of the furnace wall, equal to 65-75 degrees.

Thus, the combustion technology of a high density concentration of dust is advantageously characterized in that, the reduction in NOx emission occurs without impairing efficiency, which typical for regular schemes with low concentrated fuel-air mixture flow. In addition, since changes in the combustion conditions in the furnace relate mainly to the burners, the cost of reconstructing the combustion process in order to reduce emissions of nitrogen oxides is much lower, sometimes even by more than in comparison with typical solutions. Therefore, repowering in order to reduce NOx emissions must be started with the translation usual concentration of dust supply to the high concentration of dust supply system (HDC). In this case, it is possible to implement the technology of burning solid fuel in a highly concentrated stream.

Moreover, the transition to a highly concentrated dust burning significantly reduces the risk of slagging of combustor, since the number of primary jet fuel-air mixture flow decreases sharply.

References

1. V.A. Petrosyan, A.N. Alekhnovich, I.N. Shmigal, I.A. Sotnikov, E.A. Fedorchenko // Teploenergetika. 1991. № 6. Pp. 12-24.

2. N.A. Zroychikov, VB Prokhorov, A.M. Arkhipov, V.S. Kirichkov. Optimization of the aerodynamics of the torch and the design of tangentially directed burners on the boiler TGMP-314 / / Teploenergetika, 2011, №8, p.27-31.

3. V.I. Kormilitsyn, V.S. Yezhov. Flue gas cleaning study trapping nitrogen oxides from the combustion of natural gas // Thermal Engineering, 2013, №2, p. 71-76.

MONTHLY ZERO NET ENERGY LOSS FOR A SOUTH FACING WINDOW WITH SHUTTER, IN BUCHAREST, A REAL POSSIBILITY

Romeo Popa[1]*, Ioana Udrea**, Tudor Prisecaru*
* Thermodynamics Dept., Universitatea POLITEHNICA of Bucharest
** ASC-Romania, 9 Stefan Marinescu St., District 6, 060121, Bucharest

ABSTRACT

The monthly solar gains and heat losses for an unobstructed South window in Bucharest, having either a double non-low_e glazing or a low_e one have been calculated for three situations at night : the window without shutter, with a wooden panel shutter and with a thermal insulation panel shutter. In all three cases, the window has no shutter during daylight time. The calculation followed the monthly method for building energy of SR EN ISO 13790, that is, it produced and used a one monthly average value for the quantities involved (like the window losses or the outside temperature or incident solar radiation). The thermal correction due to mounting the window in the wall (the so-called psi_installation by Passivhaus Institut) has also been considered. Achieving zero net energy loss even in the coldest months, for a themally-good-glazing-and-frame window, consistently insulated by an exterior shutter at night, appears to be possible in the climate of Bucharest.

1. INTRODUCTION

The general strategy of lowering the cost of building energy consumption, has mainly two directions of attack : creating more energy efficient building envelopes and creating more intelligent building installations that use energy costing less. As part of the first direction, improving the energy performance of the glazed part of the building shell has continuously been targeted for several decades. Even after the invention of the insulated glazing units (IGUs), low_e glass and much more thermally efficient window frames, the race to improve the energy performance of windows continues. And one not complicated way to have better window systems is to place one or more window attachments performing a thermal function; systems that are thought of in the design phase not after the building has been raised. Well matched windows and attachments can be of real value to lower the energy consumption of a building and are desirable because in general, window attachments do not require an expensive investment and are applicable in almost any situation.

Attaching exterior shutters to windows in order to prevent the interior heat loss in cold nights is something known and common to the Romanian traditional architecture. But this knowledge appears to have been lost to a large extent in the new building design process here. Very many times when window shutters are installed, the fact is an after-building-construction consideration and action, not a consequence of a previous design process for that. Such an attitude leads to makeshift solutions and the envelope structural and thermal integrity is compromised so often.

It seems there is just one window shutter model currently sold on the Romanian market for the thermal insulation purpose, the roller type, whose slats can be all packed in a case mounted on the exterior wall above the window head . The slats are made from wood or plastic ; some can also have foam insulation inside, that is something like 5-6mm insulation for the thickest .

[1] Thermodynamics Dept., University POLITEHNICA of Bucharest, Spl. Independentei 313, Bucharest, Romania 060042, romeotraian@gmail.com

This paper probes some possible thermal consequences of a one-piece panel type shutter having thicker insulation, 3cm EPS. To operate such a shutter one needs hinges or some gliding rail system enabling the panel to move so that it covers the window when closed and does not obstruct it at all, when completely opened.

2. METHODOLOGY

The monthly net energy loss of a mobile window of standard size, height 1.48m and width 1.23m (according to EN ISO 10077), facing South, completely exposed to the sun (that is unobstructed in any way), in Bucharest, has been calculated (see Fig. 1).

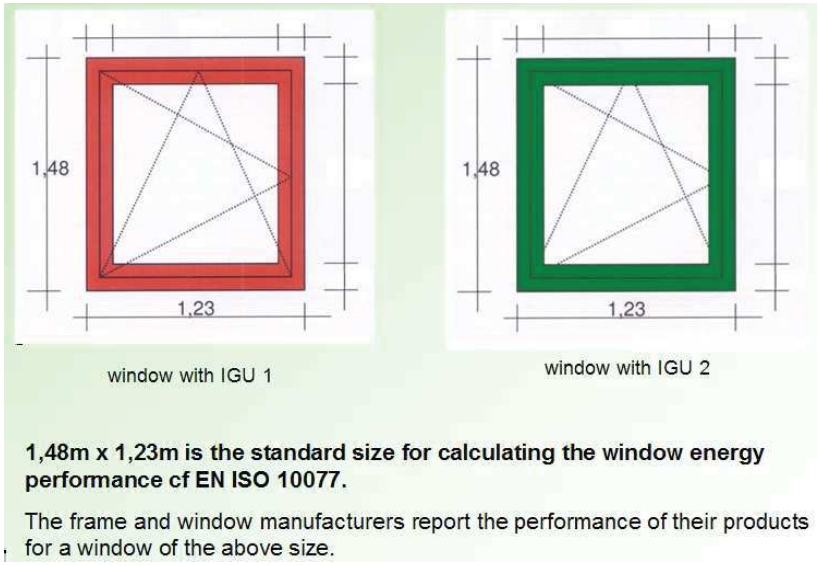

Fig. 1 The two simulated windows have an identical frame but different insulated glazing units (IGUs) : IGU 1 in the "red" window and IGU 2 in the "green" window

Some characteristics of the Saint-Gobain Glass (SGG) glass panes and the two used glazings (IGU 1 and IGU 2) made of them are shown in Fig. 2 . The pane type is either Planiclear (clear float glass, no low_e depositon on its surfaces) or Planitherm XN II (one surface is low_e). Planitherm XN II, is pane #2 (when counting from the outside to the inside) in the "good" glazing (IGU 2), see Fig. 2 (the low_e surface faces the exterior) . The exterior pane in IGU 2 is Planiclear. IGU 1 is made of two identical Planiclear layers.

Fig. 2 shows some glass technical data, the solar transmittance at normal incidence T_n , the far-infrared (FIR)/thermal emissivities of the two pane surfaces (e_1 for surface 1, to the exterior when mounted in the glazing, and e_2 for the surface to the interior) . The effect of depositing a low-e layer is striking, the FIR emissivity of untreated glass, 0.84, is lowered to the value 0.039. Another remark that should be made is some (undesired, at least for the cold season) loss in solar transmittance that accompanies this low_e deposition process, the T_n = 0.871 of Planiclear is lowered to 0.636 for Planitherm XN II (some loss in the visible transmittance, not shown, also occurs). All panes are 4mm thick and the gap between them in the IGU is filled with an Argon_90% & Air_10% mix. The thermal transmittance (the inverse of the thermal resistance) , Ug, of both IGUs is given in Fig. 2 as well as the solar heat gain coefficient of the glazing for normal incidence, g_n (accounting for various incidence angles for the solar radiation was done in the following calculation in the very crude way proposed in EN ISO 13790 [1], by taking an ajusted g as $0.9g_n$).

The used window frame, a thermally efficient model, PVC Alphaline 90 made by

Fig. 2 The two IGUs made of SGG glass panes, Planiclear and Planitherm XN II

Veka [2], see Fig. 3a and 3b, was chosen because its detailed geometry was known to us (although we did not know exactly all material properties and we had to guess some of them, our guesses proved reasonable as the calculated result in THERM, U_{frame} = 1.11 W/m2/K is practically the same with the one declared by the manufacturer).

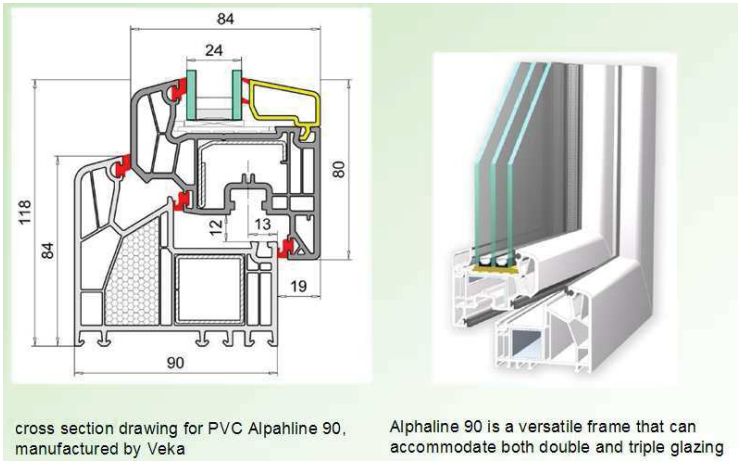

Fig. 3a and 3b A 2D drawing and a photo of the frame used in the simulations

As window attachments, exterior shutters of two kinds have been considered: 1cm thick wood panel and 1cm wood + 3cm expanded polystirene (EPS). They are assumed operated to be completely opened during daylight time but completely closed between sunset and sunrise.

Commonly, the building envelope heat transfer calculation (for both its opaque and its glazed parts) hypothesizes a 1D heat flow, accross the envelope. However, there are regions of it where, for reasonable accuracy, a 2D heat flow should be considered (in other words, linear thermal bridge corrections should be made) . The window itself has such one region, requiring a 2D calculation for it: a two "lane" strip composed of a lane neighboring the junction of the glazing and the frame, and the other being the frame itself .

Another correction is also necessary, especially for energy efficient building design, one accounting for the additional 2D heat transfer caused by mounting the window in the wall (its thermal bridge correction coefficient is the so-called psi_installation by Passivhaus Institut, Darmstadt). The strip around the outer edge of the window frame affected by this correction is illustrated in Fig. 4.

So, first after the Ug of the window glazing is determined (based on the optical and thermal characteristics of the glass panes and gas mixture it is made of), a cross section covering the above mentioned two "lane" strip of the complete window (unmounted but in a vertical position) is simulated for the 2D steady state heat flow, with adiabatic boudaries at its top and bottom, and boundary conditions for the indoors and outdoors (that is on its sides).

The softwares WINDOW and THERM [3] by Lawrence Berkeley National Laboratory (LBNL) were used for this purpose. Fig. 5a displays the cross sections prepared for simulation in THERM (after they have been drawn and heat transfer properties have been assigned to the various drawing regions, differently colored according to the material they are made from). Fig. 5b displays the results of the simulation, suggestively displaying the temperature field.

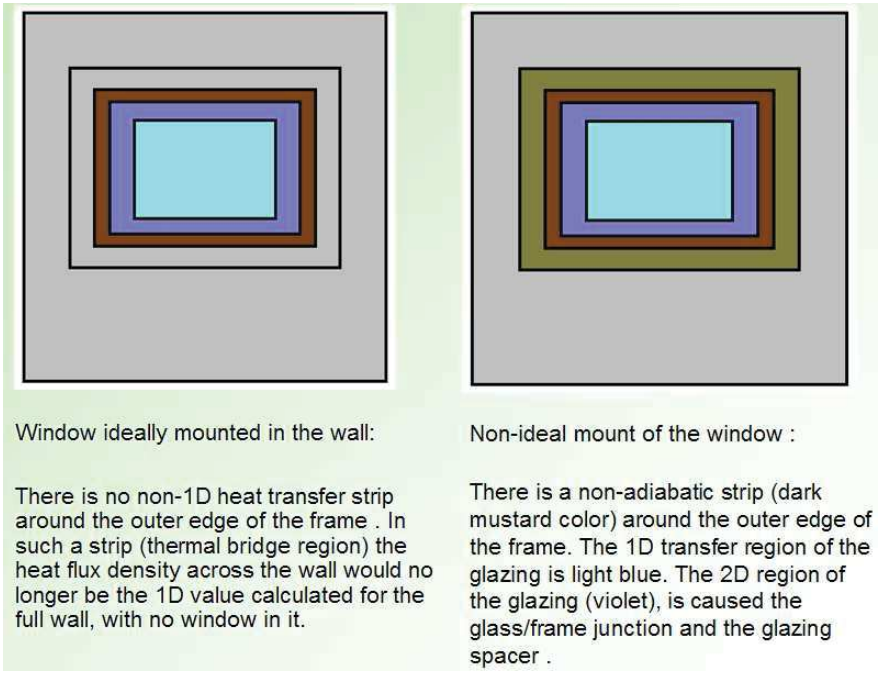

Fig. 4 Mounting the window in the wall ideally, not perturbing the heat transfer through the wall without window (very non-realistic) and considering that perturbation

The run THERM simulations produced the necesary numbers to calculate cf [4], the quantities U_w, U_{w+sh} and U_{w+ish} respectively the whole unmounted window thernal transmittance , the transmittance for the window & its wood panel shutter and the transmittance for the window and its insulation shutter. A (very optimistic for Romania) thermal bridge correction for mounting the window in the wall, psi=0.1 W/m/K was used [5].

Two heat fluxes were computed for each month from October to March included, for daylight time when the shutters are completely opened and for night when they are completely closed. They were multiplied by the total day and respectively night time of every month, taken from [6], and then added for each month to obtain the heat loss in the six cases described. Monthly mean outdoor temperature data from [7] were used and the indoor temperature value was taken 20º C .

The monthly solar gains, same for all six cases, were calculated using monthly solar

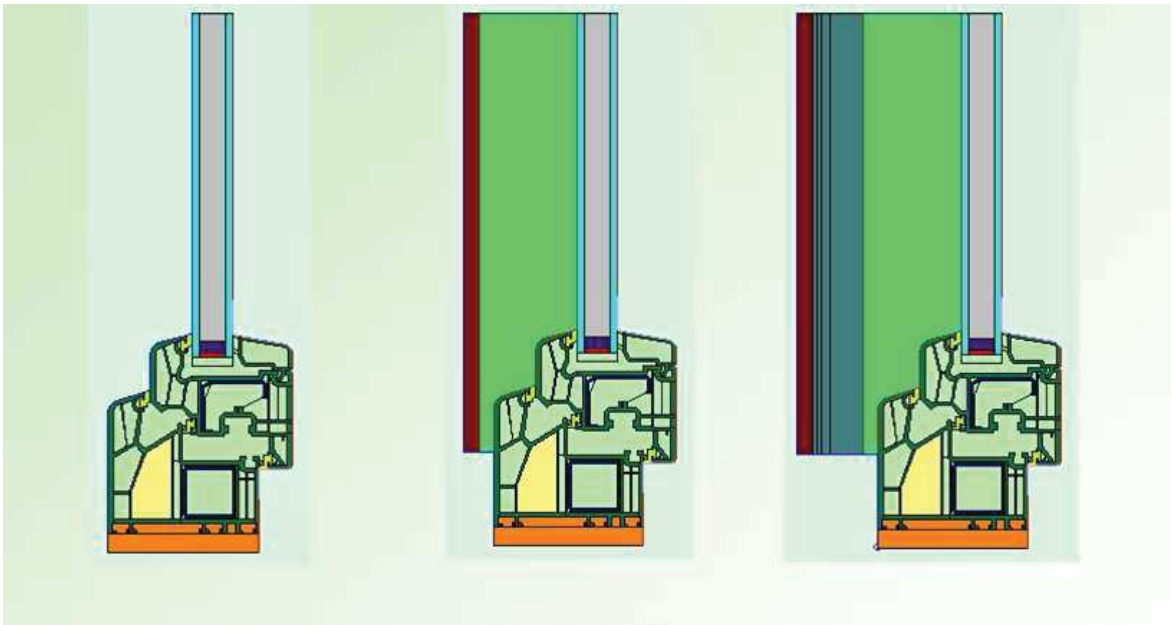

cross sections of the frame and the 2D heat transfer strip of the window glazing in the three configurations, as drawn for simulation in THERM : window with no shutter, plane wooden shutter panel window and window with a thermal insulation shutter (to the right)

Fig. 5a The three considered configurations for the unomunted window before the simulation (a 1cm insulation was additionaly placed by us at the base of the frame and thought of as part of it ; it is the orange region in the drawings)

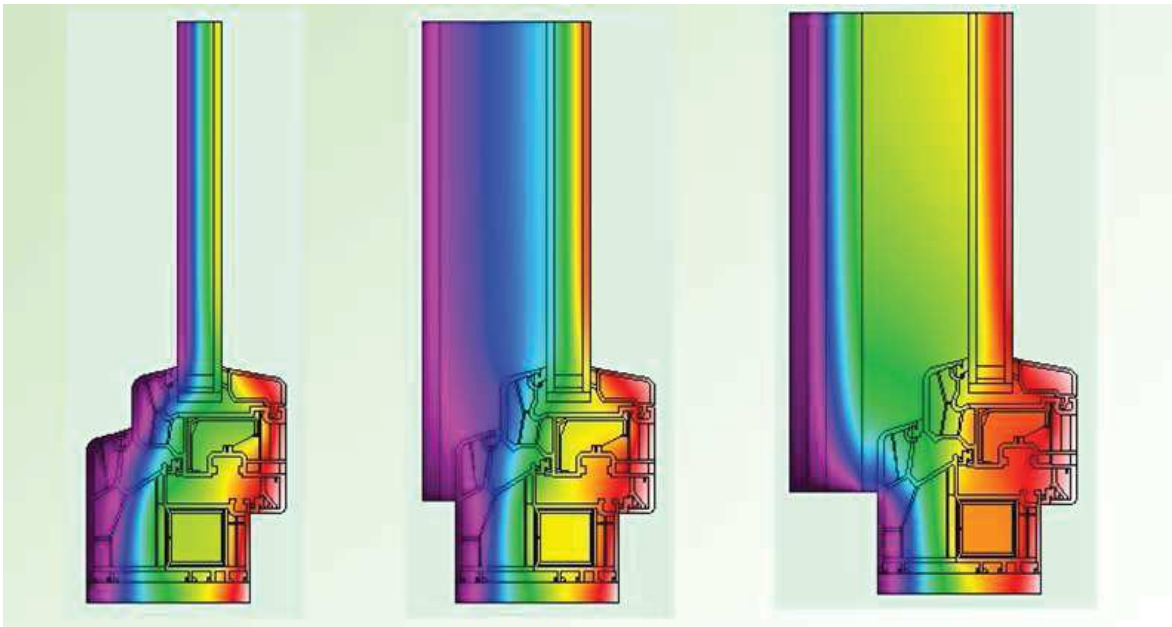

Conventional color temperature results of the simulation in THERM : the temperature range extends from red (higher temperature) to blue to dark purple (lower temperature) .

Fig. 5b A colored display of the simulation results for cases having the same glazing radiation means for Bucharest (on a vertical surface facing South), from [8] .

3. RESULTS

The results, illustrated in Figs. 6, show as expected, higher both gains and losses for the "red" window, in Fig. 6a (the biggest value is 80 kWh, the gains for October).

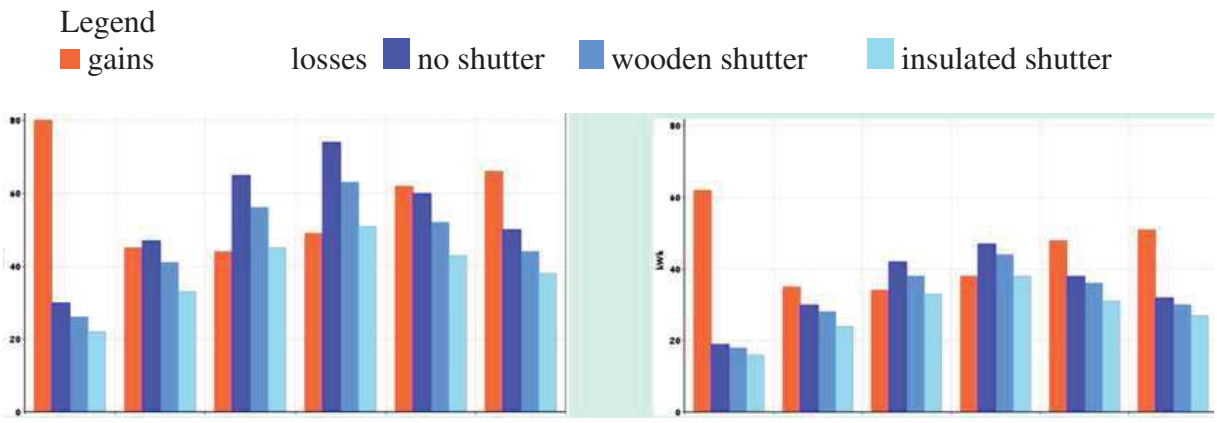

Figs. 6a and 6b Left the "red" window and right the "green" window. From left to right, gains and losses for October, November, December, January, February and March. The figures on the Y axis and horizontal grid lines are 20 kWh apart.

4. CONCLUSIONS

Even for such a South window in Bucharest, having a non-low_e glazing (the "red" one in Fig. 1) and Argon&Air mixture in its cavity and a thermally performant frame, a zero net energy loss in the most unfavorable months (December and January) seems reachable. Although it is of course expected this window requires much higher daily fluctuations in the heating and the cooling need, compared to the low_e glazing window (the "green" one).

However, a crux of the made calculation is the assumption of a very optimistic (for the Romanian construction market) psi_installation value, 0.1 W/m/K. Achieving such a quality requires very carefull planing in advance of the window mounting work and even thinking about that construction detail in the building design phase (which is laborious procedure but normal in the case of a passivhaus).

Another necessary remark is related to the air space between the shutter and the window (the intense green area in Fig. 5a) where an optimistic natural ventilation regime was assumed (the option "slight cavity ventilation" was used in THERM). Such a weak ventilation may require a closer-to-the-window mount of the shutter (the distance is 9mm in Fig. 5a), which in practice may not be very easy.

References

[1] SR EN ISO 13790, *Performanţa energetică a clădirilor, calculul necesarului de energie pentru încălzirea şi răcirea spaţiilor,* 2009
[2] Geza, Z., *Prezentare Veka : Alphaline 90*, Eurofereastra 2007
[3] LBNL WINDOW and THERM software, https://windows.lbl.gov/software/therm/therm.html
[4] EN ISO 10077-1 and 10077-2, *Thermal performance of windows, doors and shutters*, 2012
[5] Anexa K la Ordinul 1590/24.08.12 pt modificarea C 107/3, *Catalog cu punti termice specifice cladirilor*
[6] US Naval Observatory calculator, http://aa.usno.navy.mil/data/docs/Dur_OneYear.php
[7] Anexa A a SR 1907-1, *Instalatii de incalzire*, 1997
[8] Anexa 6 a NP 048, *Normativ pentru expertizarea termica si energetica a cladirlor existente si a instalatiilor de incalzire si preparare a apei de consum aferente acestora*, 2000

REALISTIC TRENDS ON AUTOMOTIVE ENGINEERING DEVELOPMENT: COMBINING HYBRID WITH CLASSIC

Alexandru Racovitză[1]

University "POLITEHNICA" Bucharest, Faculty of Mechanical Engineering
Dept. of Thermodynamics, Engines, Thermal and Refrigerant Machines

ABSTRACT

This paper highlights the benefits of using an integrated solution consisting in a combination inside the Hybrid Electric Vehicle configuration based on the electric energy supply ensured by a Direct Ethanol Fuel Cell (DEFC) and the classic propulsion furnished by a supercharged Spark Ignition Engine (SIE) with the support of a Micro-Turbine (MT) as the main motion source for the Electric Generator (EG).

Key Words: Hybrid Electric Vehicle, High Efficiency, Low Emissions, Bio-Ethanol, Direct Ethanol Fuel Cell, Supercharged Spark Ignition Engine.

1. INTRODUCTION

Nowadays, strong arguments are used by those positioning themselves on one side or another related to the key role played in the propulsion by modernised and new adapted thermal engines and the hybrid solution, in which electric propulsors are gaining a furthermore importance. The newest standards limiting the exhaust gas emissions, encouraged by the continuously greater role played by the bio-fuels are leading to solutions regarding the expectations for the engines efficiency and their emissions levels [1]. Hybrid propulsion is also considered to better fit the above described needs, but technically there are some problems not yet covered in the long therm use of the automotive applications, such as the limited operation autonomy and service assistance, less passengers room comfort due to the higher dimensions and weights of the components. In Hybrid Electric Vehicles (HEV) there are two possible configurations assembling the two propulsion types: in series and in parallel (see Fig.1 a and b) [2]. In the first case the thermal propulsor is connected to the system and in the second case both propulsors connect the transmission one at the time.

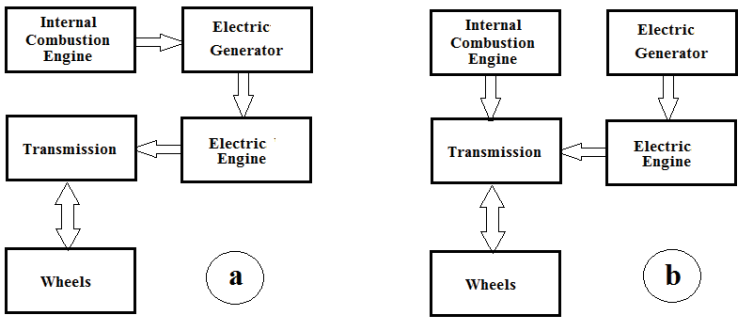

[1] 313 Splaiul Independentei, sect.6, 060042, Bucharest, tel.: 0040-21-4029451, e-mail: racovitzaalexandru@gmail.com

Figure 1: Hybrid engines configuration – in series (a) and in parallel (b) [2]

Despite the fact that Hydrogen Fuel Cells are "cleaner" than cells using other primary fuel, Direct Ethanol Fuel Cells (DEFC) [3] (see Fig.2) are more efficient and providing more safe in use [4,5]. Furthermore, bio-ethanol can be used on-board of the vehicle fueling the fuel cells as the thermal engine as well, with certain gain on CO and HC engine emissions' levels [6]. The electrical generator system which supplies the batteries of the electrical engine receives its primary motion energy from the thermal engine, and when vehicle operated from the wheels Breaking Regenerative System (BRS) [7]. Other methods to gain supplementary electric power is to use micro-turbines in the path of the exhaust gas produced by the internal combustion engine [8].

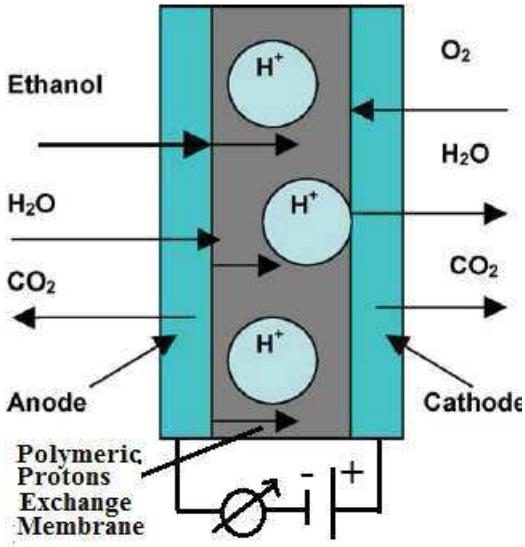

Figure 2: The schematic of the DEFC bipolar operation [3]

2. INTEGRATED CONFIGURATION USING DEFC AND MICRO-TURBINE

The schematic of the proposed solution (see Fig.3) is based on a combination between the functional elements of a classic supercharged Spark Ignition Engine (SIE) and the electric part formed by the electric engine, the electric generator, the battery and the fuel cell (DEFC). The common fuel used by both engines is bio-ethanol due to its properties requested as a fuel cell primary fuel and in the same time as a combustion fuel in the thermal engine, delivered by the injection fueling system (FS). The engines are configured to act as in the parallel scenario mentioned above and their functions sustaining each others operation. Thus, SIE is coupled to the transmission system (TS) and at the same time is delivering energy to the alternator (ALT) which is charging the battery (BT) of the electric engine (EE). On its turn, the electric engine can switch to the transmission connection and it has to furnish motion energy to the internal combustion engine compressor (C). The battery is provided with more electric energy supply from the braking regenerative system (BRS) attached to the wheels (W). The battery must cover all the necessary supply for the system, and in the first place for ECU (Electronic Command Unit). Among the most controlled sub-systems of the whole configuration the injection fueling system (FS), the spark ignition system (SI), the catalyst

systems of the fuel cell as for the exhaust gas (CT) have integrated all their specific functions. The micro-turbine (MT) mounted on the outlet path of the SIE exhaust gas delivers motion energy to the electric generator (G) and following to this situation it doesn't supply the engine air compressor as classic turbocharging group usually works. In order to limit the emissions, catalysts have been mounted downstream the micro-turbine and in the outlet collector of the fuel cell, in this particular case especially the CO_2 emissions being necessary to be filtered. Among many other functions, ECU is collecting operational data from engines and controls the regime functions of the spark ignition system (SI) and of the fueling system (FS).

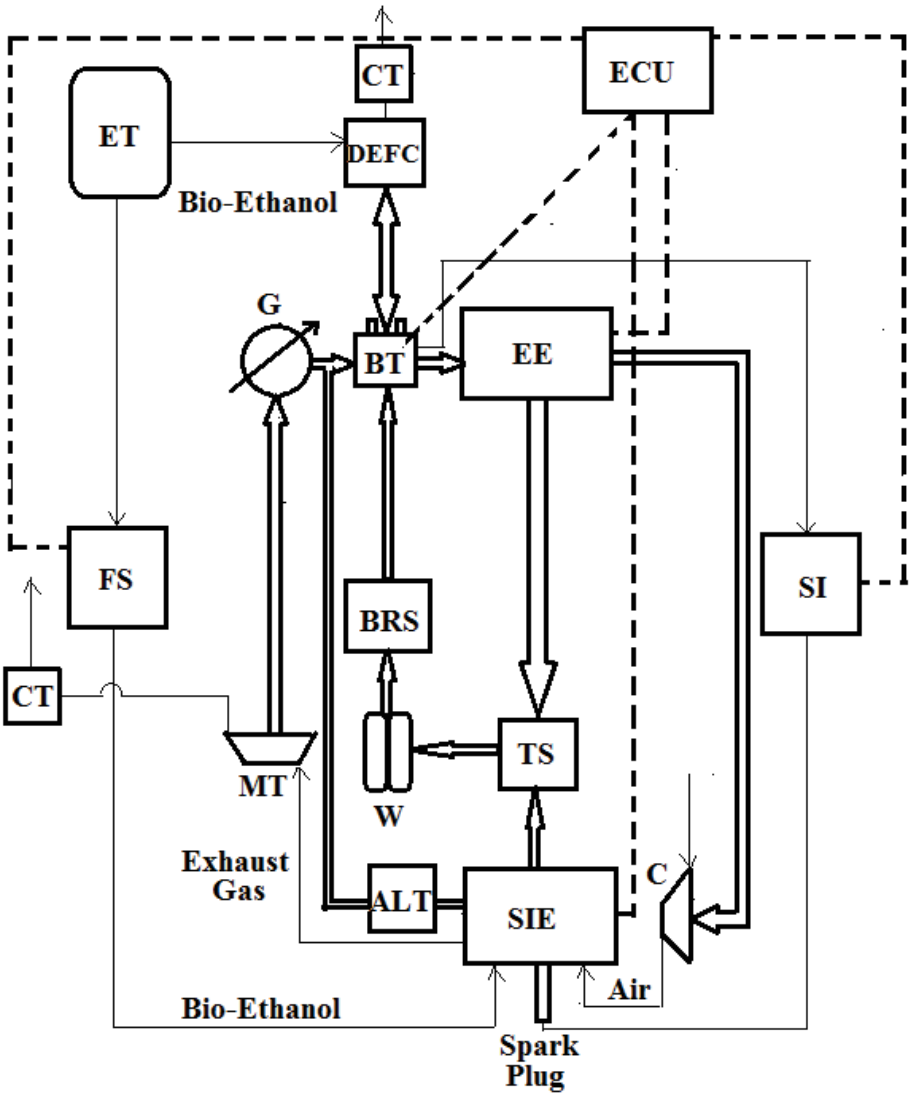

Figure 3: The schematic of the HEV solution with DEFC and Micro-Turbine

3. CONCLUSIONS

HEV configurations must provide benefits concerning both types of installations, thermal and electric. The global efficiency relies on the particularities of each part which operates under specific conditions and requests.

The adopted solution as presented above combines the advantages of using DEFC and the ICE exhaust gas micro-expander. The chosen fuel which is bio-ethanol is an appropriate fuel to be used as a primary fuel in the fuel cell and to be combustioned in the SIE, leading to an increase of the efficiency and to a drop of the emissions comparing to other classic fuels.

It remains as an assumed task for the future research objectives to theoretically investigate the influences of all the main components of the system efficiency under certain defined optimization purposes.

References

[1] Directive (EU) 2015/1513

[2] A. Paykani, M. Taghi Shervani-Tabar, *A comparative study of hybrid electric vehicle fuel consumption over diverse driving cycles*, THEORETICAL & APPLIED MECHANICS LETTERS 1, 052005 (2011), doi:10.1063/2.1105205;

[3] www.researchgate.net/figure/228616120_fig1_Fig-1-Schematic-illustration-of-a-bipolar-direct-ethanol-fuel-cell-DEFC

[4] M.Z.V. Kamarudin, S.K. Kamarudin, M.S. Masdar, W.R.W. Daud, *Review: Direct Ethanol Fuel Cells*, ELSEVIER, International Journal for Hydrogen Energy, 38 (2013), pp. 9438-9453;

[5] C.Osornio-Correa, R.C.Villarreal-Calva, A.Molina-Cristóbal, J.Estavillo-Galsworthy, S.D.Santillán-Gutiérrez, *Optimization of Power Train and Control Strategy of a Hybrid Electric Vehicle for Maximum Energy Economy*, Ingeniería Investigación y Tecnología, vol. XIV (1), 2013: pp.65-80 ISSN 1405-7743 FI-UNAM66;

[6] C.Cincu, L.Fara, A.C.Racovitză, L.Lobonț, *Bioethanol obtained from wooden biomass. An appropriate alternative fuel for spark ignition engines*, Cellulose Chemistry and Technology, no.45 (1-2)/2011, ISSN 0576-9787, pag.121-125.

[7] A.Nasri, G.Gasbaoui, B.M. Fayssal, *Novel Four Wheel Drive Propulsion System Control Using Backstepping Strategy*, ELSEVIER Procedia Technology 22(2016), pp.509-517.

[8] B.L. Arav, R.Shulman, V.A. Kozminykh, *Refinement of hybrid motor-transmission set using micro-turbine generator*, ELSEVIER Procedia Technology 129 (2015), pp.166-170.

THE DESIGN OF THE WATER DIFFUSER SYSTEM OF A TANK FOR A COGENERATION PLANT WITH RECIPROCATING ENGINES

Petrică RADAN[1,2,3], Victor-Eduard CENUȘĂ[3], Elena ARION[2,3], Adrian Andrei ADAM[2]
[2]INCDE ICEMENERG
[3]University Politehnica of Bucharest, Faculty of Power Engineering

ABSTRACT

Integration of thermal energy storage systems into cogeneration plants plays a very important role in their technical and economic operation. The use of storage systems increases the efficiency of the cogeneration plant and its flexibility in operation. The efficiency of the heat storage systems can be improved if the water inside the tank is stratified. In time, water de-stratification results in energy losses. The paper presents the integration of a heat storage system into a cogeneration plant with a reciprocating engine by means of an existing fuel oil tank. At the same time, the water diffusion system is calculated considering a four-ring octagonal system.

1. INTRODUCTION

The heat supply of consumers is the main objective of the cogeneration plants, but nowadays heat and electricity production is affected by the electricity market that leading to inconsistencies between the demand of heat and the electricity produced [1]. The heat demand is usually discontinued when the heat demand is low; the cogeneration plant will produce electricity, and the excess heat is stored to be used later when the heat demand is higher [2, 3]. Water stratification is created by the difference in density between hot water and cold water. The intermediate region between the cold water at the base of the tank and the warm water is called thermocline. The formation of the thermocline zone is determined by the volume and geometry of the tank, the water flow, the thermodynamic properties of the water, and the dimensions of the slots. There are several water diffusion systems (radial, octagonal, "H", square) on the market. The water diffusion system in the tank selected in the present paper is octagonal.

2. INTEGRATING THE TANK IN THE COGENERATION PLANT SCHEME

The analyzed cogeneration plant is equipped with two piston engines, each with a power output of 6800 kW. The recovered thermal power is of 5560 kW, and the total hot water flow rate of the two engines is Qmain pipe = 480 m^3/h (0.133 m^3/s), with a temperature difference of 20 °C.The pipeline through which this hot water flow passes has a nominal diameter of 300 mm. To cover the peak of the heat load the cogeneration plant has two hot water boilers.

Even if in winter the heat demand exceeds the thermal power produced by the two engines in cogeneration operating at maximum load, for most of the the year the engines operate at partial load. There are also periods of time in spring and in autumn when the hot water boilers are used for covering the heat demand. In order to use the engines longer periods of time at

[1]Bucharest, 0763952893, radan.petrica@yahoo.com

maximum load and to reduce the utilization time of the hot water boilers are used heat accumulation is required. Thus, the fuel utilization and the engine lifetime can be improved.

Heat accumulation involves additional investments and seeking solutions for reducing them is always a priority. Taking into account the specific characteristics of the analyzed plant, the paper proposes that an existing fuel oil tank be adapted for heat accumulation. The tank has the following geometrical characteristics: 11.4 m radius and 11.8 m height, the volume being of about 5000 m^3. The material the tank is made of is OL37, and its insulation is made of fiberglass wool.

Figure 1 presents the variant that involves the tank's integration into the analyzed cogeneration plant. The storage system involves three steps: loading, storing and unloading. The hot water tank needs the following parts: distribution / take-up (diffuser) to insert / remove water into / from the tank without creating turbulence. During the tank loading, the hot water is taken from the engine and diffused by the top horizontal diffuser, and the bottom take-up part drains the water and reinserts it into the circuit. During unloading, the top part draws in the water and sends it to the consumer, while the lower diffuser returns the water from the return of the district heating network to the base of the tank.

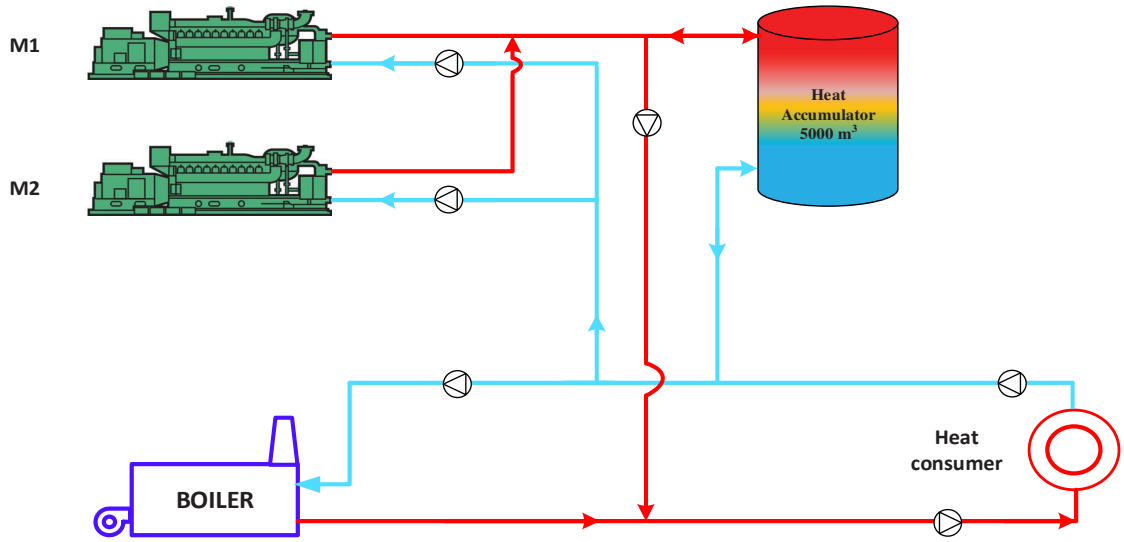

Figure 1: Integration of the tank into the cogeneration plant with piston engines

3. SYSTEM DIFFUSER DESIGN

The proposed diffusion system is octagonal, with a number n_{rings} = 4 diffusion rings, resulting in a number of $n_{diffuser\ pipes}$ = 8 • n_{rings} = 32 diffusion ducts. The diffusion system dimensioning must take into account the maximum operating regime. This is obtained by considering that the sale of electricity takes place at the top of the consumer curve when the price is high and in the conditions of a deficit of thermal consumption. This case involves the accumulation of heat produced in cogeneration by both engines at full load. Thus, the flow of hot water through each side of the octagons can be calculated by means of the relation:

$$Q_{diffuser\ pipe} = Q_{main\ pipe} / n_{diffuser\ pipes} \quad (1)$$

The water flow in the diffusion system is influenced by the inlet Reynolds number (Re_i) [4],[5],[6]

$$Re_i = q / \nu \quad (2)$$

where: - q is the volume flow rate per unit of length of the diffuser into the circumferential direction (m^2/s) (3), and
- ν is inlet kinematic viscosity (m^2/s).

$$q = Q_i / L \quad (3)$$

where: - Q_i is the inlet volumetric flow rate (m^3/s).
- L is the characteristic length of diffuser (m).

In relation (3), if $Q_i = Q_{main\ pipe}$ then L is the characteristic length of the whole diffuser system, and if $Q_i = Q_{main\ pipe} / n_{rings}$, then L is the characteristic length of one ring of system diffuser. L is calculated as the double of the perimeter of the octagon [4, 5].

Table 1: System diffuser characteristics

Design inlet temperature during charge cycle [°C]	90
Inlet kinematic viscosity, ν [m^2/s]	3.25719E-07
Length of each diffuser pipe in octagon #1 [m]	3.3
Length of each diffuser pipe in octagon #2 [m]	5.6
Length of each diffuser pipe in octagon #3 [m]	7.3
Length of each diffuser pipe in octagon #4 [m]	8.6
Characteristic length of diffuser for octagon #1 [m]	52.8
Characteristic length of diffuser for octagon #1 [m]	89.6
Characteristic length of diffuser for octagon #1 [m]	116.8
Characteristic length of diffuser for octagon #1 [m]	137.6
Re_i for octagon #1	1938
Re_i for octagon #2	1142
Re_i for octagon #3	876
Re_i for octagon #4	744

Re_i is heavily influenced by water temperature, through the strong variation with it of kinematic viscosity. Figure 2 shows this dependence. From the point of view of the flow, the cold storage installations are more advantageous than the heat storage ones, the laminar flow being easier to obtain at low temperatures.

Different diameters of the diffuser water supply pipe have been considered (0.273 m, 0.219 m, and 0.168 m) (nominal diameters by 250 mm, 200 mm, respectively 150 mm), and their corresponding water velocities have been computed obtaining the following values: 0.0712 m/s, 0.1105 m/s, and 0.187 m/s.

Considering that the ratio between the length of the diffuser pipe cross-section and the slot length is 4 the slot length (21.4 mm, 17.2 mm, and 13.2 mm) has been computed. By selecting a slot width of 1 mm, the slot area is determined. At the same time, by imposing the slot inlet/outlet velocity (for example 0.2 m/s), the flow rate of each slot can be computed and a total number of slots in diffuser pipes is obtained.

Then the number of slots in each diffuser pipe is computed. By rounding the obtained values and recomputing with the total number of slots in diffuser pipes the final number of slots in each diffuser pipe can be obtained: 10, 13, respectively 16.

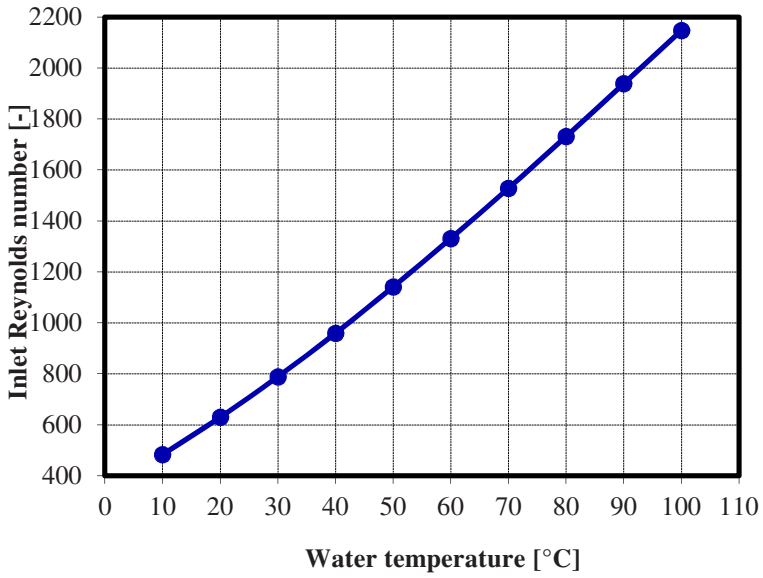

Figure 2: Inlet Reynolds number (Re_i) vs. water temperature

4. CONCLUSIONS

The paper analyzes the adaption of an existing fuel oil tank from a cogeneration plant with piston engines for storing heat. An octagon water distribution system with four water diffusion rings has been dimensioned, determining the inlet Reynolds number to establish the laminar flow and the dimensions of the water diffusion system. The highest inlet Reynolds number (Re_i = 1938) has been obtained on the inner water diffusion ring.

Acknowledgements

This work was supported by a grant of the Romanian Authority for Scientific Research, CNCS-UEFISCDI, through the "Programul 2- Cresterea competivitatii economiei romanesti prin cercetare, dezvoltare si inovare", tip proiect: Transfer de cunoastere la agentul economic "Bridge Grand", Titul proiectului: Cresterea competivitatii ENET SA Focsani prin dezvoltarea si diversificarea serviciilor eferite si optimizarea tehnologiilor modern de producere combinata a energiei electrice si termice. Numar contract: NR 66 BG/2016.

References

[1] V. Athanasovici, et al., *Treaty of thermal engineering. Heat supply. Cogeneration* (T*ratat de inginerie termică. Alimentări cu căldură. Cogenerare*), AGIR, Bucharest, 2010.

[2] Holler, S., Olbricht, M., "*Energetic performance of short term thermal storages in urban district heating networks*", The 14th International Symposium on District Heating and Cooling, September 7th, Stockholm, Sweden, 2014.

[3] Volkova, A., & Siirde, A., "*The use of thermal energy storage for energy system based on cogeneration plant*", In Recent Researches in Geography, Geology, Energy, Environment and Biomedicine: The 5th International Conference on Energy and Development-Environment-Biomedicine. Greece, Corfu, page. 71-75, July 2011.

[4] Bahnfleth, W.P., Song, J., "*Constant flow rate charging characteristics of a full-scale stratified chilled water storage tank with double-ring slotted pipe diffusers*", Applied thermal engineering, 25(17), 3067-3082, 2005.

[5] Bahnfleth, W. P., Song, J., Cimbala, J. M., "M*easured and modeled charging of a stratified chilled water thermal storage tank with slotted pipe diffusers*", HVAC&R Research, 9(4), 467-491, 2003.

[6] Chung, J. D., Cho, S. H., Tae, C. S., Yoo, H., "*The effect of diffuser configuration on thermal stratification in a rectangular storage tank*", Renewable Energy, 33(10), 2236-2245, 2008.

ENERGETIC AND EXERGETIC ANALYSIS OF COMBINED CYCLE POWER PLANT WITH SINGLE LEVEL PRESSURE HEAT RECOVERY STEAM GENERATOR

Petrică RADAN[1,2,3], Victor-Eduard CENUȘĂ[3], Elena ARION[2,3], Adrian Andrei ADAM[2]
[2]INCDE ICEMENERG
[3]University Politehnica of Bucharest, Faculty of Power Engineering

ABSTRACT

Selecting the combined cycle parameters with a single steam pressure level is a compromise between the optimal use of energy and the optimal exergetic heat of combustion gases from the gas turbine. The main parameter is the live steam pressure. In a combined cycle, high steam pressure does not necessarily mean high efficiency. It is amazing that the best efficiency is achieved even while the steam pressure is rather low. A change in the live steam pressure greatly affects the amount of heat that needs to be discharged into the condenser. The electrical power of the steam turbine increases when the steam pressure is lower because a larger amount of heat is recovered from the combustion gases and transformed into less efficient electrical energy.

1. INTRODUCTION

The main challenge in designing a combined gas-steam cycle is proper utilization of a gas turbine exhaust heat in the steam cycle in order to obtain maximum steam turbine power. Lee [1] has study the optimum design parameters of Heat Recovery Steam Generators(HRSG) to maximize the efficiency of bottom cycle of the combined cycle power plant(CCPP) by minimizing the irreversibilities. Franco and Giannini[2] obtain the main operating parameters and detailed design of the component concerning the geometric variables of the heat transfer sections for minimization of the pressure drop and overall dimensions of HRSG. In this paper it is proposed a model of energy and exergetic analysis of the combined cycle to identify the optimum steam pressure for a maximum electrical power at the steam turbine.

2. METHODOLOGY

In this paper, the CCPP has **3**xGas Turbine(GT)+**3**xHRSG+ **1** Steam Turbine (ST).The HRSG has three components: economizer, evaporator and superheater with single steam pressure. The circulation of the HRSG is natural. The energetic and exergetic analysis of the HRSG was made with the pinch-point temperature Δt_{pp}=8°C and the approach point Δt_{app}=5°C at constant value.

Table 1: Gas turbine SGT 800-50 data characteristics (in ISO conditions, natural gas)[3]

Electric power [MW]	50.500
Heat rate [kJ_t/kWh]	9410
LHV Efficiency [%]	38,26
Flue gas temperature [°C]	556
Flue gas flow rate [kg/s]	133,7

[1]Bucharest, 0763952893, radan.petrica@yahoo.com

The mathematical model implementation.

A. Computational assumptions.

1. Atmospheric conditions ISO: t=15°C, relative humidity=60%, p=1.01325bar
2. Fuel, CH_4 100%, with Low Heating Value, LHV=46798 kJ/kg;
4. Pressure, temperature and enthalpy losses on pipes are estimated to 2%;
5. The steam turbine mecanical and generator efficiency are: η_m = 99.2%; η_g = 98.5%
6. The air filter pressure drops are neglected; Steam quality > 80%
7. The specific heat it the combustion gases is considered to be constant;

B. Reference parameters for exergy:

1. Pref=0.03170 [bar];
2. Tref=298.15 [K];
3. Href=2,546.54 [kJ/kg];
4. Sref =8.556796 [kJ/kg K]

C. Main Inputs

1. Flue gas analysis: O_2, CO_2, H_2O, N_2, A_r
2. Gas turbine: D_{gas}, Cp_{gas}, $t_{gas,}$ power electric, heat rate,
3. HRSG: Δt_{sup} (dif betwen flue gas temp-steam tempe),Δt_{pp}, Δt_{app}
4. Steam Turbine: p_{min}, p_{max}, η_{ST}
5. Condenser:p_c,$t_{rau.,}$ Δt_{min}, Δt_{max}

The physical component of the exhaust gas exergy flow rate is given by[4], [5]

$$Ex_{gas} = D_{gas} \cdot [Cp_{gas} \cdot (T_{gas} - T_{ref}) - T_{ref} \cdot (Cp_{gas} \cdot ln\frac{T_{gas}}{T_{ref}})] \quad (1)$$

Then, the exergy rate of steam/water:

$$Ex_{st/w} = D_{st/w} \cdot [(h_{lst/w} - h_{ref}) - T_{ref} \cdot (S_{st/w} - S_{ref})] \quad (2)$$

Lost exergy:

$$Ex_{loss} = T_{ref} \cdot (S_{ref} - S_g) \quad (3)$$

Table 2. Exergy balance results of 3xGas turbine SGT 800-50

Exergy In [kW]	**398964**
GT fuel exergy combustor [kW]	1399234
Air exergy compressor inlet [kW]	-267.87
Exergy Out [kW]	**253461**
GT electric output [kW]	151500
GT exhaust exergy [kW]	101961
Exergy Loss [kW]	**145503**
GT compressor, combustor, and turbine exergy loss [kW]	138954
Mechanical/electrical/gear loss [kW]	6547.8

Table 3. Exergy balance results of 3xHRSG

Exergy In[kW]	**99,156.34**
Exergy in with flue gas [kW]	98,249.31
Exergy in feed water [kW]	402.28
Feed pump electric power [kW]	504.75
Exergy Out[kW]	**84,486.12**
Exergy to steam turbine [kW]	73,323.05
Exergy lost to stack [kW]	11,163.07
Exergy Loss [kW]	14,670.22
Exergy lost by heat transfer [kW]	14,670.22

Table 4: Steam turbine exergy balance results

Exergy In [kW]	**73,374.64**
Throttle steam exergy (before stop valve) [kW]	73,374.64
Exergy Out [kW]	**63,449.95**
ST electric output [kW]	58,375.53
ST exhaust steam [kW]	3,240.05
Leakages not recovered to ST [kW]	1,834.37
Exergy Loss [kW]	9,924.69
ST expansion exergy loss [kW]	9,924.69

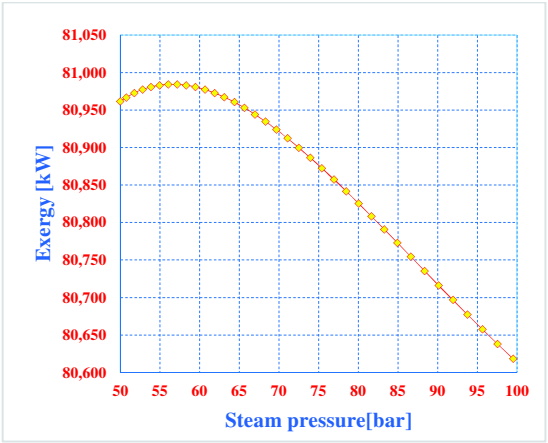

Figure.1: Maximum exergy transmitted by HRSG to steam turbine

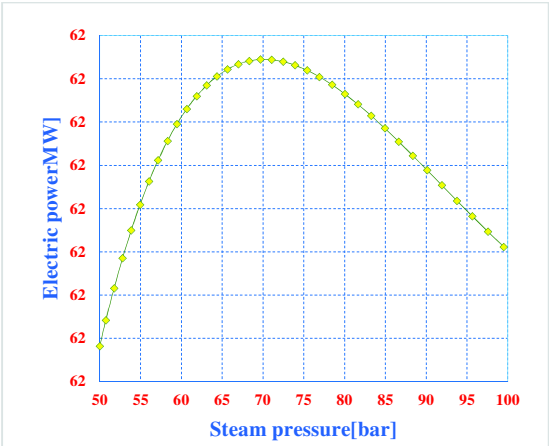

Figure.2:Inlet steam pressure vs electric power produced by steam turbine

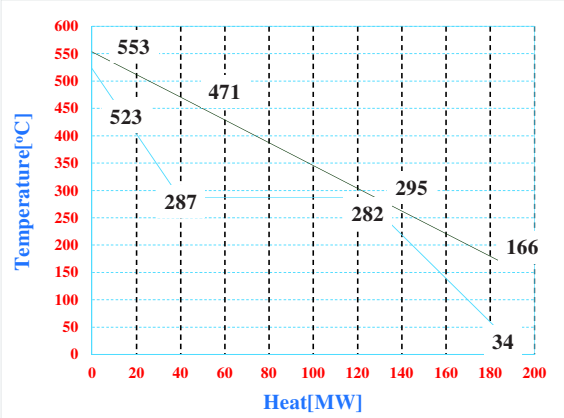

Figure.3:T-Q Diagram

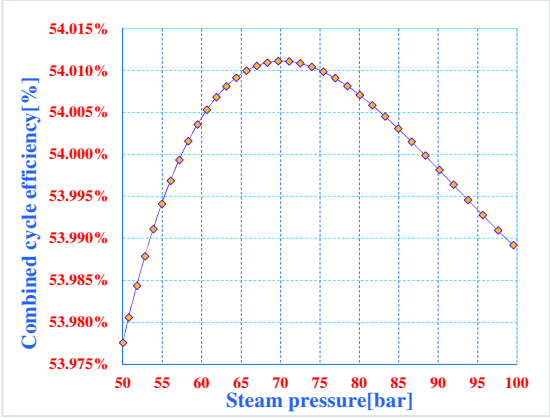

Figure.4:Combined cycle efficiency

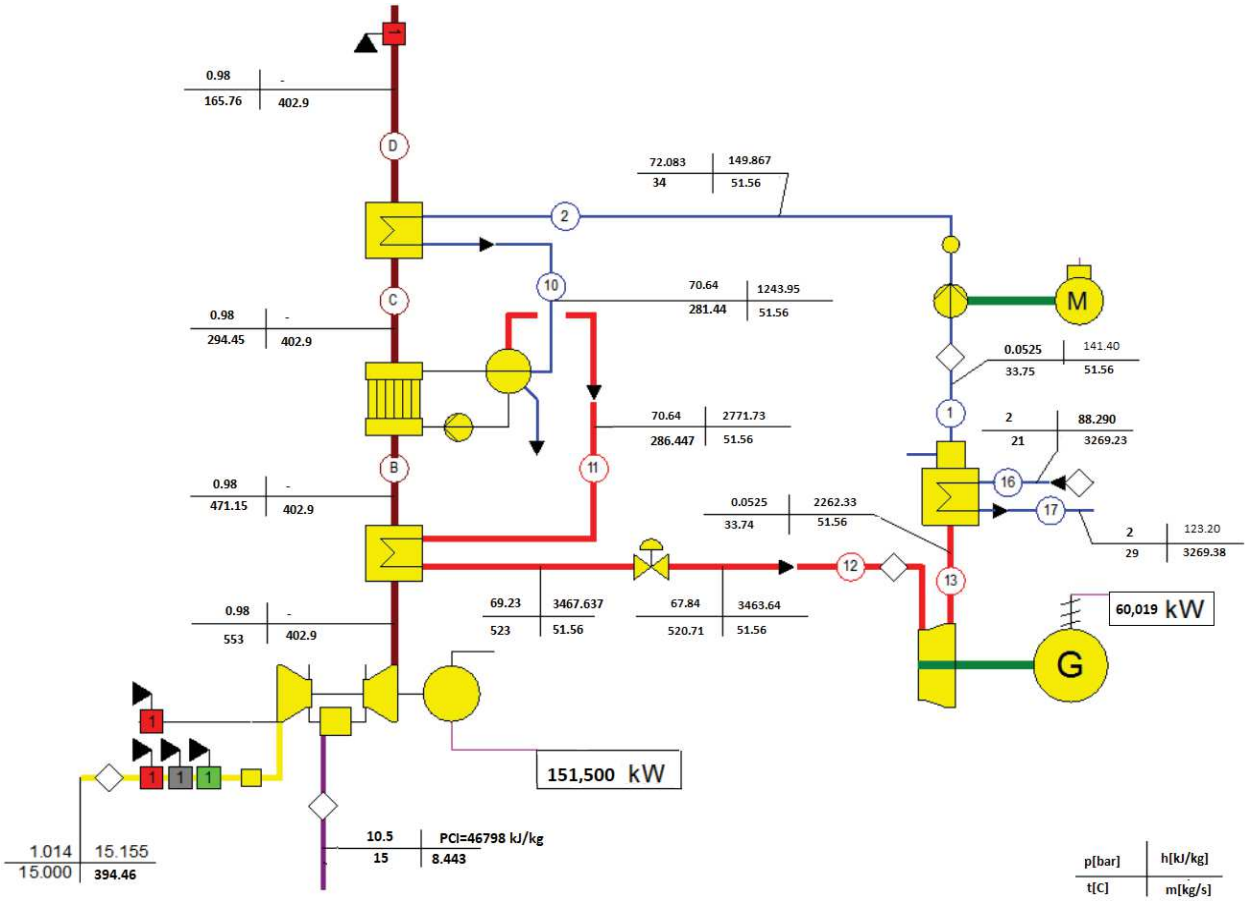

Figure. 5:Combined cycle power plant results

3. CONCLUSIONS

Optimization of the HRSG steam pressure was made in the assumption of keeping the constant steam temperature and varying the outlet pressure from the superheater. The steam pressure range is [45÷90 bar]. From the point of view of the maximum transfer of exergy recovered by the steam generator in the combustion gases, the optimization is made at a steam pressure of 56.79 bar. The maximum recovered exergy is 73.77 MW.

The maximum electrical power produced by the steam turbine is 60 MW. The steam pressure at which electricity production was maximized is p=69.23 bar, t=523 °C. The maximum steam pressure limit was conditioned by the end steam quality at the condenser inlet. The quality of steam is 87.61%, being an acceptable value. The internal turbine efficiency is 88.3%, and the specific turbine steam consumption is 3,093 tonnes of steam/MWh.

References

[1]. J. S. In and S. Y. Lee, “Optimization of heat recovery steam generator through exergy analysis for combined cycle gas turbine power plants,” Int. J. Energy Res., vol. 32, no. 9, pp. 859–869, Jul. 2008

[2]. A. Franco and N. Giannini, “A general method for the optimum design of heat recovery steam generators,” Energy, vol. 31, no. 15, pp. 3342–3361, Dec. 2006

[3] http://www.kushaindustry.com/pdf/brochure/sgt-800-gt-en.pdf

[4]. Bracco, Stefano, and Silvia Siri. "Exergetic optimization of single level combined gas–steam power plants considering different objective functions." Energy 35.12 (2010): 5365-5373.

[5]. Sanjay. "Exergy and energy analysis of combined cycle systems with different bottoming cycle configurations." INTERNATIONAL JOURNAL OF ENERGY RESEARCH 37.8 (2013): 899-912.

ANALYSIS OF PROSPECTS OF FUEL PEAT CONSUMPTION IN UKRAINE

Svitlana Radchenko, Vitalii Zubenko, Taras Antoshchuk, Anatolii Bashtovyi
[1] Institute of Engineering Thermophysics of the National Academy of Sciences of Ukraine, str. Zheliabova, 2a, Kyiv, 03680, Ukraine, +38 044 453 28 56

ABSTRACT

In the article, results of experimental investigations of peat combustion were presented as an example of effective and environmentally friendly technology. The developed installation includes the retort-type burner in which crushed heat-treated peat briquettes are burning. As a result, conditions for sustainable work of the burner with 65 kW capacity were selected and the suitable combustion regime was identified for crushed peat fuel with a moisture content of 15%, which is acceptable for implementation in the industrial equipment of various capacities.

1. INTRODUCTION

An exhaustion of fossil fuels and the problem of "greenhouse effect" make people find possibilities of improving power-generating equipment and use more renewable energy. One of perspective fuel for some regions of Ukraine may be peat.

According to the resolution №33/148 UN General Assembly (1978) peat as mineral, refers to non-traditional renewable energy sources, together with the wind, geothermal, hydropower and biological resources [1]. In 2000, European Parliament also admitted peat as renewable energy within a frame of annual increase of stocks [2]. Also in 2006, the European Parliament confirmed the status of peat as a slowly-renewable energy resource [3]. Peat was separated into an independent category of "Peat" (between the categories of "other solid fuels" and "Biomass") on the 25th session of the Intergovernmental Panel on Climate Change (IPCC) in 2006 at the suggestion of Finland, that reflect the nature and age of peat fuel [4].

Production and use of peat in the energy sector are traditional for many countries. This is because the main deposits are formed of peat with a high degree of decomposition; on the other hand, peat with low decomposition is not very popular in agriculture.

According to the authors [5] in recent years, the EU overall average annual use of peat for energy purposes was about 3640 toe (42 TW×h). Approximately 2 million people receive thermal energy from peat. The largest size of primary energy peat among the European countries is in Finland and Ireland (5-7%), significantly lower in Estonia (1.2%) and Sweden (0.6%). The largest consumers of peat are Finland (63% of total consumption in the EU), Ireland (27%), Sweden (8%). Peat is mostly burned in CHP (42% of peat consumed), the CES (39%), boilers (11%) and private households (8%).

Table 1 presents data on the consumption of peat resources in six countries of EU where the peat industry is concentrated.

Table 1: Degree of peat assimilation in EU countries

	Finland	Ireland	Sweden	Estonia	Latvia	Litvenia	Total
Resources of energy peat, th. toe	1100000	47500	370000	59000	57000	22000	1655500
Annual consumption, th. toe	2280	987	290	72	2	4	3640
%	0.207	2.078	0.078	0.122	0.004	0.018	0.22

As seen in Table 1, Finland consumes the largest amount of peat among European countries, but Ireland is the most intense in deposits using. In addition, according to the data [6], which is shown in Figure 1, in last years the consumption of peat in Finnish energy sector decreased slightly, due to the general decrease in country energy consumption, more intensive use of wood waste and significant development of wind power industry [7].

Generally, there is distinguished three types of peat fuel: milled peat (moisture content 40-50%), lumpy peat and briquette peat/pellet peat (with a moisture content of 10-20%). Usually, milled peat comes to large energy factories (CHP/CPP), lumpy peat is burned in the boilers and briquette/pellet peat is used in private households.

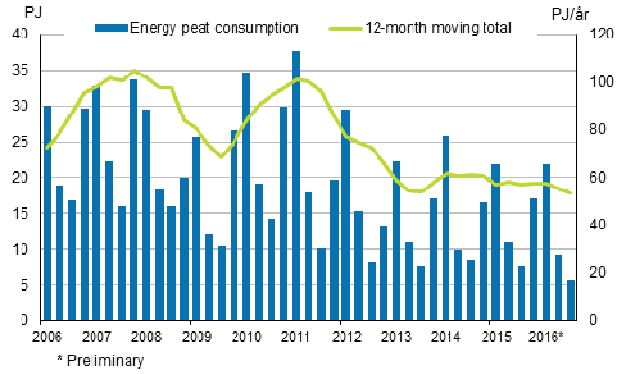

Figure 1: Consumption of peat in Finland

The main part among total annual extracted peat in the EU makes milled peat (80%), much less - lumpy peat (16%) and pelleted peat only 4%. Figure 2 shows more detailed distribution by countries. It should be noted that unlike Finland and Ireland, which produce mainly milled peat, in Sweden part of lumpy peat is quite high and is from 50 to 70%.

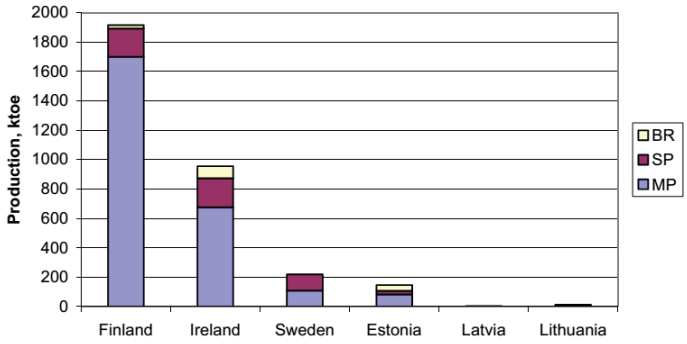

Figure 2: Production of peat

According to data [8] about 60 large factories (mainly CHP) and more than 120 boilers use peat or peat/wood mixture in Finland. According to information from [5] 20 CHP of them - is communal property, 27 belong to the CHP industry, 18 - are CPP stations. All these factories are equipped with boilers, which capacities are from 20 to 550 MWth, and produce about 7200 MW of thermal energy per year. In addition, peat share is more than 22% from fuel consumption of all Finnish CHPs, 19% from boiler houses fuel consumption and 8% of CPP consumption.

Ireland depends on imported energy on 90%. Peat in this country - is largest own fuel resources. According to [8], three CPP with 100-150 MW capacity and two CHP with 20 MW capacity are operated in Ireland, however, according to [5], the total energy output of three CPPs is about 370 MWe and share of peat in power generation - 13%.

There are 22 boiler houses and 9 CHPs using peat as fuel in Sweden. There are 3 CHP and some smaller power stations in Estonia. Peat as fuel is used in boiler houses of municipal authority and small boilers in private buildings in Lithuania. Latvia hasn't large energy plant on peat fuel, peat is used only by private households.

Figures 3 and 4 show the approximate location of objects using peat as a fuel and their subordination. The main using of milled peat occurs in powerful energy objects (Finland, Ireland) and lumpy peat is burned in boiler houses (Sweden, Estonia).

Financial performance of the industry, which consist of about 650 companies including 3 large companies, 70 medium, and others - businessmen, as follows: turnover from sales of peat on the EU internal market is about 424 million Euro and on the international market - 214 million Euro [5]. Fuel from peat can be produced in various forms in accordance with

consumer's needs – it is important for Ukrainian power industry. It means that it is advisable of CHP building and use of milled peat in areas that are relatively rich in peat and have compact site coverage, which requires electricity and heat. Prepared fuel in form of peat briquettes/pellets will be the best solution in case of dispersed private households.

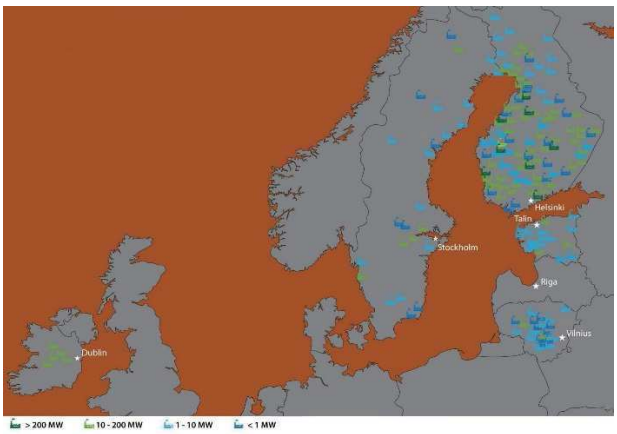

Figure 3 – Location of energy sites according to [8]

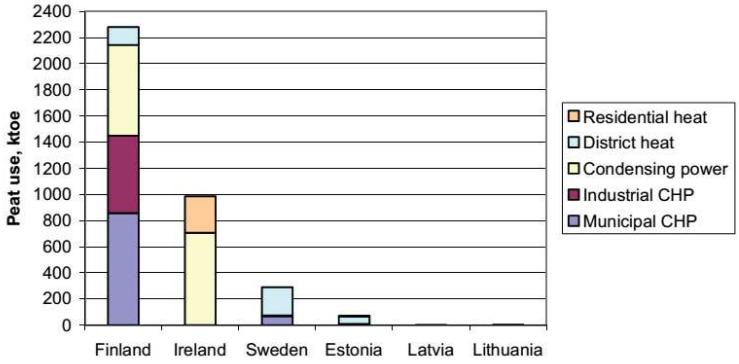

Figure 4: Distribution of energy sites [5]

Peat, which is produced annually, should be separated in a potential assessment as a renewable energy source. According to the most conservative estimates, annually about 2.5 million tons of peat (0.6 million tce/year or 0.42 million toe/year) can be used for energy targets. Now Ukrainian peat mining enterprises use about one percent of the available peat deposits. The average annual production of peat is 400 thousand tons. According to experts review, 17 million tons of peat are available for extraction till 2030.

Generally, the State balance of mineral reserves of Ukraine has recorded for more than 1,500 peat deposits with total reserves of about 1.3 billion tons in terms of dry peat. The largest number of stocks are concentrated in Volyn, Rivne and Chernihiv regions (100-200 mill tons each), Lviv, Zhytomyr, Kyiv, Sumy, Poltava (50-100 mill tons each) [10]. Traditionally, the main part of fuel peat (80%) is converted to other fuels and energy. About 15% of not treated fuel peat are used for non-energy purposes. The remaining peat is used by enterprises and organizations of other activities.

2. METHODOLOGY

The aim of this work includes the practical study of crushed peat combustion in experimental installation with retort-type burner, which was developed by the Institute of Engineering Thermophysics NASU.

The flow sheet of experimental installation with capacity up to 70 kW is shown in Fig. 5. The installation includes retort-type burner 1 with a screw feeder 2 that delivers fuel (milled peat) from the fuel hopper 3. Structurally, retort includes grating, on which biofuels is fed, and

which has distributed a supply of primary air in two areas: the first zone aimed to encourage the pyrolysis of peat and second - for post-combustion of carbonaceous residues. Torch from burner goes into fire chamber space of heat exchange unit 4, which is installed on the base 5.

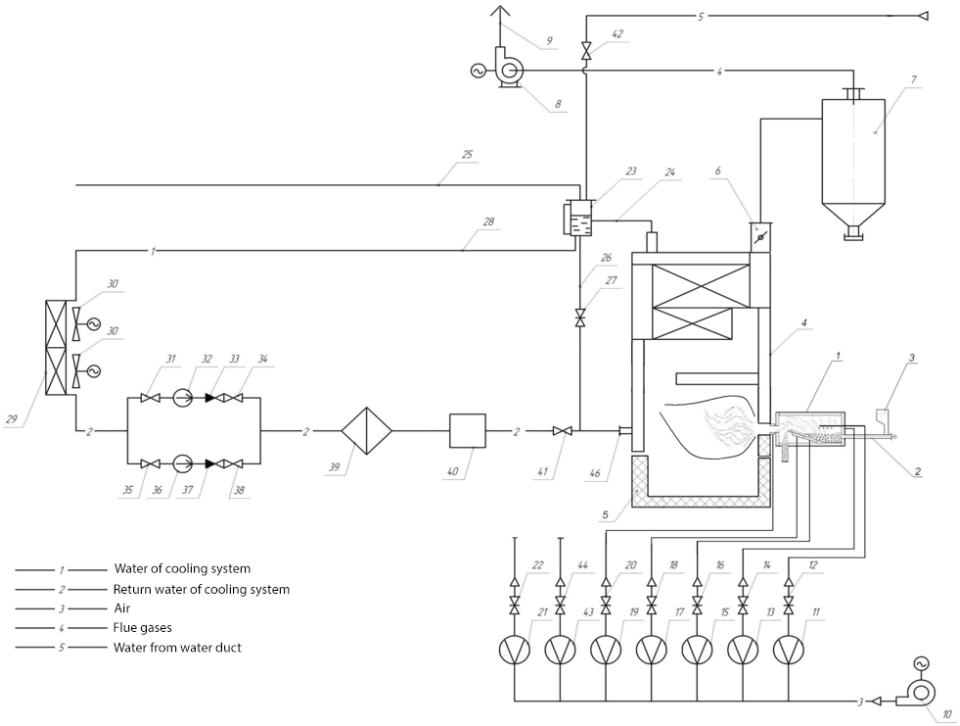

Figure 5 – Flow sheet of experimental installation:
1 – retort-type burner; 2 – screw-type fuel feeder; 3 – fuel hopper; 4 – heat-exchange unit; 5 – lined base; 6 – flue damper; 7 – cyclone; 8 – smoke exhauster; 9 – duct of flue gas removal; 10 – blow fan; 11, 13, 15, 17, 19, 21 – flow-measuring diaphragms; 12, 14, 16, 18, 20, 22, 27, 31, 34, 35, 38, 41 – cocks; 23 – extended tank; 24 – output pipe; 25 – exhaust pipeline; 26, 28 – pipelines; 29 – heater; 30 – axis fan; 32, 36 – circulating pumps;33, 37 – back valve; 39 – filter; 40 – heat energy meter; 46 – input pipeline.

A pipeline of flue gas removal from the heat exchange unit through flue dumper 6 connected by to cyclone 7 and smoke exhauster 8, the exhaust is directed to the duct of flue gas removal 9. Blow fan 10 with distribution pipelines is designed for air supply to the burner. Outdoors expansion tank 23 with water indication tube is installed at a level higher than heat-exchange unit 4. Outlet water pipe of heat exchange unit 4 is connected to pipe 24 of extended tank 23. It should be noted that closures and control valves are not installed on this pipeline. The exhaust pipeline connects the expansion tank with the atmosphere and also pipeline closures aren't installed. The installation is equipped with power and control panel, and with auxiliary equipment and other equipment.

Experimental study of the retort-type burner operation was performed using peat briquettes after heat treatment (see. Fig. 6).

To ensure the burning of such peat briquettes in developed retort-type burner with mechanical screw supply system, fuel briquettes were crushed into pieces with sized less than 30 mm. This was done manually, by hammers (Fig. 7). Fractional composition of crushed fuel peat is shown in Table 2.

Mass of crushed peat was determined by the method of bulk fuel weighing in the vessel of known volume. The data are presented in Table 3.

The results of these experiments demonstrate the functional ability of pilot burner on crushed peat and showed a sensitivity of contaminated matter emissions to variable regimes of the burner operation. The resulting values of CO and NO_x emissions at the fire chamber exit depending on the excess air ratio in terms of dry undiluted products of combustion with 0% oxygen content at fuel consumption 8.8 kg/h are shown in Figure 8. This figure also shows the

values of temperature at the burner output, depending on the total excess air ratio. These data identify possible trends of contaminated matter emissions at changing the excess air.

Figure 6: General view and dimension of peat briquettes

Figure 7: General view and dimension of crushed peat briquettes

Table 2: The fractural composition of crushed peat

Fraction size	>30…>20	>15	>10	>7	>5	>1	<1
Fraction composition, %weight	16.75	18.54	17.65	11.13	7.29	18.03	10.61

Table 3: Characteristics of crushed peat briquettes

Characteristics	Value
Moisture level in briquette, % mass.	15.0
Poured mass, kg/m^3	819.5
Higher temperature of burning, kJ/kg	17685.0
Lower temperature of burning, kJ/kg	16306.7
Theoretically necessary volume of air, nm^3/kg	6.047

According to the analysis of chemical composition of the combustion products, the residual oxygen concentration ranged without control from 3.8 to 8.9% vol., that correspond to the excess air ratio in the burner in the range of from 1.22 to 1.74.

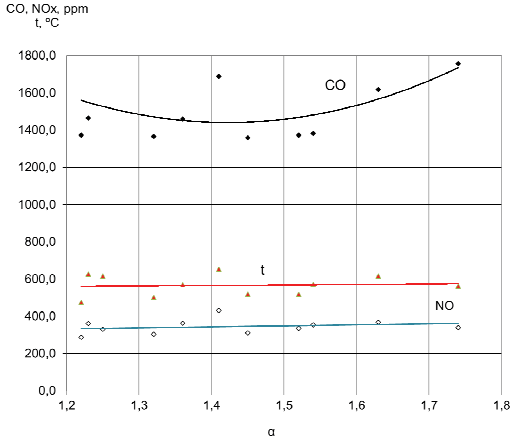

Figure 8: Emissions of CO and NO depending on the excess air ratio

The temperature of combustion products at the burner exit is ranged from 475 °C to 653 °C, in addition to that concentration of carbon monoxide is changed from 1359 to 1850 ppm at varied excess air ratio and the concentration of nitrogen oxides ranged from 287 to 431 ppm. The dependence of emission of carbon monoxide and nitrogen oxides on excess air ratio is shown in Figure 8. The trend line of CO concentration shows that CO emissions are minimal at excess air ratio from 1.35 to 1.55. The trend of NO_x concentration demonstrates a slight increase of NO_x emissions at rising of excess air ratio.

3. CONCLUSIONS

Summarizing the data presented in the review, the active use of peat as fuel is caused by not only rich peat resources but also by state policy against use of renewable energy in the energy consumption of the country. A responsible approach to the environment is required to use most of the features of effective local fuels consumption and try to expand the range of conventional combustion technologies. Experimental study of crushed peat combustion in installation with the retort-type burner is shown as an example of research for finding effective technologies and environmentally safety energy use of peat in installations with low capacity.

As a result, the conditions of stable work of burner with 65 kW capacity were discovered and regimes of combustion for crushed peat with 15% moisture content were found. Such regimes are suitable for implementation in the industrial equipment of different capacities.

References

[1] A. Belyakov A.S., Kosov V.I.,Gogin D. Yu. Peat resource potential with scientific and industrial potential of Russia in solving of heat power engineering, agro-complex and environmental protection regional problems// *Proceedings of the international conference "Peat in solution of energy, agriculture and ecology problems "*, May 29-June 2, 2006, Minsk, Republic of Belarus, pp. 16-20.

[2] V.I. Markov, N.I. Volkova Peat - renewable resources under our feet // *Ecology and Industry of Russia*, - M .: Kalvis, №1 January 2014, pp. 58-60.

[3] European Parliament resolution on a strategy for biomass und biofuels, 14 December 2006, "The European Parliament ... {78} Calls on the Commission to include peat, with regard…", http://www.europarl.europa.eu/oeil/FindByProcnum.do?lang=2&procnum=INI/2006/2082.

[4] A.V. Mikhailov, V.G. Selennov Peat in small-scale power engineering // *Academy of energy*, - St. Petersburg: Publishing House "President-Neva", No. 1 (27) 2009, pp. 48-56.

[5] Report «Peat industry in the six EU member states - summary report», which was prepared Paappanen Teuvo and Leinonen Arvo (VTT) for European Peat and Growing Media Association (EPAGMA) in 2010.

[6] Official Statistics of Finland (OSF):http://www.stat.fi/til/ehk/2016/03/ehk_2016_03_2016-12-21_kuv_005_en.html Source: The Bioenergy Association of Finland/Association of Finnish Peat Industries

[7] Official Statistics of Finland (OSF): http://www.stat.fi/til/ehk/2016/03/ehk_2016_03_2016-12-21_tie_001_en.html.

[8] EPAGMA ENERGY PEAT TRANSPARENCY POLICY 2014-2016 http://www.epagma.eu/sites/default/files/documents/epagma_energy_peat_transparency_policy_2014-2016.pdf.

[9] Law of Ukraine "On Ratification of the Nationwide Mineral Resources Base Development Program of Ukraine for the Period until the Year 2030" Date of entry into force: May 25, 2011

[10] http://plast.vn.ua/ru/0104_5.html.

TECHNICAL MONITORING RESULTS AFTER ENERGY EFFICIENCY INVESTMENT FOR A STUDENT DORMITORY IN PODGORICA

Violeta Rasheva[1], Christiyan Iliev[2], Veselka Kamburova[3], Drazen Karadaglic, Michael Velikanov[4]
[1]University of Food Technologies, Bulgaria; [2]University of Birmingham, Great Britain;
[3]University of Ruse "Angel Kanchev", Bulgaria; [4]Encon Services International, USA

ABSTRACT

Energy conservation measures (ECMs) were implemented in the Student Dormitory (Dorm) in 2013 in Podgorica, Montenegro. The Dorm has 2 buildings (Phase 1 and Phase 2 wings). The next ECMs are implemented: 1. Exterior walls thermal insulation on the Phase 2wing; 2. Energy efficient windows and doors with low U-values on all of the Phase 2 and partially of the Phase 1 wing.

The Dorm's annual energy consumption before the energy efficiency investments (i.e., the Dorm's baseline energy use) was estimated in 2012 [3].

The technical monitoring of energy consumption after investment in the Dorm indicates that the thermal ECMs provided a substantial saving of 14% for Phase 1 and 40% for Phase 2 of the Dorm. In addition, the building retrofit led to the improvements of the student room's comfort.

1. INTRODUCTION

Climate change and security of energy supply are two major challenges needing urgent actions. They have common causes and common solutions. The issue of energy consumption in buildings stands in the heart of the EU policy on energy efficiency. The energy consumption in the building sector has the largest share in the total energy consumption and the CO_2 emissions released into the environment [1]. Large part of this energy can be saved by renovation of the existing buildings and implementation of profitable energy conservation measures.

The aim of this paper is to report the results from technical monitoring after the energy efficiency investment implemented in the Dorm.

2. METHODOLOGY

Student Dormitory Buildings Characteristics (Table 1): The Dorm's main technical design documentation, including thermal engineering, was prepared 40 years ago. The buildings' thermal engineering was based on standards that largely ignored the „cost of energy use".

The Dorm was completed between 1975 and 1978: Phase 1 in 1975 and Phase 2 in 1978. Total floor area of all buildings is 10,700 m^2, while the total building envelope is 7,483 m^2. The Dorm is located within the complex of buildings of the University Engineering Faculty.

Table 1: Dorm characteristics

Characteristics	Phase 1	Phase 2	Headquarters Building: Offices, Kitchen, Restaurant	Total
Area, m^2	4,535.30	3,864.56	2,298.62	10,698.48
Heating Area, m^2	2,724	3,500	1,848	8,072
Number of inhabitants	~400	~600	-	~1000

[1] Professor PhD University of Food Technologies, Bulgaria; tel:+359897910737; e-mail: v_rasheva@abv.bg

The Dorm's Complex is the largest student dormitory in Montenegro, with two wings: Phase 1 with 181 student rooms and Phase 2 with 180 student rooms. The Phase 1 and 2 buildings accommodate up to 1,200 students. Phase 1 has 45 bathrooms and Phase 2 has 18 bathrooms. In the Phase 1, the two dorm rooms share one bathroom, while in the Phase 2, five rooms share one bathroom. Phases 1 and 2 combined have 70 corridors.

In addition, the Dorm has: Dorm Management Offices, Kitchen, Restaurant with line food service, Café bar, Student Club, Library; Internet Café, and TV Hall.

The Phase 1 and 2 buildings are used as a student dormitory almost all year. More precisely the Dorm rooms are used by students during the academic year from September 1st to June 30th of the next calendar year. Students use their rooms not only as bedrooms and living rooms, but also for studying. In addition, some students are preparing food in their rooms, ironing clothing washing in their bathrooms, etc.

The buildings are of a reinforced concrete. Concrete external walls were without thermal insulation. Doors and windows were wooden. Five years ago, some of original wooden doors and windows of the Phase 1 building were replaced with aluminum doors and windows. The flat roof is made of concrete and had no insulation.

Dorm systems: The Dorm does not have an independent space heating system. Instead, the Dorm shares its space heating system with the Engineering Faculty's other buildings. The Dorm's Buildings do not have ventilation or air conditioning systems.

University's Boiler Plant for Space Heating. Heavy-fuel oil fueled boilers, situated in the University's Boiler Room, supply space heating water to the Dorm Phase 1 and 2 buildings and other University's buildings. These boilers are not operated by the Dorm's staff. The University's Boiler Room has three heating boilers, manufactured by a company of Former Yugoslavia, now Croatia. One was produced in 1988 and has a power 3.25 MW, while another two are from 1977 and with the power of 1.9 MW each. Total power of the plant is 7.05 MW. The working regime of the system is 90/70°C with a pressure of 2.6 bars at 65°C. This information was obtained from the boiler room's main and the as-built technical design documentation.

University's Pipeline for Space Heating. The forced space heating pipe and the return pipe line have a diameter of 150 mm. The pipe run from the University's Boiler Plant to the University Engineering Faculty is 600 meters. At the distance of about 250 meters from the University's Boiler Plant, branch pipes, with a diameter of 80 mm, are welded to the main space heating and the return pipe. These branch pipes connect the University's main space heating lines to the sub-stations of the Dorm's Phase 1 and 2 buildings. Other Dorm's buildings, like restaurant, kitchen, café bar, student club, library, Internet café, and TV halls, are not connected to the University space heating lines. Space heating of these buildings is provided by individual heating units that use heating oil and by split electric-powered air conditioning units.

Before the energy efficient investment the University's Boiler Plant produced hot water for space heating from Monday to Friday for about 3 to 4 hours in the morning and 3 to 4 hours in the afternoon [3]. Heat was generated to meet heating needs of the University Engineering Faculty buildings not the Dorm's space heating needs. More precisely, the duration of the daily heating periods was primarily decided based on the heating needs of the University students attending classes. Thus, the space heating system is operated to meet classroom heating needs in the morning between 7:00 and about 11:00 and in the afternoon between 15:30 and about 17:30, for on average about 7 hours of heating per day. For the remaining about 18 hours per day, the University's Boilers are off.

During weekends (Saturday and Sunday) and during holidays and school breaks, the University's Boiler Plant is always off. On many weekdays, the Dorm's students remain in their Dorm's rooms for the entire day. Some of the students attend classes in the morning, some in the afternoon, but all of them are generally in their rooms in the evening and night. This is exactly when the University's Boiler Plant is off and heat is not provided by the University Line.

After the energy efficient investment the University space heating system operated for only 4 to 5 hours daily. Whenever the boilers are off, the Dorm's space heating is provided by in-room plug-in electric heaters and electric radiators, which are owned by the students. Often, even when the University line is operating the water temperature is far below the building's needs, and thus, the students using their electric heaters and radiators. It is likely that many students leave their electric heaters on all day for the entire heating season. The plug-in electric heaters/electric radiators have a capacity of between 1.5 kW to 3 kW each. Based on the inspection of rooms and the interviews with students and Dorm's maintenance staff, the monitoring team concluded that every one of the 381 rooms is normally equipped with at least one electric heater or radiator.

Radiators for Heating: A radiator-based heating system is used in Dorm's Phase 1 and 2 buildings. Before the energy efficiency investment the radiator's lacked control valves. Also the space heating sub-stations of both buildings were not equipped with electronic regulation or automated control systems. Radiators are 68 cm high and 10 cm wide and are in poor technical condition. The radiators in student rooms have 10 segments, in corridors they have 9 segments and in bathrooms, if they exist at all, radiators have 4 segments.

The headquarter building offices, restaurant, kitchen, etc. are heated using split air conditioners, electric heaters and other similar space heating devices.

Dorm's Maximum Heat Demand [2,4,6]. The University's Boiler of 3.25 MW is able to satisfy maximum heat demand of the Dorm. About 40% of the University's Boiler capacity is devoted to meet the Dorm's heat demand. This is based on the assessments of the monitoring consultant in close cooperation with University staff managing the space heating system

Domestic Hot Water (DHW) for the Dorm is generated by a DHW Boiler (model NP-125-MP) firing LFO oil. This Boiler is situated in the Dorm's Boiler Room in the basement of the Headquarters building near the Phase 1 building and it is equipped with a built-in fuel flow meter. The Dorm's DHW Boiler has a nominal heat capacity of 1.5 MW, nominal operational pressure of 0.5 bars, and the DHW (at nominal operational pressure) has a temperature of 100^0C. The DHW Boiler was produced by the Boiler Manufacturing Factory Metal in Preševo, Serbia, and has been operating since 1997. This information was obtained from the DHW Boiler's technical documents and was confirmed during the monitoring inspection. The DHW Boiler's flue gases are exhausted in the atmosphere using a chimney of 280 mm diameter. The Boiler has its own feeding pumps. A fan feeds air to burner. In addition to the Dorm's DHW Boiler of 1.5 MW, there are two new electric DHW Boilers produced by the Mikoterm Electronic Company. Each Boiler has capacity of 72 kW, and the total capacity of these 2 Boilers is 144 kW. The Boilers are equipped with electronic controls.

Thermal Efficiency of University's Boiler Plants [7,9]. To determine the efficiency of the boiler units operation, measurements of the operating mode of the water heating HFO boilers were performed. Analysis of the boiler's exhaust flue gas was made using a portable electronic gas analyzer Testo 350xl. The selected representative section, for the flue gas analysis, was at the horizontal gas duct after the back boiler chamber.

Boiler efficiency is derived using the following reverse balance equation:

$$\eta = 100 - (q_2 + q_3 + q_4 + q_5), \%, \quad (1)$$

where -q_2 is losses of heat with the exhaust flue gasses, %

-q_3 is heat losses due to the incomplete chemical fuel combustion, %

-q_4 is heat losses due to the incomplete mechanical fuel combustion, %

-q_5 is heat losses due to radiation into the environment, %

The temperature of the supplied air, the temperature of the exhaust gases, the excess air and other gas (i.e., CO, CO_2, O_2 and RO_2) levels in the flue gases were measured using the gas analyzer Testo 350xl. The supplied air is fed to the burner without heating or other treatment. The air's moisture content for the region of Podgorica is taken from the literature. The temperature of the fuel before the burner was measured using a thermometer. The

moisture, injected by the burner is assumed to 2 kg/kg (this value is normal for this type of burners). The Bacharach smoke number is determined using a sample of the sites HFO. The Q_5 (1.5%) losses are estimated by the team's expert based on hot water boilers with similar thermal capacity. The design power of the boiler is taken from boilers' passports (specifications). The efficiency of the University's Boiler Plant 1 is calculated to be 84.9%, and the efficiency of University's Boiler Plant 2 is calculated to be 88.1%

Thermal Efficiency of Dorm's DHW Boiler. The team's expert made efficiency measurements at the Dorm's DHW Boiler of 1.5 MW using the same portable electronic gas analyzer (Testo 350xl). The efficiency of the Dorm's DHW Boiler is calculated to be 83.6%.

3. TECHNICAL MONITORING

Thermal Energy: Based on measurements of the hot water flow rates, and the difference in temperatures of the hot water in-flow and return-flow, the daily heat energy consumption was calculated using the following formula:

$$Q = G \text{ x } (T_{in} - T_{out}) \times c \text{ x } t, \text{ kWh}, \quad (2)$$

where -G is volumetric flow rate, kg/s

-T_{in} is temperature at the inlet, ^oC

-T_{out} is temperature at the outlet, ^oC

-c is specific heat of the liquid, kJ/(kg.K)

- t is time of working of the system, h

Hot water flow rates and the temperatures of the in-flow and return-flow in the pipeline were measured 10,000 times at 2-minute intervals over the 14–day measurement period. The average outdoor temperature for the period from the 9th to the 23th December 2013 was 5.1°C.

Exterior wall U-coefficients were measured before and after investments in randomly selected rooms of the Dorm's Phase 1 and Phase 2 buildings. The U-coefficient after investment was measured using the U-value measurement device, model Testo 635-2. The results of measurements are given in Table 2.

Table 2: U-Value Measured on January 29, 2014

Measurement Site	Coefficient of Heat Transfer U, W/m^{2}K		
	Before [3]	After	Declined by
Phase 1 - Average	2.34	2.3	1.7%
Phase 2 - Average	3.22	0.64	80%

The coefficients of heat transfer of the external walls in the Phase 1 building were not changed after investment, since the external wall thermal insulation was not included in energy efficiency measures for Phase 1 building. The coefficient of heat transfer of the external walls of the Phase 2 building decreased significantly after investment. The thermal insulation included in energy efficiency measures at the Phase 2 building increased the heat resistance of the walls, thus decreasing the heat transfer coefficient by about 80%.

Building comfort is controlled by four variables [5, 7, 8]: Indoor air temperature, Surface temperatures, Relative air humidity, and Air speed (i.e. drafts). Indoor air temperature and relative humidity were measured before and after the investments, but air speed was not measured. After the investments, the average daily indoor temperatures increased from 21.1^{0}C before investment to 21.6 °C (Phase 1) and 22.8 °C (Phase 2) after investment. The average daily temperature after investment was generally above the recommended Dorm's temperature of 20°C. Humidity data were not measured before investment. After investment measurements indicate that Phase 1 and Phase 2 buildings had an average indoor air humidity of 44.28% and 41.96%, respectively. The average humidity is in the range of the recommended humidity levels of 35% to 50%.

The recent energy efficiency investments, including improvements in exterior wall insulation and windows and doors with lower U-values, should have increased interior wall surface temperature during the heating season, thereby improving building comfort. Similar improvements to exterior windows and doors should reduce infiltration losses thereby reducing drafts in the building and again should improve building comfort. Thus, the building retrofit is very likely to have improved of the Dorm's Phase 1 and 2 buildings' comfort.

The annual thermal energy consumption ($W_{g.a}$) is estimated as follows [2,4]:

$$W_{g.a} = K_{TM} * A_g * DH_{g.a}/1000, \quad (3)$$

where -A_g is total heated area;

-$DH_{g.a}$ is average annual degree hours for the heating season;

-K_{TM} is Heat Transmission Coefficient which reflects building heat transmission through walls, windows, doors and floors ($K_{TM} = 1000 \times W_{TM} / (A_g \times DH_{TM})$);

-W_{TM} is Measured thermal energy consumption;

-DH_{TM} is Degree hours during 11 days of measurements (outdoor temperature (T_{OUT}) and indoor temperatures (T_{IN}) were measured): $\sum(T_{IN} - T_{OUT})$ for 11 days.

The Dorm's energy efficiency measures led to energy savings of 14% for Phase 1 and 40% for Phase 2 (Table 3). During the monitoring period the University's space heating system operated for only 4 to 5 hours per day. To heat their rooms, the students used their electrical heaters. The Dorm Management has no information on time of electrical heaters operation and the actual consumption of student's electric space heaters. Since students do not pay electricity bills, it can be assumed that electrical heaters were even used in some rooms and some days/hours when the central space heating system was operating. If so, some measured indoor temperatures, and therefore, the estimation of the Heat Transmission Coefficient K_{TM} are likely to be impacted by electrical heaters operation. Consequently, the Dorm's thermal energy consumption estimate for space heating is likely to be under estimated.

Table 3: Annual Thermal Energy Consumption and Savings before and after Investment [3]

Indicator	Unit	Phase 1	Phase 2	Total
Thermal Energy Consumption before Investment	kWh/Year	568,959	731,041	1,300,000
Thermal Energy Consumption after Investment	kWh/Year	488,683	439,898	928,581
Thermal Energy Savings	kWh/Year	80,276	291,143	371,419
Thermal Energy Savings	%	14%	40%	29%

The electricity consumption before investments (Figure 1) shows seasonal usage changes with higher consumption from November to March and peak consumption in December. This is probably caused by the increased use of lights during the winter and the use of electrical space heaters in rooms that are under heated by the central heating system.

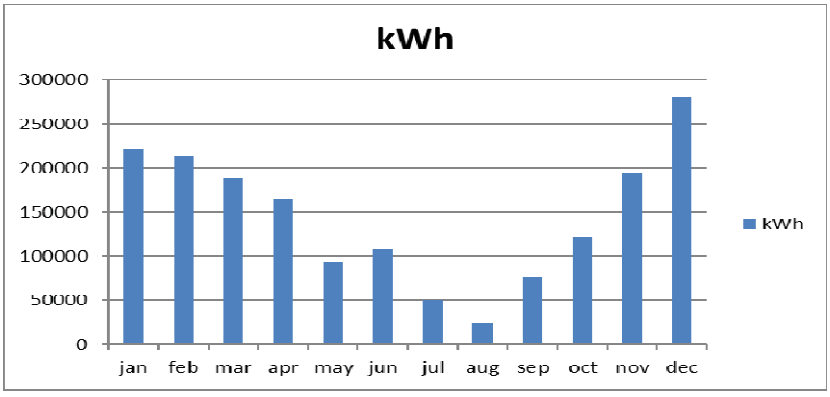

Figure 1: Total Monthly Electricity Consumption of All Dorm's Buildings in 2012

The electricity consumption data after investment (Figure 2) was collected during the 14-day technical monitoring period and for the four-month period after the investment were completed by the building owner. The after electricity consumption from October 2013 to December 2013 was higher than the electricity consumption for the same period in 2012. However, a new large Dorm's building was connected to Dorm's electricity meter (there is one electricity meter for the entire Dorm's Building Complex) and fewer hours of space heating was provided by the University's Boiler Plant so the students' electrical space heaters are assumed to have operated more.

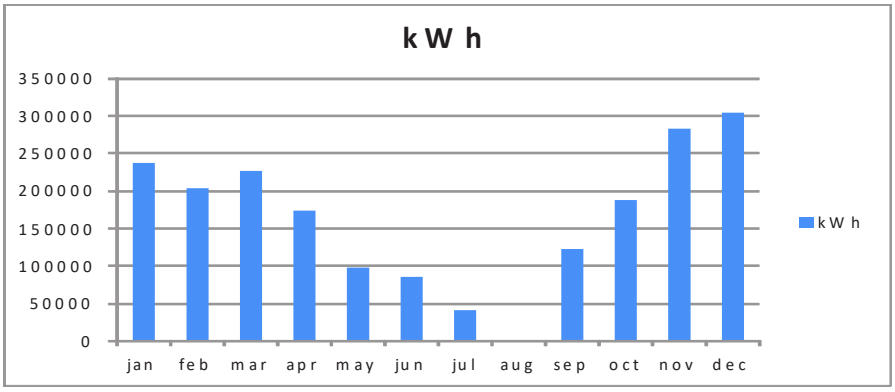

Figure 2: Total Monthly Electricity Consumption of All Dorm's Buildings in 2013

3. CONCLUSIONS

The technical monitoring and evaluation of energy consumption after investment in the Dorm indicate that the thermal energy system efficiency measures provided a substantial saving of 14% for Phase 1 and 40% for Phase 2 of the Dorm.

In addition, the building retrofit led to the improvements of the student room's comfort.

The electricity consumption in 2013 was higher than the electricity consumption for the same period in 2012. However, a new large Dorm's building was connected to Dorm's electricity meter and fewer hours of space heating was provided by the University's Boiler Plant so the students' electrical space heaters are assumed to have operated more.

References

[1] Balaras, C. A., A. G. Gaglia, E. Georgopoulou, S. Mirasgedis, Y. Sarafidis, D. P. Lalas - *European Residential Buildings and empirical assessment of the Hellenic building stock, energy consumption, emissions and potential energy savings Building and Environment*, 42 (3), (2007), pp. 1298-1314.

[2] Degree-days: theory and application. TM41:2006. The Chartered Institution of Building Service Engineers. London.

[3] Detailed Energy Audits. Monitoring Reports Before. *Available Technical Designs. Data and Information Obtained Directly from the Users of Buildings*.

[4] Iliev I, N. Kaloyanov, P. Gramatikov, V. Kamburova, A. Terziev, I. Palov, S. Stefanov, K. Sirakov. *Energy Efficiency and Energy Management Handbook, Bulgaria Energy Efficiency for Competitive Industry Financing Facility (BEECIFF): Project Preparation, Capacity Building and Implementation Support.* Sofia, Ministry of Economy, Energy and Tourism ("MoEET"), 2012.

[5] *Methodology of conducting energy audit for new and existing residential and non-residential buildings with simple and complex technical structure for the needs of technical certification of buildings (according to the Article 7-EPBD)*. EIHP Energy Institute Hrvoje Požar. Zagreb 2008.

[6] Рашева, В., *Енерго-технологичен анализ на промишлени предприятия.* Академично Издателство на УХТ, Пловдив, 2011.

[7] Reknagel H.. Sprenger E.. Schramek R.. Čeperković S.. *Heating and Air Conditioning*. Interklima-Grafika. 2004.

[8] *Rulebook on Yugoslav Standards for Thermal Techniques in Civil Engineering.(Official Journal of SFRY.* 69/87 and 54/89).

[9] Todorović B. *Design of Central Heating Facilities*. Faculty of Mechanical Engineering. Belgrade. 2005.

APPLIED MODELING for PRODUCER GAS FIRED COMBUSTION CHAMBER for MICRO GAS TURBINE

Cornel Sandu[1], Andreea Petcu Mangrea
Romanian Research & Development Institute for Gas Turbines COMOTI

ABSTRACT

This paper is an attempt of analyzing the possible conversion of a small power equipment from burning conventional liquid fuel to low calorific gaseous fuel, as producer gas.

1. INTRODUCTION

Nowadays, renewable forms of energy are constant preoccupation all over the world for many economies, regardless the level of development. This happens not only due to the reduction in the consumption of fossil fuels, with ecological benefits, but also waists from different economic activities, such as agriculture, turn into useful raw materials. It is the case of biomass, which can be converted into producer gas. At a first evaluation, the low calorific value seems to be a disadvantage, but with the new knowledge in combustion technologies it can be overcome. Considering the possible benefits, the authors took in account to derivate a shaft power gas turbine engine, Garrett model GTP 30-67, in such a way to make it able to run on producer gas. Good experience have been previously gained with this equipment when studying another nonconventional fuel[1] . In this endeavor, authors found very good inspiration in the studies [2], [3]. The most promissing result of several CFD simulation corresponding to few tehnical solutions was chosen to be presented in the following.

2. GEOMETRY

In Figure 1 the concept of the combustor, that will be part of GTP 30-67 turbo-shaft engine running on producer gas, is revealed.

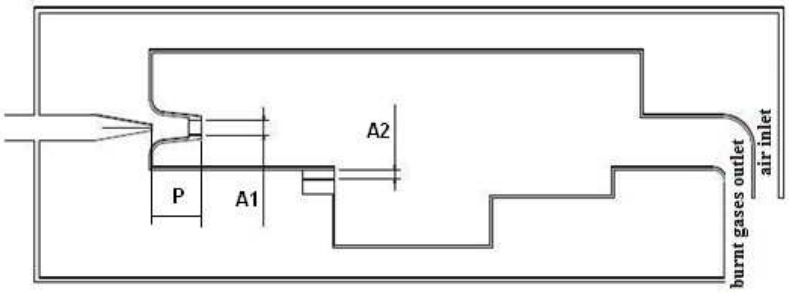

Figure 1: Physical model

It is an annular type combustion chamber in contrast with the solution used on the base engine. Because of very narrow space, resulting from back to back disposal of the compressor and turbine rotors, the reverse air flow is imposed. Air is delivered inside the flame tube in two stages. The primary stage is basically a nozzle ending with a rectangular section A1 and the secondary stage is a rectangular straight slot of A2 section.

The fuel injector is placed at the very entrance of convergent nozzle on the track of the primary air. Thus a small possible combustion zone is created. The chemical reactive gas

[1]Address: Bucharest, 164 Ion Mihalache Av., Apt. 27, Sector 1,phone:+40727113101,email:cornel.sandu@comoti.ro

mixture enters the flame tube, where it meets burnt gases coming here by recirculation. The role of recirculation products is firstly to reduce the oxygen concentration and secondly to bring an amount of heat in order to guarantee a stable burning. The reduction in oxygen concentration in this region is desirable, in order to avoid stoichiometric condition being fulfilled. The goal is to maintain the temperature under a value of 1800 K and thus to minimize the NO formation by thermal mechanism.

In the subsequent evolution inside the flame tube, reactive products reach the secondary air inlet section. Secondary air jet join the main flow, thus contributing by diffusion and mass transfer to the completion of combustion. Furthermore it adds kinetic energy, which provide a higher recirculation rate of the burnt gases. A cavity is provided just below the secondary air inlet in order to offer the necessary space to generate a swirl. This rotor behaves as a kinetic accumulator, intended to reduce fluctuation in the main flow.

Fuel injection section is a very narrow rectangular slot. Accordingly fuel exits in a flat jet, this shape being considered to fit in the best way with the geometry of the first stage burning chamber. One can also assume that a flat fuel jet mixes easier with air, especially in the confined primary zone of combustion.

Based on all above assumptions a practical solution was imagined. As shown in Figure 2 it is designed as a circular chain of identical narrow cylindrical segments. In this way, a very discreet fuel and air injection are provided, with good consequence regarding mixing and, therefore combustion characteristics.

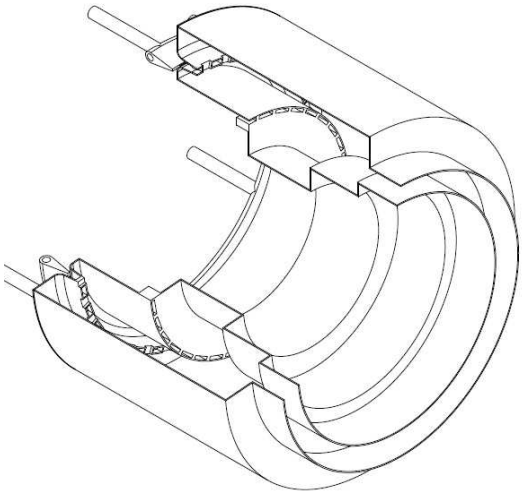

Figure 2. Constructive solution for the combustion chamber using producer gas

3. COMPUTATIONAL DOMAIN

Numerical evaluation of the proposed technical solution was carried out by using the commercial code ANSYS CFX. The geometrical CAD model is a 10 degree cylindrical sector corresponding to a base element of the circular pattern which represents the combustor. Computational mesh(Figure 3), accomplished through ICEM CFX, is in unstructured tetrahedral format, with 5,696,798 elements.

Boundary conditions :

T_{aaer}= 450 K: inlet air temperature

T_{acomb}= 288 K : inlet fuel temperature

$\dot{m}_{aer}$= 0,012 kg/s : inlet air mass flow

$\dot{m}_{comb}$= 0,0024 kg/s : inlet fuel mass flow

p_{ega}= 2 bar : outlet burnt gas relative pressure

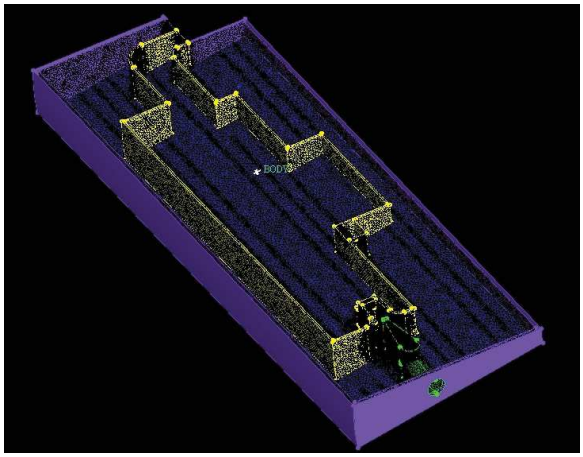

Figure 3. Computational grid

The specific models used in the numerical simulation of combustion process are presented in Table 1.

Table 1: Simulation models

Turbulence model	*k-ε*
Combustion model	*Eddy Dissipation Model (EDM)*
Reaction mechanism	*Methane Air WD2 (multi step)*
Reaction mechanism	*Hydrogen Oxygen(multi step)*
Reference pressure	*101.323 Pa*
Reference temperature	*280K*

4. RESULTS

The total temperature map corresponding to the diametrical axial plane of the combustor device is displayed in Figure 4. As seen, an uniform field of temperature was obtained in the hot region of fire tube.

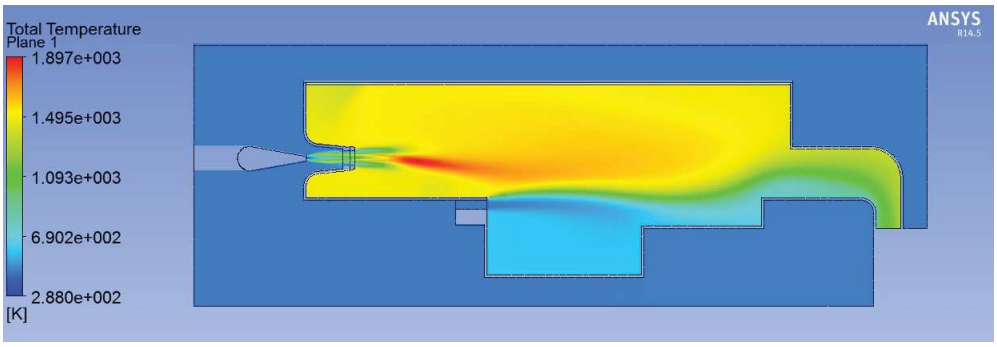

Figure 4. Total temperature map

To reveal, even more, the uniform temperature distribution, the simulation was undergone to a post processing using total temperature isosurfaces(Figure 5) . The corresponding temperature of these surfaces are (from red to green): T_1= 1850 K ; T_2= 1500 K ; T_3= 1400 K ; T_4= 900 K;

Using the same plane as for the temperature map, a velocity vector plane was processed(Figure 6). An intense recirculation of burnt gases can be observed from exit to the primary combustion zone.

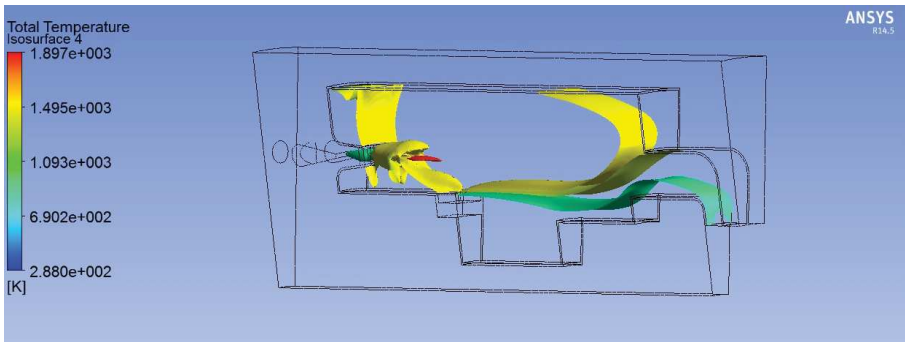

Figure 5. Total temperature isosurfaces

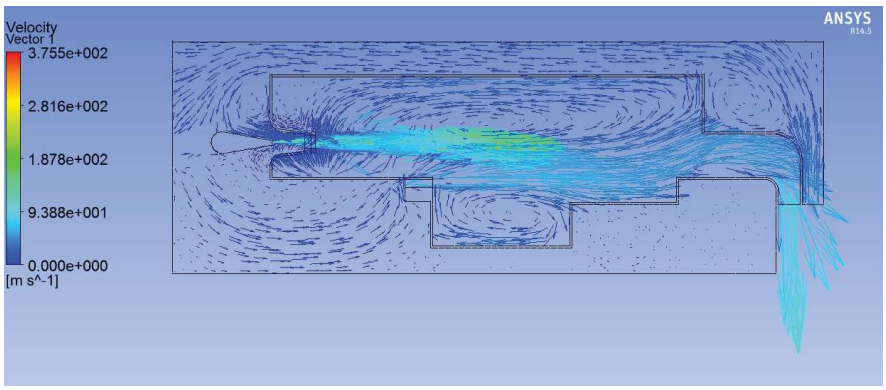

Figure 6. Velocity vector plane

The most significant parameters, resulting from simulation, are included in the following table.

Table 2 : Calculated parameters

Average outlet burnt gases total temperature	T_{ega}= *1095 K*
Average outlet burnt gases velocity	w_{ega}=*95 m/s*
CO mass fraction in outlet burnt gases	*0.17 ppm*
CH_4 mass fraction in outlet burnt gases	*0,016 ppm*
Fuel inlet velocity	w_{acomb}= *135 m/s*

5. CONCLUSIONS

An annular combustion chamber with very discrete injection of fuel and air supply is a viable solution for running a gas turbine with producer gas. Good burning feature is theoretically achieved in the combustion device, due to the intensive recirculation of flue gases and secondary air intake. Rather than being used in combustion process only, the secondary air injection is mainly used for enhancing burnt gases recirculation and obtaining an favorable temperature cross profile at the combustion chamber exit.

There are good premises to start the design of an experimental model using the computational model, in order to validate the theoretical results.

References

[1] Petcu, A.C., Sandu, C., Berbente, C., *Numerical simulations of Jet-A combustion in a gas turbine combustion chamber*, International Journal of Engineering and Innovative Technology (IJEIT) Volume 3, Issue 1, July 2013

[2] Al-Halbouni, A., et. al., Applied Modelling for Bio- and Lean Gas Fired Micro Gas Turbines, www.uni-due.de/imperia

[3] Al-Halbouni, A., et. al., New Burner Systems with High Fuel Flexibility for Gas Turbines, www.uni-due.de/imperia

HEAT RECOVERY IN METALLURGY. TECHNICAL AND ECONOMICAL ASPECTS OF USING ORC INSTALLATIONS IN ROMANIA

Associate Prof. Mircea SCRIPCARIU Ph.D.[A,1] , Lecturer Ioan BITIR-ISTRATE Ph.D[A], Associate Prof. Mihai BUȚU Ph.D.[A], Associate Prof. Radu PORUMB Ph.D.[A], Alexandru PAVEL Ph.D.[B], eng. Mariana PĂTRĂȘCAN[B]
[A]University Politehnica of Bucharest,
[B]Elsaco ESCO
[3]tel.: 0040214029846, email: mirceas1960@yahoo.com

ABSTRACT

Energy efficiency is a key factor for the sustainable development and competitiveness of the Romanian industry. In the last years the energy intensity of this sector has decreased with 43% but still has further potential. The aim of this paper is to present the conditions in which heat recovery using ORC installations is technically feasible and economically attractive in the metallurgy industry. The first section briefly presents the energy efficiency and the environmental impact aspects for this industrial sector. Next are identified processes with heat recovery potential and technical solutions using installations operating on ORC cycle for low temperature thermal energy capitalization. The economical efficiency is further analyzed, highlighting the conditions leading to successful projects in the Romanian energy market conditions. Conclusions and recommendations are drawn up using the sensitivity analysis and a comparison between different ORC equipment sizes.

Keywords-energy efficiency, heat recovery, industrial process, ORC cycle, electricity generation, economical performances.

1. OVERVIEW REGARDING ENERGY CONSUMPTION AND ENVIRONMENTAL ASPECTS IN ROMANIA

The economy primary energy consumption during 2008 thru 2015, decreased with 20.5%, recording 31844 ktep [1]. In 2015, gas consumption had the highest weight in the primary energy consumption with 31.3%.

In the same period, the final energy consumption decreased with 12.5%, mainly due to a 26% reduction in the industrial consumption. Out of the energy intensive branches, metallurgy recorded an increase in its energy consumption in 2015 compared with the year 2012 (+ 122 ktep, representing + 7.4%), while the chemical industry recorded a decrease of its energy consumption (- 244 ktep, representing - 14.7%).

The typical indicator for energy efficiency at the national level is the energy intensity. In table 1 the trend of the energy intensity for Romania during the period 2007-2014 is presented. Energy intensity recorded a drop with around 43% both due to measures taken by the industry for energy efficiency improvement and to the restructuring process that took place in the economical crises period, closing down of production capacities included. Even with a favourable trend in the analysed period, energy intensity still has values over the UE-28 average, placing Romania among the most energy intensive countries in Europe.

The energy economy potential, mainly losses reduction in Romania, is estimated at approximate 28% of the final energy consumption. For the industry, the estimate is 20% [3, 4]. Industry represents the economy branch with the highest contribution to environmental pollution, through the large quantity of gaseous, solid and liquid pollutants evacuated in air, water and soil.

[1] 313 Splaiul Independentei, tel.: 0040214029846, email: mirceas1960@yahoo.com

Table 1 Energy intensity trend, 2007-2015 [2]

Indicator	2007	2008	2009	2010	2011	2012	2013	2014
M.U.	tep/1000EUR							
Primary energy intensity	0.428	0.404	0.374	0.384	0.384	0.373	0.335	0.330
Final energy intensity	0.269	0.254	0.244	0.251	0.245	0.244	0.236	0.215
Industry energy intensity	0.361	0.336	0.252	0.230	0.216	0.210	0.208	0.206

The impact on air quality is generally caused by the IPCC[2] installations operation or by exceeding the emission limits or the ceiling values established for specific pollutants: particles, sulphur oxides, nitrogen oxides, heavy metals (e.g., zinc), volatile organic compounds (VOC). As for the water quality impact, this is caused by the installations' age, inappropriate operation of stations/installations for technological wastewater treatment/pre-treatment as well as to the inefficiency of air decontamination installations. Soil is polluted firstly by the incorrect storage of solid waste resulted from specific industrial production processes than, indirectly, through acid deposition and through exploitation of raw material resources needed by the industry.

Between 2010 and 2013, Romania recorded a decrease of GHG[3] emission with approximately 6.32%, which place it among the countries with the most important reduction of this indicator. In 2012, values reported for Romania were with 26.73% higher than the average value in EU (see figure 1). This decrease continued over the years till 2016 due to structural changes the industry is permanently showing.

Among activities with significant environmental impact for metallurgy can be mentioned [6]:

- metal production in primary forms and semi-finished, activity with air pollution impact,
- hot rolling and applying coatings of molten metal.

The actual economical situation transforms activities like ensuring of energy resources, the need for CO_2 emission reduction as well as the environmental protection in major challenges for the energy management at national level [5].

2. THE NEED AND OPPORTUNITY OF HEAT RECOVERY IN METALLURGY

Processes generating secondary energy sources like heat are frequently encountered in Romanian metallurgy. It is mainly about combustion processes for heat treatment or for waste neutralization (melting, quenching, incineration, drying, etc.) followed by warm or hot flue gases release through exhaust chimneys. Not always this secondary energy source is recovered, mainly due to technical and economical reasons.

The technological recovery direction (that assumes the use of the thermal energy in the same technological process) is limited mainly due to thermal-technical reasons.

The power generation direction (generation of warm/hot water in a heat exchanger) needs an advanced simultaneity with a consumer or the existence of a storage equipment, with an important investment requirement.

The recovery of the energy content from the secondary sources needs to pass over all the obstacles of technical or economical nature to exploit its exceptional potential regarding the improvement in energy efficiency. One of the best solutions in this direction is represented by

[2]IPCC – Intergovernmental Panel on Climate Change
[3]GHG – Greenhouse gas

the valorisation of this potential to generate a superior form of energy, electricity. In this way disappears the limitation given by the need for simultaneity of energy generation and consumption due to the permanent electricity demand on the industrial sites. In addition, it is generated an expensive resource, fact that brings positive effects in the field of energy efficiency and of environmental protection in the whole transformation chain in the national electricity grid.

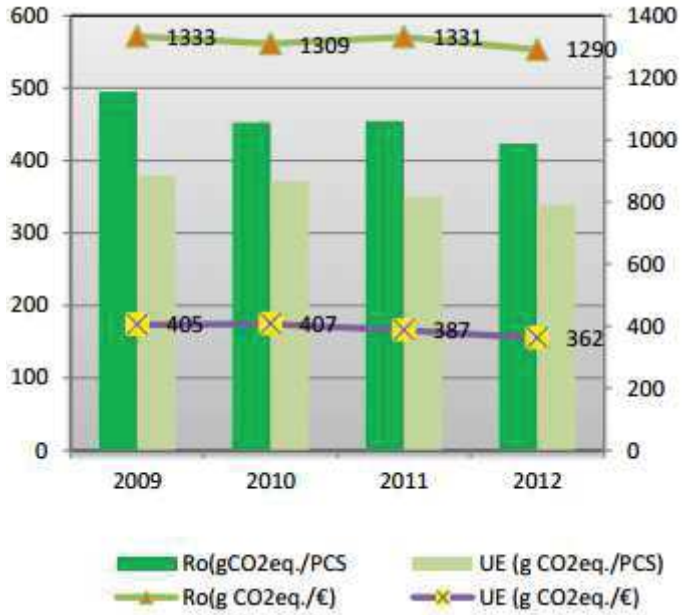

Figure 1 Trend of GHG emission for each GDP[4] unit and calorific value at EU level and for Romania [6]

3. GENERAL ASPECTS REGARDING THE TECHNOLOGY FOR ENERGY GENERATION USING INSTALLATIONS OPERATING ON ORC CYCLES

The Rankine Organic Cycle (ORC) represents, from the thermodynamics point of view, one of the most efficient technologies of heat conversion into electricity. The range of electricity output for the equipment relying on this technology is mainly between 50÷2,200 kWe, depending on the manufacturer. Yet, on the market, one can find solutions based on ORC cycle with higher installed capacities (5÷70 MWe), solutions developed mainly by manufacturers like Ormat, Enertime, Cryostar [8, 9].

The main factor that influences ORC technology parameters is the hot source temperature. Thus, in figure 2 it is shown the range of needed temperatures at the hot source for the main manufacturers developing this technology [8, 9]. As well, the electricity efficiency of the ORC based equipment and the selection of the working fluid (organic) depends on the hot source temperature.

When the ORC installation works in cogeneration (with heat generation or refrigeration energy combined or not with an additional equipment), the global efficiency is around 86÷90%.

For example in Romania, in other industries, a Turboden ORC unit has been installed in Gherla and it generates 1.4 MWe and about 5.3 MWt. Generated heat is used for the factory's wood process treatment and electricity is delivered to the grid. Sortilemn consumes heat in its process for boiling logs and in its wood presses, veneer and timber drying kilns [7].

[4]GDP=Gross Domestic Product

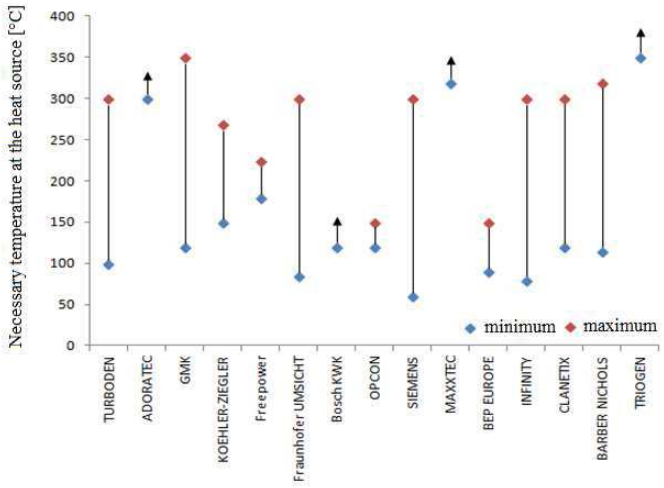

Figure 2 The range of the needed temperature at the hot source for the main ORC technology manufacturers

4. ECONOMICAL OPPORTUNITY ANALYSIS OF USING ORC EQUIPMENT IN THE METALLURGICAL SECTOR IN ROMANIA

The economical analysis using indicators highlighting costs and benefits resulting from energy efficiency improvement projects, during the entire life span of the equipment, is recommended by the energy efficiency legislation promoted at the European Union (EU) level [10] and transposed in Romania through Law no. 121/2014 [11].

For the opportunity analysis of heat recovery solutions in the metallurgical industry with ORC cycle based installations, the following indicators were used:

- NPV (Net Present Value) that quantifies the profitability over the life-cycle,
- IRR (Internal Rate of Return), useful for the financing cost analysis and ascertainment of the funding opportunity through grants (e.g. the Large Infrastructure Operational Programme-POIM that will be available in Romania until 2020),
- Cost/benefit ratio (CBR) that gives decision-makers an image on the economies that can be achieved for each spent euro,
- Simple payback period (t_r) that is useful for assessing the speed for investment recovery and, moreover, it gives a piece of information on the efficiency of such investments in comparison with those for the core business.

The technical-economical analyses were performed by the authors for a range of ORC units between 400 and 1,790 kW in two technological solutions:

- With the valorisation of thermal energy,
- Without the valorisation of thermal energy.

From technical literature and recent procurement documents it could be established ranges for the specific investment costs [12]. The valorisation of thermal energy required an increase of the specific investment cost determined by the hot water preparation installations.

The technology used for the steam turbine in the thermodynamic cycle of the ORC installations allows for a very high availability of the generation units, of about 98%. Generally speaking, these installations need only 3÷5 hours/week for maintenance works.

For the calculation of the thermal energy generated by the ORC installations, the following evaluation has been considered for the boilers working on natural gas whose production of thermal energy can be replaced: efficiency $\eta = 0.8$ and $y = 0.25$, the cogeneration index of the units with steam turbine, generating simultaneously electricity and thermal energy.

In order to calculate the economical indicators, the following avoided costs were taken into consideration:

- with the procurement of electricity,
- with natural gas.

In table 2 there are presented the results of the economical analysis for projects using ORC units for heat recovery in the metallurgical processes in the case of using the minimum values of the range for the investment costs.

The main conclusions are:

- Projects in which the thermal energy, resulting from the Rankine cycle with organic fluids, can be used on site are economically attractive,
- The development of projects in which the thermal energy resulting from the cycle is exhausted in the atmosphere are not feasible in the conditions given in Romania,
- Projects in which thermal energy from ORC units can be used on site, become attractive for units starting with installed capacities $P_i \geq 700$ kW. If the specific investment is close to the minimum level of the range, even projects with 600 kW units become economically viable.

For establishing conditions in which projects using ORC installations for heat recovery in the metallurgical sector become economically attractive were developed sensitivity analyses of the economical indicators when specific investment, annual operation hours, annual operation costs, electricity and gas prices on the market vary. They were done for the case of the 400 kW ORC unit, see table 3.

Table 2 Results of the economic analysis for projects using ORC installations for industrial heat recovery. The case of using the minimum value of the investment cost range

P_i	With the valorisation of thermal energy				Without the valorisation of thermal energy			
	NPV	IRR	t_r	CBR	NPV	IRR	t_r	CBR
kW	euro	%/year	years	-	euro	%/year	years	-
400	-1,580,682	4	8.0	0.75	-4,178,529	<0	28.6	0.27
600	218,286	13	5.4	1.07	-3,678,485	<0	17.3	0.39
700	1,872,985	20	4.1	1.38	-2,673,247	<0	12.4	0.50
970	3,043,928	22	3.9	1.46	-3,255,851	<0	11.5	0.54
1,790	7,548,338	28	3.3	1.70	-4,077,027	1	9.5	0.63

Every economical indicator proved to be very sensible to the investment cost (IC) and the annual operation hours (t_f). A variation in the annual operation costs (C_{op}) has a less significant influence on the economical performances of projects for heat recovery in the metallurgical industry with ORC equipment.

Electricity and gas prices (p_{el}, p_g) on the Romanian market that determine the avoided costs for electricity and thermal energy, have an influence on the values of NPV and IRR.

A drop in the annual operation hours to values bellow 7,800 hours/year makes only projects with ORC units over 700 kW economically attractive, if the thermal energy resulting from the thermo-dynamical cycle is used on-site.

Table 3 Results of the sensitivity analyses of the economical indicators. The case of 400kW ORC units with the valorisation of thermal energy

Criterion		NPV	IRR	t_r	CBR
Variable	IC, ↓10%	↑37%	↑59%	↓11%	↑12%
	t_f, ↓10%	↓27%	↓57%	↑13%	↓10%
	C_{op}, ↓10%	↑3%	↑6%	↓1%	↑1%
	p_{el}, ↓10%	↓10%	↓21%	↑4%	↓3%
	p_g, ↓10%	↓17%	↓36%	↑8%	↓6%

5. MAIN CONCLUSIONS AND RECOMMENDATIONS ON THE DEVELOPMENT OF PROJECTS USING ORC INSTALLATIONS FOR HEAT RECOVERY IN THE METALLURGICAL INDUSTRY IN ROMANIA

The analyses performed for this paper highlight the following recommendations that could bring a contribution to the successful development of heat recovery projects using ORC installations:

- This solution of heat recovery is advantageous on industrial sites where there is a demand low parameters heat during the whole year,
- Projects become attractive for ORC units starting with 600 kW installed capacity; projects with smaller units could become efficient only if grants are available,
- Projects were heat resulting from the ORC cycle is not used on site become feasible only if a support scheme is available,
- Along with the complete market liberalization for gas and an increase in the electricity and gas prices, we consider that a support scheme may help such projects to become attractive for decision-makers in the industry.

Authors shared in this paper their experience in working with the industry and consider that the results could help decision-makers in the metallurgical sector to become more efficient by cutting the energy costs through innovative solutions. We would like to continue our research on the benefits of using ORC installations for heat recovery in the industry with a detailed case study.

References

[1] National Institute of Statistics, *Statistical bulletins*.
[2] The Romanian Energy Regulatory Authority (ANRE) – the Energy Efficiency Department, *Trends of energy efficiency and energy policy in Romania*, September 2015.
[3] European Bank for Reconstruction and Development (EBRD), *Strategies and Policies*.
[4] The Romanian Energy Regulatory Authority (ANRE), *Reports on energy efficiency*.
[5] Ministry of energy, *Romania's energy strategy, document for public debate*.
[6] National Agency for Environmental Protection, *Annual report on the environmental status in Romania 2014*, www.anmp.ro
[7] http://www.turboden.eu/en/public/press/2011_ROMANIA_SORTILEMN_DEF.pdf
[8] https://www.environmental-expert.com/companies
[9] Reza Rowshanzadeh, *Performance and cost evaluation of Organic Rankine Cycle at different technologies* – Master thesis, Department of Energy Technology KTH Sweden, http://kth.diva-portal.org/smash/get/diva2:410363/FULLTEXT01.
[10] Directive 2012/27/EU of the European Parliament and of the Council on energy efficiency.
[11] The Romanian Parliament, *Law no. 121/2014 on energy efficiency*.
[12] Company brochures: TURBODEN, AQYLON, ElectraTherm, CALNETIX.

INSTABILITY IN OPERATION OF A SOLAR POWERED H_2O-LIBR ABSORPTION COOLING SYSTEM

Iuliana ŞORIGA[1], Adina GHEORGHIAN[1], Camelia STANCIU*[1],
Dorin STANCIU[1], Beatrice TĂNASE
University Politehnica of Bucharest, Department of Engineering Thermodynamics, Heat Engines, Thermal and Refrigeration Equipment

ABSTRACT

Daily operation of a solar powered simple effect one stage water - lithium bromide absorption cooling system is analyzed. The whole system is composed by a parabolic trough collector concentrating solar energy into a tubular receiver, a fully mixed thermal water storage tank and the absorption cooling system. Water is solar heated and stored to be used for maintaining the cooling system in operation as long as possible during the considered day. Time dependent cooling load is considered for the air conditioning of a residential two-storeys house. The aim is to correctly size the solar collector and storage tank and thus a parametric study is performed in this regard. The results emphasized high operation instability of the cooling system due to the large interval of variation for desorber temperature. Optimum dimensions of the storage tank associated to a specific solar collector dimension are determined to ensure the longest continuous startup operation of the cooling system.

1. INTRODUCTION

The main advantages of absorption cooling systems (ACS) compared to mechanical vapor compression ones (VCS) consist in the following issues: they do not use greenhouse gases (CFC) as refrigerants; are able to use other energy sources than electricity, including solar energy; they are silent. As regarding the cost, ACS are significantly more advantageous than the VCS [1, 2]. According to [3], most ACS use balanced liquid/vapor absorption cycles, particularly the ammonia/water systems for refrigeration and lithium bromide/water systems for air conditioning. In some experimental prototypes a plate or coaxial heat exchanger was introduced to reduce heat loss and dimensions, and therefore increase the system energy efficiency. A new ACS cycle (H_2O-LiBr) for cooling a house with a total area of 300 m^2, powered by solar energy, is proposed in [4]. Using storage tanks effectively balances the cooling load, enhancing the ability to provide cooling on demand. The results showed that this system can solve the problem of mismatch between solar radiation availability and demand for air conditioning. Paper [5] analyzes a solar assisted H_2O-LiBr ACS for residential buildings. In normal operation conditions, single-effect H_2O-LiBr ACS need inlet temperatures between 80 and 100°C and achieves a coefficient of performance (COP) of about 0.7. The authors concluded that the ACS using H_2O-LiBr as the working fluid are suitable for domestic applications. A commercial single-effect H_2O-LiBr ACS, with a cooling capacity of 4.5 kW, intended for domestic use, has been tested in [6], to determine its energy performance. In simulations over a period of 20 days, for inlet water temperature values between 80 and 107°C, the total energy supplied to the vapor generator has reached 1085.5 kWh, the heat removed from the evaporator was 534.5 kWh, and the average COP for the entire period was 0.49. Paper [7] presents a feasibility study of a solar power ACS, located in Tunisia. The system was modeled using TRNSYS and EES programs, based on input data regarding annual weather

*Corresponding author: camelia.stanciu10@yahoo.com

forecast in Tunisia. The authors found that the system optimized for a typical 150 m^2 building should contain a H_2O-LiBr ACS with a capacity of 11 kW, flat-plate solar collectors with a total area of 30 m^2 and a 0.8 m^3 hot water storage tank. The designing of a 11 kW H_2O-LiBr ACS, which could cover the cooling load of a typical house in Cyprus is described in [8]. The optimal system obtained by the authors from the simulations consisted of 15 m^2 parabolic collectors, inclined at 30° from the horizontal, an ACS, and a hot water storage tank of 600 l.

In this paper, instability in operation of solar assisted H_2O-LiBr ACS is emphasized due to the small range storage tank water temperatures for which the system can operate. In this context, we present here an optimization study regarding the solar collector and storage tank size coupled to a simple effect single-stage water – lithium bromide ACS. The goal of this optimization is to maximize the working period of the system during the day.

2. MODEL AND RESULTS

Figure 1 shows the schematic representation of the studied ACS. The absorption cooling system is powered by a parabolic trough collector (PTC). The PTC useful heat is stored in a fully mixed water storage tank with the role of ensuring a longer period of constant heat supply to the generator, independently of the solar irradiance fluctuations. To simulate the transient operation of the presented system, a mathematical model is proposed and implemented in Engineering Equation Solver [9]. The studied ACS cooling load is correlated to the requirements for the air conditioning of a residential two-storeys house on July 15th, in Bucharest climatic conditions [10]. It varies between 1.9 kW and 4.7 kW along the day, the maximum being attended at 2PM.

Applying the first law of thermodynamics, the following differential equation is obtained, describing the storage tank water temperature variation in time:

$$\left(m \cdot c_p\right)_{ST} \frac{dT_{ST}}{d\tau} = \dot{Q}_u - \dot{Q}_G - \left(UA\right)_{ST}\left(T_{ST} - T_a\right) \tag{1}$$

where m is the storage tank water mass [kg]; c_p is water specific heat capacity [J/(kg·K)]; T_{ST} is the tank water temperature [°C]; Q_u is the PTC useful heat rate [W]; Q_G is the heat rate transferred to the vapor generator [W]; $(UA)_{ST}$ is the overall heat conductance (product between the global heat loss coefficient and tank surface) [W/K]; T_a is the ambient air temperature [°C].

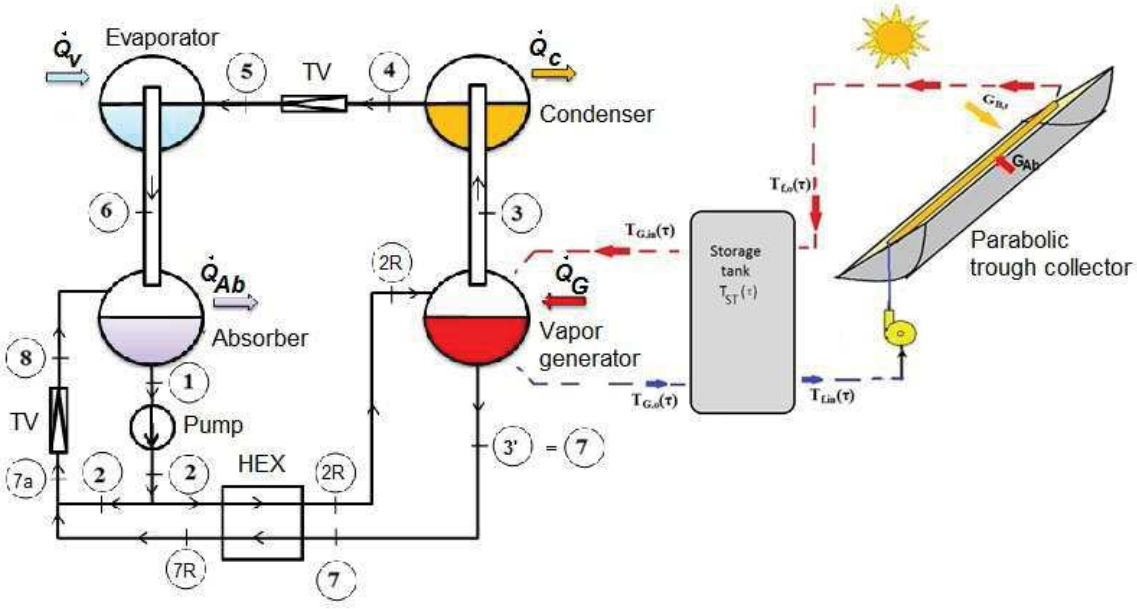

Figure 1: Absorption cooling system with H_2O-LiBr and parabolic trough collector.

The solar collector mathematical model has been thoroughly described in [10].

The thermal loads of the evaporator and condenser were determined by equations (2) and (3):

$$\dot{Q}_V = \dot{m}_0 (h_6 - h_5) \tag{2}$$

$$\dot{Q}_C = \dot{m}_0 (h_4 - h_3) \tag{3}$$

where h is the specific enthalpy [J/kg] of H_2O vapors that left the desorber; $\dot{m}_0$ is the refrigerant (H_2O) mass flow rate crossing the two heat exchangers [kg/s].

Energy balance equations for the absorber and desorber (vapor generator) are given by equations (4) and (5):

$$\begin{aligned} &-\dot{m}_0 h_6 - \left(\dot{m}_{Ab} - \dot{m}_0\right) h_8 + \dot{m}_{Ab} h_1 = \dot{Q}_{Ab} \\ &\Rightarrow \dot{Q}_{Ab} = -\dot{m}_0 \left[h_6 - h_8 + (f + a)(h_1 - h_8)\right] \end{aligned} \tag{4}$$

$$\begin{aligned} &\dot{m} h_2 + \dot{Q}_G = \left(\dot{m} - \dot{m}_0\right) h_7 + \dot{m}_0 h_3 \\ &\Rightarrow \dot{Q}_G = \dot{m}_0 \left[f(h_7 - h_2) + (h_3 - h_7)\right] \end{aligned} \tag{5}$$

where a is the recirculation factor defined as $a = \frac{\dot{m}_{rec}}{\dot{m}_0} = \frac{\dot{m}_{Ab} - \dot{m}}{\dot{m}_0}$ and $f = \frac{\dot{m}}{\dot{m}_0}$; $\dot{m}$ is the total mass flow rate of the H_2O-LiBr mixture.

Exergetic efficiency and coefficient of performance were determined by equations (6) and (7), respectively:

$$COP = \frac{\dot{Q}_V}{\dot{Q}_G + P_P} \tag{6}$$

$$\eta_{ex} = \frac{Ex(\dot{Q}_V)}{Ex(\dot{Q}_G) + P_P} \tag{7}$$

where P_P is the pump consumption power, computed as $P_P = \dot{m}_{Ab} \left|w_p\right| = (f + a)\dot{m}_0 \left|w_p\right|$ [W]; w_P is the pump specific mechanical work, [J/kg]; $Ex(\dot{Q}_V) = -\dot{Q}_V \left(1 - \frac{T_a}{T_V}\right)$; $Ex(\dot{Q}_G) = \dot{Q}_G \left(1 - \frac{T_a}{T_{Gmed}}\right)$; $T_{Gmed} = T_3$.

Initially the simulations were performed for a PTC solar collector of 6 m length and 2.9 m width, and a hot water storage tank of 0.17 m^3. At every step of calculation, the operating conditions of the absorption refrigeration system have been checked, in terms of acceptable concentrations, degassing interval, and verification of first and second laws of thermodynamics. We obtained an inappropriate variation of the water temperature in the storage tank, as its value is too small to maintain the continuous operation of the ACS module in the morning, although it is continuously functioning in the time interval 13-18. Two methods of improvement can be applied: either to use a larger surface PTC, or to decrease the amount of water in the storage tank, m_{st}. By increasing the size of the collector to a 7 m by 2.9 m PTC collector, while keeping the same hot water storage tank of 0.17m^3, significantly increased the storage tank water

temperature, T_{st}, in the morning, enough to sustain continuous operation of the ACS module (Figure 2). Because water is used as refrigerant, the maximum value can not exceed 220°C (in this case the water in the system is pressurized to 10 bar). In the case of T_{st} value greater than 220°C, the system will be turned off automatically. It is noted that the temperature in the desorber at noon (equal to the storage tank temperature, T_{st}) is greater than the upper limit of operation of the ACS module. Therefore, the ACS module stops working.

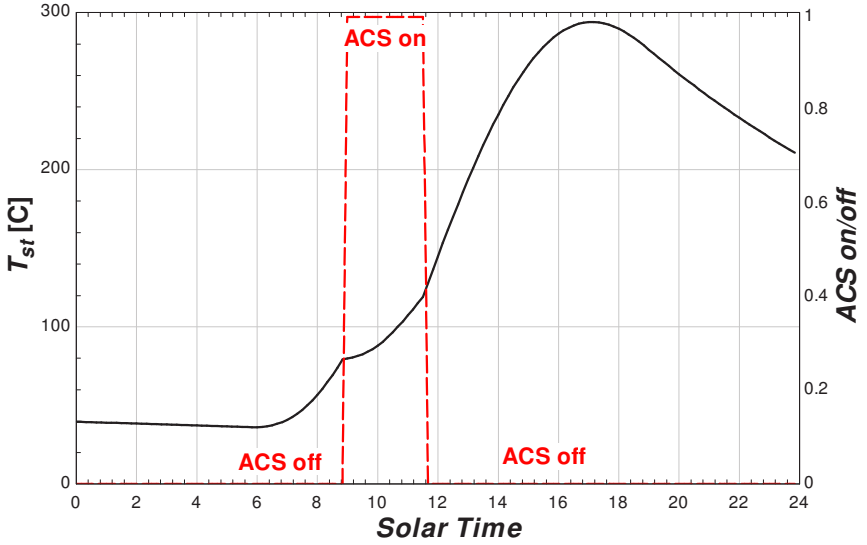

Figure 2: The storage tank water temperature and the functioning periods of the ACS; PTC surface is 7x2.9 m, and storage tank capacity is 0.17m^3.

The next step is testing the configuration with smaller amount, m_{st}, of water in the tank in order to lower T_{st} in the afternoon. At the same time this approach must be correlated with the size of the PTC collector so that T_{st} doesn't decrease in the morning. A very similar storage tank water temperature variation with the one presented in Figure 2, is obtained if we choose a PTC collector of 6 x 2.9 m, and a lower hot water storage tank volume of 0.13 m^3.

In conclusion, both options for improving the functioning of the ACS module proved to be inefficient. In addition, it has been previously shown that H_2O-LiBr ACS are able to function only in a very narrow interval of the vapor generator temperature. This simulation shows the high instability of the system when it is powered by solar energy. In this context, a compromise must be found between the size of the solar collector and the storage tank to obtain a longer period of stable operation of the ACS module. After successive attempts, these dimensions are: a PTC solar collector area of 6x2.9 m^2, and a storage tank volume of 0.22 m^3. The results for this configuration are shown in Figure 3, which reveals the increased operation period of the ACS, compared to the previous cases. Table 1 summarizes the results regarding the operation periods of the ACS module, and the sensitivity study on the size of the collector and the storage tank, respectively.

Table 1: Operating time of ACS module; sensitivity study on the size of the collector and storage tank dimensions.

	ACS ON, for the longest stable operating period	
PTC length [m] - storage tank volume [L]	On time	Off time
6-170	13:10	18:00
7-170	9:00	11:30
6-130	9:00	11:40
6-220	10:30	18:00

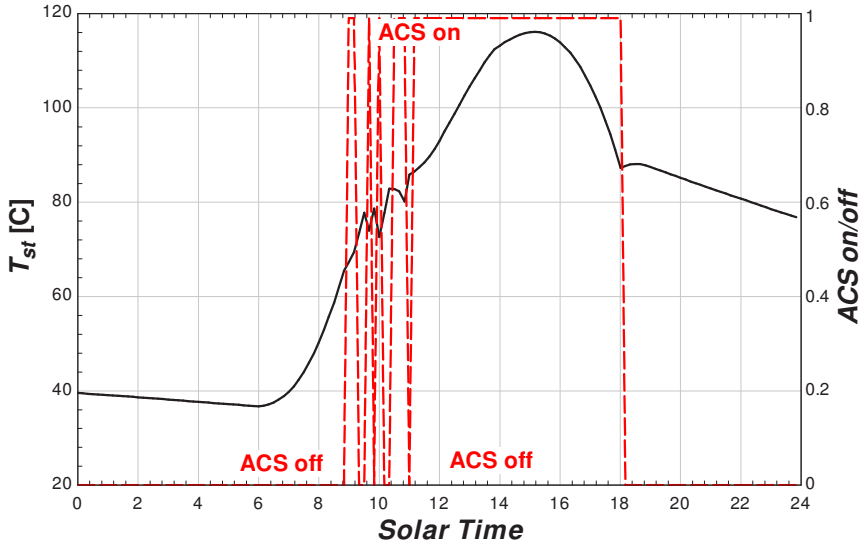

Figure 3: The storage tank water temperature and the functioning periods of the ACS; PTC surface is 6x2.9 m, and storage tank capacity is 0.22m^3.

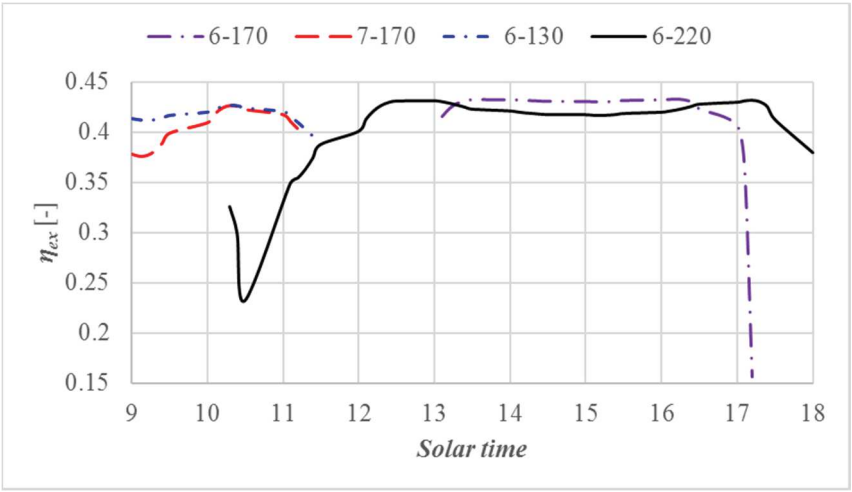

Figure 4: ACS module exergetic efficiency; sensitivity study on the size of the collector and storage tank dimensions.

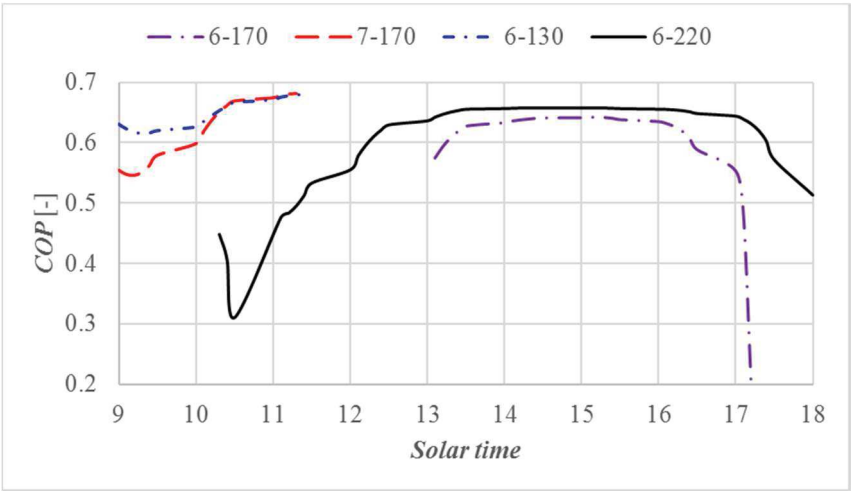

Figure 5: ACS module coefficient of performance; sensitivity study on the size of the collector and storage tank dimensions.

In Figures 4 and 5 the ACS module performance variations (exergetic efficiency and coefficient of performance, respectively) for the accomplished sensitivity study are presented. Two cases are from far better than the others considered, namely cases 6-220 (6m long PTC by 2.9 m wide and 220L storage tank) and 6-170. Note that the exergetic efficiency in the case 6-220 presents values in the upper limit, slightly lower compared to 6-170 between 13:30 and 16:30. However, the advantage of the 6-220 configuration is obvious, due to the small difference between it and 6-170, and because in this case, the ACS works for a longer period compared to the other three cases. In terms of coefficient of performance, Figure 5 reveals that it's values are maximum in the case 6-220 for an extended period (the time interval 13:00-17:00) compared to the other 3 cases.

3. CONCLUSIONS

A mathematical model was proposed to simulate the dynamic behavior of H_2O-LiBr ACS, to study the effect of various design parameters on the instability in the system operation. Thus, it was shown that for certain values of the PTC surface and the water storage tank capacity, either the ACS starts and stops too often, or it does not work at all in certain times of the day. This is because the storage tank water temperature, in direct correlation with the amount of heat received by the vapor generator, exceeds the maximum limit. In this regard, we tested different sizes of the PTC collector and storage tank volumes, to optimize them so that during the day, to obtain a longer period of continuous operation of the system. The main conclusion is that in the studied case, the best operation of the ACS module is obtained when it is coupled to a PTC collector of 6 m x 2.9 m and a storage tank of 0.22 m^3.

Acknowledgement

This work was supported by a grant of the Romanian National Authority for Scientific Research and Innovation, CNCS—UEFISCDI, project number PN-II-RU-TE-2014-4-0846.

References

[1] Raluca Porumb, Bogdan Porumb, Mugur Bălan, Baseline evaluation of potential to use solar radiation in air conditioning applications, Energy Procedia, 85, pp. 442 – 451, 2016.
[2] H. Z. Hassan, A. A. Mohamad, A review on solar cold production through absorption technology, Renewable and Sustainable Energy Reviews, 16, pp. 5331–5348, 2012.
[3] Duenas C, Pilatowsky I, Romero RJ, Oskam A, Finck AP. Dynamic study of the thermal behaviour of solar thermochemical refrigerator: barium chloride–ammonia for ice production. Solar Energy Materials and Solar Cells; 70, 3, pp. 401–13, 2001.
[4] S.M. Xu, X.D. Huang, R. Du, An investigation of the solar powered absorption refrigeration system with advanced energy storage technology, Solar Energy, 85, pp. 1794–1804, 2011.
[5] V. Boopathi Raja, V. Shanmugam, A review and new approach to minimize the cost of solar assisted absorption cooling system, Renewable andSustainableEnergyReviews, 16, pp. 6725–6731, 2012.
[6] Izquierdo M, Lizarte R, Marcos JD, Gutierrez G. Air conditioning using an air cooled single effect lithium bromide absorption chiller: Results of a trial conducted in Madrid in August 2005, Applied Thermal Engineering, 28, pp. 1074–1081, 2008.
[7] Balghouthi M, Chahbani MH, Guizani A., Feasibility of solar absorption air conditioning in Tunisia, Building and Environment; 43, 9, pp. 1459–1470, 2008.
[8] Florides GA, Kalogirou SA, Tassou SA, Wrobel LC., Modelling, simulation and warming impact assessment of a domestic-size absorption solar cooling system, Applied Thermal Engineering, 22, 12, pp. 1313–1325, 2002.
[9] Engineering Equation Solver, Academic Commercial V9.914 Version; F-Chart Software, Madison, WI 53744. www.fchart.com/ees/.
[10] Camelia Stanciu, Dorin Stanciu, Adina Gheorghian - "Thermal analysis of a solar powered absorption cooling system with fully mixed thermal storage at startup", Energies (2017) 10, 72, 10 January 2017, doi:10.3390/en10010072.

ENERGY EFFICIENCY INCREASING THROUGH SPACE MANAGEMENT. CASE STUDY IN AN OFFICE BUILDING

Ioana Udrea[*1], Tudor Trita[2], Romeo Traian Popa[3]

[1]ASC-Romania, 9 Stefan Marinescu Street, District 6, 060121, Bucharest, Romania
[2] ROFMA, 47-53 Lascar Catargiu Blvd., District 1,010665, Bucharest
[3] Polytechnic University of Bucharest, Faculty of Mechanical Engineering and Mechatronics, Thermodynamics Department, 313 Spl. Independentei 313, District 6, 060042, Bucharest, Romania

ABSTRACT

European Directives which establish energy targets for 2020 and 2030 are the main legislation when it comes to reducing the energy consumption of buildings. Energy efficiency is a large field of study, it doesn't mean only energy consumption minimization by improving measures applied to building envelope and its systems. An efficient use of energy and spaces is very important too. Facility Management (FM) is a field of study that considers all the aspects of a building in this regard. Main pieces of software in the field were reviewed in order to find the better software to use for space management analysis. A well-known software - ARCHIBUS that can integrate Building Information Models (BIMs) was chosen. BIMs are files containing physical and functional characteristics of the building and linked data, which can be exchanged or networked to support decision-making. Using a Romanian office building and its digital plans, a BIM has been done. For this BIM, a space allocation in agreement with organizational company structure, with functional company structure and with a Romanian standard, SR 1907-2, relate to design indoor temperature, was done in ARCHIBUS software. From all space classifications the methods of energy improvement are discussed.

1. INTRODUCTION

A continued reduction of energy consumption in buildings is required by European Directives, 2010 Energy Performance of Buildings Directive [1] and 2012 Energy Efficiency Directive [2]. The building sector is the main user of energy, with a percent of 40% from Union's final energy consumption. The building energy evaluation is usually made for some design temperatures and by reporting total energy consumption to useful floor area of the building. This approach is very correct and allowed a consensus of all buildings. But the real use of energy and space in building and the people behavior inside it are at least as important as classic building energy assessment. In this regard, Facility Management (FM) is a field of study that considers all the aspects of a building.

According to International Facility Management Association (IFMA) definition, FM is a profession that encompasses multiple disciplines to ensure functionality of the built environment by integrating people, place, process and technology [3]. From the definition given by EN 15221-1 [4], it can be found that FM represents "integration of processes within an organization to maintain and develop the agreed services which support and improve the effectiveness of its primary activities." A good presentation of FM field, its history and a synthesis of new relevant FM papers can be found on European Facility Management Network (EuroFM) [5]. EU FM Coalition [6] is a European organization that emphasizes the importance of energy efficiency in FM in the context of European Directives targets. Romanian Facility Management Association (ROFMA) is an important promoter of Facility Management in our country [7].

[1]Corresponding author: PhD. Ioana Udrea Tel.: +040 744 661303
E-mail address: ioana.udrea@asc-ro.com

In order to realize a building and its space analysis from FM approach the main software in the field were reviewed. FM software helps the facility managers to conduct and optimize their activities. According to an important reviews portal [8], Buildium is a finest choice of property management software, especially for residential properties and associations. It stands out for its clean and easy to navigate interface. Other recommendation is Total Management, a good commercial property management software. One of the best features is the highly customizable dashboard and its optimal multitasking capabilities. From another source of FM software classification [9], it is found DirectLine, a Web-based service that provides solutions management maintenance and inventory cost and that has 25 years of successful implementations. CAFM Explorer software is a product for organizations looking to better utilize space, improve service levels, and tighten cost control. From [9] also, ARCHIBUS software is found, it is presented as a global provider of software and services for real estate, facility, and infrastructure management. In [10] the authors realized a presentation of FM software field and it results that ARCHIBUS is one of the industry's leading software packages. The author mentions also a commercial maintenance management system, IBM - Maximo Asset Management. In [11] the authors present ARCHIBUS as a brand of internationally renowned property management software. ARCHIBUS comprises a space management tool that integrates location tracking and space management capabilities with facilities management systems or software [12] and it allows users to link design elements, such as furniture, equipment, located in a database with CAD plans of the building [13].

Some of the facility management software, including ARCHIBUS, can integrate Building Information Models (BIMs). Building information modeling is a process involving the generation and management of digital representations of physical and functional characteristics of places. BIM helps us understand the way buildings look, the way they function, and the ways in which they are designed and built. This is a worldwide trend at the moment. BuildingSMART alliance [14] is a North American organization and a council of the National Institute of Building Science that coordinates the creation of tools and standards that allow projects to be built electronically before they are built physically using Building Information Modeling. This organization develops comprehensive norms related to BIM development as United States National CAD Standard [15] and United States National BIM Standard [16]. The FM software that use BIMs implement an IWMS (Integrated Workplace Management System) that get a single, integrated real estate-focused solution that addresses all business domains. The five core functional areas are Space Management, Operations and Maintenance, Real Estate Management, Capital Project Management, Sustainability and Energy Management. Space Management module has features that permits CAD/BIM integration. An IWMS solution is based on a single platform and database repository [17]. Other Facilities Management software use CAFM system that is defined as a combination of Computer-Aided Design (CAD) and/or relational database software with specific abilities for FM [18].

In [19] the relation between BIM and FM software is discussed. Several innovative techniques were used to input the information directly in the BIM model. For this study two FM software were used, ARCHIBUS and FacilityMAX. From [20] it can be found that ARCHIBUS Space Management is the effective way of managing space and to minimize cost wastage and optimize space usage. The optimization of space management contributes to efficiency and success to most organizations. The authors analyze space management, particularly in a Malaysian University. The importance of space management within the meaning and understanding of Facilities Management is highlighted by the authors in [21]. They recommend the best methods for space management to the higher education institutions.

From its good space analysis method and its integration capabilities ARCHIBUS software was chosen for present study.

The aim of this paper is to present a real case of interdisciplinary use of the same BIM. That means a time economy and a systematization of the data and efficient space utilization can be

made. More than this, in this study, it is for the first time when a new space classification is realized in ARCHIBUS in order to allocate the design temperatures to the rooms.

2. METHOD

2.1. Studied building description

The building chosen for this research is named MultiGalaxy and it is rented by OMV Petrom Global Solutions SRL. The height regime of the building is 3S + P + 9E, its gross area is over 15.000 sqm and the construction year is 2008. MultiGalaxy is an A class office building, according to BOMA [22] and has a very good add on factor 3.7% (difference between the usable area and the rentable area of an office building expressed as a factor of the rentable area). The building has two generators of 700 kW power and last generation security and protection systems. It is provided with curtain walls composed of glass type Guardian and Schuco structure. The HVAC system is realized by a three pipes heating/cooling plant type Sanyo with VRF (Variable Refrigerant Flow) with ecological Freon agent. This kind of system, with three pipes presents the advantage that they can operate simultaneously in heating or cooling regime. The ability to simultaneously heat certain zones while cooling others is realized by a heat recovery system has. The input power of the system is achieved by acting the heating pumps compressors using a thermal engine with gas fuel. This kind of system can be used at nominal capacity for outdoor temperatures up to -21 degree.

Fig. 1. The studied building, MultiGalaxy, rented by OMV Petrom Global Solutions SRL

2.2. ARCHIBUS software description

ARCHIBUS is produced by ARCHIBUS, Inc. of Boston, Mass. ARCHIBUS is a Real Estate and Facilities Management software that offers a variety of platform options to accommodate the organization's needs - from single users within a department to worldwide access via the Internet for every industry. The need to extract, duplicate, or e-mail data and files is eliminated by the new Run Anywhere architecture [23]. ARCHIBUS software is an IWMS platform that permits a workspace customization and a continuous development of the software. As any IWMS, ARCHIBUS integrates main business domains, but in this research, Space Planning&Management domain presents interest. ARCHIBUS can operate with digital building plans and links them to its database. Thus, a lot of information and classifications related to CAD plans can be made. Any further modifications of the plans will lead to automate database modification. These kinds of space management allow a good and accurate room inventory, employee assignment to organizational space allocation, internally bill departments for their space usage and other benefits.

2.3. *Spaces assignment*

Fig. 2. MultiGalaxy building, groound floor, organizational space structure by divisions

Fig. 3. MultiGalaxy building, groound floor, functional structure of spaces according to EN 15221-6

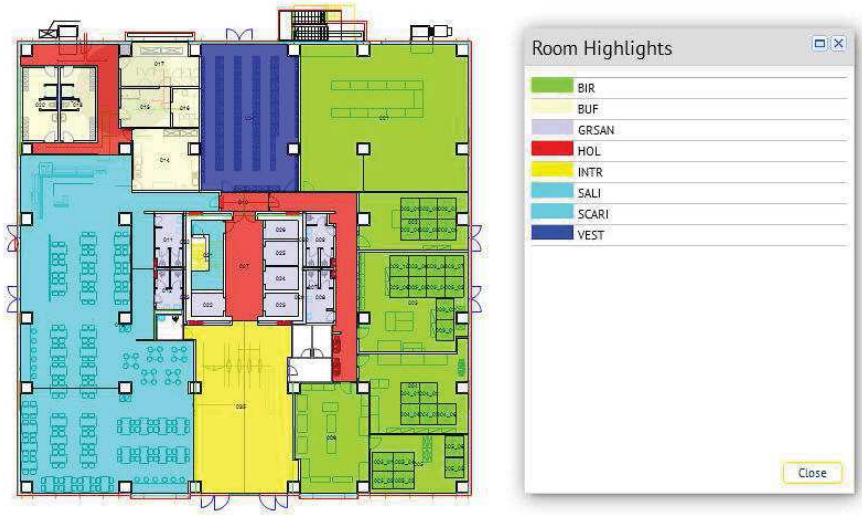

Fig. 4. MultiGalaxy building, groound floor, space structure according to SR 1907-2

From the definitions related to BIM, in this paper its main definition is considered, "a model that contains characteristics of the building and linked data which can be exchanged". Thus, although, generally BIM refers to 3D models, in this paper, respecting its basic definition, a BIM is used.

3. RESULTS AND DISCUSSIONS

The energy consumption in buildings can be reduced by classical method that means modernization solutions of the building and its systems or by rational use of energy and spaces. By rational use of energy it is understood the compliance with comfort temperature requirements, compliance with intermittent heating or cooling program. Where possible, the change of classical comfort temperatures with adaptive comfort temperatures [26] represents a decreasing of energy consumption. And it is not least important the rational use of space that means the reduction of the space allocated to a person. Based on industry studies, many organizations, both public and private sector alike, have been found to underuse office space. And more than this, efficient and effective space usage will be controlled at an expenditure cost and level of productivity [20].

The organizational space structure by divisions can be seen in figure 2. An efficient usage of the spaces is accomplished by employee assignment to the organizational structure of the building. Thus, the energy consumption can be reported to the employee instead of sqm, and it is significantly reduced. In figure 3 a functional classification of the spaces is presented. The space use is carefully watched and the common area, for example, can be reduced and thus, the energy used, reported to sqm of rented area, can decrease.

In figure 4 a space classification according to SR 1907-2 is made; the rooms are grouped according to indoor conventional air temperatures. The room's areas corresponding to different temperatures were exported from ARCHIBUS to EXCEL as xls file. In table 1 the data is systemized and the indoor reduced temperature is computed. This temperature can be used further in energy evaluation programs in order to find energy use for the studied building. Those indoor conventional air temperatures must be the set point temperatures for the HVAC system sensors.

At the end of this paper a comparison between indoor conventional air temperatures proposed by SR 1907-2 indoor comfort temperature recommended by European standard EN 15251 [27] is made. In European standard the temperatures are classified according to comfort category (A, B and C). In EN 15251 the temperatures are structured according to type of building/space and they are not at the same detail level as is SR 1907-2. As can be noticed in Table 1 the mean comfort temperature (for category B) is of 20 ºC in EN 15252 case and the mean reduced (design) temperature is of 18.4 ºC in the case of SR 1907-2.

Table 1. Indoor reduced temperature computation for MultiGalaxy building, ground floor

	BIR	HOL	GRSAN	BUF	INTR	SALI	SCARI	VEST		
Supr [m^2]	519.1	54.4	84.3	115.6	123.5	376.0	12.2	105.8	1390.9	TOTAL
T_i (SR 1907-2)[ºC]	20	15	15	20	12	18	15	22	18.4	T_i_red
T_i (EN 15251)[ºC]	20	20	20	20	20	20	20	20	20.0	T_i_comf

4. CONCLUSIONS

In conclusion, space management is one of the essential components in FM and in building energy efficiency.

In this paper it is for the first time when, in ARCHIBUS software, such an interdisciplinary space classification is made, all of these classifications are related to energy efficiency in the building. In the project that includes MultyGalaxy building, the possibility of space classification according to European norm EN 15221-6 was made by software customization. A new space classification, accordingly to SR 1907-2 is realized. It can be used in further computations for building energy assessment and for the centralization of room's set point temperatures used by the HVAC system.

For the studied building, a comparison between the indoor conventional air temperatures recommended by Romanian norm and indoor comfort temperatures proposed by European standard was made. A significant difference, of 1.6 ºC can be noticed. Although the EN 15251comfort temperatures are partially transposed in Romanian norm I5 [28] we recommend to update indoor conventional air temperatures proposed by Romanian

norm SR 1907 according to our day room types. The indoor air temperature is different from comfort operative temperature and also it is important in design and HVAC set point.

Acknowledgements

The authors thank to Mr. Dipl. Eng. Mircea Dobre, Department Manager - Facility Services, OMV Petrom Global Solutions SRL for useful information about MultiGalaxy building.

References

[1] DIRECTIVE 2010/31/EU OF THE EUROPEAN PARLIAMENT AND OF THE COUNCIL of 19 May 2010 on the energy performance of buildings, URL: http://eur-lex.europa.eu/legal-content/EN/ALL/;ELX_SESSIONID=FZMjThLLzfxmmMCQGp2Y1s2d3TjwtD8QS3pqdkhXZbwqGwlgY9KN!2064651424?uri=CELEX:32010L0031, [accessed: March 2015];

[2] DIRECTIVE 2012/27/EU OF THE EUROPEAN PARLIAMENT AND OF THE COUNCIL of 25 October 2012on energy efficiency, URL: http://eur-lex.europa.eu/legal-content/EN/TXT/?qid=1399375464230&uri=CELEX:32012L0027, [accessed: March 2015];

[3] IFMATM, International Facility Management Association, URL: https://www.ifma.org/about/what-is-facility-management, [accessed: March 2016];

[4] EN 15221-1:2006, Part 1: Facility management. Terms and definitions

[5] EuroFM, European Facility Management Network, URL: http://www.eurofm.org/index.php/what-is-fm, [accessed: March 2016];

[6] EU FM Coalition, European Facility Management Coalition, URL: http://www.eufm.org/, [accessed: May 2016];

[7] ROFMA, Asociatia Romana de Facility Management, URL: http://www.rofma.ro/, [accessed: April 2016];

[8] Property Management Software Reviews, URL: http://www.reviews.com/property-management-software/, [accessed: March 2016];

[9] Capterra, Top Facility Management Software Products, URL: http://www.capterra.com/facility-management-software/, [accessed: March 2016];

[10] Lee S., Akin O., Augmented reality-based computational fieldwork support for equipment operations and maintenance, Automation in Construction 20 (2011) 338–352;

[11] Chang C. Y., Tsai M. D., Augmented reality-based computational fieldwork support for equipment operations and maintenance Knowledge-based navigation system for building health diagnosis, Advanced Engineering Informatics, Volume 27, Issue 2, April 2013, Pages 246–260

[12] Floris, D.B. and Puybaraud, M.C., Space management system and method, US Patent App. 12/397,143, Google Patents, 2009, https://www.google.com/patents/US20090300174

[13] Hart, M.A., Office management solution, US Patent App. 12/009,327, Google Patents, 2008, https://www.google.com/patents/US20080183483;

[14] Building SMART alliance – a council of the National Institute of Building Sciences, URL, http://www.nibs.org/?page=bsa, [accessed: March 2016];

[15] United States National CAD Standard – V6, a product of National Institute of Building Sciences buildingSMART alliance;

[16] National BIM Standard – United States, an initiative of the National Institute of Building Sciences buildingSMART alliance;

[17] Planon – Aim for the Optimum, URL: http://planonsoftware.com/uk/glossary/cafm/, [accessed: March 2016];

[18] WBDG – Whole Building Design Guide, a program of the U. S. National Institute of Building Sciences, URL: https://www.wbdg.org/om/cafm.php, [accessed: March 2016];

[19] Sattenini A., Azhar S., Thuston J., Preparing a Building Information Model for Facility Maintenance and Management, Proceedings of the 28th ISARC, Seoul, Korea, p. 150-155

[20] Ibrahim I., Yusoff W. Z., Sidi N. S. S., Space Charging Model: Cost analysis on classrooms in higher education institutions, Procedia - Social and Behavioral Sciences 28 (2011) 246 – 252

[21] Ibrahim I., Yusoff W. Z., Sidi N. S. S., A Comparative Study on Elements of Space Management in Facilities Management at Higher Education Institutions, 2011 International Conference on Sociality and Economics Development IPEDR vol.10 (2011)

[22] Office Buildings: Standard Methods of Measurement - English Version (ANSI/BOMA Z65.1—2010)

[23] Zawadski C., 2010, Latest Version of ARCHIBUS Software Helps Reduce Carbon Footprint and Lower Real Estate, Infrastructure, and Facilities Management Costs, URL: http://archibus.com/press-release/1114/, [accessed: March 2016];

[24] EN 15221-1:2006, Part 1: Facility management. Area and Space Measurement in Facility Management

[25] SR 1907-2/1997 – Romanian Norm, Heating systems. Conventional calculation indoor temperatures;

[26] de Dear, R. J., Brager, G. S., and Cooper, D., Ashrae rp-884; Developing and adaptive model of thermal comfort and preference. Technical report, The American Society of Heating, Refrigeration and Air-Conditioning Engineers, Inc., and Environmental Analytics, editor. Atlanta, 1997

[27] EN 15251:2007, Indoor environmental input parameters for design and assessment of energy performance of buildings addressing indoor air quality, thermal environment, lighting and acoustics. Brussels: CEN (European Committee for Standardization);

[28] I5:2010 - Standard for the design, execution and operation of ventilation and air conditioning systems, approved by Order of the Minister of Regional Development and Tourism no. 1659 of 22 June 2011, published in the Official Gazette of Romania, Part I, no. 504 bis of July 15, 2011

ABOUT WIND ENERGY CONVERSION SYSTEMS FOR SMALL-SCALE APPLICATIONS

Krisztina Uzuneanu
„Dunarea de Jos" University of Galati
Faculty of Engineering

Abstract

In the current context characterized by the alarming increase in pollution caused by energy produced by burning fossil fuels, it is becoming increasingly important to reduce the dependence on these fuels and wind energy is a viable alternative. The paper presents some possibilties to use wind energy conversion systems for isolated areas.

1. Introduction

The convertion systems of wind energy into electrucity can be connected to the network or systems generating electricity for isolated areas.

A system of wind energy conversion into electricity connected to the network consists in (Fig. 1):

- wind turbine (1);
- axial or radial electric generator (alternator) that can be single phase or three phase (2);
- single -phase or three- phase rectifier bridge (3);
- circuit breaker (battery - turbine isolation) (4);
- controller to supervise charging of the battery unit and alternator protection (keeping battery in good condition) (5);
- battery unit (6);
- circuit breaker (battery-charge isolation) (7);
- DC to AC converter (8);
- consumers (9);
- electric meter (10).

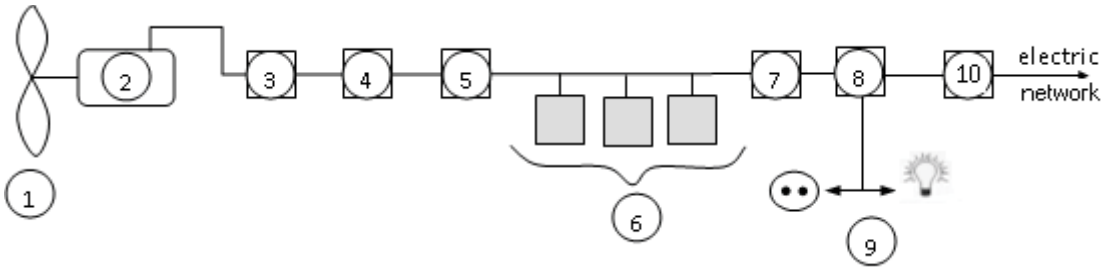

Fig. 1 System of wind energy conversion into electricity [1]

These systems connected to the networked can be systems for production of electricity on a large scale (eg. high power wind turbines), in which case components 5, 6 and 7 are missing from the scheme in Fig. 1. Also connected to the network may be the systems producing low power energy which, although connected to the network , are not mainly intended to supply electricity to the network. In this system the electricity produced is used locally (a household supplied in this way) but when producing an energy surplus, it can be "pumped" into the

national electricity grid/network (this can be done only if the parameters of the produced electricity correspond to the parameters of the network).

Small turbines are attractive to people who need something above 100-200 W to power their homes, offices or houses isolated from the mains power supply. Unlike photovoltaic panels that have virtually the same cost per watt regardless of the panel size, wind turbines are cheaper with increased size.

For a 300 W power, the cost of a wind turbine is 2,5 $/W, while a photovoltaic panel is $ 5 / W. For 1500 W, the wind system costs 2 $/W and at 10000 W the wind generator cost (without electronics) is 1.5 $ / W. [2]. The cost of regulators and controllers is the same with wind turbine and photovoltaic panel. Surprisingly, the cost of the wind turbine tower is equivalent to the cost of the support and tracking system of the photovoltaic panel.

2. Electricity Generating System for Isolated Areas

This system incorporates one or more turbines of different powers. The turbines provide variable power which turns, inside the inverter, into steady AC voltage 230 V and constant frequency 50 Hz, further used to supply AC consumers. The power excess is accumulated in batteries until they are charged. In periods of weak wind, the energy stored in batteries supply the consumers via the inverter.

If the battery voltage falls below a certain preset level, the backup Diesel generator starts automatically and works while the batteries are charged.

Battery charging is controlled by the very feature of this type of inverter to be bi-modal (DC-AC or AC-DC). In larger systems, the inverter can be synchronized with the backup generator for the high load peak uptake. In this way, the operation time of the generator is kept to a minimum and the fuel is used optimally during the operation of the backup generator. Alternative output voltages can be 230 V AC single-phase or 380 V AC and 50 Hz three-phase.

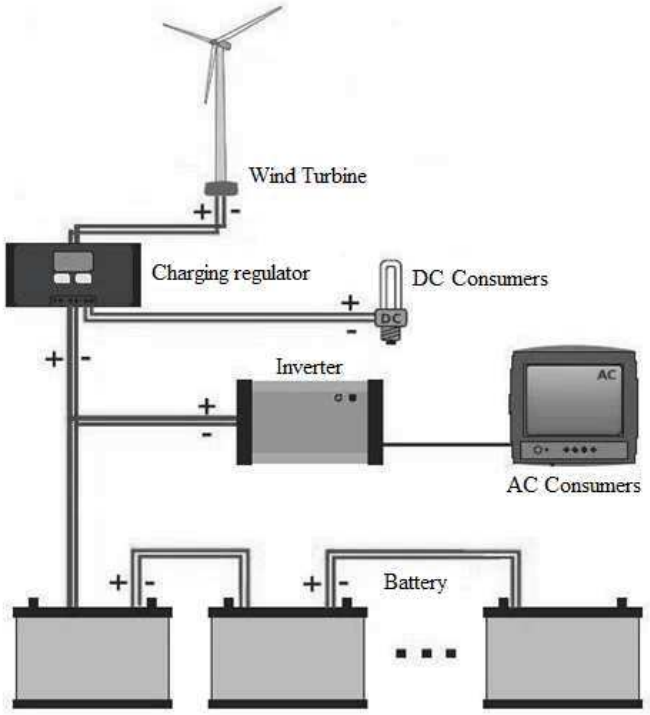

Fig. 2 Electricity generating system for isolated areas

Wind turbines can also be used to heat homes. The energy generated, that can be 230 V AC single-phase or 400 V AC three-phase, supplies the heating resistors in a battery power tank on the house heating network.
Energy is generated in a low speed alternator driven directly by permanent magnets. The turbine speed is maintained almost constant by the process computer, therefore as long as the wind is blowing, there is a voltage of 240 V or 400 V AC of variable power across the terminals [3].
If use is made of a sufficiently strong turbine, eg. 11 kW, full heating can be provided to a house of 200 m^2 in windy periods.
The energy surplus produced can be sold to an energy supplier through a complex processor of synchronous IGBT Inverter (GridTek Power Procesor). System operation is automatic.[4, 5].

3. Water Pumping System by means of a Wind Turbine

In areas where water is limited, but there is deep groundwater and regular winds (typical situation for desert or dried areas), a wind turbine can be successfully used to pump water to the surface for its subsequent use. As a matter of fact, one of the prevailing uses of wind turbines prevailed since their emergence was water pumping. Water pumping can be done directly using the mechanical force of the wind turbine (Fig.3) or using the wind power installation for the production of electricity which is subsequently used to power an electric water pump (Fig. 4).

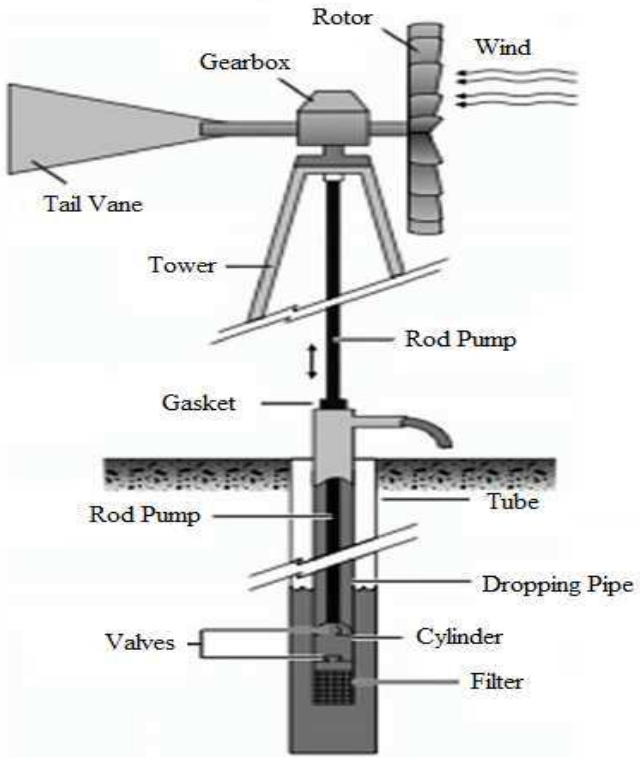

Fig. 3 Wind system for pumping water by a mechanical pump

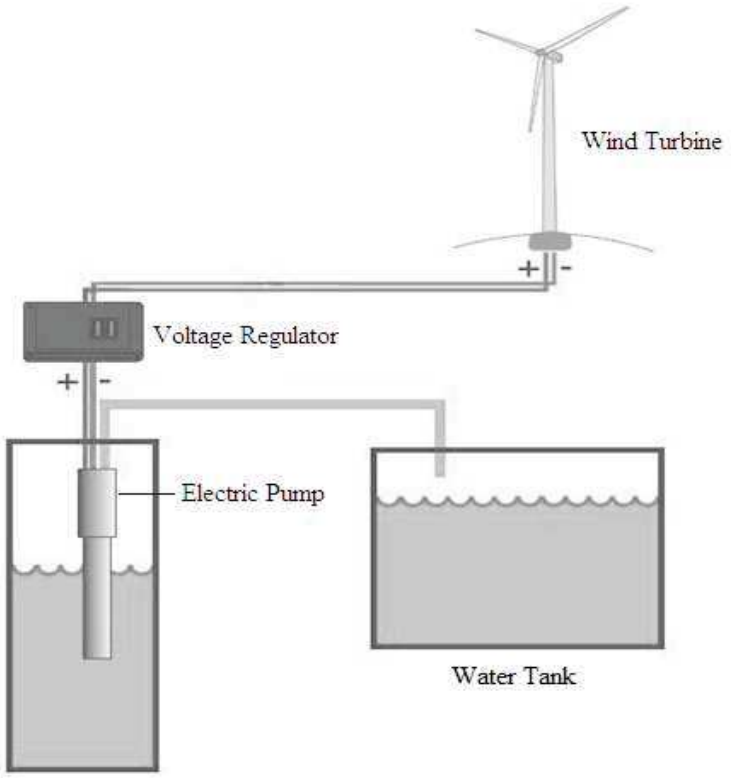

Fig.4 Wind system for pumping water by an electrical pump

These systems are also used in agriculture for irrigation of dry areas, for pumping water from rivers, etc. Basically, the operation of such wind systems for water pumping is almost free, except for possible costs of servicing and maintenance. The costs of the initial investment must be analyzed in the context of the economic and social importance attached to such investment, which can solve a number of serious problems caused by water shortage in some regions.

Conclusions

Wind energy has already been proven to be a very good solution to global energy problems. Using renewable resources refers not only to energy production, but by the particular way of generating it, also reformulates the model of development by decentralizing the sources. Wind energy is one of the particular forms of renewable energy that is suitable for small-scale applications.

References

1. Vaughn, N., - Wind Energy Renewable Energy and the Environment, CRC Press Taylor & Francis Group, London, New York, 2013.
2. Burton,T., Sharpe, D., Jenkins,N., Bossanyi,E., Wind Energy Handbook John Wiley & Sons, LTD, Chichester, New York ,Weinheim ,Brisbane , 2011.
3. Piggott, H.,Windpower Workshop, Building Your Own Wind Turbine, Centre For Alternative Technology Publications, London, 2010.
4. Flowers, L., Wind Energy Update, National Renewable Energy Laboratory, 2013 Reno, NV.
5. The Economics of Wind Energy By the European Wind Energy AssociationMarch 2009.

ENERGY EFFICIENCY IN WASTE WATER HEAT UTILISATION AND AUTOMATION OF DYEING PROCESS

Nikolay Zlatov[1], Christiyan Iliev[2], Michael Velikanov [3]

ABSTRACT

The paper presents the investigation and analysis of the energy efficiency project envisages the building of a waste water heat utilization system as well as automation of the dyeing process in the dyeing workshop of the company Bulgaria - K Jsc. As a result of this work a list of energy efficiency measures was developed. The most promising measures were selected for analysis. It includes the estimated energy savings and the CO_2 reduction, due to the use of innovative automation production processes in dyeing as part of the company business.

1. INTRODUCTION

The present investigation is the basis of detailed preliminary engineering studies, carried out about the working process of the industrial steam generators, type KM-12, analysis of the waste waters and working process of the dyeing workshop in Bulgaria - K Jsc.
The Energy Efficiency Project envisages the building of a waste water heat utilisation system as well as automation of the dyeing process in the dyeing workshop. The research results are presented along with the Energy Audit performed by specialists of EnCon Services.
The company Bulgaria - K Jsc is situated in the territory of the town of Kazanlak. The following production units are positioned on the site: Mechanical Treatment Workshop, Dyeing Workshop and Finishing Workshop.

An independent boiler station, including three industrial steam boilers type KM– 12, is located on the main site. The steam generators are operating and supply the site of the company by means of a heat carrier consisting of saturated steam 0.5 MPa only for process needs and preparation of hot water according to the requirements of the production process.

The burned fuel for one year is as follows: heavy fuel oil - 2,835 tons and light fuel oil as supporting fuel - 43 tons. The boiler station has also consumed 435,186 kWh of electric energy for the BS's own needs as well as 20,225 m^3 of softened water (including hot water preparation). The operational costs for salaries, insurance, repair and maintenance in the boiler station amount to EUR 34,800.

The dyeing of the threads includes processes as boiling-off, washing, neutralising, bleaching, dyeing, mercerising, and drying. Most of these processes require considerable quantities of heat. The processes of dyeing, using KRANTZ apparatuses are accomplished manually, which provokes imperfection in the maintenance of the technological regimes. The result is about 30% bad quality dyed threads, which have to be re-dyed, thus increasing the operational costs of the production.

[1] Professor, Institute of Mechanics, BAS, BG, zlatov@imbm.bas.bg
[2] Student, University of Birmingham UK
[3] Dr. Sc, Encon Services International LLC USA3

Nearly 1,500 m^3 of waste water at an average temperature of 35-40^{0}C, as a result of the processes in the Dyeing Workshop, are discharged daily into the sewage system. The operational costs of the process of dyeing for materials, consumables, salaries, spare parts and maintenance for one-year amount to EUR 261,618

Company Bulgaria - K consumed electricity for process needs in the amount of 4,452 MWh, which costs EUR 187,131.

The heavy fuel oil consumption was 2,835 tons, costing EUR 749,396. The light fuel oil consumption amounts to 43 tons at the amount of EUR 26,576. The water consumption in this period was 324,479 m^3, amounting to EUR 6,333.

The value of the purchased electricity amounts to 19.3% of the total energy costs for one year, the heavy fuel oil costs are 77.3%, the light fuel oil costs are 2.7%, while water costs are 0.7%.
Figure 1 presents the energy costs breakdown at Bulgaria - K Jsc for one-year period.

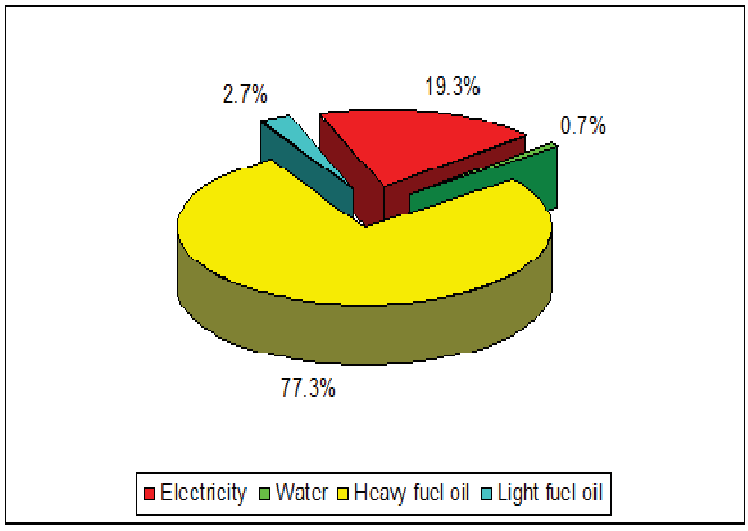

Figure 1 Energy Costs Breakdown at Bulgaria - K Jsc for one year

Figure 1 shows that the relative share of the heavy fuel oil is significant. This is due to the considerable consumption of heat energy, needed for the production processes. In the same time important quantities of warm waste water is poured out in the sewage system.

2. DESCRIPTION OF RECOMMENDED TECHNICAL MEASURES

The main goal of this energy efficiency project is to decrease the energy costs of Bulgaria - K Jsc. This will be achieved through the implementation of the following two groups of proposed technical measures:

- Waste water heat utilisation;
- Automation of the dyeing process.

2.1. Waste water heat utilisation

The project provides building of a waste water heat utilisation system as follows:
The warm waste water at a temperature of about 35-38^{0}C, actually discharged into an open waste water reservoir in order to be purified, is pumped to the Heat Utilisation Station, where it passes

through an automatic self-cleaning filter LEFCO – France, type LST-04 before entering a heat exchange group. The heat exchange group consist of two plate & gaskets heat exchangers GEA – Ecoflex, type NT100X HV situated in parallel. After giving its heat, the cooled waste water (at about 15^0C) is discharged into the sewage system.
The softened cold water with temperature of about 10^0C is pumped down from a water tank with capacity of 180 m^3 by means of an insulated pipeline to the Heat Utilisation Station, where it passes through the heat exchange group.
After heating (up to about 30^0C) the water is transferred through an insulated pipeline to a warm water tank of 100 m^3. The warm water from the tank is pumped to the heat exchangers of the sub-stations of the Dyeing Workshop in order to be heated up, in accordance with the technological requirements.
The system provides local control at operative management of the whole process of heat utilisation.
The local level controls the parameters (flow, pressure, temperature) of the water, the level of water in the tanks and the state of the pumps.
The operative management is realised through a personal computer, situated in the Operative Control Centre. Specialised system software ensures the connection with the local controls and visualises the information.
The system optimises the waste water heat utilisation system functioning and ensures the maximum utilisation of the waste water heat.

The alculation data about the energy savings from heavy fuel oil, light fuel oil, electric energy and water, resulting from the building of the waste water heat utilisation system at Bulgaria-K is shown in Table 1.

ECO 1 Waste water heat utilisation

1. Base conditions	Value	Unit	Sources
Working hours	4,380	h/yr	Bulgaria-K
Boiler station's electric energy consumption	435,186	kWh/yr.	Calculation
Boiler station's energy consumption	1,567	GJ/yr	
Heavy fuel oil consumption	2,835	ton/yr	Bulgaria-K
Light fuel oil consumption	43	ton/yr	Bulgaria-K
Water consumption	20,225	m^3/yr	Bulgaria-K
Steam boiler efficiency	85%	%	Measurement
Heavy fuel oil energy consumption	95,908	GJ/yr	
Light fuel oil energy consumption	1,517	GJ/yr	
Total fuel energy consumption	97,425	GJ/yr	
Operational costs	34,800	EUR/yr.	Bulgaria-K

2. Expected conditions	Value	Unit	Sources
Working hours	3,456	h/год.	Calculation
Boiler station's electric energy consumption	344,932	kWh/год.	Calculation
Boiler station's energy consumption	1,242	GJ/год.	Calculation
Heavy fuel oil consumption	2,386	ton/год.	Calculation
Light fuel oil consumption	36	ton/год.	Calculation
Water consumption	13,825	m^3/год.	Calculation
Heavy fuel oil energy consumption	80,733	GJ/yr	
Light fuel oil energy consumption	1,277	GJ/yr	
Total fuel energy consumption	82,010	GJ/yr	
Operational costs	45,160	EUR/yr.	Calculation

3. Savings		
Electricity savings	90,254	kWh/yr.
Heavy fuel oil savings	449	t/yr.
Light fuel oil savings	7	t/yr.
Water savings	6,400	m3/yr.
Operational cost savings	-10,360	EUR/yr.

Table 1 Energy Savings Data for the Energy Carriers - ECO 1 in Bulgaria - K Jsc

2.2 Automation of the dyeing process

The project provides installing of automated systems for full management of the technological process for dyeing of thread coils on 9 dyeing apparatus KRANTZ.

The Glauber's salt is introduced in the beginning of the process. The dye is stirred in a special vessel with heating up to 60^0C and mixing with a propeller agitator, and then introduced lightly for 20 min.

The other components (Na_2CO_3, NaOH or Egazol or TC-fix) are dosed precisely by quantities and by adding time. A precise maintenance of the desired parameters and gradients is ensured. The system maintains a great number of technological regimes, indicated by Bulgaria-K technologists.

Each system contains:

- Operating controller and software by Rockwell Automation – Allen-Bradley;
- Operator's panel Easy View 5,7 for selection of the dyeing regime;
- Electro commuting devices;
- Temperature and level probes;
- Pneumatic valves with their accessories;
- Installation boards by Rittal;
- Vessel with propeller agitator and washing system of stainless steel X18H9T for dye stirring;
- Vessel for NaOH of stainless steel AISI316;
- Dosing NaOH pump by Prominent;
- Tubing connections.

Controllable pneumatic valves replace all existing manual valves, needed for the automatic regime.

The module controller Micrologix 1200, the operator's panel Easy View, the operator's manual regime panel and the commuting and pneumatic accessories are disposed in the operating control board.

The preliminary assigned technological regimes are selected and controlled on the operating control board. Switching to manual regimes is realised by using a password.

The system is extendible with operating computer, inquires and archives. The system ensures the high quality of the dyeing process and minimizes the waste, i.e. avoids re-dyeing of thread coils.

The calculation data about the energy savings from heavy fuel oil, light fuel oil, electric energy and water, resulting from the installation of the system of automation of dyeing process at Bulgaria– K Jsc is shown in Table 2.

ECO 2 Automation of the dyeing process			
1. Base conditions	**Value**	**Unit**	**Sources**
Electric energy consumption	681,861	kWh/yr.	Bulgaria-K
Heavy fuel oil consumption	152	ton/yr	Bulgaria-K
Light fuel oil consumption	2	ton/yr	Bulgaria-K
Water consumption	3,036	m^3/yr	Bulgaria-K
Steam boiler efficiency	85%	%	Measurement
Heavy fuel oil energy consumption	6,058	GJ/yr	
Light fuel oil energy consumption	96	GJ/yr	
Total fuel energy consumption	6,154	GJ/yr	
Operational costs	261,618	EUR/yr.	Bulgaria-K
2. Expected conditions	**Value**	**Unit**	**Sources**
Electric energy consumption	524,509	kWh/yr.	Calculation
Heavy fuel oil consumption	117	ton/yr	Calculation
Light fuel oil consumption	2	ton/yr	Calculation
Water consumption	2,335	m^3/yr	Calculation
Steam boiler efficiency	85%	%	Measurement
Heavy fuel oil energy consumption	4,660	GJ/yr	
Light fuel oil energy consumption	74	GJ/yr	
Total fuel energy consumption	4,734	GJ/yr	
Operational costs	211,244	EUR/yr.	Calculation
3. Savings			
Electricity savings	157,353	kWh/yr.	
Heavy fuel oil savings	35	t/yr.	
Light fuel oil savings	1	t/yr.	
Water savings	701	m^3/год.	
Operational cost savings	50,373	EUR/yr.	

Table 2 Energy Savings Data for the Energy Carriers – ECO 2 in Bulgaria - K Jsc

Detailed technical specifications for the main energy equipment and auxiliary facilities are present. The cash savings and avoided operational costs to be realised after the project implementation are shown at the diagram of Figure 2.

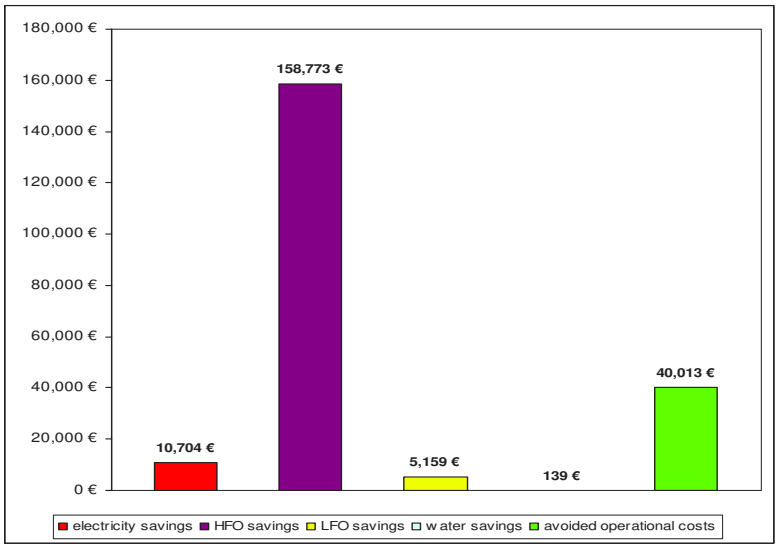

Figure 2 Savings and Revenues Resulting from Project Implementation

The analysis shows that the decrease of the project assets energy expenses after the project implementation will be 14.2%, compared to current operations, which meets the EBRD requirements for achieving minimal savings in energy consumption of 10%, compared to the baseline.

2.3. Operational costs breakdown. Project cash Flow.

The direct annual operational costs of Bulgaria - K include all current costs, related to the operation of the new waste water utilisation system as well as to automation of the dyeing processes in the dyeing workshop and are presented by the following components:

- Salaries and social security payments of the operation personnel;
- All costs, related to the consumables, spare parts and maintenance of the equipment.

The annual operation and maintenance costs of Bulgaria - K are estimated at EUR 30,160. The total operation costs include EUR 20,160 for salaries and social security payments of the operational staff and EUR 10,000 for consumables, spare parts and maintenance of the equipment.

Table 3 shows the allocation of the operational and maintenance costs.

	(EUR)
Costs for working salaries and social security payments of the operational personnel	20,160
Costs for consumables, spare parts and maintenance of the equipment	10,000
Total	**30,160**

Table 3 Operation and Maintenance Costs of Bulgaria-K Jsc

2.4. Revenues such as energy and other savings, revenues from electricity sales, Carbon Credits and/or Tradable Green Certificates

The annual savings as a result of the project implementation are given bellow:

- Electricity savings amounting to EUR 10,704;
- Heavy fuel oil savings amounting to EUR 158,773;
- Light fuel oil savings amounting to EUR 5,159;
- Softened water savings amounting to EUR 139;
- Cash savings from operation costs at the amount of EUR 40,013.

The net savings of the project implementation at Bulgaria - K Jsc amounts to EUR 214,788.

3. CONCLUSIONS

According to the Agreement with European Bank for Reconstruction and Development EBRD, the eligible energy efficiency projects are to be investments whereby the financing of the sub-project can be repaid from the resulting benefits and savings of no less than 10% achieved. As a result of the present project completion, Bulgaria - K Jsc will reduce the energy expenses for the assets subject to the project by 14.2%. The cash flow generated from the avoided energy expenses is sufficient.

The developed energy efficiency measures create energy savings and the CO2 reduction, due to the use of innovative technology of waste water heat utilization and automation of production processes in dyeing.

References

[1] Integrated Pollution Prevention and Control Reference Document on the Best Available Techniques for Waste Incineration, European Commission (2006)

[2] U.S. Department of Energy, Energy Efficiency and Renewable Energy, Clean Cities Fact Sheet- Low Level Ethanol Fuel Blends April 2005

[3] J.B.H. Nielsen, P.O. Popiel, Biogas a Promising Renewable Energy Source for Europe. AEBIOM Workshop European Parliament, Brussels (2008)

[4] Nikolay Zlatov, Energy & the Environment Wind Power London 2014, ISBN 978-619-7135-03-9

BIOREFINING – A PERSPECTIVE SOLUTION FOR BIOMASS USE

Ph.D. Eng. Alexandru Isabela Doina[1] – INMA Bucharest

ABSTRACT

Reducing dependence on non-renewable resources is a priority in the European Union. A number of renewable fuels that have the potential to reduce greenhouse gas emissions and dependency on fossil fuels are available to consumers in rural areas: biogas, solid biomass and liquid biofuels.

Biorefining is the process of converting biomass into fuel, heat and chemicals. In this context, biorefinery is a new concept, similar to oil refinery (fuel and oil products), but based on bio-resources.

Classification of different biorefineries may consider: the raw material, the platform (intermediate product) the process or the product.

1. INTRODUCTION

Bioeconomy includes the production of renewable biological resources and their conversion as well as that of waste streams into value-added products, such as food, feed, bioproducts and bioenergy.

The European Union launched in 2012, the Bioeconomy Strategy 2020 – "A Bioeconomy for Europe", as programmatic expression of the strategic initiative for sustainable growth through innovation of the European economy to overcome the effects of global economic crisis and, in particular, of predictable crises caused by climate change and fossil energy stocks depletion. This strategy proposes to economic and business environment a radical transformation of the current European economic paradigm, based essentially on the use of fossil energy, in an economy based mainly on the exploitation of renewable biological resources.

The main European strategic objectives in bioeconomy field aim the following societal challenges: food security, sustainable management of natural resources, reducing dependence on non-renewable resources, climate change mitigation and adaptation to climate change, creating jobs and maintaining European competitiveness.

In terms of reducing dependence on non-renewable resources to remain competitive, the EU needs to develop into a society with low carbon intensity, where the bioproducts and bioenergy contribute together to green growth and competitiveness. Bioeconomy strategy will contribute to understanding the availability and demand for biomass, including ease of access to alternative sources of carbon and energy (e.g. agricultural and forestry residues, waste) and promoting research in renewable resources field, such as microalgae [1].

2. METHODOLOGY

Rural regions have different characteristics in terms of access and use of energy compared to intermediate and urban areas.

Nowadays, there are several sustainable energy solutions available for households, enterprises and agriculture, which offer particular advantages for rural areas such as energy efficient use, reducing air and soil pollution as well as reducing associated greenhouse gas emissions.

Solutions on obtaining energy available to rural areas can be divided into three distinct categories: a) energy efficiency measures for buildings, b) energy conversion technologies, and c) renewable fuels with low carbon emissions.

[1] INMA Bucharest, 6 Ion Ionescu de la Brad Blvd, 0721436534, alexandruisa@yahoo.com

A number of renewable fuels that have the potential to reduce greenhouse gas emissions and dependence on fossil fuels are available to consumers in rural areas. They include biogas, solid biomass and liquid biofuels [2].

Biogas provides the opportunity to use energy sources available at a local or regional level because it is produced by conversion of animal waste and organic matter in methane and has properties similar to those of the natural gas. Refined biogas can be a source for producing electricity, heat or it can be used in transport.

Biogas can be produced from organic or animal waste, widely available in rural areas and often considered to have a low value.

Biogas

Solid biomass

Biofuels

Solid biomass is the oldest and most widely used renewable energy source. It includes wood fuel such as wood chips, pellets and split logs and is used for space or water heating.

There are, however, limits regarding biomass supply, both in terms of sustainability and lands available, which is why Europe strives to increase the share of energy from renewable sources.

Biofuels is the generic name refined liquids, derived from plants, vegetable waste and in some cases animal origin waste products. Biofuels are used in pure form or, more frequently, in conventional liquids blends of fossil fuels. Usually, they are used in transport. As in case of solid biomass, the sustainability and land use play an important role, limiting their production potential. To develop a productive and sustainable bioeconomy is needed an appropriate infrastructure.

Petrochemical processes in refineries produce a large variety of products, fuels and energy from fossil resources. Biorefineries replace these fossil resources with renewable energies (including waste), creating new sources of income and jobs in agriculture, forestry, fishing and aquaculture sectors.

Biorefining is a sustainable processing of biomass in a large gouge of vendible products (food, forage, materials, chemical products) and energy (fuels, power, heat). This requires the integration of different technologies and methods.

Biorefinery process consists in pre-treatment and biomass preparing like such as separation of biomass components (primary refining) and subsequent conversion steps/processing (secondary refining).

Primary refining involves separation of the biomass components in intermediary products (e.g. cellulose, starch, sugar, vegetable oil, lignin, vegetable fibres, biogas and synthesis gas.

In secondary refining more stages of conversion and processing generate a great number of intermediary products. Product resulted from primary and secondary refining are used in provided energy process or are processing and then processing in food or fodder.

Term of biorefinery has been used to describe the production capacities that are used for biological systems in order to effectively catalyse the basic chemical transformations taking place in that system. Biorefineries may be considered as being production capacities very adaptable, that do not limit only to producing one product, which can processed a large

variety of raw materials and can use different processes to obtain a large products variety, with a minimum waste quantity obtaining [3].

Fig. 1 Biorefinery (Copyright: Fraunhofer UMSICHT)

Clasification of different biorefineries is focused more or less systematically on some aspects. Thus, classification may take in consideration :

→ raw material material (for cereals cultures, grass, straw, wood, whole culture, algae),

→ intermediary product (for example : synthesis gas, lignocellulose, vegetable oil),

→ process (for example: thermochemical, biotechnological or

→ product (for example: bio-ethanol, fuel).

The basis of a classification system for biorefineries, with a systematically approach have been developed for the first time as part of IEA Task 42. This classification system is focused on intermediary as biorefinery platform, what allows a bigger in raw materials allocation and products and lead to a great number of achievable platforms.

Systematization is carried out in accordance with the four structural elements: raw material, platform (intermediate products that are able to connect different systems and their processes of biorefineries) products and processes. The core of the system consists of the intermediates which occur in the process of primary refining and serving as platform for the secondary refining. The terms of raw materials and products are then added to this platform. The link elements are processes. Number of platforms involved gives an indication of the complexity of the system.

Table 1 presents an assemble image of the theoretic possibilities of establishing a biorefinery.

Table 1 – The elements of biorefinery classification [4]

Raw material	**Agricultural biomass**	**Aquatis biomass**	**Biogenic residual and waste materials**
	– oil crops – starch crops – sugar crops – grasses – wood – woody biomass	– algae	– agricultural and forestry residues (e.g. straw, manure, wood residues, fruit peel, slurry) – biogenic residual materials from processing (e.g. whey, pulp, stillage, spent grains) – biogenic waste materials (e.g. yellow grease, waste wood)

Platform	– low molecular weight carbohydrates (e.g. lactose, sucrose) – polymeric carbohydrates (e.g. starch, inulin, pectin) – lignocellulose components (lignin/cellulose/ hemicellulose) – proteins – vegetable oils, lipids – pyrolysis oil – biogas – syngas		
Products	**Materials** – chemicals – materials – feedstuff* – foodstuff*	**Bioenergy** – solid, liquid, gaseous sources of bioenergy – electricity – heat	
Processes	– physical, including mechanical processes – thermochemical processes – chemical processes – biotechnological processes		

* *as a coproduct*

In the present, many biorefinery concepts are developed and implemented. Some of these concepts are simple, using a raw material (for example vegetable oil) out of which two or three products are achieved (biodiesel, animal food, glycerine) with the current, technologies. However, other biorefineries concepts are sometime very complex, using different raw materials (e.g. : algae, Mischantus and wood chips for coproducing a large products spectrum (bioethanol, phenol, omega-3 fatty acids, biodiesel) using technologies which still need time to be commercially available in the next years.

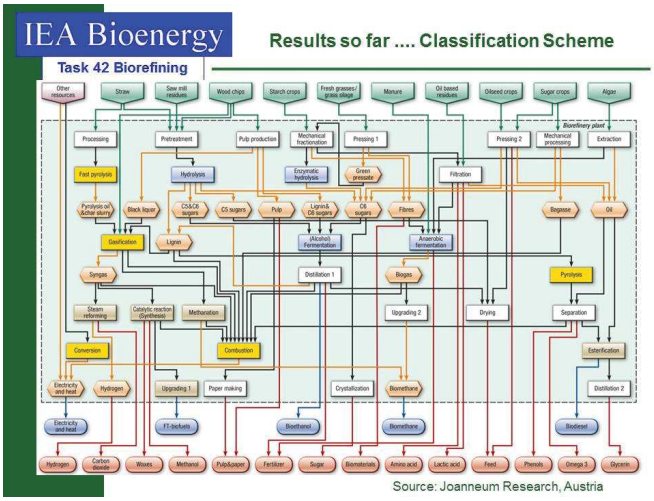

Fig.1 Classification of biorefineries [5]

Success implementing on market of integrated birefineries needs reliably processing units combined with economically profitable production chains and environmental acceptable. Development and applying the biorefinery concept have to include plants cultivating and selection of cultures, efficient conversion of biomass, minimizing thus raw materials requirements and in the same time strengthening economical of the market sectors.

In the present, at EU level there are biorefineries in countries like Austria, Belgium, Denmark, Finland, France, Deutschland, Italy, Ireland, Norway, Holland, Spain, Sweden, Hungary, UK.

In an absolutely arbitrary mode, in table 2 are presented some kinds of biorefineries.

Table 2 [6]

Austria						
Name	Company	IEA 42 Biorefinery Classification				Model
		Platforms	Products	Feedstocks	Processes	
Pischelsdorf	AGRANA	Starch, C5/C6 sugars	Starch and gluten, bio-ethanol, animal feed, CO_2	Cereals		Sugar and starch biorefinery
Germany						
Biowert	Biowert GmbH	Organic solutions (green juice and fibres), biogas, electricity and heat	High-quality cellulosic fibres, nutrients and biogas	Grass	Pressing, drying, separation	Green biorefinery
Italy						
Crescentino Bioethanol Plant	Beta Renewables	C5/C6 sugars, lignin, power & heat	Bioethanol and animal feed	Giant reed, miscanthus, switch grass, agricultural waste (straws)	Giant reed, miscanthus, grass, agricultural waste (straws)	Ligno-cellulosic biorefinery
Netherlands						
Rotterdam Biorefinery	Neste oil	Oil	Hydro-treated Vegetable Oil (HVO	Vegetable oil, waste animal fat	Hydro-treatment	HVO Biorefinery
Norway						
Sarpsborg Biorefinery	Borregaard	C5/C6 sugars, lignin, biogas	Bioethanol, lignin, cellulose, vanillin, biogas	Ligno-cellulosic crops or residues	Cooking, fermentation separation	Forest biorefinery

3. CONCLUSIONS

Biorefineries were established more time ago in food industry, for non-food products. The reasons consists in the fact that some of the key technologies, such as, the product fractioning and separation which belong to integrated biorefineries are not yet sufficient mature to apply them on commercial market. The market sectors which should collaborate for developing and commercialisation of biomass along value chain, sometimes don't do this and still there is a lack of knowledge and expertise regarding to advantages of the biorefinary processes for optimal using of biomass.

Nevertheless, by accelerating the biomass producing, especially in biorefinery approach, socio-economic and environment effects are optimised, resulting a more cost effective production of food products ingredients for animal food, chemicals, materials and bioenergy (fuels, power, heat) reducing the emissions of greenhouse gases, as well as the efficient use of available resources (raw materials, minerals, water).

References

[1] Communication from the Commission to the European Parliament, the Council, the European Economic and Social Committee and the Committee of the Regions innovating for sustainable growth: a bioeconomy for Europe strategy for "innovating for sustainable growth: a bioeconomy for Europe"
[2] http://www.rural-energy.eu Sustainable-Energy-Solutions-for-Rural-Europe
[3] Teodor Vintilă-Biorefineries, the plants of the future. Production units which use biological systems, to catalyse the the base chemical transformation. Biorafinariile, uzinele viitorului. Unitatile de productie care folosesc sisteme biologice, pentru a cataliza transformarile chimice de baza-Club Agriculturamanager.ro
[4] Biorefineries Roadmaps part of the German Federal Government action plans for the material and energetic utilisation of renewable raw materials
[5] Brochure IEA Bioenergy Task 42 Biorefinery
[6] Biorefineries Blog info@biorefinno.com

THE INFLUENCE OF PROCESSING PARAMETERS ON YIELD AND QUALITY OF VEGETABLE OIL OBTAINED BY THE MECHANICAL PRESSING OF SUNFLOWER OILSEEDS

Adrian-Ovidiu Arișanu[1], Florean Rus[1], Horia-Gheorghe Schiau[1]
Department for Engineering and Management in Food and Tourism, Faculty of Food and Tourism, *Transilvania* University of Brașov

ABSTRACT

The extraction of vegetable oils from sunflower oilseeds (*Helianthus annuus L.*), can be done by various methods: by mechanical pressing (mechanical oil expression), by solvents (solvent extraction), by supercritical fluids, by GAME (Gas Assisted Mechanical Expression) method, by combining the previously mentioned methods under different forms. Irrespective of the chosen extraction procedure, it should allow, besides high oil yields, low energetic consumptions and low production costs, obtaining high-quality end products that are appreciated and preferred by consumers. Among the above mentioned extraction methods, the extraction by mechanical pressing is the one that integrates such characteristics the best. By mechanical pressing, best quality end products are obtained, the energy consumption is low, and the purchase costs for the equipment are low. The biggest downside of mechanical pressing, as compared to the other extraction methods, refers to the low oil yield (extraction degree). In this sense, we have tried to emphasize in this paper the manner in which the main parameters involved in the pressing process (pressure, temperature, time) influence the oil yield. The raw material that was the object of the experimental researches was of three types: unpeeled sunflower seeds, partially peeled sunflower seeds and sunflower oilseed kernels, pressing of such products being done by a hydraulic press.

1. INTRODUCTION

Worldwide, especially in industrialized countries, there is increasing trend in human consumption of vegetable oils, which can be explained by the advantages they pose in terms of food, compared with animal fats:

- are more easily assimilated (predominantly unsaturated fatty acids as to the saturated ones);
- are nutritionally superior due to the presence of polyunsaturated fatty acids;
- contain less cholesterol for the human body;
- are more suitable for food products (mayonnaise, sauces, dressings etc.) [4].

In nature, all plant tissues contain vegetable fats in certain amounts (0.01...70%), which would theoretically mean that there is a variety of vegetal sources from which oils for human consumption can be extracted [3]. Practically speaking, things are very different because in industry oils are extracted only from the parts of the plant that contain vegetal fats in economically acceptable quantities (at least 15...20% of the vegetable fats, commonly found in seeds, fruits, kernels, tubers or germs).

Related to the extraction methods used, although experiments are done for the development of extraction procedures of vegetal oils by supercritical fluids (especially supercritical CO_2), but also by using GAME (Gas Assisted Mechanical Expression) methods,

[1] Department for Engineering and Management in Food and Tourism, Transilvania University of Brașov, Castelului Street, no. 148, Brașov 500014, e-mail: arisanu_ov@yahoo.com, 0751 925 480

currently, at international level, we can speak about the existence of two enshrined procedures: extraction by mechanical pressing (in screw presses or in hydraulic presses) and solvent extraction [7]. Such procedures may be applied independently or successively, depending on the type and characteristics of the oilseed raw material, its oil content, required extraction degree, but also depending on the final destination of the extracted oil. For instance, in Romania, for vegetable oils extraction from oilseed crops, the combined procedure is used in most of the cases: oilseed material pressing, by which a separation of oil of up to 80…85% can be done, followed by solvent extraction, by which the rest of the oil is separated (up to 99…99.5%) [3].

Irrespective of the chosen extraction procedure, besides high oil yields, low energy consumptions and low production costs, it should allow obtaining high quality products that are appreciated and preferred by the consumers. Studying and analysing in detail the previously mentioned extraction methods (extraction by mechanical pressing, solvent extraction, extraction by supercritical fluids and extraction by using GAME method), it has been noticed that extraction by mechanical pressing is the method that integrates the best such characteristics. Therefore, best quality products are obtained by mechanical pressing, the energy consumption is low, and the purchase costs of the equipment are low. Another advantage of the extraction by mechanical pressing refers to the fact that no chemicals are used during this process, obtaining oils with tastes and smells specific to the seeds they were extracted from. The oils that were extracted as such can be eaten directly, with no other „grooming" or quality improvement procedures [3].

The biggest downside of mechanical pressing, as reported to the other extraction methods, refers to the low oil yield (accomplished extraction degree) [1], [2], [7]. In this sense, in this paper we have tried to emphasize the manner in which the main parameters involved in the pressing process (pressure, temperature, time) influence the oil yield.

2. MATERIALS AND METHODS

The raw material that was the object of experimental researches were sunflower oilseeds (*Semen Helianthi*). This choice was done considering that in Romania, sunflower (*(Helianthus annuus L.)* is one of the most important oil plants, annually growing on large surfaces. Moreover, we must mention that Romania is one of the biggest world exporters of sunflower oilseeds with a value of exports for 2014 of 452.5 million Euros. Moreover, Romania, next to Bulgaria and France, covers around 50% of the global export offer, Romania's contribution being nearly 18%.

Studied sunflower seeds (fig. 1), with black pericarp, were purchased from Brasov (45°38' N and 25°35' E), Romania. Following the removal of impurities in the seed mass, in view of providing their physical purity, the oilseed material was maintained for two weeks at a temperature of 18°C, to reach the physiological maturity.

Figure 1: Sunflower seeds

To determine the moisture of the physiologically mature seeds, an electronic Granomat type moisture meter was used, with the following technical characteristics: voltage – 110/230 V, 50/60 Hz; sizes – around 420 x 360 x 390 mm; weight – around 18 kg. Except for moisture, this device (fig. 2), also allows the determination of other quality indexes, such as: electrical capacity (dielectric constant), weight, sample temperature etc. For studied samples, the indicated relative moisture was of 6%, for a temperature of 18.3°C.

Figure 2: Granomat moisture meter

Two new categories of oilseed products were obtained by manual decortication (peeling) of two thirds of the samples whose moisture was previously determined: sunflower kernels (by total decortication) and partially peeled sunflower seeds (by partial decortication), that together with the remained unpeeled seeds made the object of subsequent experimental researches. Partial and total seed decortication was necessary to cover a wider range of oil products submitted to extraction by mechanical pressing.

Further, the oil products were pressed, using for this purpose a laboratory mini-press (fig. 3a), attached to a big hydraulic press (fig. 3b).

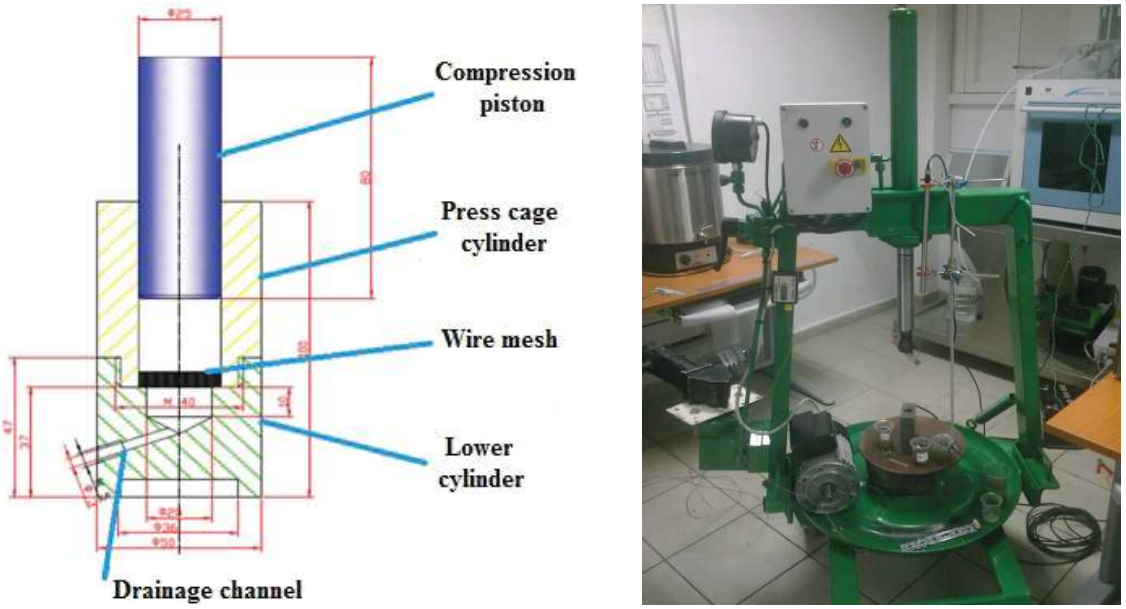

a) b)

Figure 3: Mechanical expression rigs – a) scheme of the laboratory mini-press; b) hydraulic press

We must mention that researches took place in Building R of University *Transilvania* from Brasov, at the Faculty of Food and Tourism.

3. RESULTS AND DISCUSSION

Determinations at temperatures of 30, 60 and 90 Celsius degrees were done at maximum applied pressures of 50, 100, 150, 200 and 250 bars were done for each category of oilseed material. The maximum pressures were reached gradually, for the oilseeds not to tamp immediately and therefore not to block oil evacuation.

To obtain cogent results, three pressing modalities of oilseed products were tested: continuous pressing, by which the pressure applied to seeds was gradually increased, but without ceasing to move the active organ in the pressing chamber; 3 steps pressing (50-150-250 bars), implying the gradual increase of the pressure applied to seeds, but ceasing to move the active organ in the pressing chamber for periods of 30, 60 or 90 seconds for each pressure step separately (basically, after reaching a pressure step, for instance 50 bars, the oil material was submitted to a relaxation phenomenon); 5 steps pressing (50-100-150-200-250 bars), that was done similarly to 3 steps pressing, except that in this case the oilseed material was submitted more often to the relaxation phenomenon.

We must mention that heating oil seeds at temperatures of 30, 60 and 90 degrees Celsius were done by a microwave oven, and each sample of oilseed material submitted to extraction by pressing weighted 10g.

In figure 4 we can see the results obtained following continuous pressing of the three categories of oilseed products. It can be noticed that the maximum yield in oil was obtained when pressing the oilseed kernels at temperatures of 90 degrees Celsius and at a maximum applied pressure of 250 bars. There are no important differences between the results obtained in the case of oilseed kernels pressing and those obtained in the case of partially peeled oilseeds. The oil yield was minimum for unpeeled oilseed pressing, for pressures of 50 bars and temperatures of 30 degrees Celsius. From the point of view of quality and aspect of the extracted vegetable oil, the best results were obtained for the partially peeled oilseeds pressing and for oilseed kernels pressing at temperatures of 30 degrees Celsius and generally at maximum applied pressures as low as possible.

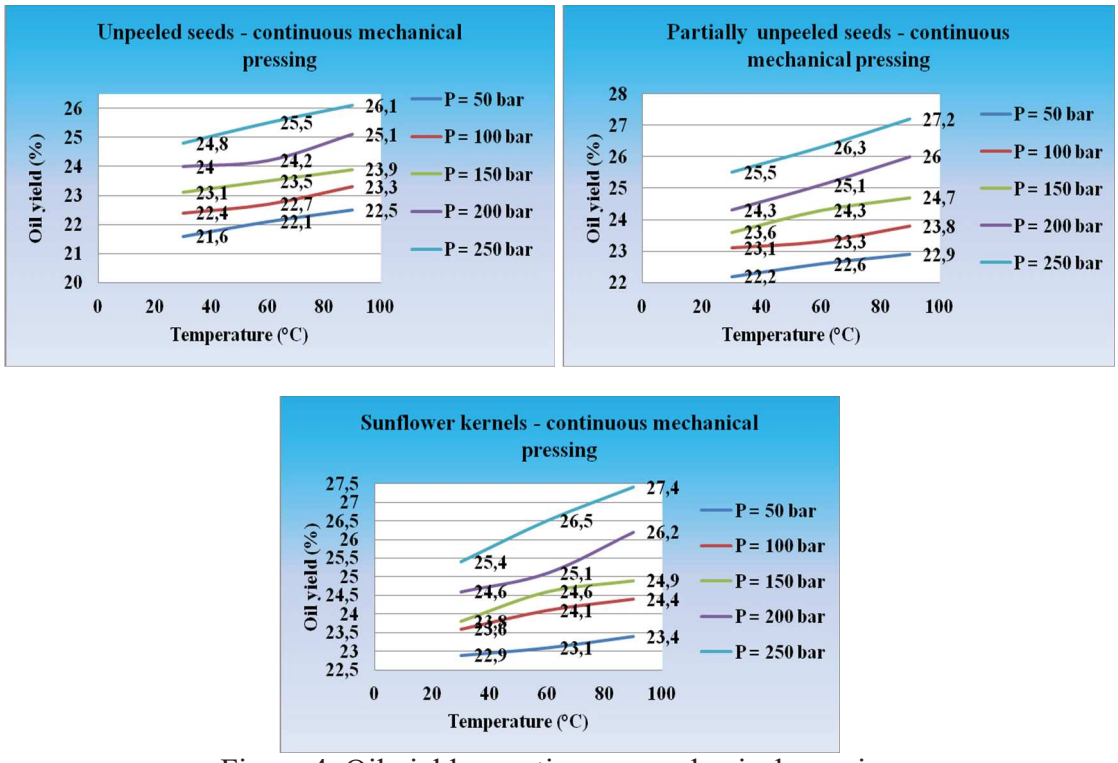

Figure 4: Oil yield – continuous mechanical pressing

As it can be noticed, in order to get best oil yields, high temperatures of the oilseed raw material and working pressures are necessary, but all these lead to an oil losing its qualities in comparison with the oil obtained by pressing at low temperatures.

In figure 5 we can see the results obtained following 3 steps pressing of the oilseed products, and in figure 6 we can see the results obtained following 5 steps pressing of oilseed products.

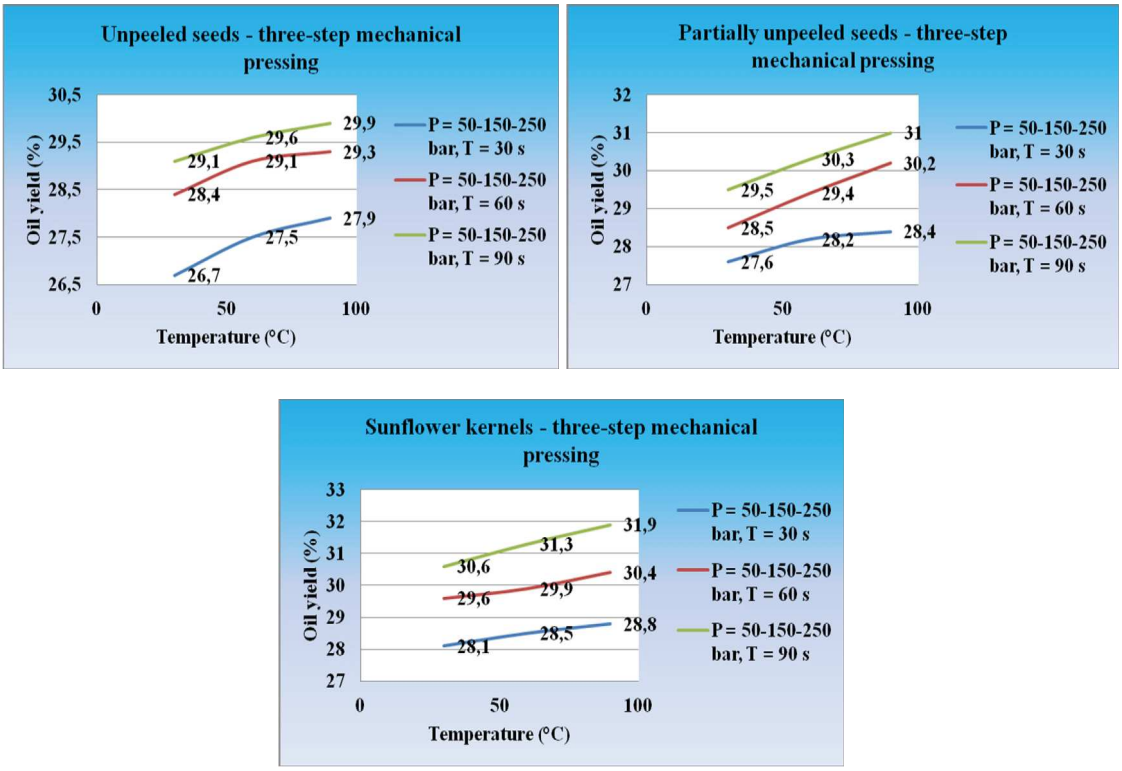

Figure 5: Oil yield – three-step mechanical pressing

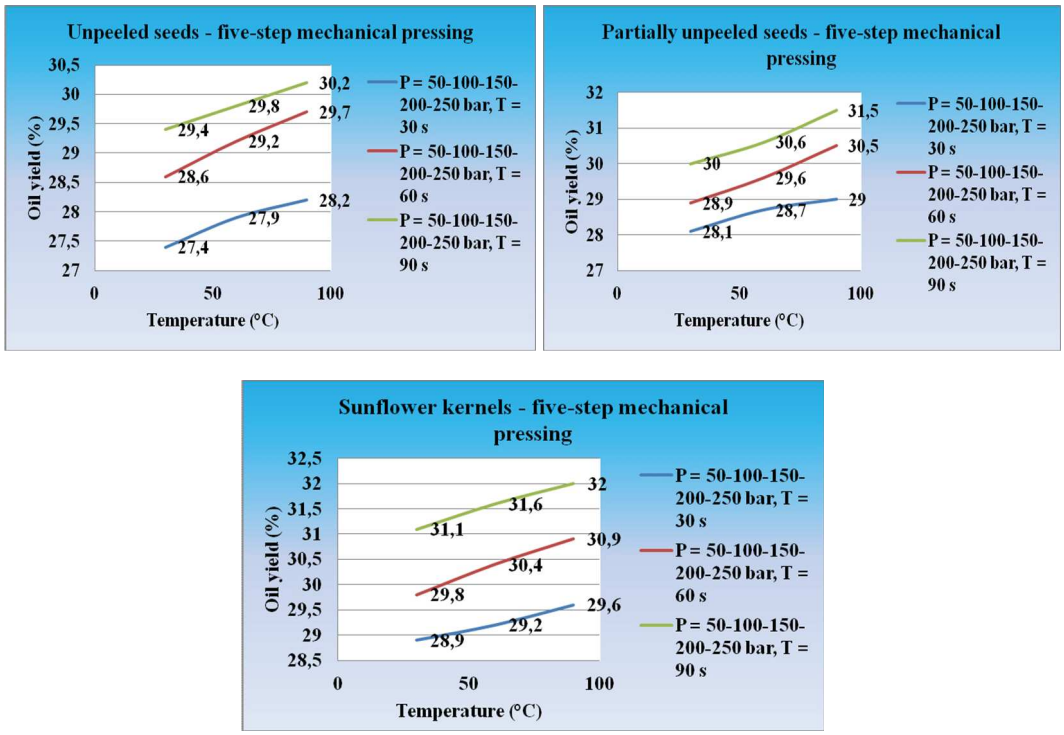

Figure 6: Oil yield – five-step mechanical pressing

As it can be noticed, staged pressing leads to high oil yields, in comparison with continuous pressing, but the length of the pressing process is much higher and it must be analysed if this is profitable from the economic point of view.

Also in the case of staged pressing, the maximum oil yields were obtained for high temperatures and pressures.

4. CONCLUSIONS

- For the extraction of vegetable oils from oilseed crops there are two established procedures: extraction by mechanical pressing and solvent extraction, but also two procedures becoming more and more popular at industrial level: extraction by supercritical fluids and extraction by GAME method.
- Irrespective of the chosen extraction procedure, besides high oil yields, low energy consumptions and low production costs, it must allow obtaining high quality end products.
- Extraction by mechanical pressing allows obtaining high quality vegetable oils that may be consumed directly, with no previous „grooming" or quality improvement processes.
- The biggest downside of extraction by mechanical pressing, reported to the other extraction methods, refers to low oil yields.
- Following the experiments, for sunflower seeds, it has been noticed that the oil yield is directly proportional with the temperature of oil raw material and maximum applied pressure.
- Regarding the quality and aspect of the extracted vegetable oil, the best results were obtained in the case of oilseed pressing at low temperatures and at low pressures.
- Oilseed staged pressing leads to high oil yields in relation to continuous pressing, but the length of the pressing process is much higher and must be analysed if this is profitable from the economic point of view.

Acknowledgement

This paper is supported by the Sectorial Operational Programme Human Resources Development (SOP HRD), financed from the European Social Fund and by the Romanian Government under the contract number POSDRU/107/1.5/S/76945.

References

[1] Adeeko, K.A., Ajibola, O.O., *Processing factors affecting yield and quality of mechanically expressed groundnut oil*, Journal of Agricultural Engineering Research, vol. 45, pp. 31-43, 1990.
[2] Ajibola, O.O., Owolarafe, O.K., Fasina, O.O, *Expression of oil from sesame seeds*, Canadian Agricultural Engineering, vol. 35, pp. 83-88, 1993.
[3] Arișanu, A.O., Hodârnău, E., *Particularities of oil extraction by pressing hulled and hydrothermally processed sunflower seeds*, Journal of EcoAgriTourism, vol. 7, pp. 32-37, 2011.
[4] Banu, C., *Food industry between fraud and truth*, ASAB Publishing House Bucharest, Romania, 624 p., 2013.
[5] Brătfălean, D., Cristea, V.M., Agachi P.Ș., *Improvement of sunflower oil extraction by modelling and simulation*, Revue Roumaine de Chimie, vol. 53(9), pp. 881-888, 2008.
[6] Găgeanu, P., Păun, A., Zaica, A., *Technology and technical equipments for obtaining vegetable oils*, INMATEH – Agricultural Engineering, vol. 29(3), pp 70-75, 2009.
[7] Khan, L.M., Hanna, M.A., *Expression of oil from oilseeds – A review*, Journal of Agricultural Engineering Research, vol. 28, pp. 495-503, 1983.
[8] Olaniyan, A.M., *Effect of extraction conditions on the yield and quality of oil from castor bean*, Journal of Cereals and Oilseeds, vol. 1(2), pp. 24-33, 2010.

GENERAL ASPECTS REGARDING OILSEED PLANTS SPREAD BOTH IN ROMANIA AND AT INTERNATIONAL LEVEL

Adrian-Ovidiu Arișanu[1], Florean Rus[1], Horia-Gheorghe Schiau[1]
Department for Engineering and Management in Food and Tourism, Faculty of Food and Tourism, *Transilvania* University of Brașov

ABSTRACT

Within the vegetable world, there are various species of plants that can gather significant quantities of lipids in various organs, usually between 35 and 70%, such plants being known as oleaginous plants or oil plants. The main purpose of oleaginous plants cultivation is the extraction of fats and edible and industrial oils, following both high extraction yields and also obtaining high quality end products. As a consequence of their special importance, oilseed plants are cultivated all around the planet, the share of each plant modifying depending on the geographical area.

1. INTRODUCTION

In the vegetable world, there are many species of plants that can gather in their component parts (in seeds, fruits, kernels, tubers, germs etc.), significant quantities of lipids, usually between 35 and 70%, such plants being known as oleaginous plants or oil plants. Taking into consideration their chemical composition, the above mentioned plants are also known as oil and protein rich or "oleoproteic" plants in the specialized literature, because usually, besides lipids, they also contain significant quantities of proteins (generally, between 12 and 42%) [2].

The main purpose of oilseed plants cropping is the extraction of food and industrial (technical) fats and oils. Nevertheless, at industrial level, we can speak of typical, proper or exclusive oilseed plants, especially cropped for the extraction of vegetable oils and about oilseed plants with mixed use, secondarily used for obtaining vegetable oils, the main use field being other than separation of fats and oils (the production of vegetable fibres and proteins, the production of natural juices etc.). Moreover, we should mention that in vegetable oils industry only those species are considered typical oilseed plants that have a minimum content of 30...35%, except for soybeans, which, even with an oil content of nearly 20% is considered a typical oilseed plant [2].

2. CLASSIFICATIONS

The number of oil plants is very high. Therefore, from nearly 100 species of known oleaginous plants, around 40 species, grouped in 16 important botanic families are currently highlighted at international level, and these are: family Compositae or Asteraceae (sunflower, safflower), family Cruciferae or Brassicaceae (colza, camelina), family Fabaceae (soybean, groundnut), family Euphorbiaceae (castor oil plant, tung oil tree), family Malvaceae (cotton), family Papaveraceae (poppy), family Rosaceae (almond), family Pedaliaceae (sesame), family Juglandaceae (walnut), family Arecaceae (oil palm tree, coconut tree), family Oleaceae (olive tree), family Linaceae (linseed), family Cucurbitaceae (pumpkin), family Cannabaceae

[1] Department for Engineering and Management in Food and Tourism, Transilvania University of Brașov, Castelului Street, no. 148, Brașov 500014, e-mail: arisanu_ov@yahoo.com, 0751 925 480

(hemp), family Solanaceae (tobacco, tomatoes) and family Vitaceae (grapevine) [3].

Depending on their *origin*, oilseed raw material can be classified as follows:

- typical oilseed plants;
- textile-oilseed plants (mixed oilseed plants);
- oilseed weeds;
- oilseed fruits of the cultivated trees;
- oilseed fruits of uncultivated trees;
- sub products and oilseed waste.

The chemical composition and the peel content of oilseed raw material are mentioned in table 1.

Table 1: Chemical composition and peel content of oilseed raw material [2]

Raw material	Peel content, %	Chemical composition, %					
		Moisture	Oil	Proteins	Unassured extractive substances	Cellulose	Ash
Sunflower seeds	14...28	9…11	44...48	18...20	10...15	14...18	2...3
Soy beans	7...12	11...13	17...19	33...36	20...23	4...5	3...5
Linseeds	4...6	9...11	35...38	25...27	20...23	4...5	3...4
Canola seeds	4...6	6...8	35...42	25...28	17...20	4...6	3...5
Castor seeds	22...25	6...9	44...52	14...18	15...17	15...18	2...4
Safflower seeds	48	7	33...40	14...15	8...9	38...40	3
Sesame seeds	8	5...7	36...58	12...24	10...29	2...11	3...8,5
Cotton seeds	31	8	17...23	22...23	26	17	4
Hemp seeds	20...25	5...12	28...34	15...27	15...25	12...16	3...5
Pumpkin seeds	24	9...11	35...54	28...30	15...20	13...20	4...5
Tobacco seeds	15	6...10	34...44	30	15	20	4...6
Wheat germs	-	11...15	10...12	28...39	17...21	10	4
Maize germs	-	6...11	20...52	20...28	18...30	4...6	3...4

We must mention that, for the same oilseed raw material (for the same variety or hybrid), there are relatively high differences regarding the oil content indicated in different sources in the published literature, absolutely normal differences, since the accumulation of fat substances directly depends on the applied agrotechnics, as well as on pedoclimatic conditions. For instance, in Romania, pedoclimatic conditions where sunflower is cultivated may determine oscillations of the oil content between 8 and 10% for the same variety or hybrid. From numerous experimental data, we could notice that the oil percentage in

sunflower seeds grows, as soil moisture grows. Moreover, the oil percentage increases noticeably under the influence of phosphorus and potassium and decreases under the influence of large quantities of nitrogen in the soil. A special influence on the chemical composition have the factors related to oilseeds conservation and storage, from the cropping moment to the industrial processing moment [2].

3. IMPORTANCE AND SPREADING

As a consequence of their special importance, oilseed plants are cultivated all around the planet, the share of each plant modifying depending on the geographical area. Internationally, after the productions registered in 2014, in accordance with the details provided by the Department of Agriculture in the United States of America (USDA) and by the Food and Agriculture Organization (FAO), the most important typical oilseed plants are the following: soybeans, with a production of 308.4 million tons, canola, with a production of 70.9 million tons, groundnuts, with a production of 42.3 million tons and sunflower, with a production of 41.3 million tons. In Europe, soybeans, canola and sunflower are the first within typical oilseed plants, this time, on the first two places almost equally being sunflower and canola, with productions of 29.46 million tons and respectively of 28.89 million tons, followed in this hierarchy by soybeans, with a production of 9.01 million tons, figures that were also registered in 2014. Regarding vegetable oil production, oil palm has the highest share among oilseed raw material, with a share of 34.39% from the world oil production, followed by soybeans, with a share of 26.75%, canola, with a share of 15.28% and sunflower, with a share of 7.64%. In Europe, canola comes first, with a share of 38.82% of the oil production, followed by sunflower, with a share of 33.72% and soybeans, with a share of 11.84% [6].

In Romania, depending on the cultivated surface and the total seed production, the main oilseed plants are: sunflower, canola and soybeans [3].

Regarding sunflower, it has been noticed that year 2013 was a peak year in terms of cultivated surface (1072 thousand hectares), but as a consequence of the average hectare yield (1998 kg/hectare), lower than the one in 2014 (2193 kg/hectare), the total yield of sunflower seeds has a maximum value in 2014 (the highest value in the history of Romania, according to the statistic data of FAO). Therefore, with a total production of 2.18 million tons of sunflower seeds, representing 5.27% from the world production and 7.39% from the European production, Romania was ranging forth in the world in 2014, after Ukraine (10.13 million tons), the Russian Federation (9.03 million tons) and the People's Republic of China (2.38 million tons), third in Europe and first in the European Union [6].

Considering the above mentioned aspects, we must mention that Romania is one of the biggest world exporters of sunflower seeds, with a value of exports of 452.5 million Euros in 2014. Moreover, Romania, next to Bulgaria and France, provides around 50% of the global export offer, the contribution of Romania being of nearly 18%.

Nevertheless, during 2007...2014, Romania runs up considerable losses regarding the average yield for hectare (1566.1 kg/hectare – the average of the eight years), nearly 15% lower than the level registered in the European Union. Although the production capacity of sunflower hybrids currently cultivated in Romania is much higher than reflected in the average yield per hectare, the production deficit can be explained by the variation of pedoclimatic conditions and crop years. Therefore, the production potential of hybrids is diminished because of less favourable physical-chemical characteristics of some soils sunflower extended to during the last period of time, but also because of the lack of moisture, that cannot be provided in certain years at the level of the plant requirements, but only under irrigation conditions [2].

For canola, the largest cultivated surface was in 2010 (527.1 thousand hectares), while the total seed yield reached the maximum value in 2014 (1.0591 million tons), this number representing a historical maximum for Romania, according to the statistic data provided by FAO. With a value export of 338.3 million Euros in 2014, Romania is still in the top of the biggest seven world exporters of canola seeds [6].

Regarding soybeans, the surface cultivated with this oilseed plant during these the eight years (2007...2014) oscillated between 109.3 thousand hectares in 2007 and 46.1 thousand hectares in 2008, while the total production peaked as the maximum of the studied period in 2014 (202.8 thousand tons). The share of Romania in global soybeans exports is low, nearly 0.08%. Nevertheless, Romanian soybeans exports increased during the last years, totalizing 21.4 million Euros in 2014 [6].

4. CONCLUSIONS

- In the vegetable world, there are many species of plants that can gather in their component parts, significant quantities of lipids, usually between 35 and 70%, such plants being known as oleaginous plants or oil plants.
- The main purpose of oleaginous plants cultivation is the extraction of fats and edible and industrial oils, following both high extraction yields and also obtaining high quality end products.
- As a consequence of their special importance, oilseed plants are cultivated all around the planet, the share of each plant modifying depending on the geographical area.
- Internationally, after the productions registered in 2014, the most important typical oilseed plants are the following: soybeans, with a production of 308.4 million tons, canola, with a production of 70.9 million tons, groundnuts, with a production of 42.3 million tons and sunflower, with a production of 41.3 million tons.
- Regarding vegetable oil production, oil palm has the highest share among oilseed raw material, with a share of 34.39% from the world oil production, followed by soybeans, with a share of 26.75%, canola, with a share of 15.28% and sunflower, with a share of 7.64%.
- In Romania, depending on the cultivated surface and the total seed production, the main oilseed plants are: sunflower, canola and soybeans.

Acknowledgement

This paper is supported by the Sectorial Operational Programme Human Resources Development (SOP HRD), financed from the European Social Fund and by the Romanian Government under the contract number POSDRU/107/1.5/S/76945.

References

[1] Ajibola, O.O., Owolarafe, O.K., Fasina, O.O, *Expression of oil from sesame seeds*, Canadian Agricultural Engineering, vol. 35, pp. 83-88, 1993.
[2] Arișanu, A.O., Hodârnău, E., *Particularities of oil extraction by pressing hulled and hydrothermally processed sunflower seeds*, Journal of EcoAgriTourism, vol. 7, pp. 32-37, 2011.
[3] Banu, C., *Food industry between fraud and truth*, ASAB Publishing House Bucharest, Romania, 624 p., 2013.
[4] Khan, L.M., Hanna, M.A., *Expression of oil from oilseeds – A review*, Journal of Agricultural Engineering Research, vol. 28, pp. 495-503, 1983.
[5] Pearson, C.H., Rath, D.J., *A hydraulic press for extracting fluids from plant tissue samples*, Industrial Crops and Products, vol. 29, pp. 634-637, 2009.
[6] http://www.fao.org

NANOTECHNOLOGY APPLIED IN WASTEWATER TREATMENT FIELD

Covaliu Ileana - Cristina[1], Zăbavă Bianca Ștefania[1], Toma Laura[1], Ilie Filip[2], Vlăduț Valentin[3], Matache Mihai Gabriel[3], Moga Corina Ioana[4], Paraschiv Gigel[1], Biriș Sorin Ștefan[1]

[1] Department of Biotechnical Systems, University Politehnica of Bucharest, 313 Splaiul Independenței street, București, Romania
[2]Department of Machine Elements and Tribology, Polytechnic University of Bucharest, 313 Spl. Independentei, 060042 Bucharest, Romania
[3] National Institute of Research-Development for Machines and Installations Designed to Agriculture and Food Industry, 6 Ion Ionescu de la Brad, Bucharest, Sector 1, Romania
[4] SC DFR Systems SRL, 46 Drumul Taberei Street, ap. 23, Sector 6, Bucharest, Romania

ABSTRACT

Flotation is acknowledged to be the most important process in use at the present time for the removal of some pollutants from water such as particles and fats. Flotation is used in the processing of the bulk of the world's non-ferrous metals, as well as of a growing proportion of its iron, non-metallic minerals and coal. Chemical collectors are routinely added to ground ore slurries before using the flotation process. Collectors selectively bind to mineral-rich particles, increasing their hydrophobicity thus promoting selective flotation. Conventional collectors are small surfactants with a short hydrocarbon tail (2-6 carbons) and a head group, such as xanthate. The present paper is intended to present much larger hydrophobic polystyrene nanoparticles that are evaluated as potential flotation collectors.

1. INTRODUCTION

Flotation can be considered as physical and chemical separation process of solid products, by establishing a contact in three phases: the floating mineral, the liquid phase and air. This is an important separation technique nowadays, with its applications ranging from selective separation of minerals to microorganisms and even ions. Flotation is used in the processing of the bulk of the world's non-ferrous metals, as well as of a growing proportion of its iron, non-metallic minerals, and coal [1].

Flotation works efficiently only if the particles which will be subject to flotation are fully liberated from the other phases. The mixture of appropriately sized and liberated particles from which the selected particles will to be floated is first conditioned with the appropriate reagents. This suspension constitutes the flotation pulp. This pulp is then placed and agitated using impellers in a suitable container called a flotation cell, as shown in Figure 1.

Air is drawn in or sometimes fed into the cell near the impeller to form fine bubbles. These fine bubbles collide with the particles, attach to those particles which have the acquired hydrophobicity, and rise to the surface where they form a froth, which is removed as a flotation concentrate by skimming.

The hydrophilic particles that are not floated with the bubbles remain in the pulp. The hydrophobic and hydrophilic character of the surfaces can be changed using surfactants.

A surfactant which makes the surface hydrophobic, is called a *collector* and possesses at least one non-polar group. The non-polar group is usually represented by a hydrocarbon but it may be a fluorocarbon or a siloxane.

Chemical collectors are routinely added to ground ore slurries before using the flotation process. Collectors selectively bind to mineral-rich particles, increasing their hydrophobicity

[1] Splaiul Independentei 313, Sector 6, Bucharest, cristina_covaliu@yahoo.com, 0722791791

thus promoting selective flotation. Conventional collectors are small surfactants with a short hydrocarbon tail (2 – 6 carbons) and a head group, such as xanthate.

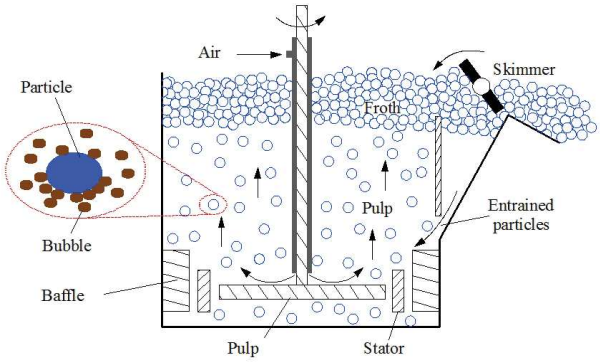

Figure 1 - Schematic diagram of an agitation-type flotation cell [2]

Applications of nanoparticles in water management can provide new values compared with conventional methods applied worldwide in drinking water treatment processes and wastewater treatment. An important role in the development of new technologies provides nanometer-scale materials that exhibit completely different from the same material of macroscopic dimensions. The ability of nanoparticles to induce flotation has been demonstrated by floating hydrophilic, negatively charged glass beads with cationic polystyrene nanoparticle collectors. Mechanisms and key parameters such as nanoparticle hydrophobicity and nanoparticle adsorption density have been identified. Coating with nanoparticles allows the beads to attach remarkably firmly on the air bubble. As little as 10% coverage of the bead surfaces with the most effective nanoparticles could promote high flotation efficiencies, whereas conventional molecular collector requires 25% or higher coverage for a good recovery.

2. METHODOLOGY

Flotation, or more formally froth flotation, is possible only when the surface of the particles to be floated is hydrophobic. Flotation involves pulverizing ore consisting of the desired mineral and unwanted gangue, into a wet slurry of particles approximately 100 μm in size, then adding a chemical reagent known as the "collector". The collector selectively binds to valuable metal-rich particles, increasing their hydrophobicity and thus promoting bubble/mineral attachment. The treated particle laden bubbles then rise to the surface of the slurry, where they are skimmed off.

Flotation reagents are the most essential component of the flotation process. In the early days of developing commercial flotation, the major advances resulted from acquiring more effective flotation reagents. On the basis of the function in flotation, flotation reagents are divided into collectors, frothers, modifiers, depressants and flocculants.

Collectors - The importance of hydrophobicity has been emphasized in both flotation theory and practical operation. The purpose of the collector is to selectively form a hydrophobic layer on a given mineral surface without binding to the gangue materials in flotation slurry; thus allowing the hydrophobized particles to attach to air bubbles, which can be recovered in the froth product. The general composition of a conventional molecular collector is a hydrocarbon chain with a reactive or functional head group [5].

S. Yang et colab., in the study "Nanoparticle Flotation Collectors: Mechanisms Behind a New Technology", have described a new technology where hydrophobic nanoparticles adsorb onto much larger, hydrophilic mineral particle surfaces to facilitate attachment to air bubbles in flotation. They showed that the role of nanoparticles is to

facilitate mineral-bubble attachment and/or to minimize detachment. The goal of the following analysis is to consider the influence of nanoparticle parameters on the various stages of mineral particle flotation with a view to identifying the critical role of nanoparticles and to optimize nanoparticle properties. In the study it was found that smaller and more hydrophobic nanoparticles are the most efficient flotation collectors and the forces required to pull a nanoparticle-coated sphere from the air/water interface of a bubble into the water was determined via micromechanical measurements. The maximum pull-off force ranged from 0.0086 μN for a clean 55 μm glass bead to 1.9 μN for a bead bearing adsorbed 46 nm diameter polystyrene spheres.

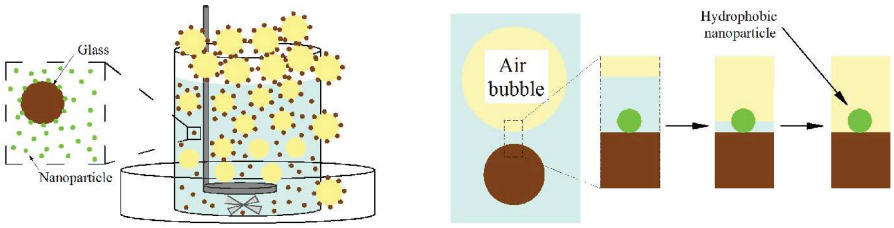

Figure 2 - Thinning and rupture of the liquid film between a mineral particle with adsorbed nanoparticles and an air bubble [7]

Hydrophobicity - Most mineral processing operations include multiple stages of froth flotation to concentrate and isolate the desired product. Typically, ore is ground to give particles that are ~100 μm in diameter with compositions varying from nearly pure samples of the desired mineral to unwanted gangue. The desired mineral particles are selectively treated with a short-chain, water-soluble surfactant to render the particles sufficiently hydrophobic to attach to air bubbles in the flotation cell.

In the study "*Nanoparticle Flotation Collectors II: The Role of Nanoparticle Hydrophobicity*", Songtao Yang and Robert Pelton determined the relationship between nanoparticle hydrophobicity and flotation recovery. They used the measurements of the contact angle to relate the nanoparticle surface properties to their ability to promote the froth flotation of hydrophilic glass beads.

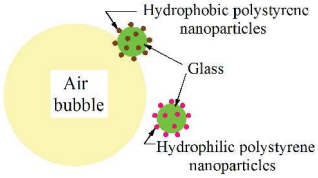

Figure 3 - Nanoparticle Hydrophobicity [3]

The results showed that the wetting behaviors of nanoparticle-decorated glass depend upon the sample history. Starting with dried surfaces, classic sessile drop measurements, θ_a, gave high advancing angles and indeterminable receding angles because of pinning. By contrast, when the glass surfaces were never dried after hydrophobic nanoparticle deposition, the corresponding receding water contact angles that formed by attached bubbles, θ_r, were reproducible. The minimum advancing water contact angle (dried, nanoparticle- decorated glass) for high flotation recovery with nanoparticle collectors was in the range of 30 – 40°, which is in accord with published results for molecular collectors. Poor flotation recoveries were observed when the nanoparticles were too hydrophilic or when the coverage was too low. Conventional flotation models suggest that the small 43 μm glass beads failed to attach to air bubbles in these cases. Figure 4 is showing combinations of the mineral particle size and contact angle capable of flotation based on the analysis of Scheludko23 using R = 5343 μm for Dmax, β = 25 μm for Dmin was chosen to divide low and high recovery data.

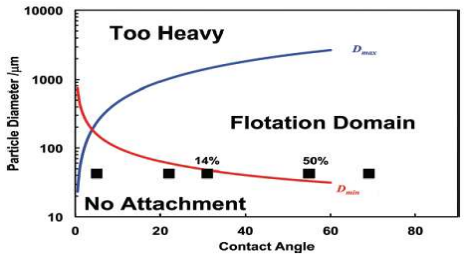

Figure 5 - Flotation domain showing combinations of the mineral particle size and contact angle capable of flotation [6]

Frothers - Frothers are used to reduce bubble size in the flotation cell and to enable the formation of a stable froth on the surface of the slurry. A stable froth is necessary in order to maintain bubbles long enough for mineral removal from the cell to maximize flotation performance.

Modifiers - The pH regulators and activators are usually classified as modifiers in flotation. The main function of modifiers is to facilitate the adsorption of collectors onto desired mineral surfaces and thus to govern flotation selectivity. The pH regulators are usually acids and alkalis.

3. CONCLUSIONS

Flotation is acknowledged to be the most important process in use at the present time for the concentration of minerals. Flotation, or more formally froth flotation, is possible only when the surface of the particles to be floated is hydrophobic.

Flotation reagents are the most essential component of the flotation process. In the early days of developing commercial flotation, the major advances resulted from acquiring more effective flotation reagents. On the basis of the function in flotation, flotation reagents are divided into collectors, frothers, modifiers, depressants and flocculants.

Frothers are used to reduce bubble size in the flotation cell and to enable the formation of a stable froth on the surface of the slurry. The ability of nanoparticles to increase flotation efficiency has been demonstrated by floating hydrophilic, negatively charged glass beads with cationic polystyrene nanoparticle collectors. The results sustain further researches in this field.

Acknowledgement

This work was supported by a grant of the Romanian National Authority for Scientific Research and Innovation, CNCS/CCCDI – UEFISCDI, project number PN-III-P2-2.1-PTE-2016-0183 and "Excellence Research Grants" Program, UPB – GEX "Bionanotechnology application in industrial wastewater treatment", contract number: 44/26.09.2016.

References

[1] Edwards, C.; Kipkie, W.; Agar, G., The effect of slime coatings of the serpentine minerals, chrysotile and lizardite, on pentlandite flotation. Int. J. Miner. Process. 1980, 7, (1), 33-42.
[2] Heiskanen, K.; Kirjavainen, V.; Laapas, H., Possibilities of collectorless flotation in the treatment of pentlandite ores. Int. J. Miner. Process. 1991, 33, (1-4), 263-274.
[3] Nguyen, A.; Schulze, H.; Ralston, J., Elementary steps in particle--bubble attachment* 1. Int. J. Miner. Process. 1997, 51, (1-4), 183-195.
[4] Pietrobon, M. C.; Grano, S. R.; Sobieraj, S.; Ralston, J., Recovery mechanisms for pentlandite and MgO-bearing gangue minerals in nickel ores from Western Australia. Miner. Eng. 1997, 10, (8), 775-786.
[5] Senior, G.; Thomas, S., Development and implementation of a new flowsheet for the flotation of a low grade nickel ore. Int. J. Miner. Process. 2005, 78, (1), 49-61. a New Technolog, McMaster University, Canada
[6] Yang S., Pelton R., Nanoparticle Flotation Collectors II: The Role of Nanoparticle Hydrophobicity, Ontario, Canada, 2011
[7] Yang S., Pelton R., Raegen A., Montgomery M.,. Dalnoki-Veress K., Nanoparticle Flotation Collectors: Mechanisms Behind, Ontario, Canada, 2011.

LIGNOCELLULOSIC SUBSTRATES BIODEGRADATION BY SOME STRAINS OF FILAMENTOUS FUNGI

Mirela Dincă[1], Mariana Ferdeș, Gigel Paraschiv, Mariana Munteanu, Nicoleta Ungureanu
University Politehnica of Bucharest, Faculty of Biotechnical Systems Engineering

ABSTRACT

Currently, lignocellulosic biomass represents the most used renewable resource for biogas production. The main components of lignocellulosic biomass are cellulose, hemicellulose and lignin, which are linked into a complex matrix highly resistant to chemical and biological conversion. However, lignin contained in lignocellulosic biomass is hardly biodegradable, thus representing a major obstacle for maximum methane production. A lot of microorganisms are capable of degrading cellulose and hemicellulose as carbon and energy sources.

In the present paper there were tested four types of filamentous fungi, namely *Trichoderma harzianum*, *Trichoderma viridae*, *Sporotrichum pulverulentum* and *Polyporus squamosus* on three types of lignocellulosic substrate consisting of wheat straw, corn stalks and sawdust.
There were evaluated specific parameters playing an important role in the process of biodegradation, such as: concentration of sugar, content of total soluble solids (TSS), dry matter in solid part and pH.

1. INTRODUCTION

Lignocellulosic biomass such as agricultural plant residues are available in large quantities and can be used for biofuel production without the risk of competition with arable land [1]. Using lignocellulosic biomass for energy recovery does not raise competition with alimentary products unlike first generation energy crops such as sugar beet, wheat or maize [2]. Biomass in general consists of 40 - 50% cellulose, 25 - 30% hemicellulose and 15 - 20% lignin and other extractable components [3]. Bioconversion of lignocellulosic biomass is limited by the protective structure of recalcitrant lignin.

In experimental researches, physical, chemical and biological pretreatment methods have been tested in order to break down the lignin and increase the biodegradation of cellulose and hemicelluloses which bear the biomethane potential of the material [4].
Biological pretreatment uses wood degrading microorganisms, including white-, brown-, soft-rot fungi, and bacteria to modify the chemical composition and structure of the lignocellulosic biomass so that the modified biomass is more flexible to enzyme digestion. The biological pretreatment is a promising technique with important advantages, such as low energy input, mild environmental conditions and environmentally friendly working manner [5, 6].

A lot of microorganisms are able of degrading and utilizing cellulose and hemicellulose as carbon and energy sources, but a much smaller group of filamentous fungi have the ability to break down lignin, the most recalcitrant component of plant cell walls. The most used are white-rot fungi which have the ability of degrading lignin to CO_2 [7].

Based on these considerations, the objective of the present paper was to investigate the efficiency of four types of filamentous fungi, namely *Trichoderma harzianum (TH)*, *Trichoderma viridae (TV)*, *Sporotrichum pulverulentum (SP)* and *Polyporus squamosus (PS)* on lignocellulosic biomasses (wheat straw (WH), corn stalks (CS) and sawdust (SD)).

The effects of fungal pretreatment were assessed by analysing the samples before and after incubation for content of total soluble solids (TSS %), pH and concentration of sugar.

[1]University Politehnica of Bucharest, Faculty of Biotechnical Systems Engineering, phone no: 0761938017, email: mirela_dilea@yahoo.com

2. METHODOLOGY

Samples preparation

The tested biomass composed by wheat straw, corn stalks and sawdust were collected from Teleorman County, an agricultural region in Romania.

Biomass samples were grinded at 1 mm using the laboratory mill Pulverisette 19 (Fig. 1a). 3 g of each tested substrate were placed in 500 mL Erlenmeyer flasks containing 200 mL of water. The Erlenmeyer flasks were then autoclaved at 120°C for 15 min, cooled at room temperature and inoculated with 10 mL of the four types of filamentous fungi, namely *Trichoderma harzianum*, *Trichoderma viridae*, *Sporotrichum pulverulentum* and *Polyporus squamosus.* Control flasks were prepared in the same manner.

After that, all flasks were placed in the orbital incubator (Fig. 1b) for a week at a temperature of 30 °C and the mixing rate was set at 150 rpm.

Fungal cultures of *Trichoderma harzianum*, *Trichoderma viridae*, *Sporotrichum pulverulentum* and *Polyporus squamosus* were cultivated on Potato Dextrose Agar in tubes at 25°C for 7 days.

Flasks sterilization had two purposes: destruction of contamination microorganisms and release of nutrient compounds from the vegetal substrate that pass into the solution.

Trichoderma harzianum was isolated from the tree bark from the University Politehnica of Bucharest Park.

All the fungal strains belong of the Microbiology Laboratory from Faculty of Biotechnical Systems Engineering.

Trichoderma harzianum and *Trichoderma viridae* are known for their capacity to produce cellulolytic enzymes that contribute to the degradation of lignocellulosic plant material [9].

The white – rot group of fungi have in common the capacity to degrade lignin as well as all other major wood components. They also have the ability to produce laccase which oxidizes phenolic compounds related to lignin. The white-rot fungi normally attack cellulose and lignin simultaneously when degrading wood [10]. The white – rot fungus *Sporotrichum pulverulentum* is one of the microorganisms that are able to degrade the polysaccharides and the lignin present in lignocellulosic biomass. It was demonstrated that *Sporotrichum pulverulentum* produces extracellular enzymes capable of oxidizing cellulose to cellobionolactone [11].

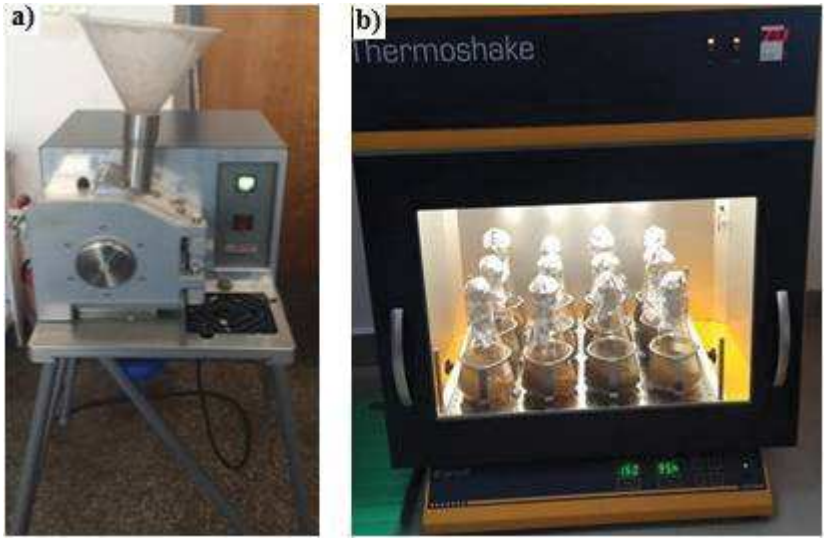

Figure 1: The laboratory mill Pulverisette (a) and the orbital incubator (b)

Polyporus squamosus together with other types of white rot fungi like *Pleurotus ostreatus, Auricularia auricular* secrete extracellular ligninolytic enzymes (lignin peroxidase, manganese peroxidase and laccase) that biodegrade lignin [12].

Methods of analysis

After incubation, the solid part from each flask was separated from the liquid part in order to conduct the laboratory tests.

The dry samples were weighed and the mass was compared to initial mass to determine the total solids biodegradation. The masses of the samples after incubation included the associated fungal biomass which could not be separated from the solids. This caused an overestimation of the residual masses of substrates.

The pH of liquid samples taken at certain intervals of time was determined using a Hanna pH-meter. The total soluble solids (TSS) were determined on a thermobalance, after centrifugation of initial samples at 5000 rpm and then filtering through a membrane with pores of 0.45 μm. The TSS represents a decisive factor for the development and growth of microorganisms. The total soluble solids have been expressed in term of dry matter (g).

Sugars concentration was achieved by the method in which is used the 3.5-dinitrosalicylic acid (DNS) [8]. All measurements were done using a T92+ UV-VIS spectrophotometer. The absorbances were measured at 540 nm and in figure 2 can be observed the calibration curve.

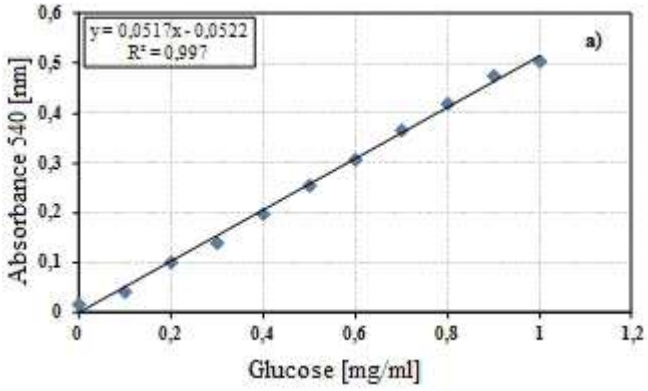

Figure 2: Calibration curve for sugar concentration

3. RESULTS

Mass balance evaluation and dry matter of substrates biodegradation in fungal pretreatment are presented in table 1. It was observed that for all tested substrates were recorded reduction of dry matter between 2.11 g and 2.78 g. The highest values, 2.78 g, were recorded for sawdust substrate in the presence of *Trichoderma harzianum.*

The total soluble solids contain soluble sugars, soluble proteins, mineral salts and water-soluble compounds that are used as nutritive substrate for different groups of microorganisms involved in anaerobic digestion and biogas production.

The final dry matter is composed both from vegetal material remained unhydrolyzed and from fungal biomass that has developed by using sugars and other nutrients from the culture medium. These sugars are resulted both from initial sugars coming from sterilized medium and after enzymatic hydrolysis produced by fungal strains on tested substrate.

Table 1: Substrate characterization after 7 days of fermentation

Sample	Type of fungi	Final mass [g]	Dry matter [g]
1	Wheat straw + TH	14.50	2.73
2	Corn stalks + TH	12.44	2.42
3	Sawdust + TH	13.61	2.78
4	Wheat straw + TV	15.34	2.50
5	Corn stalks + TV	14.00	2.77
6	Sawdust + TV	16.86	2.28
7	Wheat straw + SP	18.00	2.31
8	Corn stalks + SP	17.80	2.52
9	Sawdust + SP	10.95	2.21
10	Wheat straw + PS	18.41	2.68
11	Corn stalks + PS	20.70	2.24
12	Sawdust + PS	12.24	2.11

Mass loss was determined as follows:

$$Mass\ loss\ (\%) = \frac{initial_{mass} - dry_{matter}}{initial_{mass}} \times 100 \quad (1)$$

In figure 3 can be observed the mass loss for each type of tested substrate and each fungal strain.

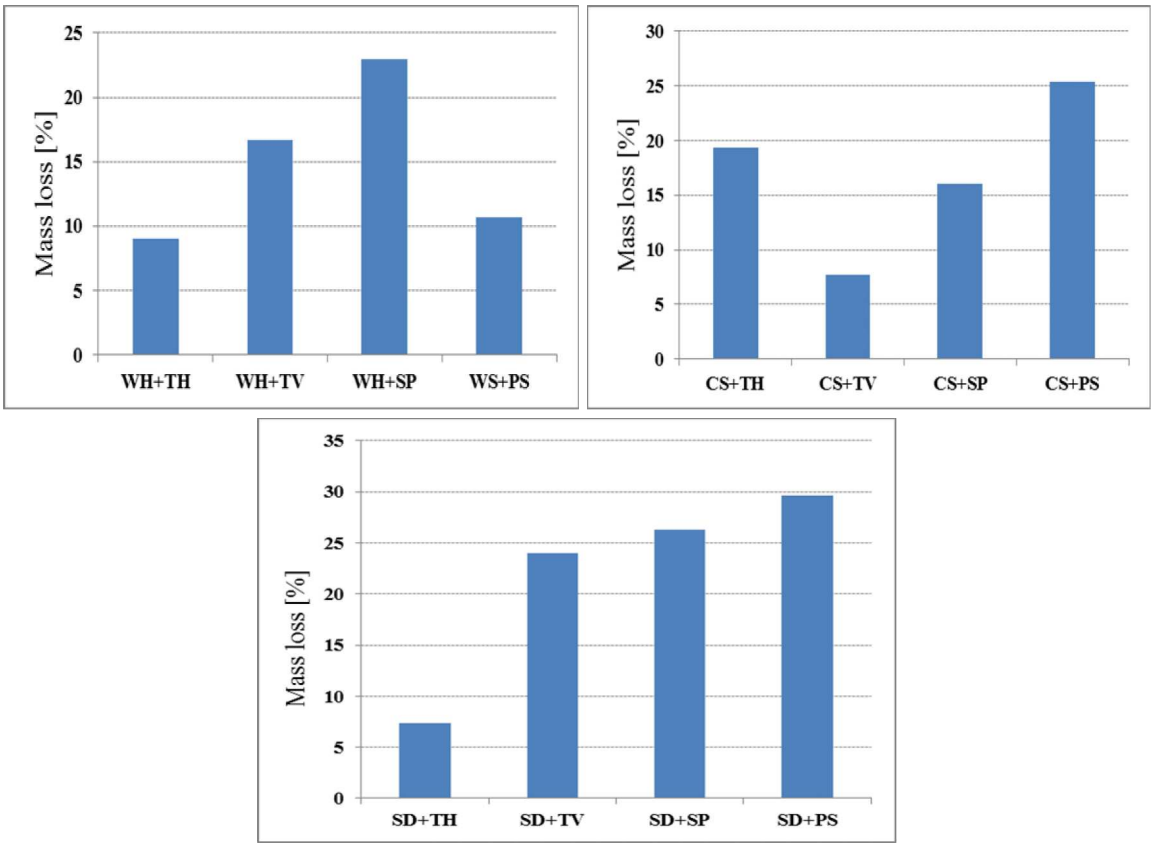

Figure 3: Mass loss for each substrate after 7 days of incubation

In figure 3 is presented the variation of pH with time of incubation for each tested substrate. The pH variation is inconclusive for this experiment; generally, the pH values had an increasing tendency and have changed with at most one unit.

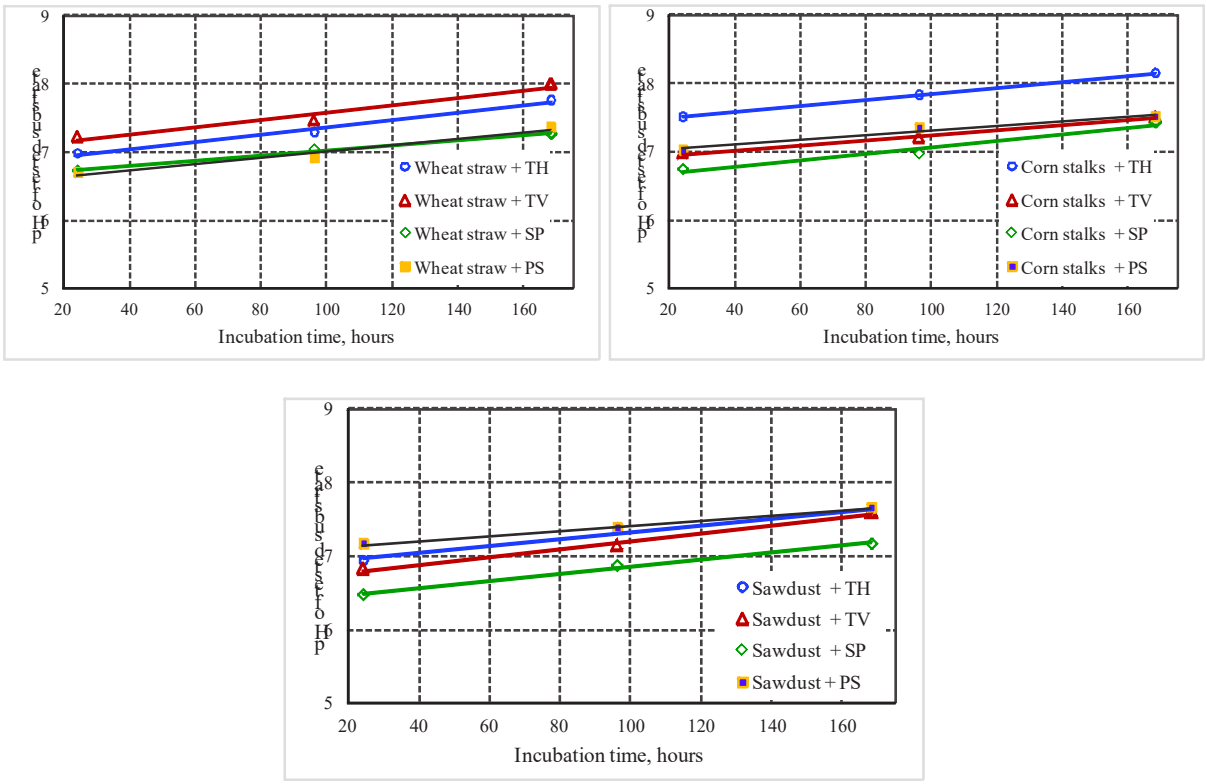

Figure 3: Variation of pH with time of incubation, for each tested substrate

Sugar concentration is mainly due to hydrolyze process of sugar in water and less to microorganisms activity, beginning to adapt to the environment and multiply.
In this case, regarding sugar concentration, there are two simultaneous phenomena: production of sugars by microorganisms through enzymatic hydrolysis and their consumption as forming. In table 2 there are presented the results after 168 h of incubation.

The determined values are between 0.470 mg/ml and 0.616 mg/ml and are comparable with the initial values (wheat straw – 0.500 mg/ml, corn stalks – 0.585 mg/ml, sawdust – 0.665 mg/ml). This fact is due to the sum of production and consumption process in the presence of fungal strains.

Table 2: Sugar concentration after 7 days of fermentation

Sample	Type of fungi	After 168 h [mg/ml]
1	Wheat straw + TH	0.521
2	Corn stalks + TH	0.544
3	Sawdust + TH	0.525
4	Wheat straw + TV	0.470
5	Corn stalks + TV	0.515
6	Sawdust + TV	0.572
7	Wheat straw + SP	0.616
8	Corn stalks + SP	0.511
9	Sawdust + SP	0.556
10	Wheat straw + PS	0.537
11	Corn stalks + PS	0.566
12	Sawdust + PS	0.503

4. CONCLUSIONS

Lignocellulosic residues from wood, agricultural, forestry and wastes are abundant in nature and have a big potential for bioconversion. Lignocellulosic biomass is hardly biodegradable, thus representing a major obstacle for maximum methane production in anaerobic digesters. The most frequently studied biological pretreatment of lignocellulosic biomass focusses on filamentous fungi activity. In this context, the present study showed that the effects of fungal pretreatment strongly depend on the nature of the considered lignocellulosic substrate.

It was proved that all the microorganisms had a stronger or weaker action on all the tested substrates as a result of extracellular enzymes production (cellulose and laccase) in culture medium.

References

[1] Sun, L., *Biogas production from lignocellulosic materials*, Doctoral Thesis, Swedish University of Agricultural Sciences, 2015.

[2] Liu, X., Hiligsmann, S., Gourdon, R., Bayard, R., *Anaerobic digestion of lignocellulosic biomasses pretreated with Ceriporiopsis subvermispora*, Journal of Environmental Management 193, p.154 – 162, 2017.

[3] Rao, M., Menon, V., *Trends in bioconversion of lignocellulose: Biofuels, platform chemicals & biorefinery concept*, Progress in Energy and Combustion Science 38, p. 522-550, 2012.

[4] Zheng, Y., Zhao, J., Xu, F., Li, Y., *Pretreatment of lignocellulosic biomass for enhanced biogas production*, Prog. Energy Combust, 42, p.35-53, 2014.

[5] Salvachúa, D., Prieto, A., López-Abelairas, M., Lu-Chau, T., Martínez, A.T., Martínez, M.J., *Fungal pretreatment: an alternative in second-generation ethanol from wheat straw*, Bioresour Technol, 102, p. 7500-7506, 2011.

[6] Menon, V., Rao, M., *Trends in bioconversion of lignocellulose: Biofuels, platform chemicals & biorefinery concept*, Progress in Energy and Combustion Science 38, p. 522-550, 2012.

[7] Sanchez, C., *Lignocellulosic residues: Biodegradation and bioconversion by fungi*, Biotechnology Advances, 27, p.185–194, 2009.

[8] Miller, G.L., *Use of Dinitrosalicylic acid reagent for determination of reducing sugar*, Analytical Chemistry, 31, pp. 426 – 428, 1959.

[9] Strakowska, J., Blaszczyk, L, Chelkowski, J., *The significance of cellulolytic enzymes produced by Trichoderma in opportunistic lifestyle of this fungus,* J. Basic Microbiol. 54(S1), p. S2-S13, 2014.

[10] Eriksson, K.E., Enzyme mechanisms involved in cellulose hydrolysis by the rot fungus *Sporotrichum pulverulentum* - Biotechnology review, Biotechnology and Bioengineering, vol. XX, p. 317 – 332, 1978.

[11] Morpeth, F.F, *Some properties of celiobiose oxidase from the white-rot fungus Sporotrichum pulverulentum*, Biochem. J., 228, p. 557-564, 1985.

[12] Raghavendra, M.P., Chandra, Nayaka S., Gupta, V.K, *Microbial enzymes for conversion of biomass to bioenergy* in Microbial enzymes in bioconversion of biomass, Gupta V.K. (ed.), Biofuel and Biorefinery Technologies 3, Springer International Publishing Switzerland, 2016, DOI 10.1007/978-3-319-43679-1_1.

METHODS OF SOLID WASTE DISPOSAL – A REVIEW

Mirela Dincă[1], Iulia Găgeanu, Georgiana Moiceanu, Bianca Zăbavă, Mariana Ionescu
University Politehnica of Bucharest, Faculty of Biotechnical Systems Engineering

ABSTRACT

Solid waste management is a major challenge throughout the world. Without an effective and efficient waste management program, the waste generated from various activities (human and industrial), can result in health hazards and have a negative impact on the environment. Waste management includes all the activities and actions required to manage waste from its inception to its final disposal. This includes waste collection, transport, treatment, recovery and disposal. In the present paper there are presented the conventional methods that are widely used for the treatment and of municipal solid waste: landfilling (dumping), sanitary landfills, incineration (combustion), pyrolysis, gasification, composting and anaerobic digestion.

1. INTRODUCTION

According to World Bank [1], in 2012, around the world were generated 1.3 billion tones of solid waste per year and because of urbanization, municipal waste generation is expected to rise to 2.2 billion tonnes by 2025. In Europe, the amount of municipal solid waste produced in 2014 was 475 kg/capita on average, which is a reduction compared to that in 2000 (523 kg/capita) [2].

The definition of "**waste**" was originally derived from the European Community Waste Framework Directive (*75/442/EEC 1975*) as "any substance or object, which the holder/producer discards or intends to discard" [3].

Waste management term has been widely accepted as a sum of measures and solutions for waste avoidance, treatment, recovery, reuse and least but not last, final disposal with consideration to ecological and economical aspects [4].

A correct waste classification is the foundation for ensuring that the collection, transportation, storage and treatment of waste are carried out in a manner that provides protection for the environment and human health [5]:

- municipal waste: the totality of waste generated in the urban and rural areas, which comes from households, institutional and commercial sources, street waste collected from public spaces, parks, green spaces, construction and demolition waste, sludge from the treatment of urban waste waters;
- waste generated by industrial activities: non-hazardous production waste and hazardous production waste;
- waste generated by medical activities;
- agricultural waste and residues.

2. METHODOLOGY

Conventional methods that are widely used for the treatment and management of municipal solid waste are [6]: landfilling (dumping), sanitary landfills, incineration

[1]University Politehnica of Bucharest, Faculty of Biotechnical Systems Engineering, phone no: 0761938017, email: mirela_dilea@yahoo.com

(combustion), pyrolysis, gasification, composting and anaerobic digestion. In the following, each of the methods listed above are presented.

Landfilling (dumping) is the most common method of solid waste disposal due to very low costs. Waste disposal through landfills causes severe environmental issues, such as: uncontrolled release of methane into the atmosphere (a gas that has 20 to 23 times higher greenhouse gases potential than CO_2), production of leachate that contaminates the soil and the ground water, unpleasant odors and spread of pathogenic microorganisms [7, 8].

Sanitary landfills are designed and constructed with systems that protect the environment from contaminants which may be present in the solid waste, wastes are compacted with compaction equipments in order to reduce their volume and deposited in thin layers [9]. Several layers are placed and compacted on top of each other to form a cell (up to 3 metres) [10] and at the end of each day, the compacted cell is covered with a layer of soil in order to prevent odours and windblown debris [11]. When the landfill is completed, a final topsoil cover is placed and compacted and various forms of vegetation may be planted (Fig. 1) [10].

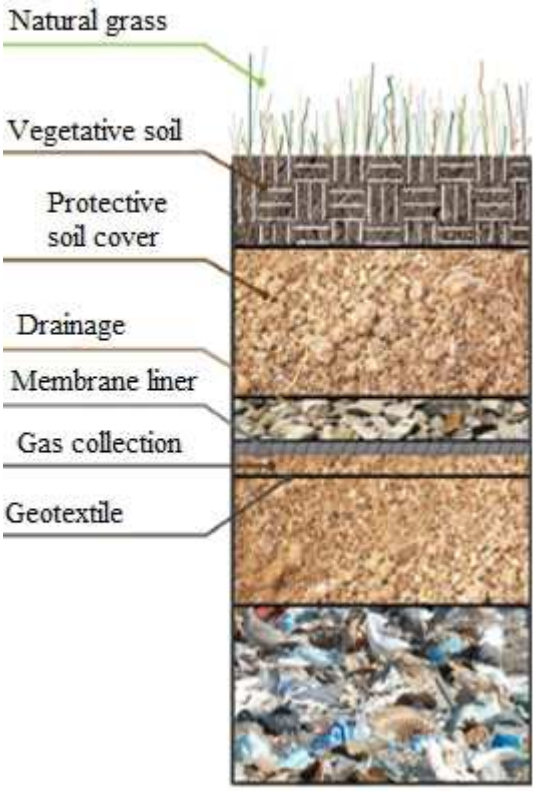

Figure 1: Landfill final cover system [12]

Incineration (combustion) is a rapid, exothermic reaction between a fuel and oxygen (O_2). The objective of waste incineration, in common with most waste treatments, is to treat waste so as to reduce its volume and hazard, whilst capturing or destroying potentially harmful substances [13]. In the incinerations plants the temperature range is between 850º–1400º C. In figure 2 can be observed the main operations included in a typical waste incineration plant [14]. The main advantages and disadvantages of incineration process are presented further.

Incineration advantages [15, 16]:

- ✓ incineration offers the option of treating residual waste and recovering energy;
- ✓ is an efficient way to reduce the waste volume;
- ✓ save landfill space and costs;
- ✓ neutralization of harmful compounds of waste and

✓ energy from waste provides a substitute for fossil fuel combustion.

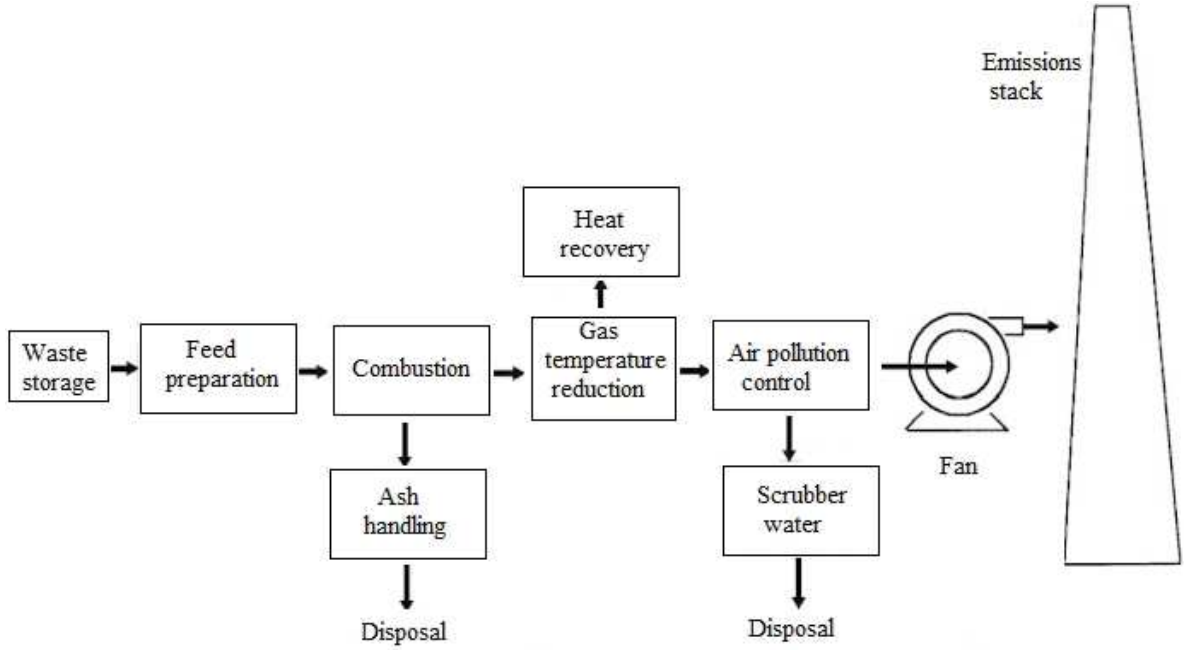

Figure 2: Scheme of typical waste-incineration [14]

Incineration disadvantages [17]:

- an incineration plant involves high investments and high operating costs;
- the residues from the flue gas cleaning can contaminate the environment if not handled appropriately;
- resulting fly and bottom ashes can contain high concentrations of hazardous trace elements such as Cd, Pb, Zn, As, Cr, Cu and other harmful substances;
- if not properly managed, these can pose a serious threat to human health and environment by releasing trace elements into soil and ground water.

In contrast to combustion, **pyrolysis** is the thermal degradation of waste in the absence of oxygen. This process requires an external heat source to maintain the temperature required. Pyrolysis is a recycling technique in which organic polymers are converted into **liquid oil, char and gases** at high temperatures via thermal decomposition (Fig. 3). Pyrolysis studies were carried out at different temperatures ranging from 300 to 900°C, however typical optimum temperatures for plastic waste were around 500–550°C [18].

Gasification can be considered a process between pyrolysis and combustion in that it involves the partial oxidation of a substance. Gasification converts solid and liquid waste to a usable synthesis gas or syngas and instead of producing just heat and electricity, as is done in an incineration plant, the syngas produced by gasification can be turned into higher value commercial products such as transportation fuels, chemicals and fertilizers [20]. The temperatures in a gasifier for municipal solid waste typically range from 600 to 1000ºC. Feedstock can include wood waste (sawdust and bark), crops, agricultural waste (corn stalks), wastewater treatment plant biosolids, municipal solid waste, animal wastes and blends of the various feedstocks. In figure 4 is presented the scheme of a downdraft gasifier [21].

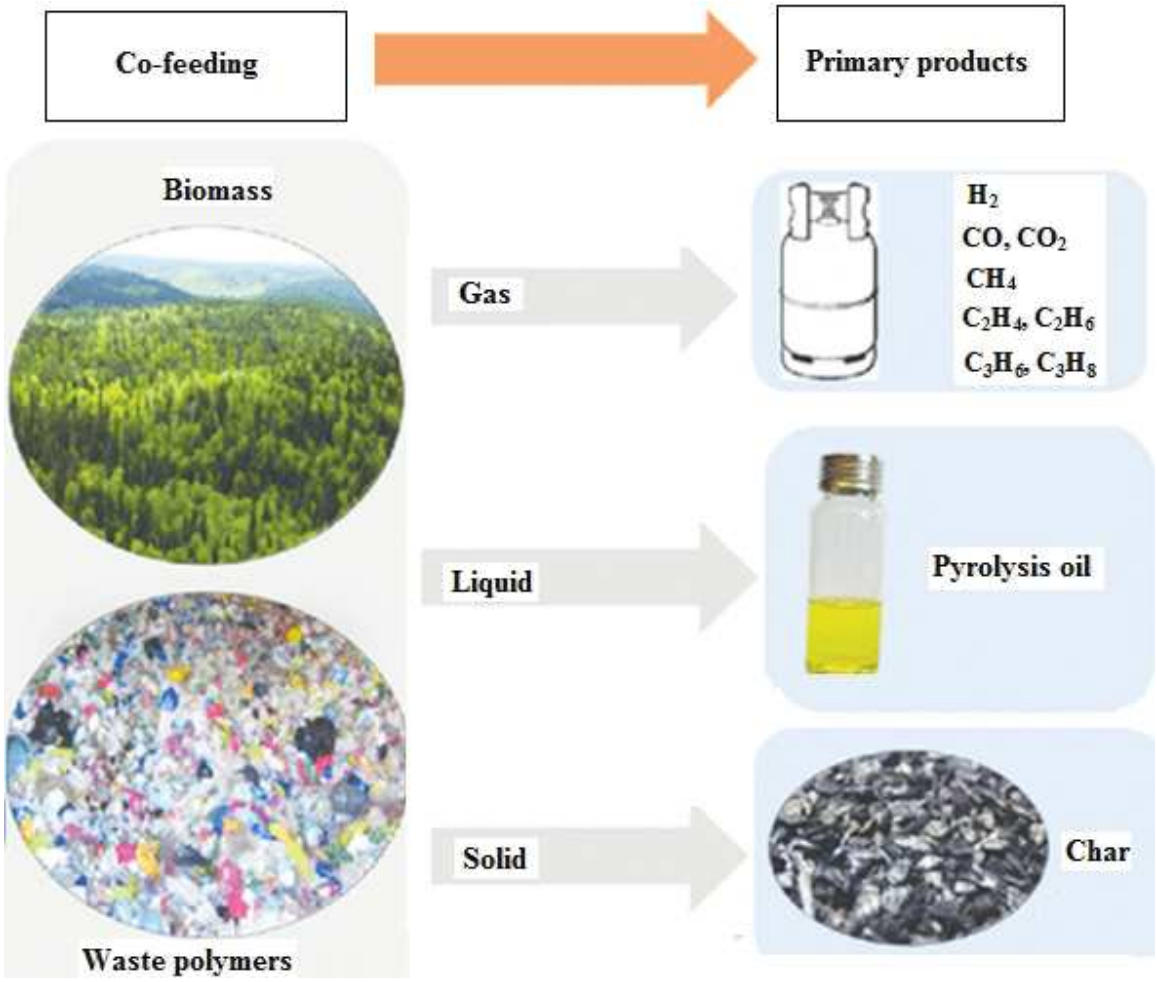

Figure 3: Final products resulted from pyrolysis [Adapted from 19]

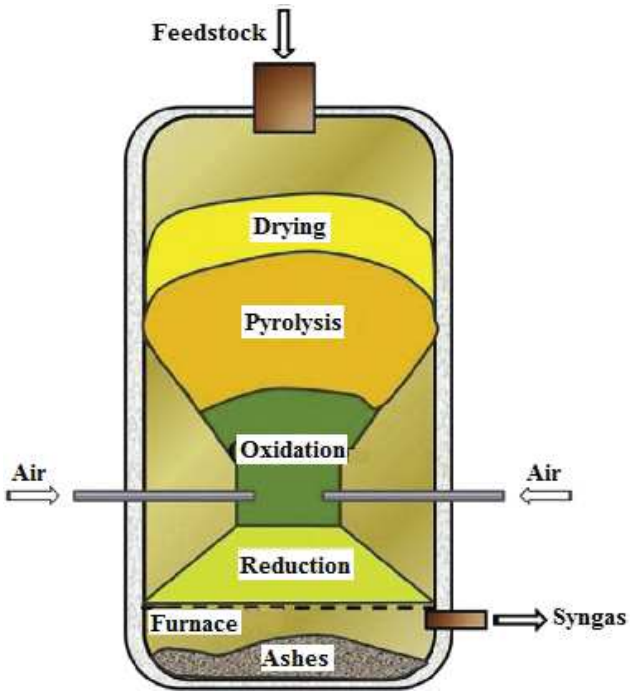

Figure: 4 Scheme of a downdraft gasifier [21]

Composting is a biological process in which a succession of microbial populations converts organic material into a biologically stable product [22]. Composting decomposes waste aerobically into CO_2, water and a humic fraction. The final product is stable, free of pathogens and plant seeds and can be beneficially applied to land [23]. One of the many benefits of adding compost to the soil is that the nutrients in it are slowly released to the soil and are then available for use by plants [24].

The process of anaerobic digestion represents a biochemical process, by which complex organic substrates (vegetal biomass, animal manure, organic waste, wastewater and sludges from sewage system) are degraded, in the absence of oxygen, to the stage of biogas and digestate by various types of anaerobic bacteria [25]. This process is considered to be a key technology for the sustainable use of biomass and involves a series of metabolic reactions: hydrolysis, acidogenesis, acetogenesis and methanogenesis, which are conducted by various groups of microorganisms [26].

3. CONCLUSIONS

The increasing amount of municipal solid waste represents a challenge throughout the world, because of their correct handling in order to minimize the environmental impact. Traditional methods of waste management such as landfilling and incineration present a negative environmental impact. The new methods for waste management that transform waste in valuable products (biofuels) include both biological and thermochemical (gasification and pyrolysis) conversion.

Mechanical–biological treatment of the organic solid waste is now the main strategy to reduce biodegradable municipal solid waste in Europe [27]. It consists of mechanical pre-treatment followed by an aerobic (composting-like process) or anaerobic process, so that waste impacts are reduced. The composting process produces a harmless product that can be used as organic fertilizer, while the anaerobic decomposition (fermentation) produces biogas (renewable energy) and digestate (which, enriched with compost, results in a high quality fertilizer) [28].

References

[1] The World Bank, *Solid Waste Management*, Available at http://www.worldbank.org/en/topic/urbandevelopment/brief/solid-waste-management, 7 April 2017.

[2] Eurostat Statistics Explained, Available at http://ec.europa.eu/eurostat/statistics-explained/index.php/Municipal_waste_statistics.

[3] http://ec.europa.eu/environment/waste/framework/framework_directive.htm.

[4] Waste disposal, Chapter VII, Available at http://www.invent.hs-bremen.de/e-learning_Dateien/Handbook_chapters/chapter_7.pdf.

[5] National Waste Management Strategy - Ministry of Environment and Water Management, Available at http://www.mmediu.ro/img/attachment/37/strategii-planuri-studii-54786035a7ea7.pdf.

[6] Hoornweg, D., Bhada-Tata, P., *What a Waste: A Global Review of Solid Waste Management*, World Bank, no. 15, 2012.

[7] Matsakas, L., Rova, U., Christakopoulos, P., S*trategies for enhanced biogas generation through anaerobic digestion of forest material - An overview*, BioResources, 11, p.5482–5499, 2016.

[8] Păunescu, I., Paraschiv G., *Installations for waste recycling*, Ed. Agir, 2006.

[9] Bolyard, S.C., Reinhart, D.R., *Application of landfill treatment approaches for stabilization of municipal solid waste*, Waste Management, 2016.

[10] Sanitary landfill, Available at https://www.britannica.com/technology/sanitary-landfill, 2010.

[11] University of Wisconsin, *Landfilling principles*, http://www.bvsde.paho.org/bvsair /e/repindex/repi49-50/lesson2/lesson2.html.
[12] ***http://www.liteearth.com/about/.
[13] European Comission, *Waste incineration*, http://eippcb.jrc.ec.europa.eu/reference/BREF/wi_bref_0806.pdf.
[14] Waste Incineration & Public Health, National Research Council (US) Committee on Health Effects of Waste Incineration. Washington (DC): National Academies Press (US); Available at: https://www.ncbi.nlm.nih.gov/books/NBK233627/, 2000.
[15] Melikoglu, M., Lin, C., Webb, C., *Analysing global food waste problem: Pinpointing the facts and estimating the energy content*, Open Eng, 3, p.157–164, 2013.
[16] Rand, T., Haukohl, J., Marxen, U., *Municipal solid waste incineration*, The International Bank for Reconstruction, 2000.
[17] Saqib, N., Backstrom, M., *Distribution and leaching characteristics of trace elements in ashes as a function of different waste fuels and incineration technologies*, Journal of Environmental Sciences, 36, p. 9 - 21, 2015.
[18] Miandada, R., Barakata, M.A., Aburiazaizaa, A.S., Rehanb, M., Nizamib, A.S., *Catalytic pyrolysis of plastic waste: A review*, Process Safety and Environmental Protection 102, p.822–838, 2016.
[19] Zhang, X., Lei, H., Chen, S., Wu, J., *Catalytic co-pyrolysis of lignocellulosic biomass with polymers: a critical review*, Green Chem., 18, 4145-4169, 2016.
[20] Waste to energy gasification, http://www.gasification-syngas.org/applications/waste-to-energy-gasification/.
[21] Gagliano, A., Nocera, F., Patania, F., Bruno, M., Castaldo D.G., *A robust numerical model for characterizing the syngas composition in a downdraft gasification process,* Comptes Rendus Chimie, 19(4), p. 441 – 449, 2016.
[22] Alberta Environment, *The Composting Council of Canada, Mid-scale Composting Manual*, 1st edition, no. T/506, ISBN 0-7785-0943-5 (on-line), http://esrd. alberta.ca/waste/composting-at-home/documents/MidscaleCompostingManual-Dec1999.pdf, 1999.
[23] Artola, A., Barrena, R., Font, X., Gabriel, D., Gea, T., Mudhoo, A., Sanchez, A., *Composting from a sustainable point of view: respirometric indices as key parameter*, Global Science Books, Dynamic Soil, Dynamic Plant, pp. 1 – 16, 2009.
[24] Raabe, R.D., *The rapid composting method*, University of California, Vegetable Research and Information Center, http://vric.ucdavis.edu/pdf/compost_rapidcompost.pdf.
[25] Al Seadi, T., Rutz, D., Prassl, H., Köttner, M., Finsterwalder, T., Volk, S., Janssen, R., *Biogas – Handbook*, University of Southern Denmark, ISBN 978-87-992962-0-0, 2008.
[26] Khanal, S.K., *Anaerobic biotechnology for bioenergy production: principles and applications*, United States: John Wiley & Sons, Inc. 2008.
[27] Scaglia, B., Adani, F., *An index for quantifying the aerobic reactivity of municipal solid wastes and derived waste products*, Sci. Total Environ. 394, p.183–191, 2008.
[28] Adani, F., Tambone, F., Gotti, A., *Biostabilization of municipal solid waste*, Waste Manag. 24, p. 775–783, 2004.

INCREASING ENERGY AUTONOMY IN ISOLATED AREAS THROUGH COMBINED USE OF RENEWABLE RESOURCES

Valeriu DULGHERU[1], Liliana DUMITRESCU[2], Ana-Maria POPESCU[2],
Marian BLEJAN[2], Radu RADOI[2]
[1]Technical University of Moldova, Mechanical Faculty, Chişinău, Republic of Moldova
[2]National Institute for Optoelectronics - Subsidiary Hydraulics and Pneumatics Research Institute, INOE 2000-IHP, Bucharest, Romania

ABSTRACT

Romania has significant amounts of renewable energy, with potential for transformation into electric and thermal energy; especially in the electricity production sector, over the past few years important steps have been taken, adding new production capacities, which exploit solar and wind sources mainly. Besides these, the use of hydraulic energy, an area with tradition in Romania, has resulted in 2016 in more than 42% of the electricity being produced from renewable sources. Most of the currently installed conversion systems are of high power; lately, with the fall in production prices and rise in awareness of the negative environmental impact of fossil fuel consumption, especially in isolated areas has become viable the use of smaller conversion systems, at the level of a household or workplace. This paper presents a solution to ensure the energy needs using mostly solar energy, which, however, can be combined with wind or hydro power.

1. INTRODUCTION

Production and use of electricity in a traditional system, that is using fossil fuels, is increasingly criticized for its negative impact on the environment, which in turn has important economic and social consequences (Food pollution, crop reduction, population health damage, etc.). Replacing traditional with renewable sources for energy production significantly diminishes this negative impact. The means for converting energy from renewable sources Can be used both as centralized energy sources, high power, and, to a large extent, decentralized sources, particularly advantageous for rural or isolated consumers, which perfectly corresponds to the European trend to decentralize energy distribution [1,2].

Romania has aligned itself with this trend supporting, by an economic policy of European inspiration (facilities, grants, etc.), the utilization of renewable energy, especially wind and solar. In recent years, many wind and solar farms have appeared which has contributed to increasing the share of electricity produced from renewable sources in the total energy produced. In 2016, 42.38% of electricity produced was obtained from renewable sources and 57.62% from conventional sources. Share of primary energy sources in electricity production is shown in the graph in Figure 1 [3].

If at national level the situation is good, at local level, for isolated households, farms, or for special target locations, little has been done in the use of renewable sources. On the other hand, isolated households which are not connected to the common electricity network still use costly and polluting energy solutions (electric generators powered by gasoline or diesel engines).

[2]14 Cutitul de Argint, 040558, Bucharest, Romania, +40727391783, dumitrescu.ihp@fluidas.ro

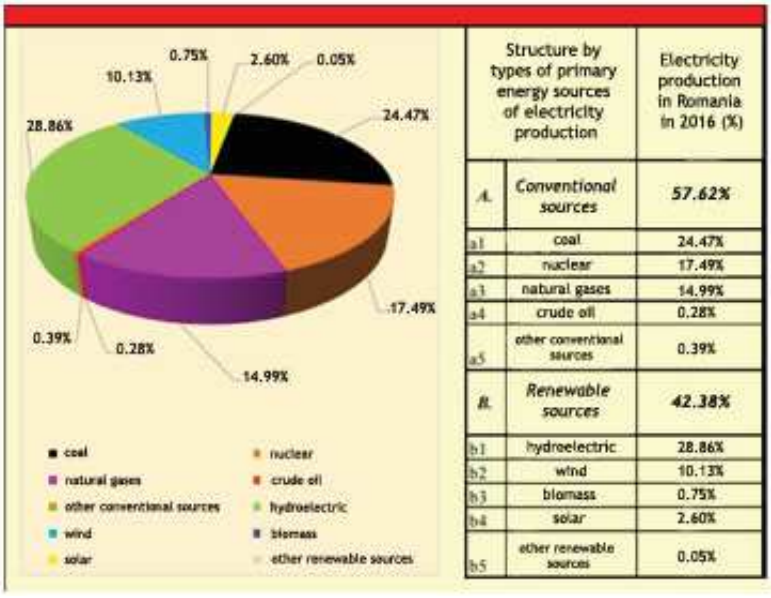

	Structure by types of primary energy sources of electricity production	Electricity production in Romania in 2016 (%)
A.	*Conventional sources*	*57.62%*
a1	coal	24.47%
a2	nuclear	17.49%
a3	natural gases	14.99%
a4	crude oil	0.28%
a5	other conventional sources	0.39%
B.	*Renewable sources*	*42.38%*
b1	hydroelectric	28.86%
b2	wind	10.13%
b3	biomass	0.75%
b4	solar	2.60%
b5	other renewable sources	0.05%

Figure 1: Share of primary energy sources in electricity production

Below is a solution proposed for powering an isolated location with a daily consumption of 26.4 kWh. This amount has been reached considering an average hourly consumption of 1 kW, to which we add a reserve of 10% (24 h x 1 kW + 2.4 kWh = 26.4 kWh).

2. ANALYSIS DIRECTIONS FOR SOLUTION SETTING

When discussing ensuring energy autonomy in isolated areas, the first step is assessing the potential (qualitative and quantitative) energy sources; the next one is choosing the means of conversion, and, at the end of the design phase, evaluating by simulation the amount of energy produced by the proposed system. All of this is based on the initial knowledge of consumption needs.

The types of renewable energy with real potential for utilization on the territory of Romania are: solar energy, wind energy and hydraulic energy. In addition, biomass energy can be used in particular to produce thermal energy.

Using solar energy. On the territory of Romania, solar energy is available in most areas, with values in the range 1000...1500 kW/m^2/year; For this reason, solar energy is first taken into account when designing a system for producing electric or thermal energy, in most areas of the country. Converting solar energy into thermal energy to produce domestic hot water is relatively simple and it is performed directly and with high efficiency. Regarding the conversion means, particularly for photovoltaic panels, there are 2 favorable trends: increasing conversion performance and lowering the price. Currently, panels available on the market have an efficiency of 14...21% and a price of 100...300 €/m^2, depending on efficiency [4]. The other components of an electricity generation system (batteries, inverters, controllers, etc.) also show a tendency to lower cost prices and increase performance.

Using wind energy. In order to be exploited with good results, wind energy must be associated with wind speeds greater than 5 m/s. This condition, coupled with the need for lack of environmental turbulence (vegetation, various constructions, etc.), reduces the possibilities of using wind turbines. Nevertheless, they can be combined with photovoltaic solar panels for charging batteries during periods of good wind speeds or during periods when photovoltaic panels have low productivity (at night or on cloudy days). There are also areas where wind turbines can provide the electricity needed on their own; this requires first consulting the wind potential maps at national and local level, as the one in Figure 2 [5].

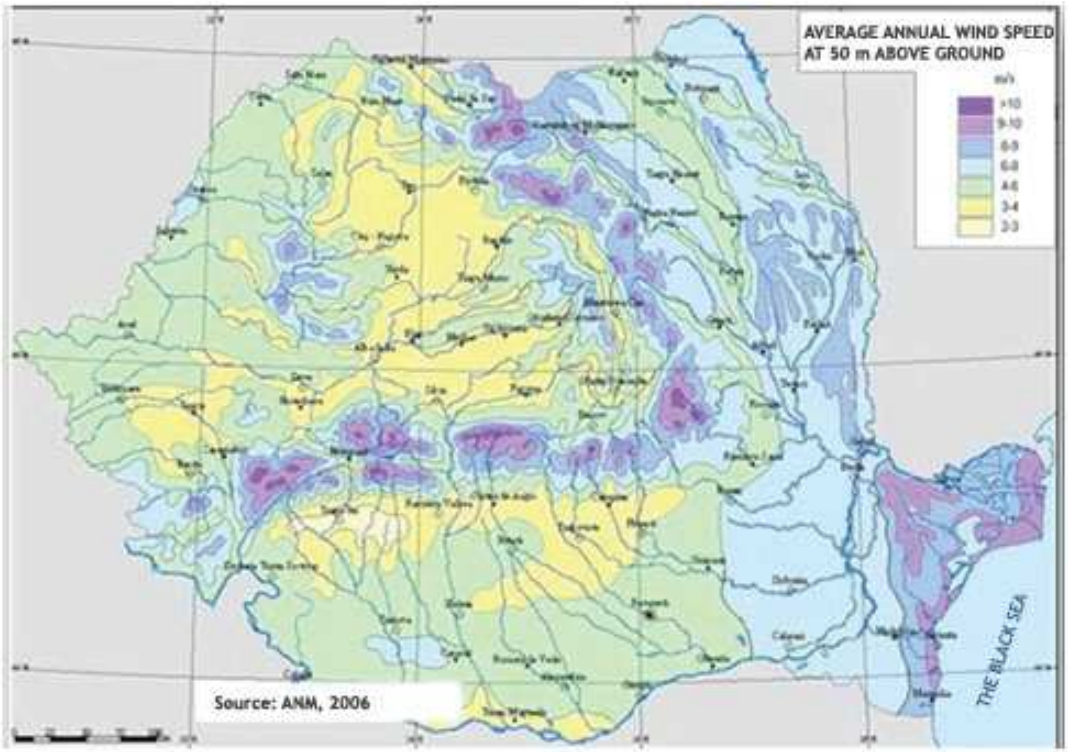

Figure 2: Romania's wind potential map

For the utilization of **hydraulic energy** in isolated areas the conversion means under the category of micro- and pico-power plants should be analyzed. Their analysis showed that there are reserves to increase the efficiency of the currently used turbines. Betz's coefficient, theoretically equal to 0.593, is the maximum theoretical conversion efficiency of hydraulic energy. Most existing systems provide a coefficient of use of the kinetic energy of water in the range of 0.1...0.2. In this respect there are sufficient reserves to streamline the hydraulic flow turbines, which are becoming increasingly tempting for engineers and inventors in the industry both in terms of higher energy density of water (compared to density of air) and in terms of its 24-hours-a-day availability for consumers located near rivers. To avoid building a dam, the kinetic energy of a river can be used using water current turbines. Such turbines are easy to install, are operated easily and their maintenance costs are affordable. A current speed of l m/s represents an energy density of 500 W/m^2 of the cross section [6]. But only part of this energy can be extracted and converted into useful electrical or mechanical energy, and this depends on the type of rotor and blades. The speed is particularly important, because doubling the water speed results in an increase of eight times in the energy density. However, the use of hydraulic energy is conditioned by the existence of a water stream near the target location to be supplied. On the other hand, the kinetic energy of the watercourses provides a permanent and constant source, less subject to natural variations. It should also be mentioned that the means of converting hydraulic energy are less widespread in the market because of higher complexity compared to the types of energy presented above.

In conclusion, for the isolated areas of Romania the renewable energy with the highest potential for use is solar energy due to its availability on most of the country's surface. Solar energy can easily be converted into electric and thermal energy, without the need for special construction works. Solar (photovoltaic or thermal) panels have an affordable price, a long service life and require minimal maintenance. For these reasons, the solution proposed below for the production of electricity is based on solar energy; other types of energy can be combined with it, depending on the natural availability of sources.

3. PRESENTATION OF THE PROPOSED SOLUTION

Starting from the amount of 26.4 kWh required to be provided per one day, all parts of an installation having the conceptual diagram shown in Figure 3 are dimensioned.

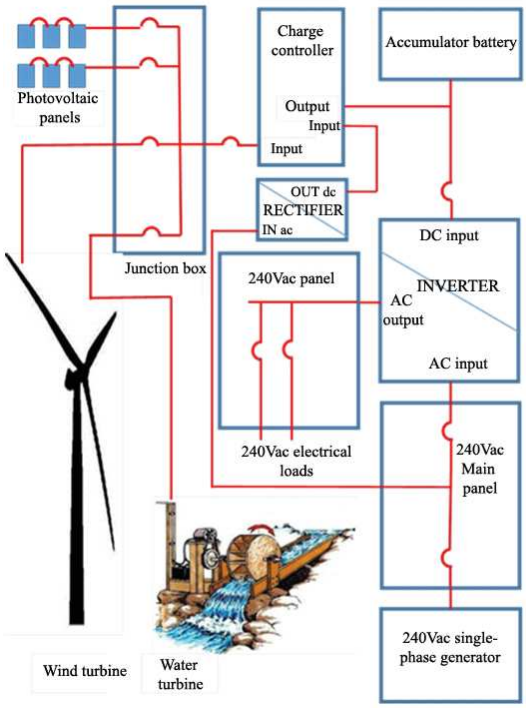

Figure 3: Conceptual diagram of the conversion facility

The battery of accumulators will be designed to be able to store the electricity supplied by the photovoltaic panels (and consumed) in one calendar day and provide a reserve of approx. 25%. By choosing the 24 V value for the DC voltage used in the electrical system, which is a typical value used in industrial systems, the current required for a load of 1.1 kW from a voltage of 24 V is:

1.1 kW / 24 V = 45.83 A, (1)

So the capacity of the battery of accumulators in order to provide this current value for a day long is:

45.83 A * 24 hours = 1100 Ah. (2)

A typical accumulator used for photovoltaic systems is the 12 V - voltage and 205 Ah - capacity one, operating in loading / unloading cycles from 50% to 100% of its capacity; therefore, the number of accumulators required to make up the battery is:

(1100 Ah / 205 Ah) * (24 V / 12 V) * 100%/50% = 21.5 accumulators. (3)

In order to have a storage reserve, one chooses the value of 24 accumulators with capacity of 205 Ah.

Calculation of photovoltaic panel area

The needs for electricity provided daily by the photovoltaic panel area has been presented in the above, and it has the value of 26.4 kWh per day. To calculate the required electrical power amount of photovoltaic panels an online calculator provided by the European Commission under "EU Science Hub – Joint Research Center" has been used [7]; the necessary data, including the location for which the calculation is made, has been entered into this instrument. The calculation showed that 1 kW of installed power produces a daily average of 3.36 kWh. It follows that for the daily needs of 26.4 kW the required installed power is:

26.4 / 3.36 = 7.85 kW, (4)

value which can be rounded to 8 kW. The number of required solar panels that have a maximum power of 250 W is:

8 kW / 250 W = 32 panels. (5)

Using an online simulation environment which is available on http://pvwatts.nrel.gov/pvwatts.php [8], a reverse check can be made, obtaining the amount of energy produced by the group of photovoltaic panels which have the above characteristics.

RESULTS

Print Results

9,669 kWh per Year *

Month	Solar Radiation (kWh / m² / day)	AC Energy (kWh)	Energy Value ($)
January	1.64	351	N/A
February	3.03	578	N/A
March	3.99	820	N/A
April	4.96	943	N/A
May	6.12	1,154	N/A
June	6.56	1,182	N/A
July	6.79	1,236	N/A
August	6.30	1,152	N/A
September	4.82	890	N/A
October	3.34	655	N/A
November	1.89	380	N/A
December	1.53	327	N/A
Annual	4.25	9,668	0

Figure 4: The result of simulating the amount of electricity produced

This simulation environment gives a value of 9668 kWh/year for the energy produced by a system of photovoltaic panels of polycrystalline type, with an installed capacity of 8 kW. Thus, the energy produced daily by the system will be: 9668 kWh / 365 days = 26.5 kWh/day.

As the amount of energy varies over a year, it is recommended to install an electric generator driven by a thermal motor (electro generator set), which can also be found in the structure shown in Figure 3.

Economic evaluation of the solution

After choosing the components, an estimate of the price of such a system has been made. The result is summarized in the table below.

Table 1: Estimate of the price for the proposed system [4, 9, 10]

Item no.	Component name	Pcs.	Price/ pcs (lei)	Total value (lei)	Notes
1	Photovoltaic panel	32	911.54	29,169.50	Heckert Solar 250 W, NeMo series
2	Battery pack	24	1787.40	42,540.24	Trojan 12V 205Ah J185 – 1500 cycles
3	Inverter	1	10,675.80	10,675.80	Victron Multiplus
4	Charge controller	1	4,320.00	4,320.00	Victron SmartSolar
5	Programmable logic controller	1	3,446.40	3,446.40	Twido – Schneider Electric
6	Various electrical accessories	1	5,000.00	5,000.00	
7	Electro generator set	1	10,000.00	10,000.00	
	Total of materials for electrical system			**104,248 lei, VAT inclusive or ~ 19,250 € + VAT**	

For photovoltaic panels, which are the main component of the system, an average variant, as price and power, has been chosen, of about 1.000 lei / pcs. and a capacity of 250 W, produced by a known company; if one chooses a cheaper version, also available on the market, the price for the group of panels may drop by 20...25%. In the same way one can reduce the price for the battery pack. To present a situation as close as possible to reality, prices have been updated in May 2017.

4. CONCLUSIONS

The paper presents a variant of a power generation system based on a group of photovoltaic panels, to which a wind turbine or a small hydro power turbine can be added.

The system is dedicated to isolated areas where there is no possibility of feeding from the common power supply network. To ensure electricity also for periods when solar energy is lower (cold season, cloudy days, etc.), the work diagram is completed with an electro generator set.

The system allows powering a location where daily recorded consumption is of about 26.4 kWh or a location which has an installed power of 1.1 kW. If consumption is lower, the system, based on components in the same category, can be resized, with favorable implications on the final price.

The current trend of increasing the efficiency of photovoltaic modules and reducing the production price makes the proposed solution more and more accessible from a financial point of view.

Acknowledgement

This paper has been developed in INOE 2000-IHP, as part of a project co-financed by the European Union through the European Regional Development Fund, under Competitiveness Operational Programme 2014-2020, Priority Axis 1: Research, technological development and innovation (RD&I) to support economic competitiveness and business development, Action 1.1.4 - Attracting high-level personnel from abroad in order to enhance the RD capacity, project title: *Establishing a high level proficiency nucleus in the field of increasing renewable energy conversion efficiency and energy independence by using combined resources*, project acronym: CONVENER, Financial agreement no. 37/02.09.2016.

References

[1] Maican, E., *Sisteme de energii regenerabile*, Printech, Bucharest, 2015.
[2] Bostan, I., Dulgheru, V., Sobor, I., Bostan, V., Sochirean, A., *Sisteme de conversie a energiilor regenerabile*, Tehnica-Info, Chisinau, 2007.
[3]http://www.green-report.ro/mix-ul-perfect-in-energie-42-din-productia-de-energie-electrica-a-romaniei-asigurata-din-surse-regenerabile/, accesat la 18.04.2017
[4] https://www.esolar.ro/panou-cu-celule-monocristaline-benq-330w.html, accesat la 20.04.2017
[5] http://add-energy.ro/potentialul-eolian-al-romaniei/, accesat la 20.04.2017
[6] Bostan, I., Dulgheru, V., Bostan, V., Sochireanu, A., Ciobanu, O., Ciobanu, R., *Micro-hydropower station for kinetic energy conversion of flowing water,* "HIDRAULICA" no. 3-4/2012, ISSN 1453 - 7303
[7] http://re.jrc.ec.europa.eu/pvgis/apps4/pvest.php?lang=en&map=europe, accesat la 20.04.2017
[8] http://pvwatts.nrel.gov/pvwatts.php, accesat la 21.04.2017
[9] http://www.westech-solare.ro/panou-fotovoltaic-poli-250w-made-germany-p-339.html
[10] http://www.heckertsolar.com/

DISCOLORATION OF WATER CONTAINING SYNTHETIC DYES BY FOUR STRAINS OF *ASPERGILLUS*

Mariana Ferdeș[1], Mirela Dincă, Gigel Paraschiv, Laura Toma
University Politehnica of Bucharest, Faculty of Biotechnical Systems Engineering

ABSTRACT

The ability of fungi to decolorize synthetic dyes in industrial wastewaters by bioaccumulation/biosorption or enzyme production mechanisms represents an eco-friendly method that offers many advantages over traditional approaches. The present study demonstrates the potential of some fungal strains to decolorize three coloring solutions containing Basic Fuchsin, Crystal Violet and Methylene Blue. The experiments were carried out in liquid media, using four microbial strains namely *Aspergillus niger* ATCC 20107, *A. niger* ATCC 22343, *A. oryzae* CMI 126842 and *A. terricola* F86. The decrease of absorbance in all samples has been assessed, showing remarkable values in the culture of *Aspergillus niger* ATCC 20107, where the percent of discoloration was more than 90%. This study demonstrates the capacity of fungal biomass to degrade the synthetic dyes and can be considered a promising alternative to conventional technologies.

1. INTRODUCTION

Microbiological treatments of industrial wastewater could be less expensive alternative techniques compared to the physical and chemical methods. These techniques are based on treatment processes of polluting agents by biosorption, bioaccumulation or by enzyme biotransformation [1, 2]. The presence of dyes in water effluents reduces the sunlight passing through water, reaching with difficulty in lower volumes; it affects the photosynthesis activities of aquatic flora, lowering the concentration of dissolved oxygen, with negative effects on aquatic flora and fauna [3, 4]. Dyes are recalcitrant organic molecules, resistant to aerobic digestion and are stable upon exposure to light. The problem of colored effluents has worsened with the use of reactive dyestuffs [5].

Effluent treatment processes in the textile industry are presently achieved by various techniques including methods of sedimentation, filtration, flotation, coagulation, osmosis, solvent extraction, adsorption, incineration, etc [5, 6]. The treatment done solely by one of these methods proved to be insufficient leading to the need for their combination.

Different species of fungi have been successfully used in bioremediation of effluents coming from the textile industry [7, 8], which are capable of producing various iso-forms of extracellular oxidases including laccase, lignin peroxidase and Mn peroxidase, enzymes involved in lignin degradation and various xenobiotic compounds including textile dyes [9]. Different species of *Aspergillus, Trametes* [10] and *Phanerochaete chrysosporium* [11] were tested in the biodegradation processes of industrial effluents.

The objectives of the present work were to identify active fungal strains able to decolorize synthetic dyes in aerate solutions and to analyze their biodegradation potential in time expressed as percentage of discoloration.

[1] University Politehnica of Bucharest, Faculty of Biotechnical Systems Engineering, phone no: 0729821256, email: marianaferdes@yahoo.com

2. METHODOLOGY

Fungal strains

The discoloration of synthetic dyes was assayed for four fungal strains: *Aspergillus niger* ATCC 20107, *A. niger* ATCC 22343, *A. oryzae* CMI 126842 (Commonwealth Mycological Institut Kew, England) and *A. terricola* F86 from the culture collection of Microbiology Laboratory, Faculty of Biotechnical Systems Engineering.

The fungal strains were cultivated on Potato Dextrose Agar (potato extract 4.0 g/L, glucose 20.0 g/L, agar 15.0 g/L) and stored at 4ºC. The fungal submerged cultures were carried out in Czapek Dox Broth (sucrose 30.0 g/L, $NaNO_3$ 3.0 g/L, K_2HPO_4 1.0 g/L, $MgSO_4$ 0.5 g/L, KCl 0.5 g/L, FeSO4 0.01 g/L, final pH 7.3).

Synthetic dyes

The discoloration activity of the fungal biomass was assessed using three dyes:

1. Basic Fuchsin (molecular formula $C_{19}H_{17}N_3 \cdot HCl$, molecular weight 323.82 g/mol) belonging of triarylmethane class, used as textile dye, disinfectant, and in microbiology
2. Crystal violet or gentian violet (molecular formula $C_{25}H_{30}ClN_3$, molecular weight 407.99 g/mol), belonging of triarylmethane class, used in medicine.
3. Methylene blue (molecular formula $C_{16}H_{18}ClN_3S$, molecular weight 319, 852 g/mol), belonging of thiazin class, used in medicine.

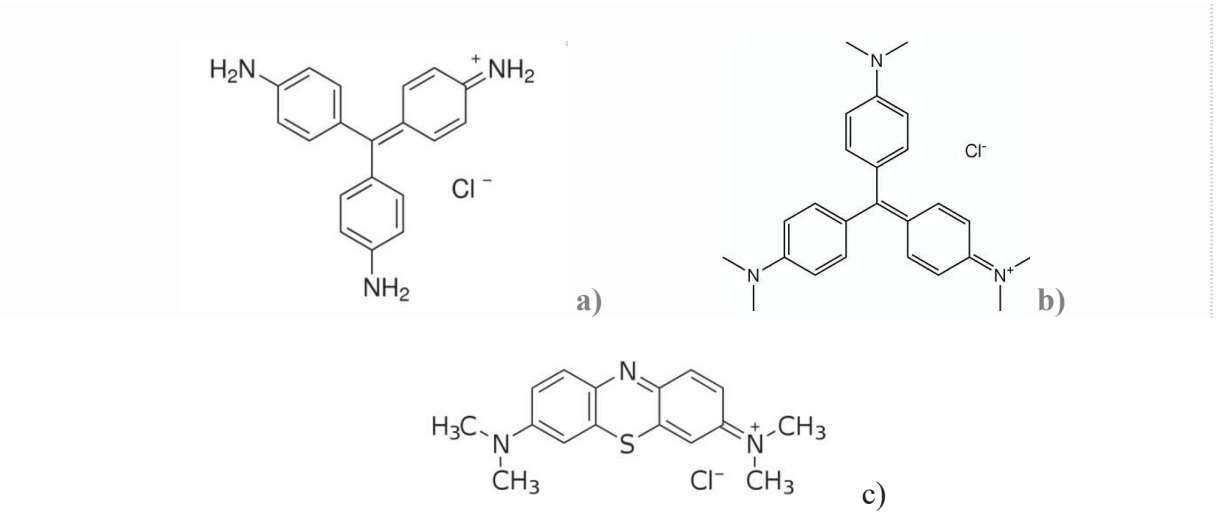

Fig.1 Structural formulas of a) Basic Fuchsin b) Crystal Violet
c) Methylene Blue

The absorption spectra in VIS domain were recorded for all three synthetic dyes and the wavelength for maximum absorbance (λ_{max}) was measured. A calibration curve (absorbance at λ_{max} against known concentration) was plotted to determine the concentration of each dye in samples.

Assay of dyes discoloration

Quantitative discoloration studies were carried out using the fungal cultures grown in 500 mL Erlenmeyer flasks containing 200 mL of Czapek Dox medium, on a rotary shaker at 150 rpm, 30^{O}C. The flasks were inoculated with 10 mL of 72 h old culture in Czapek Dox medium for each fungal strain.

After 3 days of incubation the synthetic dyes were added in the cultures as single dye solution. The specific absorbance of each sample was determined using a UV-VIS spectrophotometer (T92+, PG Instruments) at different time intervals. The percentage of discoloration was calculated using the following formula:

$$Discoloration\ (\%) = \frac{Ai - Af}{Ai} \times 100$$

where *Ai* is the initial absorbance, after adding the dye, and *Af* is the final absorbance.

3. RESULTS

Four *Aspergillus* strains were selected in order to assess the potential of degradation of synthetic dyes: *A. niger* ATCC 20107, *A. niger* ATCC 22343, *A. oryzae* CMI 126842 and *A. terricola* (F86) from the culture collection of Microbiology Laboratory, Faculty of Biotechnical Systems Engineering.

The absorption spectra of the synthetic dyes were recorded and the characteristic wavelengths for maximum absorbance were determined: 543nm for Basic Fuchsin, 575 nm for Crystal Violet and 664 nm for Methylene Blue. The concentrations of residual dyes were determined using the calibration curves shown in figure 2.

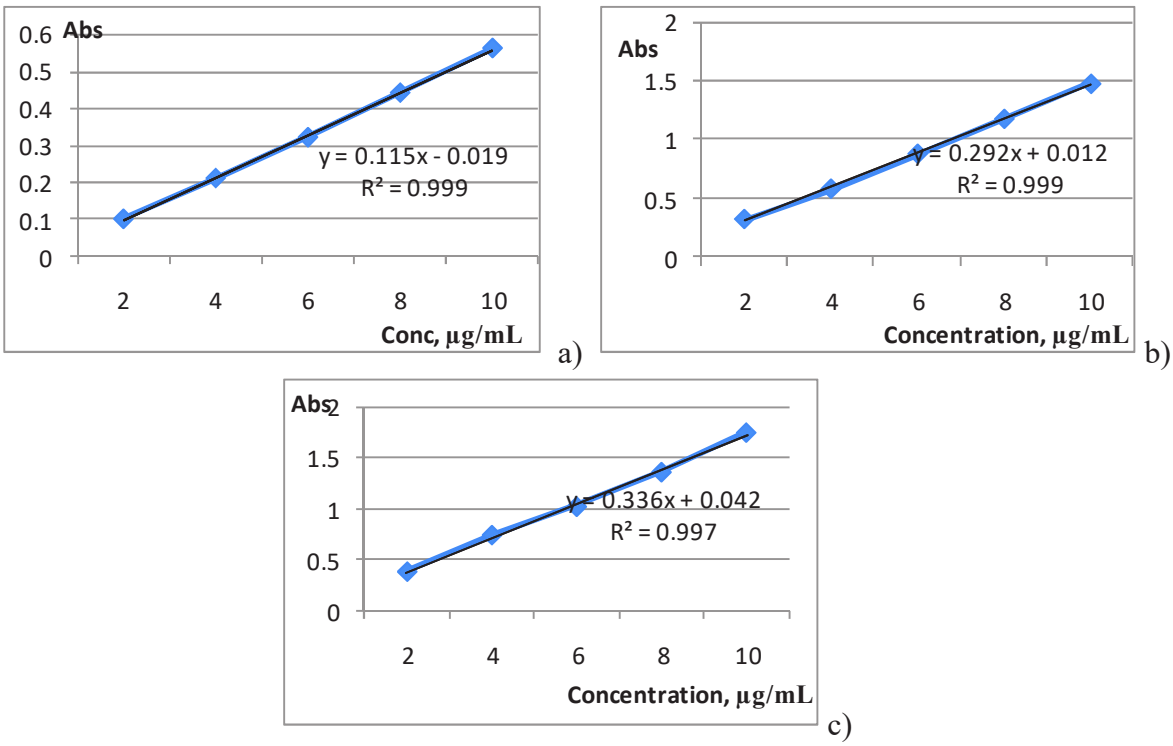

Fig.2. Calibration curves for a) Basic Fuchsin b) Crystal Violet c) Methylene Blue

After 3 days of incubation at 25 °C on orbital shaker, the fungal strains have grown as filamentous structures, in the form of pellets 1 – 3 mm in diameter.

In order to assess the discoloring activity of the four fungal strain, the solutions of synthetic dyes have been added in a concentration of 5 µg/mL.

The characteristic dye absorbance for each dye was determined at different intervals (1, 2, 4, 24, 48 hours) in the culture filtrate. The results are shown in figure 3 a, b, and c and

demonstrate that even after the first 4 hours of incubation the absorbance decreased considerably in all samples.

The obtained results demonstrate that all dyes undergone a partial or quite total biodegradation in the fungal cultures, after 2 days. The specific absorbance decreases suddenly in the first 4 hours but slowly in the next time interval. This discoloration of synthetic dyes is probably due to the fungal enzymes action and to the absorption of pigments on the fungal biomass.

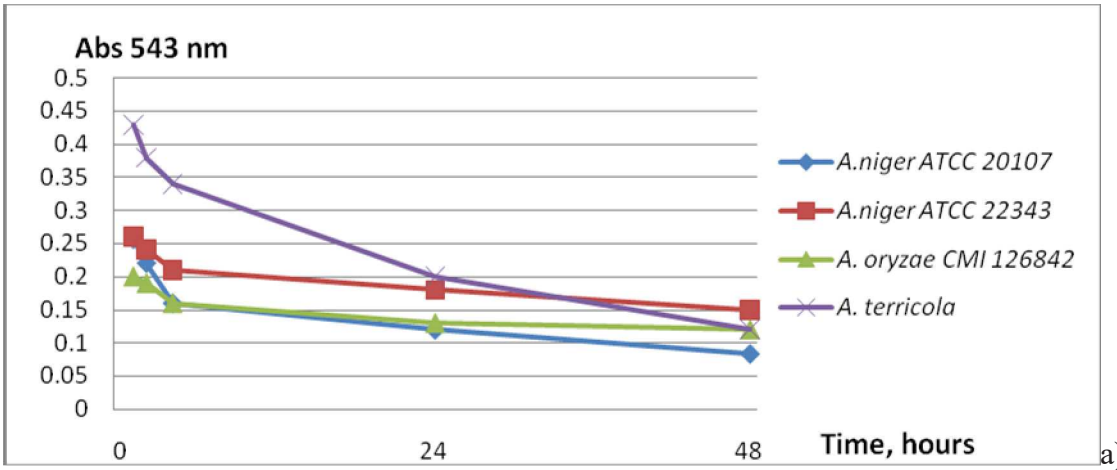

a)

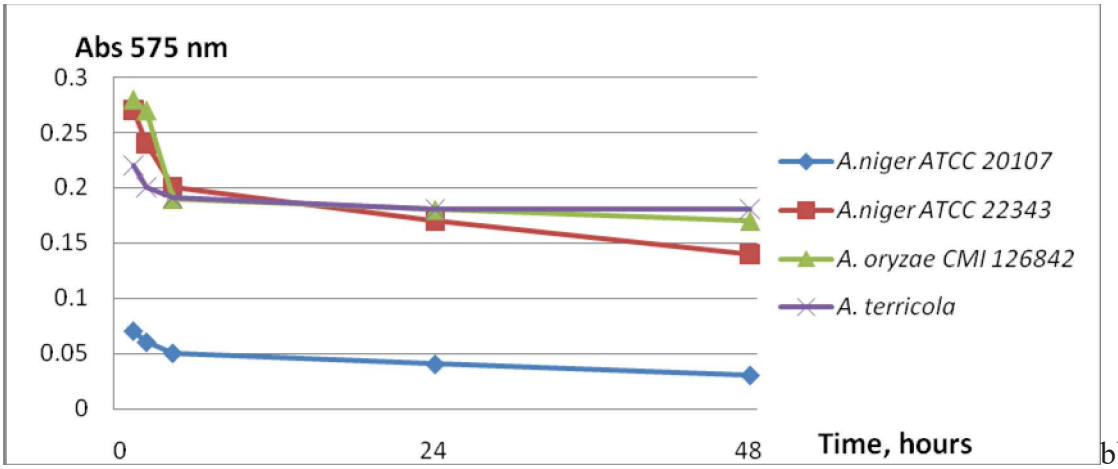

b)

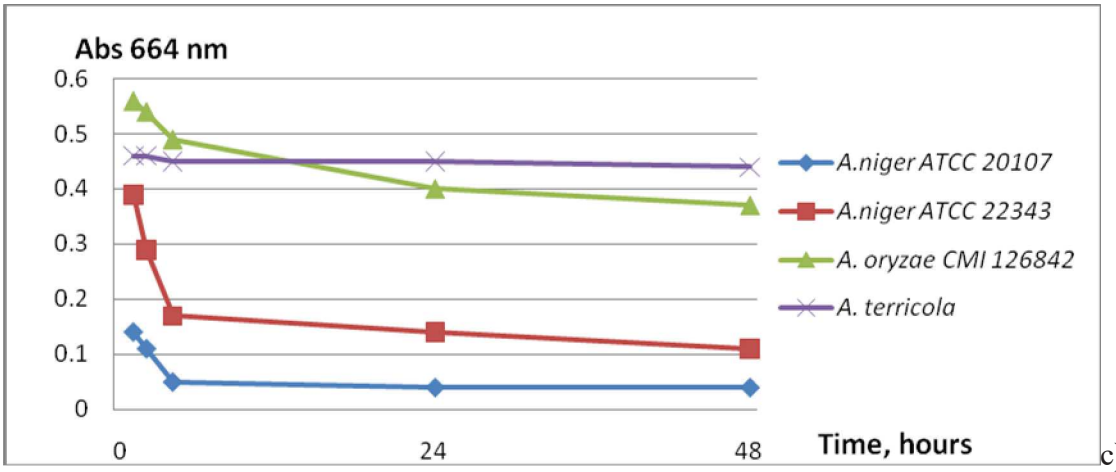

c)

Fig.3 Absorbance values in fungal cultures containing
a) Basic Fuchsin b) Crystal Violet c) Methylene Blue

The greatest degree of biodegradation for all dyes has been observed in the cultures of *Aspergillus niger* ATCC 20107. For example, the concentration of basic fuchsine decreases from 5 µg/mL to about 1.5 µg/mL in the presence of this fungal strain. In the samples with Crystal Violet the concentrations has varied from 5 µg/mL to 0.2 µg/mL and the concentration of Methylene Blue decreases at 0.23 µg/mL. In the cultures of *A. niger* ATCC 22343, *A. oryzae* and *A. terricola* the decrease of dye concentration was not so great, but higher than 50%. The weakest degradation activity was shown in the cultures of *A. terricola* for all dyes.

The percentage of discoloration for all fungal cultures after 2 days is illustrated in figure 4. The discoloration depends on the fungal strain and type of synthetic dye. After 2 days of incubation the discoloration ranges between 46% and 70% for Basic Fuchsin, 75% and 96% for Crystal Violet, 49% and 95% for Methylene Blue, the greatest values being determined in the cultures of *Aspergillus niger* ATCC 20107.

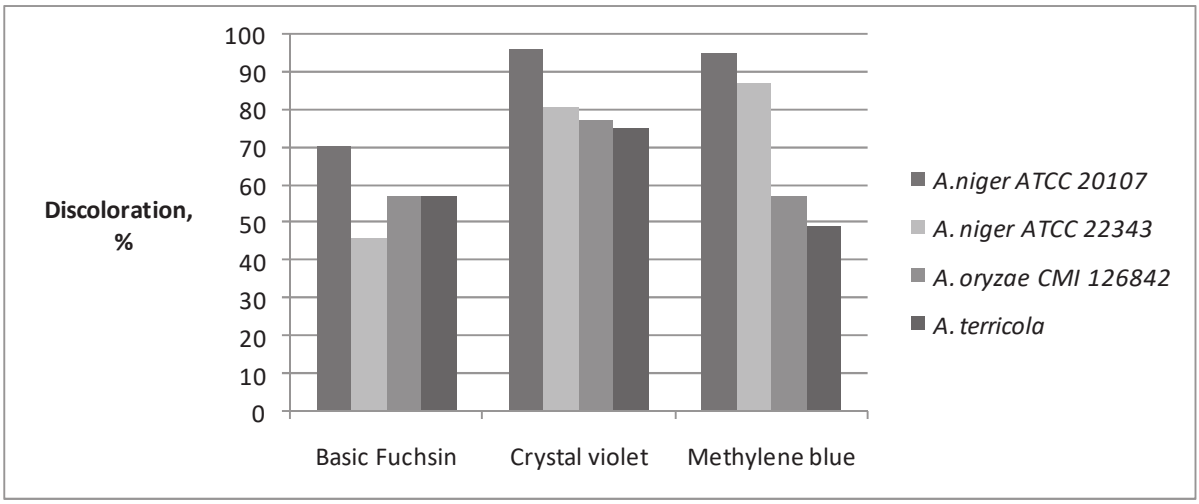

Fig. 4. Discoloration percents of synthetic dyes in the cultures of *Aspergillus niger* ATCC 20107, *A. niger* ATCC 22343, *A. oryzae* CMI 126842, and *A. terricola* F86

4. CONCLUSIONS

An interesting future perspective regarding biological methods for colored wastewater treatment is the use of fungal biomass able to degrade synthetic dyes by biosorption, biosorption and bioaccumulation or by enzyme biotransformation.

Four fungal strains namely *Aspergillus niger* ATCC 20107, *A. niger* ATCC 22343, *A. oryzae* CMI 126842 and *A. terricola* F86 were cultivated in Czapek Dox broth supplemented with synthetic dyes after 120 hours of cultivation.

The assessment of discoloration percentage demonstrated that all fungi were able to biodegrade Basic Fuchsin, Crystal Violet, and Methylene Blue after 2 days of incubation at 30°C in submerged, shaken cultures.

The degree of discoloration depends on the fungal strain and the structure of synthetic dye. The discoloration ranged between 46% and 70% for Basic Fuchsin, 75% and 96% for Crystal Violet, 49% and 95% for Methylene Blue, the greatest values being determined in the cultures of *Aspergillus niger* ATCC 20107.

References

[1] Khehra M.S., Saini H.S., Sharma D.K., Chadha B.S., Chimni S.S., *"Decolorization of various azo dyes by bacterial consortium"*, Dyes Pigm. 67:55–61, 2005.

[2] Ogugbue C.J., Sawidis T., *"Bioremediation and Detoxification of Synthetic Wastewater Containing Triarylmethane Dyes by Aeromonas hydrophila Isolated from Industrial Effluent"*, Biotechnology Research International vol.201, DOI 10.4061/2011/967925, 2011.

[3] Nilsson I., Moller A., Mattiasson B., Rubindamayugi M.S.T., Welander U., "*Decolorization of synthetic and real textile wastewater by the use of white-Rot fungi"*, Enzyme and Microb. Technol. 38: 94-100, 2006.

[4] Ibrahim M.B., Poonam N., Datel S., Roger M., "*Microbial decolorization of textile dye-containing effluents: a review"*, Bioresource Technol. 58(3): 217-227, 1996.

[5] Archna Lokesh K.N., Kiran S.R.R., "*Biological methods of dye removal from textile effluents - A review"*, J. Biochem. Tech. 3(5): S177-S180, 2012.

[6] Robinson T., McMullan G., Marchant R., Nigam P., *"Remediation of dyes in textile effluent: a critical review on current treatment technologies with a proposed alternative"*, Bioresource Technol. 77 (12): 247-255, 2001.

[7] Kaushik P., Malik A., "*Fungal dye decolourization: Recent advances and future potential"*, Environ. Int. 35(1): 127-141, 2009.

[8] Przystaś W., Zabłocka-Godlewska E., Grabińska-Sota E., "*Biological Removal of Azo and Triphenylmethane Dyes and Toxicity of Process By-Products"*, Water Air Soil Pollut. 223 (4):1581-1592, 2012.

[9] Wesenberg D., Kyriakides I., Agathos S.N., "*White-Rot fungi and their enzymes for the treatment of industrial dye effluents"*, Biotechnol. Adv. 22(1-2):161-87, 2003.

[10] Ramírez-Montoya, L.A., Hernández-Montoya V., Montes-Morán M.A., Cervantes F.J., "*Correlation between mesopore volume of carbon supports and the immobilization of laccase from Trametes versicolor for the decolorization of Acid Orange 7"*, J. Environ. Manage. 162: 206–214, 2015.

[11] Espinosa-Ortiz E.J., Rene E.R., van Hullebusch E.D., Lens P.N.L., "*Removal of selenite from wastewater in a Phanerochaete chrysosporium pellet based fungal bioreactor",* Int.Biodeterior. Biodegradation, Vol. 102,pp. 361–369, 2015.

RESEARCHES ON THE INFLUENCE OF BIOMASS RECIPES ON THE PELLETIZING PROCESS

Găgeanu Iuliana[1)], Voicu Gheorghe [2)], Mirela Dincă[2)], Vlăduț Valentin [1)], Matache Mihai [1)], Voicea Iulian[1)], Rădulescu D.L.[3)], Caba I.[1)]
[1)] INMA Bucharest / Romania; [2)] University Politehnica of Bucharest / Romania;
[3)]UASVMB – Faculty of Management, Economic Engineering and Rural Development / Romania

ABSTRACT

Biomass is the most abundant source of renewable energy on the planet that can be used by anyone without requiring special treatment or equipment. However, biomass deteriorates easily in open air, and due to difficulties in transportation and storage, it is necessary for it to be processed in order to reduce its volume and improve handling. One of the most common ways of processing biomass and turning it into biofuel is represented by the pelletizing process. The paper presents a series of researches conducted for determining the influence of biomass recipes used on the final quality of pellets resulting from the pelletizing process.

1. INTRODUCTION

In a broad sense of the word, biomass is represented by plant organic matter, animal metabolic residues (manure) as well as microorganisms. In a strict sense, agricultural biomass includes secondary products from the plants cultivated such as: straws, corn cobs, stalks (sun flower, soy, corn), leaves (beet, vine), pods (soy, beans, peas), shells (walnuts, peanuts), pits (plum, peach, apricot) and manure from animal farms [1]. Besides the agricultural biomass sources, the most important biomass sources come from forestry: primary and secondary material from exploiting forests and resinous and deciduous plantations. [2,3]

Usually, biomass is burned in its original state to generate heat and electricity, or it can be used as raw material for the production of biofuels (liquid biofuels such as biodiesel and bioethanol, or solid biofuels, such as pellets and briquettes) and some chemical compounds. Biomass is a biodegradable and renewable energy resource. Biomass production represents an expanding field due the increasing interest in alternative energy sources. [4, 5,6]

The use of biomass as a source of renewable energy represents a sustainable option for the use of fossil fuels and is one of the easiest to use sources of renewable, because it does not require special equipment for being transformed into energy, being possible to be combusted in conventional equipment used for the combustion of fossil fuels.

One of the most used methods for processing biomass is represented by the pelletizing process. The process consists in grinding biomass materials to small particle sizes (<8-10 mm) and forcing it through the orifices of a die in a special equipment (pelletizing machine). When the biomass material passes through the die, it is compressed and bound together due to the heat that occurs during pelletizing. The heat activates the lignin in the biomass and it acts as a binding agent that maintains the shape of the pellets after cooling.

The quality of pellets is greatly influenced by the materials used. The paper presents a series of researches conducted in order to determine the influence of biomass mixes and recipes used on the quality of pellets produced.

[1]6, Ion Ionescu de la Brad Blvd., tel.: +40762676642, e-mail: iulia.gageanu@gmail.com

2. METHODOLOGY

In order to determine the influence of biomass recipes used on the final quality of the products, a series of tests were conducted on pellet samples. All pellets were produced using the same pelleting machine (a ring die pelleting machine with 8 mm orifices in the die) and the same particle sizes for all biomass materials, respectively <8 mm, obtained by grinding the biomass in a hammer mill.

Figure 1 shows the pellet samples used for tests.

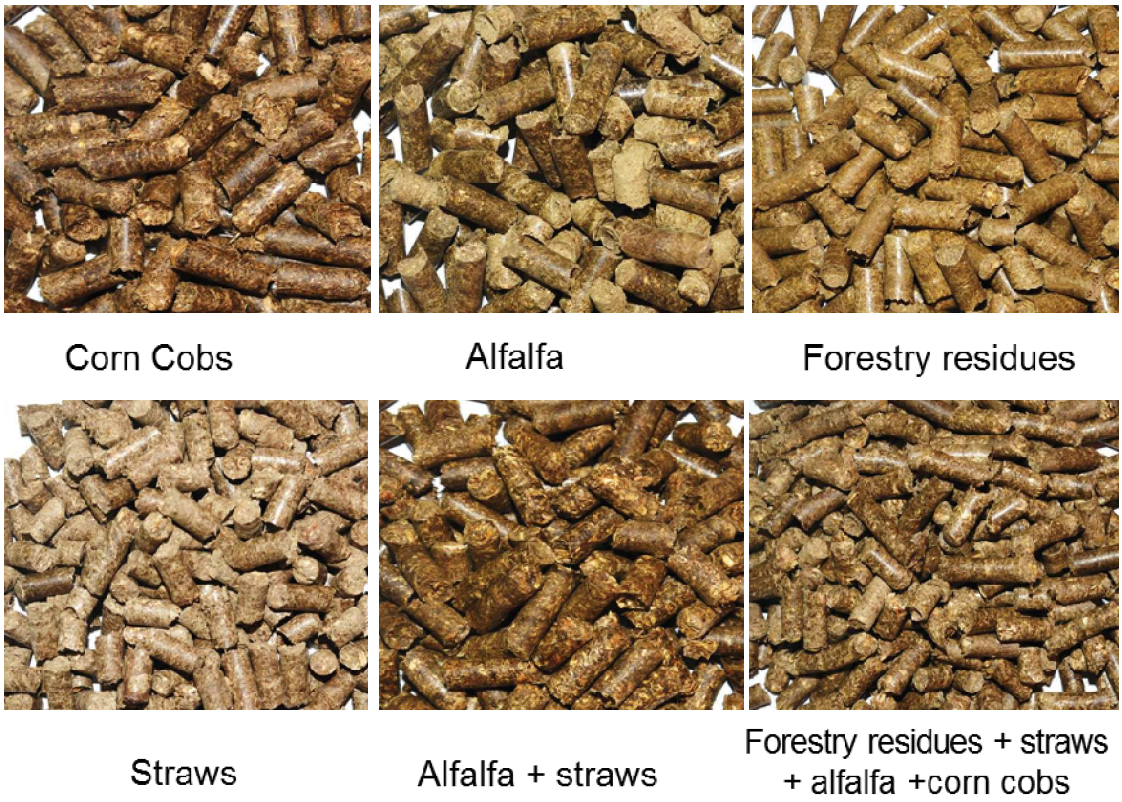

Figure 1: Pellet samples used for determinations

The determinations were conducted on pellets obtained only from one material (corn cobs, alfalfa, forestry residues and straws) as well as on two type of pellets obtained from mixes between these materials, in order to assess the differences between using only one material and using the same materials in combination. Pellets made from the combination between alfalfa and straws had a 50% material from both biomass types. Pellets from forestry residues + straws + alfalfa + corn cobs had 25% from each type of biomass material.

The following quality parameters were determined for the final products: moisture, lower calorific value, ash content, volatile matter content.

Moisture was determined on a wet basis, using the method described in standard ISO 18134-1:2015 “Solid biofuels - Determination of moisture content - Oven dry method - Part 1: Total moisture – Reference method” [7].

The ash content was determined by introducing the pellet samples in the calcination furnace, according to the method described in standard ISO 18122:2015 “Solid biofuels - Determination of ash content” [8].

The content of volatile matters was also determined by introducing the pellet samples in the calcination furnace, according to the method described in standard ISO 18123:2015 “Solid biofuels - Determination of the content of volatile matter” [9].

The inferior calorific value was determined combusting the pellet samples in the calorimeter, according to the method described in standard CEN - EN 14918 – "Solid biofuels - Determination of calorific value" [10].

The quality parameters of pellets were determined using the following laboratory equipment shown in table 1.

Table 1: Equipment used for determinations

Equipment/type	Measure domain / division
Precision weighing scales /AW 220, with self-calibration	0÷200 g / 0,1 mg
Furnace with temperature adjustment /MEMMERT-UFE 500	0÷260 ºC / 1 ºC
Calorimeter /CAL 2k;	0,001 Mj/kg
Naberterm Calcination oven, with P 320 controller	0 ÷ 1400 ºC / 10 ºC

The results from the determinations are shown in table 2. The data in table represents the average value from two determinations conducted on the same type of pellet samples.

Table 2: Results from the tests conducted on biomass pellets

No.	Pellet sample	Moisture [%] *(105ºC)*	Inferior calorific value [Mj/kg]	Ash content [%] *(550ºC)*	Volatile matter content [%] *(900ºC)*
1.	Corn cobs	8.8	13.724	8.53	74.52
2.	Alfalfa	9.38	16.236	6.47	77.42
3.	Forestry residues	7.34	16.021	7.74	76.51
4.	Straws	10.91	15.654	6.94	72.42
5.	Alfalfa + straws	9.05	16.128	6.32	78.03
6.	Forestry residues + straws + alfalfa + corn cobs	9.84	15.892	7.21	78.23

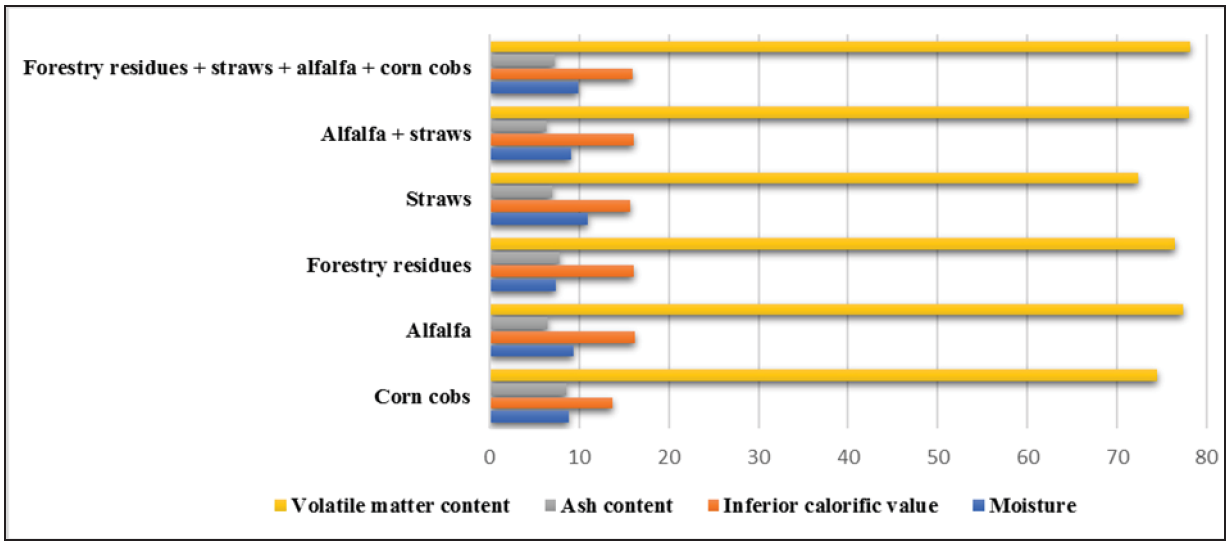

Figure 2: Comparison between the most important quality parameters

From table 2 and figure 2 it results that when combining different types of materials, we obtained good results in terms of inferior calorific value, ash content and volatile matter content, compared to the pellets obtained only from corn cobs or from straws.

3. CONCLUSIONS

Every year, a very important quantity of biomass is wasted, especially the one represented by secondary products in agriculture that are left or are burned on the field. Densification represents a good way to use biomass as renewable energy source in a sustainable manner, ensuring green solid biofuels that can be used by a large range of consumers.

Based on the experimental data resulted, the following conclusions can be given:

1. The combinations between two or more types of biomass materials that were tested showed that it is better to use materials such as corn cobs or wheat straws in combination with other materials to obtain pellets with better quality;
2. By using biomass materials with low lignin content (straws, alfalfa) in combination with woody biomass (forestry residues), which has high lignin content that causes better material binding and increased pellet durability, is ensured that secondary products from agriculture, which otherwise would we wasted, are valorised and transformed into energy without compromising the final quality of pellets obtained;
3. The use of residues from agriculture as well as from forestry for producing pellets represents an activity with good future prospects, contributing to a sustainable development and use of energy, without affecting human and animal food necessities.

Acknowledgement

This work was funded by the Executive Agency for Higher Education, Research, Development and Innovation Funding, within the project entitled "Optimizing the composition of biomass mixtures for obtaining high quality pellets", ctr. 24 BG / 2016 (code PN-III-P2-2.1-BG-2016-0266).

References

[1] Ion V.I., Ion D.I. (2006) - Energy from Biomass, Theoretical considerations. Energy, no. 7(38), pg. 14-30;
[2] Danciu A. et al. (2010). Technology for solid agricultural and forestry biomass capitalization for obtaining clean energy and reducing greenhouse effect gas emissions. Research Report, contract 21-008, INMA Bucharest;
[3] Găgeanu I., Voicu Gh., Bunduchi G, Brăcăcescu C. "Experimental Research on the Process of Pelleting Salix Viminalis Depending on Humidity and Granulation" - Proceedings of 15th International Scientific Conference Engineering for Rural Development – Jelgava, 2016, pp. 624-628;
[4] Berkesy L., Begea M., Berkesy C., Crăciun M., Suciu L. Qualitative aspects regarding biomass destined for heating, Ecoterra, no. 30, 2012, pp. 64;
[5] Voicea I., Vladut V., Cardei P., Matache M., Gageanu I., Voicu Gh., Popescu C., Paraschiv G.,Kabas O. - Compacting process and mathematical analysis of miscanthus briquettes expansion, Proceedings of the 43rd International Symposium on Agricultural Engineering, ISSN 1848-4425,2015, Opatija – Croatia;
[6] Stelte W., Sanadi A.R., Shang L., Holm J.K., Ahrenfeldt J., Henriksen U.B. Recent developments in biomass pelletization – A review. BioResources 7(3), 2012, pp. 4451-4490;
[7] ISO 18134-1:2015 "Solid biofuels - Determination of moisture content - Oven dry method - Part 1: Total moisture – Reference method";
[8] ISO 18122:2015 "Solid biofuels - Determination of ash content";
[9] ISO 18123:2015 "Solid biofuels - Determination of the content of volatile matter";
[10] CEN - EN 14918 – "Solid biofuels - Determination of calorific value".

MODELING AND SIMULATION OF MASS DOSING PROCESS TO PRODUCE PELLETS WITH EXCEL VBA PROGRAMING

George IPATE[1], Gheorghe VOICU, Cristian DUMITRESCU, Erol MURAD, Filip ILIE
University POLITEHNICA of Bucharest

ABSTRACT

In this paper, we develop a program Excel for the study mass dosing process simulation components of a mixture of biomass to manufacture pellets. The program was developed using the VBA programming language, in which Runge-Kutta numerical method applied (RK4) system for solving differential equations describing the mass dosing. This program has a very user friendly interface, as users only need to enter only relevant information to calculate complete system solution differential equations. This program can be an extremely effective tool academic community of professors and students, and others. Application of numerical methods in solving various engineering problems is perceived as being extremely practical nowadays. Our objective is to show how the development of interactive computing modules, with good graphics capabilities can improve the study of the concepts of modeling and simulation in different areas.

Keywords: modeling and simulation, biomass dosing system, mathematical models, differential equations

1. INTRODUCTION

Simultaneous differential equation systems are commonly used in modeling engineering problems in the surrounding world. These equation systems are a mathematical model that can be easily used by engineers in understanding behavior and solving real world problems. Solving differential equation systems using numerical methods is a very interesting topic, because depending on the method used, the accuracy of the obtained solution may vary, and through this it could increase the level of understanding of the studied problems. In this way, it becomes obvious the necessity of deepening the studies that lead to the realization of easy-to-use tools in solving the systems of differential equations.

Tay et. al [1] demonstrated how to solve a system of two first-order ODEs via the RK4 method using Microsoft Excel using VBA programming. Oliveira et al [2] demonstrated teaching the numerical solutions of the oscillatory movement of a mass-spring system and its general solution. They used a spreadsheet as structured tools to support the modelling and the analysis of the results. Tay et. al [3] develop a spreadsheet calculator using VBA code for solving ODEs using Euler's numerical methods. Rosen [4] uses a similar approach to display the solution of a model of the earth's carbon cycle.

The purpose of this paper is to achieve a mass-dosing simulation program using the Excel VBA language to study the influence of changes on the physical / process parameters involved and the effect these changes make on the corresponding graphs. Program codes are very easy to use, with direct application to solve real engineering problems, and increase students' motivation to do something to recognize, process and apply the information they receive [5]. According to Mohammad et al. [6], a good teaching process is a process of combining various methods of teaching and teaching approaches to achieve optimal teaching effect.

[1]Corresponding author email : ***puiuipate@yahoo.com***

2. METHODOLOGY

The study of the dynamic behavior of physical systems and processes is done with mathematical models in the form of ordinary, linear or non-linear differential equations.

To solve ordinary differential equations, many computer programs use the 4th Runge-Kutta method, being very widespread because of its increased efficiency. It uses a weighted average of four estimates of gradients multiplied by the x-spacing **h** to deduce the y-increment [5]. This numerical solutions involve time-stepping from initial conditions forward in the time-direction. Fourth-order Runge-Kutta method is widely used in computer solutions to differential equations because it is accurate, stable, and relatively easy to program.

To determine the approximate solution of the linear order differential equation of the form:

$$\frac{dy}{dx} = f(x, y), \text{with given initial condition y at x } = 0, \quad (1)$$

the RK4 method is defined by the formulas:

$$y_{n+1} = y_n + \frac{1}{6}(k_1 + 2k_2 + 2k_3 + k_4) \quad (2)$$

where

$$k_1 = h * f(x_n, y_n) \quad (3)$$

$$k_2 = h * f(x_n + \frac{1}{2}h, y_n + \frac{1}{2}k_1) \quad (4)$$

$$k_3 = h * f(x_n + \frac{1}{2}h, y_n + \frac{1}{2}k_2) \quad (5)$$

$$k_4 = h * f(x_n + h, y_n + k_3) \quad (6)$$

where - h is the integration step ($h = x_{i+1} - x_i$, $i = 0 \ldots n-1$) and the ends of the interval belonging to the independent variable x are: $x_0 = a$, $x_n = b$.

The main advantage of the RK4 method over other numerical methods to solve differential equation systems is that it ensures the further improvement of precision and truncation error on an integration step.

Microsoft Excel, a program present on most personal computers, has the same capabilities to solve mathematical problems or process and display graphical results as well as more sophisticated computing programs like Matlab or Mathcad. Visual Basic for Applications, or VBA, is a "dialect" of Microsoft's Visual Basic programming language embeded in Excel, that allow the programmer to work with Excel's workbooks, worksheets, cells and charts [8]. The numerical integration technique the fourth order Runge-Kutta can be incorporated easily in a standard MS Excel© spreadsheet by the VBA function to perform the numerical integration.

3. NUMERICAL EXAMPLE

Gravitational batch dosing is widely used in industry and agriculture. The components required to make the recipe are stored in the hopper, from which they are extracted and flowed simultaneously into the mixing bowl provided with a dosing scale. Principally a recipe and a total mass of the batch (m_{batch}) are required. The recipe is usually given as the weight ratio p_i of the component "i" of the total mass of the batch:

$$m_{batch} = \sum_{i=1}^{n} p_i = \sum_{i=1}^{n} p_i * m_{batch} \quad (7)$$

and thus results:

$$\sum_{i=1}^{n} p_i = 1 \quad (8)$$

where - *n* is total number of components of the recipe.

The gravitational mass dosing process starts when the automatic dosing control system controls the starting of the extractors or the opening of the component storage hopper flaps.

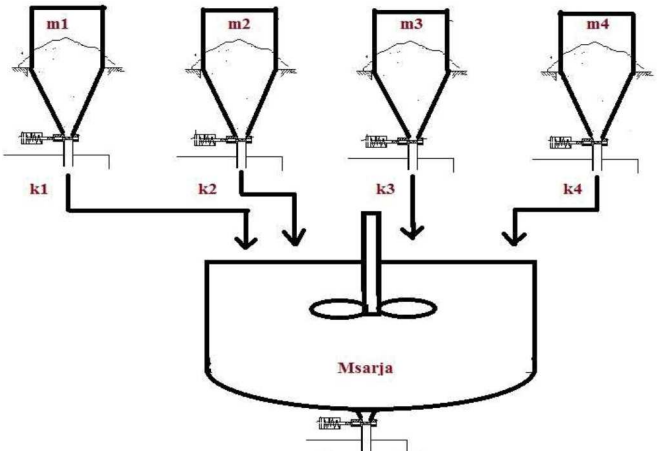

Figure 1: Schematic of gravity mass dosing process

The mixing vessel is supported on the sensitive elements of a weight transducer which during the flow of the components gives a signal to the automatic dosing control system. When this signal reaches a value equal to the reference value (total mass of the batch) programmed to mix the mixture, the automated control system gives the component flow stop command and the exhaust flap opening of the mix packing it in bags.

The mass dosing process described in the scheme in Figure 1 below can be modelled, according to the law of mass action, by the following system of first-order differential equations:

$$\frac{dm_i(t)}{dt} = p_i * m_{batch} - m_i(t)\,, m_i(0) = 0 \qquad (9)$$

where - i is the component (i=1..4); p is the weight ratio; m_{batch} is total mass of mixture and m is the component mass.

The simulation results can be compared with the exact analytic solution:

$$m_i(t) = p_i * m_{batch}(1 - \frac{1}{e^{tsim}}) \qquad (10)$$

where - t_{sim} is total time of dosing process.

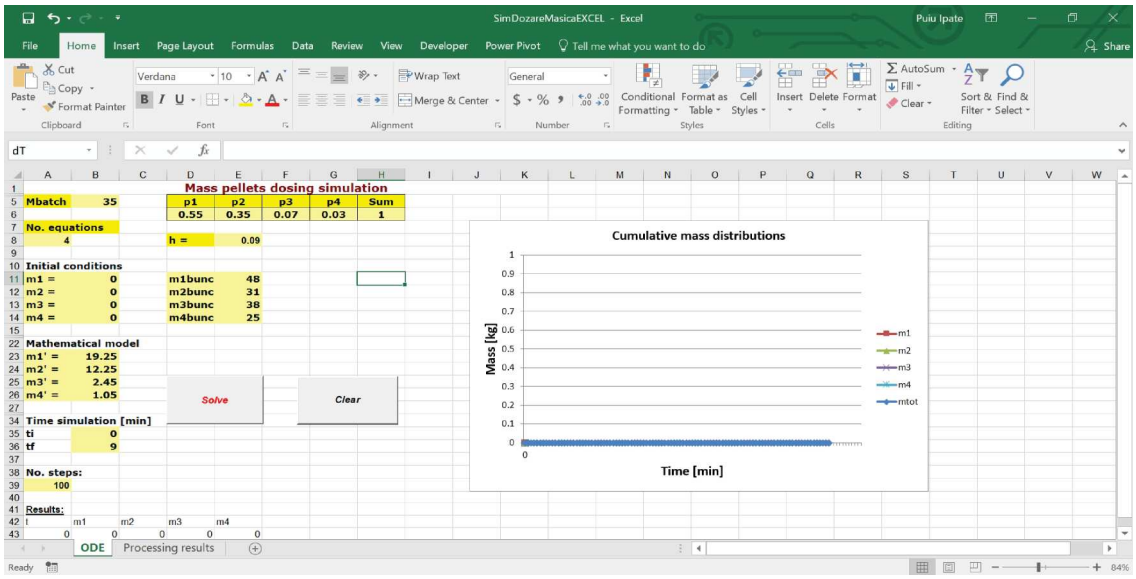

Figure 2: User interface program

Using the simulation program, we can obtain the graph of the previous solution of $m_i(t)$ which expresses the relationship between time t, from the initial moment t_0 to the final t_{sim} and

the mass of the components of the mixture $m_i(t)$ in the mixing vessel and in the feed hopper. It is also possible to display the so-called state curve that graphically represents the mass flows of the components at each time of the dosing process as well as the dosing error.

As a numerical example, we will analyze the mass dosing process of the biomass pelleting mixture by extrusion consisting of mixed solid particles after the recipe: 0.55 parts of corn cobs, 0.35 parts of wheat straw, 0.07 parts of wood sawdust and 0.03 binders. The mixture will be packed in 35 kg raffia bags.

Figure 2 illustrates the friendly user interface program of mass dosing simulation model. By modifying the data in mathematical model (cells B23-B26) for $dm_i(t)/dt$, (for time t_0=0 to final time t_{sim}=9 min in cells B35-B36) different component mass levels can be predicted for future. Firstly, users can select principal parameters total mass batch in B5 to input the required information ODE's.

The model parameters weight ratio $\boldsymbol{p_i}$ starting in D6 are defined to the top of the main spreadsheet. The number of equations to be solved (n) and the step size for the integration (h) are specified under process parameters (A8, respectively, E8). The initial values of the four dependent variables $m_i(t)$ are specified on the columns B, rows 11-14 for the mixing vessel, respectively columns E, rows 11-14 for the feed hoppers. The main table begins in location A43 with the time simulations array *t*. The amount of material from each component added to the mixing vessel (B43-E43) is calculated from the initial values (B11-B14). Once the "Solve" button is clicked, the simulation run and the process values will be calculated automatically based on the integration time step. Solve button is associated with VBA code that is written to compute the solution of the system of ODE's using RK4 method. The full solution is shown in Figure 3. By pressing the "Clear" button, the results obtained by running the simulation program are deleted.

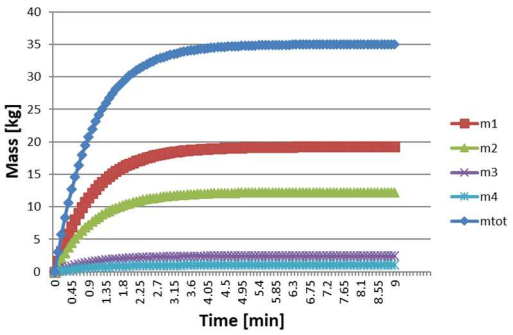

Figure 3: Cumulative mass distribution in mixing vessel

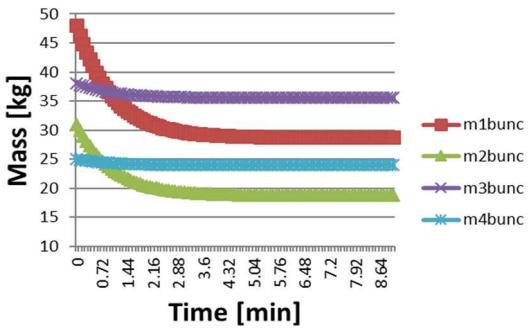

Figure 4: Cumulative mass distribution in feed hoppers

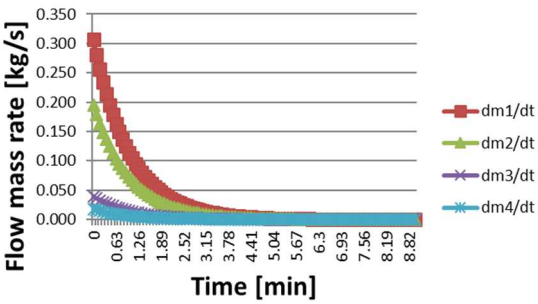

Figure 5: Flow mass rate distributions

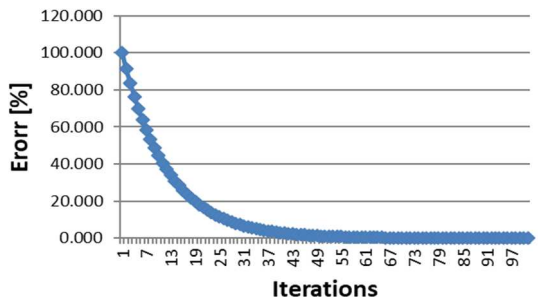

Figure 6: Dosing error versus iteration number

Excel provides a viable alternative for performing routine calculations, such as processing the results from the simulation. Table 1 shows the values of the processing of the data obtained by numerical solving of the differential equation system. Figure 4 shows the graphic for the

cumulative mass distribution in feed hoppers as a function of time, for the parameters and initial conditions earlier defined. In figure 5 we can see the flow mass rate distributions of raw material. To complete the application, we include the dosing error curve shown in figure 6. The dosing error can be calculated whit relation:

$$error[\%] = \frac{m_{batch} - m_{batch}(t)}{m_{batch}} * 100 \qquad (11)$$

The results can be compared considering the different values of the process parameters. This can be done with the VBA code shown in Figure 7.

Table 1: Processing results from simulation data

Processing results

time	m1bunc	m2bunc	m3bunc	m4bunc	mtot	dm1/dt	dm2/dt	dm3/dt	dm4/dt	error
0	48.000	31.000	38.000	25.000	0.000	0.307	0.195	0.039	0.017	100.000
0.09	46.343	29.946	37.789	24.910	3.012	0.280	0.178	0.036	0.015	91.393
0.18	44.829	28.982	37.596	24.827	5.766	0.256	0.163	0.033	0.014	83.527
0.27	43.445	28.101	37.420	24.752	8.282	0.234	0.149	0.030	0.013	76.338
0.36	42.180	27.297	37.259	24.683	10.581	0.214	0.136	0.027	0.012	69.768
0.45	41.024	26.561	37.112	24.620	12.683	0.196	0.124	0.025	0.011	63.763
0.54	39.968	25.889	36.978	24.562	14.604	0.179	0.114	0.023	0.010	58.275
0.63	39.002	25.274	36.855	24.509	16.359	0.163	0.104	0.021	0.009	53.259
0.72	38.120	24.713	36.743	24.461	17.964	0.149	0.095	0.019	0.008	48.675
0.81	37.314	24.200	36.640	24.417	19.430	0.136	0.087	0.017	0.007	44.486
0.9	36.576	23.730	36.546	24.377	20.770	0.125	0.079	0.016	0.007	40.657
0.99	35.903	23.302	36.460	24.340	21.995	0.114	0.073	0.015	0.006	37.158
1.08	35.287	22.910	36.382	24.307	23.114	0.104	0.066	0.013	0.006	33.960
1.17	34.725	22.552	36.310	24.276	24.137	0.095	0.061	0.012	0.005	31.037
1.26	34.210	22.225	36.245	24.248	25.072	0.087	0.055	0.011	0.005	28.365
1.35	33.740	21.926	36.185	24.222	25.927	0.080	0.051	0.010	0.004	25.924
1.44	33.311	21.652	36.130	24.199	26.708	0.073	0.046	0.009	0.004	23.693
1.53	32.918	21.403	36.081	24.177	27.421	0.066	0.042	0.008	0.004	21.654
1.62	32.560	21.174	36.035	24.158	28.074	0.061	0.039	0.008	0.003	19.790
1.71	32.232	20.966	35.993	24.140	28.670	0.055	0.035	0.007	0.003	18.087
1.8	31.932	20.775	35.955	24.124	29.215	0.051	0.032	0.006	0.003	16.530
1.89	31.658	20.601	35.920	24.109	29.712	0.046	0.029	0.006	0.003	15.107
1.98	31.408	20.441	35.888	24.095	30.168	0.042	0.027	0.005	0.002	13.807
2.07	31.179	20.296	35.859	24.082	30.583	0.039	0.025	0.005	0.002	12.619
2.16	30.970	20.163	35.833	24.071	30.964	0.035	0.023	0.005	0.002	11.533

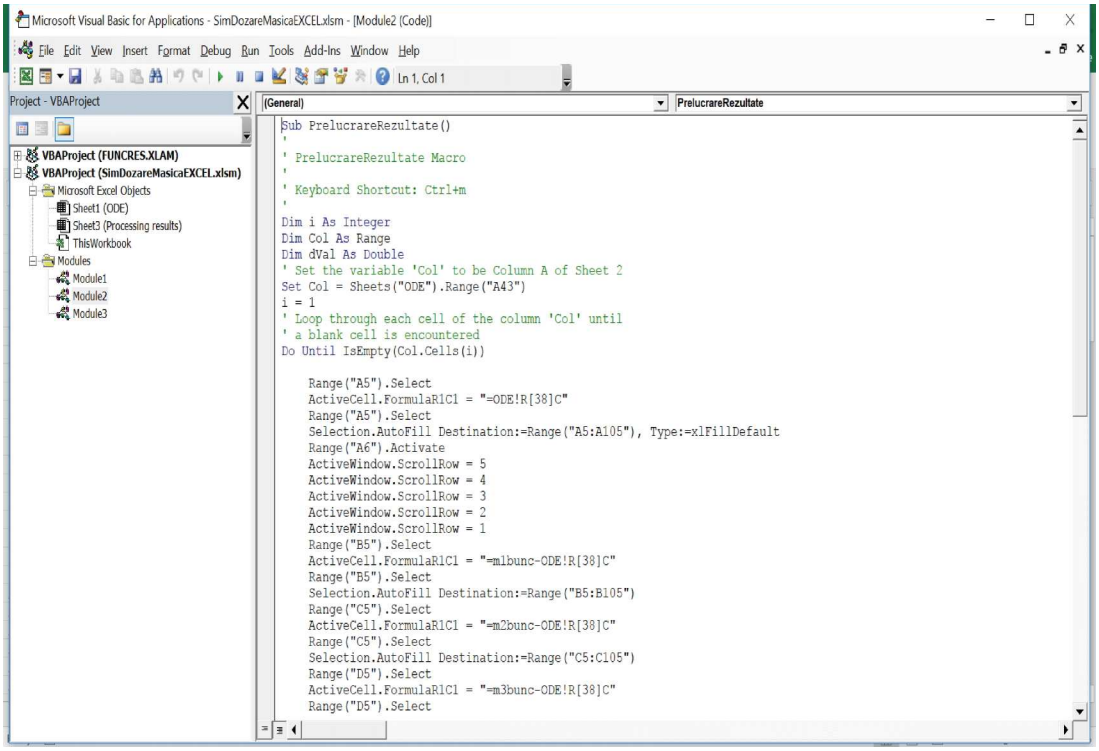

Figure 7: VBA code for processing results from simulation

4. CONCLUSIONS

This paper presents how to implement the 4th Runge-Kutta numerical method in solving the differential equation systems in the VBA Excel programming environment to study the gravitational mass gravity dosing process of raw materials used in pelleting. The VBA programming language is very easy to use because users only need to enter the relevant data to get the complete solution, which will be displayed later, of the mathematical model of the process. Excel spreadsheets allow teachers and students to build their own numerical computing applications based on an approach that focuses primarily on stimulating creativity and innovation to solve modeling problems in real world processes or systems.

Acknoledgement

The work has been funded by Ministry of National Education and Research through the Executive Agency for Higher Education, Research, Development and Innovation Funding, within the project entitled „Optimizing the composition of biomass mixtures for obtaining high quality pellets", BG 24 / 2016.

References

[1] Tay, K.G., Cheong, T.H., Lee, M.F., Kek, S.L., *A fourth-order Runge-Kutta (RK4) Spreadsheet Calculator For Solving A System of Two First-Order Ordinary Differential Equations Using Visual Basic (VBA) Programming*, Spreadsheets in Education (eJSiE), Vol. 8, Iss. 1, Art. 5, 2014.

[2] Oliveira, M.C., Nápoles, S., *Using a Spreadsheet to Study the Oscillatory Movement of a Mass-Spring System*, Spreadsheets in Education (eJSiE), Vol. 3, Iss. 3, Art. 2, 2010.

[3] Tay, K.G., Kek, S.L., Cheong, T.H., Abdul-Kahar, R., *The Euler's Spreadsheet Calculator Using VBA programming For Solving Ordinary Differential Equations*, ARPN Journal of Engineering and Applied Sciences, Vol. 11, No. 20, October, 2016.

[4] Rosen, E., *Using VBA as an Alternative*, 2009.

[5] Lilley, D.G., *NME: Some Useful Excel/VBA Codes for Numerical Methods in Engineering*, 48th AIAA Aerospace Sciences Meeting Including the New Horizons Forum and Aerospace Exposition, Orlando, Florida, 4 - 7 January 2010.

[6] Mohammad, N., Yasin, R.M., Ana, E., *Creative Teaching in Design and Technology Curriculum: Using Structural Equation Modeling*, Procedia - Social and Behavioral Sciences 204, pp 240 – 246, 2015.

[7] Hood, D., *Numerical solution of ordinary differential equations using an MS Excel© spreadsheet*, MSOR Connections, Vol. 9, No. 3, October, 2009.

[8] Billo, E.J., *Excel@ for Scientists and Engineers - Numerical Methods*, Published by John Wiley & Sons, Inc., 2007.

THE ASSESSMENT OF ENVIRONMENTAL IMPACT DUE TO THE TRAFFIC IN BUCHAREST

Istrate Irina Aura[1], Cocârță Diana Mariana[2]
[1]University POLITEHNICA of Bucharest, Faculty of Biotechnical Systems Engineering, Department of Biotechnical Systems
[2] University POLITEHNICA of Bucharest, Faculty of Power Engineering, Department of Energy Production and Use

ABSTRACT

In Romania, noise is an increasingly worrisome factor, especially in the Romanian capital, which becomes more and more crowded every day. According to recent studies, it seems that road traffic is the main cause of noise pollution in Bucharest. The inhabitants of the city are exposed, with or without their will, to the noise. Romania is one of the most "noisy" countries in the European Union. In the big cities in Romania from the noise levels point of view, Bucharest is the in the first place, while at the end of this classification is Iasi, with only 16% of the population affected by noise. This paper aims to study the noise level at an intersection in Bucharest and to interpret the results according to STAS 10009-88 Admissible Limits of Noise in Cities. As far as the experimental activity is concerned, it consisted in the development of measurements at one of the busiest intersections in Bucharest where it is observed that all the over ground means of transport are intersecting.

1. INTRODUCTION

The sounds are part of our lives and surround us everywhere. Man, whatever it does, it produces noise, more or less. He is blustering, and any activity is accompanied by a sound. Whether he talks, go by car, it feeds, builds a block, he must be heard. The sound follows us everywhere that we do not realize anymore what its functions are.

From physiological point of view, the sound represents the sensation produced on the auditory organ by the vibration of material bodies and transmitted through acoustic waves.

In the opposite direction of sound is defined notion of noise. According to the explanatory dictionary of the Romanian language the noise represents “a sound or the mixing of discordant sounds, strong, that impressive the hearing in an unpleasant way. Clamor, uproar." Noise is characterized by two important qualities: the intensity, measured in decibels [dB], and the frequency, measured in Hertz [Hz].

1.1. Legislation regarding noise

Directive 2002/49/EC (the Environmental Noise Directive – END) is considered the main European Union (EU) instrument used for the identification of noise pollution levels. This legal act is the one that trigger the necessary action both at Member State and at EU level. According to the [1], the Member State have to prepare and publish, every 5 years, noise maps and noise management plans for:

[1]Splaiul Independentei 313, Bucharest, Romania, +40723 542 609, ia_istrate@yahoo.com

- agglomerations with more than 100,000 inhabitants;
- major roads (more than 3 million vehicles a year);
- major railways (more than 30.000 trains a year);
- major airports (more than 50.000 movements a year, including small aircrafts and helicopters);

At European level, Environmental noise is also regulated at the source of the noise, with legislation on issues such as harmonized noise limits for motor vehicles, outdoor equipment and other noise-generating products. The list below outlines key legislation in the field of noise at source [1].

- **Road traffic noise (follow-up by** EC DG for Internal Market, Industry, Entrepreneurship and SMEs **)**
  - Motor Vehicles - Regulation No 540/2014
  - Motor Cycles - Regulation No 168/2013 and Commission Delegated Regulation No 134/2014
  - Tyres for motor vehicles and their trailers and their fitting - Directive 2001/43/EC
- **Aircraft noise (follow-up by** EC DG for Mobility and Transport **)**
  - Limitation of the noise from airplanes - Regulation No 216/2008 and Regulation No 748/2012
  - Operating restrictions at Community airports - Regulation No 598/2014
  - Regulation of chapter 3 civil subsonic airplanes - Directive 2006/93/EC
- **Railway noise (follow-up by** EC DG for Mobility and Transport**)**
  - Railway interoperability - Directive 2008/57/EC
  - Technical Specification for Interoperability (TSI) on Noise - Regulation (EU) No 1304/2014
  - Noise charging - Regulation (EU) 2015/429
  - Connecting Europe Facility - Regulation (EU) 1316/2013

Road traffic is the most dominant source of environmental noise in Europe. It is estimated that 125 million people are affected by noise levels from road traffic greater than 55 decibels (dB) Lden, including more than 37 million exposed to noise levels above 65 dB Lden [1].

1.2. Health effects of noise

According to the findings of the World Health Organization (WHO), noise is the second largest environmental cause of health problems, just after the impact of air quality (particulate matter) [2].

The World Health Organization's Night Noise Guidelines for Europe present evidence of the health damage of night-time noise exposure and recommend threshold values above which adverse effects on human health are observed [2]. An annual average night exposure not exceeding 40 decibel (dB) has been recommended in the Guidelines. Sleepers that are exposed to night noise levels above 40dB on average throughout the year can suffer health effects like sleep disturbance and awakenings. Above 55dB long-term average exposure, noise can trigger elevated blood pressure and lead to ischemic heart disease [2].

A study commissioned by DG Environment on the Health implication of road, railway and aircraft noise in the European Union found that exposure to noise in Europe contributes to [2]:

- about 910 thousand additional prevalent cases of hypertension,
- 43 thousand hospital admissions per year, and

- at least 10 thousand premature deaths per year related to coronary heart disease and stroke.

2. METHODOLOGY

Reducing exposure to noise should be based on the general principles of prevention, starting from the source up to the minimum possible value. There are three methods for noise reduction:

I. Methods for the control of noise at source;

II. Methods of combating the noise propagation paths;

III. Methods of combating the noise at receiver.

In figure 1, it can be seen the noise map of Bucharest. On the main roads, the noise levels are exceeding the values of 80 dB[A].

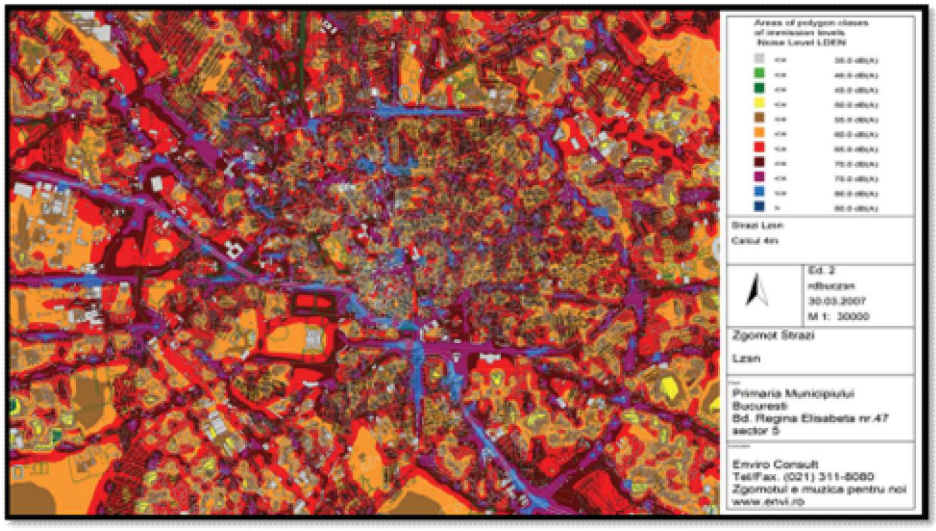

Figure 1: Noise map in Bucharest [3]

For the experimental research, it was decided to have a series of measurements in a crowded intersection, were different types of streets. Thus, the presented intersection encompasses category 1 street - Mihai Bravu, with category 2 streets -Blvd. Baba Novac and Dristor Street, with category 3 street Traian Popovici.

The measurements were made using a sound level meter type Solo. The sound level meter is an electronic device that measure the intensity of the sound waves, in particular the noise. This device is designed to respond to sound in about the same manner as a human ear in order to obtain objective, reproducible measurements of sound pressure level. The measurements campaign was performed according to the legislation, both during the day (07:00-23:00) and at night (23:00-07:00) at different times, as follows:

- Interval no. 1 -> **06:00 – 08:00**;
- Interval no. 2 -> **08:00 – 10:00;**
- Interval no. 3 -> **16:00 – 18:00;**
- Interval no. 4 -> **23:00 – 01:00.**

The ranges were chosen to highlight the level of noise involved in moments of urban life, namely transit to and from work, for the first time intervals, and the last interval was chosen in order to make a comparison with a period which in theory is supposed to be quieter

(night). The intersection is the one that brings together the streets: Baba Novac, Mihai Bravu, Traian Popovici, Dristor as shown in Figure 2.

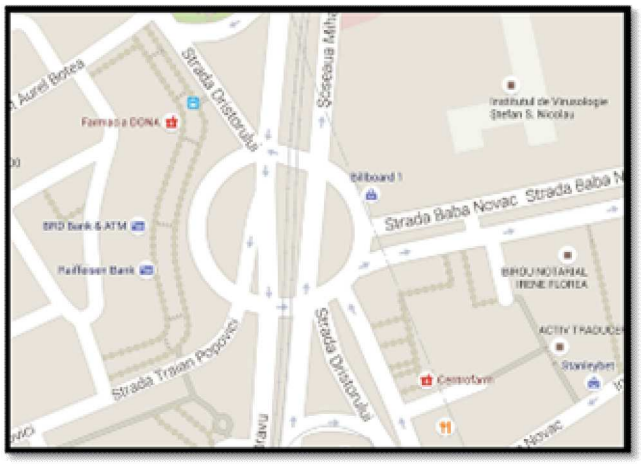

Figure 2. The intersection were the measurements have been performed

The measurement campaign is divided for each street in three measurement points:

- Point in the intersection (0 m from the main intersection);
- Point at 50 m from the main intersection;
- Point at 100 m from the main intersection.

The idea was to assess the noise at different distances from the main intersection in order to have values for the human health risk assessment.

From the sound level meter, all the data were downloaded and then processed. An example for the data obtained from the measurement device is presented in figure 3 (a and b).

File	BN50.CMG					
Start	09.06.16 06:39:23					
End	09.06.16 06:42:23					
Channel	Type	Wght	Unit	Leq	Lmin	Lmax
#443	Leq	A	dB	66,6	52,8	77,0

a)

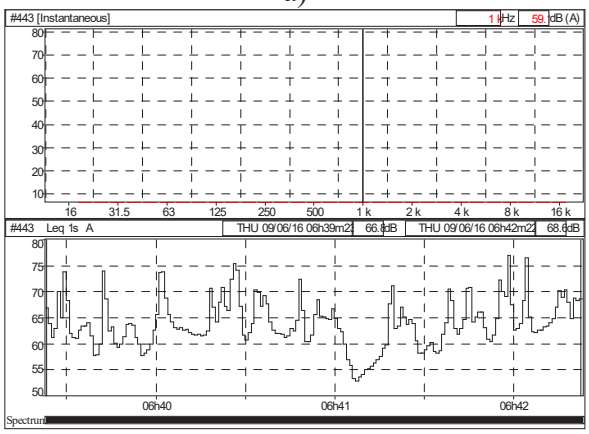

b)

Figure 3: The data collected in the measurement point placed at 50 m from the main intersection: a) the main data registered in the sound level meter; b) sound level evolution during 3 minutes of measurement.

The results obtained after all the measurements are presented in figure 4.

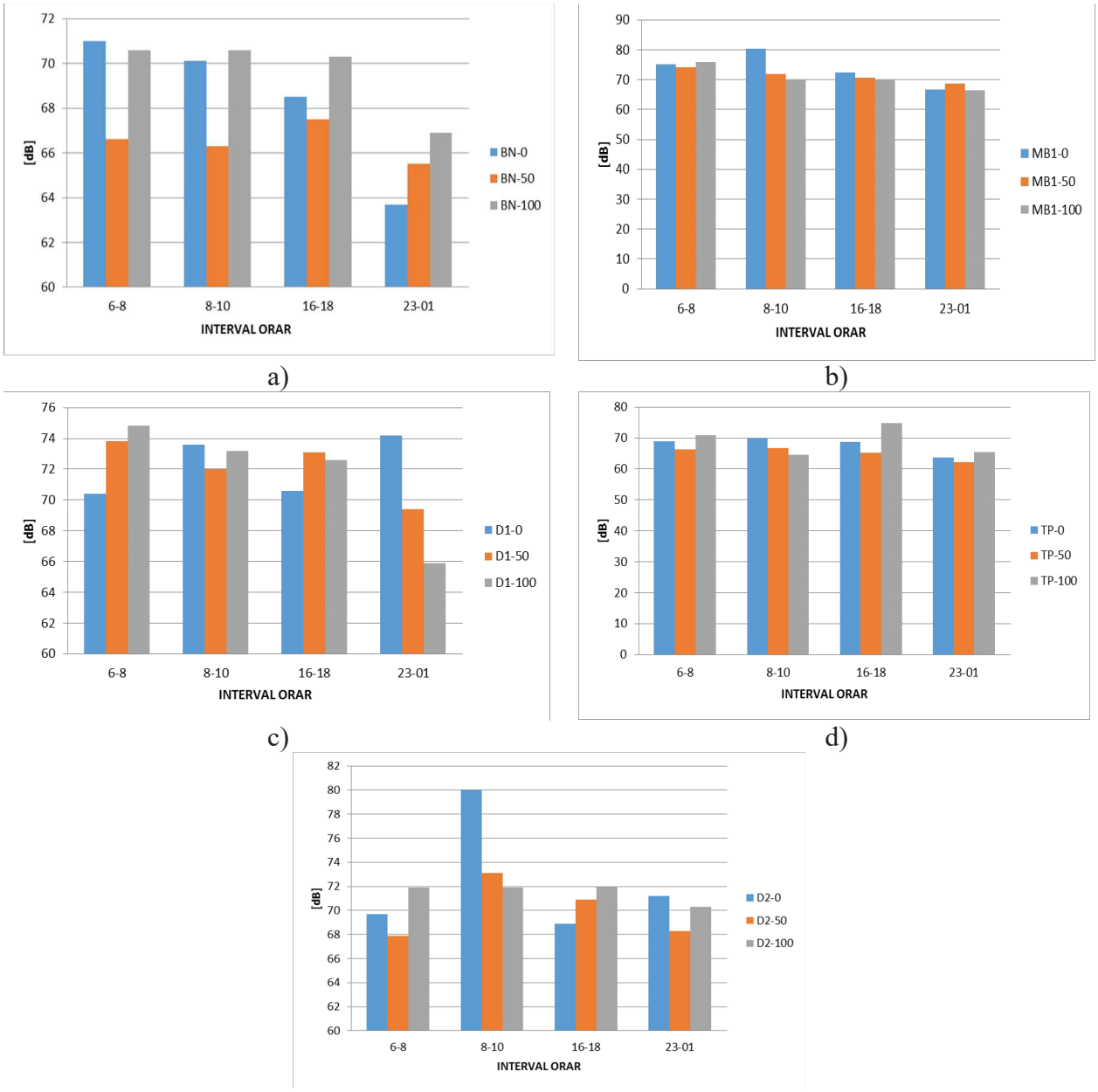

Figure 4. Noise level variation for: a) Baba Novac Street, b) Mihai Bravu_1 Street; c) Dristor_1 Street; d) Traian Popovici Street; e) Dristor_2 Street

3. CONCLUSIONS

This paper had as main aim the study of noise in an intersection in Bucharest, and interpretation of the results according to STAS 10009-88 permissible noise Limits. As regards the experimental work, consisted in the development of sets of measurements in one of Bucharest's congested intersections where it is observed that all of the ground transportation intersect.

Figure 4 is very suggestive for the analyzed time period. Social life in the capital is active in this interval, and the noise level is highest on the Dristor Street, connecting with the Centre

of the capital. Thus it appears that the highest level for this interval is Leq (D1_0) = 74.2 dB(a) which for this time of day should be a maximum of 65 dB (A).

The Romanian legislation stipulates that the maximum allowable limits on a day to be regarded with 10dB (A) less during the night, in this case, the maximum allowable under the law should be 55dB (A). Therefore, it is concluded that during the night, the noise level measured is very high relative to the maximum allowable limit, showing that people living on the Dristor street can be influenced at night especially during the summer when the windows open. The most present effects on the population is low quality sleep at night, the high level of stress, heart palpitations, and headaches.

Acknowledgement

The authors would like to thank you Mrs. Titileci Laura, for the support given during the experimental campaigns.

This work has been funded by University Politehnica of Bucharest, through the "Excellence Research Grants" Program, UPB – GEX. Identifier: UPB–EXCELENȚĂ–2016, Research project title: Utilizarea ozonului în tratarea solurilor contaminate organic/ The use of ozone for the treatment of organic contaminated soils, Contract number 42/26.09.2016 (acronym: OZOSOL) and under National Funds – Young research teams, REMPET project "Decision making for the remediation of contaminated sites with petroleum products using source -path - receiver model and cost-benefit analysis" (2015-2017).

References

[1] Directive 2002/49/EC of the European parliament and of the Council http://eur-lex.europa.eu/legal-content/EN/TXT/PDF/?uri=CELEX:32002L0049&from=EN (accessed in April 2017)
[2] European Commission, http://ec.europa.eu/environment/noise/health_effects_en.htm (accessed in April 2017)
[3] Bucharest Town Hall, www.pmb.ro

CONSIDERATIONS REGARDING THE SOIL COMPACTIBILITY EVALUATION IN ORCHARDS

Marin E.[1], Mateescu M., Manea D., Gheorghe G., Caba I.
INMA Bucharest

ABSTRACT

The main purpose of this paper is to present some research for the compilation of the soil compaction map in conditions of local humidity in orchards by using a modern methodology, which uses methods and techniques specific for precision farming. The obtained results will help the management improvement, through the information provided the compacted areas and the depth of soil compaction as a result of the repeated passage of the orchards machinery, to apply recovery measures only in those areas. So, it will be done substantial increase in production, reducing start-up costs and substantial support in substantiating the decisional processes taking place at the fruit farm management level.

1. INTRODUCTION

Penetration resistance is one of the physical indicators of soil quality, along with other features such as structure, apparent density, water infiltration rate, water retention capacity, being used as an indicator of soil compaction.

The energy invested in the working process carried out by the working organs of agricultural machinery is a particular interest for the rational design and development of these elements of agricultural machinery for soil working execution [2].

Determination of penetration resistance is a simple method of assessing soil compaction, much used in research on soil works and other agro-technical elements, to highlight the seasonal dynamics of the physical state of the soil. This dynamics results, on the one hand, from the variation during the year and under the influence of different agro-technical measures of apparent density, especially in the arable layer, and on the other, from the seasonal dynamics of humidity. So, the penetration resistance determinations can provide a combined image of the effect of compaction and humidity. However, if is to be studied only the effect of the compaction condition, it is necessary to perform measurements on similar humidity [3].

To know if the soil of a land is or not subject to compaction, the farmer has to ask questions about intensity, expansion, spatial and temporal variation, depth, thickness and time of compacting, which requires a direct on-site investigation. Only a correct local monitoring and adequate mapping of compacted areas allow us an optimal soil processing, because the depth of machining can be optimized according to the depth of compaction. Soil information is also needed in precision agriculture to drive and understand plant growth and land behavior at repeated passes of agricultural machinery [4].

To assess the physical state of the soil at one time, to determine the correlation between the state of soil compaction with the resistance opposite by the working organs of the soil-working machines to the execution of agricultural works or to the development of the roots of the horticultural crops, respectively for the determination of the load capacity of the terrain, it

[1]Bucharest, Bvd. Ion Ionescu de la Brad, Division 1, +04212693269 and marin_43eu@yahoo.com

is used the technical procedure to measure "in situ" the resistance opposite by an "undisturbed" ground to penetration with a standard metal body.

The use of penetrometers as devices for the determination of resistance to soil penetration has been taken into account by researchers over the last forty years [1]. One of the problems in compaction measuring and other soil features is the lack of a fast and accurate method of making measurements. The two problems on the use of most soil penetrometers are the laborious processes of manually pushing the cone into the ground and recording the individual readings obtained at specified intervals. Another problem encountered on penetrometers manually operated is the difficulty of obtaining a constant penetration speed when the cone is pushed into the ground.

The mapping of the soil by means of an electronic penetrometer, consisting of a rod ending with a cone, which is pushed into the ground by a hydraulic cylinder, provided with a force transducer, assures the measurement of applied force and a displacement transducer who is measuring the depth penetration. Data collected, together with the positions corresponding to the evidence, measured by a GPS receiver, can be transferred to a personal computer's memory, where the computer system processes them on the basis of specialized software, to finally generate maps of the soil compaction state.

2. METHODOLOGY

The study material was represented by monitoring the compaction state in conditions of local soil humidity on the field plot at the Pomicola Research and Development Institute of Bucharest. In the experimental procedure implemented has been used an Eijkelkamp Penetrologger electronic penetrometer with digital display equipped with a humidity sensor Eijkelkamp Thetaprobe [1], connected to the electronic module of the penetrometer (Figure 1).

Figure 1: Electronic penetrometer with digital display Eijkelkamp Penetrologger equipped with a humidity sensor Eijkelkamp Thetaprobe

Conducting experimental research in the field assumed the following:

- Identify the location of the batch by locating in GPS coordinates, determining the size of the batch surface, identifying the type of soil;
- Carrying out the mapping plan, identifying the points of interest or points where measurement of various parameters is desired, setting the coordinates (lines, columns, density of sampling points);
- Inserting mapping plan data into the electronic penetrometer memory;
- Measuring and plotting the compaction state and local humidity of the soil on the monitored lot.

Collecting data focused on the sampling, analysis and recording of soil samples by manual methods. The press pressure and local humidity in the monitored plot soil was recorded by slow penetration with the Eijkelkamp Penetrologger penetrometer equipped with a humidity sensor Eijkelkamp Thetaprobe (Figure 2). With the integrated GPS, the measuring point has been accurately recorded.

Figure 2: Measurement of press pressure and local humidity

3. RESULTS

For each measuring point (total 13 points), was performed a series of 13 records (Figure 3) representing the press pressure and humidity values at ground level, that have been provided in the form of electrical signals whose levels have been tracked on the digital display and recorded in the device memory, after which they have been downloaded to a computer to be appropriately processed.

On Google Earth Maps [1] it is possible to perform measurements and thus, verifying the spatial distribution of measurement locations with the field measurements, of course taking into account the marking absolute errors of the GPS device (± 1 m).

Figure 3: Location of the experiment on the raster map - Google Earth

The penetration resistance of soil or superficial subsoil, measured by penetrologger, is a compacting measure or the load capacity of the land (0 ... 200 N uncompacted land, 200 ... 300 N land subject to compaction, over 300 N compacted land).

The penetration resistance F was calculated with the formula:

$$F = p \times S, [N] \quad (1)$$

where:

p is the press pressure in MPa measured with the Eijkelkamp Penetrologger penetrometer;
S - penetration cone surface in mm^2.

The ThetaProbe sensor measures volumetric soil humidity content, θv, by the well-established method of responding to apparent dielectric constant changes. These changes are transformed into a DC voltage practically proportional to the humidity content of the soil over a wide range of work. The volumetric soil humidity content is the ratio between the volume of water present and the total volume of the sample. This is a non-dimensional parameter, expressed either as a percentage (% vol) or a ratio ($m^3.m^{-3}$). Thus, 0.0 $m^3.m^{-3}$ corresponds to a completely dry soil and pure water of 1.0 $m^3.m^{-3}$.

With the help of the data obtained, after making the calculations, were plotted graphs of compaction resistance on a 30 cm depth with MATCHAD. Processing of experimental data and realization of spatial distribution maps of the experimental lot parameters (compaction under local humidity conditions), as decision support for management, were made by moving from the hexadecimal geographical coordinate system to decimal places with the help of the on-line coordinate converter.

Table 1: Soil compaction values, in MPa, at the measurement points

Measurement point	1	2	3	4	5	6	7	8	9	10	11	12	13
Depth of measurement [cm]	30	30	30	30	30	30	30	30	30	30	30	30	30
The press pressure [MPa]	2	2.5	3	3	2	1.6	1.8	2.5	1.8	1.2	2	2.2	2.5

Table 2: Soil humidity values, in %, at the measurement points

Measurement point	1	2	3	4	5	6	7	8	9	10	11	12	13
Depth of measurement [cm]	60	60	60	60	60	60	60	60	60	60	60	60	60
Soil humidity [%]	29	28	26	26	30	34	26	28	27	30	29	30	28

Using the obtained data, after calculating with Excel, for the penetration cone area of 100 mm^2, was determined the penetration resistance, in N, at each measuring point.

Table 3: Penetration resistance values, N

Measurement point	1	2	3	4	5	6	7	8	9	10	11	12	13
Penetration cone area, [mm^2]	100	100	100	100	100	100	100	100	100	100	100	100	100
Penetration resistance, [N]	200	250	300	300	200	160	180	250	180	210	220	250	180

To achieve the modern system for development land compaction maps, were carried out the following activities:

1. Conversion of hexadecimal geographical coordinates into decimal coordinates by direct calculation or using available utility software;
2. Form an ASCII file that contains on columns data obtained by measurements and calculations for latitude, longitude, penetration resistance and local soil humidity;

3. Choosing mathematical computing software, eg MATCAD;
4. Import the ASCII file formatted into MATCAD, using the command: Insert-> DATA-> FILEINPUT-> filename.txt;
5. Marking as data vector every column in the ASCII file;
6. Statistical processing of imported data: average, standard deviation, etc.;
7. Obtaining the 3 coordinate diagrams with the Surfaceplot or ContourPlot function;
8. Import the graphics image into the raster map obtained from the Google Earth archive (The tools and materials used are not required; instead of Google Earth, you can use any other archive of maps with numeric and aerial or satellite imagery information. Also, instead of Excel, Mathcad, etc. any other numerical analysis programs may be used and with graphical possibilities.)

The graphical representations of penetration resistance based on the decimal coordinates (longitude and latitude) are shown in Figure 4 (**a**-graph in points, **b**-graph in plan and **c**-graph of the surface).

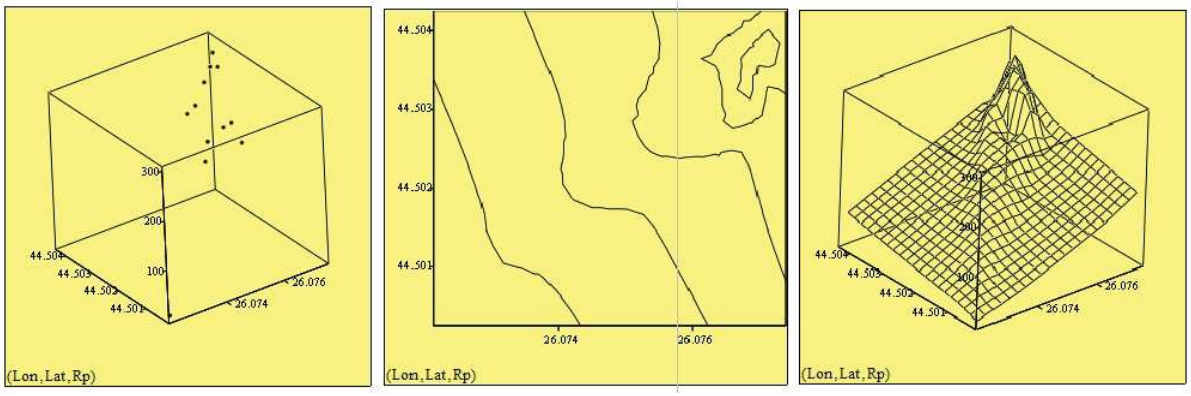

a. **b.** **c.**

Figure 4: Graphical representations of penetration resistance according to decimal places (longitude and latitude)

Overlaying the penetration distribution map over the aerial image, taken from the Google Earth image archive, of the experimental batch is shown in Figure 5.

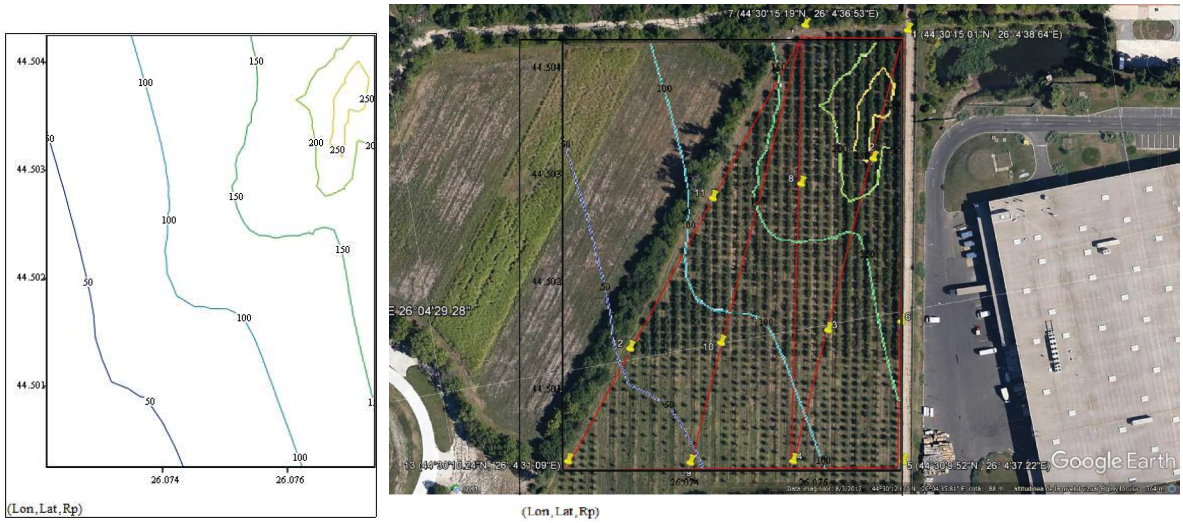

Figure 5: Overlay of the penetration resistance distribution map over the aerial image of the experimental batch

4. CONCLUSIONS

Land compaction of agricultural crops is a form of soil degradation, being an undesirable accompanying phenomenon occurring during the execution of agricultural works, the phenomenon being impossible to avoid, but which can be kept under control by appropriate management, for which it is necessary to monitor the causes of land compaction.

Accentuated compaction condition leads to the difficult circulation of substances in the soil, the destruction of organic matter, a sharp decrease in porosity (which in fact generates much of the other problems).

Values of soil resistance to penetration are important in land classification, and the soil penetration resistance profile together with depth are required for quantification the degree of soil compaction.

It also contributes to providing a common system to characterize the soil properties from which it may be possible to determine the number of passes of agricultural machinery, in order to predict traction performance.

The novelty of the research is that, with regard to the classic use of digital models and the production of maps, the introduction of an accompanying map with overlapping aerial photographic images, in the background, facilitates the rapid identification of areas requiring repairs, both in terms of compaction and local humidity of the soil.

Information and preparation of compactness maps under conditions of local humidity from the soil have the ability to be synthesized, giving users the information they need.

Using the method for compiling the soil compaction map in conditions of local humidity in orchards offers the possibility of identifying degraded lands, using a complex and comprehensive set of spatial analysis tools necessary in the future for the complete computerization of the cadastre system.

Acknowledgement

This work was funded by the Ministry of Research and Innovation, within the project entitled "PN 16 24 02 01: "*Innovative technology for the maintenance of tree plantations situated in rural areas through soil works, root cuts and precision foliar fertilization*", ctr. 8N/09.03.2016 / Ad. No. 1/2017.

References

[1] Bengough A.G., Campbell D.J., O'Sullivan, M.F., *Penetrometer techniques in relation to soil compaction and root growth. In Soil and Environmental Analysis. Physical Methods. 2nd Edition*. Eds. KA Smith, CE Mullins. pp. 377-403. Marcel Dekker: New York, 2001.

[2] Saracin I, Pandia O., Gheorghe M., Chiriac A., *Apparatus for determination soil penetration resistance for establishing work index parameters of agricultural machines,* Metalurgia International, Volume: 15, Issue: 11, pages: 94-96, 2010.

[3] Rus, F., Csatlos, C., *Techniques and equipments for the evaluation of physical and mechanical characteristics of soils*, Transylvania University Publishing House, Brasov, 2010.

[4] Sulewska, Maria Jolanta, *The control of soil compaction degree by means of LFWD*, Baltic Journal of Road and Bridge Engineering, Volume: 7, Issue: 1, pages: 36-41, DOI: 10.3846/bjrbe.2012.05, 2012

[5] Gracia, C., Estivill, J., Bautista, I., *Compaction of a horticultural soil by passage of heavy vehicles. Effect on the resistance to penetration*, VII Congreso iberico de agroingenieria y ciencias horticolas: innovar y producir para el futuro. Innovating and producing for the future, pages: 524-529, 2014

[6] https://en.eijkelkamp.com/products/field-measurement-equipment/functional-specs-penetrologger-set-a.html.

[7] https://www.google.com/earth/

THE CAE STUDY OF THE AIR VELOCITY OVER A GREENHOUSE FOR THE INSTALLATION OF A WIND TURBINE

Mateescu Marinela[1], Gheorghe Gabriel[1], Manea Dragos[1], Marin Eugen[1], Persu Catalin[1], Bota Marius[2]
[1]INMA, Ion Ionescu de la Brad Blv. No. 6, Sector 1, Bucharest, 004021-269.32.55, gabrielvalentinghe@yahoo.com
[2] BUILD PR CONSULTING SRL Cluj Napoca 0040747090869, msbota@yahoo.com

ABSTRACT

This paper presents the study of the air velocity in the vicinity of a greenhouse using the SolidWorks software, the Flow Simulation module, to find out the ideal position for mounting a wind turbine for greenhouse energy independence. This methodology is based on TRIZ (Theory of Solving Inventive Problems) priciples. The article presents the diagrams for different air velocities in the vicinity of a greenhouse. These charts will be generated using CFD (Computational Fluid Dynamic), which is a necessary tool for reducing the passivity and the idle time of the wind turbine.

1. INTRODUCTION

The wind is one of the four elements (sun, earth, water and wind) that decides directly in the realization of renewable energies, is a vector element in time and space, extremely variable.

Within the Romanian Plain, the highest values are located in these eastern part and in the Plain of Oltenia. Similar values are specific to the largest part of the Plateau of Moldova and Dobrogea, the western extremity of the Western Plain and the South of Banat [2].

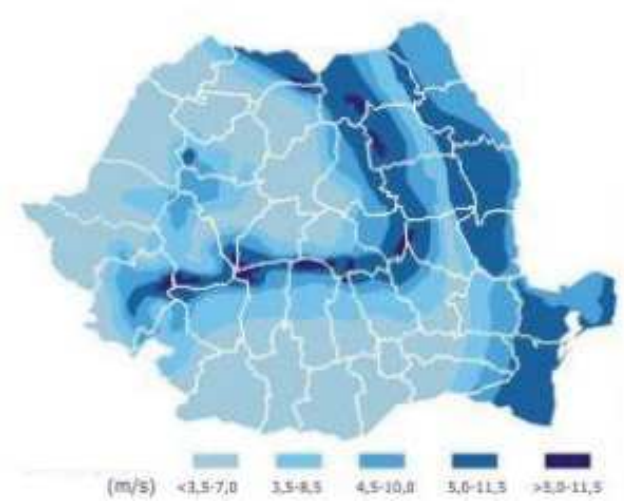

Figure 1: Average air velocity on Romania's territory [2]

CFD simulates fluid (either liquid or gas) passing through or around an object. The analysis can be very complex—for example, containing in one calculation heat transfer, mixing, and unsteady and compressible flows. The ability to predict the impact of such flows on your product performance is time consuming and costly without some form of simulation tool.

2. METHODOLOGY

Conceptual Analysis of Flow Simulation

Conceptual analysis for a flow analysis problem using finite element analysis reveals that the following logical steps and sub-steps are needed:

- Pre-processing (building the model), wich includes:
    1. Geometry creation
    2. Material property assignment
    3. Boundary condition specification
    4. Mesh generation and setting the computational domain
- Solution (running the simulation)
- Post-processing (getting results)

2.1 Pre-processing (building the model)

The geometry of the model is defined in the geometry creation step. After the solid geometry is created like in figure 2, the material properties of the solid are specified in the material property assignment step. The material properties required for the FEM analysis depends on the type of analysis. In this flow analysis problem will produce the same results regardless of the material. Material properties become relevant when dealing with flow analysis when a roughness factor is introduced or the thermal fluid properties are being examined.

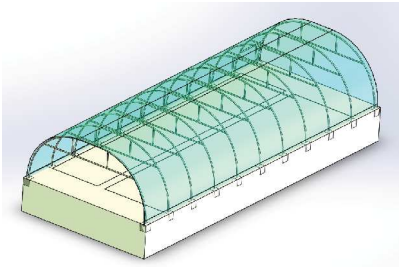

Figure 2: Geometry model of the greenhouse who will be analyzed

SolidWorks Flow Simulation has two options to create a new project: using the configuration wizard (figure 3) and creating a new project with default settings. In this situation, the project configuration will be used to specify the initial conditions. The initial conditions include temperature which is 293,2 K, pressure which is 101325 Pa and velocity, which is 6 m/s in this situation. The direction of the velocity is along the x-axis, however the x-axis points in the opposite direction so the velocity needs to be “6 m/s” to correctly apply the boundary condition.

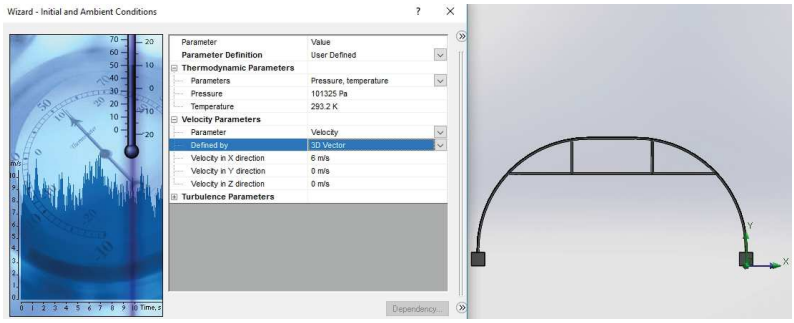

Figure 3: Initial velocity, temperature, and pressure conditions

Since this is an external flow problem, most of the boundary conditions were defined in the project wizard. The next step will set goals for the simulation before it runs, which allows us to select the exact goals they are interested in and decreases the calculation time for the software. Flow Simulation can be used to find goals such as velocity, mass flow, etc. at a point, surface, volume, or globally. In this case, the simulation needs to find parameters at the surface of the greenhouse so “surface goals” will be used (figure 4).

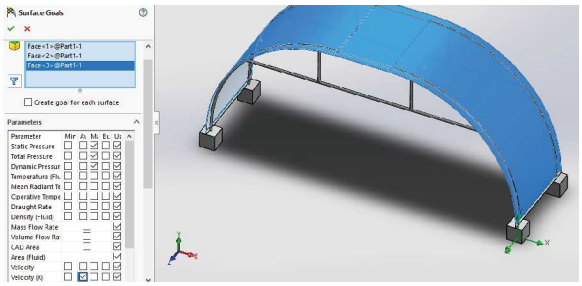

Figure 4: Selecting the goals for the simulation software

The purpose of the Mesh Generation sub-step is to discretize the part into elements. The flow simulation software also has a computational domain, which will also be examined in this section. The simulation software will only solve for parts within the computational domain, so it is important to include enough of the model to acquire good data without overloading the software. To simplify the problem and reduce calculation time, this model will be analyzed as a 2D model instead of 3D.

2.2 Solution (running the simulation)

The Solution is the step where the computer solves the simulation problem and generates results for use in the Post-Processing step and just need to click on the run button.

2.3 Post-processing (getting results)

The first plot in the post-processing step is setting up flow trajectories. Flow trajectories trace the flow of the fluid from a set starting point to the edge of the computational domain. The plot will show output such as velocity or pressure at specified intervals along the fluid path. With SolidWorks Flow Simulation, the number of trajectories can be defined along with the display type. In this case, 100 flow trajectories will be inserted at the edge of the computational domain and the default lines with arrows configuration will be used and the result can be seen to figure 5.

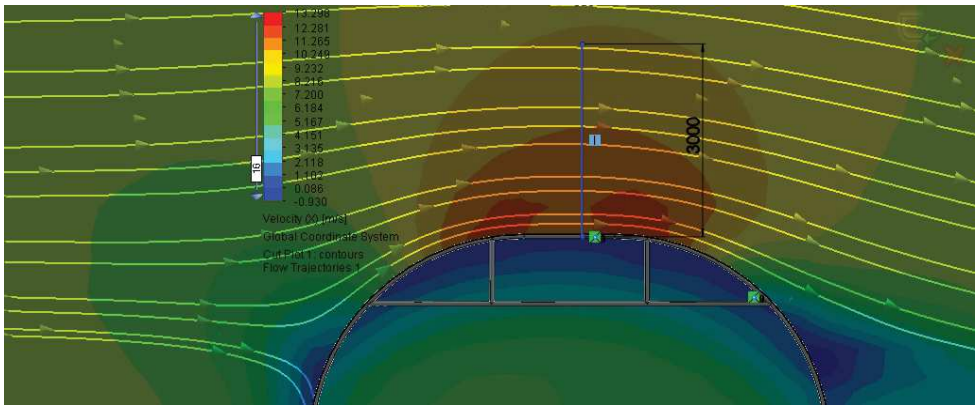

Figure 5: Flow trajectories around greenhouse

Due to this study we can see that over a distance of 3000 mm above the greenhouse which has a height of 3000 mm, we have an air velocity of 12 m / s, which is twice the atmospheric conditions initially introduced and is sufficient for mounting a wind turbine with the technical specifications in Table 1.

Table 1: Technical specifications wind turbine [3]

MODEL	600M2
NOMINAL POWER [kW]	0.6
MAXIMUM POWER [kW]	0.63
NOMINAL VOLTAGE [V]	24
WIND SPEED, FOR START [m/s]	2.5
WIND SPEED, NOMINAL [m/s]	13
WIND SPEED, SURVEILLANCE [m/s]	45
MAXIMUM WORKING TEMPERATURE [°C]	80
MINIMUM WORKING TEMPERATURE [°C]	-30
AIRSCREW DIAMETER [mm]	1750
BLADES NR. [buc]	3
WEIGHT [kg]	15.5
GENERATOR TYPE	Three-phase, synchronous with permanent magnet
HEIGHT TOWER [m]	6

3. CONCLUSIONS

Due to the structure of the greenhouse, it behaved like a deflector and it was possible to obtain a nominal speed for commissioning of an eolienne even if the speeds in the plain are not generous.

Thanks to this study, wind turbines can be installed in areas with low wind power, but some forms of deflectors must be mounted to increase the speed.

Acknowledgement

This work was funded by the The Ministry of Research and Innovation, within the project PN 16 24 01 01 - *Intelligent system for condensation irrigation in greenhouses and solariums*, Ctr. 8N / 09.03.2016, Ad. no. 1/2017.

References

[1] A. Ducoina, M.S. Shadloob, S. Royc, Direct Numerical Simulation of flow instabilities over Savonius style wind turbine blades, Renewable Energy, Volume 105, May 2017, Pages 374–385

[2] Analysis of the wind energy potential at the level of the center region in the perspective of sustainable economic development, Editor: Agency for Center Regional Development

[3] Wind turbines Technical book, Romstal, www.romstal.ro

[4] Guihua Zhu, Yuzhu Zhang, Jiliang Ren, Tuanhui Qiu, Tao Wang, Flow Simulation and Analysis in a Vertical-Flow Sedimentation Tank, Energy Procedia, Volume 16, Part A, 2012, Pages 197-202

[5] K.K. Padmanabhan, Study on increasing wind power in buildings using TRIZ Tool in urban areas, Energy and Buildings, Volume 61, June 2013, Pages 344–348

WASTE GAZIFICATION TECHNOLOGY USING A FIXED-BED GASIFIER – review

Georgiana Moiceanu[1], Gigel Paraschiv[1], Gheorghe Voicu[1], Mirela Dincă[1], Mariana Ferdeș[1], Laura Toma[1], Nicoleta Ungureanu[1]
University Politehnica of Bucharest, Faculty of Biotechnical Systems Engineering
*E-mail: moiceanugeorgiana@gmail.com

ABSTRACT

All the different standards that apply today for the assurance of a high standard of living had led to a drastic increase in waste generation. The variation rate if municipal solid waste (MSW) is a consequence of the lack of information between environmental policy-makers, manufactures and stakeholders, along with demography, climate, socio-economic and industrial development. In the present paper we studied the gasification technology, mainly fixed bed gasifiers that are used today in order to convert solid waste to a gaseous fuel. The fixed bed gasifier has been the traditional process used for gasification, in solids move either counter current (updraft) or concurrent (downdraft) to the flow of a gas as reaction takes place, and the solids are converted to gases.

1. INTRODUCTION

The most important service a city can provide for its people is municipal solid waste management, regardless the income of the city/country. In order to maintain a high life style standard it is necessary to manage effectively municipal solid waste otherwise risking a severe impact on health, local and global environment, and economy. Improperly managed waste usually results in down-stream costs higher than what it would have cost to manage the waste properly in the first place [5].

According to World Bank by 2025 the number of urban residents will increase to 4.3 billion thus generating about 1.42 kg/capita/day of MSW (2.2 billion tons per year) [5]. Also waste generation will more than double in the next 25 years in lower income countries. Out of all the waste generated about one fourth is being recycled and three-fourth are disposed of in landfills [11]. For example out of 389 million tons of MSW generated by the United States only 36.5% is recycled [11]. Waste composition is influenced by factors such as culture, economic development, climate, and energy sources; composition impacts how often waste is collected and how it is disposed. Low-income countries have the highest proportion of organic waste. Paper, plastics, and other inorganic materials make up the highest proportion of MSW in high income countries [5].

Landfilling and thermal treatment of waste are the most common methods of MSW disposal in high-income countries. In early 1970's the "waste management hierarchy" appears on Ontario's Pollution Probe. At first the hierarchy represented three options: reduce, reuse and recycle, but as years passed by and the need for an optimum waste management and for the insurance that in future generation are not affected by our actions, another "r" word appeared "recover".

After trying a number of methods for waste disposal and considering the need for more energy and faced with an expensive problem, many countries turned to gasification, a way for turning waste into energy [11]. For example with mass-burn incinerators a ton of MSW is turned into 550 kilowatt-hours of electricity, while a tone of MSW can produce 1000 kilowatt – hours of electricity using gasification. Gasification is a unique process that transforms a

carbon-based material, such as MSW or biomass, into other forms of energy without actually burning it [11].

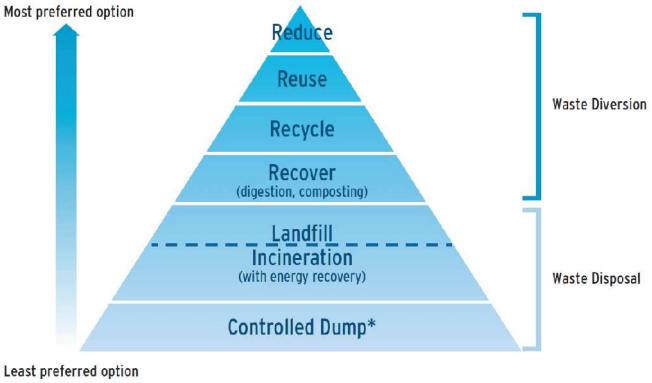

Figure 1: Waste hierarchy[5]

Using chemical reaction solid and liquid waste materials are converted into gas. The materials components are broke down into simple molecules, primarily a mixture of carbon monoxide and hydrogen. It results a synthesis gas (syngas) that can be converted into electricity and valuable products.

Although there have been substantial research involving gasification of MSWs, sugarcane bagasse and other different types of wastes, the process simulation studies on gasification are still limited. Recently, Mavukwana et al. [7] performed simulation of sugarcane bagasse gasification using the Advanced System for Process ENgineering (Aspen) Plus software and they compared the model data with experimental results published in the literature. The overall data were found to be in good agreement.

Another study has been done by Chen et al. [2] on two different types of fixed bed reactor for MSW simulation. The aim of the research was to observe the effect of flue gas from the combustion section on the composition and lower heating value (LHV) of syngas, heat conversion efficiency, and carbon conversion at different gasification temperatures and air equivalence ratios. Researchers developed simulation models for their specific feedstocks, therefore an integrated model which can be used for a number of feedstocks is necessary. They worked on an integrated and generalized model applicable for different feedstocks.

There are many types of gasifiers for waste gasification. As mentioned before in the present paper we studied the gasification technology, mainly fixed bed gasifiers that are used today in order to convert solid waste to a gaseous fuel. The fixed bed gasifier has been the traditional process used for gasification, in solids move either counter current (updraft) or concurrent (downdraft) to the flow of a gas as reaction takes place, and the solids are converted to gases.

2. METHODOLOGY

Gasification is a partial oxidation process at elevated temperatures (500-1400 ºC) that results in producer gas consisting of CO, H_2, CO_2, CH_4, traces of higher hydrocarbons such as ethane and ethene, water vapors, nitrogen (if air is the oxidizing agent) and various contaminants such as small char particles, ash, tar and oil. The gasification process is mainly done in fixed and fluidized bed.

In 1839 Bischaf patented a simple process for gasifying coke, the first commercial updraft fixed bed gasifier. The fixed bed gasifier system uses a reactor/gasifier with a cooling and cleaning system. It also has a bed of solid fuel particles through which the gas moves either up or down [3]. The fixed bed gasifier is the simplest type of gasifier. It consists from a

cylindrical space for fuel and gasifying media, a fuel feeding unit, an ash removal unit and a gas exit. As gasifying process occurs the fuel bed moves down the reactor. These equipment's operate high carbon conversion, low gas velocity, long solid resistance time and low ash carry over [1, 9]. A disadvantage of fixed bed gasifiers is tar removal.

Different types of fixed bed gasifiers can be classified by taking into consideration the way the gasifying agent enters the gasifier: updraft, downdraft, crossdraft.

Updraft gasifier

Updraft gasifiers are the simplest forms of fixed bed gasifiers. The fuel enters the gasifier from the top of the reaction chamber and the agent (air, oxygen or mixture) enters from the bottom of the unit. As the fuel is consumed it flows down the reactor through the drying, pyrolysis, gasification and combustion zones. The gas temperature when it exits is between 80 -300°C and it contains oil and tar (10-20%).

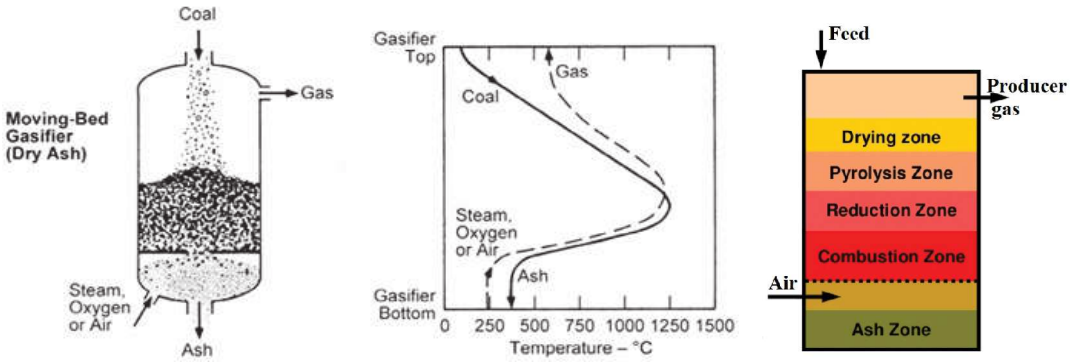

Figure 2: Updraft fixed bed gasifier [12, 13]

In order to use updraft gasifiers on a wide range of feedstocks, including waste such as sludge, it is used a high temperature agent gasification (1000°C).

In order to better understand the updraft gasifiers a serious of test were done by scientists. For example A. Surjosatyo et. al. (2014) studied modified updraft gasifier with recirculation of the pyrolysis gases back to the combustion zone and the gas outlet at the reduction zone. The fuel used was woody biomass that had a moisture content of 10.24%. The gasification process included a gasification reactor with a diameter of 0.22 m and a length of 0.63 m and constructed of stainless steel. The results showed tendencies to reduce the amount of tar produced do to flow increase of the pyrolysis gases to the combustion zone [10].

In paper [8] scientists studied a modified updraft fixed bed gasifier. In this study feedstock feeding system was adjusted. The material used was woodchips that were fed continuously through a conduit in the base of the reactor over the grate. After experiments they concluded that the quality of the gas obtained was better in this design; because was possible to generate producer gas with very low tar content with minimum losing in efficiency. Also, the CH_4 and CO were a higher concentration in producer gas than in a typical updraft gasifier.

Other scientist studied a one-dimensional steady state mathematical model for the simulation of a small scale fixed-bed gasifier. The model used is based on a set of differential equations describing the entire gasification process of softwood pellets and is solved by a two-step iterative method. The gasifier used was a laboratory-scale fixed-bed updraft gasifier. Furthermore, simulations for different air to fuel ratios and varying power inputs have been performed using the adapted model. With higher power input temperature profiles increase due the improved char combustion as well as the CO yield increase corresponding to

decreasing CO_2 values. This may conclude that the gasification efficiency increases with the power input [6].

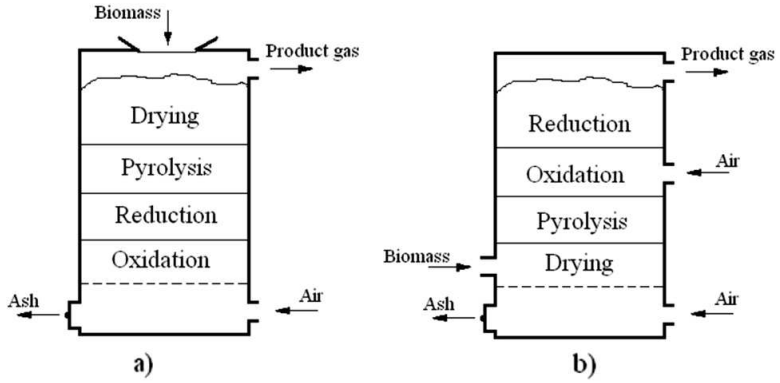

Figure 3: Updraft gasification reactor: a. typical design; b. modified design[8]

Regarding municipal solid waste in Chen et al. studied Simulation of municipal solid waste (MSW) gasification with air in two different types of fixed bed reactors. One type is an updraft fixed bed reactor with very well defined sections (drying, pyrolysis, gasification, and combustion), and the other type is different in the last two sections that the flue gas from the combustion section is not introduced into the gasification section. The results indicated that the introduction of flue gas from combustion section into the gasification section improved the heat conversion efficiency and the lower heat value of syngas. Also no differenceces were found between the concentration of each component in syngas for both higher and lower air equivalence ratio [2].

Downdraft Gasifiers

A downdraft gasifier is similar to updraft gasifier, the air is introduced at a mid or top part of the reaction zone from above decomposing the combustion gases and burning most of the tars and syngas is removed from the bottom part of the chamber. These gasifiers are well defined areas, drying, pyrolysis, combustion and reduction zone. Downdraft gasifiers are not ideal for waste treatment because they typically require a low ash fuel such as wood, to avoid clogging [14].

On their way down the acid and tarry distillation products from the fuel must pass through a glowing bed of charcoal and therefore are converted into permanent gases H, CO_2, CO and CH_4. Depending on the temperature of the hot zone and the residence time of the tarry vapors, a more or less complete breakdown of the tars is achieved. A main advantage of downdraught gasifiers represents the possibility of producing a tar-free gas suitable for engine applications. A major drawback of downdraught equipment lies in its inability to operate on a number of unprocessed fuels. In particular, fluffy, low density materials give rise to flow problems and excessive pressure drop, and the solid fuel must be pelletized or briquetted before use [16].

The downdraft gasifiers are preferred to updraft gasifiers in IC engines or for direct heating applications where purity of gas is a critical [17].

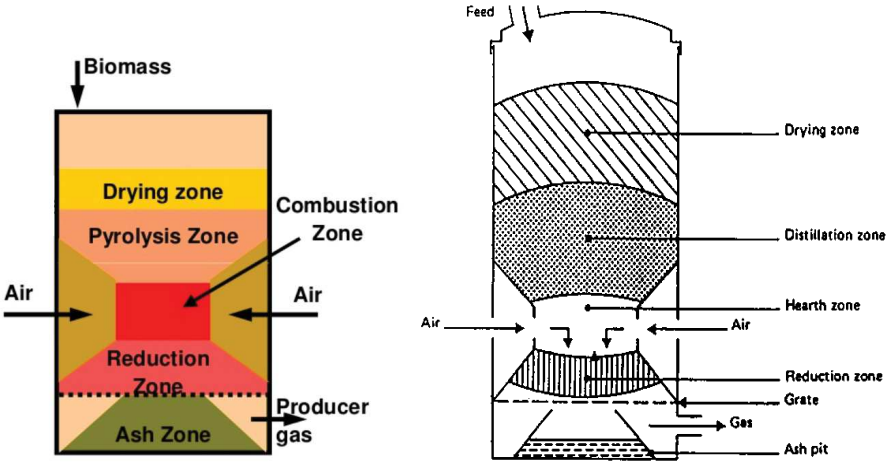

Figure 4: Downdraft fixed bed gasifier [15, 16]

A study regarding downdraft gasifiers aimed to observe the thermal behavior of an existing 5 kW_e downdraft biomass gasifier (DBG) unit on various zones along with different equivalence ratios (ER). The results shown that producer gas increased with increase in equivalence ratio. Also another conclusion could be drown regarding tar formation that was found to decrease with increase in equivalent ratio [4].

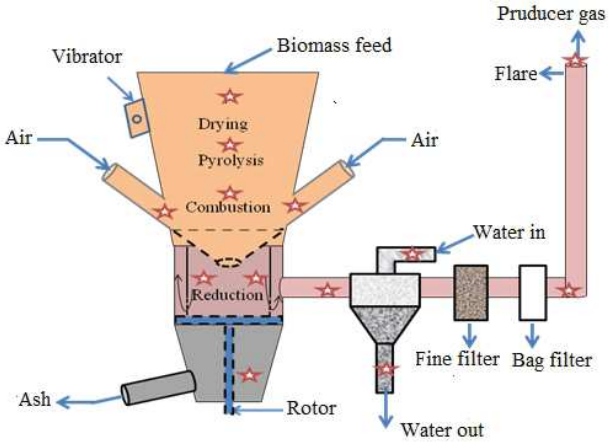

Figure 5: Downdraft gasifier [4]

Crossdraft gasifier

The air inlet and the gas outlet are on the opposite sides in the middle of the chamber of the gasifier. Crossdraft gasifiers are known for high operating temperatures, high exit gas temperatures, high gas velocity do to gasifiers design. Startup of these gasifiers is faster that downdraft gasifiers and the reduction of CO_2 is low. Unlike updraft and downdraft gasifiers the ash bin, fire and reduction zones are separate. This type of gasifier design limit the type of fuel usage restricted to only low ash fuels such as wood, charcoal and coke. Cross draft gasifier operates well on dry air blast and dry fuel [18].

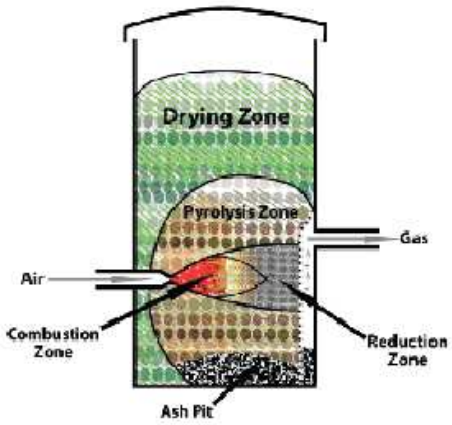

Figure 6: Crossdraft gasifier [18]

3. CONCLUSIONS

In order to obtain a solution to municipalities waste problems a strategy that includes a number of technologies such as waste reduction, recycling, landfilling and waste-to-energy is needed. An area that has to be developed is waste-to-energy that converts the non-recyclable and combustible portion of the waste to electricity, prevents contamination of nature and lessens the dependence on fossil fuels for power generation. Improvement of waste sorting and pre-treatment methods would increase the viability of waste gasification. If mechanical processes like shredding and sorting of the waste could be simplified and more effective, gasification would become even more advantageous. A good recycling practice implemented by the municipalities can improve waste gasification [14].

References

[1] Carlos, L., *High temperature air/steam gasification of biomass in an updraft fixed batch type gasifier*. Ph.D. thesis. Royal Institute of Technology, Energy Furnace and Technology, Stockholm, Sweden, 2005.

[2] Chen, C.; Jin, Y.Q.; Yan, J.H.; Chi, Y., *Simulation of municipal solid waste gasification in two different types of fixed bed reactors*. Elsevier - Fuel, 103, pp. 58–63, 2013.

[3] Chopra S., Jain A., *A Review of Fixed Bed Gasification Systems for Biomass*, Agricultural Engineering International: the CIGR Ejournal. Invited Overview No. 5. Vol. IX., April 2007.

[4] Gajanan N. S., Mahanta P., Patil R.S., *Experimental Studies on Thermal Behavior of Downdraft Gasifier*, Proceedings of the World Congress on Engineering 2014 Vol II, WCE 2014, London, U.K, July 2 - 4, 2014.

[5] Hoornweg D., B-T. Perinaz – *What a waste, A global review of solid waste Management*, Urban Development Series Knowledge Papers, No. 15, March 2012.

[6] Mandl C., Obernberger I., Biedermann F., *Modelling of an updraft fixed-bed gasifier operated with softwood pellets,* Elsevier, pp. 3795-3806, http://www.sciencedirect.com/science/article/pii/S0016236110003613, 2010.

[7] Mavukwana A., Jalama K., Ntuli F.; Harding K., *Simulation of Sugarcane Bagasse Gasification Using Aspen Plus*. In Proceedings of the International Conference on Chemical and Environmental Engineering (ICCEE), Johannesburg, South Africa, pp. 70–74, 15–16 April 2013.

[8] Pedroso D.T., Machín E.B., Silveira J.L., Nemoto Y., *Experimental study of bottom feed updraft gasifier*, Elsevier – Renewable Energy, pp311-316, https://www.researchgate.net/publication/257415112_Experimental_study_of_bottom_feed_updraft_gasifier, 2013.

[9] Reed T. B., Das A., *Handbook of biomass downdraft gasifier engine systems*, Colorado: Solar Energy Research Institute, 1988;

[10] Surjosatyo A., Vidian F., Nugroho Y.S., *Experimental Gasification of Biomass in an Updraft Gasifier with External Recirculation of Pyrolysis Gases*, Journal of combustion, Vol. 2014, Art Id 832989, p://dx.doi.org/10.1155/2014/832989, 2014.

[11] Gasification The Waste-to-Energy solution, Gasification Technologies Council, www.gasification.org.

[12] https://www.netl.doe.gov/research/coal/energy-systems/gasification/gasifipedia/fmb.

[13] https://www.slideshare.net/reddyas/biomass-gasification-58749293.

[14] http://www.altenergymag.com/content.php?issue_number=09.06.01&article=zafar.

[15] https://www.slideshare.net/reddyas/biomass-gasification-58749293.

[16] http://www.fao.org/docrep/t0512e/T0512e0a.htm.

[17] http://www.eai.in/ref/ae/bio/bgt/type/fixed_bed_gasifier.html.

[18] http://www.enggcyclopedia.com/2012/01/types-gasifier/.

CRITERIA FOR WATER MANAGEMENT OPTIMIZATION IN AGRO-TOURISMUS

Marco Ragazzi[1], Precazzini Ilaria[1], Ramona Giurea[1/2], Rada Elena Cristina[3], Moise Ioan Achim[4], Irina Aura Istrate[5]

[1] University of Trento, Department of Civil Environmental and Mechanical Engineering, via Mesiano 77, Trento, Italy, marco.ragazzi@unitn.it; ilaria.precazzini@gmail.com
[2] University "Lucian Blaga" of Sibiu, Department of Industrial Engineering and Management, Emil Cioran 4, Sibiu, Romania, ramona.giurea@ulbsibiu.ro
[3] University of Varese, Department of Theoretical and Applied Sciences, via G.B. Vico, 46, Varese, Italy, elena.rada@unitn.it
[4] University 1 Decembrie 1918 of Alba Iulia, Department of Exact Sciences and Engineering, Bibliotecii 5, Alba Iulia, Romania, achimmoise@yahoo.com
[5] University Politehnica of Bucharest, Department of Biotechnical Systems, Splaiul Independenței 313, Bucharest, Romania, ia_istrate@yahoo.com

ABSTRACT

Water management optimisation is a topic that concerns many sectors. The present paper gives a contribution to understand the approach that can be adopted in the agro-tourism sector, often characterised by decentralised structures. The technological level to be adopted for water management depends on the local context. Solutions are already available for losses prevention, water separation aimed to optimised management, treatment and recovery. The difficulty is their integration.

Keywords: agro-tourism; reuse; treatment; water.

1. INTRODUCTION

Tourism has become one of the most important global industries nowadays with a major economic activity in the European Union (EU) with wide-ranging impact on economic growth, employment, social development and impact on the environment [1, 2]. The year 2016 marked the seventh consecutive year of growth for European tourism. Europe is the most visited region in the world welcomed 620 million international tourist arrivals in 2016 [3]. International tourist arrivals worldwide are expected to increase by 3.3% a year between 2010 and 2030 to reach 1.8 billion by 2030, according to UNWTO's long-term forecast report Tourism Towards 2030 [4].

Agro-tourism has been acknowledged world-wide since the early twentieth century [5-7]. The specific literature reveals numerous definitions for agro-tourism [8-12]. In the 90's the EU showed a clear attitude of the Community to tourism in rural areas, and agro-tourism was formed. The policy of rural development and of the development of agro-tourism must be compatible with the rules set by the EU, thanking into account that the development is active environment protection, landscape care and preserving the local culture and traditions [13].

Romania and Italy are two of the countries with a agro-tourism heritage. In Italy, agro-tourism was born as a spontaneous hospitality, and then it developed as a tightly connected and complementary activity to the mains activities of cultivation, forestry and breeding [14]. Since

1990, it has undergone a gradual and progressive separation from agriculture [15]. Romania, beginning with the 1989, after the communist period, started to implement the legislation in this sector [16]. In Figure 1 and Figure 2 the number of bathing waters in Italy and Romania is shown [17].

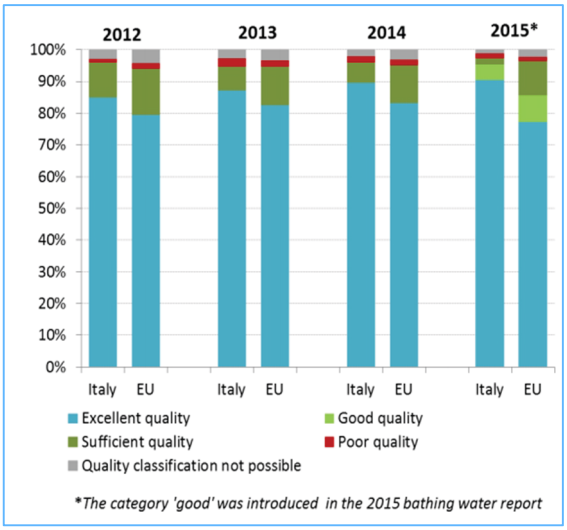

Figure 1: Bathing water quality 2012-2015, IT

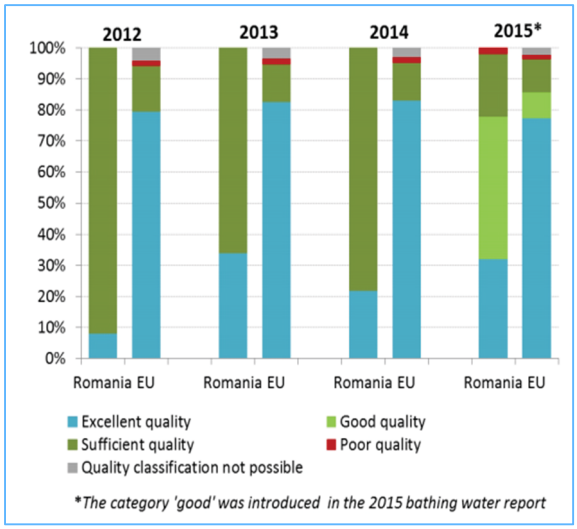

Figure 2: Bathing water quality 2012-2015, RO

2. WATER CONSUMPTION AND RECOVERY

Agro-tourisms facilities are generally characterized by ***significant drinking water consumption***, which is due to domestic household pickups in kitchens, for cleaning and washing linen, but mainly for the provision of sanitation in the rooms or in the accommodations. The classic water consumption can then be added, depending on the specific reality, the use of irrigation water for gardens, gardens and crops.

A careful management of the water consumption requires a proper maintenance of hydraulic systems and taps in terms of seals control and pressure monitoring in the plant. The presence of small but continuous losses results in negligible consumption without any service being provided to the user. Additionally, feeding the hydraulic system with pressures higher than the recommended one's entails significantly higher fuel consumption as the pressure rises at the same lifetime.

These are various types of ***water-saving devices*** such: mixers that allow the flow temperature and flow to be adjusted more rapidly; friction-jet devices that mix air out of the air with air by increasing the power of the jet, but at the same time reducing the amount withdrawn; flow reducers designed essentially to reduce the flow rate and timer; low or differential flow using less litters depending on the button; timing taps or photocells. The use of high-efficiency washing machines and dishwashers also combines the reduced energy consumption required by the appliance with reduced water consumption.

Various practical technologies can lead to water savings to the agro-touristic structures but are effective and only allow for real differences if they are accompanied by correct behaviours from the part of the guests and those working at the facility. It is therefore important to involve guests in the environmentally-friendly management systems chosen by the agro-touristic structure, stimulating conscious behaviours to avoid frustrating the efforts put into practice.

The internal consumption of the structure often adds irrigation water, which, in addition to being preferably carried out in the absence of direct irrigation and outside the warmer hours, to avoid rapid evaporation, can be optimized by adopting programmed irrigation and preferably drop wise so as to distribute where necessary the water with the right amount without dispelling it unnecessarily.

Remarkable savings in water drainage can then be achieved by installing storage systems and plumbing systems that allow the reuse of rainwater for non-sanitary and non-drinking purposes, which however represent a significant fraction of the daily water requirement. Although the common habit is to use drinking water for all purposes, almost half of the water needs of agro-tourism structures do not require water with potable characteristics.

Rainwater is a precious and free resource, can be collected, filtered and reused for various purposes that do not require drinking water such as irrigation of gardens, gardens, car wash, agro-tourism machinery and paved areas but also use inside the building as cleaning and for toilet flushing. There are also commercially available washers equipped with a double attachment for rainwater and drinking water, which allow to use rainwater during the washing process while rinsing with the drinking water. To ensure better water retention quality, it is possible to add traditional UV filtering filters to eliminate the dangers of bacteria in the collected waters. In the case of reuse of meteoric water for irrigation purposes and other non-sanitary uses outside the building, simple systems for the collection and storage of water can be adopted in tanks.

In Figure 3 a typical pattern of collection, storage and subsequent reuse of meteoric water for exterior and interior purposes to the building is presented. Reuse of limited rainwater to off-site uses do not require changes to the traditional hydraulic system, and therefore presents lower economic investment.

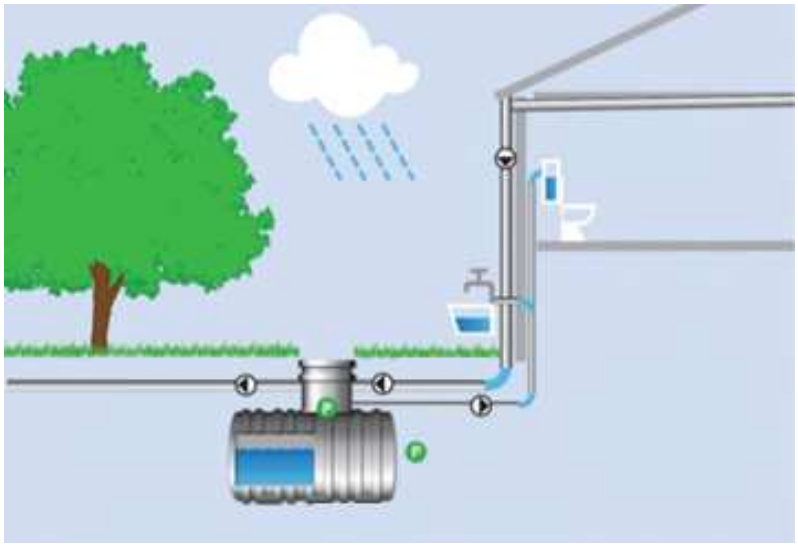

Figure 3: Example of a typical pattern of rainwater reclamation and storage with subsequent reuse for exterior and interior purposes to the building

In the *agro-tourisms facilities* water consumption with showers, baths and sinks make up the bulk of all withdrawals. Precisely in this type of structure using *gray water treatment systems* for re-use could make a significant contribution to reducing drinking water consumption. The gray waters come from sink drains, bathtubs, showers, washing machines

and dishwashers and can be properly treated and re-used for purposes that do not require drinking water, such as irrigation, outdoor washing or rinsing of the toilet, the black waters have a low organic load and nutrients.

The use of heat exchangers for the recovery of heat from effluent discharges is a possibility not to be overlooked since the drained ***gray waters*** reach temperatures of 24-30°C [18]. The development and diffusion of such technologies are aimed at increasing the energy efficiency of buildings by transforming what was previously seen only as something to be disseminated as soon as possible, into a resource to be exploited.

3. STRATEGIES

The *agro-tourisms facilities* can be connected to the municipal sewerage system and the purifier. If these structures are located in very remote locations, generally a septic tank (see Figure 4a) is used, possibly followed by damp areas built as aging thrown together (the flow pass from one chamber to the other but holds the settling solids and the floating substances). The septic do not allow the introduction of rainwater. The main pollutant removal rates referring to two main used system, using literature data are shown in Table 1 [19]. The Imhoff system have two superimposed and communicating environments that allow sedimentation and biological digestion process (Figure 4b).

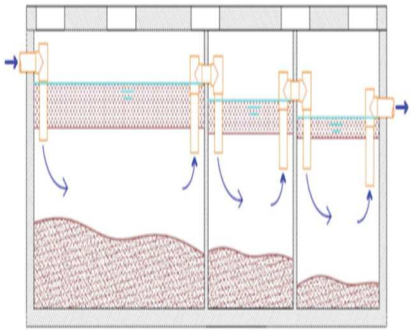

Figure 4a: Tricameral septic tank

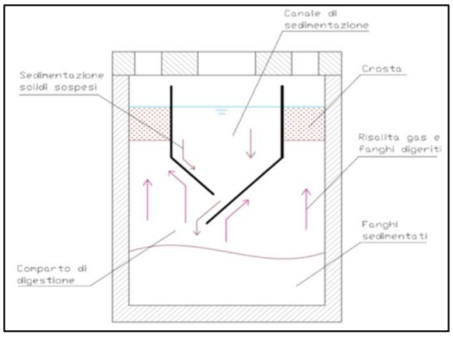

Figure 4b: Imhoff system

Table 1: Percentages main pollutant abatement [19]

	septic tanks	Imhoff
	%	%
COD	28-56	25-35
BOD_5	18-54	25-35
TKN	0-22	-
P_{tot}	0-40	-
Suspended Solids	48-98	55-56
Settling solids	92-100	85-90

The Imhoff system, compared to conventional septic tanks, has the advantage that the shape of the tank is such as to prevent the formation of gas produced in the lower compartment up to the upper compartment by altering the sedimentation process; and also allows digestion in the lower environment under more controlled conditions than septic tanks [21].

Both systems are suitable as a pre-treatment that can be followed by a phytodepuration.

The phytoremediation systems can be easily integrated into the landscape and become an integral part of it.

Although phytoremediation can be achieved through solutions of different types, it is preferable to realize a sub-surface flow that allows the flow to remain below the level of the fill material so that no surface water is present. A sub-surface phytoremediation system can be realized either horizontally or vertically.

The horizontal flow configuration allows to create a saturated system where predominantly anoxic processes are performed and therefore the nitrification reaction does not occur which allows the oxidation of the NH_4 present in the nitrite and nitrate reflux. However, the absence of oxygen makes possible reactions by particular bacteria that can use nitrates instead of oxygen. Vertical flow configuration instead provides discontinuous power from above; in this way an unsaturated system is created and the presence of air in the porosity makes possible the nitrification reaction. The bed must be made of certified material with a given granulometry and washed in such a way as to eliminate the particles of limes and clay which otherwise could risk obstructing the porosity.

Combination in series of the Imhoff as pretreatment upstream of a phytoremediation system consisting allows a good reduction of pollutants. Exiting effluent from the biological phase crosses the filling material.

4. CONCLUSIONS

Water management optimisation is a topic more and more important in the management of the environment. In Europe a steady attention is put to that in order to complete a pathway that today guarantee high standard for surface water. In the present paper some aspects were discussed to understand the approach that can be adopted in the agro-tourism structures, often decentralised in the territory. Decentralisation needs site specific solutions. As a consequence in this sector the Imhoff tank can give play an important role yet. The technological level to be adopted for water management depends on the local context, thus other solutione are available. In teh whole, the management criteria concerns solutions available for prevention of losses, for water separation (black and gray water, etc.) for treatment and recovery. A comprehensive vision of the targets in compulsory to guarantee an integrated management of all the types of water used or „polluted" at the structure.

References

[1] European Commission, Tourism, https://ec.europa.eu/growth/sectors/tourism_en, 2017.

[2] Giurea, R., Ioan, A.M., Ragazzi, M., Cioca, L.I. Focusing agro-tourism structures for environmental optimization, Quality - Access to Success, 18, 115-120, 2017.

[3] UNWTO Tourism Highlights - 2016 Edition, http://www.eunwto.org/doi/book/10.18111/9789284418145.

[4] UNWTO Tourism Towards 2030. Global Overview, http://www.wise.co.th/wise/Knowledge_Bank/References/Tourism/UNWTO_Tourism_Toward_2030.pdf, 2011.

[5] Busby, G., & Rendle, S., *The transition from tourism in farms to farm tourism. Tourism Management*, 21, 2000.

[6] McKenzie, N., & Wysocki, A., *Agritainment: A viable option for Florida producers,* IFAS Extension e University of Florida, 2002.

[7] Wicks, B., & Merrett, C., *Agritourism: an economic opportunity for Illinois. Rural Research Report*, 14(9), 2003.
[8] Barbieri, C., & Mshenga, P. M., The role of the firm and owner characteristics on the performance of *agritourism farms*, Sociologia Ruralis, 48, 166–183, 2008.
[9] McGehee, N. G., *An agritourism systems model: a Weberian perspective*, Journal of Sustainable Tourism, 15, pp. 111–124, 2007
[10] McGehee, N. G., & Kim, K., Motivation for agri-tourism entrepreneurship, ournal of Travel Research, 43, 161–170, 2004.
[11] Sharpley, R., & Sharpley, J., *Rural tourism: An introduction*. Thomson Business Press, 1997.
[12] Wall, G., *Agrotourism*, In J. Jafari (Ed.), Encyclopaedia of tourism, pp. 14–15, London: Routledge, 2000.
[13] Sznajder, M., Przezbórska, L., Scrimgeour, F., *Agritourism*, Wallingford, UK ; Cambridge, MA, 2009
[14] Law 730/1987.
[15] Ciervo, M., *Agritourism in Italy and the local impact referring to Itria Valley. The organic firm "Raggio Verde" and its ecological agritourism project*, Agritourism Between Embeddedness and Internationalization. Proceedings, pp. 11-26, 2012.
[16] ANT - Autoritatea Nationala pentru Turism (National), Available: http://turism.gov.ro/legislatie/, 2017.
[17] European Commission, European Environment Agency, State of bathing water country reports –Italy and Romania, 2016.
[18] IRIDRA S.r.l., Il riuso delle acque reflue: realizzazioni e prospettive http://www.iridra.com//
[19] Meggers et al., 2011.
[20] FarinaR., *Nuovestrategieperl'usoefficientedell'acquanegliedificiresidenziali,tecnologie di recupero del calore*, 2013.
[21] Masotti L., Verlicchi P., *Depurazione delle acque di piccole comunità*, Hoepli, 2005.

MANAGEMENT OF EXCESSIVE METEORIC WATER IN RURAL RESIDENTIAL AREAS

Safta Victor-Viorel[1], Gîrleanu Iulian-Cezar[1], Zăbavă Bianca-Ştefania[1], Boureci Adrian[2]
[1]University POLITEHNICA of Bucharest, Department of BIOTECHNICAL SYSTEMS
[2]Captain NICOLAE PLEŞOIANU High School of Râmnicu Vâlcea

ABSTRACT

Excess water coming from melting snow or heavy rainfall is a problem for rural households because it may occur puddles or runoff that affect negatively spaces within them, both in terms of functionally and aesthetically.

This paper presents several measures to manage excess meteoric water in rural households based on creating conditions for water absorption into soil or by plants.

These measures, which besides being particularly effective, can create aesthetically arrangements in terms of landscape.

Keywords: rural households, excess rainwater, infiltration – percolation, absorption by plants

1. INTRODUCTION

Excess water coming from melting snow or heavy rainfall is a problem for rural households because it may occur puddles or runoff that affect negatively spaces within them, both in terms of functionally (damage or flooding of access roads and spaces in households, flooding of areas in homes or outbuildings, transport and accumulation of silt, especially in households in slope) and aesthetically. These phenomena are manifested mainly in spring and during rainy periods in summer or autumn.

To counteract these phenomena particularly troublesome it requires a correct management of the excess water which implies to create conditions for excess water absorption in soil or by plants.

The absorption of the water by the soil is a natural process by which the water penetrates the soil surface and then follows a downward movement which ends in the saturation zone, in the groundwater. The process has two distinct phases, namely: the water penetration through the surface of the soil, phase called *infiltration*, and the descendant movement of water (mainly on vertical direction) through the unsaturated zone of the soil up to the first piezometric level that marks the upper limit of aquifers groundwater, phase called *percolation*.

The process of infiltration-percolation of water into the soil is dominated by the complex interactions between the three phases present in the process, namely:

- *the solid phase* represented by the pattern of mineral formations from the unsaturated zone of the soil through which occurs the infiltration and the percolation;
- *liquid phase* represented by meteoric water;
- *gaseous phase* represented by the air present in the unsaturated porous space of the soil.

The determinant forces in the phenomenon of infiltration-percolation are the gravity and the capillary, that move the water from wet areas to those with lower moisture content. As a resistant forces occur: the friction of the water with the mineral particles surfaces and the

[1] Splaiul Independentei 313, Sector 6, Bucharest, 0724017310, saftavictorviorel@yahoo.com

backpressure exerted by the air contained in the soil. As secondary factors which influences the infiltration-percolation phenomenon can be mentioned: the viscosity of the water influenced by temperature and the mineralization of the water (the content of dissolved salts).

In the initial stage of the process of infiltration-percolation, the action of capillary forces from the unsaturated zone of the soil is more important than that of the gravity, and this is the reason for which the current lines, which indicates the water movement route, can be deviated in all directions. The capillary effect decreases with the wet front advancement, so at depths of the order of one meter, the gravitational percolation becomes dominant, developing in depth with a speed relatively uniform. An important role in the dynamics of infiltration-percolation is played by the air from the soil. At the beginning, when the wet front advances unevenly, the air is evacuated in different directions and the speed of water percolation decreases due to the energy consumption. If the process of percolation continues, a part of the air is dissolved in the water and can recorded even an increase of the percolation speed [1].

In their turn, the plants absorb water from the soil for their needs of growth and development and then, they evacute a part ot the water by evapotranspiration into the atmosphere.

After the absorbtion of the excess water by the soil and plants this is biologically cleaned and discharged into groundwater and atmosphere. It is worth mentioning that the soil's property of water purification has been exploited by the creation of extensive infiltration-percolation fields used for domestic wastewater treatment.

For the purpose of a suitable management of the excess water, they can be taken several measures, which, besides the fact that they are highly efficient, can create very aesthetic arrangements from the landscape viewpoint.

2. MEASURES TO ELIMINATE EXCESS METEORIC WATER FROM HOUSEHOLDS

In present, a series of measures to eliminate the excess of meteoric water have been developed and applied, namely:

- the use of permeable paving to the construction of the access roads (see Figure 1), made

Figure 1 – Examples of permeable paving

of modular pavers (stone, cobbles or porous asphalt), interspaced with gravel or sand or planted with mosses, allowing the water in excess to infiltrate into the soil;

- the construction of drainage trenches or swales (see Figure 2), filled with stones or gravel, in the areas where runoffs are formed after the precipitation, and which act as buffers for the excess of meteoric water, before it gradually infiltrate into the soil;

Figure 2 – Examples of drainage trenches filled with stones or gravel

- the establishment of artificial obstacles or terraces on slope terrains (see Figure 3) in order to stop or to slow down the streams that appear after the rainfalls, thus creating favorable conditions for the infiltration-percolation of the excess water into the soil;

Figure 3 – Examples of artificial obstacles or terraces on slope terrains

- also for the slopes, the creation of stones riverbeds or waterfalls, for conducting of the streams and biological ponds into depressions areas, for the storage of the excessive meteoric water (see Figure 4);

Figure 4 – Examples of routing courses or excess meteoric water storage ponds

- the constitution of infiltration fields with grass or even of "rain gardens" (see Figure 5), which are lower areas where the excess water is leaking, cultivated withe certain species of plant which absorb intensively the water, thereby facilitating the gradual infiltration of excess water into the soil.

Figure 5 – Examples of infiltrating fields with grass and rain gardens

Otherwise, a pleading for the use of grassy fields in role of excess water infiltration field was the construction on the roof of the new Visitors Center of the Brooklyn Botanical Garden (see Figure 6) of an infiltration fields with grass, which facilitates natural filtration and controls the excess meteoric water connected with the city`s sewerage system. This roof design conceived like an extension of the garden, joins the architecture with the landscape and redefines the

physical and philosophical relationships between visitors and garden, exhibition and movement, culture and nature. By the fusion of the engineering technologies with sustainable landscaping, the Visitors Center marks the 100th anniversary from the inauguration of the botanical garden, a hundred years of offered public services and education, demonstrating involvement in environmental issues.

Figure 6 – Grassy field on the roof of the new Visitors Center of Brooklyn Botanical Gadren

3. CONCLUSIONS

Excess water from snow melting or from heavy rainfall represents a problem for rural households that can cause puddles or runoff that affect negatively spaces within them, both in terms of functionally and aesthetically..

In order to counteract these particularly troublesome phenomena, it is necessary to have a correct management for the excess of meteoric water, which involves the creation of conditions for excessive water absorption in the soil or by the plants.

For this purpose, a series of measures can be taken, such as the permeable paving at the construction of access roads, the construction of drainage trenches and swales filled with stones or gravel in the areas where runoffs are formed, the creation of artificial obstacles or terraces on slopes terrain and the creation of stones riverbeds or waterfalls, for conducting of the streams and biological ponds into depressions areas, for the storage of the excessive meteoric water and the constitution of infiltration fields with grass or “rain gardens”.

These measures, besides the fact that they are highly efficient, can create very aesthetic arrangements from the landscape viewpoint.

References

[1] Aoyagi C. - Infiltration and percolation. FormuLa Landscaping - http://www.formlainc.com/resources/beautiful-water-conservation/

[2] G. Allen Burton, Jr., Ph.D. RobertE. Pitt, Ph.D., P.E. – Stormwater effects handbook, A toolbox for watershed managers, scientists, and Engineers, Lewis Publishers

[3] R. Pitt, M. Lilburn. S.R. Durrans, S. Burian, S. Nix, J. Vorhees, and J. Martinson - **The** Beneficial Uses of Stormwater in Urban Areas and the Need for Change in Urban Water Management - *Guidance Manual for Integrated Wet Weather Flow (WWF) Collection and Treatment Systems for Newly Urbanized Areas (New WWF Systems)*. U.S.Environmental Protection Agency, Urban Watershed Management Branch, Edison, New Jersey. Dec. 1999.

[4] Robert L. Siegrist, Ph.D., John E. McCray, Ph.D., and Kathryn S. Lowe - *Wastewater infiltration into soil and the effects of infiltrative surface architecture* - Small Flows Quarterly, Winter 2004, Volume 5, Number 1
[5] Safta V.V., Gîrleanu I.C., Zăbavă Bianca-Ştefania, Boureci Adrian - *Infiltration -percolation extensive systems for urban wastewater treatment* - 5th International Conference on Thermal Equipment, Renewable Energy and Rural Development (TE-RE-RD - 2016), Golden Sands, Bulgaria, 2-4 June 2016, ISSN 2457 – 3302.
[6] ***,Faculty of Land and Food Systems, The University of British Columbia – Watershed Science - The Hydrological Cycle - http://ubclfs-wmc.landfood.ubc.ca/webapp/IWM/course/watershed-science-3/hydrological-cycle-16/
[7] ***, New Jersey Stormwater Best Management Practices Manual February 2004 Chapter 9.7: Standard for Pervious Paving Systems February 2004 Page 9.7-14 http://www.state.nj.us/dep/stormwater/bmp_manual/NJ_SWBMP_9.7.pdf
[8] ***, Infiltration trench – Villanova University – College of engineering – Villanova urban stormwater partnership - https://www1.villanova.edu/villanova/engineering/research/centers/vcase/vusp1/research/infiltration-trench.html
[9] ***, Introduction to soil science – e-courses for B. Sc.(Agriculture) degree program – Retention of water by soil - http://eagri.tnau.ac.in/eagri50/SSAC121/
[10] ***, http://www.archdaily.com/235079/brooklyn-botanic-garden-visitor-center-opens-to-the-public
[11] ***, Soak It Up: How to Manage Stormwater in Your Landscape - houzz - https://www.houzz.com/ideabooks/44218826/list/soak-it-up-how-to-manage-stormwater-in-your-landscape

INTEGRATION OF RENEWABLE ENERGY SOURCES ON ELECTRICITY MARKET USING TEP OPTIMIZATION

Catalina Alexandra Sima[1], George Cristian Lazaroiu[1], Virgil Dumbrava[1], Mihai Tirsu[2], Victor Galbura[2]
[1]University POLITEHNICA of Bucharest, Splaiul Independentei 313, 060042 Bucharest, Romania
[2]Institute of Power Engineering, Academy of Sciences of Moldova, Moldova
catalina.sima@yahoo.com, cristian.lazaroiu@upb.ro, v_dumbrava@yahoo.com

ABSTRACT

Transmission expansion planning has the purpose to ensure two important objectives: economic trade and engineering reliability and also, in this paper, it establishes the optimal expansion decisions in a large real network with classical generators and high share of RESs.

The proposed problem is a mixed-integer nonlinear programming problem (MINLP) that is resolved using a deterministic model considering a threshold budget for new transmission lines that are possible to be built.

The objective of the mathematical model presented in this paper is to decrease the entire operational cost of the power system. The considered model was solved using GAMS (General Algebraic Modeling System) optimization software and it can be modified to enable the independent system operator (ISO) to adjust to future electrical network modifications.

1. NOMENCLATURE

Indices:
d – demands
h – hydro energy generation units
t – thermal energy production units
w – wind energy production units
l – transmission lines
b – buses
Sets:
d_b – demand supplied from bus b
h_b – hydro energy production unit located at bus b
t_b – thermal energy production unit located at bus b
w_b – wind energy production unit located at bus b
l_p – transmission lines possible to be build
$r(l)$ – receiving node
$s(l)$ – sending node
Parameters:
C_l – maximum capacity for transmission line l [MW]
B_l – susceptance of transmission line l [S]
G_h – generation capacity of hydro unit h [MW]
G_t – generation capacity of thermal unit t [MW]
G_w – generation capacity of wind farm w [MW]
L_d – consumption of demand d [MW]
c_{LS}^d –load shedding cost of demand d [€/MWh]

c_h – cost of production of hydro unit h [€/MWh]
c_k – cost of production of thermal unit t [€/MWh]
c_w – cost of production of wind unit w [€/MWh]
BI_p^{ib} – annualized budget for investing in construction of new transmission lines [Euro]
CI_p^{im} – annualized cost for investing in new transmission lines *l* [Euro/MW]
Binary variables:
u_l – Binary variable that is 1 if a possible line *l* is built, and 0 if a possible line *l* is not built.
Variables:
LS_d – load shedding of demand *d* [MW]
P_h – power produced by hydro unit h [MW]
P_t – power produced by hydro unit t [MW]
P_w – power produced by hydro unit w [MW]
PF_l – power flowing through transmission line l [MW]
V_b – voltage level at bus *b* [rad]
γ – time period [hours].

2. INTRODUCTION

In Romania, in Dobrogea aria are installed many renewable energy sources especially wind and photovoltaic. Considering atmospheric conditions for RESs, the location of the RESs is not consistent with the demands of the power system. It is necessary to take into consideration the interconnection of RESs into the existing power system in order to avoid the overloads [1-3], [6].

The results of the mathematical model that solves transmission expansion planning (TEP) problem helps the system operator to decide which is the best solution for the reinforcement of the existing grid. The solution of the model is regarding the balance between producers and consumers, the capacity of the transmission lines (perspective ones and the existing ones), the capacity of the generators. It is important, for the system operator to be able to take the best decisions regarding reinforcements in order to increase the reliability and safety of the power system in an uncertain environment [1], [5-6].

TEP has the purpose to ensure two important objectives: economic trade and engineering reliability and also, in this paper, it establishes the optimal expansion decisions in a large real network with classical generators and high share of RESs [7-9].

The proposed problem is a mixed-integer nonlinear programming problem (MINLP) and it is solved using a deterministic model considering a threshold budget for new transmission lines that are possible to be built. The model is applied on a large real network that contains 18 generating units, 16 demands, 29 existing transmission lines and 3 new transmission lines that are possible to be built.

The objective of the mathematical model presented in this paper is to minimize the cost associated with building new electrical transmission lines, the operating cost of production units and the load-shedding cost.

3. MATHEMATICAL MODEL

The proposed model is nonlinear considering the products between binary variables and continuous variables. In order to linearize the model, the nonlinear constraints are substitute with equivalent mixed-integer linear sets. The resulted mathematical model is a linear one and in this article, it is solved using a deterministic method [5].

The objective function of the mathematical model that is proposed in this paper is minimizing the total operational cost of the large real system which is located in the south aria of Romania. The decision that the ISO is taking, regarding the reinforcement of the existing power system is constrained also by the threshold budget. The minimization of the total costs is referring to the minimization of the cost needed for building the new transmission lines, the operation cost of the generating units and load-shedding cost.

$$min \sum_{l \in l_p} CI_p^{im} u_l + \gamma \left\{ \left[\sum_{gk} c_t P_t + \sum_{d} 1000 \cdot LS_d \right] + \left[\sum_{gw} c_w P_w + \sum_{d} 1000 \cdot LS_d \right] + \left[\sum_{gh} c_h P_h + \sum_{d} 1000 \cdot LS_d \right] \right\} \quad (1)$$

Subjected to:

$$\sum_{l \epsilon l_p} CI_p^{im} u_l \leq BI_p^{ib} \quad (2)$$

$$u_l = \{0,1\}, \forall l \in l_p$$

$$\sum_{t \in t_b} P_t + \sum_{h \in h_b} P_h + \sum_{w \in w_b} P_w - \sum_{l \backslash s(l)=n} PF_l + \sum_{l \backslash r(l)=n} PF_l = \sum_{d \in d_n} (L_d - LS_d), \forall b \quad (3)$$

$$PF_l = B_l \left(V_{s(l)} - V_{r(l)} \right), \forall l \backslash l \in l_p \quad (4)$$

$$-C_l \leq PF_l \leq C_l, \forall l \backslash l \in l_p \quad (5)$$

$$-u_l C_l \leq PF_l \leq u_l C_l, \forall l \backslash l \in l_p \quad (6)$$

$$-(1 - u_l)M \leq PF_l - B_l \left(V_{s(l)} - V_{r(l)} \right) \leq \leq (1 - u_l)M, \forall l \in l_p \quad (7)$$

$$0 \leq P_t \leq G_{t,} \forall t \quad (8)$$

$$0 \leq P_h \leq G_{t,} \forall t \quad (9)$$

$$0 \leq P_w \leq G_{w,} \forall w \quad (10)$$

$$0 \leq LS_d \leq L_d, \forall d \quad (11)$$

$$-\pi \leq V_b \leq \pi, \forall b \quad (12)$$

$$V_b = 0, reference\ bus \quad (13)$$

Where 1000 is load-shedding cost.

As mentioned before the Dobrogea power system contains 18 generating units, 16 demands, 29 existing transmission lines and 3 new transmission lines that are possible to be build.

In the figures below it can be seen the data for the thermal generating units and wind generating units that were used in the proposed problem. The generated power that is produced at the hydro power plant is 210 [MW].

In this article, the optimal decision of the system operator is based on a future demand forecast. It is considered that the power requested by the demands is the largest expected at each node.

The mathematical model considered in this paper was solved using GAMS (General Algebraic Modeling System) optimization software and it can be modified to enable the ISO to adjust to future electrical network modifications.

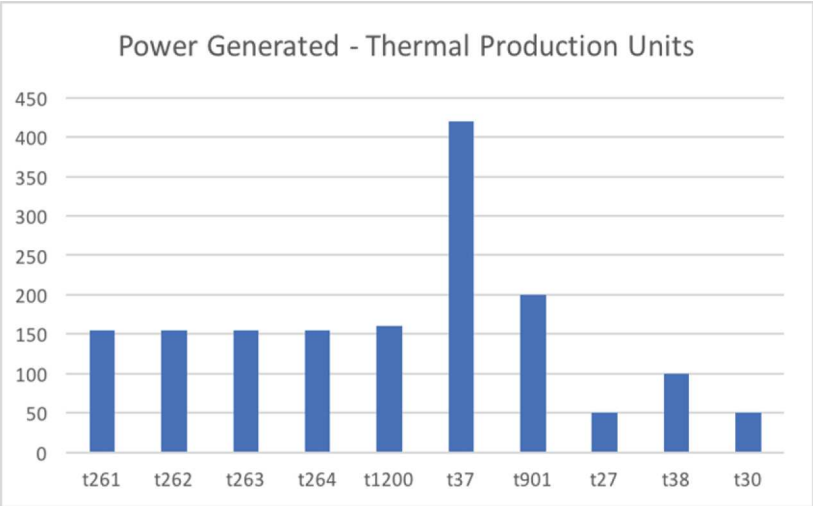

Figure 1: Data for Thermal Generating Units

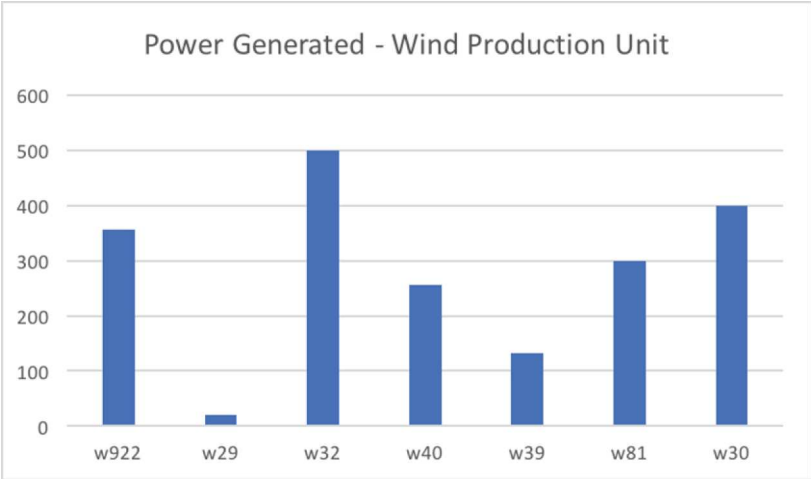

Figure 2: Data for Wind Generating Units

4. CASE STUDY RESULTS

As mentioned before, the real test network that is located in south of Romania, contains 18 generating units, 16 demands and 29 existing transmission lines. Regarding the construction of the new lines, only 3 new lines are possible to be built in the considered time horizon.

The construction of the new lines is constrained also by the threshold budget that is varying between 15 million Euros and 25 million Euros.

The results given after compiling the program are the optimal results for the reinforcement of the power system. The number of the new transmission lines that are possible to be build are constrained by the threshold budget.

In Figure 3 it can be seen the optimal decision for the reinforcements of the existing power system function of investment budget. With the threshold budget of 15 million Euros only l_{19} is possible to be built, and the threshold budget of 25 million Euros lines l_{13} and l_{19} are possible to be built.

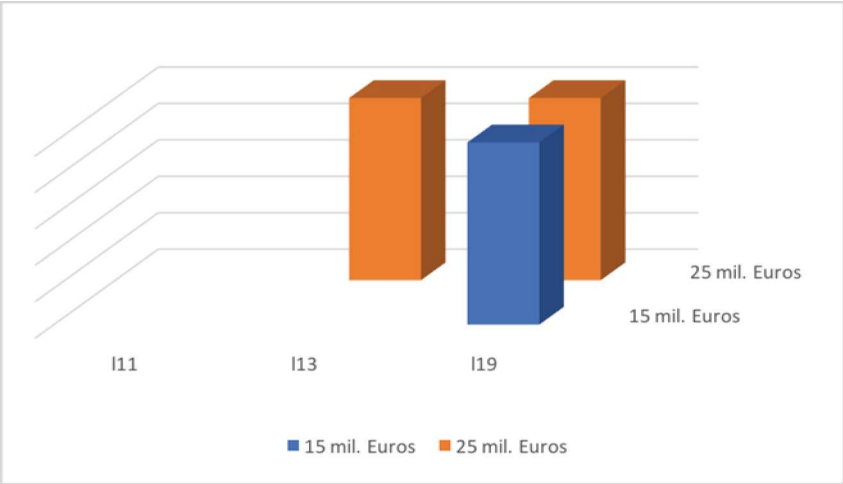

Figure 3: The optimal solution for the reinforcements

5. CONCLUSIONS

In order to avoid grid overload, it is necessary to take into consideration the expansion of the existing power system. Transmission expansion planning can increase the competitiveness of the market participants and provides reliability and safety of the power grid.

In this article, it is proposed a mixed-integer nonlinear programming problem that is solved using a deterministic method. The results of the problem will determine the optimal solution for the expansion of the grid.

The threshold budget is varying between 15 million Euros and 25 million Euros and it denotes the number of the new transmission lines that are possible to be built. For an investment budget of 15 million Euros, fewer transmission lines will be built then if it is considered an investment budget of 25 million Euros. With the increasing of the investment budget and the construction of the new lines the cost associated with load shedding decreasing.

The objective function of the mathematical model is to decrease the entire operational cost: the cost required in order to build the new transmission lines, the load shedding cost and operation cost of the generating units.

The proposed model can be modified to enable the ISO to adjust future electrical network modifications.

Acknowlegment

This work was supported by a grant of the Romanian National Authority for Scientific Research and Innovation, CCCDI – UEFISCDI, project number 37BMPNIII-P3-199/02.09.2016 and and 16.80013.5807.12/RO.

References

[1] N. Golovanov, H. Albert, St. Gheorghe, N. Mogoreanu, G.C. Lazaroiu, Renewable sources in power systems, AGIR: Bucharest, 2015, pp. 37-52

[2] N. Golovanov, G. C. Lazaroiu, M. Roscia, D. Zaninelli, "Integrating RES into the Romanian transport system," Proc. 2009 PowerTech, pp. 1-5, 2009

[3] V. Dumbrava, G. Bazacliu, B. Nicoara, G.C. Lazaroiu, D. Zaninelli, "Load profiling for the electricity market," Proc. 43rd Univ. Power Eng. Conf., pp. 1-5, 2008

[5] S. de la Torre, A.J. Conejo, J. Contreras, "Transmission expansion planning in electricity markets," IEEE T. Power Syst., vol. 23, issue 1, pp. 238–248, February 2008

[6] C. Rathore, R. Roy, “Impact of wind uncertainty, plug-in-electric vehicles and demand response program on transmission network expansion planning,” Electr. Pow. Syst. Res., vol. 75, pp. 59–73, 2016
[7] F. Ugranl, E. Karatepe, “Multi-objective transmission expansion planning considering minimization of curtailed wind energy,” Electr. Pow. Syst. Res., vol. 65, pp. 348–356, 2015
[8] D.Z. Fitiwi, L. Olmos, M. Rivier, F. de Cuadra, I.J. Pérez-Arriagak, “Finding a representative network losses model for large-scale transmission expansion planning with renewable energy sources,” Energy, vol. 101, pp. 343-358, February 2014
[9] M. Sedghi, A. Ahmadian, M. Aliakbar-Golkar, “Assesment of optimizations algorithms capability in distribution network planning: Review, comparison and modification tehniques,” vol. 66, pp. 415–434, August 2016

MONITORING OF AIR QUALITY IN ROMANIAN-BULGARIAN BOARD REGION

Assoc. Prof.Phd.Eng. Gabriela Anca Cristina Simion, Spînu Florentina
University Politehnica of Bucharest
gacsimion@gmail.com

ABSTRACT

Last years an important problem is the fact that countries sharing the same border must exchange information in order to monitor transboundary transport of air pollutants. This paper presents automatic monitoring system implemented at the Romanian-Bulgarian border, project PHARE CBC RO/BG 1999. It is created a joint monitoring network on monitoring air quality in cities bordering the lower Danube basin.

1. INTRODUCTION

Monitoring Air Quality in the Romanian – Bulgarian Border Area of Danube River is an important problem for sustainable protection of the environment in region. The harmful effects on human health, vegetation and ecosystems, determined by their exposure to air pollution, impose a join approach of all European countries regarding the ambient air quality assessment. The air quality assessment in cross border area imposes a joint approach of both countries because the air pollution is not a local problem. In this case an important target is the continuous and in real time information of decision factors regarding the air quality. Environmental policy plays an important role among EU concerns and it represents nowadays one of the most important political aspects at EU level.

Specific results identified after analyzing the monitoring network will be presented and plans and measures for developing the air quality monitoring network in cross-border region will be proposed. The data will be posted on a web-site available in languages: Romanian, Bulgarian, and English. The air quality assessment will be done on the basis of criteria and methods common for all EU states, with a view to create the premises necessary for issuing consistent and solid decisions and policies for pollution control. The project proposed to connect the physical infrastructure of the common border on air quality monitoring and communication services as a basis for effective cooperation, in accordance with the program strategy. Current links between the two countries on air quality in a cross-border context were reinforced by the Phare Cross Border Cooperation projects (CBC) from 1999 to 2003. This activity aims to ensure a positive significant impact, sustainable change and durable improvement within the eligible areas in both countries Romania and Bulgaria.

2.METHODOLOGY

Air is an important environment factor, because it ensures rapid transport of the pollutants in the atmosphere. The policy principles governing the protection of ambient air quality are connecting to health of the population prevails. It must be protected against the danger of illness due to atmospheric pollution .Applying the "polluter pays" principle is necessary.

Awareness and change in the behavior of economic agents regarding the promotion of best available techniques and good management practices is made in order to reduce atmospheric pollution .Increase awareness of the populations from both countries in pollution problems is very important.

Automatic monitoring system implemented at the Romanian-Bulgarian border follows the evolution of the pollutants as SO_2, NO_2, $PM_{10,}$ Pb, O_3, CO, C_6H_6 in towns near the border:

Turnu Magurele – Nikopol,

Zimnicea –Rostov,

Giurgiu -Ruse,

Calarasi – Silistra.

Each automatic air quality monitoring station consisted of:

- DOAS (Differential Optical Absorption Spectroscopy) system for monitoring the indicators: C6H6, NO2, SO2, O3, CO2, C6H5 -OH, C6H5 -CH = CH2, C6H5 -CH3, C6H4 (CH3) 2, NO.

The basic principle was the optical determination of various chemical pollutants along an open optical path of up to several hundred meters, using differential absorption spectrometry as a method of analysis.

The monitoring station was equipped with two transmitters and two long-range receivers up to 500 m and short track up to 200 m.

They were designed to measure and analyze the atmospheric gases released into the environment. These transmitters / receivers were used in combination with the AR 500 Analyzer. The light beam from the emitter was directly directed toward the receiver, and on its way through the atmosphere the intensity was affected by dispersion and absorption into molecules and particles found in ambient air. Depending on the pollutants in the atmosphere, the light was received differently by the receiver.

From the receiver, the captured light was led through an optical fiber to the analyzer, which was a spectrometer equipped with signal processing equipment.

Point Monitor for SO2 is ML 9850B Analyzer. It is based on ultraviolet fluorescence along with a converter furnace for H2S measurements

SM 200 sampling machine is an automatic sampling machine for PM10, which offers automatic harvesting of these powders.

The station was equipped with weather sensors that provided information on: temperature, relative humidity, solar radiation, wind direction and speed.

Data and information to the public were displayed on a display by displaying graphical media representing the limit value for each monitored pollutant, toxicological effects and weather data. This panel was located in front of the Giurgiu City Hall, so that every citizen had access to the information received from the monitoring stations.

Since 2010, besides the 2 monitoring stations, three stations were located in Giurgiu and another in the rural area - these new stations being part of the National Air Quality Monitoring Network (NNMC).

At present the monitoring of the ambient air quality is carried out through the National Air Quality Monitoring Network (NNMCA), an objective of national public interest, managed by the central public authority for environmental protection. The RNMCA includes sampling and measuring instruments located at fixed locations and related laboratory equipment, as well as equipment necessary for collecting, processing, transmitting data and informing the public about ambient air quality.

In Giurgiu, Giurgiu Environmental Protection Agency continuously monitors air quality through 4 stations, which have been integrated into the National Air Quality Monitoring Network.

Automatic monitoring stations is located as follows:

GR1 - traffic station located on Bucharest Highway, at the entrance to Giurgiu Municipality, the respective location being considered opportune from the point of view of the traffic flow. The monitored parameters are: SO2, NO, NOx, NO2, CO, BTX, PM10;

GR2 - urban background station located in the Students Park, adjacent to Transylvania Street, located in an area not directly exposed to traffic and local industry. The monitored parameters are: SO2, NO, NOx, NO2, O3, CO, BTX, PM10 and weather parameters;

GR3 - industrial station, located in the yard of the Giurgiu Weather Station, the Slobozia Highway, located in an industrial zone including the thermoelectric power station of Giurgiu Municipality. The monitored parameters are: SO2, NO, NOx, NO2, CO, PM10 and weather parameters;

GR 4 - suburban rural station located in Branistea village, Oinacu commune, located away from all major pollution sources. The monitored parameters are: SO2, NO, NOx, NO2, O3, CO, BTX, PM10 and weather parameters;

The limit values for the monitored indicators are established according to the Law no. 104/2011 on ambient air quality.

Trends in annual average concentrations of certain atmospheric pollutants are analyzed.

The evolution of air quality is presented for the period 2011 - 2015, using the monitoring data recorded at the stations of the National Air Quality Monitoring Network, for all the indicators having data capture higher than 75%.

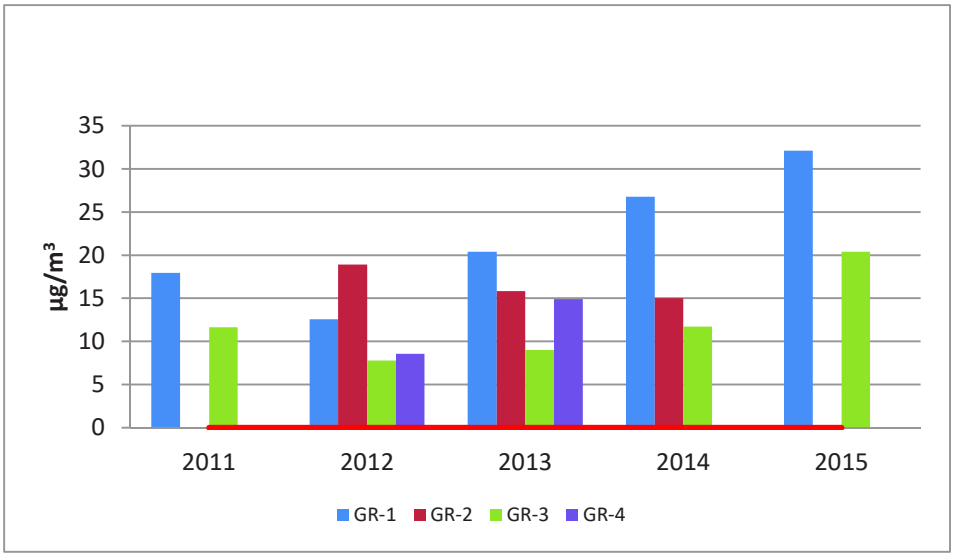

Figure 1:SO_2 Annual Concentration Evolution

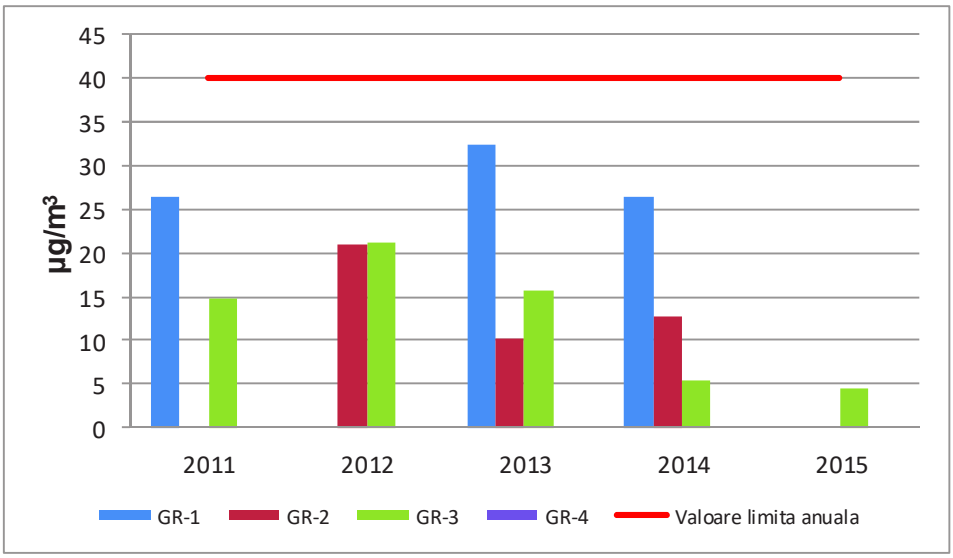

Figure 2: NO_2 Annual Concentration Evolution

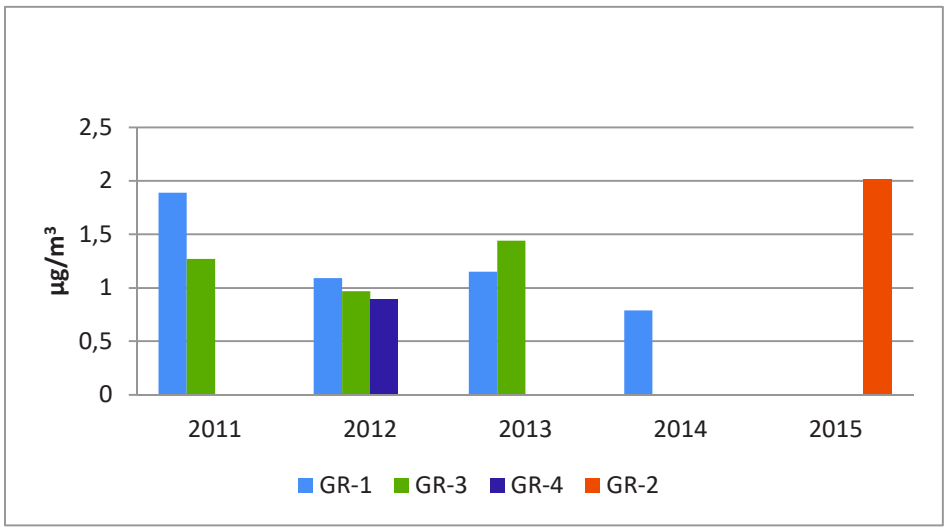

Figure 3: CO Annual Concentration Evolution

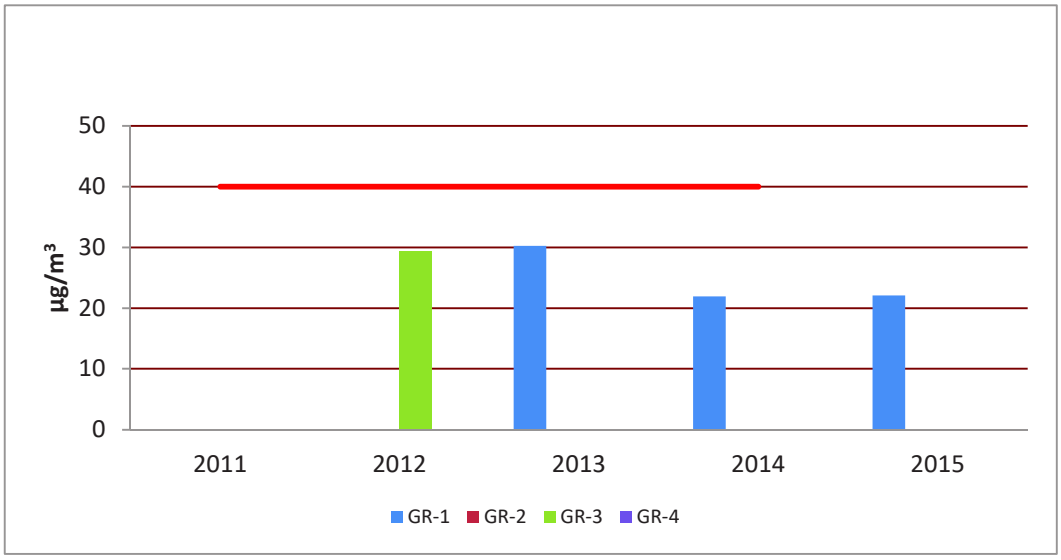

Figure 4: PM10 Annual Concentration Evolution

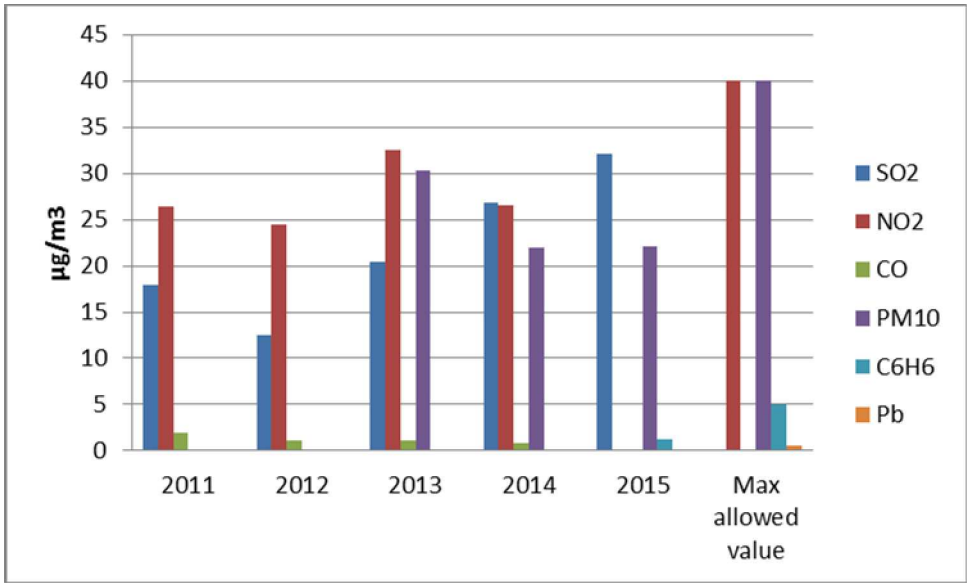

Figure 5: Evolution of annual average concentrations of air pollutants recorded at traffic stations

3. CONCLUSIONS

The actions and measures that are required for the reduction of the atmospheric emissions in the city of Giurgiu are:

- improvement of road infrastructure in order to reduce dust emissions into the atmosphere;
- replacement of solid and liquid fuels with natural gas in households and by economic agents;

- efficiency of heat consumption;
- extension of green areas;
- use of renewable energy resources;
- encourage research activities aimed at improving parameters for combustion plants (burners) and flue gas installations;
- self-monitoring of emissions by economic operators and reporting of self-monitoring data to APM Giurgiu.

Measures have been taken to reduce emissions from the industry and housing sectors in Giurgiu by connecting to the gas network, which has significantly reduced the emissions from combustion.

The inhabitants of Giurgiu met the importance of thermal insulation of homes and measured their thermal energy, which reduced energy losses.

Transport infrastructure ensures bypassing residential areas, reducing the impact on the population.

There has been a significant increase in interest in the efficiency of heat consumption and the use of alternative energy.

References

[1] Simion,G.C, *Monitoring and Control of Environment*, MatrixRom, Bucharest, 2012.
[2] Annual Report of Giurgiu Agency for 2010-2015 apmgr.anpm.ro/ calitatea aerului.
[3] The Local Environmental Action Plan (PLAM) of Giurgiu County apmgr.anpm.ro

CONSIDERATIONS REGARDING THE IMPORTANCE OF MELISSA CULTURE IN TERMS OF BENEFITS AS A MEDICINAL PLANT

Elena Sorică [1)], Mihai Matache [1)], Cristian Sorică [1)], Iulian Voicea [1)],
Augustina Pruteanu [1)], Ion Grigore [1)]

[1)] National Institute of Research - Development for Machines and Installations Designed to Agriculture and Food Industry - INMA, Bucharest, Romania, postelnicu.elena@yahoo.com

ABSTRACT

This paper presents the importance of melissa culture (lemon balm) for the pharmaceutical and cosmetic industry, in terms of benefits as medicinal plant. The active principles (active substances) contained within medicinal plants are those who give the therapeutic effect. Each plant, in principle, presents an interest for a particular active substance, which may be isolated by various methods. Melisa is an important source of volatile oil, its main component being citral.

This paper presents the experimental evaluation of the extraction degree of active principles from melissa. Measurements were performed within INMA using a percolator for obtaining extracts of medicinal and aromatic plants. The results are important for the plant processors and for the producers of phyto-pharmaceutical products.

1. INTRODUCTION

Melissa (fig. 1), also known as lemon balm, is one of the oldest medicinal plants cultivated on small surfaces since antiquity. [1]

The name of the plant comes from the Greek "melissophyllon" meaning "honey-leaf", because melissa is a plant with sweet perfume and extremely appreciated by bees. [6]

The plant is cultivated for preparing teas and in some places as a honey plant.

Besides the medicinal qualities, melissa is a valuable plant for the essential oil which is obtained after distillation of its leaves, Oleum Melissae, an oil rich in citrol, very aromatic. Essential oil content in the leaf reaches 0.4 – 0.5%. The oil is used in pharmaceutics and cosmetics.

Apart from the essential oils it contains: citral, in terpenes class, citronellol, tannins, resins, saponins, succinic acid, caffeic acid, vitamin C (up to 15% of dry matter), geraniol and a bitter principle.

Melissa is among the most utilized plants in the world and is used in the form of: powder, infusion, cataplasm, tincture and oil. [9]

Figure 1: Melissa [5], [8]

Melissa is a perennial plant, with lignified rhizome, and it looks like the dead-nettle. Like dead-nettle, it forms numerous straight and highly branched stems, which give a dense shrub aspect, 50-60 cm high. The leaves are oval, petiole, of an intense green. They are thin, with a paper-like consistency and the surface covered with a network of fine veins, slightly sunken, which gives a reticulated aspect. The leaves wither and fall in late autumn and appear again the following year, usually in April. The flowers, yellowish-white or pale mauve, form bunches, which are not numerous, sheltered by leaves. The plant blooms from June to August. [5]

Melissa has sedative, antispasmodic, analgesic, stomachic, choleretic, cholagogic, carminative, antiseptic, mild anti-diarrheic and antiherpes effects. Melissa has a beneficial effect on the nervous system and is recommended as herbal remedy for headaches that occur on the background of stress and strain, but also for insomnia and digestive disorders.

Also, melissa is an excellent long term remedy against Alzheimer's disease, reduces agitation and improves post-traumatic memory disorders. Melissa also removes depression, has positive effects on the psyche, favours optimistic thinking, enhances mental and psychological tone. This plant is used in the treatment of anorexia nervosa, cholecystitis, cholelithiasis, viral hepatitis and thyroid disease. Meanwhile, melissa favours fighting most forms of rheumatism, has anti-inflammatory joint effect, slows or even stops the degenerative processes. [3]

Melissa grows in the spontaneous flora in many countries of southern Europe, western Asia and northern Africa. At first, spontaneous flora was the only source of raw material.

In Romania, melissa can be found in the spontaneous flora of southern and western areas, where it grows dispersed in calcareous places, grasslands and oak forest clearings. [1]

Depending on maintenance, melissa resists in the same place 3-8 years, it can be cultivated outside crop rotation, choosing for this the most pristine lands. As preplants, very suitable for growing melissa are maslins for the green mass and hay, early legumes for grains and cereals.

Soil preparation is made depending on the preplant and the degree of soil water supply. So, after early preplants, under enough humidity conditions, is performed directly the 28-30 cm deep plowing. The plow in aggregate with stellar harrow will be used. If the soil is dry and the plowing cannot be carried out, right after the land is cleaned, the discing is performed for weed control and plowing will be made after the first rainfall. After late preplants, the deep plowing is performed directly. [1]

2. MATERIAL AND METHOD

The plant can be propagated by using seeds (Fig. 2), sown directly in the field, seedling, also by separating old bushes or by rooting green cuttings.

Sowing directly in the field is the cheapest propagation method, but can only be applied on very clean fields and in areas with wet springs. The success of crops sown directly in the field is conditioned by the way of preparation, seedbed uniformity and the presence of humidity in the surface layer of the soil. Field rolling must be made both before and after sowing.

Figure 2: Melissa seeds [7]

Seedling propagation is an expensive method, but much safer. Seedling production is performed in cold beds, prepared like the vegetable ones.

Propagation by separating old bushes is achieved by eliminating the old plantations; this is a cheap method with the help of which very good results can be obtained.

Propagation by rooting green cuttings (Fig. 3) is used only in the works of improvement for rapid multiplication of extremely valuable forms.

Figure 3: Melissa cuttings [6]

3. RESULTS

Medicinal plant species owe their phytotherapeutic action to the presence of bioactive components, also called active principles, with effects in the metabolism of the whole human or animal body. In relation to the presence of certain active principles, plants have specific effects, enhanced by their synergetic action, with both food quality, as well as therapeutic or preventive ones. Useful substances from medicinal plants are obtained from plant bodies, in general, either by means of water (usually hot), or by using a solvent (e.g. the alcohol).

The degree of extraction of active principles from plants is strongly influenced by the following factors:

- humidity of cut and selected plants;
- samples consistency (leaves/stems/peels/seeds/etc.);
- percolation time;
- percolation pressure;
- used solvent.

In order to determine the degree of extraction of the active principles, a percolator was used. It (Fig. 4) is the technical equipment operating in the technological line of medicinal and aromatic plants primary processing. The percolator functions on solvent and percolation under pressure, in two phases. It has two compartments for introducing the plant charge, being mounted on the floor of the room. The entire extraction process takes place automatically, its parameters being prescribed, controlled and displayed by a PLC with display. It is designed to extract the active principles from the plant material, dried or freshly harvested to pre-established sizes.

Figure 4: Percolator [4]

Table 1: Percolator technical characteristics [4]

Type of energy source	Electricity network
Volume of extraction chambers [l]	12 / 24
Maximum air pressure [bar]	8
Maximum power consumption [W]	500
Dimensions: ✓ length [mm] ✓ width [mm] ✓ height [mm]	 1.000 600 1.350
Mass [kg]	175

Before being introduced into the percolator, the plants are weighed (Fig. 5) in order to achieve the correct plant-solvent ratio:

Figure 5: Preparing the material for percolation (dosing)

The plants from which the active principles are extracted, weighed and dosed are put in a bag of a special and very fine mesh, and then introduced into the compartment that will be used for percolation (Fig. 6).

Figure 6: Introducing the material into the percolation compartment

Over these plants is added the solvent used for extracting the active principles (distilled water, alcohol, vinegar, etc.) up to a level at the bottom of the compartment.

After introducing the material from which active ingredients are extracted and the solvent into the percolation compartment and after all preparatory operations for starting the percolator were made, the time of the percolation operation and its maximum pressure are set, the START button is pressed.

After the percolation is completed, samples (fig. 7) were taken in special capsules and were put in the oven to accurately determine the percentage of active substance extracted in the process. [2]

Figure 7: Capsule of the material undergoing percolation

The percentage of active principles extracted was calculated after the sample was kept inside the oven with the temperature set at 105^0C (Fig. 8) as long as it is stipulated in the current standards, for the material undergoing percolation being determined the percentage of active principles extraction from the plant.

Figure 8: Setting temperature for drying the material

In order to extract the active principles from melissa plant, the following results, shown in Table 2, were obtained:

Table 2: Results obtained from melissa

Parameter determined	**Value**
Test time [min]	60
Chopped material mass undergoing extraction [kg]	0.20
State of raw material undergoing extraction	dried
Humidity of the sample undergoing extraction [%]	7.03
Active principles extraction degree [%]	18.04

4. CONCLUSIONS

Melissa is one of the oldest medicinal plants known for its sedative, antispasmodic, analgesic, stomachic, choleretic, cholagogic, carminative, antiseptic, mild anti-diarrheic and antiherpes effects.

This plant is used in the treatment of anorexia nervosa, cholecystitis, cholelithiasis, viral hepatitis and thyroid disease. Meanwhile, melissa favours fighting most forms of rheumatism, has anti-inflammatory joint effect, slows or even stops the degenerative processes.

The degree of extraction of active principles from plants is strongly influenced by the following factors: humidity of cut and selected plants; samples consistency; percolation time; percolation pressure; used solvent.

After processing experimental data, it was found that the degree of active principles extraction for dry melissa is 18.04%, with 7.03% humidity.

References

[1] Emil, P., Aurel, M., Anela, D., Maria, V., Oltea, C., *Treaty of medicinal and aromatic plants, vol. II, Publishing House of the Socialist Republic of Romania, 1986* / *Tratat de plante medicinale şi aromatice*, vol II, Editura Academiei Republicii Socialiste, Bucureşti, 1988.

[2] INMA – *Methodology for testing the Percolator used for obtaining extracts with active principles from medicinal and aromatic herbs* (MET-04), Bucharest, 2011.

[3] http://www.ziuaconstanta.ro/divertisment/sanatate/sanatate-melisa-proprietati-si-beneficii-526528.html.

[4] INMA – *Testing report – Percolator used for obtaining extracts with active principles from medicinal and aromatic plants / Raport de experimentare - Percolator utilizat pentru obţinerea de extracte cu principii active din plante medicinale şi aromatice*, Bucharest, 2011.

[5] http://www.ecovazon.md/informatii/melisa.

[6] http://www.farmacianaturii.ro/magazin/butasi-de-melisa-ecologica/

[7] http://www.e-gradinarit.ro/plante-aromatice/roinita/

[8] http://decostyle.mayra.ro/legume/plante-medicinale/melisa/314/

[9] http://sanatate.bzi.ro/9-indicatii-terapeutice-ale-melisei-2255

CONSIDERATIONS ON THE INCINERATION OF MUNICIPAL SOLID WASTE

Nicoleta UNGUREANU[1], Mihaela NIȚU[2], Valentin VLĂDUȚ[2], Mirela DINCĂ[1], Bianca-Ștefania ZĂBAVĂ[1], Iulian VOICEA[2], Ioan CABA[2]
[1]Politehnica University of Bucharest, Faculty of Biotechnical Systems Engineering, Romania;
[2]INMA Bucharest, Romania

ABSTRACT

As a result of growing concerns about groundwater contamination, decreasing availability of land for waste disposal, respectively public health and aesthetic issues related to landfills, incineration represents an alternative method for the treatment of municipal solid waste. The paper presents the theoretical aspects related to waste incineration and its residues, namely gas emissions into the atmosphere, fly ashes and bottom ashes. Also, there are presented some mass balances obtained at the incineration of municipal solid waste and current possibilities for the recovery of bottom ashes.

1. INTRODUCTION

Wastes are a heterogeneous mixture of residues of all kinds, whose composition depends on variables such as socio-economic conditions, cultural and climatic differences. Waste composition varies over time due to additional recycling or economic growth in the collection area, and these two factors can change significantly the amount of waste and their calorific value [12].

According to Eurostat, in the EU member states, the amount of municipal waste generated by a person in 2013 was 481 kg, of which 470 kg/person were treated by various methods: 31% landfilled, 28% recycled, 26% incinerated and 15% composted [8].

In most countries in the developing world, the frequent practice of waste management is still the landfilling, but in industrialized countries in Europe, and also in Japan, USA and Canada, the proportion of waste burnt in incinerators is very high (up to 100%) [10]. Due to increasing concerns on groundwater contamination, decreasing availability of land in many areas, and also the aesthetics and public health aspects regarding landfills, incineration is regarded as a valid method of disposal for municipal waste and for industrial applications [5].

Incineration (combustion) is a process of thermal decomposition by exothermic oxidation at high temperatures (850-1100°C), whereby the waste is converted into a non-hazardous material, with low volume, at the same time generating thermal energy that can be recovered in the form of heat (hot water / steam), electricity or a combination of those.

Some attractive features of incineration are given by the facts that it reduces the initial volume of combustible waste by 80-95%, and for the disposal of a tone of burned waste is needed an area of only 0.1 m^2. Incineration is also characterized by stabilization, pathogen elimination, and recycling. The time of reaction is short, so the waste can be treated rapidly.

Modern incinerators offer a proven way to route waste away from landfills and at the same time facilitate the recovery of energy contained in the waste [2]. Residual waste contains a substantial amount of energy. In terms of the possibility to use their heat of combustion, wastes are classified as [20]: combustible (paper, plastic, wood, leather, rubber, foods, gardening residues, textile fabrics) and non-combustible (glass, ceramic, stone, metal).

[1]Splaiul Independenţei 313, sector 6, Bucharest, 0724086492, nicoletaung@yahoo.com

The calorific value of mixed waste ranges from 7.500 to 11.000 kJ/kg. Mainly in the last years, the calorific value of municipal waste increased due to the efforts to recycle the glass, metals and kitchen waste. Figure 1 presents the percentage composition of MSW collected in the member states of the European Union in 2012.

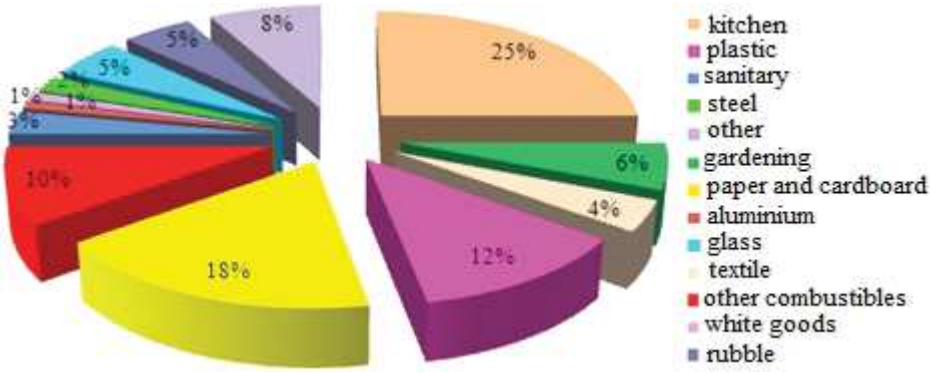

Figure 1: The composition of municipal solid waste in the EU, in 2012 [21]

Incineration with energy recovery is considered a process of recovery and incineration without energy recovery is a disposal process [20]. According to Eurostat, in 2010, in the 27 Member States of the European Union, 87.7 million tons of waste (of which, approximately 1.5 million tons in Romania) were incinerated with energy recovery, and 41.44 million tons of waste (of which, 74.520 tons in Romania) were incinerated without energy recovery [18].

2. METHODOLOGY

Figure 2 presents the simplified model of a solid waste incinerator. The most important part of the incineration plant is the furnace, whose role is to ensure the continued, controlled and complete incineration of waste.

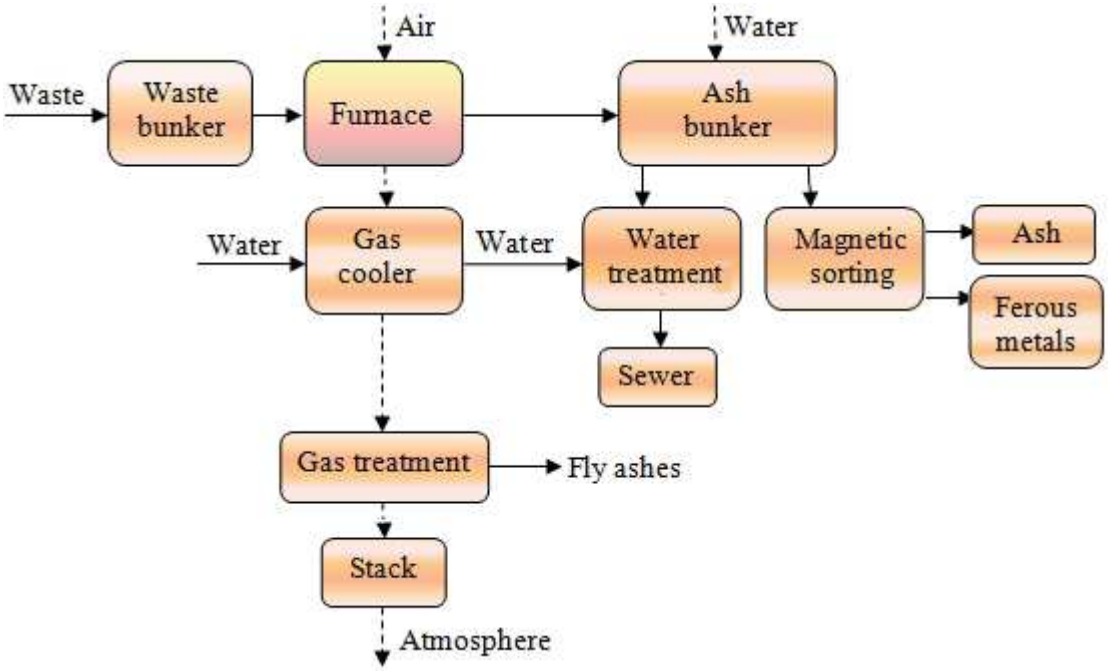

Figure 2: Simplified model of a waste incineration plant [15]

Therefore, a basic requirement is to introduce an air under the incineration grate and to ensure its proper control. Combustion temperature should be kept at 850-1100°C and furnaces

must be massive and high to ensure good turbulence of the air (this is a prerequisite for proper combustion). In order to start the ignition, is necessary the use of a support flame.

In such incinerator, the combustion processes are carried out with the following characteristic steps [14]:

a) *drying*: under the action of heat radiated in the furnace, the air introduced, in the majority of cases pre-heated, and the recirculated hot combustion gases, a large part of the moisture of waste is converted to steam which is then removed in mixture with flue gas;

b) *conversion*: by uniform application of heat, relatively large amount of various volatile substances and semicoke gases are eliminated from the waste. The characteristic of these gases is that they ignite at relatively low temperatures (250ºC). Waste incineration will begin immediately after ignition of evolved gases;

c) *combustion*: by enabling the proper conditions, waste will burn continuously without the addition of auxiliary fuel. The burning rate of the emitted gas depends on the thermal conductivity, the loading capacity of the combustion grate, the amount of air introduced into the furnace. The burning rate can be increased by reducing the amount of waste contained in the grate and by preheating the air introduced into the incinerator;

d) *post-combustion* is the last stage of the incineration, when the particulate matter fallen from the combustion grate continues burning on an additional grate (post-combustion grate) mounted in the extension of the main grate, or are are placed in a vertical well mounted at the lower end of the combustion grate and through the layer of waste is injected from the bottom up a stream of air, optionally with the addition of steam. In some cases it can be used the solution in which the slag (the matter subjected to the post-combustion) is introduced into a post-combustion rotating drum with very low rotation speed (4-8 revs/h).

Figure 3 shows the input and output parameters specific to waste incineration: yellow represents the residual materials, blue indicates the negative outputs (the environmental costs), and green represents the positive outputs of incineration (the environmental benefits).

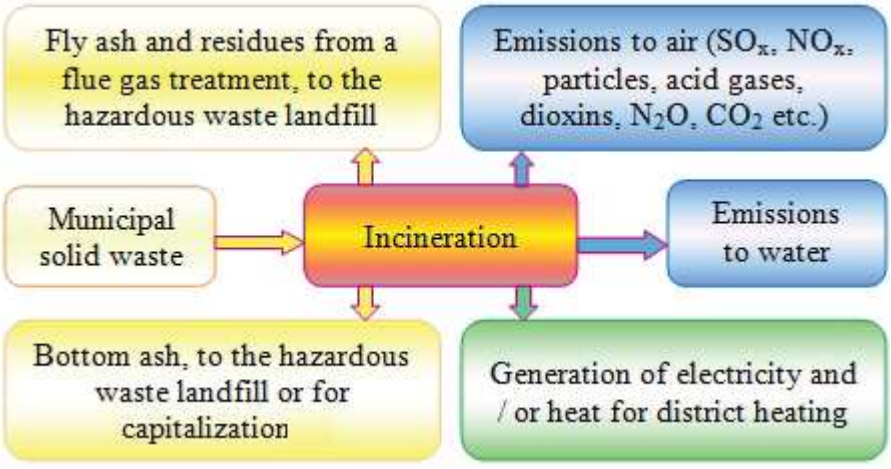

Figure 3: Input and output parameters specific to waste incineration [6]

Incineration of municipal waste involves the generation of greenhouse gases in the atmosphere: carbon dioxide (CO_2), nitrous oxide (N_2O), nitrogen oxides (NO_x), ammonia (NH_3), carbon monoxide (CO), volatile organic compounds (COV), and persistent organic pollutants (e.g. furans and dioxins) and certain heavy metals (Pb, Cu, Cd, Cr, Ni, Hg) [7].

Dioxins are highly toxic chemicals that may occur in the incineration of household waste containing plastic or wood treated with chlorine chemicals. Furans are combinations of

organic liquid chemicals resulting from the distillation of pine resins and they are used as an important intermediate in the synthesis of plastics and in the pharmaceutical industry.

In the incineration, the dioxins / furans are formed by the so-called "de novo" synthesis, from various non-extractable carbon structures, or by forming the precursor / reactions of the structures derived from incomplete aromatic oxidation or cyclization of hydrocarbs fragments. Generally, the formation of these toxic substances takes place in the presence of a surface or structure of carbon (e.g., the fly ash), organic or inorganic ions of chlorine, copper or iron (as a catalyst), in an oxidizing atmosphere and, ideally, at temperatures of 250 - 450 °C [3].

Usually, the normal operation of waste incineration plants does not generate methane (CH_4). The methane only occurs in exceptional cases and in small quantities (from the fermentation of waste remaining in the waste bunker) so that in quantitative terms the CH_4 generated by incineration is not considered dangerous for the climate.

Carbon dioxide is the chief climate-relevant emission of waste incineration and is higher by 10^2 than other emissions. The incineration of 1 Mg of municipal solid waste is associated with the release of about 0.7 to 1.2 Mg of carbon dioxide [10].

The solid residues of waste incineration are fly ash, bottom ash and air-pollution control residues. Fly ash ranges from 1.6 to 8.7% of the incinerated waste, depending on the waste input and combustion technology. Bottom ash is the residual material in the combustion chamber and it contains the non-combustible constituents of the waste feed (stones, bricks, glass, ceramic, plastic and wood) and metals that can be recovered and recycled. The amount of bottom ash is influenced by the level of waste pretreatment.

In the European Union, the impact of waste incineration on the environment (air, water, soil) is assessed by the Directive on the limitation of air emissions of pollutants from large incineration plants (Directive 2001/80/EC) and the impact of energy generation from waste treatment processes is mitigated by the Waste Incineration Directive (Directive 2000/76/EC).

In recent years, owners of waste incinerators were forced to improve their systems to reduce emissions of particulate and gaseous pollutants from flue gases released into the atmosphere. Equipment such as electrostatic precipitator, fabric filter, wet scrubber or dry /semi-dry absorption systems as well as catalytic or non-catalytic reduction in various combinations guarantee emissions that remain safely below the legal requirements.

3. RESULTS

The mass balance of a waste incineration plant has shown that by the incineration of 1 ton of waste, which requires the injection of 4000-4500 m^3 air, were obtained: 220 kg bottom ash, 30 kg fly ash and 30 kg metals (which is a reduction by 280 kg of the initial mass of waste) [4].

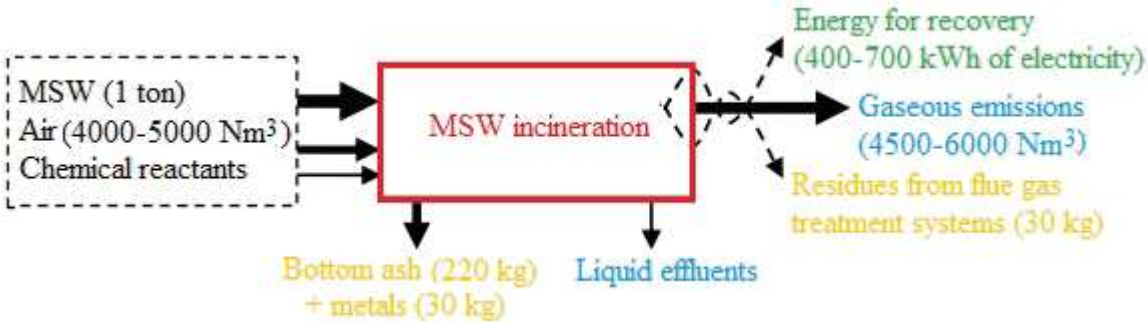

Figure 4: Mass balance at the incineration of a ton of municipal solid waste [16]

The volume of flue gas varies between 4600–6000 Nm^3/ton of waste, and the recovered

energy is 400–700 kWh as electricity, respectively 1205 kWh as heat. At the exit from the stack, the flue gases contain 11–19 g dust, 40–50 g SO_2, 800–900 g NO_x, 30–40 g HCl and 5–40 mg Hg [17]. The amount of solid residues (slag and ash), based on the amount of waste represents 10 - 15% by volume and 20-50% of the mass of waste. The residual bottom ash amounts for about 80% of the solid residues generated after incineration (bottom ash, fly ash, boiler ash, etc.).

Similar amounts are obtained at the incineration of a ton of waste from a grate incineration plant for municipal solid waste, consisting in grate firing, multistage flue gas cleaning, liquid and solid residue treatment. In this case, solid residues consist of 220 kg slag, 25 kg metals, 20 kg fly ash, 5 kg gypsum and 1 kg filter cake. The solid residues from residual waste incineration only make up 25 - 30% of the untreated residual waste volume. Due to the high density of these residues, the landfill volume required is only 10% of the original volume [13].

Figure 5: Mass balance for solid residues from a grate incineration plant [13]

Another example for the specific mass flows of a fluidized bed combustion plant with the annual throughput of 80.000 tons, shows that by incinerating 1 ton of waste (910 kg residual materials and 90 kg sewage sludge), are obtained 93 kg bed ash, 137 kg boiler ash, 25 kg filter particulates, 0.4 kg neutralization sludge and 0.1 kg gypsum, which is 255 kg of solid residues [13].

There are various possibilities to recover some of the residues from waste incineration. A significant amount of the solid residues can be recovered for recycling (e.g. metals or gypsum).

Bottom ash contains CaO, SiO_2, Fe_2O_3 and Al_2O_3. Metal recovery from bottom ash generally has the highest priority due to prices and environmental considerations. The mineral fraction in the bottom ash is used in the production of cement and concrete, road pavement, glass, ceramics, adsorbents and zeolite. After proper treatment for the removal of heavy metals, the ash can be used in agriculture, because its content of phosphorus and potassium may partly replace the commercial fertilizers, and the lime in fly ash can reduce soil acidity [11]. In some European countries (e.g. Denmark, Germany and the Netherlands) the use of mineral fraction is very high (up to 98%). Other countries do not gain the full benefits of bottom ash, which is instead landfilled [1].

By concentrating the inorganic substances in certain residue streams (e.g. particulate matter or filter cake with an increased heavy metal content), they can be prepared for mechanical treatment with the aim of metal recovery, or at least controlled landfill disposal [13].

However, given the evidence of heavy metal contamination of the bottom ash and the toxicity of fly ash, their capitalization poses serious concerns about environmental contamination and threats to human health [4].

4. CONCLUSIONS

The incineration of municipal solid waste plays an important role in all waste management systems, mostly because it is an advantageous method of waste treatment in the context of constant production growth and rapid world-wide urban expansion.

Incineration reduces substantially the mass and volume of the solid waste, and this implies a lower need for landfilling. The heat produced during incineration is further used for steam generation.

Special attention should be paid to the effectiveness of the systems for flue gas treatment, because these gases contain furans and dioxins.

Bottom ashes are solid residues that can be capitalized mainly as construction materials, but they can contain high concentrations of hazardous substances that would be a serious threat for human health and environment, if they are not properly managed.

References

[1] Allegrini, E., Maresca, A., Olsson, M., E., Holtze, M.,S., Boldrin, A., Astrup, T., F., *Quantification of the resource recovery potential of municipal solid waste incineration bottom ashes*. Waste management, vol. 34, pp. 1627-1636, 2014.

[2] Astrup, T., Pedersen, A., J., Hyks, J., Frandsen, F., J., *Residues from waste incineration*, Final report PSO-5774, Technical University of Denmark, 2010.

[3] Batterman, S., *Assessment of small-scale incinerators for health care waste*, Completed for Water, Sanitation and Health Protection of the Human Environment World Health Organization, 2004.

[4] Bell, L., Bremmer, J., *Burning waste for energy it doesn't stack-up. Exposing the push towards unsustainable waste to energy technology in Australia*, 2013.

[5] Bontoux, L., *The incineration of waste in Europe: issues and perspectives*. Institute for Prospective Technological Studies Seville. EUR 18717 EN, 1999.

[6] Economic Analysis of Options for Managing Biodegradable Municipal Waste. Final Report to the European Commision. Eunomia Research & Consulting.

[7] EMEP/EEA emission inventory guidebook, Municipal waste incineration, NFR 5.C.1.a. Incineration of domestic or municipal waste (without energy recovery), 2013.

[8] Environment in the EU, 54/2015, http://ec.europa.eu/eurostat/documents/%202995521/6757479/8-26032015-AP-EN.pdf.

[9] Flue gas cleaning. Steinmüller Babcock Environment. Nippon Steel & Sumikin Engineering Group.

[10] Good practice guidance and uncertainty management in national greenhouse gas inventories. Emissions from waste incineration, pp. 455-468.

[11] Lam, C.,H.,K., Ip, A.,W.,M., Barford, J.,P., McKay, G., *Use of incineration MSW ash: a review*, Sustainability Journal, vol. 2, pp. 1943 – 1968, 2010.

[12] Municipal solid waste incineration. World Bank Technical Guidance Report, Washington D.C., 1999.

[13] Neubacher, F., Kurz, G., *Technical requirements for incineration of residual waste*, A guideline in good practice, Edited by Bulgarian Ministry for Environment and Water, 2013.

[14] Păunescu, I., Paraschiv, G., *Installations for waste recycling*, Agir Publishing, Bucharest, 2006.

[15] Pode, V., *Waste management and incineration*. Politehnica Publishing, Timişoara, 2005.

[16] Quina, M.,J., Bordado, J.,M., Rosa, M., Quinta-Ferreira, R.,M., *Air pollution control in municipal solid waste incinerators. The impact of air pollution on health, economy, environment and agricultural sources*. Edited by Dr. Mohamen Khallaf, published by InTech, pp. 331 – 358, 2011.

[17] Tang, P., Florea, M.,V.,A., Spiesz, P., Brouwers, H.,J.,H., *Characteristics and application potential of municipal solid waste incineration (MSWI) bottom ashes from two waste-to-energy plants*, Construction and Building Materials, vol. 83, pp. 77-94, 2015.

[18] http://appsso.eurostat.ec.europa.eu/nui/submitViewTableAction.do.

[19] http://ec.europa.eu/eurostat/web/waste/waste-generation-and-management/management/incineration.

[20] http://fluid.wme.pwr.wroc.pl/~spalanie/dydaktyka/combustion_MiBM/waste/waste_incineration_plants.pdf

[21] https://www.zerowasteeurope.eu/2012/05/the-european-parliament-votes-in-favour-of-almost-zero-waste-for-2020/

EXPERIMENTAL RESEARCHES ON ANALYSING THE COMPOSITION OF BIOGAS RESULTED FROM THE PROCESS OF ANAEROBIC DIGESTION

PhD. Eng. Voicea Iulian[1)], PhD. Stud. Eng. Găgeanu Iuliana[1)], PhD. Eng. Matache Mihai[1)], PhD. Stud. Eng. Cujbescu Dan[1)], PhD. Stud. Eng. Persu Cătălin[1)], PhD. Eng. Dilea Mirela[2)] PhD. Eng. Ungureanu Nicoleta[2)], Eng. Bota Sorin Ovidiu[3)], PhD. Eng. Caba Ioan[1)]
[1)] INMA Bucharest, [2)]University Politehnica of Bucharest
[3)] BUILD PR CONSULTING SRL Cluj Napoca

ABSTRACT

Anaerobic digestion is a biochemical process through which, complex organic substrates (plant biomass and waste, manure, organic waste, wastewaters, sludge from sewage systems, etc.) are decomposed in the absence of oxygen to the point of biogas and digestate, by various types of bacteria. Within the paper was achieved a monitoring of the composition of biogas resulted after a 35 days anaerobic fermentation cycle. Thus, compared to other biofuels, biogas requires the lowest contribution of technological water, an important aspect in the view of the envisaged water crisis, expected in many regions of the world.

1. INTRODUCTION

The fight against global warming represents one of the main priorities of European policies for energy and environment. European directives on the production of renewable energy, on reducing greenhouse gas emissions and on sustainable waste management are based on the commitment of member states to implement adequate measures for fulfilling them. The production and use of biogas from anaerobic digestion has the potential of complying with all three directives simultaneously, [1, 2].

One of the main advantages of biogas production is the capacity to transform waste into valuable resources, by using them as raw materials for the process of anaerobic digestion. Many EU countries are confronted with huge problems, associated to an overproduction of organic waste resulted from the industry, agriculture as well as from household activities. Biogas production represents a very good way to satisfy national and European regulations in the fields, which are becoming more and more restrictive, and also of using organic waste for producing energy, followed by recycling them in the form of fertilisers, [3]. Biogas production technologies contribute to reducing waste volume, as well as costs determined by their removal.

A biogas installation does not only constitute an energy supplier. The biomass resulted from the process of anaerobic digestion, called digestate, represents a valuable soil fertilizer, rich in nitrogen, phosphorus, potassium and micronutrients, and can be applied on the field using normal equipment that are also used for liquid manure. Compared with raw manure, the digestate shows an improved efficiency as fertilizer, due to its high homogeneity and to the high availability of nutrients, a good C/N ratio and the almost complete lack of unpleasant odour, [4].

Nutrient circuit, through the process of biogas production – from the production of raw materials until applying the digestate as fertilizer – is a closed one. Carbon (C) compounds are

[1], National Institute of Research - Development for Machines and Installations Designed to Agriculture and Food Industry INMA, Bucharest, Romania, tel: 0752161780, e-mail: voicea_iulian@yahoo.com

reduced in the process of anaerobic digestion, methane (CH_4) being used for producing energy, while carbon dioxide (CO_2) is released into the atmosphere, from where it is taken by plants, during photosynthesis. Some carbon compounds remain in the digestate, improving the carbon content of soils when the digestate is used as fertilizer, [5]. Biogas production can be fully integrated in the activity of conventional or organic farms, where the digestate replaces common inorganic fertilizers, produced with high consumption of fossil energy.

In the last years, the international biogas market has grown by 20 up to 30% every year. In Europe, countries such as Austria, Denmark, Germany and Sweden are among the most experienced ones when it comes to biogas technologies and have managed to establish competitive national markets in the field. To develop these markets, intense R&D researches were conducted, and biogas sectors have received considerable governmental subventions and have benefitted from public support. The involved farmers, operators of biogas factories as well as investors have accumulated important knowledges, private technical information and expertise regarding biogas technologies. Besides the traditional types of raw materials, in countries such as Germany and Austria was initiated the cultivation of energetic plants for biogas production. Important research efforts were made in the direction of increasing the productivity and diversity of energetic plants, as well as for evaluation their potential for biogas, [6]. A series of new agricultural practices, new systems for crop rotation, intercrop and combined crop were defined, making the object of intensive research and development. In the last years, important researches were conducted regarding technologies for converting raw materials into biogas. New types of digesters, feeding systems, storage facilities as well as an entire series of other equipment were introduced and adapted. Both dry AD systems as well as wet ones are continuously improved, through high level research activities that are focused both on ensuring the stability of operations and processes, on performances, as well as on finding new substrate combinations.

The use of biogas for the combined production of heat and electricity (CHP) has become the standard application for the greater part of biogas projects in Europe. In countries such as Sweden, The Netherlands and Germany, improved biogas was also used as biofuel for transportation. In these countries distribution networks were established and stations for improvement and packaging were built. Improving biogas and feeding the natural gas network represents a relatively new application, and the first installations for feeding the natural gas network with biomethane were achieved in Germany and Austria. The newest biogas use is in the field of electric piles, which already represents an evolved and commercially available technology, operating in countries such as Germany.

Anaerobic digestion represents a biochemical process through which, complex organic substrates (plant biomass and waste, manure, organic waste, residual water, sludges from sewage systems, etc.) are decomposed, in the absence of oxygen, up to the state of biogas and digestate, by various types of anaerobic bacteria, [7].

The substrates of the AD process can be classified depending on their origin, dry matter (DM) content, methane production as well as other criteria. Substrates with dry matter content smaller than 20% are used for the so called wet digestion (named wet fermentation). This category includes manure and also organic waste from the food industry. When the dry matter content is higher than 35%, the digestion type is called dry digestion (dry fermentation). Dry digestion is typical in the case of energy crops and silage materials. Choosing the type and quantity of raw material for obtaining the substrate mixture subjected to anaerobic digestion depends on the content of dry matter, as well as on its content of sugars, fat and proteins, [8].

During the process of anaerobic digestion, a very small quantity of heat is released, compared to the case of aerobic decomposing (in the presence of oxygen), for example composting. The energy contained in the chemical bonds of the substrate mainly remains stored in the biogas produced, in the form of methane. The process of forming biogas is the

result of successive stages in which the initial substances are continuously decomposed into smaller and smaller molecules. In each stage, specific groups of microorganisms are involved. A process of anaerobic digestion comprises four main stages, namely: hydrolysis, acidogenesis, acetogenesis and methanogenesis.

Theoretically, hydrolysis is the first stage in the process of anaerobic digestion, during which complex organic substances (polymers) are decomposed into smaller substances, called mono or oligomers. Polymers such as sugars, fats, nucleic acids and proteins are transformed into glucose, glycerol, purines and pyrimidines. Hydrolytic bacteria release hydrolytic enzymes, transforming biopolymers into smaller soluble compounds. In the hydrolysis process, a large variety of bacteria is involved, the process being achieved through the means of bacterial exoenzymes attacking the particulate undissolved matter. The products resulting from hydrolysis are further decomposed/digested by the bacteria involved in the process and will be then used within their own metabolism.

During the acidogenesis stage, the hydrolysis produces are transformed by acidogenic (fermentative) bacteria into methanogenic substrates. Simple sugars, amino acids and fatty acids are degraded to acetate, carbon dioxide and hydrogen (70%) as well as to volatile fatty acids (VFA) and alcohols (30%).

During acetogenesis, the products resulted from acidogenesis that cannot be directly transformed into methane by methanogenic bacteria are transformed into methanogenic substrates. VFA and alcohols are oxidised to methanogenic substrates, such as: acetate, hydrogen and carbon dioxide. Both VFA and alcohols with chains of carbon atoms longer than one unit are oxidised to acetate and hydrogen. Hydrogen occurrence leads to the increase of its initial pressure. This can be seen as a "residual product" of acetogenesis and inhibits the metabolism of acidogenic bacteria. During methanogenesis, hydrogen is transformed into methane. Acidogenesis and methanogenesis usually take place at the same time, as symbiosis of two groups of microorganisms.

Methanogenesis represents a critical stage of the entire digestion process, also consisting in the slowest biochemical reactions of the process. Methanogenesis is strongly affected by the operating conditions. The composition of raw materials, charging rate, temperature and pH are examples of factors influencing methanogenesis. Overloading the digester, temperature variation or a massive inlet of oxygen usually determines a stop in methane production. The production of methane and carbon dioxide from intermediary reaction products is achieved by methanogenic bacteria. 70% of the methane formed originates from acetate while the rest of 30% is produced through hydrogen and carbon dioxide conversion.

2. METHODOLOGY

Therefore, in order to solve current problems raised by the high quantities of waste generated within a micro agro-zootechnical farm, within the project "*INNOVATIVE TECHNOLOGY FOR OBTAINING BIOGAS THROUGH ADVANCED METHANOGENESIS*" was achieved an experimental model of an installation for obtaining bioenergy through dry and wet advanced methanogenesis – MGA. ***The experimental model (EM)*** *of modular installation for obtaining bioenergy through dry and wet advanced methanogenesis – MGA, is composed of the* ***following parts****:*

- Modular container (fig. 1);
- Digester for the process of dry anaerobic digestion (fig. 2);
- Digester for the process of wet anaerobic digestion (fig. 3);
- Heating system (electric boiler) (fig. 4);
- Green energy supply system (photovoltaic panels) (fig. 5);
- Monitoring and control system for the MGA modular installation (fig. 6).

Figure 1: Modular container

Figure 2: Digester for dry anaerobic digestion process

Figure 3: Digester for wet anaerobic digestion process

Figure 4: Heating system

Figure 5: Green energy supply system

Figure 6: MGA Monitoring and control system

The raw material used for the process of dry anaerobic digestion was represented by chopped miscanthus mixed with silage corn. The active control and monitoring of the modular experimental installation for obtaining bioenergy through methanogenesis of organic waste (MGA) was achieved using a programable logic controller (PLC), programmed through the means of a graphic operator interface represented by an operating terminal – OT.

The parameters of the dry anaerobic digestion process that were chosen to be monitored and controlled using the installation's automation system were the following ones:

- The temperature of the process of anaerobic digestion was 39ºC;
- The pH of the process was set and maintained at the value of 7;
- The time of retention in the digesters was 35 days;
- The C/N ratio achieved in the two digesters was 20;
- The moisture of the mix achieved in the digester with dry fermentation was 45%.

The experimental research of analysing the composition of biogas resulted through the process of dry anaerobic digestion was achieved using a COMBI IR system for determining biogas composition. The Mentor/ComIR Series uses the latest miniature infrared technology for the detection of CH4 and CO2. Each sensor has a 0-100% Volume range which is necessary for the biogas application. The use of infrared sensors means that the level of CO2

can be measured accurately and the CH4 sensor cannot be poisoned if high levels of H2S are present. The unit is fitted with following sensors: 0-100% Volume CH4 (infrared), 0-100% Volume CO2 (infrared), 0-200 ppm H2S.

Figure 7: System for analyzing biogas composition

The testing methodology involved the determining of biogas composition 3 times per day, for 35 days while the experiment was conducted. The average CH_4 volume, the average H_2S, respectively the average CO_2 percentage were determined per fermentation day. In figure 8 are presented the average experimental data obtained for the composition of biogas obtained through the process of dry anaerobic digestion.

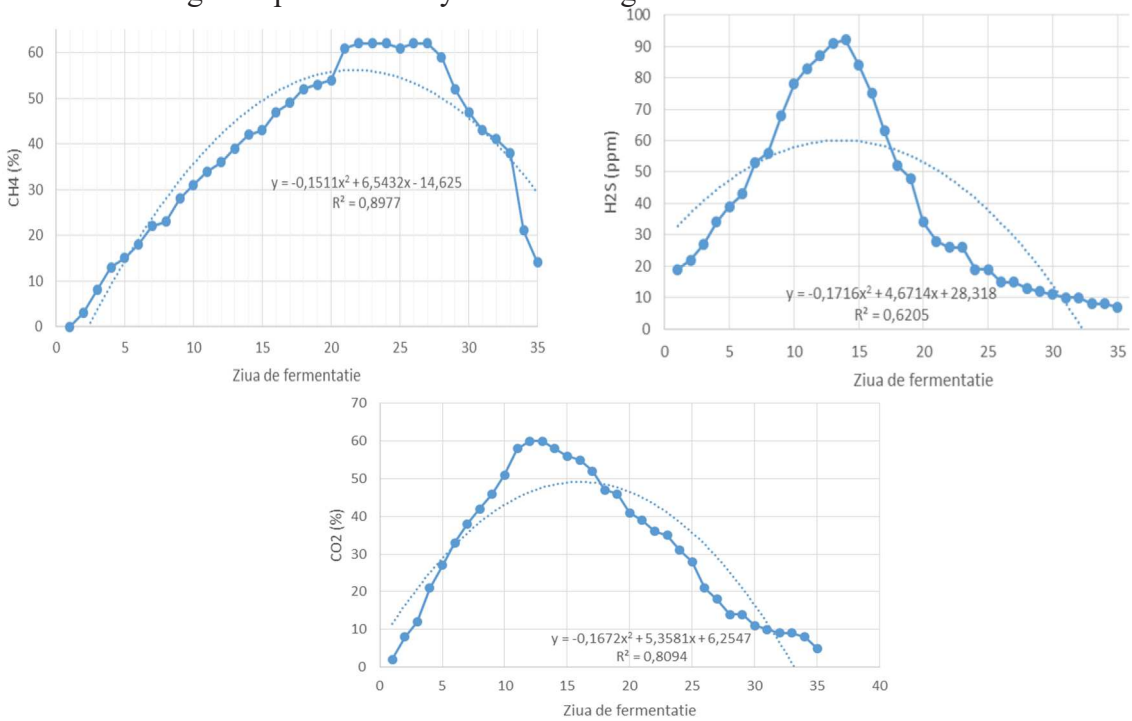

Figure 8: Experimental research on the analysis of the composition of biogas resulted from the process of dry anaerobic digestion

3. CONCLUSIONS

Based on the experimental data resulted, the following conclusions can be given:

1. The maximum CH_4 concentration in the composition of biogas obtained through the process of dry anaerobic fermentation was 64% and the fermentation period was recorded

to be between days 21 and 27. The average CH_4 value recorded in the composition of biogas in the 35 days of dry anaerobic digestion was 42%.

2. The maximum H_2S concentration in the composition of biogas obtained through the process of dry anaerobic fermentation was 92 ppm and the fermentation period was recorded to be between days 12 and 15. The average H_2S recorded in the biogas composition in the 35 days of dry anaerobic digestion was 36 ppm.
3. The maximum CO_2 concentration in the composition of biogas obtained through the process of dry anaerobic fermentation was 60% and the fermentation period was recorded to be between days 12 and 13. The average CO_2 recorded in the biogas composition in the 35 days of dry anaerobic digestion was 34%.
4. Biogas resulted from the process of dry anaerobic digestion using the experimental model for obtaining bioenergy through advanced dry and wet methanogenesis – MGA showed an adequate CH_4 content that allowed it to be successfully burned in the biogas generator and to be converted into electric energy that was used for the energetic independence of the installation.

Acknowledgement

This work was funded by the Executive Agency for Higher Education, Research, Development and Innovation Funding, within the project entitled "PN 16 24 04 03**:** Innovative technology for obtaining biogas through advanced methanogenesis " ctr. 8N/09.03.2016 / Act. Ad. nr.1/2017.

References

[1]. Ahlberg-Eliasson K., Nadeau E., Leven L., Schnurer A., *Production efficiency of Swedish farm-scale biogas plants*, Biomass and Bioenergy 97, pp. 27 – 37, 2017;

[2]. Demirel B., Scherer P.*, Trace element requirements of agricultural biogas digesters during biological conversion of renewable biomass to methane*, Biomass and Bioenergy 35 (3), pp. 992 – 998, 2011;

[3]. Hejnfelt A., Angelidaki I., *Anaerobic digestion of slaughterhouse by-products*, Biomass and Bioenergy 33 (8), pp. 1046 – 1054, 2009;

[4]. Mata-Alvarez J., Dosta J., Romero-Gueiza M.S., Fonoll X., Peces M., Astals S., *A critical review on anaerobic co-digestion achievements between 2010 and 2013*, Renewable Sustain. Energy Rev. 36, pp. 412 – 427, 2014;

[5]. Moeller H.B., Sommer S.G., Ahhring B., *Methane productivity of manure, straw and solid fractions of manure,* Biomass and Bioenergy 26 (5) , pp. 485 – 495, 2014.

[6]. Nielsen – Holm J.B., Seadi T. Al., Oleskowicz-Popiel, *The future of anaerobic digestion and biogas utilization*, BioResources Technology 100(22), pp. 5478 – 5484, 2012;

[7]. Ward A.J., Hobbs P.J., Holliman P.J., Jones D.L., *Optimisation of the anaerobic digestion of agricultural resources*, BioResources Technology 99 (17), pp. 7928 – 7940, 2008;

[8]. Westerholm M., Hansson M., Schnurer A., *Improved biogas production from whole stillage by co-digestion with catle manure*, BioResources Technology 114, pp. 314 – 319, 2012;

CONSIDERATION ON THE CONSTRUCTIVE FACTORS OF CLARIFIERS AND THEIR INFLUENCE ON THE SETTLING PROCESS EFFICIENCY – A REVIEW

B.Șt. Zăbavă[1], Gh. Voicu[1], N. Ungureanu[1], M. Dincă[1], M. Ionescu[1], M. Munteanu[1], A. Pruteanu[2]
[1] Politehnica University of Bucharest, Faculty of Biotechnical Systems Engineering, Romania
[2] INMA Bucharest, Romania

ABSTRACT

Nowadays, the destruction and pollution of our environment has produced a growing awareness worldwide of the need for more effective wastewater treatment. Sedimentation is the oldest and most widely used unit operation in water and wastewater treatments. Sedimentation is the process of removing solid particles heavier than water by gravity settling. The terms sedimentation, settling, and clarification are used interchangeably. The unit sedimentation basin may also be referred to as a sedimentation tank, clarifier, settling basin, or settling tank. In wastewater treatment, sedimentation is used to remove both inorganic and organic materials which are settleable in continuous-flow conditions. This paper presents the results obtained in some research focused on wastewater decanting processes using different constructive variants of settling tanks.

1. INTRODUCTION

Sedimentation is perhaps the oldest and most common water treatment process. The principle of allowing turbid water to settle before it is drunk can be traced back to ancient times. In modern times a proper understanding of sedimentation tank behavior is essential for proper tank design and operation. Generally, sedimentation tanks are characterized by interesting hydrodynamic phenomena, such as density waterfalls, bottom currents and surface return currents, and are also sensitive to temperature fluctuations and wind effects [1].

Sedimentation (settling) is the separation of suspended particles that are heavier than water. The sedimentation of particles are based on the gravity force from the differences in density between particles and the aid. Sedimentation is widely used in wastewater treatment systems. A successful sedimentation is crucial for the overall efficiency of the plant [2].

Sedimentation tanks are divided into two main categories in type and concentration of sludge and particles which are available in them. Primary settling tanks have low influent concentration. Flow field in them is not much influenced by concentration field and buoyancy effects can be negligible. However, secondary or final-settling tanks have higher influent concentration. They usually are placed after primary tanks and activation tanks. So they usually contain activated sludge and as a result of this, size of particles would grow and flow-field is influenced by the concentration distribution [3].

The settler has two functions; clarication and sludge separation. That is to remove essentially all of the solids from suspension and to concentrate theses solids (eg for recycling to the aeration basin). Depending on the particles concentration and the interaction between particles, four types of settling can occur, see also figure 1:

- *discrete particle settling*. The particles settle without interaction and occurs under low solids concentration. A typical occurrence of this type of settling is the removal of sand particles.
- *flocculent settling*. This is defined as a condition where particles initially settle independently, but occulate in the depth of the clarification unit. The velocity of settling

[1] Splaiul Independentei 313, Sector 6, Bucharest, 0731538941, bianca.dragoiu@yahoo.com

particles are usually increasing as the particles aggregates. The mechanisms of occulent settling are not well understood.

- *hindered settling*. Inter-particle forces are sufficient to hinder the settling of neighboring particles. The particles tend to remain in a fixed positions with respect to each others. This type of settling is typical in the settler for the activated sludge process (secondary clarifier).
- *compression settling*. This occurs when the particle concentration is so high that so that particles at one level are mechanically in uenced by particles on lower levels. The settling velocity then drastically reduces.

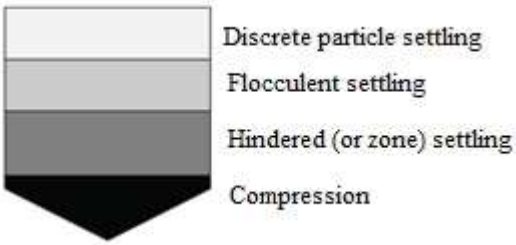

Figure 1: Settling phenomena in a clarifier [2]

2. METHODOLOGY

Enhancing the efficiency of the settling tanks is one of the most economical approaches for refining water. There are many works that have been published regarding simulation of settling process. The most representative are presented below.

D. Zârnoianu and al. studied the decantation processes for wastewater on an experimental plant formed by two constructive varieties for the clarifiers with tangential inlet and spillway threshold: without a device for removing decanted sludge and equipped with device for removing sludge.

In figure 2 are presented the compared variations in time for the efficacy of separating for the two types of decantors (without scraper and with scraper) and in figure 3, the variation of the suspension's concentration in mud for the two types of clarifiers (without scraper and with scraper).

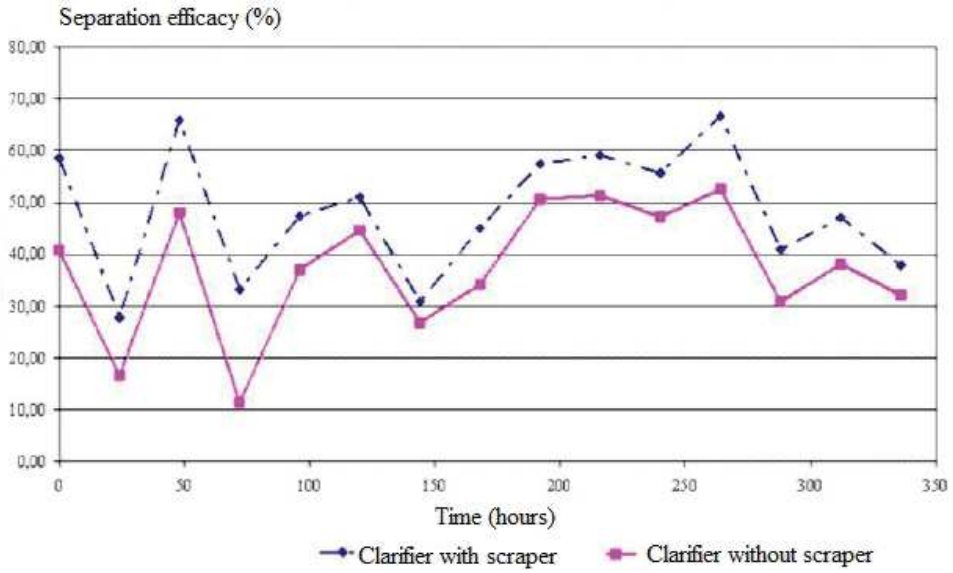

Figure 2: Variation in time of the efficacy of separating impurities in the clarifier with scraper and without scraper [4]

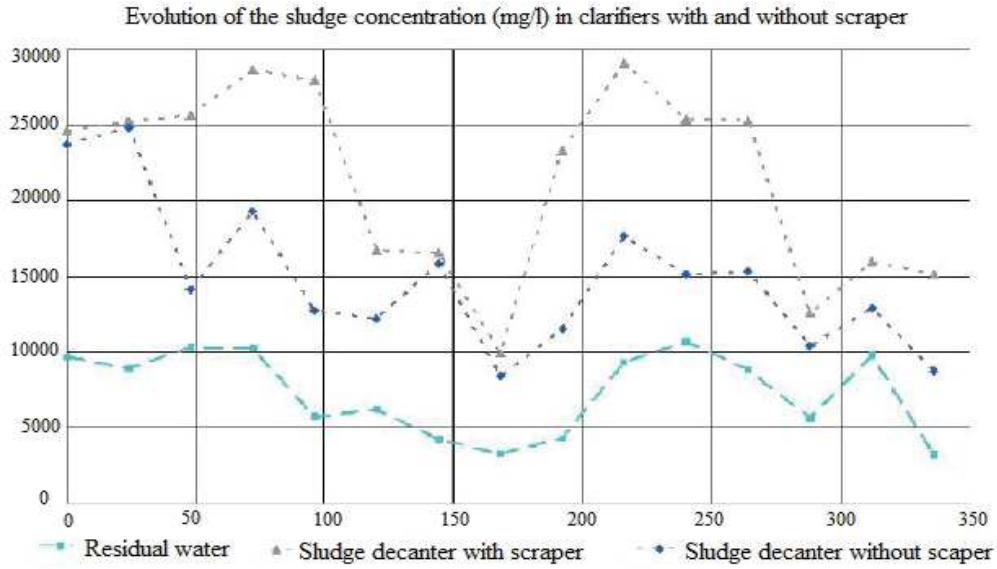

Figure 3: Variation in time of the suspension's concentration of mud for the two types of clarifiers [4]

Results showed that the efficiency of separating suspensions from residual waters is superior for the clarifiers with devices for scraping, compared to the one of the clarifiers without scraping devices, a fact leading to the reduction of solids concentration in the discharged (clear) water. Therefore, it is recommended to use clarifiers with tangential inlet and spillway threshold equipped devices for scraping the sludge, which come into operation automatically after filling the clarifier.

Another study made by D. Zârnoianu and al. was focused on wastewater decanting processes in a pilot test rig using 3 constructive variants of decanters: with tangential inlet and free exit, with tangential inlet and a discharge threshold and with deflection plates and a discharge threshold, respectively. Each decanter model used for testing was operated at three distinctive temperatures (100^0C, 85-90^0C and 75^0C) and also at four distinctive values of the wastewater feeding flow rate ($3m^3$ /h, $4m^3$ /h, $5m^3$ /h and $8m^3$ /h, respectively).

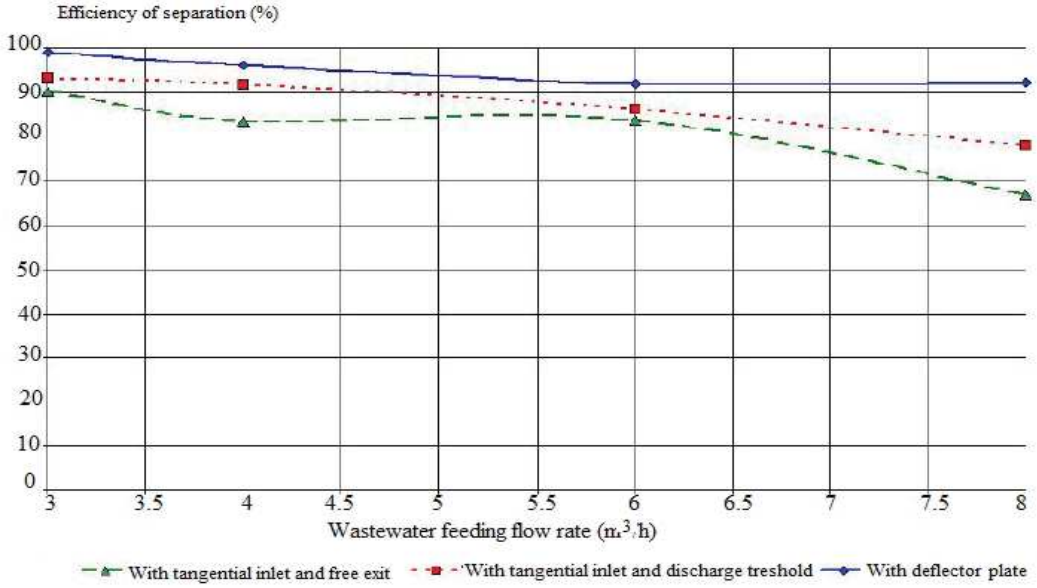

Figure 4: Evolution of the separation efficiency versus flow rate at 100^0C, for various types of decanters [5]

In the graph of figure 4 it can be observed that at a temperature of 100^0C a slight decrease of the separation efficiency with the increase of the decanter feeding flow rate occurs regardless of decanter type, and that the decanter with deflection plate presenting the best sedimentation efficiency and in the graph of figure 5 it can be seen that at medium temperatures (85-90^0C) the separation efficiency decreases visibly with increasing decanter feeding flow rate, regardless of its type, the best sedimentation efficiency being that of the decanter with deflection plate.

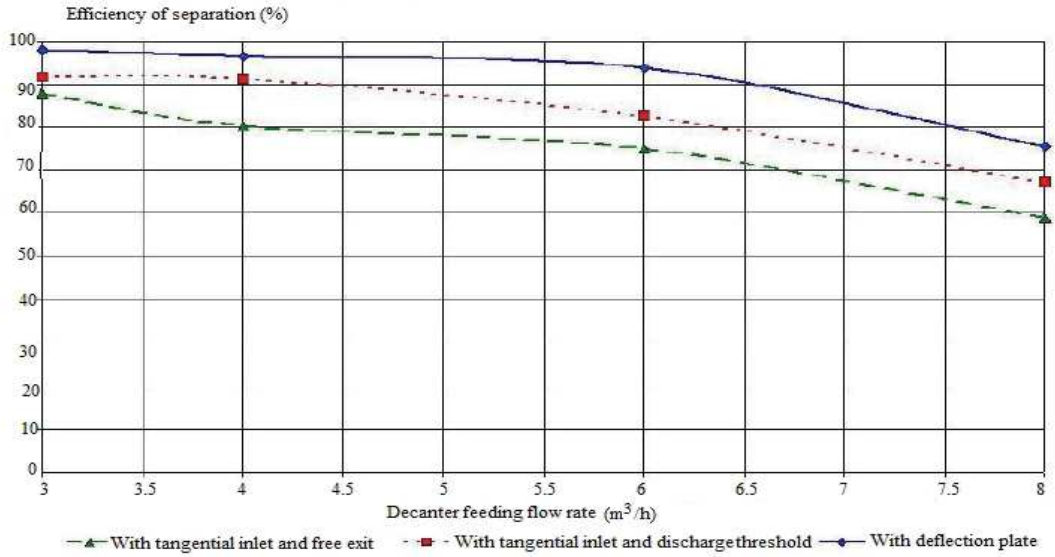

Figure 5: Evolution of the separation efficiency versus flow rate at 85-90^0C, for various types of decanters [5]

In the graph of figure 6 it can be seen that at a lower temperature (75^0C) a significant decrease of the separation efficiency occurs with increasing decanter feeding flow rate, regardless of its type, the best sedimentation efficiency being that of the decanter with deflection plate.

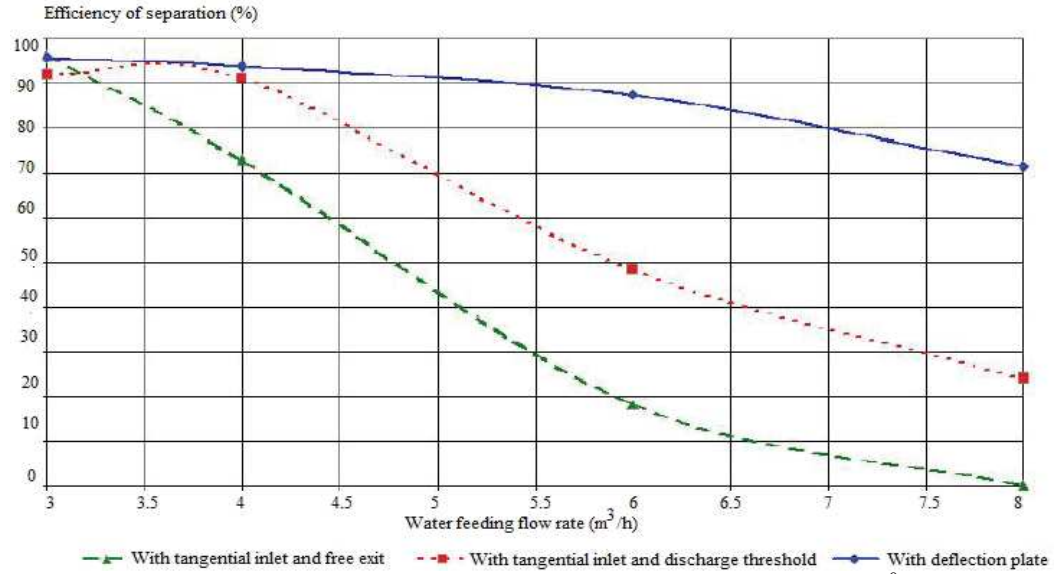

Figure 6: Evolution of the separation efficiency versus flow rate at 75^0C, for various types of decanters [5]

The results shows that the separation of the suspended particles by means of decanting wastewater is the more efficient the higher the inlet temperature and the smaller the feeding flow rate into the decanter are. Regardless of the flow rate magnitude and the temperature of the decanted water, the best efficiency is that of the decanter with deflection plate.

Circulation regions always exist in settling tanks. These regions would result in short-circuiting enlargement of the dead zone and high flow mixing problems and avoid optimal particle sedimentation. Therefore, the main objective of the tank design process is to avoid formation of the circulation zone, which is known as dead zone. Experiments show that the tank performance can be improved by altering the geometry of the tank which leads to a different velocity distributions and flow patterns.

The presence of a baffle and its effect on the hydrodynamics of the flow field has been investigated in a primary settling tank by A. Razmi et al. Hydrodynamics of the flow field in these basins is sophisticated. Therefore a numerical simulation has been provided to discover such flow field.

The experiments were conducted in a rectangular channel with and without baffles. In this study, a baffle was located in different distance from the inlet, s/L= 0.125, 0.15, 0.5 (figure 7).

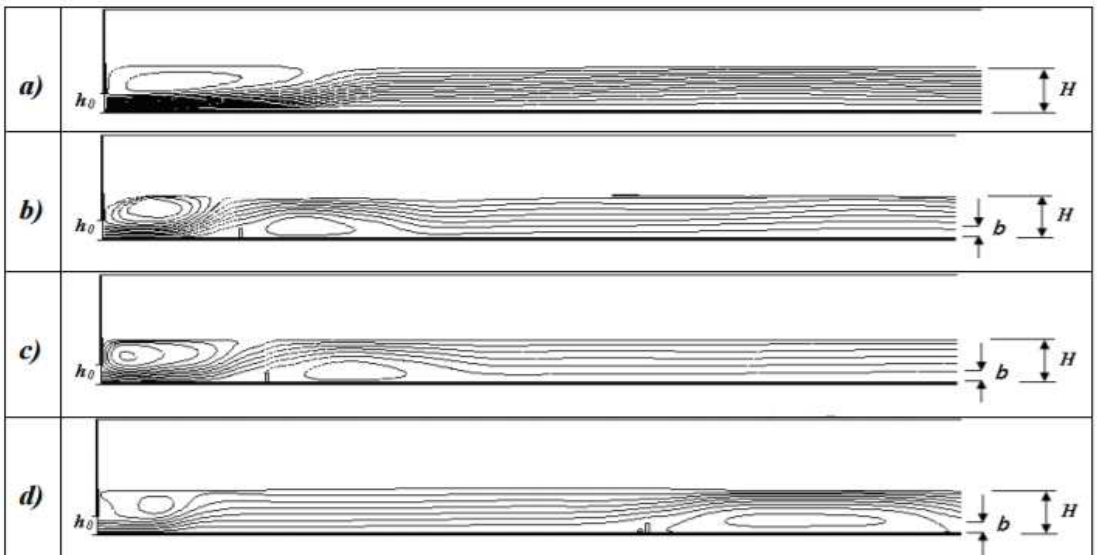

Figure 7: Streamlines of different baffle locations in settling tank from above: a) No baffle, b) s/L=0.125, c) s/L=0.15, d) s/L=0.5. [6]

Following experimental studies, it is observed that the best results were obtained by placing baffles in the vicinity of the inlet wastewater, optimal placement position of the baffle being at the s/L = 0.125.

Results show that this baffle can reduce the size of the dead zones and turbulent kinetic energy in comparison with the no-baffle condition.

Additionally, the formation of circulation regions reduced the efficiency of the sedimentation tank by short circuiting and this negative phenomenon is improved by proper position of the baffle. In other words, locating a baffle at an appropriate part of the tank prevents from formation the bottom jet moving to the surface of the basin and overflows at the outlet.

3. CONCLUSIONS

Sedimentation is perhaps the oldest and most common water treatment process. Sedimentation (settling) is the separation of suspended particles that are heavier than water.

Enhancing the efficiency of the settling tanks is one of the most economical approaches for refining water. In fact, many factors influence the tank's efficiency, amongst which the tank geometries is of primordial importance.

Experimental results showed that the efficiency of separating suspensions from residual waters is superior for the clarifiers with devices for scraping, compared to the one of the clarifiers without scraping devices and the separation of the suspended particles by means of decanting wastewater is the more efficient the higher the inlet temperature and the smaller the feeding flow rate into the decanter are.

The formation of circulation regions reduced the efficiency of the sedimentation tank by short circuiting and this negative phenomenon is improved by proper position of the baffle. Studies show that this baffle can reduce the size of the dead zones and turbulent kinetic energy in comparison with the no-baffle condition.

References

[1] A. H. Ghawi, J. Kriš "*A Computational Fluid Dynamics Model of Flow and Settling in Sedimentation Tanks*", Slovak University of Technology, Slovakia, 2005

[2] [B. Carlsson "*An introduction to sedimentation theory in wastewater treatment*" , Systems and Control Group Uppsala University Nov 96, rev Okt 98

[3] *A. Razmi , B. Firoozabadi , and G. Ahmadi* "*Experimental and Numerical Approach to Enlargement of Performance of Primary Settling Tanks*", Department of Mechanical and Aeronautical Engineering, Clarkson University, Potsdam, NY 13699, USA. April , 2008

[4] D. Zârnoianu , S. Popescu , C. Brăcăcescu "*Theoretical and experimental research on the separation process of impurities from waste water through decantation",* 6 th International Conference ″Computational Mechanics and Virtual Engineering ″ COMEC 2015, Brasov

[5] D. Zârnoianu, S. Popescu, M. Radu "*The influence of constructive factors and working conditions of decanters on wastewater processing efficiency*", 3 rd International Conference ″Research & Innovation in Engineering ″ COMAT 2014, Brasov

[6] A. Razmi, B. Firoozabadi, G. Ahmadi "*Experimental and Numerical Approach to Enlargement of Performance of Primary Settling Tanks*", Journal of Applied Fluid Mechanics, Vol. 2, No. 1, 2009

ASPECTS ON THE EFFICIENCY OF ROLL-OVER PROTECTIVE STRUCTURES TESTING

Sorin-Ştefan BIRIŞ[1], Edmond MAICAN[1], Nicoleta UNGUREANU[1],
Cătălin PERSU[2], Mihai MATACHE[2], Marius OPRESCU[2]
[1]Politehnica University of Bucharest, Faculty of Biotechnical Systems Engineering, Romania
[2]INMA Bucharest, Romania

ABSTRACT

All ROPS tests aim to ensure the ROPS will safely absorb a certain minimum level of strain energy during loading, without the risk of structure failing or deflecting into the safety „clearance" zone, or the zone most likely to be occupied by the operator. The level of test loading is directly related to the mass of test tractor because during a rollover, the greater the weight of the vehicle, the greater will be the forces and impact energy applied to the ROPS. At present, most testing procedures for cabins are destructive, and if the resistance structure is inadequate, it is necessary to redesign the cabin and to retest it, in order to reach its validation. This entails high costs and this is why in the validation cycle of a resistance structure of the cabin has also been introduced a virtual test phase using the finite element method. This paper presents a validation procedure where the phase of virtual analysis using the finite element method is of particular importance for reducing costs and the time required to validate a resistance structure for an agricultural tractor.

Keywords: ROPS (Roll-Over Protective Structure), testing, FEM (Finite Element Method), cabin

1. INTRODUCTION

The risk of tractors rolling over depends on the tractor characteristics, working environment and terrain. This is the main reason for which, in the design and development of tractors it became of prime importance the need to protect the operator from the risk of being injured or causing death due to a roll-over. The development of standards has been outpaced by the continuous evolution of the tractors, and countries all over the world have set standards to address the safety of the operators which the tractors need to conform [5].

The design and testing requirements for ROPS have been studied by many agricultural engineering research institutes and universities. This was achieved by a research, testing and examination of tractor roll-over accidents. In most tests, tractor roll-overs were recreated under relatively controlled conditions, to allow the study of loadings applied to the ROPS and the subsequent behaviour of the structures [14]. The resulting national ROPS testing standards were harmonized over time, to create those known today, allowing OECD to be at the forefront of ROPS test standards development. Initially, the validation tests of ROPS performance were conducted using a sequential combination of „Dynamic" swinging (pendulum-type) mass impacts from the rear, side and possibly the front of the structure. These were complemented by gradually-applied crushing loads to the upper „roof" of the ROPS. This testing procedure is embodied by OECD Code 3, which was first introduced in 1966 [14]. All ROPS tests aim to ensure that the ROPS will safely absorb a certain minimum level of strain energy under loading, without the risk of structure failing or deflecting into the safety „clearance" zone, which is most likely to be occupied by the operator. The level of test loading is directly related to the mass of the test tractor, given that during a rollover, the heavier the vehicle, the greater will be the forces and impact energy applied to the ROPS [14].

[1]Bucharest, Splaiul Independentei, 313, sector 6,+40744756832, biris.sorinstefan@gmail.com

In the late 1960's and early 1970's, tractor power and mass increased and it became clear that the „Dynamic" ROPS test procedure had some limitations for testing of the ROPS equipping heavier tractors. Thus, it became difficult to apply the mass-related dynamic loading in a controlled and safe way as tractor mass increased. However, in 1983, this problem was solved by the development and introduction of the „Static" ROPS test procedure (OECD Code 4). As a result of numerous researches in different countries, it was developed a test procedure which replaced the swinging pendulum mass with a series of slowly-applied loadings. The direction and sequence of loadings, and also the vertically applied crushing loads were retained. Figure 1 presents the loading sequence for OECD Code 4. The loading / strain energy levels which the ROPS must withstand are directly related to mass of the test vehicle [14].

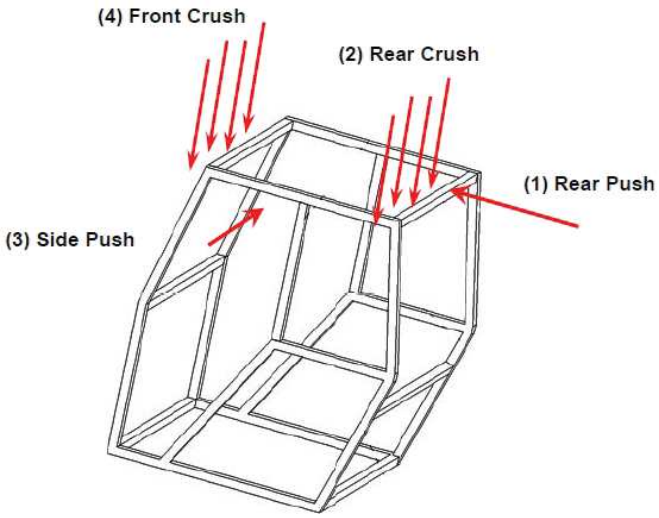

Figure 1: Typical OECD Code 4 'Static' ROPS test loading sequence [14]

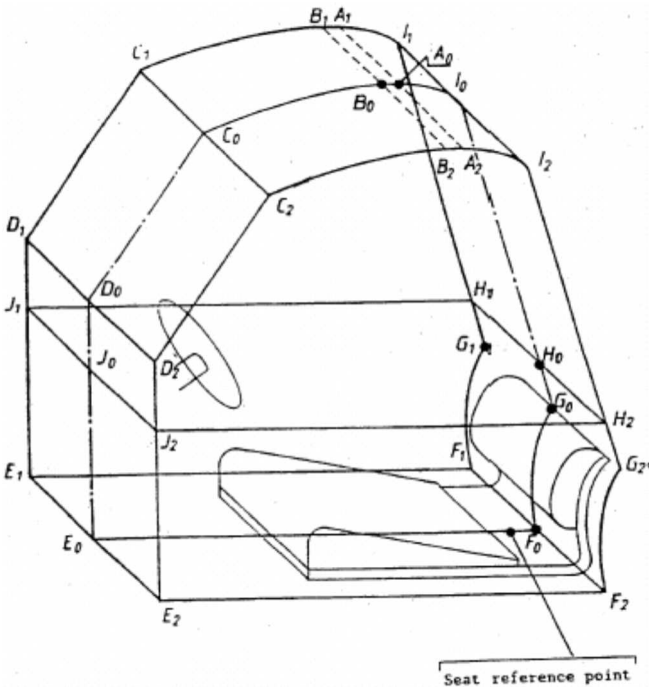

Figure 2: Clearance zone of the driver

According to Directive 2003/37/EEC, tractors weighing over 800 kg can be homologated using the OECD standard code for the official testing of protective structures on agricultural and forestry tractors (static test), which is known as Code 4. It has been designed a ROPS

attachable to the rear axle of various models of tractors, and has been developed a computer program for the calculation of the ROPS design [2]. During loading, no parts can interfere into the driver's clearance zone (Fig. 2), or the area occupied by the driver during the rollover, when the driver stays in the seat and holds onto the steering wheel [2].

2. METHODOLOGY

Since their release in the 1980's, ROPS Test Codes have not changed significantly. However, the family of OECD ROPS Codes has increased so that presently it includes test procedures for Narrow-Track (wheeled, vineyard and orchard) tractors (Codes 6 and 7), plus Crawler (track lying) tractors (Code 8) and Telehandlers (self-propelled variable reach all-terrain forklift trucks for agriculture) (Code 9). Less dynamic ROPS tests are performed today, most of them being carried out by „static"-type procedures. In these tests, Code 4 is the most frequently used. Yet, unlike other OECD Test Codes, the ROPS test is related to the particular structure tested, which could be adapted to a range of different tractor models. A structure is usually tested with loadings to fit the heaviest model in the vehicle range, in the safe knowledge that the requirements of the lighter models will be satisfied. The results of OECD ROPS tests are not available to the public. Instead, they are kept confidential to the vehicle / ROPS manufacturer and the testing station which performed the test. After the testing, a test report is completed; this report is subsequently checked by the OECD Coordinating (Quality Control) Centre and, if the report is appropriate, an OECD Approval Number is issued for the ROPS to prove that it has met the test requirements [14].

Figure 3 shows the complex diagram for determining the continuous roll-over behaviour of a laterally overturning tractor with a front mounted roll-over protective structure (ROPS) [13] where: Version B1 refers to the Point of impact of ROPS behind longitudinally unstable equilibrium point; Version B2 refers to the Point of impact of ROPS near longitudinally unstable equilibrium point; Version B3 refers to the Point of impact of ROPS in front of longitudinally unstable equilibrium point.

The loss of stability resulting in a rollover is caused by the slope of the ground but is also due to other causes. More than half of lateral rollovers are caused by tractors slipping into ditches or bumping against obstacles (Chisholm, 1972). Seeking to limit the risk of an overturn, various active devices (mobile ballasts and inclinometers) have been experimentally tested (Fabri and Ward, 2002) [2]. Currently, the computer simulation modeling is widely used [14].

Impact tests are designed to represent the most frequent type of road crash, resulting in serious or fatal injury. The calculation of impact forces during various collisions is by the following principle: *The change in the kinetic energy of an object is equal to the net work done on the object. This fact is referred to as the Work-Energy principle and is often a very useful tool in mechanics problem solving*. It is derivable from conservation of energy and the application of equations for work and energy, so it is not independent of the conservation laws. In case of a straight-line collision, the performed net work is equal to the average force of impact times the distance travelled during the impact [6].

The load sequence consists in a combination of loads, with the application based on an energy target, and crushing tests with a vertical application based on a force target. Code 4 stipulates to apply one longitudinal load, asymmetrical with respect to the longitudinal axis of the ROPS, two crushing tests (one on the front and one on the rear of the ROPS), and one lateral load applied at a position defined with respect to the seat index point (SIP) [4]. The ISO standard establishes a lateral load at a position defined with respect to the deflection-limiting volume (DLV), one crushing test applied in the center of the structure and one longitudinal load.

Another factor that recommends the choice of Code 4 is the wide lateral clearance zone compared to other standards. The lateral clearance zone defined by Code 4 includes the

deflection-limiting volume of the ISO standard and extends to the front of the steering wheel to create a large volume around the driver. In terms of the frontal view, the ISO standard is more conservative at the shoulder point. The magnitudes of longitudinal and lateral loads stated by the two standards are also different. Thus, Code 4 establishes a defined energy to be absorbed by the ROPS, while the ISO 3471 standard establishes the energy and force for the lateral load and a force for the longitudinal load [4].

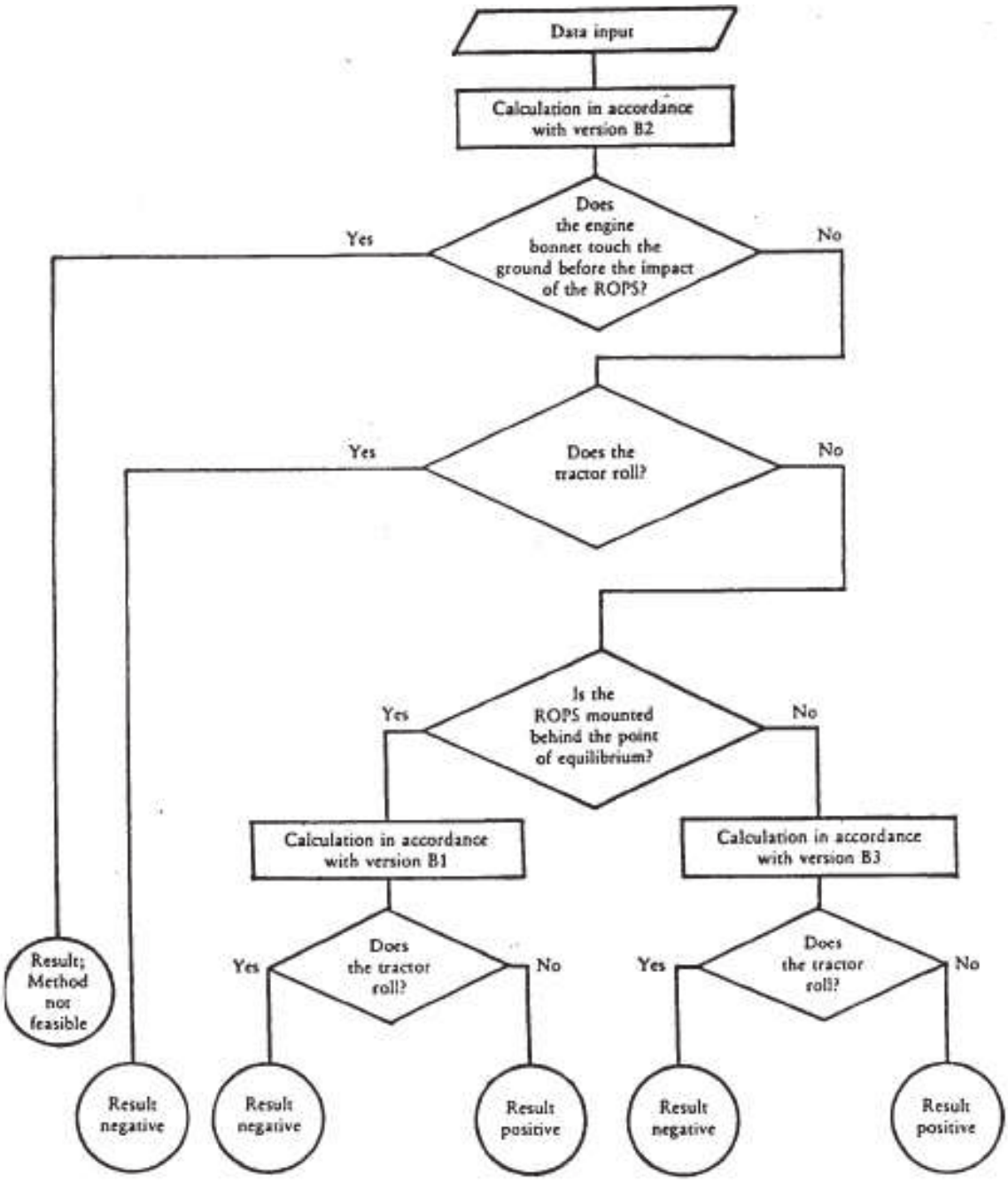

Figure 3: Flow diagram for determining the continuous roll-over behaviour of a laterally overturning tractor with a front mounted roll-over protective structure (ROPS) [13]

The flow diagram for the classical method of testing-homologation is shown in Figure 4 and the flow diagram proposed for the testing-homologation using the analysis by the finite element method of the cabin resistance structure is shown in Figure 5. Because the analysis will show the limits imposed by model size and the geometry will be notably simplified, this research should highlight the issues, limits and constraints in the procedure proposed by the

standards. It could be used as a general guideline for future enhancements of design and to estimate the limits of products being put into service in the future.

The rear part and one side of the tractor's structure were pushed by hydraulic cylinders. The longitudinal loading was stopped when the energy absorbed by the protective structure was equal to or higher than the required energy input established by Code 4.

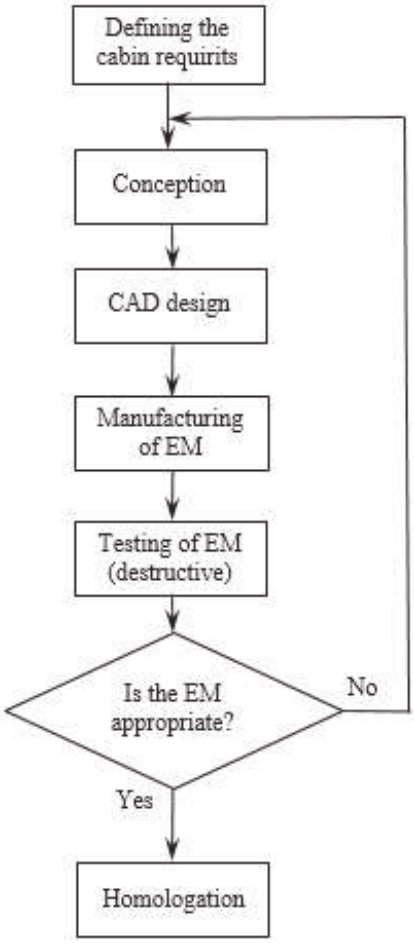

Figure 4: Flow diagram for the classical method of testing-homologation

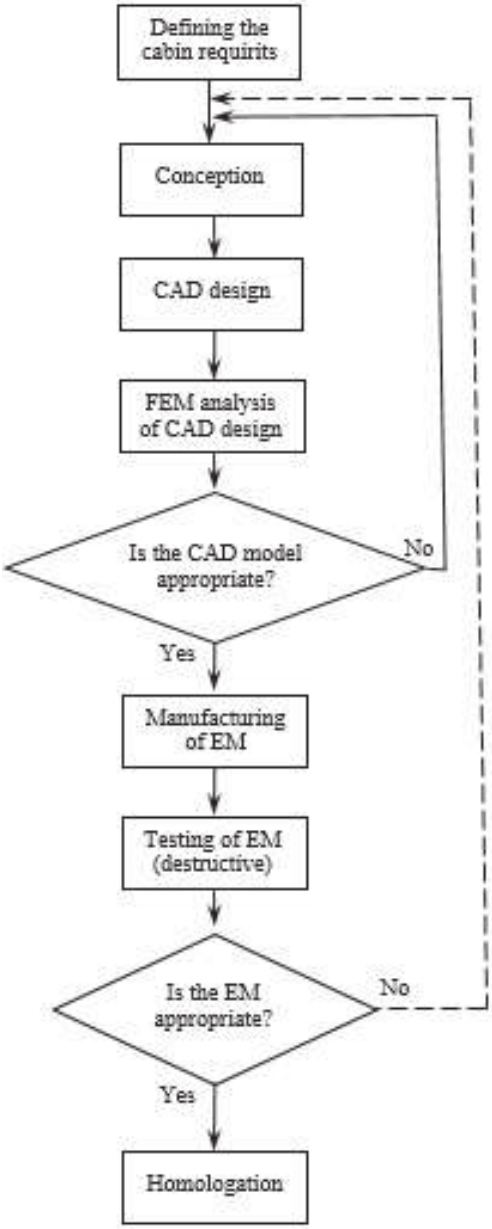

Figure 5: Flow diagram proposed for the testing-homologation by FEM

The ROPS are accepted if they fulfill the following conditions during and after completion of the tests: no part will enter the clearance zone or crash the seat during the tests, respectively the clearance zone (as defined and located by Code 4) is not outside the protection of ROPS. Any part touching flat ground when the tractor rolls over toward the direction from which the test load is applied will be considered "outside the protection of the structure". To assess this, width settings of the tires and tracks should be the smallest standard fitting specified by the manufacturer. Furthermore, at the point where the required energy absorption is found in the

horizontal loading tests, the force must be higher than $0.8 \cdot F_{max}$, which is the maximum resistance measured during the test.

3. CONCLUSIONS

By comparing the diagrams in Figures 4 and 5 it can be seen that, although more complex, the variant in Figure 5 allows the spectacular decrease in the costs of homologation of a resistance structure for the cabin of agricultural tractor. Effective testing of the experimental model is only carried out after it is established that the CAM model corresponds, following the FEM analysis. The total time required for homologation is decreasing. The accuracy of the test results increases using the diagram in Figure 5.

Acknowledgement

This work was supported by UEFISCDI based on 25BG/2016 financing program.

References

[1]. Abhay Kumar, Arun Mahajan, S Prasanth, Sudhir Darekar, Jagadeesan Chellan, K Ashok Kumar, and Jeya Kumar RanjithKumar, *Agricultural Tractor Cabin Structure Design for Durability and Rollover Protective Structure Test*, 2015 SAEInternational.

[2]. Mangado J., I. Arana, C. Jarén, P. Arnal, S. Arazuri, J. L. Ponce de León, *Development and Validation of a Computer Program to Design and Calculate ROPS*, Journal of Agricultural Safety and Health 13(1): 65−82, 2007.

[3]. McKenzieE. A., Jr.,J. R. Harris, *Increasing Tractor Operator Protection through NIOSH CROPS Research*, 2010 ASABE Annual International Meeting, Pittsburgh, PennsylvaniaJune 20 – June 23, 2010.

[4]. MolariG., M. Badodi, A. Guarnieri, M. Mattetti, *Structural Strength Evaluation of Driver's Protective Structures for Self-Propelled Agricultural Machines*, Journal of Agricultural Safety and Health, 20(3): 165-174, 2014.

[5]. Sachin R. Shende, V.P.Kshirsagar, Ganesh R. Shelke, *Design and Optimization of Tractor Roll OverProtective Structure*, International Journal of Engineering Development and Research, Vol. 4(3), pp. 933-939, 2016.

[6]. Saini Amandeep Singh, *To Study Weld Strength and Strain Energy Absorption of Roll Over Protection Structure of an All Terrain Vehicle*, IOSR Journal of Mechanical and Civil Engineering (IOSR-JMCE), Volume 10, Issue 2 (Nov. - Dec. 2013), pp. 27-31.

[7]. Thambiratnam, D. P. and Clark, B. J. and Perrera N. J., *Performance of a roll over protective structure for a bulldozer*. Journal of Engineering Mechanics,135(1), 2009, 31-40.

[8]. Thambiratnam, David P. and Clark, Brian J. and Perera Nimal J., *Dynamic Response of a Rollover Protective Structure*. Computer-Aided Civil and Infrastructure Engineering, 23(6), 2008, 448-464.

[9]. ***, Directive 2009/75/EC of the European Parliament and of the Council of 13 July 2009 regarding roll - over protection structures of wheeled agricultural or forestry tractors.

[10]. ***, The delegated regulation (EU) no. 1322/2014 of Commission of 19 September 2014 for completion and amending and amending the Regulation (EU) No 167/2013 of the European Parliament and of the Council with regard to the construction of vehicles and general requirements for the type-approval of agricultural and forestry vehicles.

[11]. International Standard ISO8082-1, Self-propelled machinery for forestry — Laboratory tests and performancerequirements for roll-over protective structures, 2009.

[12]. Society of Automotive Engineers (SAE), 2009. SAE J2194 Roll-Over protective structures(ROPS) for wheeled agricultural tractors.

[13]. OECD Standard code for the official testing offront mounted roll-over protective structures on narrow-track wheeled agricultural and forestry tractors, CODE 6 – July 2012.

[14]. OECD Tractor Codes Brochure, January 2013, http://www.oecd.org/tad/tractor

METHODOLOGY FOR ESTIMATING FUEL CONSUMPTION AND PRODUCTION NORMS (WORKING CAPACITY) BY POWER CLASSES, DEPENDING ON THE AGRICULTURAL WORKS OF HOEING AND APPLYING HERBICIDES

Bolintineanu Gh.[1], Cujbescu D.[1], Matache M.[1], Vlăduţ V.[1], Persu C.[1], Găgeanu I.[1], Muscalu A.[1], Caba I.[1], Vlad C.[2], Popescu C.[3)]
[1]INMA – Bucharest, [2]ICEADR Bucharest; 3) SC Hofigal SA Bucharest

ABSTRACT

The paper aims to establish methodologies for estimating fuel consumption and production norms (working capacity) by power classes, depending on the agricultural works of hoeing and applying herbicides, in plain areas. First, 5 main tractor classes were identified, broken down depending on the type on agricultural exploitation, and for each tractor class were identified the representative tractors for the power range *P*, as well as the average specific fuel consumption in g/HPh (g/kwh). The average working speeds were established for each tractor class (tractor with minimum and maximum power in the power class), for hoeing and applying herbicides, as well as the theoretical working widths. depending on them, calculation formulas were determined for fuel consumption per hectare and for the working capacity (productivity).

1. INTRODUCTION

The hoeing work is very important for managing water in the soil, having a role in cutting weeds from underneath, at small depths, the plants remaining on the surface of the soil and impeding water losses. Simultaneously, the crust and capillaries through which water losses occur are destroyed. At the same time, the cracks in the soil, which constitute real ventilation channels causing the loss of water from the deep soil layers, are covered. [3]

The basic work for fighting weeds is constituted by hoeing. Three mechanical hoeing works between plant rows and two manual hoeing works on row are recommended.

Hoeing has a double role of completing the action of herbicides (in numerous cases herbicides don't ensure the complete destruction of weeds), of improving soil structure and of favouring the development of the young crop. [6] Crop hoeing influences plant growth and crop level in a decisive manner. The first hoeing is done immediately that sun flower rows are well distinguished and the first two real leaves are formed. Mechanical hoeing is performed first, followed by manual hoeing and then the second mechanized hoeing needs to be performed at a short interval (10-12 days) immediately after the weeds appear. At an interval of approximately 15 days, a third mechanical hoeing is performed. The last hoeing is done when plants are 60-70 cm high, a delay making it impossible to enter the field with the cultivator because they hit the plants, which are very sensitive to breakage. The protection area during hoeing increases from 8-10 cm during the first hoeing to 14-15 cm during the last because leaves are rigid and break easily. The working speed is established so that soil is not thrown on the row. The working depth of the cultivator's active bodies needs to ensure the destruction of all weeds. [4] A too deep soil mobilizing, from which result soil lumps of slices that favour water loss and cause plant covering with soil, will be avoided. Soil working depth is 15 cm, all the cultivator's stations need to operate at the same depth. Manual hoeing is performed after the first and second

[1]bolintineanu_gh@yahoo.com

mechanized hoeing, with extra care not to cut or harm plants. From researches conducted, it was proven that only mechanical hoeing, without applying herbicides, increase sun flower production with 470-800 kg/ha, a manual hoeing brings an additional increase of 430-470 kg/ha and a second manual hoeing bring an increase of another 200-370 kg/ha.

Figure 1: Hoeing machine [5]

Excessive use of chemicals in agriculture leads to soil balance disturbance and to the accumulation of mineral substances in the soil and in the groundwater (eg. nitrites, which have a methemoglobinizing effect for humans and animals and destroys atmospheric nitrogen fixation bacteria).

Pesticides, mostly non-biodegradable, concentrate along trophic chains, being toxic to plants and animals. Pests also become resistant to pesticides, requiring the creation of new, more effective synthesis substances, which also have the disadvantage of being more toxic to the environment.

An alternative solution for reducing soil pollution is biological pest control. [2] Due to pesticide pollution, over 300 million hectares are in a high degree of degradation, thus the phenomenon is considered to be irreversible. Bioproducts are biological means made on the basis of microorganisms that are useful for crop plants based on natural compounds (herbal extracts). Due to their biological nature, bioproducts have a complex action on crop plants, the most correct term being not of biopreparations used in plant protection, but biopreparations for agricultural use.

The use of herbicides in weed control is based on their ability to produce in weeds the deregulation of vital processes such as photosynthesis, respiration, absorption and metabolism of nutrients. Researches on the efficacy of these substances have been performed under different climatic conditions and have been aimed at establishing the conditions of use (dosage, application time) in order to achieve maximum efficacy in weed control without affecting the normal growth and development of sunflower plants. [1]

Figure 2: Sprayer machine [7]

Herbicides are chemical substances that exhibit phyto-toxic action on weeds in crops, fruit and wine plantations, etc. [8] The work of applying herbicides is designed to prevent the growth of weeds and, implicitly, to avoid populating soil with their seeds. Not applying weed control treatment generates massive reductions in spring crop yields and inefficient use of water existing in the soil.

2. METHODOLOGY

The methodology for estimating fuel consumption and production norms (working capacity) by power classes, depending on the agricultural works of hoeing and applying herbicides comprises the following stages:
1. A classification of tractors in made, taking into account the National Strategy for Rural and Agricultural Development for the years 2014-2020 and the Code of Good Agricultural Practices, starting from Law 37/2015, as follows:

Exploitation	Tractor range (HP)
Subsistence farms	<45
Semi-subsistence farms	46÷80
Small exploitation	81÷120
Average exploitation	121÷200
Large exploitation	201÷360

2. For each tractor class were identified the representative tractors for the power range *P* as well as the average specific fuel consumption in g/HPh (g/kwh).

Nominal tractor power (CP)	Diesel fuel consumption (g/kwh)	Diesel fuel consumption (g/HPh)
<45	330	242.64
46	300	220.58
80	292	214.70
81	292	214.70
120	288	211.76
121	280	205.88
200	261	191.91
201	259	190.44
360	250	183.82

3. For the hoeing work and for the work of applying herbicides, the average working speeds were established for each tractor class, depending on the statistical data available for them:

Tractor range (CP)	**Average working speed *v* (km/h) for hoeing**	**Average working speed *v* (km/h) for applying herbicides**
I		
<45	4.6	5,8
II		
46	5,2	7,3
80	6.1	8,1
III		
81	6,4	9,0
120	8,1	11,2
IV		
121	8,7	13,3
200	10.8	14,1
V		
201	11,8	16,7
360	12,7	18,1

4. The estimation of theoretical working width *l (m)*: was considered between 1.6 - 1.7 m for hoeing and between 6 - 36 m for applying herbicides.
5. The load of the tractor was of 35% for hoeing and 30% for applying herbicides. For estimating fuel consumption per hectare, the following calculation formulas were used:

- for hoeing

$$q_p = \frac{0.35Pc}{85vpl} \tag{1}$$

- for applying herbicides

$$q_e = \frac{0.3Pc}{85vpl} \tag{2}$$

where -*dv* is fuel consumption (l/ha);
-*P* is tractor nominal power (CP);
-*c* is the specific fuel consumption (g/HPh) for each tractor class (minimum and maximum power tractor in the power class);
-*v* is the average working speed (km/h);
-*l* is the working width (m);
-*p* is the skidding correction coefficient (%).

For skidding, an average value of 20% for hoeing and 5% for applying herbicides was chosen, therefore the working speed was pondered by a correction coefficient $p = 0.8$ for hoeing and a correction coefficient $p = 0.95$ for applying herbicides.

6. For estimating the working capacity (productivity) W, the following formula was used:

- for hoeing

$$W = \frac{vpl}{10} k_{pr} \quad (3)$$

- for applying herbicides

$$W = \frac{vpl}{10} k_{er} \quad (4)$$

Where W represents the working capacity (ha/h) and k_{pr}, k_{er} represent correction coefficients.

For the work of applying herbicides, the parcels were divided on sizes depending on the type of agricultural exploitation, applying the correction coefficients of the working capacity:

Exploitation type	**Correction coefficient**
SMALL exploitation	
Subsistence and semi-subsistence agricultural exploitation	0.74
Parcel length <250	0.83
AVERAGE exploitation	
Parcel length 250-500 m	0.91
LARGE exploitation	
Parcel length 500-800 m	1
Parcel length >800 m	1.05

Observation: The estimation of fuel consumption and working capacity (productivity) was achieved taking into account the ***actual time worked***, disregarding the following: helping time (the time for turning at the end of rows, the time for empty runs, movement from one parcel to another, servicing the machine), the time for technical maintenance (adjustments during operation, daily technical maintenance, replacing active bodies during operation), fuel supply, preparation and ending time, time for resting and natural necessities, etc.

3. CONCLUSIONS

The methodology aimed at developing a rapid method for calculating fuel consumption per hectare and the working capacity (productivity), helping farmers to properly size their tractor and agricultural machinery park depending on the size of their exploitation, to establish the staff necessary to serve it and to make an economic calculation on the cost-effectiveness of the chosen solution.

References

[1]. Dobre P., *Energetic base and horticultural machines*, Bucharest, 2010;
[2] Hoy M., *Biology Control in Agriculture IPM System,* Imprint: Academic Press, eBook ISBN: 9780323144759, 1985;

[3] Onisie T., Zaharia M., *Farm practices,* University of Agricultural Sciences and Veterinary Medicine "Ion Ionescu de la Brad", Faculty of Agriculture, Iași, 2002;
[4] Stehle T., Griepentrog H. W., Holpp M., Anken T., *Study on a machine vision based guidance system for hoeing in row crops,* LAND.TECHNIK AgEng 2015, 6.-7. VDI-Verlag, Düsseldorf, Germany, pp.493-498, ISSN 978-3-18-092251-5, Germany, 2015;
[5] http://agronotizie.imagelinenetwork.com/agrimeccanica/2011/09/22/il-terreno-respira-con-rotosark/14004;
[6] https://www.mondomacchina.it/en/operations-the-importance-of-hoeing-machines-c1690;
[7] http://nhresourcecenter.com/applying-herbicides-corn-longer-viable-2/;
[8] https://www.sciencedaily.com/terms/herbicide.htm.

CONSIDERATIONS CONCERNING THE GROWTH AND DEVELOPMENT OF HORTICULTURAL PLANTS IN ACQUAPONIC CROPS

PhD. Eng. Caba Ioan Ladislau, Phd. Stud. Eng. Laza Evelin-Anda, PhD. Eng. Pop Augustin, Phd. Stud. Eng. Cujbescu Dan, Lecturer PhD.Eng. Ungureanu Nicoleta.
INMA Bucharest – Sucursala Timisoara / Romania
Tel: 0256.499.336 E-mail:inmatm_caba@yahoo.com

ABSTRACT

Aquaponics is considered a successful combination of: aquaculture (fish growth) and hydroponics (plant growth on water), being considered from the antiquity to the present day the agriculture of the future. Due to the living components of the system, assures the ideal environment, cleaning each other's water and sustaining its existence. For this reason, the costs of plant and fish production are considerably reduced. Vegetable plants: salads, special herbs have low nutrient requirements and are well suited to aquaponics.

The present paper aims at making the fish growing and the cultivation of leguminous plants profitable and efficient in aquaponic systems. Aquaponic can be defined as a combination of aquaculture and hydroponic systems whereby waste water rich in nutrients from the aquaculture system is transferred to another system called hydroponic plant. Plants absorb nutrients from wastewater and thus improve or purify water in the aquaculture system. This method offers an ecological and sustainable system.

1. INTRODUCTION

Aquaponic systems are more complex than the systems designed only for growing plants or fish breeding, because optimum conditions for each group of active organisms participanting in the production process - plants, fish and nitrifying bacteria, are not identical.

Aquaponics is an intensive production system herse several cultures are produced with reduced inputs of water and fertilizers and it is very suitable for small agricultural producers targeting local markets and agritourism opportunities. For practicing efficient aquaponics increased attention is necessary regarding consumer demands, food security and economic efficiency, through continuous development of new technologies.

Aquaculture as well as hydroponics have already become agri-food sectors with the fastest growth worldwide, representing an important potential for supplying the world population with aquaponic products, namely vegetables and fruits, healthy and of high quality. Their combinație is still at the beginning, being subject of research to innovative development of many specialized institute [5,6].

These practices have appeared centuries ago in ancient China, [5] spread throughout the world, and yet their combination is still at the beginning, being the object of research for the innovative development of many specialized institutes [6,7]

In aquaponic systems, a variety of horticultural plants such as any salad, Chinese cabbage, parsley, basil, thyme, mint, roe, chives, rosemary, beetroot, rucola, basil, mint, bush, chives, various tropical plants. Horticultural plants that harvest (tomatoes, peppers, cucumbers, beans, peas, pumpkins) have high nutrient requirements, so they need nutrient-rich, very stable systems. Plants that are used for their fruits (tomatoes, peppers, cucumbers) have a higher nutritional demand and have better performances in a well-stocked and stable aquaponic system. Greenhouse tomato varieties are better suited to low light conditions, high humidity in greenhouses than field varieties. [4]

A component of the aquaponic system is aquaculture, which involves the existence of fish and one or more pools of their growth. In their tanks, fish receive fresh water and food to grow. As a result of the fish feed process, the water in the tank will contain residues and scraps of unconsumed food. Water is treated with specific bacteria, which transforms waste into nutrients for plants, thus favoring their natural and ecological growth.

Consumption of nutrients in the water by the "layers" of vegetables cause the water to become usable again for the fish, so that it is directed by gravity or pumped back to the fish basin and the recirculation continues.

The wastewater from the fish tanks led by irrigated pipes plants that rest on another tank, rooted in water, on a bed of gravel (or other materials), then returns to the fish tank in a continuous stream. In hydroponic crops, the plants are sown either on floating artificial substrates or in a sterile, porous substrate with high water permeability.

This way plants receive nutrients and fish water is naturally filtered. Effluents from fish contain nitrates and bacteria that favor the natural and ecological growth of vegetables [1,2].

In fish tanks, ammonia exists in two forms, which together are called total ammonia nitrogen [3]. The nitrification process represents the two-step biological oxidation of ammonia to nitrate. The process is carried out by autotrophic bacteria that use ammonia and nitrites as growth substrates to generate energy for cellular and reproductive activity [1,2].

The effectiveness of the nitrification process is dependent on oxygen concentration, temperature, biomass retention time, alkalinity and pH. Nitrifying bacteria are strictly aerobic, they can only nitrify in the presence of dissolved oxygen (OD).

The process of biological denitrification is the conversion of nitrates to nitrogen gas in the absence of oxygen. This process is carried out by some of the heterotrophic bacteria, called denitrifying heterotrophic bacteria, which have the ability to use nitrates and nitrites as an acceptor electron in the oxidation process of organic matter.

The efficiency of the denitrification process is affected by the absence of dissolved oxygen, the presence of a suitable and active population of denitrifying bacteria, pH, temperature, nutrients and redox potential [6,7].

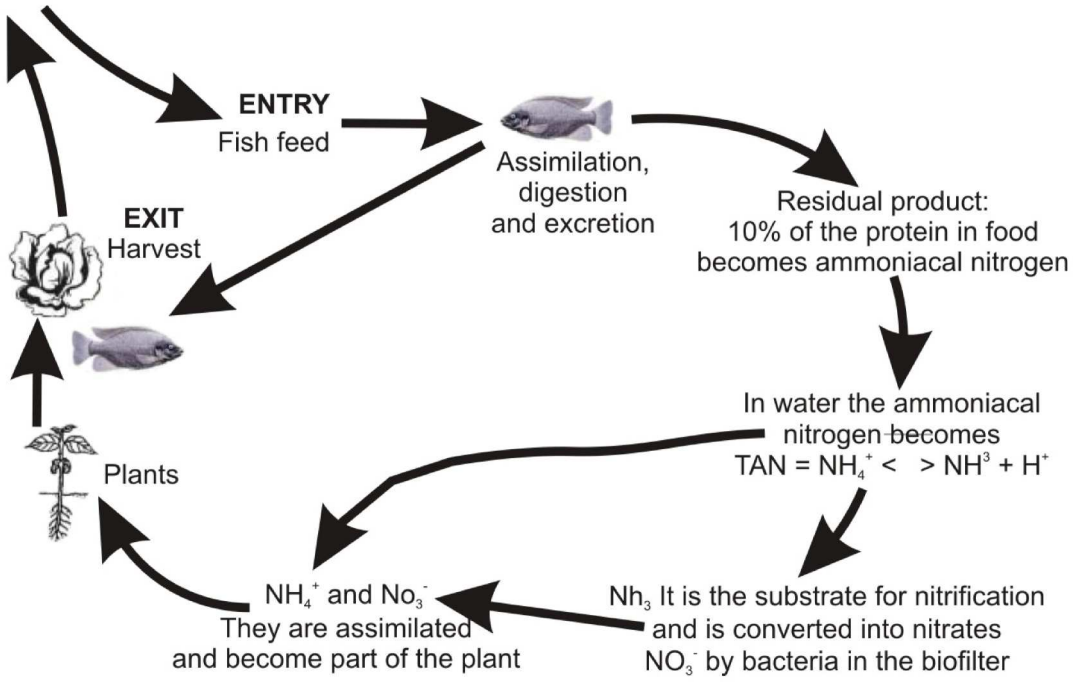

Fig. 1 Circuit of obtaining horticultural plants in aquaponics cultures

2. METHODOLOGY

The hydroponic subsystem have the following main components:

- two hydroponic tanks, placed on two metal supports. The water coming from acuaculture subsystem, supplies, in parallel, each of the two tanks, being introduced at one of their ends and then removed at the poposita end;
- floating supports for plants, made of expanded polystyrene, presenting holes where the lettuce seedlings are planted;
- devices for regulating water level in hydroponic tanks;
- taps for regulating water flow rate in hydroponic tanks;
- plant lighting panels, placed over the hydroponic tanks, so that the distance to plants be adjustable, have the role to ensure the light necessary for photosynthesis.

Connecting the hydroponic system to the aquaponic one is made using fittings and fixtures so that water supply for hydroponic tanks can be ensured either through the outlet pipe or the supply pipe of the biological filter. Water removal from hydroponic tanks will be made through the supply pipe of the mechanical filter.

Determining water quality, in different phases of the technological process, will be made by taking periodical samples and their analysis in laboratory.

The denitrifying installation from aquaponic cultures that will be used during the experiment has the following main characteristics:

- Type of culture ..... aquaponic
- Fish species bred in recirculating acuaculture systems (RAS).....sturgeons and pike-perch
- Hydroponic culture vegetables .....lettuce
- Hydroponic culture surface……..... ……....8 m^2
- Culture density (lettuce) ……12...14 piece/m^2
- Average water need for lettuce growing .....1,5 m^3/day
- Lighting type …….....…..... LED lamps
- Energy source ……..……..... photovoltaic panels.

Quality evaluation from the chemical point of view was made on lettuce (*Lactuca sativa)* within the first research experiment.

The quality of the two rehearsals was compared with conventional control culture production under natural conditions.

Chemical analysis was performed on a number of 5 plants from each repetition and on a number of 5 control culture plants. The plants selected for the purpose of laboratory chemical analyzes were those of potential marketing, which have a maximum degree of development in terms of quantitative characteristics and which have faithfully respected the phenotypic characteristics of the cultivated variety. At the same time, the root parts of the plants were also evaluated.

Root chemical evaluation was made on total amount of roots. Three root samples were taken:

sample 1 – the roots of the 5 plants chemically assessed from repetition 1,
sample 2 - the roots of the 5 plants chemically assessed from repetition 2,
sample 3 - the roots of the 5 plants chemically assessed from control culture.

This chemical analysis focused on the amount of ammonia (NH_4^+), nitrate (NO_3^-) and phosphorus as phosphorus pentoxide (P_2O_5) in plants, respectively in roots.

Determining the amount of ammonia (NH_4^+), nitrate (NO_3^-) and phosphorus as phosphorus pentoxide (P_2O_5) in plants was made in acetic acid extract [2].

Basic descriptive statistical indexes for chemical variables studied in the case of lettuce from aquaponic module and lettuce conventional growing under natural conditions are presented in the following table where:

X – Medium value;
NH_4R_1 – Ammonia level from repetition 1 (mg/kg fresh product);
NO_3R_1 – Nitrate level from repetition 1 (mg/kg fresh product);
$P_2O_5R_1$ – Phosphorus pentoxide level from repetition 1 (mg/kg fresh product);
NH_4R_2 – Ammonia level from repetition 2 (mg/kg fresh product);
NO_3R_2 – Nitrate level from repetition 2 (mg/kg fresh product);
$P_2O_5R_2$ – Phosphorus pentoxide level from repetition 2 (mg/kg fresh product);
NH_4M – Ammonia level from control culture (mg/kg fresh product);
NO_3M – Nitrate level from control culture (mg/kg fresh product);
P_2O_5M – Phosphorus pentoxide level from control culture (mg/kg fresh product).

Table 1: Basic descriptive statistical indexes for chemical variables studied in the case of lettuce from aquaponic module and lettuce conventionally grown under natural conditions

		X	Min	Max	S	S^2	CV%	S_X
Rep. no.1	NH_4R_1	1,77	1,55	2,00	0,24	0,05	10,98	0,10
	NO_3R_1	811,69	776,25	865,89	34,59	1228,43	4,15	15,10
	$P_2O_5R_1$	349,12	321,65	378,90	27,59	761,56	7,91	12,32
Rep. no.2	NH_4R_2	1,70	1,41	2,10	0,29	0,12	16,49	0,09
	NO_3R_2	810,79	740,95	896,00	63,91	4082,17	7,97	29,50
	$P_2O_5R_2$	374,32	356,00	410,11	17,38	301,69	4,68	7,78
Control Version	NH_4M	2,12	1,90	2,65	0,28	0,08	11,29	0,15
	NO_3M	111,75	89,66	137,90	16,66	246,31	15,14	5,56
	P_2O_5M	206,23	184,23	239,03	19,10	329,76	9,78	9,10

Basic descriptive statistical indexes for variables studied in the case of lettuce from aquaponic module and lettuce conventionally grown under natural conditions where:

X - Medium value;
$GradR_1$ – Root mass from repetition 1 (g);
$GrfrR_1$ – Leaf rosette mass from repetition 1;
$NrfrR_1$ – Number of leaves per plant from repetition 1;
$GradR_2$ – Root mass from repetition 2 (g);

GrfrR2 – Leaf rosette mass from repetition 2;
NrfrR2 – Number of leaves per plant from repetition 2;
GradM – Root mass from control culture (g);
GrfrM – Leaf rosette mass from control culture;
NrfrM – Number of leaves per plant from control culture

Table 2: Basic descriptive statistical indexes for chemical variables studied in the case of lettuce from aquaponic module and lettuce conventionally grown under natural conditions

		X	Min	Max	S	S^2	CV%	S_X
Rep.no. 1	$GradR_1$	4,09	2,89	6,12	1,42	1,99	29,56	0,73
	$GrfrR_1$	35,21	20,30	55,38	15,10	199,80	29,95	6,41
	$NrfrR_1$	17,66	13,00	25,01	4,55	21,30	25,70	2,06
Rep.no. 2	$GradR_2$	6,65	4,10	12,74	3,59	12,59	43,53	1,68
	$GrfrR_2$	51,07	36,62	74,78	14,47	218,71	28,39	6,56
	$NrfrR_2$	22,03	17,00	29,10	4,38	19,60	19,91	1,99
Control Version	GradM	4,09	2,80	6,35	1,34	1,87	29,83	0,65
	GrfrM	34,58	25,33	50,25	10,30	105,99	29,87	4,68
	NrfrM	11,62	8,00	15,10	2,75	7,35	20,93	1,18

3. CONCLUSIONS

Modern Aquaponics, a branch still at the beginning, which combinase aquaculture with hydroponics, judiciously applied, can sum up the benefits, and elen more, can mutual neutralize some major problemist of the two, uș chi as the unse as nutrients, by plants, of noxious products fish generated.

For operating a fish aquaponic breeding system in a recirculating acvacole system and hydroponic plant production, it is essential to maintain an optimal quality of recycled water. This is achieved, mainly, through efficient filtration, treatment and denitrification of waste water.

Regarding the assessment of the chemical characteristics of lettuce obtained in aquaponic module and conventional technology under natural conditions, it has Ben observând that terne are differences between NH_4^+ levels identified in plant roșește in repetition 1 and repetition 2 and but they are not significant. There are significant differences between the NH_4^+ level found in plant rosettes from repetition 1 and the NH_4^+ level from control culture. There are also significant differences between the NH_4^+ level found in plant rosettes from repetition 2 and the NH_4^+ level from control culture. P_2O_5 levels identified in plant rosettes from repetition 1 and 2 are different, but not significant.

In respect to the assessment of organoleptic characteristics of lettuce obtained in aquaponic module and conventional technology under natural conditions it was found that plants obtained in aquaponic module were not so appreciated in terms of taste, plant health,

odor and color. In conclusion, the conventional production plants are valued more by consumers compared to the plants produced in aquaponic module.

In conclusion, although the level of nitrate is significantly lower in control culture than in aquaponic productions, they do not exceed the maximum limit admitted for human consumption.

References

[1] Blidariu F.**,** *Increase of economic efficiency and sustainability of fish breeding in recirculating systems by the intermediary of aquaponic cultures*, Timişoara, (2013).

[2] Cristea F., Radulov I., Lato F., Agrochemistry-analysis method, Ed. Euro, Timisoara,(2011).

[3] Francis-Floyd, R., C. Watson, D. Petty and D. Pouder, Ammonia in aquatic system, University of Florida Fisheries and Aquatic Sciences Dept. Document TA16, (2012).

[4] Hughey T.W. Barrel , Ponics, a.k.a. Aquaponics in a Barrel,(2005).

[5] MacKay K.T. Rice, Fish Culture in China, International Development Research Center, PO Box 8500, Ottawa, ON, Canada K1G 3H9, http:web.idrc.ca/openebooks/313-5/09,10,2011, (2011).

[6] Martan E., Polyculture of fishes in aquaponics and Recirculating Aquaculture, Aquaponics Journal, (2008).

[7] Şumălan R., Plant physiology - Plant physiology elemente applied in horticulture, Ed. Eurobit, Timişoara, (2009).

THE LIFTING DRUMS IMPORTANCE IN CONSTUCTION OF SELF LOADING WAGONS

PhD. Eng. Caba Ioan Ladislau[1)], Phd. Stud. Eng. Laza Evelin-Anda[1)], Phd. Stud. Eng. Cujbescu Dan[1)], PhD. Eng. Voicea Iulian[1)], Phd. Stud. Eng. Gageanu Iuliana[1)], Lecturer PhD.Eng Ungureanu Nicoleta[2)], Eng. Dumitru Iulian[1)], Eng. Oprescu Marius[1)], PhD. Eng. Eng. Vlăduţ Valentin

INMA Bucharest / Romania; [2)]U.P. Buchrest / Romania
Tel: 0256.499.336 E-mail: *inmatm_caba@yahoo.com*

ABSTRACT

It is known that the global livestock feeding were made machines, with increased working capacity, high efficiency operation. These equipments are prominently self-loading and transported fibrous feed wagons.

These trailers, in addition to their numerous advantages includes, presents some technical drawbacks motivate operating their small spread in Romanian agriculture.

In order to improve the workflow of self loading and transported fibrous feed wagons, propose equip them with lifting drums.

1. INTRODUCTION

It is known that all the works in agriculture are connected to the weather. In some cases the campaigns with harvesting feed or hay production are partially compromised by the vagaries of weather. It requires harvesting, conditioning, transport, storage of fiber feed in maximum safety, in the shortest time possible, in strict compliance with the agro-livestock requirements. On the international markets the offer of high quality equipments with outstanding working performances, which are capable to achieve in good condition and with increased speed the fibrous feed harvesting, transporting, conditioning and storage. Some of these equipments allow the merging of several operations at a single pass, such as the mowing with the crushing of the green feed material, the loading with the shredding, etc.

Under the conditions of the Eastern European agriculture development, a perspective machine for small and medium farmers is the fibrous feed self loading wagon trailer.

This machine can perform simultaneously several operations such as:

- cutting feed
- raising them in furrow
- shredding
- transportation to the livestock farms
- administration of the feed directly into animals' paddocks

2. METHODOLOGY

Studying different types of fibrous feed self loading wagons trailers (Fig. 1, 2), with maximum power requirement for operating of 100 HP, we found some shortcomings in their functioning, such as:

- duet to the reduced force of the tractor, they don't allow fibrous feed proper shredding,

- some models, in their construction are not fitted with shredding system in order to maintain the low price of the machine,
- at low moisture, with values between 30-40% the transport channel becomes clogged if more chopping cuttlers are used,
- the low reliability of the feed raised mechanism, which at the majority of equipments is elevator scrapers chain with finger.

3. RESULTS

4. After studying the possibilities of improving the functioning of fibrous feed wagons trailers, we proposed the rethinking of the shredding system of these machines.
5. Researching the technical possibilities that could solve the problems raised in the proper functioning of this type of equipment, we designed a device type lifting drum.
6. In the followings we present the functioning and operating mode of this lifting drum. The lifting drum takes over the fibrous feed material from the raised device from the furrow of type drum with resilient fingers or as the case from the mowing device with rotary drums, it chops them and stores them in the floor of the trailer.

Fig.1. Self loading wagons trailers from Pottinger company [2], [3]

Fig.2. Self loading wagons trailers from SIP company [4]

Fig.3. Self loading wagons trailers from Pottinger [4]

It is rugged built, without multiple elements in moution that could cause the device failure. The turning speed of the lifting drum is calculated so that the fibrous feed cutting to be possible at any value of moisture. Due to the reversing switch incorporated in the revolving mechanism, the drum can also rotate in inverse proportion than the direction of lifting – shredding of the fibrous feed material flow.

The lifting – shredding drum, conceived and presented in Fig.4, has the following components:

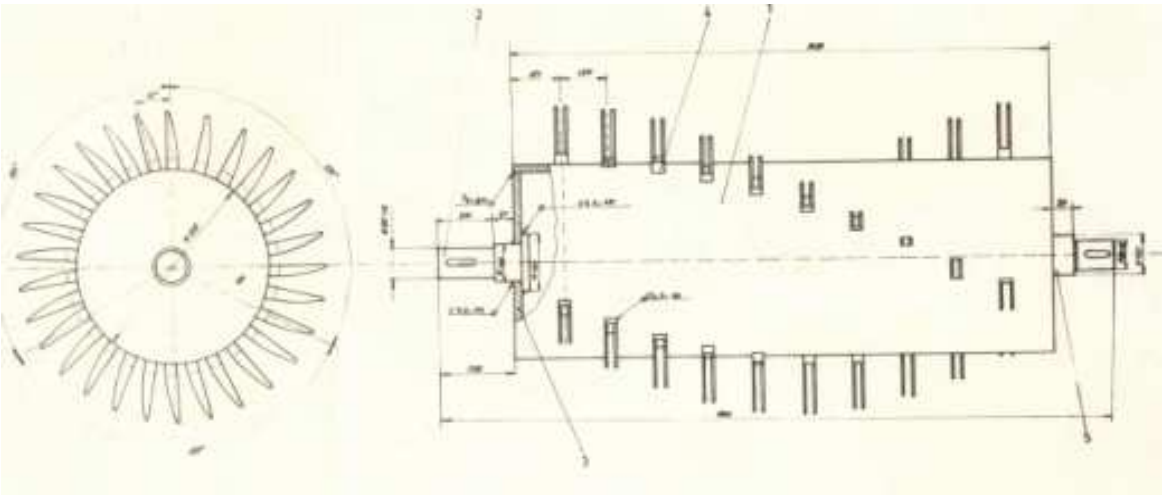
Fig. 4. Lifting drum [1]

1. The body of the drum, which is made of steel tube with a diameter of 500 mm,
2. The supportive and gearing axis of the drum,
3. The side walls,
4. The lifting – shredding fingers, mounted on the circumference of the drum,
5. Spacer.

It can be seen that the drum's lifting fingers are in the form of a "U" with the slight ray of connection to the top, which thus allows the achievement of the cuts with sliding to reduce the operating force.

It is known that this type of cutting is performed with the lowest energy consumption.. The fingers' arrangement has been made after a three-propeller beginnings to reduce the shocks during the operation of the lifting – shredding device. In total on the drum's body are willing thirty fingers, each row having ten piece.

7. CONCLUSIONS

The application of the lifting drum in construction of fibrous feed wagons trailers solved the problems related to the equipment reliability of this type, the vibrations disappeared during their operation, the problems related to the clogging of the transport channel with faded fibrous materials have been eliminated, the shredding - chopping cutlers number was increased due to application of cutting with sliding which is achieved with a low power consumption. Among other advantages of lifting drum using we can also mention the reducing of the equipment‘s weight.

References

[1] Caba, I. L, 1988. Lifting drum. Certificate of innovative Nr.879 / 05/06/1988.Romania;
[2]. https://www.poettinger.at/en_us/Produkte/Kategorie/14/silage-loader-wagons
[3]. https://www.poettinger.at/en_ie/Produkte/Detail/225/euroboss-loader-wagons;
[4]. http://www.sip.si/forage-wagons/items/senator-22-9
[5]. http://www.andresenmaskin.se/wp-content/uploads/2014/07/129.02.0611_Jumbo_combiline_en.pdf

OPEN SOURCE PARADIGMS IN URBAN AND RURAL DEVELOPMENT

Alexandru Calcatinge, PhD[1]
"Ion Mincu" University of Architecture and Urbanism, Bucharest, Faculty of Urbanism,
Department of Urban Planning and Territorial Development

ABSTRACT

What does open source has to do with rural development, one might ask? Well, basically open source would have to be the very foundation for the future urban and rural living and development. In this respect, this paper will emphasize on the ideas of open source urbanism, open source ecology, open source hardware design and the relations between those that will eventually lead to the possibility of a global villages network based on a globally integrated village environment.

1. INTRODUCTION

It is my conviction that we live in a world of data and ideas. Besides nature, which is also based on data and which was slowly created on this planet since it's inception (or in other terms, by God), all other creations are basically data operations that lead to ideas being created and materialised. I am an architect and I believe that what the human kind ever creating is basically big chunks of data that was being modelled and interpreted. Nevertheless, without getting into too much details, all this basic data is actually open sourced. The planet and the universe doesn't know any other kind of data, only the human kind decided that this data should be closed sourced in order to produce revenue. That is until recently, when open source and big data started to win in critical sectors of our existence. Now, perhaps that "economy" should have been a better word, but I carefully chosen the other one: existence - it is based on big data interpretation and its development and use. Economy is only a part of it, essential for the societies to evolve and prosper.

Having said this, now we can make direct reference to the main ideas that shape the open source paradigm in the urban/rural development area. We will discuss aspects like open source urbanism, open source ecology, open source hardware design and a possible global villages network. Some ideas have been pinpointed last year at the TE-RE-RD conference, but now it is time to evolve and bring more light into it.

2. THE OPEN SOURCE CULTURE

I believe that most of you already heard about open source. This term became notorious due to the free software movement in computer science from the end of the last Century. Thus, open source became almost a culture synonymous to freedom. But, as life showed us, open is not always similar to free (as in free of charge), so you should not make the mistake and consider those synonyms. Open means freedom, not free as in no cost involved. With regard to free software, there are several unique freedoms, such as: freedom to run the software, freedom to copy and redistribute the software, freedom to study and change the software and the freedom to improve it. All those freedoms can be used in the case of other open source "paradigms" like urbanism, ecology and hardware design.

All these are governed by a "global paradigm of interconnectivity"[1] that forms an open system which is the foundation of all open source paradigms, being at small hardware level, urban, rural or ecological.

---

[1] UAUIM, str. Academiei nr. 18-20, 010014, Bucureşti, România.

As we look at this matter from a macro to micro perspective, those open source ecosystems can be layered as follows: (1) at the macro level we have the ecology, (2) then the urbanism and (3) the hardware design. We will be equally interested in all three of them in this paper. Starting in a top-down manner, we will discuss the open source ecology paradigm, followed by the open source urbanism and big data related to the ideea of smart cities. In the last part we will develop on the open source hardware design with a direct emphasize on rural development.

3. OPEN SOURCE ECOLOGY PARADIGM

Marcin Jukabowski stated that the open source ecology paradigm "is an idea that the open source economy is a route to human prosperity in harmony with natural life support systems" [2]. The main idea of this paradigm is to facilitate open access to information and technology in ways that will empower local communities. In this respect, the Open Source Ecology movement has developed a Civilization Starter Kit, which gives detailed information about DIY projects that could determine local prosperity and community development. There is also a Global Village Construction Set available, in order for people to "survive and thrive with a high quality of life that is not dependent on global supply chains, human exploitation, and environmental degradation" [3].

The open source ecology paradigm is based on the creation of alternatives that have a foundation based on the following: thinking, learning, sharing, making, intervening, working, living [4]. The Agents of Alternatives consider these founding elements to be "intertwined worlds" [5] and offer working definitions for each. Reading these definitions will determine you to think that they can equally apply to the open source culture and paradigm too. And it is true.

4. OPEN SOURCE URBANISM PARADIGM

The term open source is also used in conjunction with the term urbanism. What it means is best described by Saskia Sassen, but before getting to that, we should first take a short look at other paradigms that led to this open source paradigm.

Quiet recently, in a meeting with the heads of the departments, the Dean and the Vice Rector at our Faculty, we discussed on the issues of what urbanism has become nowadays. In the contemporary realm, the urbanist became amongst the least involved in the urban planning and design process, because almost everyone became a "specialist" in dealing with urban related issues. Everyone has an opinion, a suggestion or an idea, and they only use the urbanist to materialize that idea. This is because the urbanism became open source, thus being available to everyone, no matter what their competences are in this matter.

The open source model in urbanism is not even close to similar to the model that the free software movement is based on. At least in the free software movement, even though you are not a programmer or have no prior computer science training, you at least should gain some computer related competences in order to be able to understand the open source code that you are about to modify or improve. Even though you can manage this, your code will not be directly accepted into the upstream repositories until it is checked, verified and controlled by manual or automated systems.

The urbanism's open source model lets you bring your ideas, and even implement them, depending on where you live, but some sort of control and regulations are also implied. This type of citizen-led urbanism is also known as Tactical Urbanism. Besides this type of openness, there is another one, based on big data – it defines the smart cities. The openness of the city determines its dynamic character and the fact that it is in a never-ending state of transformation.

In this context of continuous transformations, the contemporary main actor is the big data. This big data, translated to the realm of our urban living, determines the frontier of innovation, competition and productivity – for short: development. And all this with the benefit of the community. But what does it take for a city to be smart? Rob Kitchin brought all the definitions from the literature down to only two important terms [6]: (1) the notion of "everyware" that is given by all the interconnected devices built into the urban environments and (2) "knowledge economy and governance" that is driven by the smart people living in the cities and that through creativity, innovation and entrepreneurial actions are building a new kind of city upon technology platforms of all kind. Kitchin also states that those two basic ways to reduce the idea of a smart city are actually developing upon "prioritisation of data capture and analysis as a means for underpinning evidence-informed policy development, enacting new modes of technocratic governance, empowering citizens through open, transparent information, and stimulating economic innovation and growth" [7]. Thus, all this open source information that the city is generating is actually a new way to generate growth and wealth to it's citizens, eventually.

Saskia Sassen sees this openness as incompleteness of the city [8], based on small open interventions that make an impact to the entire, and complete, system. Those interventions would be based on small talk-back scenarios of the city system – communities opposing some official decisions that crossed the thin red line of eligibility, individual trials against the administration, infrastructure issues that determine some redesigns and many other examples. This is only a part of what open source urbanism means. Sassen explains the openness and talk-back of the city as a result of certain conditions that were not satisfactory for the community, which in some cases could take time to offer a new solution, from several years to decades, or perhaps only days or months.

There are several examples that Sassen gives when she emphasizes on the works of urbanists and technologists in the city. Amongst those, important ones are the Network Architecture Lab at Columbia University [9] and SENSEable City Lab at MIT [10]. Those are experimental academic projects that enable data collected from the city in order to determine future interventions. Besides those, I could add a special case of ICT involvement in the city development, in the case for blind and visually impaired people. This is a project that is conducted by CEIT ALANOVA in Austria and one of their papers on this project was published in one of my edited books back in 2014 [11]. This is a very interesting project that I would advice you to read.

Nevertheless, all these projects are working with big data and open source data. Nowadays, everything that generates growth and development paths is based on tremendous volumes of [open source] data. Rob Kitchin determined [12], based on the existing literature, that the cities had generated a continuously increasing amount of data, based on the consumers and companies traits. The numbers are extraordinary, according to Kitchin's references: 35 zetabytes of data to be generated by 2020 globally, as 1.7 million billion bytes are generated every minute, globally [13]. Only think about how much of this data could be channelled back to the local development. Most of these data consists of geospatial locations, embedded machines, IoT devices and even CCTV and surveillance equipment.

One good example of how big data can be used for local development is the case of Amsterdam city, where the administration is using all the big data it collects to create a series of interactive maps with detailed information on general urban information, urban development, sustainability, vacant space availability, green distribution, nature and farming, traffic and infrastructure, architecture and history and neighborhood and amenities [14].

All this data being generated by all kind of devices, big and small, determines us to continue the discussion on a macro level, bringing in the open source hardware issue, in the following sub-chapter.

5. OPEN SOURCE HARDWARE PARADIGM

What is open source hardware, through? It is a set of physical objects that are generated by free and open designs, documentation, assembly materials and eventually, running software. But, before getting into more details, should we ask what is the impact of open source hardware to the ongoing hardware development and community grow? Referring to the data amounts that we presented earlier, one should know that this kind of data is generated by closed and open hardware alike, but the calculations were not divided by those types. While closed hardware is reserved for the larger tech companies, the open hardware is mainly created by smaller companies and are targeted to the community.

Thus, a paper presented at the 2016 PICMET (Technology Management for Social Innovation) conference showed how the open source hardware impacts the social innovation spectrum [15]. The authors interpreted a series of open source surveys targeting software and hardware users, and the conclusions were that "the rise of open-source movement goes along with a paradigm shift in (industrial) value creation. (…) It is characterized by networking, knowledge sharing, collaboration, co-creation and decentralization" [16]. The overall winner is the community, which, in a study conducted in 2013 came out to be formed of hobbyists, programmers and engineers, designers, students, inventors, entrepreneurs and researchers in various percentages [17].

The most important aspect to be taken into account while developing open source hardware is the hardware patent, which can be a bottleneck in open-source production. Nevertheless, once a producer has a hardware patent issued, it can grant open access to the patent technology and let anyone use it and/or change it, or create a trademark [18].

Out of all the open source hardware devices, I consider the 3D printers and Arduino to be of great importance with regard to the urban and rural development.

The idea of a 3D printer is in itself based on the philosophy of open source and sharing – its main purpose is to create new things. While there are many closed source printers around, the open source printing is gaining a lot of traction right now. Therefore, Tom Callaway from Red Hat reviewed the best open source 3D printers from 2016 on the opensource.com website [19]. Among the printing innovations there are the Prusa i3 MK2 by Josep Prusa from RepRap, Mechaduino from Tropical Labs (a servo motor), the Bricoleur Clay Extruder (a special clay printer based on RepRap), the Lulzbot TAZ 6 by Lulzbot, and a bio-printer by Ourobotics. All of the above mentioned 3D printers bring innovation in their respective fields.

For more information I advise you to read the opensource.com article on this, as we will not get into much more detail on these models. What we are interested in is how to use this with respect to urban are rural development. Open source ecology has a project for an open source hardware 3D printer called "The Distributive Enterprise 3D printer" that is modular and can be extended by the users' needs and thus used to produce objects of various sizes.

Besides those 3D printers, the start of the open source hardware "show" is the Arduino platform. The Mechaduino from Tropical Labs is one of the fewer 3D printers servo motor that are built on Arduino. Mechaduino has reached the 3rd prototype stage and the producers had put together a manual that is also free to download [20]. The Arduino offers a relatively low cost open source platform for hardware development and thus can be used in a variety of projects run by the community. A simple visit to the official Arduino website will just make you want to build some cool stuff, using as few money as you can. Arduino hardware boards comes in many forms, covering several levels, from entry level, enhanced features, IoT, education, wearable and 3D printing [21].

Nevertheless, you should keep in mind that no hardware, being it closed or open source, can not run without an appropriate software platform. This is where Arduino brings into the "battle" a great suite based on a web editor and a desktop IDE, and the process of using those only implies creating an Arduino developer account and starting right up.

Besides the Arduino platform, there is the Raspberry Pi platform, which is as important as the first one. It was produced in order to create a low cost platform that has a small form factor and could compete with the larger personal computers in terms of computing power and operability, but giving the opportunity to experiment and learn with it more than a usual computer could. The Raspberry Pi has reached version 3 model B, which was released back in 2015, with a quad core 64bit ARM based processor, 1GB of RAM and for the first time, integrated wireless and Bluetooth connectivity, at the

price of 35$. It runs on Raspbian, a version of Debian Linux specially crafted for it, but there are spins of Ubuntu Linux, Fedora Linux and openSUSE Linux for this platform too.

6. OPEN SOURCE AND DIY IN URBAN/RURAL DEVELOPMENT

Thus, having a concise presentation of what open source is with regard to ecology, urbanism and hardware, now is time to highlight some implications of using open source hardware projects in rural development.

First of all, how can open source be embraced in the development of various rural or urban areas? The main argument is its costs, and this is perhaps the most important asset of contemporary economy. But, in order to implement this kind of technology we need open minded administrators, councillors and mayors that will invest in the hardware and the "minds" behind it. They need to shift the focus to the community, which is really hard to do considering that once they have the power, they start to feel the taste and are not able to let the community to rule. This is called citizen-driven innovation, and open source technology plays an important and primary role. The World Bank's study on citizen-driven innovation considers the most important elements of future development to be IoT, cloud computing and open data that will be the base on idea generation, cooperative design and services [22].

Therefore, once you can get the community into it, one more think you have to do is to build specific community networks based on governance and policy and social connectivity. Thus, basically community network is an "alternative bottom-up approach, based on community-driven infrastructure development, as a substitute (…) to the classic top-down operator-driven paradigm" [23]. Community involvement is the fuel of innovation, and this is best seen in the rural development projects around the world. Amongst those, the ones implemented in developing countries are the best examples in the innovation department.

Open hardware and software is used in intensive and integrated agricultural and farm systems (most based on Arduino) [24], and also in the case of assisting the farmers in their farming operations [25]. In the case of various large developing sectors such as healthcare, climate change, pollution or energy, most of the hardware used is not open source and big names as CISCO play a major role in delivering components, expertise and software. Leaving aside the open source aspect, the CISCO research into IoT and big data involvement in global development has some interesting findings. Thus, big data leads to a reduced cost of computing in general, cheaper sensors and a bigger emphasize on software development and accuracy [26], and its use will increase in sectors like healthcare of developing countries, water and sanitation, agriculture, resiliency, energy consumption and production and natural resource management. In this respect, the conclusions of the study were as follows: to create a master plan and policy framework for the adoption of IoT, creating an enlarged hardware network for connectivity and spectrum specific to IoT, promote an ecosystem for community development and innovation, create data centres and specific standards, and all these must be built on trust and confidence in the adopting technology [27].

7. CONCLUSIONS

The main conclusion of this short paper is that open source is the very future of rural and urban development. Open source hardware is gaining traction amongst hobbyists and professionals alike. On the other part, open source software is highly available and can be used in running the hardware part, free of charge. By no means does this paper cover all the aspects of open source involvement in rural and urban development, but it can easily form a foundation for future discussions on the subject of open source, community management and hardware solutions for local development. The paradigms presented here are the base for a possible global villages network based on a globally integrated village environment, which will consist of open source data and hardware. Thus, in the near future, the most important asset for developing projects specific to rural areas will be the ability to coordinate, manage, create and code open source specific hardware and software.

References

[1] Kovats, S., The future of open systems solutions, now. UNESCO WSIS+10 review, Berlin, 2013, p.6.
[2] Jakubowski, M., *Open Source Ecology: Civilization Starter Kit v.0.01*, p.6.
[3] OSE team, Open Source Ecology. Factor E Farm in five minutes, p.1.
[4] Fuad-Luke, A., Hirscher, A-L., Moebus, K., *Agents of Alternatives. Re-designing our realities*, Berlin, 2015, pp.18-19.
[5] Fuad-Luke, A., Hirscher, A-L., Moebus, K., *Agents of Alternatives. Re-designing our realities*, Berlin, 2015, p.18.
[6] Kitchin, R., *The real-time city? Big data and smart urbanism*. In: GeoJournal no 79:1-14, Springer, 2014, pp:1-2.
[7] Kitchin, R., *The real-time city? Big data and smart urbanism*. In: GeoJournal no 79:1-14, Springer, 2014, p.2.
[8] Sassen, S., Open Source Urbanism, op-ed on Domus.it: http://www.domusweb.it/en/op-ed/2011/06/29/open-source-urbanism.html.
[9] Netlab project of Columbia University can be found at: http://www.networkarchitecturelab.org/
[10] The SENSEable City Lab from MIT can be found at: http://senseable.mit.edu/
[11] Neuschmid, J., Gajevic, L., Schrenk, M., Wasserburger, W., *The blinds's critical space and the role of modern ICT*, in: Calcatinge, Al. (ed.), Critical Spaces. Contemporary perspectives in urban, spatial and landscape studies, LIT Verlag, Vienna 2014, pp. 179-206.
[12] Kitchin, R., *The real-time city? Big data and smart urbanism.* In: GeoJournal no 79:1-14, Springer, 2014, p.4.
[13] Kitchin, R., *The real-time city? Big data and smart urbanism*. In: GeoJournal no 79:1-14, Springer, 2014, p.4.
[14] The interactive maps of Amsterdam can be accessed at: http://maps.amsterdam.nl/.
[15] Moritz, M., Redlich, T., Grames, P. P., Wulfsberg, J. P., *Value creation in open-source hardware communities: case study of Open Source Ecology*. In: 2016 Proceedings of PICMET'16:Technology Management for Social Innovation.
[16] Moritz, M., Redlich, T., Grames, P. P., Wulfsberg, J. P., *Value creation in open-source hardware communities: case study of Open Source Ecology*. In: 2016 Proceedings of PICMET'16:Technology Management for Social Innovation, p. 2368.
[17] Moritz, M., Redlich, T., Grames, P. P., Wulfsberg, J. P., *Value creation in open-source hardware communities: case study of Open Source Ecology*. In: 2016 Proceedings of PICMET'16:Technology Management for Social Innovation, p. 2369.
[18] Moritz, M., Redlich, T., Grames, P. P., Wulfsberg, J. P., *Value creation in open-source hardware communities: case study of Open Source Ecology*. In: 2016 Proceedings of PICMET'16:Technology Management for Social Innovation, p. 2370.
[19] Tom Callaway's article on opensource.com can be accessed at: https://opensource.com/16/12/yearbook-3D-printing-innovations.
[20] The Mechaduino manual can be downloaded from the address: https://cdn.hackaday.io/files/11224480207616/MechaduinoManual.pdf.
[21] Check the official arduino boards at: https://www.arduino.cc/en/Main/Products.
[22] Eskelinen, J., Robles, A. G., Lindy, I., Marsh, J., Muente-Kunigami, A., (Eds.), *Citizen-Driven Innovation. Guidebook for city mayors and public administrators*. World Bank and the European Network of Living Labs, 2015.
[23] Belli, L., Echaniz, N., Iribarren, G., *Fostering connectivity and empowering people via community networks: the case of AlterMundi*. In: Belli, L., (ed.), Community connectivity: building the Internet from scratch. Annual report of the UN IGF dynamic coalition on Community Connectivity, FGV Direito Rio, 2016, p.32.
[24] Ruane, J., Dargie, J.D., Mba, C., Boettcher, P., Makkar, H.P.S., Bartley, D.M., Sonnino, A., (Eds.), Biotechnologies at work for smallholders: case studies from developing countries in crops, livestock and fish, Food and Agriculture Organization of the United Nations, 2013.
[25] Narechania, A., An android-arduino system to assist farmers in agricultural operations, Proceedings of IRF International Conference, New Delhi, India, 2015.
[26] Harnessing the Internet of Things for Global Development. A contribution to the UN Broadband commission for Sustainable Development by CISCO and ITU.
[27] Harnessing the Internet of Things for Global Development. A contribution to the UN Broadband commission for Sustainable Development by CISCO and ITU, p.47.

CONVERGENCE STUDY FOR PARABOLIC NON -STATIONARY STRUCTURAL MODELS

Cardei Petru[1], Sfiru Raluca
INMA Bucharest

ABSTRACT

This article gives an example of a study of the convergence of a structural parabolic non - stationary model. In this case, apart from spatial variables, the convergence study must take account, also, by the behavior of the solution over time. We chose for the convergence study, the numerical simulation of a process of diffusion of a fluid into the soil. From a physical point of view, the model is elementary. This mathematical model can be the basis of a more complicated construction (simulators) for complex studies for the distribution and absorption of fluids in the soil of some plantations, especially those arranged for different agricultural crops. The mathematical model used is that of the plane fluid diffusion, into the soil. The results consist of the evolution of the fluid concentration, in the soil, depending of time and of the two spatial variables. The article only exposes the organization of data and the estimation of the convergence of the results.
.

Key words: convergence, structural, model, non -stationary phenomenon, FEA

1. INTRODUCTION

Convergence studies for structural models already have an appreciable length of time, perhaps in the order of several decades. These studies aim to achieve optimal meshing for the numerical solution of the problem, allowing for a solution that is sufficiently precise, with less computational effort. In [1], I have tried to enunciate some possible mathematical definitions of the convergence of structural models. This notion is fundamentally different from mathematical convergence. In [2], we have diversified the range of types of convergence notion for structural models, introducing convergence in the set of the structural models of the same phenomenon. The convergence study first appeared from structural engineers, mechanics specialists (metal structures, machine building industry).

2. METHODOLOGY

To study the convergence of the numerical solution, the material (the subject) used is the classical mathematical model of diffusion on a geometric model inspired by the practice of arranging agricultural plantations. Geometry is taken from strawberry plantations, with the soil shape, obtained through formation of ridges, [8]. We simulate the effect of slow irrigation in a normal section in the direction of the ridges and on the soil surface. The simulation is done only for the case that water level in the ridges interval has stabilized to half the height of the ridge.

The geometric model is given in Figure 1. The ground area is bounded by the polygon line: ABCDEFGHIJKLM. The QBA, EFGH and KPL polygons are water areas. These areas contribute to the calculation, through the conditions to the boundaries AB, EFGH and KL. The initial water concentration in the soil occupied field was considered ideally null. Changing the initial concentration (humidity) can modify the coefficient of water diffusivity in the soil.

[1]INMA Bucharest, Bd. Ion Ionescu de la Brad, no. 6, , 0726142837, petru_cardei@yahoo.com

Border conditions (concentrations) are given in Table 1. Border conditions are also ideal. These conditions can be refined, taking into account experimental measurements.

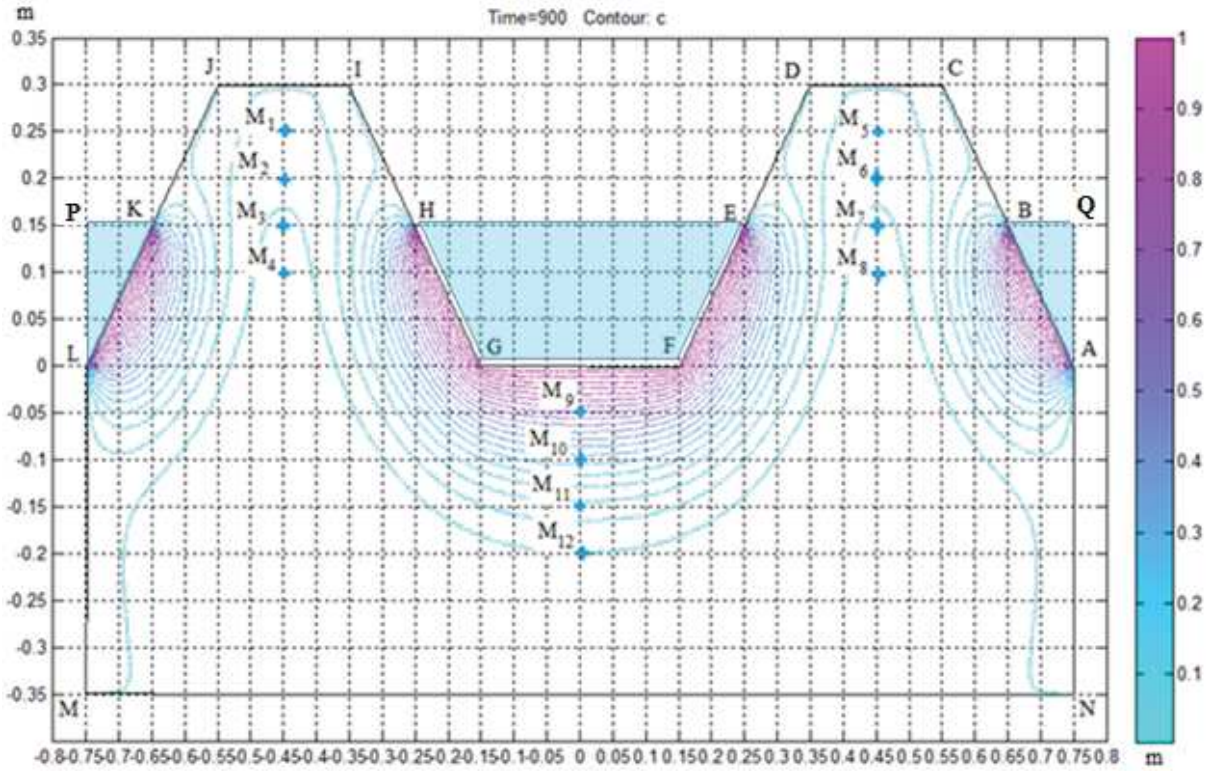

Figure 1: Mathematical model of the diffusion of water in the soil: geometry, border conditions, point of reporting of the water concentration. The contours correspond to the water concentration constant values.

Table 1: List of the concentrations on the boundary of the considered soil domain.

Segment	concentration	Segment	concentration	Segment	concentration	Segment	concentration
AB	1.00	EF	1.00	IJ	0.10	LM	0.08
BC	0.15	FG	1.00	JK	0.15	MN	0.05
CD	0.10	GH	1.00	KL	1.00	NA	0.08
DE	0.15	HI	0.15				

The model and solving is based on the package for solving the partial differential equations, which belong to the MATLAB software [9]. The equation which modeling the diffusion phenomenon is the simplest possible:

$$\frac{\partial c}{\partial t} - \mathrm{div}(D\mathrm{grad}c) = Q \tag{1}$$

where c is the water content in the soil, D is the diffusion coefficient, and Q is the volume sources flow, considered null in this model. Obviously, the model is very simple, appropriate to the purpose of exemplifying the convergence study for a non -stationary, structural model.

Method of study of convergence

The points of the diffusion field, where the results are tracked are marked on the model in Figure 1: M1,…, M12. The points M1, ... M4 and M5, ..., M8 correspond to the axis of symmetry of the ridges, and are located approximately on the direction of the root of the plants. The points M9, ..., M12 are on the axis of the interval between the ridges. For the study, in each of the M1, ..., M12 points, the concentrations and the time at which they were recorded were collected. Four reference times were considered: initial time, 0 s, 300s, 600s, and 900s. The above data was selected for each of the eight mesh networks considered.
The convergence study method was the same as in other convergence studies, [1], [2], [3]. The density of the spatial mesh has gradually increased, until the concentration values at all control points, M1, ..., M12, have an asymptotic tendency.
After each spatial meshing and running program, the concentration values were read at the M1, ..., M12 points for the moments of time: 0, 300, 600, and 900 seconds. These values were stored in the tables and then represented graphically as in Figure 2, 3 and 4. The control points were chosen so that the water content in the soil in the neighborhood of these points was significant for plant roots at some stage of their development. Such points are M1, ..., M4 and M5, ..., M8. Control points M9, ..., M12 are important for knowing the maximum concentration of water in the soil, which is partly responsible for compaction phenomena.

Results
Verification of the solution's convergence was made both by the asymptotic behavior of the solution in relation to the meshing, but also by checking the symmetry of the solution values in relation to the symmetry axis of the geometry of the field. The symmetry of the solution, on a geometry domain having a symmetry axis and symmetrical loads on the border, is a qualitative aspect which, in such cases, needs to be verified. For the initial time, t = 0, we did not give the graphical representations, because, except for some values of the meshing density (116, 464 and 994 finite elements), in other cases the solution is identically null.
At any of the three measuring times (300, 600 and 900 s), the asymptotic character of the solution is present in all control locations, starting with the meshing that includes 28,852 elements.
In Figure 2, at a depth of 5 cm from the horizontal area of the ridges (control locations M1 and M5), after 300 seconds of water dissipation, the water concentration reaches a value of 0.042 (or 4.2%). In the same locations, after 600 and 900 s from the beginning of the phenomenon, the water concentration reaches 0.065 and 0.08 respectively (Figures 3 and 4). The distribution of the concentrations values in the two ridges of the geometric domain considered shows a clear symmetry (Figures 3 and 4).

Observations
The structural model proposed in this article serves only to demonstrate the need for a convergence study for diffusion and mass and energy transfer problems, all the more complicated, as the phenomena under consideration are not stationary. The chosen example is a simple one because the diffusion is only a small component of the interaction between soil and water. Apart from the other phenomena of this interaction, the phenomenon is easier to understand. In addition, if this model is considered separately one and is proves the need for a convergence study, then, for more complex models, the need for this study is obvious.
Interaction between soil and water can have a starting point in this model. In order to achieve a fidelity to make such a model useful, the phenomenon of water transfer through the soil, and the phenomena of compaction and erosion caused by the movement of water in the soil and in the irrigation channels must also be taken into account. Therefore, in addition to the

phenomenon of diffusion and mass transfer (substance), the general model should be supplemented with the equations of the fluids movement in the channels, with the equations

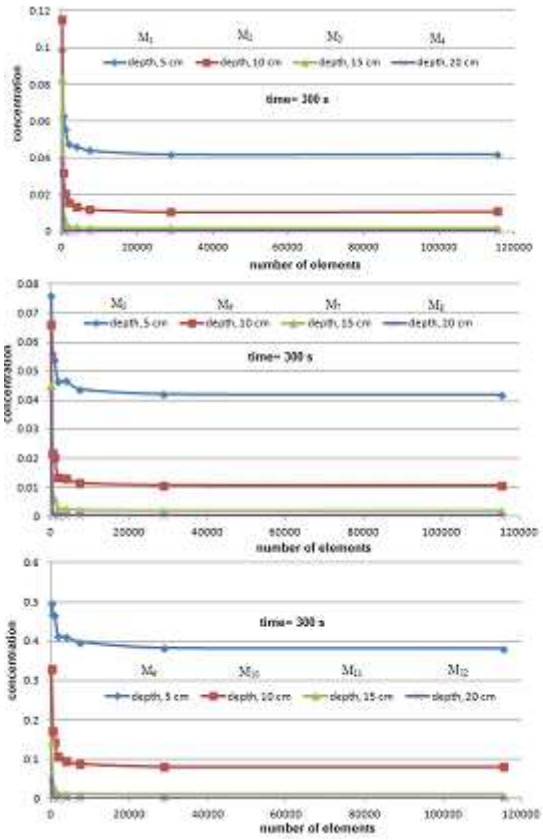

Figure 2 The water concentration variation in the control points depending on the number of finite elements, at the time 300 seconds from the beginning of the diffusion simulation.

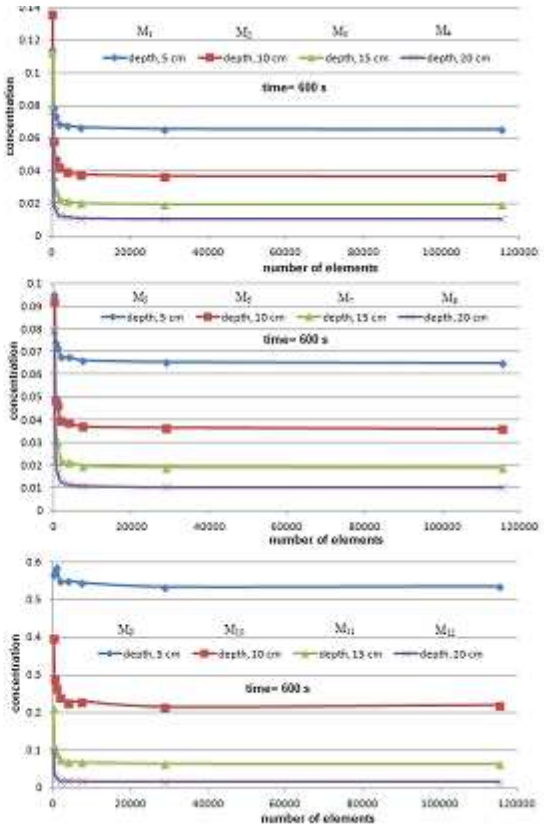

Figure 3 The water concentration variation in the control points depending on the number of finite elements, at the time 600 seconds from the beginning of the diffusion simulation.

of the stability of the soil ridges modeled on the surface of the plantation and, with equations that characterize the erosion of these forms. Such a complex model will be able to estimate plant irrigation (efficiency, irrigation speed but also the maximum allowable water velocity in the channels), lifetime of soil modeling (optimal in the sense of lifetimes equal to plant life, from planting to harvesting). Such mathematical models are found, combined in various complex programs for the management of agricultural soils (WEPP, [10], RUSLE, [11], etc.). Within these expert programs, there are other mathematical models that predict the behavior of agricultural crops based on weather forecasting and financial resources.

3. CONCLUSIONS

The results presented in this article show that the convergence study is mandatory for diffusion and mass and energy transfer issues. The convergence study of these problems is further complicated by the fact that, generally, these phenomena, characterized by hyperbolic operators, are no -stationary. For this reason, the asymptotic behavior in relation to mesh density must be checked at many various times. Depending on the meshing pattern over time, the convergence study can get complex issues, especially when the physical phenomenon present instability due to some physical parameters. Was not the case for the simple example examined

in this article. It is noted that there is a limit of meshing density of the spatial domain, from which the asymptotic character of the solution manifests clearly for any discretization with a number greater than the mentioned limit. For the domain considered in the concrete example examined, this limit can be taken between 25,000 and 30,000 finite elements (the penultimate meshing considered was 28852 items). The last meshing considered, with a total of 115,408 elements, led to a practically identical solution to that, obtained, using the mesh with 28,852 elements for the spatial domain. On the structural model considered, the symmetry of the solution was also, tested, and taking into account the geometric and physical symmetry of the model. We find that the solutions obtained for mesh with the number of elements between 20000 and 25000, show a very good symmetry. This assertion is made, given the accepted tolerance limits on soil humidity.

The model considered is only a modest component to be considered in a significant model of the interaction between water and soil (agricultural or other soil).

In essence, the study shows users of such models that they should not stop at the first mesh, but try to get the asymptotic behavior of the solution. Obtaining this asymptotic behavior of the solution is the minimum guarantee of some very likely results, in line with the reality. However, as we have pointed out in each article related to these aspects, the final verdict, validation of the model, can be done only by comparison with experimental results (and those that are well developed and, even in this case, are, ideally, insufficient).

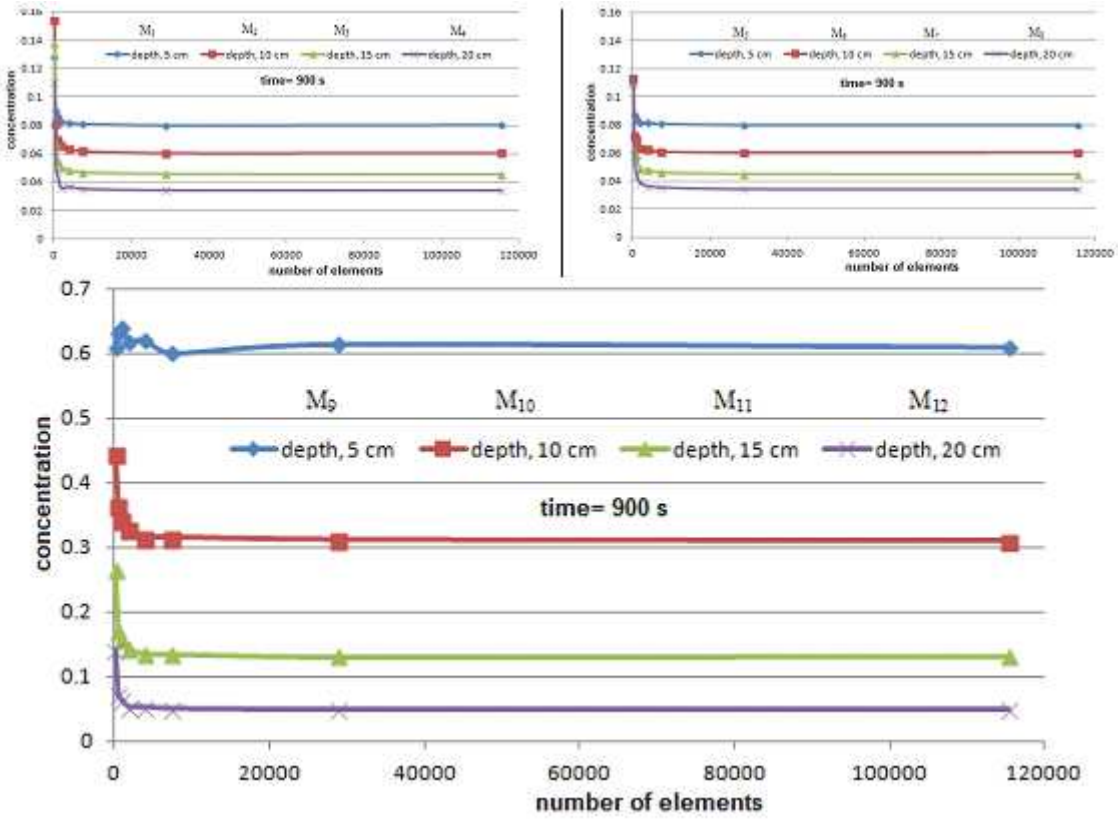

Figure 4 The water concentration variation in the control points depending on the number of finite elements, at the time 900 seconds from the beginning of the diffusion simulation.

Acknowledgement

This work has been done within the project "*Advanced computer and digital research of conception and development, in order to efficiency the intelligence technology systems for agricultural works*" within the NUCLEU 2016 - 2017 Program. Code PN 16.24, founded by the Government of Romania - Ministry of National Education and Scientific Research.

References

[1] Cardei, P., *Considerations on the convergence of structural analysis results*, *performed by finite element method*,https://www.researchgate.net/publication/312595676_Considerations_on_the_convergence_of_structural_analysis_results_performed_by_finite_element_method, 2017.
[2] Cardei, P., *The Convergence analysis of the mathematical models of a phenomenon in the structural analysis*, https://www.researchgate.net/publication/314113468_The_Convergence_analysis_of_the_mathematical_models_of_a_phenomenon_in_the_structural_analysis, 2017
[3] Cardei P., Sfiru R., Muraru S., Muraru V., *The convergence of structural models used in the geotechnical software*,https://www.researchgate.net/publication/315712564_THE_CONVERGENCE_OF_STRUCTURAL_MODELS_USED_IN_THE_GEOTECHNICAL_SOFTWARE, 2017
[4] Li Z., Reed M., B., *Convergence analysis for an element-by-element finite element method*, Computer methods in applied mechanics and engineering, ELSEVIER, vol. 123, issues 1-4, 1995.
[5] Gaevskaya A., Iliash Y., M. Kieweg, Hoppe R.H.W., *Convergence Analysis of Adaptive Finite Element Method for Distributed Control Problems with Control Constraints*, Conference Paper, Control of Coupled Partial Differential Equations, pp. 47-68, 2005.
[6] Shen R. W., *Convergence Study On Explicit Finite Element for Crashworthiness Analysis*, SAE International, Technical Paper, 2006.
[7] Rauch J., *On Convergence of the Finite Element Method for the Wave Equation*, SIAM Journal on Numerical Analysis, 1985.
[8] http://fermadecapsuni.ro/bilonare/21.htm , 2017.
[9] Mathworks Documentation, https://www.mathworks.com/help/pde/index.html , 2017.
[10] USDA-Water Erosion Prediction Project Hillslope Profile and Watershed Model Documentation, NSERL Report #10, https://www.ars.usda.gov/midwest-area/west-lafayette-in/national-soil-erosion-research/docs/wepp/wepp-model-documentation/ , 1995
[11] http://fargo.nserl.purdue.edu/rusle2_dataweb/RUSLE2_Index.htm , 2017.

IDENTIFYING SHAFT SURFACE DEFECTS USING VIBRATION ANALYSIS

Crăița CARP-CIOCÂRDIA[1], Răzvan-Adrian BECHERU[1], Georgiana DUNCA[1],
Diana Maria BUCUR[1], Ioan MAGHEȚI[1], Marin ANICA[2]
[1]University POLITEHNICA of Bucharest, Romania
[2]Digitline Automatizări, Romania

ABSTRACT

This paper presents an identification method of the surface defects of a rotating system. The necesity to study this subject comes from the importance to determine the influence of the defect influence over the vibration signal.

A burr on the shaft was simulated using an aluminum foil tape. The vibration was measured using two orthogonal displacement probes at different operation regimes (low and high rotational speeds). The vibration analysis revealed some specific features for the simulated defect.

The experimental tests were conducted in the Mechanical Vibration Laboratory from University POLITEHNICA of Bucharest.

1. INTRODUCTION

A slow roll is defined as the functioning of a machine in a speed interval at which no significant dynamic forces act on the machine such as unbalance forces, or forces induced by other defects such as bearing defects [1].

Acquiring data at slow roll speeds is critically important because it allows us to distinguish shaft surface imperfections (scratches, burrs, residual magnetism) that appear at such speeds from other malfunctions that yield similar data at full-speed conditions.

Slow-roll speeds are typically 5% or less of the full operating speed of the machine, or its first balance resonance if the machine operates above it.

Vibration analysis of a rotating machine is widely used to discover different defects that can appear during the machines operation modes. In the same time, it is used to monitor the parameters of a machine in real time. The purpose in this case is to find faults in the early stages of their developement.

Usually, measurements are made using displacement, speed or acceleration sensors, as well as an optical rotational speed transducer.

2. METHODOLOGY

This study focuses on identifying surface defects of rotating machinery shafts. The experimental setup (Fig. 1) used consisted in of a cylindrical weight attached to a steel shaft resting on three bearings, actioned by an electrical motor. The shaft is represented in this case by the cylindrical disc. The defect will be simulated by an aluminum foil tape, with a thickness of 0.6 mm, placed on the disc's surface.

The drive unit is a three-phase asynchronous motor with cage rotor, power of 0.37 kW, and maximum speed through frequency converter up to 100 Hz is 6000 rpm. The drive unit has the possibility to change rotation direction. The control unit of the setup can vary continuously

Romania, Bucharest, 313 Splaiul Independentei, 0040214029250, craita.carp@upb.ro

the rotational speed from 0 to 6000 rpm.

One pair of displacement sensors was set on the shaft, on vertical and horizontal directions (Fig. 1). The rotational speed was measured using an optical sensor.

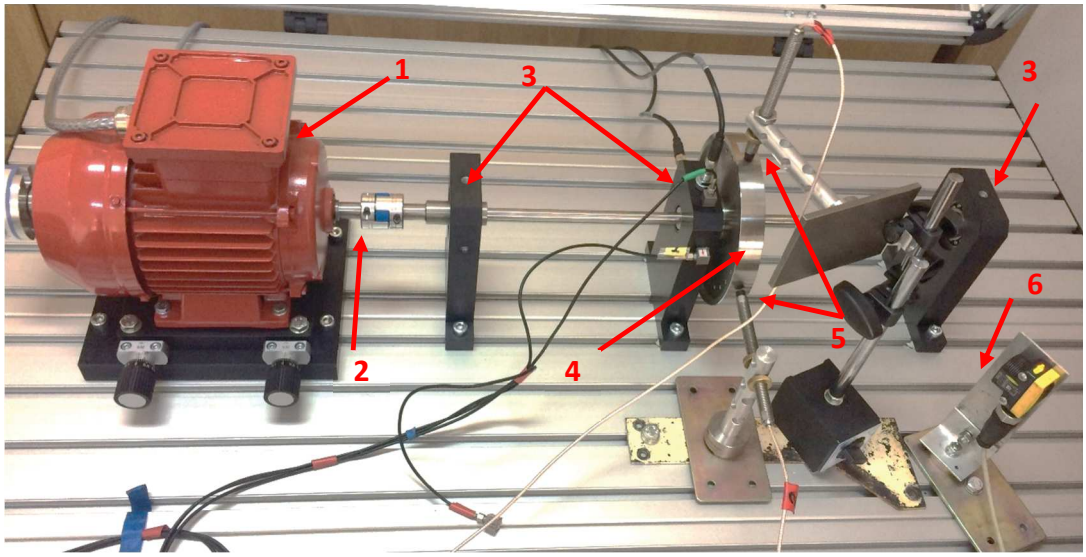

Figure 1: Experimental setup – 1. Drive unit; 2. Coupling; 3. Bearings; 4. Disc (Shaft); 5. Displacement sensors; 6. Optical rotational speed transducer

The results from the vibration analysis are presented for the parameters recorded simultaneously using an acquisition system with 25 kHz frequency on each channel and 0.1% accuracy.

Measurements were made at different rotational speeds and during speed decrease from 3000 rpm to 80 rpm, with and without the defect. In this paper the results for two rotational speeds (80 and 1500 rpm) and during speed decrease will be presented. The rotational direction is clockwise and the duration of each acquisition is 20 s.

3. RESULTS ANALYSIS

The vibration analysis includes the time-domain and the frequency-domain analyses. In most cases, the examination of the time domain behavior of a machine is fundamental to the analysis of that equipment [2].

Time domain analysis is representative for the actual "sequence of events" which occurs on process machinery. However, there are situations when the complexity of the dynamic signals exceed the data processing capabilities of an oscilloscope. In these cases, frequency domain analysis is required for detailed study of the signals.

This is achieved using Fourier analysis techniques to separate a time domain signal into discrete frequency components. The frequency spectrum of the complex signals generated by machines is characteristic for each machine, representing an unique pattern, referred to as the "machine signature" [3].

The frequency domain analysis in the present study is carried out on a number of 2^{15} samples. The sampling period is 0.04 ms, which corresponds to a “cutting frequency” of 12.5 kHz.

Figure 2 presents the shaft orbits. The orbits for the shaft without the defect (Fig. 2a and 2b) have a typical form, with a circular-eliptical shape. The orbits for the shaft with the defect (Fig. 2c and 2d) point out two orthogonal deformations. These are due to the defect that was

observed succesively by the two displacement sensors as impulses (the deformations are oriented outside the general orbit shape).

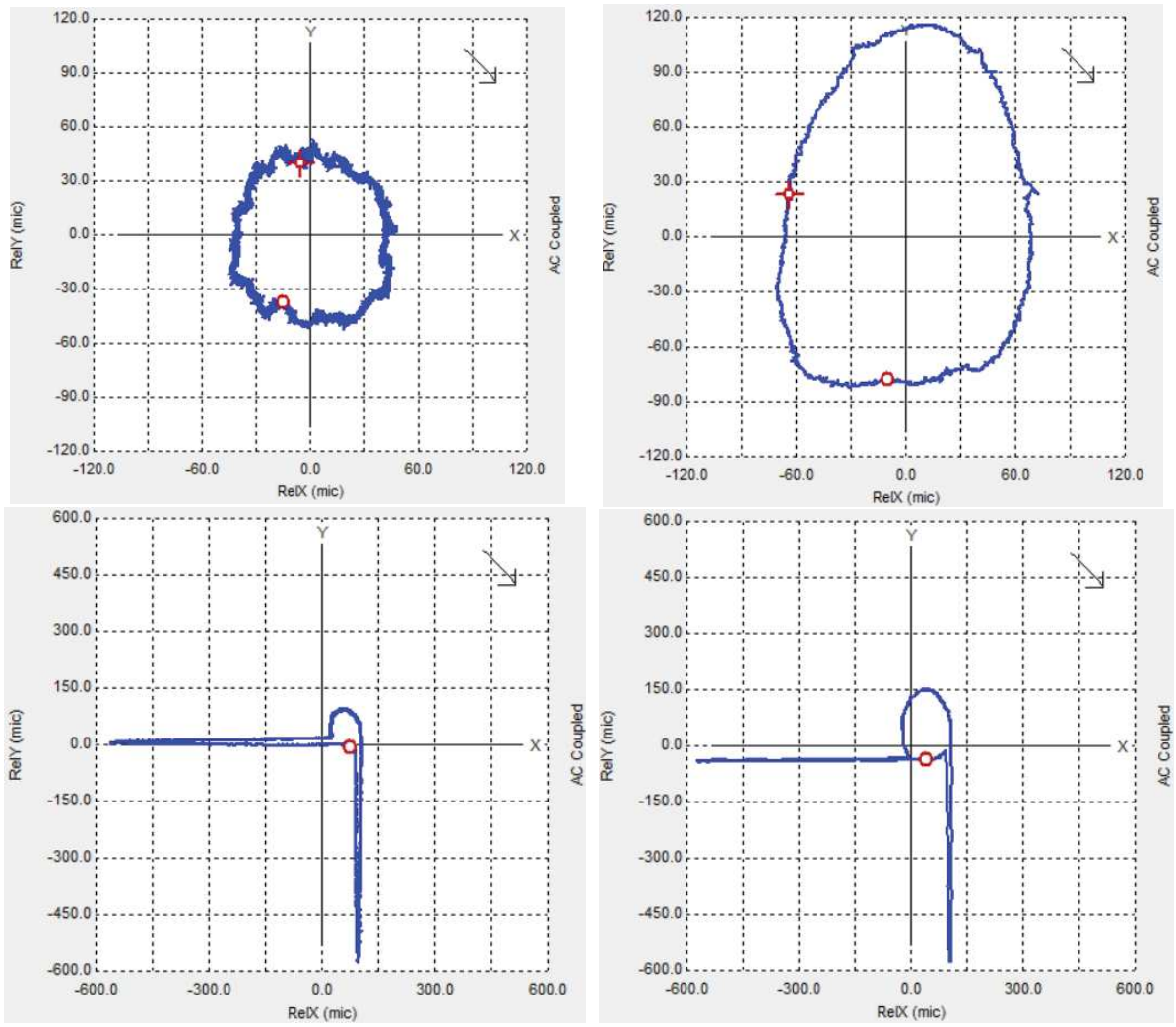

Figure 2: Shaft orbits a) 80 rpm, without defect b) 1500 rpm, without defect c) 80 rpm, with defect d) 1500 rpm, with defect

In figures 3 and 4 the spectral analysis of the displacement sensors signals at 1500 rpm, without and with defect, are presented. The spectre in figure 3 show that the 1X harmonic is dominant, meaning that the vibration of the shaft without the defect has an almost sinusoiudal shape. The same conclusion can be drawn from figure 5a. In figure 4, it can be seen that introducing the defect on the shaft has the effect of increasing the number of harmonics with significant amplitudes. The presence of the defect can be also observed in the waveforms of the signal from figure 5b.

The frequency analysis of the signal recorded during the speed decrease, with and without the defect, is represented as two cascade plots (Fig. 6). It can be seen that for the case with defect (Fig. 6b) multiple harmonics are present in the spectrum. Also, the amplitude of the vibration at higher harmonics is almost the same during the entire recording period. This is a confirmation of the results from [1], stating that a burr (or a scratch) can cause the apparition of harmonics with nearly constant amplitudes at all shaft speeds.

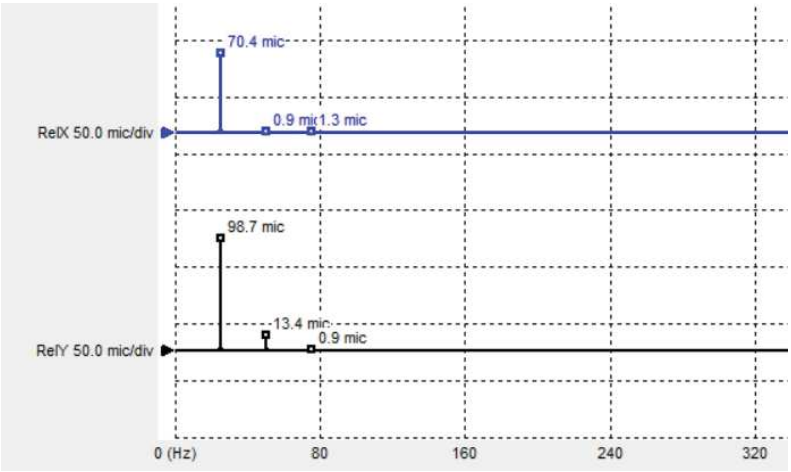

Figure 3: FFT at 1500 rpm, without defect

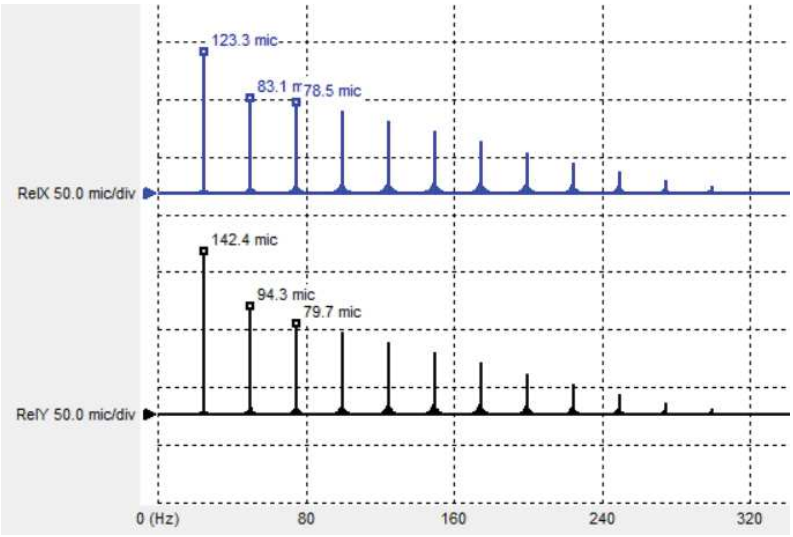

Figure 4: FFT at 1500 rpm, with defect

During the speed decrease, the system passes through its critical frequency (around 2500 rpm), as it can be seen in the cascade plots of both scenarios (for 1X harmonic). In the case of the shaft with defect, the maximum amplitudes in the spectrum (Fig. 6b) have values over 200 μm. When the shaft is without defect the maximum amplitudes are around 100 μm. This difference is due to the introduction of the defect on the shaft.

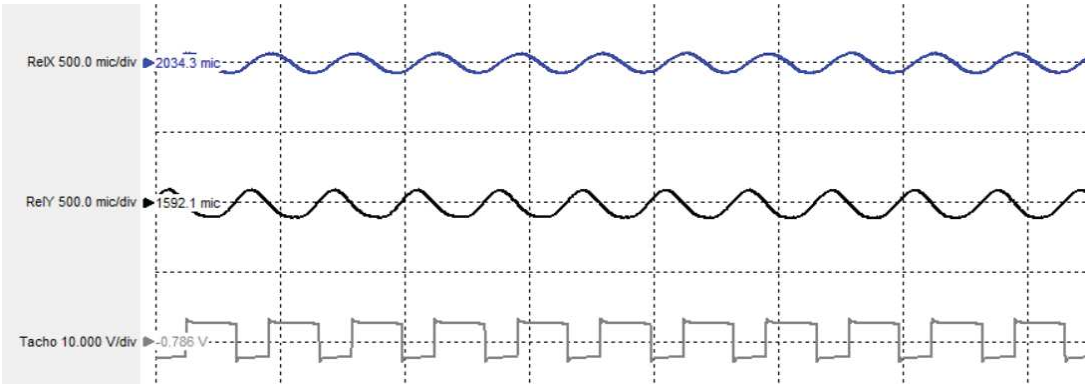

Figure 5: a) Signal waveform at 1500 rpm without defect

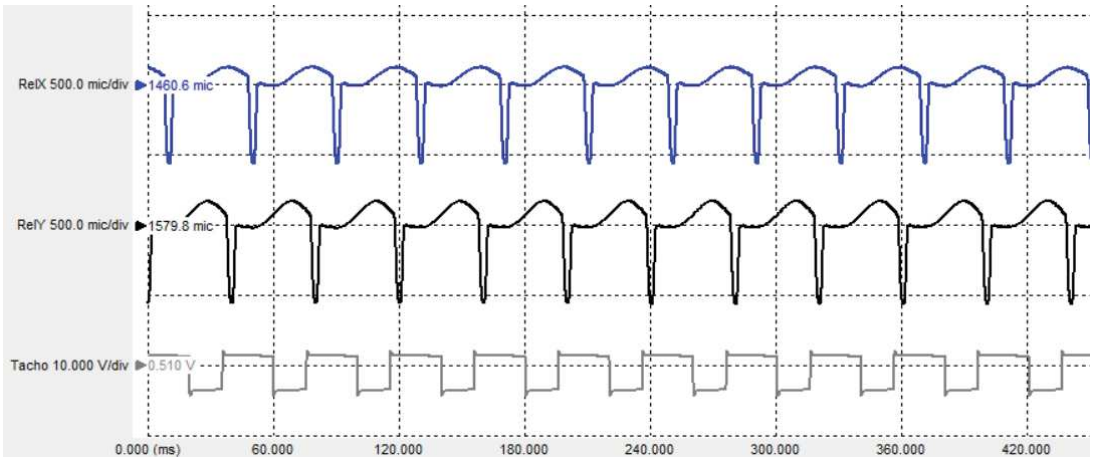

Figure 5: b) Signal waveform at 1500 rpm with defect

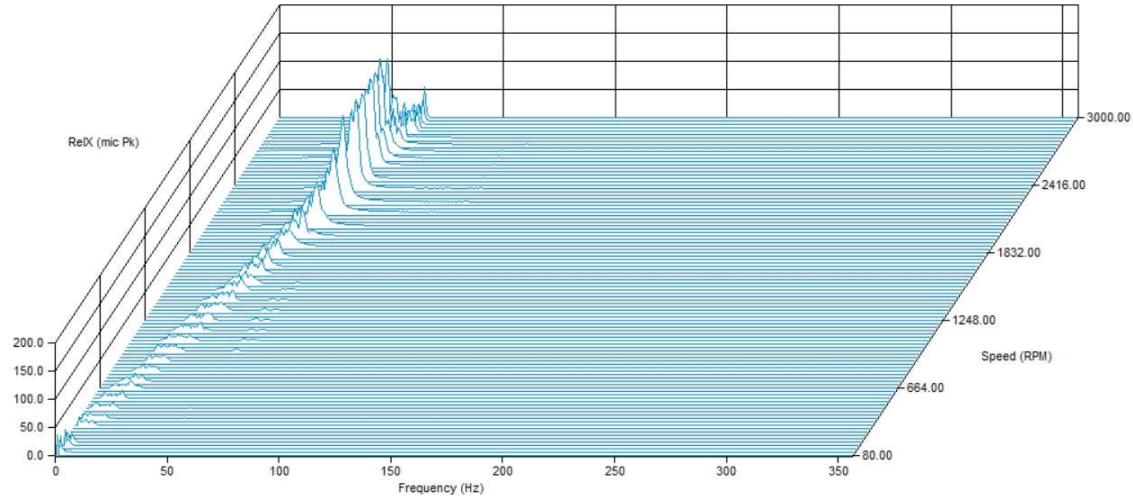

Figure 6: a) Cascade plots during speed decrease without the defect

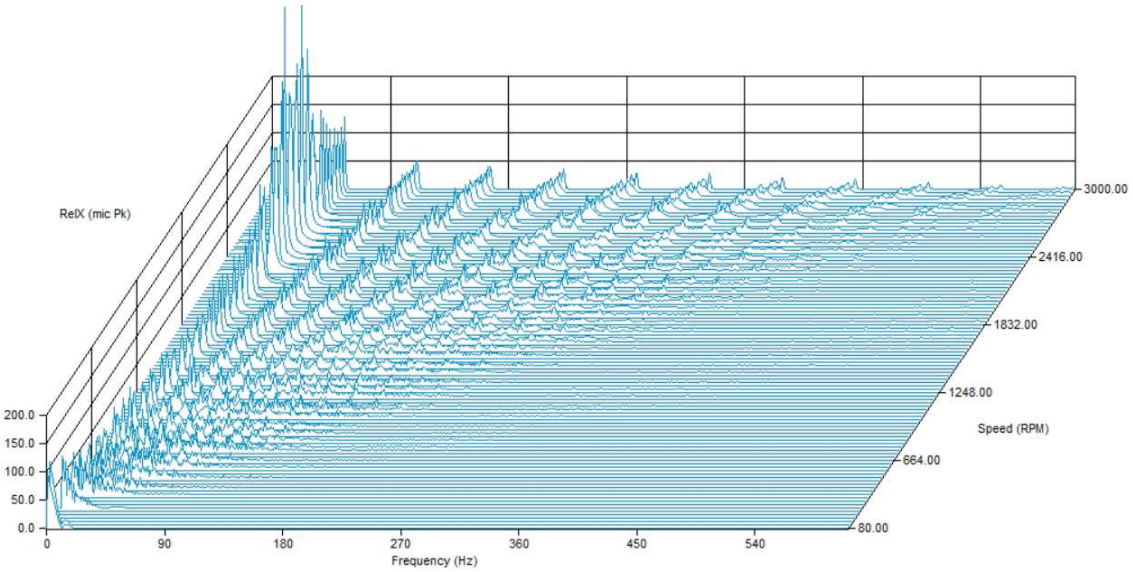

Figure 6: b) Cascade plots during speed decrease with the defect

4. CONCLUSIONS

The paper presents an experimental approach regarding the influence of the surface defects over the dynamic behavior of a rotating system. A burr was simulated using an aluminum foil tape fixed on the shaft. The analyzed experimental tests were conducted with and without defect, for two rotational speeds (80rpm and 1500 rpm) and for the speed decrease regime.

From the analysis of the recorded signals of the displacement sensors orbits and FFT diagrams were represented.

The influence of the defect over the measured displacement was found in the waveforms, orbits and FFT diagrams. The orbit of the shaft with defect is specific to the burr, which is important for vibration diagnosis.

The amplitude of the vibrations in the scenario with defect was higher than without defect.

In addition it was confirmed that a burr can cause the apparition of harmonics with nearly constant amplitudes at all shaft speeds.

Acknowledgements

The experimental data was processed using FastView Software, by courtesy of Digitline Automatizari Company.

References

[1] Maalouf, M. G., *Slow Speed. Vibration Signal Analysis,* ASME Turbo Expo 2007, Montreal, Quebec, Canada, May 14–17, 2007, published in ORBIT Magazine, Vol.27, No.2, pp.4-16, 2007.

[2] Eisenmann, R. C. jr., Eisenmann, R. C. sr., *Machinery malfunction diagnosis and correction,* Prentice Hall PTR, New Jersey, 1997

[3] Bannister, R., Donato, V., *Signature analysis of turbomachinery*, Sound and Vibration, No. 9, 1971

THE INFLUENCE OF THE SPEED OF REVOLUTION OF A HAMMER MILL ON ENERGETIC WILLOW CHIPPINGS

Mihai Chițoiu[1], Gheorghe Voicu[1], Georgiana Moiceanu[1], Gigel Paraschiv[1], Mirela Dincă[1,*], Găgeanu I.[2], Valentin Vladut[2]
University Politehnica of Bucharest, Faculty of Biotechnical Systems Engineering
*E-mail: chitoiu_mihai@yahoo.com

ABSTRACT

Increasing concerns about fossil fuel depletion and CO_2 increase in air that enhances greenhouse effect on the planet have made biomass an alternative energy resource that has two main characteristics: its eco-friendly, and it is renewable. High volume of biomass represents an impediment in its usage as a final product. Each stage of the preparation process was studied by researchers both for establishing the influence of biomass properties on the process as well as for designing the equipment used for preparation process. In this paper experimental research regarding the influence of the speed of revolution of a hammer mill on energetic willow chippings were done. For testing a hammer mill – TCU equipped with an inclined plan (material feeding chamber), collecting the hash in bags, through a two way evacuation system, hash was directed with the help of a shutter was used.

1. INTRODUCTION

Nowadays major worldwide concerns are climate change and fossil fuel resource depletion. To limit the impact of climate change, to replace fossil fuel resources and to reduce green gas emissions, renewable energy resources must be developed and studied further. One of these studies showed that biomass crops are important bioenergy sources [8, 9, 10, 11, 12].

A very important issue nowadays is represented by the question "how to cut down on costs in order to offer the consumer a lower price range?". In order to answer it the attention is now focused on reducing the cost resulted from biomass grinding. It is the process with the highest costs of all. There are many biomass grinding equipments, but when we consider purchase costs, maintenance costs and energy consumption, hammer mills seem to be the best option.

The hammer mills grinding process consists of hitting the material by hammers articulated on a rotor. A parameter that must be taken into consideration when designing such equipment is represented by the percussions applied on the hammers that are not supposed to be transmitted to the articulation. The percussion given by collision with the particles of material is applied in the center of percussion, without this fine tuning connection percussions appear and produce supplementary perturbations. Not taking into consideration there it will have a negative effect on both energy saving and grinded material [3].

Later on the processing process of biomass the quality of the grinded material influences the processes involved in pellet production [7].

Better material binding and high equipment efficiency in the pelletizing process can be achieved with small and medium particle sizes, this conducting to a decrease in the overall production costs [5, 6].

According to different studies energy willow is an agricultural plant that can be grown both on high moisture soils and on clay soils, its calorific power being very large compared to other plants (4900kcal/kg). Energy willow can be processed, obtaining a significant quantity of solid biofuels (chippings for energy plants, briquettes, pellets) [13].

The first preparation process of energetic willow happens during harvesting. The plant can be harvested on the field with specially designed equipment that not only cut the willow stems, but also grinds them into large chippings [4].

Thus considering the size of chipping in this paper experimental research regarding the influence of the speed of revolution of a hammer mill on energetic willow chippings was done.

2. METHODOLOGY

Experiments that are presented in this paper were carried out in November 2015 in a specialized laboratory at the National Research - Development Institute for Machines and Installations Designed to Agriculture and Food Industry – INMA Bucharest. For testing a hammer mill – TCU equipped with an inclined plan (material feeding chamber), collecting the hash in bags, through a two way evacuation system, hash was directed with the help of a shutter was used. Energetic willow stems chipping were realized through hitting and shearing between hammers mounted on the hammer disk, and counter knives. The main characteristics of the hammer mill are: electric motor power: 22 kW, electric motor speed: 2.940 rot/min, milling capacity: 900 m^3/h, interchangeable grinder sieve with different hole sizes.

Figure 1: TCU hammer mill [14, 1]

For experimental tests it was used a sieve with holes ϕ10, a two-step hammer, a speed of revolution of 3000rpm (50 Hz), 2850 rpm (47.5 Hz), 2700 rpm (45Hz), 2550 rpm (42.5 Hz) and 2400 rpm (40 Hz) and samples of 6 g. The speed was varied using a frequency convertor.

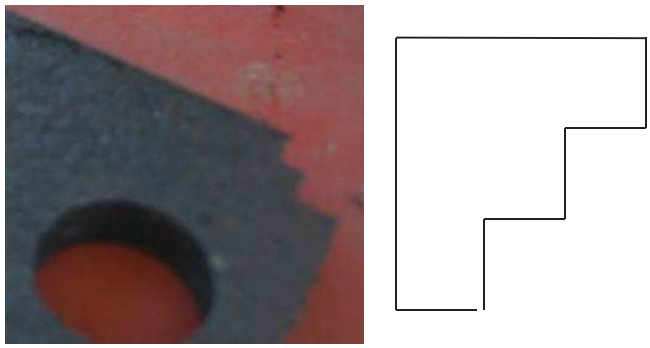

Figure 2: Hammer used during tests

Results obtained after testing are presented in Table 1.

Table 1: Experimental data obtained during testing

Sample no.	Chipped material size/quantity for each dimension				Speed of revolution [rpm]
	< 4 mm [g]	4÷7 mm [g[	7÷10 mm [g]	> 10 mm [g]	
1	1,0815	2,2642	1,5695	1,0848	3000
2	0,8508	2,204	1,9272	1,018	2850
3	0,9441	1,9499	1,937	1,169	2700
4	0,9865	1,9266	1,8404	1,2465	2550
5	1,0138	2,1135	1,6915	1,1812	2400

Experimental results were interpreted with the help of Microsoft Excel program, applying regression analysis for each specific particle dimension obtained after chipping process. The influence of revolution speed on chipped material quantity was shown by drawing variation curves. In figure 3 it is shown the material distribution for every speed of revolution after subjecting it to screening with a sieve with ϕ10 holes.

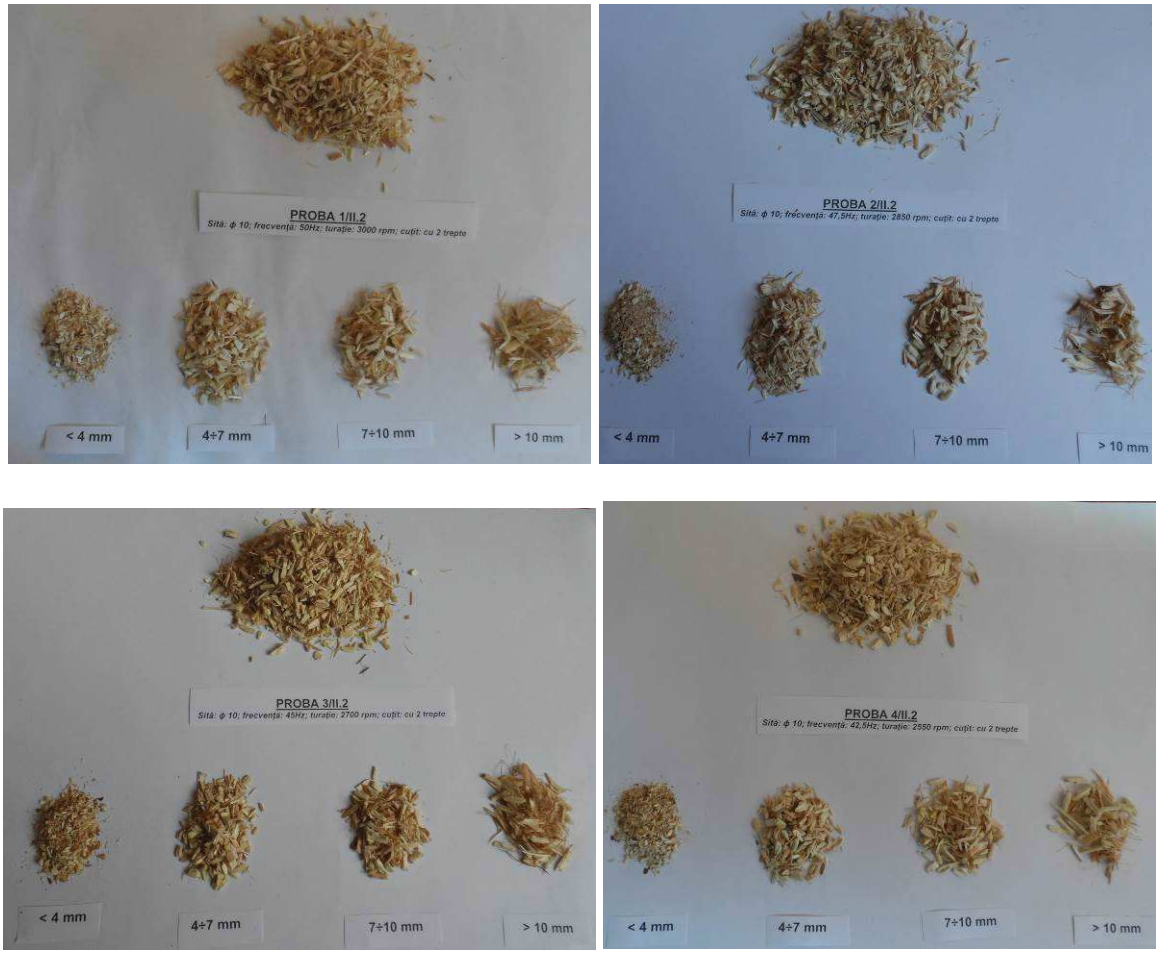

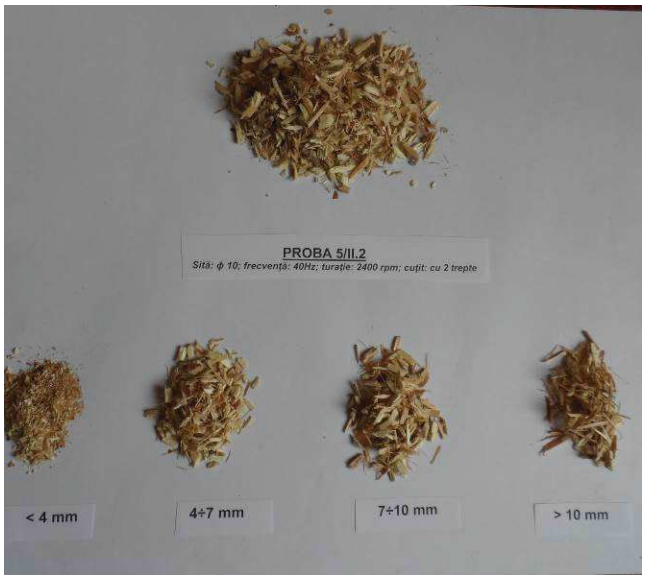

Figure 3: Sample distribution after material screening

Variation curves resulted are presented in figure 4.

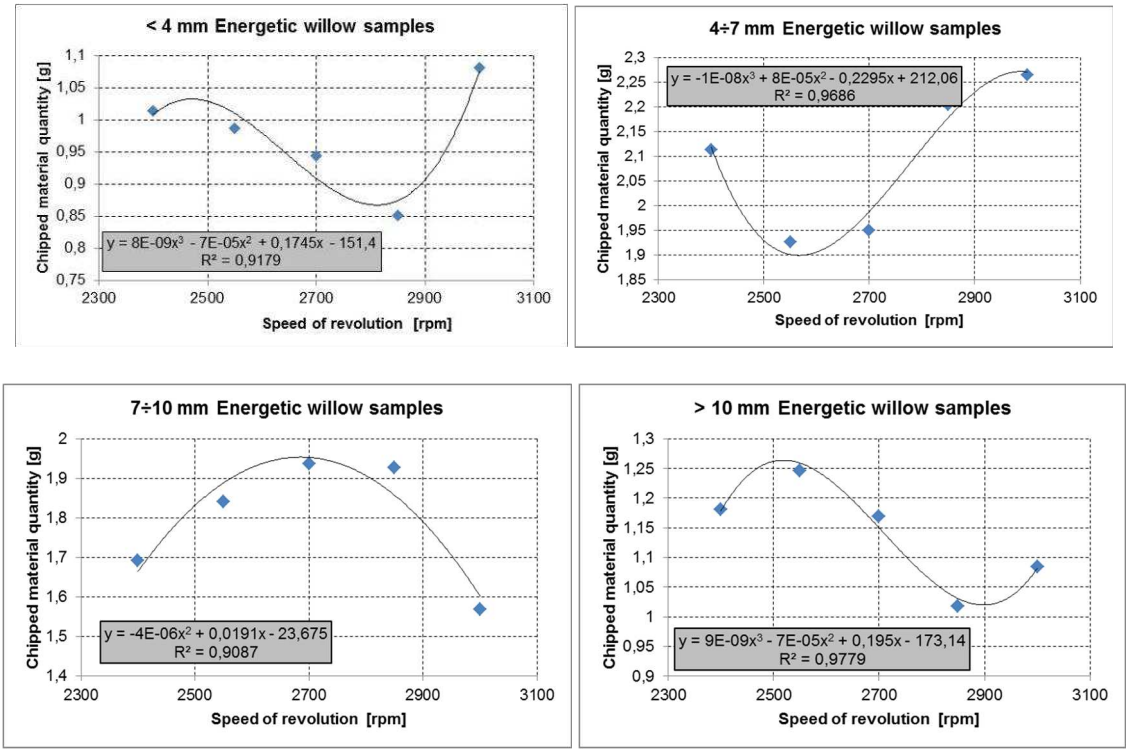

Figure 4: Variation curves between speed of revolution and chipped material quantity

As it can be seen for the correlation between speed of revolution and chipped material quantity for < 4 mm energetic willow particle size distribution on the sieves the coefficient correlation is R^2=0.9179. The regression function used was a third degree polynomial regression. The sieve with the highest degree of particles was registered for the speed of revolution 2400 rpm.

In the case of the correlation between speed of revolution and chipped material quantity for 4÷7 mm energetic willow particle size distribution on the sieves it can be said that the largest quantity of material was registered for the speed of revolution of 3000 rpm while the smallest quantity of material was registered for the speed of revolution of 2550 rpm. In this case the

correlation coefficient R^2=0.9686.

Regarding the 7÷10 mm energetic willow particle size distribution on the sieves it can be mentioned that a second degree polynomial regression function was applied. The data resulted shown a correlation coefficient of R^2=0.9087. The highest quantity of material remained on the sieve was registered for the speed of revolution 2700 rpm.

A third degree polynomial regression function was applied in order to correlate the speed of revolution and chipped material quantity for > 10 mm energetic willow particles. The distribution showed that for a speed of revolution of 2550 rpm the quantity of material was the highest. Also the smallest quantity was registered for a speed of revolution of 2850 rpm. In this case the correlation coefficient was R^2=0.9779.

3. CONCLUSIONS

In order to obtain a clear view on the process and the equipment used for energetic plant processing, experimental research are conducted all around the world. A better understanding of the entire process helps us achieve the goal of limiting the impact we have today on climate change. Thus, with this in mind a small part of this process was studied in this paper by using a TCU hammer mill. The influence of revolution speed on chipped material quantity was shown by drawing variation curves. As it could be seen from figure 3 all the correlation coefficients for the aspects analysed were higher than $R^2 \geq 0.9087$. Considering that these parameters were also studied in a different paper for miscanthus samples and that the results obtained shown a correlation coefficient above 0.8587, we can say that a connection between the analysed parameters was demonstrated [2].

Future studies in this field with various biomass samples will help find better correlations between revolution speed and chipped material particle size, this leading to a decrease in energy consumption and better size reduction process.

Acknowledgement

This work was partially supported by the strategic grant POSDRU/159/1.5/S/137070 (2014) of the Ministry of National Education, Romania, co-financed by the European Social Fund – Investing in People, within the Sectoral Operational Programme Human Resources Development 2007-2013.

References

[1] Chiţoiu M., Voicu Gh., Paraschiv G., Moiceanu G., Vlăduţ V., Matache M., Marin E., Bunduchi G., Danciu A., Voicea I., Găgeanu I.- *Energy consumption of a hammer mill when chopping miscanthus stalks*, Proceedings of The 44 International Symposium On Agricultural Engineering "Actual Tasks on Agricultural Engineering", pp. 215-224, ISSN 1333-2651, Opatija–Croaţia 2016.

[2] Chiţoiu M., Voicu Gh., Paraschiv G., Moiceanu G., Vlăduţ V., Matache M., Marin E., Bunduchi G., Danciu A., Găgeanu I., *the influence of the speed of revolution of a hammer mill on miscanthus chippings* , Annals of the University of Craiova - Agriculture, Montanology, Cadastre Series, Vol. XLV 2015.

[3] M. Fenchea, Design of hammer mills for optimum performance, Journal of Vibration and Control

[4] Lundquist L., Willi F., Leterrier Y., Manson J.A. E. - Compression Behavior of Pulp Fiber Networks, Polymer Engineering and Science, 2004.

[5] Tabil L., Adapa P., Kashaninejad M. - *Biomass Feedstock Pre-Processing* – Part 2: Densification, Biofuel's Engineering Process Technology, August, 2011.

[6] Tumuluru J. S, Wright C. T., Kenny K. L., Hess J. R. - A Review on Biomass Densification Technologies for Energy Application, The INL is a U.S. Department of Energy National Laboratory, August 2010.

[7] N. Yancey, C.T. Wright & T.L. Westover, „*Optimizing hammer mill performance through screen selection and hammer design*", ISSN: 1759-7269 (Print) 1759-7277 (Online) Journal homepage: http://www.tandfonline.com/loi/tbfu20.

[8] Greenpeace, Scénario de transition énergétique, 27 p, 2013.
[9] Eurelectric, *Power choices pathways to carbon-neutral electricity in Europe by 2050*, Full Report, Union of the Electricity Industry, 100 p, 2011.
[10] EREC, *RE-thinking 2050, a 100 % renewable energy vision for the European Union*, 76 p, 2010.
[11] ECF, *Roadmap 2050: a practical guide to a prosperous, lowcarbon Europe*, Technical Analysis, 100 p, 2010.
[12] IEA/OECD, *Perspectives des Technologies de l'Energie, Scénarios et Stratégies à l'horizon 2050, Synthèse et Implications Stratégiques*. International Energy Agency (IEA), 15 p, 2006.
[13] http://greenenergy.org.ro/index.php?language=en&page=23
[14] www.inma.ro.

TURBO-GENERATOR SET SIMULATION IN DYNAMIC CONDITIONS

Dana-Alexandra Ciupăgeanu, Gheorghe Lăzăroiu
University Politehnica of Bucharest

ABSTRACT

The aim of this paper is to analyze the influence of a sudden load variation at the terminals of a turbo-generator set on the behavior of its constituent elements, with focus on synchronous generator modeling. For this purpose, the steam turbine including the speed governor, the excitation system together with the automatic voltage regulator and the round-rotor synchronous generator were modeled using Simscape Power System components, in Matlab. The blocks parameters were calculated based on polynomial functions, determined by regression, considering the rated electrical power of the generator as the independent variable. The data on which rely the regressions belongs to the machines in the IEEE 300 Bus System. Given that the blocks parameters were determined depending on the mentioned independent variable, the presented model can be used to simulate the dynamic response of turbo-generators sets of different sizes.

1. INTRODUCTION

Electricity market requirements increasingly target operating flexibility due to the continuing shift towards renewable energy integration. Dynamic simulation is a cost-efficient tool for improving the flexibility of dispatchable power generation in transient operation such as load changes.

The operating flexibility of thermal power plants is limited by technical constraints such as ramp rates and minimum load limit. Existing power plants can be retrofitted with optimized components and control circuits to mitigate these constraints and to meet enhanced adaptability requirements. Thermal power plants flexibility in service is therefore an essential factor for reliable grid stability and for economic operation.

Simulation in dynamic conditions offers an effective tool for optimizing the power plant performance and control structures as well as for assessing capabilities and limitations of the system with regard to process, materials, emissions or economics. The accurate description of automation structures and control devices are essential in order to obtain a realistic dynamic response [1].

2. METHODOLOGY

2.1. Mathematical model of the synchronous generator

In synchronous generator modeling, the three stator windings are considered 120 electrical degrees apart and the rotating structure having an excitation winding and one or more equivalent rotor body windings. The magnetic axis of the excitation winding is defined as the direct axis (d) and perpendicular to it is defined the quadrature axis (q). The equivalent rotor circuits reflect induced current paths in the damper winding [2]. Using Park's transformation, the three-phase stator quantities, which are variable in time, are converted to corresponding two-axis quantities that are time invariant under steady state conditions.

The mathematical model of the synchronous generator used by Simscape Power Systems is the standard model [3], [4] which shall be presented forward.

$$v_s = -R_s \cdot i_s + \omega \cdot P \cdot \Psi_s + \frac{d}{dt}\Psi_s \tag{1}$$

where: v_S is the stator voltage; R_s is the stator resistance; i_s is the stator current; ω is the electrical angular speed; P is Park's transformation; Ψ_s is the stator flux linkage.

The stator flux linkage in d-q axes are given by the following equations:

$$\Psi_d = -(L_{ad} + L_l) \cdot i_d + L_{ad} \cdot i_{fd} + L_{ad} \cdot i_{1d} \tag{2}$$

$$\Psi_q = -(L_{aq} + L_l) \cdot i_q + L_{aq} \cdot i_{1q} + L_{aq} \cdot i_{2q} \tag{3}$$

$$\Psi_0 = -L_0 \cdot i_0 \tag{4}$$

where: Ψ_d, Ψ_q and Ψ_0 are the d-axis, q-axis and zero-sequence stator flux linkage; i_d, i_q and i_0 are d-axis, q-axis and zero-sequence stator currents (which are related to phase stator currents on the terminal of the synchronous generator through Park's transformation); i_{fd}, i_{1d}, i_{1q} and i_{2q} are the currents flowing in the field circuit, d-axis damper winding 1, q-axis damper winding 1 and 2 respectively; L_l is the stator leakage inductance; L_{ad} and L_{aq} are the mutual inductances of the stator direct (d) and quadrature (q) axis; L_0 is the zero-sequence stator inductance.

$$v_r = R_r \cdot i_r + \frac{d}{dt}\Psi_r \tag{5}$$

where: v_r is the rotor voltage; R_r is the rotor resistance; i_r is the rotor current; Ψ_r is the rotor flux linkage.

With respect to rotor flux linkage, they are defined through the equations (6)-(9):

$$\Psi_{fd} = L_{ffd} \cdot i_{fd} + L_{f1d} \cdot i_{1d} - L_{ad} \cdot i_d \tag{6}$$

$$\Psi_{1d} = L_{f1d} \cdot i_{fd} + L_{11d} \cdot i_{1d} - L_{ad} \cdot i_d \tag{7}$$

$$\Psi_{1q} = L_{11d} \cdot i_{1q} + L_{aq} \cdot i_{2d} - L_{aq} \cdot i_q \tag{8}$$

$$\Psi_{2q} = L_{aq} \cdot i_{1q} + L_{22q} \cdot i_{2q} - L_{aq} \cdot i_q \tag{9}$$

where: L_{ffd}, L_{11d}, L_{11q} and L_{22q} are the self inductances of the rotor field circuit, d-axis damper winding 1, q-axis damper winding 1 and 2 respectively; L_{f1d} is the rotor field circuit and d-axis damper winding 1 mutual inductance.

The electromechanical equations governing generator's behavior are:

$$2H\frac{d\omega}{dt} = m_t - m_e \tag{10}$$

$$\frac{d\delta}{dt} = \omega - \omega_s \tag{11}$$

where: H is the inertia constant of the turbo-generator set; m_t and m_e represent the mechanical and electromagnetic momentum; δ is the electric angle; ω_s is the steady-state angular speed.

The electromagnetic momentum depends on d-q axes flux linkage and currents according to (12):

$$m_e = \Psi_d i_d + \Psi_q i_q \tag{12}$$

2.2. Presenting the turbo-generator set model used in the simulation

The turbo-generator set's components and the load connected to its terminals were modeled using Simscape Power Systems, as shown in figure 1. To simulate the dynamic conditions, a step load change was considered. The round-rotor synchronous generator terminal voltage is controlled by an Automatic Voltage Regulator (AVR). The system also includes a speed governor, which adjusts the turbine's prime mover intake in order to regulate the mechanical power output for maintaining its stability and performance.

The solver configuration used is typical for stiff models.

The load variation was considered $\pm 0.1 p.u.$ out of the constant load and both were determined depending on generator's rated electrical power.

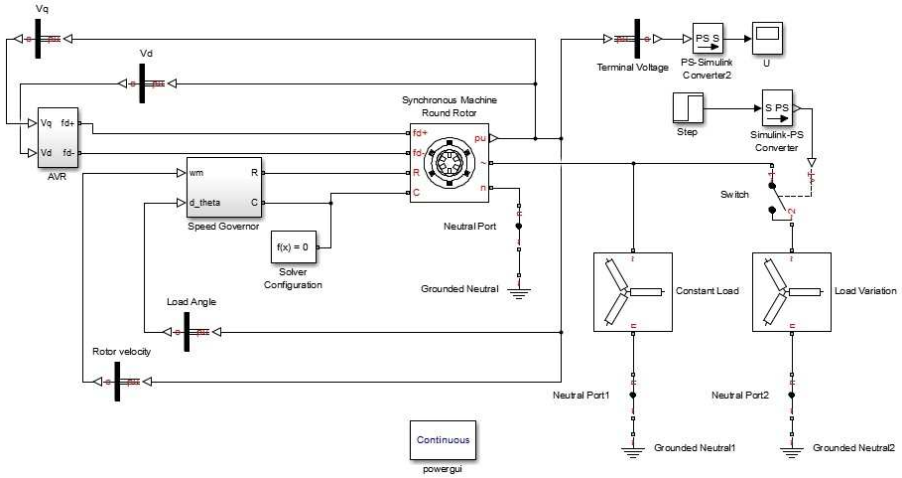

Figure 1: Simulation system diagram in Simulink

A. Synchronous generator parameters and characteristic quantities

Direct axis (x_d) and quadrature axis (x_q) synchronous reactance, in p.u., represent the quotient of the sustained value of that fundamental AC component of armature voltage, which is produced by the total correspondent axis primary flux due to armature current, and the value of the fundamental AC component of this current, the machine running at rated speed.

Direct axis (x''_d) and quadrature axis (x''_q) subtransient reactance, in p.u., are defined as the quotient of the initial value of a sudden change in that fundamental AC component of armature voltage, which is produced by the total correspondent axis armature winding flux, and the value of the simultaneous change in fundamental AC component of armature current, the machine running at rated speed.

Direct axis (x'_d) and quadrature axis (x'_q) transient reactance, in p.u., are defined similar to the subtransient reactance, excluding the high decrement components during the first cycles.

The connection between the reactance and the inductance (from paragraph 2.1.) of a circuit is given by equation (13), and for obtaining the value in p.u. it shall be divided by the base impedance:

$$X = \omega L \tag{13}$$

Direct axis (T''_{d0}) and quadrature axis (T''_{q0}) subtransient open circuit time constant, in seconds, represent the time required, following a sudden change in operating conditions, for

the rapidly changing component of the open-circuit armature winding voltage which is due to corresponding axis flux, to decrease to 1/e, that is 0,368 of its initial value, the machine running at rated speed.

Direct axis (T'_{d0}) and quadrature axis (T'_{q0}) transient open circuit time constant, in seconds, represent the time required, following a sudden change in operating conditions, for the slowly changing component of the open-circuit armature voltage, which is due to correspondent axis flux, to decrease to 1/e, that is 0,368 of its initial value, the machine running at rated speed.

The leakage reactance (x_l) takes into account the leakage of the field winding, on load and in the over-excited region, which is used in place of the armature leakage reactance to calculate the excitation on load by means of the Portier method.

The above mentioned quantities and parameters were assessed based on fifth order polynomial regressions using IEEE 300 Bus Test System machines data. The independent variable considered was the rated electrical power of the generator.

In Table 1 are presented the values calculated for a rated electrical power of the synchronous generator of 450 MW. Excepting the subtransient open circuit time constants, on both direct and quadrature axes, all the other calculated values fall within the limits set by the representative values for the round rotor synchronous generator, in accordance with the scientific literature.

Table 1: Values of the round-rotor synchronous generator block parameters

Quantity	Symbol and measurement unit	Calculated value	Representative values	
			Minimum	Maximum
Inertia constant	H [s]	2.8499	2.5	6
Armature resistance	r_a [p.u.]	0.0038	0.0015	0.005
Unsaturated d axis synchronous reactance	x_d [p.u.]	1.6969	1.0	2.3
Unsaturated q axis synchronous reactance	x_q [p.u.]	1.6597	1.0	2.3
Unsaturated d axis transient reactance	x'_d [p.u.]	0.2681	0.15	0.40
Unsaturated q axis transient reactance	x'_q [p.u.]	0.6553	0.3	1.0
Unsaturated d axis subtransient reactance	x''_d [p.u.]	0.2087	0.12	0.25
Unsaturated q axis subtransient reactance	x''_q [p.u.]	0.2087	0.12	0.25
Leakage (Portier) reactance	x_l [p.u.]	0.1585	0.01	0.20
d axis transient open circuit time constant	T'_{d0} [s]	3.0962	3.0	10.0
q axis transient open circuit time constant	T'_{q0} [s]	0.5839	0.5	2.0
d axis subtransient open circuit time constant	T''_{d0} [s]	0.0186	0.02	0.05
q axis subtransient open circuit time constant	T''_{q0} [s]	0.0132	0.02	0.05

B. Excitation system and Automatic Voltage Regulator block parameters

The excitation and AVR subsystem is represented in Figure 2. The Excitation System block implements an IEEE type 1 synchronous machine voltage regulator combined to an exciter. The block's V_d and V_q (direct and quadrature axes stator voltage, in p.u.) inputs are connected to the p.u. output of the synchronous generator block. The output of the block is the field voltage, v_{fd}, in p.u., which is applied, through the controlled voltage source, to the electrical conserving port $f_d +$ of the synchronous generator block.

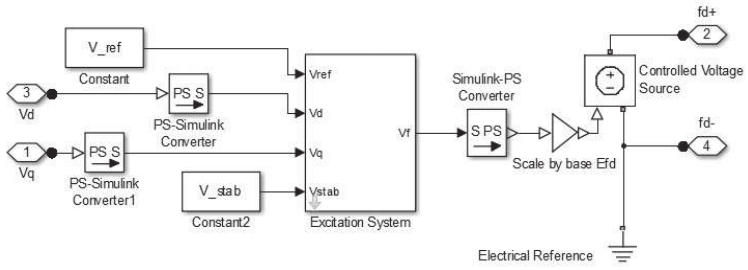

Figure 2: AVR subsystem diagram in Simulink

The values in Table 2 were obtained as presented in section A and for the same value of the generator's rated electrical power, 450 MW.

Table 2: Values of the excitation system block parameters

Quantity	Symbol and measurement unit	Calculated value
Regulator input filter time constant	T_r [s]	10^{-4}
Regulator gain	K_a [p.u.]	279.6751
Regulator time constant	T_a [s]	0.2674
Exciter self-excitation at full load field voltage	K_e [p.u.]	1.0779
Exciter time constant	T_e [s]	0.2471
Regulator stabilizing circuit gain	K_f [p.u.]	0.0593
Regulator stabilizing circuit time constant	T_f [s]	0.9280

C. Steam Turbine and Governor block parameters

The Steam Turbine and Governor block implements a complete tandem-compound steam prime mover, including a speed governing system, a four-stage steam turbine, and a shaft with up to four masses. The speed governing system consists of a proportional regulator, a speed relay, and a servomotor controlling the gate opening. The steam turbine has four stages, each modeled by a first-order transfer function. The subsystem is represented in Figure 2.

Regarding power system stability studies, the important aspect of the turbine's governor dynamics is the initial response, in the first seconds following a disturbance. A clear example is the concept of fast-valving. This control is characterized by the sudden action to close the intercept valves on a steam turbine following a nearby fault to reduce the mechanical power on the generator shaft and thus minimize the acceleration of the shaft and likelihood of rotor angle instability [5].

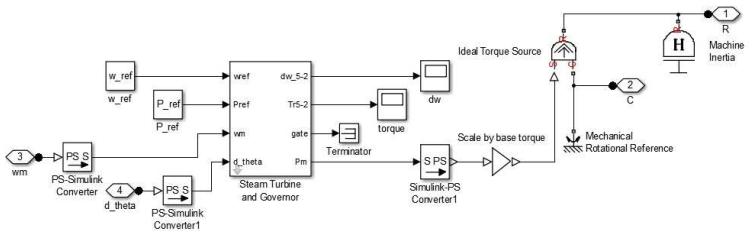

Figure 3: Speed Governor subsystem diagram in Simulink

Similar to previous sections were determined the speed governor parameters, presented in Table 3.

Table 3: Values of the speed governor block parameters

Quantity	Symbol and measurement unit	Calculated value
Turbine steady-state droop	R_p [p.u.]	0.0078
Servo-motor time constant	T_{sm} [s]	0.2186

3. RESULTS AND CONCLUSIONS

The model's parameters and characteristic quantities were determined depending on the rated electrical power of the generator and therefore it can be used to simulate the behavior of turbo-generator sets of different sizes in many cases, by adjusting the constant load magnitude, the percent, time and lasting of load variation.

Figures 4a and 4b show the response of a turbo-generator set having the parameters previously determined, according to paragraph 2.2. The constant load connected to its terminals is 0.85 p.u., the load variation occurs at t=5s, is 0.1 p.u. and is permanent during the simulation, which lasts for T=30s. Both responses stabilize.

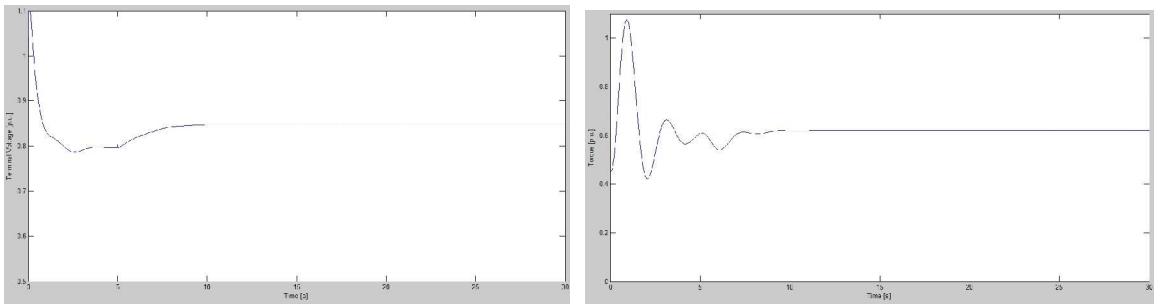

(a) (b)

Figure 4: (a) Terminal Voltage [p.u.] and (b) Mechanical Torque [p.u.]

References

[1] Alobaid, F., Mertens, N., Starkloff, R., Lanz, Th., Heinze, Ch., Epple, B., *Progress in dynamic simulation of thermal power plants,* Progress in Energy and Combustion Science, Vol. 59, 2016

[2] *IEEE Guide for Synchronous Generator Modeling Practices in Stability Analyses*, IEEE Standard 1110-1991

[3] Spoljaric, Z., Miklosevic, K., Jerkovic, V., *Synchronous Generator Modeling Using Matlab*, SiP 2010 28th International Conference Science in Practice.

[4] Lăzăroiu, Gh., *Modelarea şi simularea proceselor şi componentelor centralelor electrice,* Teza de doctorat, 1997

[5] *Dynamic Models for Turbine-Governors in Power Systems Studies*, IEEE Power&Energy Society Technical Report PES-TR1, 2013

ANALYSIS OF STRESSES ARISING IN A SCARIFIER EQUIPMENT WITH FIVE WORKING BODIES

Croitoru Şt.[1], Caba I.[2)], Matache M.[2)], Persu C.[2)], Voicea I.[2)], Marin E.[2)], Vlăduţ V.[2*)], Ungureanu N.[3)], Bungescu S.[4)], Hărmănescu M.[4)], Cujbescu D.[2)], Dumitru I.[2)], Brăcăcescu C.[2)]

[1)]University of Craiova, [2)]INMA Bucharest, [3)]U.P. Bucharest; [4)]USAM Timişoara

ABSTRACT

Soil loosening is an operation that must be carried out at least every five years, in order to decompact and loosen the soil. Without this regular operation, the soil becomes compacted due to intensive agricultural works (repeated passages over the same surface), rains, animals, etc., thus reducing the yields per hectare by up to 50%. The equipment that performs these operations are massive and robust, to withstand the extremely high stresses that arise in the resistance structure and others. The paper presents an analysis of the stress that occur in a soil scarifying equipment with five working bodies, taking into account the main factors influencing these stresses.

1. INTRODUCTION

The works of deep soil loosening are carried out according to some pedological criteria, such as the alternate presence of rainfall excess and deficiency periods of moisture in the soil during plant growing period, respectively of a deficient total porosity [2, 4, 5].

Deep loosening is generally appropriate on non-sloping fields or without an alternation of layers that favors the lanslides, on fields subjected to alternations of moisture excess and deficiency, with or without in-ground water, leakage, floods, etc.

This type of soil work is suitable when practicing an intensive agriculture in order to ensure high crop yields, being effective on podzolic soils, reddish browns, vertisols, lacquers and heavy alluvial soils, chernozems, brown soils and medium alluvial soils.

Subsoiling works are not performed on sandy soils, with pebbles and hard superficial rock, on flooded fields and on fields where the underground water is found below 1 m deep, on fields with slopes over 15% and on landsliding fields or coastal springs.

The optimum moisture at which is recommended to carry out deep loosening of soil is 60-90% of the active moisture range, which is found between the wilting coefficient and field water capacity.

In terms of the placement of the working bodies, the requirements stipulate that when their number exceeds the unit, two of them shall be arranged so that to ensure the loosening of wheel ruts of the tractor, to annihilate the secondary effect of soil compaction produced by them [5].

The graduation of soil loosening depth is based on the climatic criterion, and the corresponding indicator for this is the sum of precipitation from November to April (interval without significant quantitative evapotranspiration). Based on this requirement, soil loosening must be carried out to the depth at which is achieved the correspondence between the amount of precipitation falling within the mentioned and that of the minimum total porosity. Generally, the average working depth is between 50 and 60 cm.

Soil works ensure:

♦ accumulation and storage into the soil of all water from precipitation during summer and autumn;

[1]University of Craiova, Tel: 0721.254.608; E-mail: valentin_vladut@yahoo.com

♦ the accumulation into the soil of as much nitrate as possible by intensifying the nitrification processes;
♦ the obtaining of a loose layer of soil, but at the same time placed, to ensure a good rooting of the plants and to avoid the process of unrolling;
♦ the obtaining of a lump-free seedbed, so that the seed can get intimate contact with the soil and to be able to grow up in the shortest possible time.

2. METHODOLOGY

Regardless of the method of soil work, for a good growth and development, the cultivated plants need to achieve an optimal ratio between capillary and non-capillary porosity and a most favorable regime of water, air and food in the soil.

The equipment for which the structural analysis was performed [1, 3] is intended for deep soil loosening equipment and has five chisel-type active bodies (Figure 1).

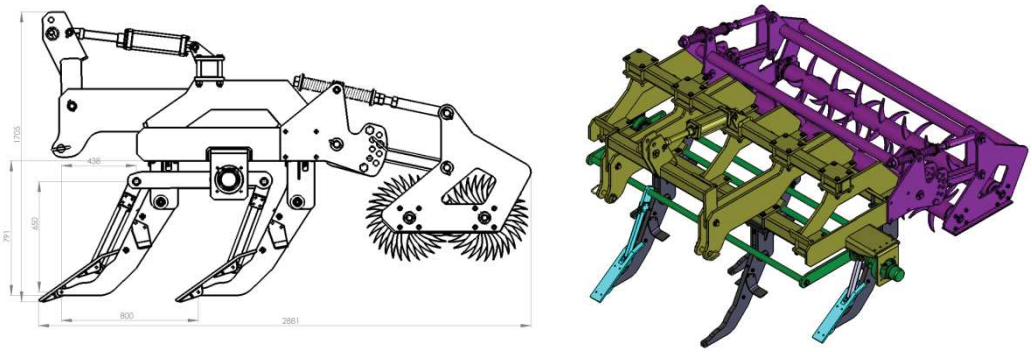

Figure 1: SCAR5 equipment for deep loosening of soil

The measurement of the coupling forces between the tractor and the technical equipment (tensile strength F_t) was performed using a device with tensometric transducers (tensometric frame) shown in Figure 2.

Figure 2: Device with tensometric transducers (tensometric frame)

To save the data measured directly in the field, was used an MGCplus data amplification and acquisition system, with 16 analogue input channels and 16 digital output channels and an ML455 HBM amplification module. The power supply to the MGCplus system was a lead-acid battery of 12 Volt.

For transferring obtained data to a portable computer, the specialized CATMAN software for data acquisition and processing was used, which allowed to filter the signals received from the transducers and to determine their minimum, maximum and average values. The signals recorded and saved to the computer's memory, in ASCII type files, were processed using the Microsoft Excel software, and presented as graphs, which were processed, eliminating the transient working regimes (at the beginning and completion of the experimental samples).

Figure 3 shows the graphical recordings for the field movement of the tractor in the 5th gear and the working depth of the equipment set at 0.50 m.

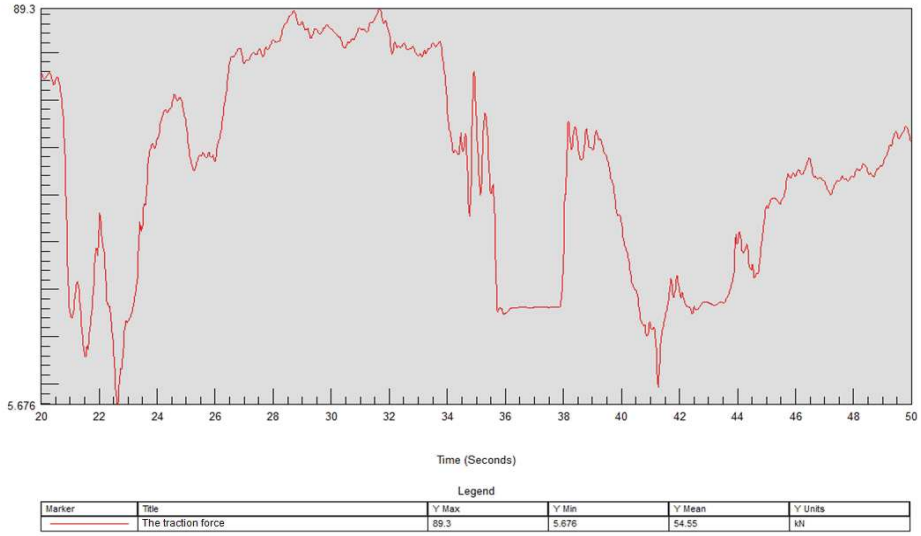

Figure 3: Traction force determined at 0.50 m working depth of the equipment (in the 5th gear)

3. RESULTS

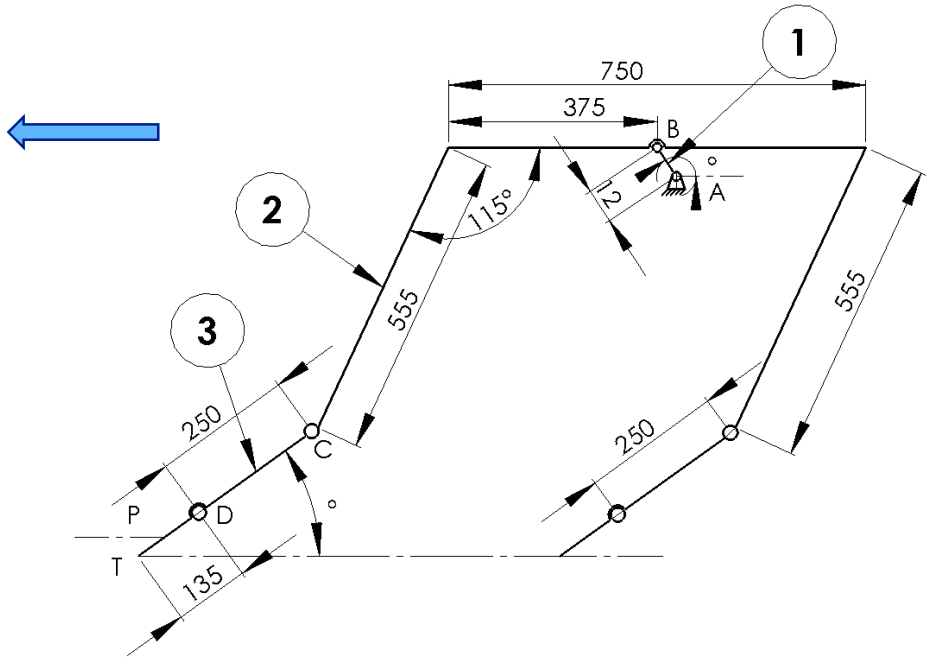

Figure 4: The kinematic scheme of the scarifier's mechanism

INITIAL DATA FOR THE SCARIFIER MECHANISM

AB = 0.012 m
BC = 0.930 m
CD = 0.250 m
CT = 0.485 m
Masses for only a mechanism:
M1=12.75 kg
M2=28.26 kg
M3=7.33 kg
Thickness of the coulter = 0.016 m
Position of the point of application of the resistant force = 0.775 m
Soil friction coefficient = 0.4
QMAXI1=70.39 kN
QMAXI2=75.71 kN

According to Figure 5, there are two mechanisms on the front bar, respectively 3 mechanisms on the rear bar.

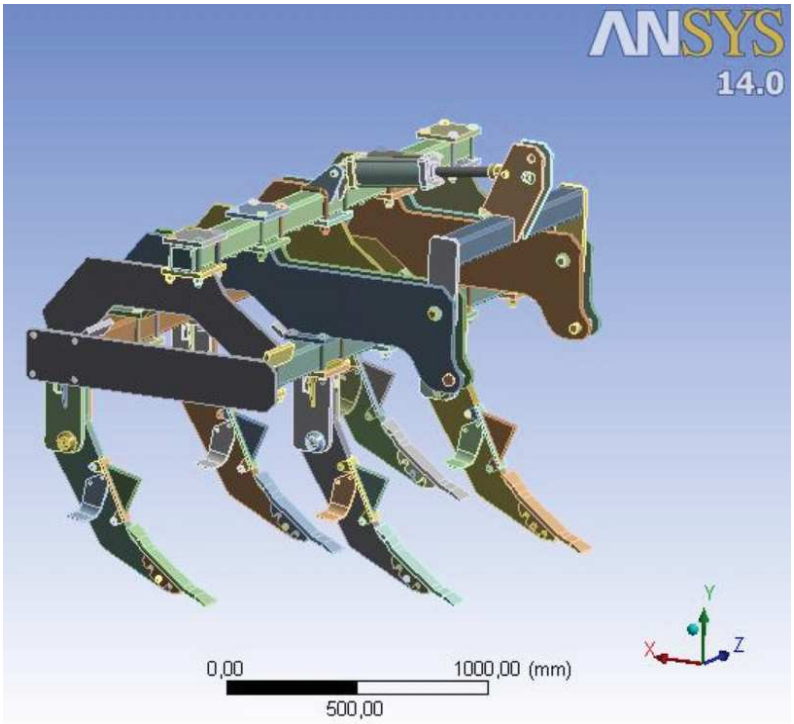

Figure 5: SCAR-5 equipment for deep loosening

Model (B4) > Geometry	
Object Name	*Geometry*
State	Fully Defined
Definition	
Source	D:\Anghel\SCAR\scar_simulation model.x_t
Type	Parasolid
Length Unit	Meters
Element Control	Program Controlled
Display Style	Body Color
Bounding Box	
Length X	1663,6 mm
Length Y	1701,9 mm
Length Z	2352, mm

Properties	
Volume	1,468e+008 mm³
Mass	1152,4 kg
Scale Factor Value	1,
Statistics	
Bodies	577
Active Bodies	425
Nodes	1098734
Elements	556995
Mesh Metric	None

The data obtained from measurements of the tensile force were processed with the GliphWorks software, thus obtaining the diagram for the variation of the traction force duriwhile moving into the soil at a depth of 30 cm (Figure 6).

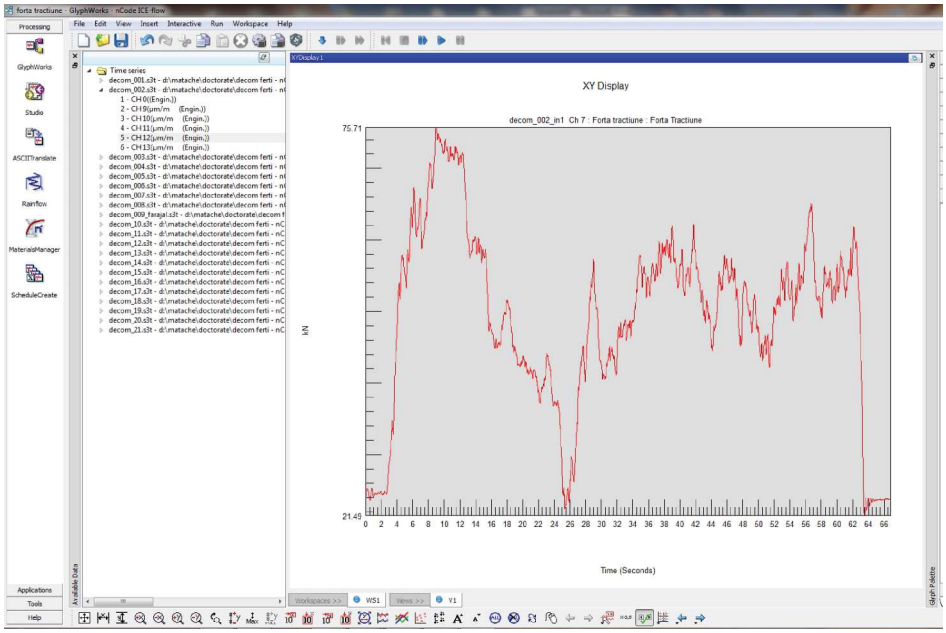

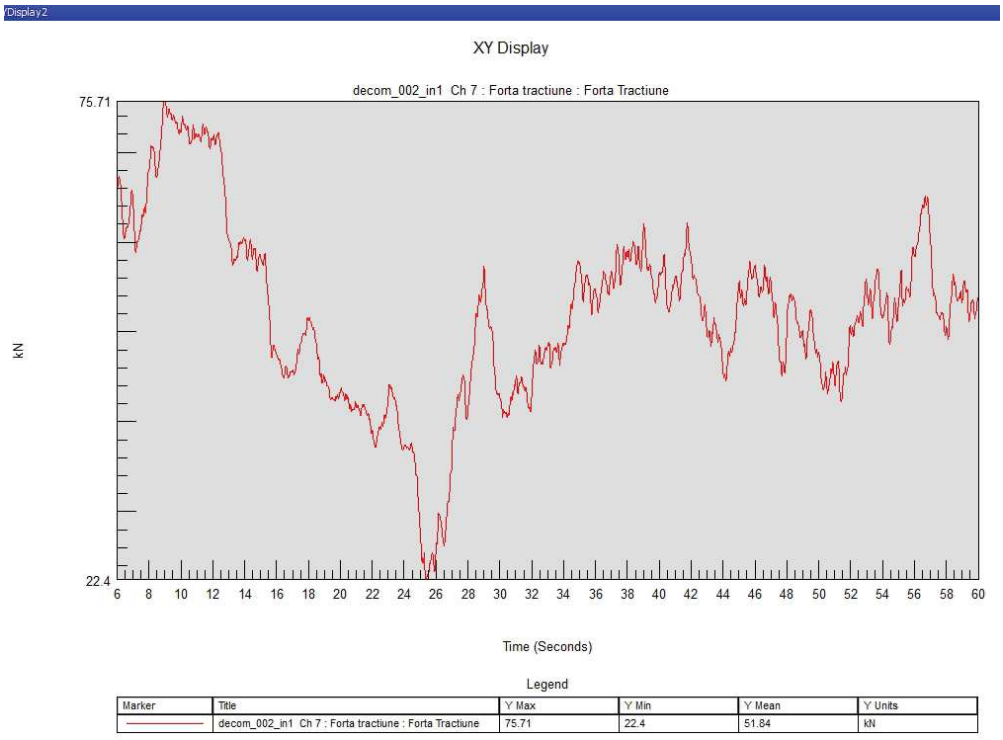

Figure 6: Data processing in GliphWorks software

4. CONCLUSIONS

Considering the mentioned above, it can be concluded that:

- This type of loosening equipment is well suited for soil decompaction but it requires high power tractors (over 250 HP);

- The traction force varies proportionally to the working depth, and increases with increasing the working depth.

Acknowledgement

This paper has been funded by Ministry of Research and Innovation through the UEFISCDI, within the projects entitled "***Conservative tillage technology***", contr. 181/2014 and "***Enhancing the competitiveness of SC ARTECOM SRL by optimizing an equipment for deep processing of soil***", contr. 78BG/2016.

References

[1] Calle, G., Quintero, H., Diaz, A., Henao, E. *Graphic-analytical method for the kinetostatic analysis of a fourth-class Assur group,* 13th LACCEI Annual International Conference "Engineering Education Facing the Grand Challenges, What are we doing?", Santo Domingo, Dominican Republic, 2015, pp. 1-2;

[2] David, A., Voicu, Gh., Persu, C., Gheorghe, G. *The determination of the resistant forces for deep loosening of soil machines with active organs*. INMATEH – Agricultural Engineering, vol. 42(2), 2014, pp. 21-28.

[3] Durango S., Calle G., Ruiz O. *Analytical method for the kinetostatic analysis of the second-class RRR Assur group allowing for friction*. J. Braz. Soc. Mech. Sci. & Eng., vol. 32, (2010), pp. 200-207

[4] Hakansson I. *Machinery - induced compaction of arable soils. Incidence –consequences – counter - measures.* Reports from the division of soil management, no. 109. Department of Soil Sciences Uppsala. ISSN 0348-0976, ISRN SLU-JB-R-109-SE, 2005.

[5] Marin E., Pirnă I., Sorică C., Manea D., Cârdei P. *Studies on structural analysis of resistance structure as a component of equipment with active working parts driven to deeply loosen the soil*. INMATEH – Agricultural Engineering, vol. 36(1), 2012, pp. 13-20.

CONSIDERATIONS ON THE ESTIMATION OF FUEL CONSUMPTION AND PRODUCTION NORMS (WORKING CAPACITY) BY POWER CLASSES, DEPENDING ON THE AGRICULTURAL WORK OF SOWING

Cujbescu D.[1], Matache M.[1], Bolintineanu Gh.[1], Vlăduţ V.[1], Persu C.[1], Găgeanu I.[1], Gheorghe G.[1], Caba I.[1], Voicu Gh.[2], Vlad C.[3]
[1]INMA – Bucharest, [2]PU – Bucharest, [3]ICEADR – Bucharest

ABSTRACT

The estimation of fuel consumption is important for estimating the budget and possibilities of achieving certain specific agricultural works. The objective of this paper is to develop a method for the estimation of fuel consumption and of production norms (working capacity) by power classes, depending on the agricultural work of sowing.

1. INTRODUCTION

The value of tractor is measured by the amount of work achieved in relation with the cost incurred for achieving that work.

The efficient operation of agricultural tractors includes:

- maximizing engine fuel efficiency and the mechanical efficiency of the drive train;
- maximizing the traction advantage of traction devices;
- choosing an optimum movement speed for a particular tractor. [3]

Along with increasing the emphasis of fuel preservation, it is desirable to foresee that the use of fuel is achieved at a higher degree of precision. [4]

Mechanized sowing represents an important link through which man controls the biological cycle of plants used for their biological contribution. By sowing agricultural crops in general, we understand the incorporation of seeds in the soil at distances and depths established through scientific and experimental researches, where, in favourable conditions of moisture, heat and aeration, they germinate, resulting in new plants. Sowing machines have as destination to achieve the sowing work consisting in evenly distributing the seeds of different species in the soil, at an adequate depth, in the view of exposing them to optimum conditions of germination and development for the future plants. [1]

In order to obtain a quality sowing work, the channels need to be opened at the optimum depth, seeds need to be distributed evenly, collinear in those channels, and in the end to be covered with soil.

Sowing crops on rows is achieved by universal machines that ensure seed distribution in continuous flow on equidistant rows. This method is practiced at large scale for straw cereals, peas, mash, linen, flax, hemp, perennial cereals and legumes, fodder, etc. [5]

Machines for seeding in pockets, also called precision sowers, are used for sowing hoeing crops (corn, sun flower, beans, soy beans, melons, cucumbers, etc.). These machines perform seed by seed sowing, one or more seeds per pocket. [2] This implies an even distribution of seeds at fixed distances on rows, resulting in ensuring an optimum nutrition space for plants and reducing the quantity of seeds per surface unit.

[1]dcujbescu@yahoo.com

2. METHODOLOGY

Starting from the objectives of the National Strategy for Rural and Agricultural Development for the years 2014-2020, the Code of Good Agricultural Practices, Law 37/2015 and from the situation of the park of tractors and agricultural machinery existing at 31.12.2014 in Romania, a classification of tractors divided depending the type of agricultural exploitation was made, as follows:

Table 1: Classification of tractors depending on the type of agricultural exploitation

Exploitation	**Tractor range (HP)**
Subsistence farms	<45
Semi-subsistence farms	46÷80
Small exploitation	81÷120
Average exploitation	121÷200
Large exploitation	201÷360

Next, for each tractor class were identified the main tractors that are representative for the power range *P* as well the average specific fuel consumption in g/HPh (g/kwh), taking into consideration the tractors with minimum and maximum power in the power class, thus establishing the average working speed.

Table 2: Average working speeds

Tractor range (HP)	**Average working speed *v* (km/h) for sowing on rows**	**Average working speed *v* (km/h) for sowing hoeing plants**
I		
<45	4.0	4.0
II		
46	6.0	4.2
80	6.4	6.4
III		
81	8.1	8.6
120	10.8	10.8
IV		
121	12.0	12.0
200	13.8	13.8
V		
201	15.6	15.6
360	17.4	17.4

The estimation of theoretical working width *l* (m), was conducted depending on the sowing method (sowing on rows or sowing hoeing plants), taking into consideration that the distance between two rows of straw plants is 0.125 m, and the distance between two rows of hoeing plants is 0.7 m. [6]

Estimating that for the sowing work, the tractor uses 45% of its nominal power, the calculation of fuel consumption per hectare q is determined as follows:

$$q = \frac{0.45Pc}{85vpl} \quad (1)$$

where -dv is fuel consumption (l/ha);
-P is tractor nominal power (CP);
-c is the specific fuel consumption (g/HPh) for each tractor class (minimum and maximum power tractor in the power class);
-v is the average working speed (km/h);
-l is the working width (m);
-p is the skidding correction coefficient (%).

An average value of 10% was estimated for skidding, therefore the working speed was pondered by a correction coefficient p = 0.9.

Table 3: Specific fuel consumption for each tractor class (minimum and maximum power tractor in the power class)

Tractor nominal power (HP)	**Diesel fuel consumption (g/kwh)**	**Diesel fuel consumption (g/HPh)**
<45	330	242.64
46	300	220.58
80	292	214.70
81	292	214.70
120	288	211.76
121	280	205.88
200	261	191.91
201	259	190.44
360	250	183.82

The estimation of the working capacity (productivity) W is achieved using the following formula:

$$W = \frac{vpl}{10} k_p \quad (2)$$

where -W is the working capacity (ha/h);
- k_p is the correction coefficient for the working capacity.

The parcels were divided on sizes depending on the type of agricultural exploitation, applying the correction coefficients for the working capacity:

Table 4: Working capacity correction coefficients

Exploitation type	Correction coefficient
SMALL exploitation	0.83
Parcel length <250	
AVERAGE exploitation	
Parcel length 250-500 m	0.91
LARGE exploitation	
Parcel length 500-800 m	1
Parcel length >800 m	1.05

CONCLUSIONS

The method of estimating fuel consumption developed can be improved if other perturbing factors are taken into consideration, such as:

- Preparation and ending time for the sowing work;
- The time for turning at the end of the row;
- The idle time;
- Movement from one parcel to another;
- Servicing the sowing machine;
- Seed supplying;
- Adjusting the sower during operation;
- Daily technical maintenance;
- Replacing active bodies during operation;
- Fuel supply;
- Rest time and natural necessities, etc.

Acknowledgment

The work has been funded by Ministry of National Education and Research through the National Agency for Scientific Research, within the project entitled “Innovative technology for weeding crop establishment through mulching using degradable film”, PN 16 24 04 02.

References

[1]. Căproiu St., *Agricultural machines for working the soil, sowing and crop maintenance,* Didactic and Pedagogic Publishing House, Bucharest, 1982;
[2]. Dobre P., *Energetic base and horticultural machines*, Bucharest, 2010;
[3] Grisso R. D., Kocher M. F., Vaughan D. H., *Predicting tractor fuel consumption,* American Society of Agricultural Engineers ISSN 0883−8542, Vol. 20(5), pp. 553−561;
[4] Grisso R. D., Vaughan D. H., Roberson G. T., *Fuel prediction for specific tractor models,* Applied Engineering in Agriculture, American Society of Agricultural and Biological Engineers ISSN 0883-8542, Vol. 24(4), pp. 423-428, 2008.
[5] Onisie T., Zaharia M., *Farm practices,* University of Agricultural Sciences and Veterinary Medicine “Ion Ionescu de la Brad”, Faculty of Agriculture, Iași, 2002;
[6] *Production and diesel fuel consumption norms, Rates for remunerating mechanizers*, Ministry of Agriculture and Food Industry, General Economic Direction for the Mechanization of Agriculture, 1985.

PRODUCTION AND CONSUMPTION OF WHOLESALE MEAT

Duţu Mihaela-Florentina[1], Begea Mihaela, Duţu Iulian Claudiu, Cîrîc Alexandru
University Politehnica of Bucharest

ABSTRACT

This paper aims to review a selected passage consumption of beef, pig and poultry worldwide. Selected European Union there is a growing trend in meat consumption which generates and intensification of intra and extra-Community product. This paper will study the use of different meats selected world and selected Romania and will try to see what will be the consumption of this product selected Romania.

1. INTRODUCTION

Meat is a basic food source in human nutrition. The TROFIN balanced chemical composition with high biological value, complete protein, fat, minerals and vitamins, high digestibility and quality dietetico - appreciable cooking, the meat is essential to human nutrition food. [1, 2]

In most communities, the meat served over time an important role in food items due to reasons including taste, tradition, plus nutritional aspects.

In the EU and in the world there is a growing trend in meat consumption, which generates and intensification of intra and extra-Community product.

In international trade, they are representative quantities of beef, swine, sheep and poultry. World production of beef is 235 million tons. International trade represents about 12% of world production. The main exporters of meat are: 18% Australia, New Zealand 8%, Brazil 4.5% and 17% of the main importers are the U.S., Japan 9% [3, 6].

Meat producers' efforts should be directed not only towards the requirements of population growth, but also to those caused by increased consumption of meat per capita.

The amount of meat consumed in different countries vary very widely, depending on the influence of social, political, economic, religious and depending on demographic differences. Thus, in meat-producing countries such as Argentina, Uruguay, Australia, it was reported an average consumption of meat of 300 g / day / person, compared to 10 g / day / person in India or Indonesia [14].

2. STUDY OF DIFFERENT TYPES OF MEAT CONSUMPTION WORLD

Consumption of beef in the world

Consumption of beef in 2009 averaged 11.12 kg / head / year, with a minimum of 0.3 kg / head / year registered in Liberia and a maximum of 54.1 kg / head / year in Argentina. In Figure 1 can be seen consumer categories. Thus, one state had a consumption of over 50 kg / head / year.

There are 14 countries in the world which has a consumption of between 25.1 and 50.0 kg / head / year, with their average of 31.5 kg / head / year. Also, the member 56 presents a consumption of between 10.1 and 25.0 kg / head / year (mean 16.5 kg / head / year), 50 states are included in consumer 5,1- 10.0 kg / head / year, 55 states have a consumption of less than 5 kg / head / year beef [5, 6].

[1]Spl.Independentei, no.313, sect.6, Bucharest, 0214029637, dutumihaelaflorentina@gmail.com

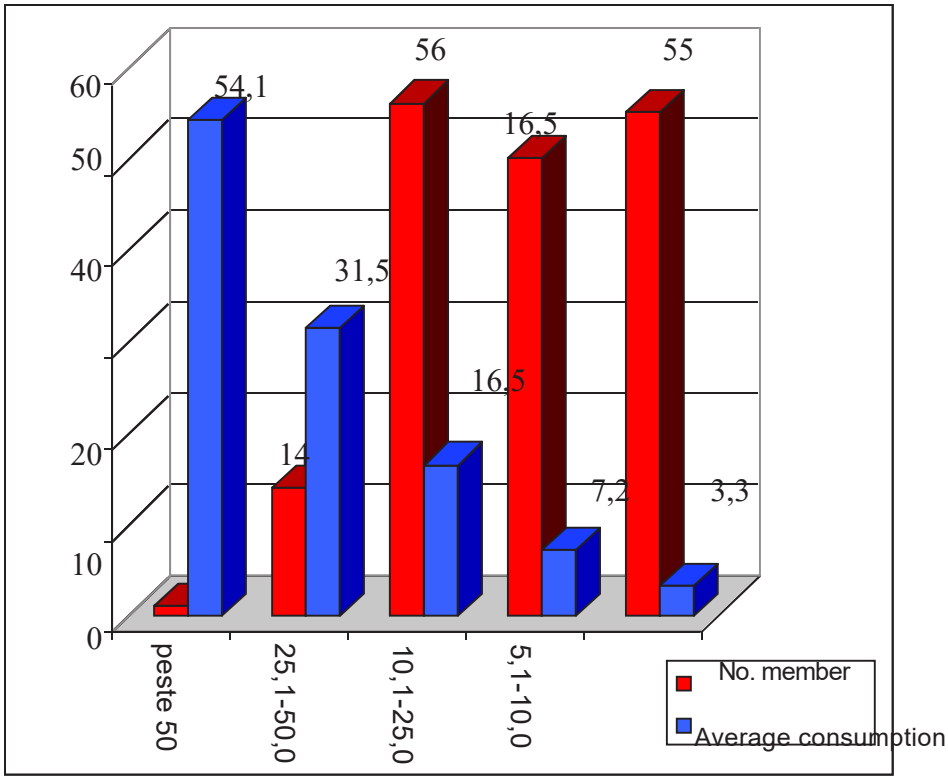

Figure 1: Categories consumption of beef, the number of countries in the world included in each category and average consumption for each category (FAOSTAT, 2012)

Consumption of pork in the world

Consumption of pork in 2009 was on average 15.0 kg / head / year, with a minimum of 0.1 kg / head / year registered in Chad, Nigeria, Sri Lanka and Turkmenistan and a maximum of 65.6 kg / head / year in Austria. In Figure 2 can be seen consumer categories. Thus, the two states have a consumption of 50 kg / head / year (mean 60.1 kg / head / year). In the world there are 34 countries which have a consumption between 25.1 and 50.0 kg / head / year, with their average of 36.59 kg / head / year. Also, the member 42 presents a consumption of between 10.1 and 25.0 kg / head / year (mean of 16.67 kg / head / year), 22 states are included in the category of consumption 5,1- 10.0 kg / head / year (average of 7.45 kg / head / year) and 56 states have a consumption of less than 5 kg / head / year swine meat (with an average of only 1.86 kg / head / year) [5, 6].

Consumption of poultry meat in the world

Consumption of poultry meat in 2009 averaged 29.78 kg / head / year, with a minimum of 0.2 kg / head / year registered in Rwanda and a maximum of 97.5 kg / head / year in Kuwait . Can be seen in Figure 3 categories of consumption for poultry meat. Thus, eight states had a consumption of over 50 kg / head / year, with an average of 64.51 kg / head / year.

In the world there are 41 countries which have a consumption between 25.1 and 50.0 kg / head / year, with their average of 34.82 kg / head / year. Also, 66 states presents a consumption of between 10.1 and 25.0 kg / head / year (average 16.99 kg / head / year), 15 states are included in the category of consumption of 5.1 to 10 , 0 kg / capita / year (average of 7,61kg / head / year) and 47 states have a consumption of less than 5 kg / head / year poultry (average 2.38 kg / head / year) [5, 6].

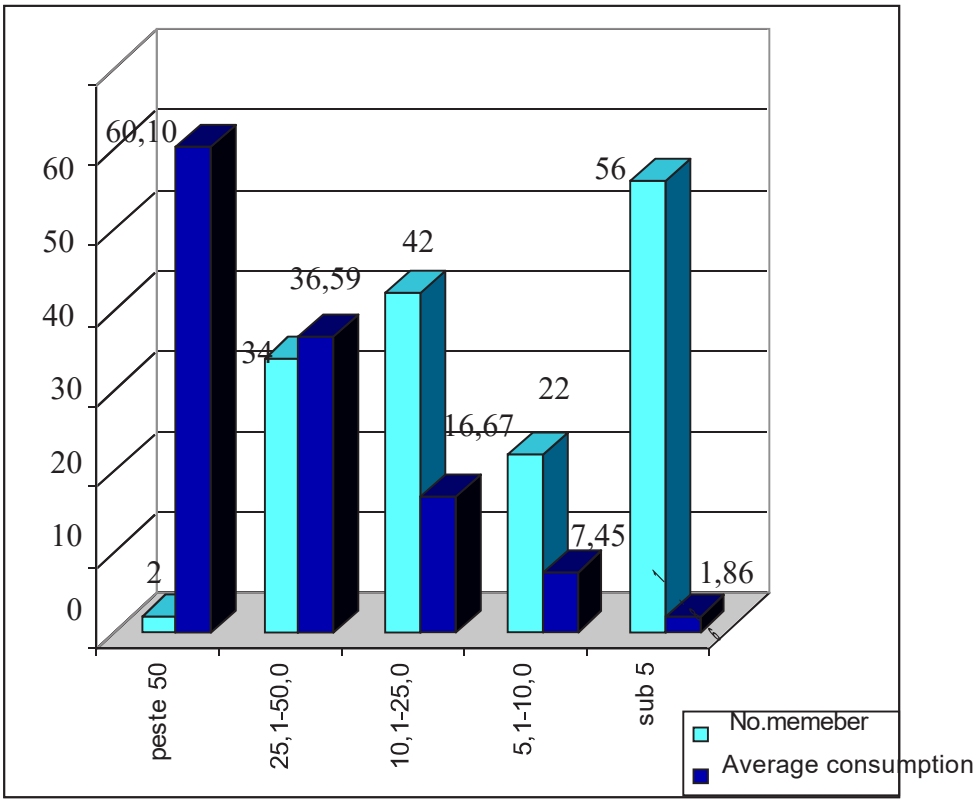

Figure 2: Categories consumption of pork, the number of countries in the world included in each category and the average consumption for each category (FAOSTAT, 2012)

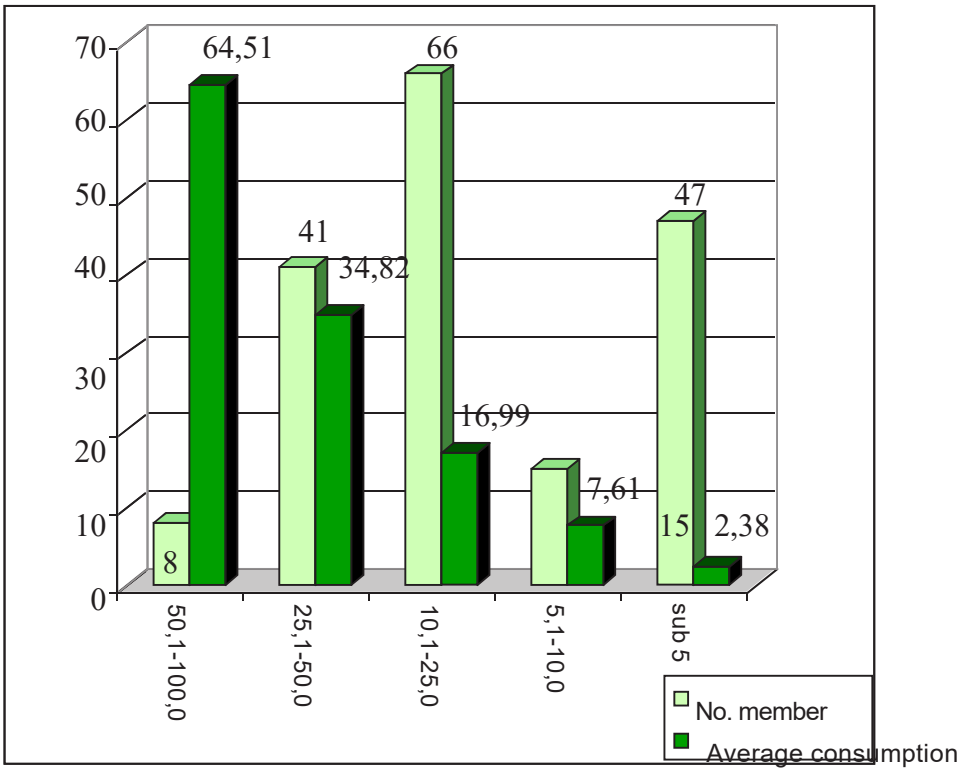

Figure 3: Categories of poultry consumption, the number of countries in the world included in each category and the average consumption for each category (FAOSTAT, 2012)

Consumption of beef, pork and poultry in Romania

In Romania, between 2000 and 2009, meat consumption, depending on the species of origin, can be summarized as follows:

- an average of 7.9 kg / head / year, with a minimum of 6.7 kg / capita / year (2001) and a maximum of 10.0 kg / head / year (2005) for beef cattle;
- an average of 28.3 kg / head / year, with a minimum of 23.1 kg / head / year (2001) and a maximum of 32.0 kg / head / year (2008) for pork;
- an average of 18.5 kg / head / year, with a minimum of 13.0 kg / head / year (2000) and a maximum of 21.0 kg / head / year (2009) for poultry (Figure 5) [4, 5]

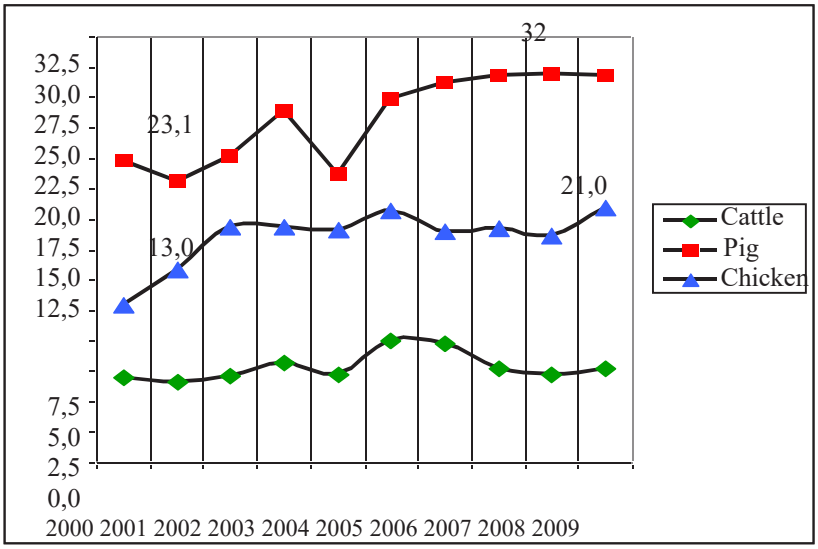

Figure 4: Consumption of beef, pork and poultry in Romania between 2000 and 2009, with minimum and maximum values (FAOSTAT, 2012)

3. CONCLUSIONS

Consumption of beef in 2009 averaged 11.12 kg / head / year, Romania with consumption of beef under this average.

Selected world pork consumption in 2009 was on average 15.0 kg / head / year, Romania with a consumption of 28.3 kg / head / year which was above the average consumer in the world. Consumption of poultry Romania was below the average consumption selected developed world.

References

[1] Darabă Aura, *Evaluarea calității cărnii*, Editura Didactică și Pedagogică, București 2007

[2] Diaconescu Ion, Ardelean Dorina, Diaconescu Mirela, *Merceologie alimentară: Calitate și siguranță*, Editura Universitară, București.2007

[3] Turek Rahoveanu Adrian și colaboratorii, *Analiza filierei sectorului carne în România*, Editura Ars Academica, București, 2009

[4]Mihaiu Mihai și colaboratorii (2009*), Controlul sănătății produselor de origine animală*, Editura Risoprint, Cluj – Napoca.

[5] ***http://www.codexalimentarius.org

[6] ***http://www.efsa.europa.eu

[7] ***http://www.faostat.fao.org

DESIGN OF MACHINE FOR SEPARATION AND PROCESSING THE RECYCLABLE SOLID WASTE

Nadhim Mejbil Faleh[1]
University of Mustansiriah (IRAQ)

Iulia Adriana Grafu[2]
Polytechnic University of Bucharest

ABSTRACT

The accumulation of garbage in Baghdad and the statistical reviews show that starting with the year 2003 the city was forced to bury the solid waste in vast tracts. The study we did seek alternative methods of waste management and waste diversion by recycling. Alternative methods are having environmental and health impacts so research explore the potential for solid waste management. Increased recycling provides an attractive option since it also eliminates reservation land used in landfill and other disposal requirements. Environmental impacts are big reducing pollution, conserving energy and can create jobs by building more manufacturing industries that can be a very good economic opportunity. The local government in Baghdad, confirmed that the waste produced by the Baghdad daily rate is about 11 thousand tons, which is equivalent to more than 4 million tons per year. The authorities explain that the work of the stations is limited to waste pressing only, without any separation operations or recycling process. An experimental system for separation of the waste that could handle three type of waste: PVC, glass and paper is made in this article. The steps within this system are designed to be as automated as possible to can increase speed of operations and reduce costs.

1. INTRODUCTION

Recycling is a plausible path to reduce the amount of waste generated in the country in a sustainable way [1]. Global waste has increased about 28% from 5.6 Mt in 1997 to 7.65 Mt in 2007 and is estimated to further increase by 30% in 2020 [2, 3]. Solid waste is generated in many forms by human activities (industrial, domestic, commercial and construction) and animals. Some of the waste fall out of the commercial use i.e. cannot be utilized. Parts of this waste (specially the industrial part) are considered hazardous to the environment and natural resources. Continuous population growth and increase of standard of living, solid waste is increasing in tremendous amounts. This fact enforced a major problem facing the world [4]. Waste treatment includes a lot of different processes. Besides from the organizational, structural and technical monitoring information of waste treatment should also be considered the procedures Thermal, Biological and Mechanical. Processing falls under the heading of physical treatments by using physical techniques to modify the composition and form of the waste and is having differences between thermal and mechanical treatment. Anytime make a recycling process mean a conversion of the material mean secondary production of a new material named raw material mean used material transformed in useful goods. Recycling process conduce to reduce the amount of waste from landfill so the goal is to use and reuse material from garbage to minimized and important is first the way garbage is separate; because a good separation of the garbage from start help and support the next steps and give efficacy of the facilities which deals with the waste. Mechanical treatment is defined like the process of sorting and separation aggregates with the purpose to separate for reuse single materials from the waste stream of the city's solid waste can be process like size reduction, classification, separation and compaction. Typical aggregates in mechanical separation need different types of sorting and separation

[1] Iraq, Baghdad, 009647709778646, dr.nadhim@uomustansiriyah.edu.iq
[2] Polytechnic University of Bucharest, 0040767296500, grafu.iulia@gmail.com

methods: (1) Some aggregates for size reduction, classification, separation and compaction of the waste. (2) Pre-treat the waste stream and collect recyclables out of the waste stream. (3) Separate ferrous/ nonferrous metals, light fractions, different types of plastics, glass, inert materials fast and easy.

2. METHODOLOGY

This study is concerned with analyzing of information on the annual rate of waste in Baghdad, and the analysis of its components, in preparation for the design and construction scheme of the system processor for the problem. Iraq is known as one of the most populous Arab countries with population exceeding 32 million. Rapid economic growth, high population growth, increasing individual income and sectarian conflicts have led to worsening solid waste management problem in the country. Iraq is estimated to produce 31,000 tons of solid waste every day with per capita waste generation exceeding 1.4 kg per day. Baghdad alone produces more than 1.5 million tons of solid wastes each year. Rapid increasing in waste generation production is putting tremendous strain on Iraqi waste handling infrastructure which been heavily damaged after decades of conflict and mismanagement. In the absence of modern and efficient method for handling and disposal infrastructure most of the wastes are disposed in unregulated landfills across Iraq, with little or no concern for both human health and environment. Spontaneous fires, groundwater contamination, surface water pollution and large-scale greenhouse gas emissions have been the hallmarks of Iraqi landfills.

3. SEPARATION PROCEDURE

Gravity separation method uses differences in specific gravity (SG) between various minerals to achieve a separation and is a wet process although examples of dry gravity separators exist. Gravity separation method works best when there is a big difference in the SG in the minerals that is need to be separated, and the particle size is the same and not excessively fine, and shape is circular.

In this study, the experiments are designed to have operating conditions that can produce the separation applications. This study attempted to use a local analysis to identify the relatively composite percent in the waste in Baghdad, a combination of plastic waste 52%, aluminum cans 34% and rest of paper, dust and food crumbs, were identified. A choice of the separation method based this analysis. The system described in Figure 1, consists of Vibrated Beam; Part 1, which is based on the principle of size separation, at the end of which small-scale waste is disposed of. The plastic waste is after separated from aluminum cans by rotor in the separation unit no.4.

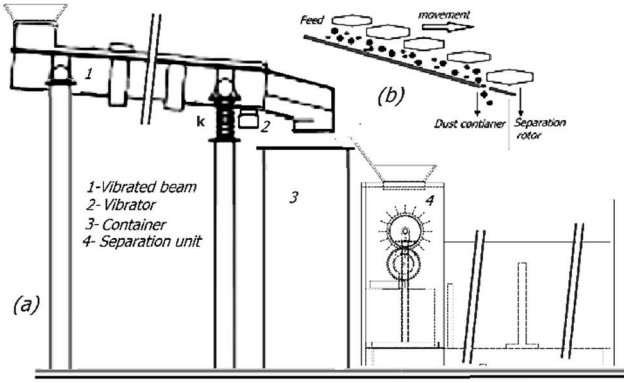

Figure 1: Separation system

Williams [5] has stated that when a big particle get to be localized at the base of a vibrated container, the particle will rise always and reach a height in the belt that depends on vibration strength. However, as quantities are not precisely defined, it is difficult to obtain more than a qualitative picture because it is unclear in which limit this experiments was done. Williams found that the large particle rises above critical amplitude and reaches an equilibrium height that depends on the vibration strength [6]. A sketch of the particle positions is shown in figure1.

In the regime where vibration frequency is small, the system does not remain fluidized throughout the cycle even for large amplitudes. This shaking is assumed to do a local rearrangement, and geometry plays a dominant role in determining the properties of vibrated granular materials. This is the regime in which the MC simulations were applied to make size separation [7]. But first let us consider the gravity and density of variation for a set of multi sized particles in a vibrated beam. For a normal case, the volume and density are well-defined However, the behavior of separation is based on two things: (1) the normal frequency of the system, and then the frequency emitted by the vibrator. Therefore, the oscillator was being represented as shown in Figure 2, and the covering equations of the application were studied.

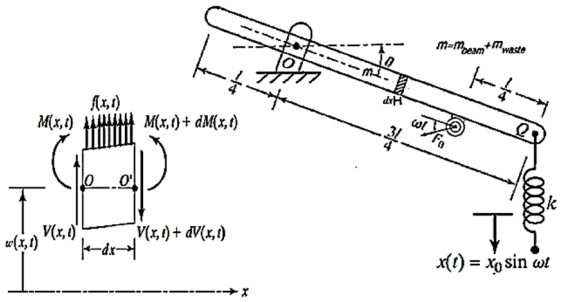

Figure 2: Modeling of vibrated beam

E is the elastic modulus, I is the second moment of area and *f (x,t)* is the applied external force. The beam with length *l*, and with conditions as shown in Figure 2, that is given by:

From the FBD as shown in Figure 2, and according to newton's 2nd law we have:

$$-(V+dv)+V+f(x,t)dx=\rho A(x)dx\frac{\partial^2 w}{\partial t^2} \qquad (1)$$

Where *W(x,t)* is the transverse displacement of the beam, ρ is the density of the beam, A is the cross sectional area,

$$\sum Mo=0$$

$$M+dM-(V+dv)dx+V+f(x,t)dx\frac{dx}{2}-M=0 \qquad (2)$$

$$dV=\frac{\partial V}{\partial x}dx \quad and \quad dM=\frac{\partial M}{\partial x}dx$$

Disregarding terms involving second powers in dx (1) and (2) can be written as

$$-\frac{\partial V}{\partial x}(x,t)+f(x,t)=\rho A(x)dx\frac{\partial^2 w}{\partial t^2}(x,t) \qquad (3)$$

$$\frac{\partial M}{\partial x}(x,t)-V(x,t)=0$$

Sub in eq. (3) become:

$$-\frac{\partial^2 M}{\partial x^2}+f(x,t)=\rho A(x)\frac{\partial^2 w}{\partial t^2} \qquad (4)$$

From the elementary theory of bending of beams (also known as the Euler-Bernoulli), the relationship between bending moment and deflection can be expressed as:

$$M(x,t)=EI\frac{\partial^2 w}{\partial x^2}(x,t) \qquad (5)$$

where E is Young s modulus and I(x) is the moment of inertia of the beam cross section about the y-axis. Inserting Eq. (5) into Eq. (4) we obtain the equation of motion for the forced lateral vibration of a no uniform beam:

$$\frac{\partial^2}{\partial x^2}\left[EI(x)\frac{\partial^2 w}{\partial x^2}(x,t)\right] + \rho A(x)\frac{\partial^2 w}{\partial t^2}(x,t) = f(x,t) \qquad (6)$$

For a uniform beam, and for free vibration Eq. (6) reduces to

$$c^2\frac{\partial^4 w}{\partial x^4}(x,t) + \frac{\partial^2 w}{\partial t^2}(x,t) = 0 \qquad Where \quad c = \sqrt{\frac{EI}{\rho A}} \qquad (7)$$

The free-vibration solution can be found using the method of separation of variables as

$$W(x,t) = W(x)T(t) \qquad (8)$$

Substituting Eq. (7) into Eq. (8) and rearranging leads to:

$$\frac{d^4W(x)}{dx^4}\frac{c^2}{W(x)} = -\frac{1}{T}\frac{d^2T(t)}{dt^2} = a = -\omega^2 \qquad (9)$$

Equation (9) can be written as two equations:

$$\frac{d^4W(x)}{dx^4} - \beta^4 W(x) = 0$$

$$\frac{d^2T(t)}{dt^2} + \omega^2 T(t) = 0$$

Where

$$\beta^4 = \frac{\omega^2}{c^2} = \frac{\rho A\omega^2}{EI}$$

$$\therefore T(t) = A\cos\omega t + B\sin\omega t \quad and W(x) = C1\cos\beta x + C2\sin\beta x + C3\cosh\beta x + C4\sinh\beta x$$

where A and B are constants that can be found from the initial conditions, C1, C2, C3, C4, are different consta5nts can be found from the boundary conditions. Due to Singiresu [8] Equation. (8.85) the natural frequencies of the beam are computed as:

$$\omega = \beta^2\sqrt{\frac{EI}{\rho A}} = (\beta l)^2\sqrt{\frac{EI}{\rho A l^4}}$$

Now applying the boundary conditions:

$$\frac{\partial W(x)}{\partial x} = -C1\beta\sin\beta x + C2\beta\cos\beta x + C3\beta\sinh\beta x + C4\beta\cosh\beta x$$

$$\frac{\partial^2 W(x)}{\partial x^2} = -C1\beta^2\cos\beta x - C2\beta^2\sin\beta x + C3\beta^2\cosh\beta x + C4\beta^2\sinh\beta x$$

$$\frac{\partial^3 W(x)}{\partial x^3} = C1\beta^3\sin\beta x - C2\beta^3\cos\beta x + C3\beta^3\sinh\beta x + C4\beta^3\cosh\beta x$$

At x=L/4=1/4

Deflection=*W=o* , bending moment $EI\frac{\partial^2 W(x)}{\partial x^2} = 0$

At X=L

$EI\frac{\partial^2 W(x)}{\partial x^2} = 0$ and $\frac{\partial}{\partial x}\left(\frac{\partial^2 w}{\partial x^2}\right) = kw$

$W(l/4) = C1\cos l\beta/4 + C2\sin l\beta/4 + C3\cosh l\beta/4 + C4\sinh l\beta/4 = 0$ *E B.C 1*

$$\frac{\partial^2 W(l/4)}{\partial x^2} = 0$$

$-C1\beta^2\cos l\beta/4 - C2\beta^2\sin l\beta/4 + C3\beta^2\cosh l\beta/4 + C4\beta^2\sinh l\beta/4 = 0$ *E B.C.2*

$$\frac{\partial^3 w(4)}{\partial x^3} = kw(4)$$

$C1\beta^3\sin 4\beta - C2\beta^3\cos 4\beta + C3\beta^3\sinh 4\beta +$
$C4\beta^3\cosh 4\beta = C1k\cos 4\beta + C2k\sin 4\beta + C3k\cosh 4\beta + C4k\sinh 4\beta$ *E B.C.3*

$$\frac{\partial^2 W(l)}{\partial x^2} = 0$$

$$-C1\beta^2 \cos l\beta - C2\beta^2 \sin l\beta + C3\beta^2 \cosh l\beta + C4\beta^2 \sinh l\beta = 0 \qquad E\,B.C.4$$

From above four equations we can find C1, C2, C3, and C4

The steady state response of forced vibration can be expressed as:

$$EI \sum_{n=1}^{\infty} \frac{d^4 W(x)}{dx^4} q_n(t) + \rho A \sum_{n=1}^{\infty} W_n(x) \frac{d^2 q_n(t)}{dt^2} = f(x,t) \qquad (10)$$

Where $q_n(t)$ is the generalized coordinate in the nth mode.

$$\sum_{n=1}^{\infty} \omega_n W_n(x) q_n(t) + \sum_{n=1}^{\infty} W_n(x) \frac{d^2 q_n(t)}{dt^2} = \frac{f(x,t)}{\rho A} \qquad (11)$$

Now multiply both sides of above Eq. by $W_m(x)$ ((where $W_m(x)$ orthogonal with $W_n(x)$. And integral from 0 to l

$$\sum_{n=1}^{\infty} \omega_n q_n(t) \int_0^l W_n(x) W_m(x)\, dx + \sum_{n=1}^{\infty} \frac{d^2 q_n(t)}{dt^2} \int_0^l W_n(x) W_m(x) dx = \frac{1}{\rho A} \int_0^l W_n(x) f(x,t) dx$$

But from orthogonal property ($(\int_0^l W_n(x) W_m(x)\, dx = 0)$) for any n≠m

$$W_n^2 q_n(t) + \frac{d^2 q_n(t)}{dt^2} = \frac{1}{\rho A b} Q_n(t)$$

Where:

$$b = \int_0^l W_n^2(x) dx$$

$$Q_n(t) = \int_0^l W_n(x) f(x,t) dx \qquad (12)$$

where $Q_n(t)$ is called the generalized force corresponding to $q_n(t)$:

$$q_n(t) = A_n \cos \omega_n t + B_n \sin \omega_n t + \frac{1}{\rho A b \omega_n} \int_0^l Q_n(\tau) \sin \omega_n (t - \tau) d\tau$$

With this fabrication from Figure 1, we go on for with size separation in the vibrated granular matter, dust, and food crumbs which leave at the end of the vibrated beam, while the water bottles and juice containers all get for the rotor of separation unit like is shown in Figure3. Equation (12) determines the size of vibrated gate produced, based on the factors and specifications specified in Equation (1) and unbalanced mass in vibrator. We often need a value of W(x,t) at the right end of beam, that not exceeding 6 mm, to ensure dust and granules are disposed of, without bottles and containers. Separation unit that uses a track and a rotor to sort waste as shown in Figure 2. This method been chosen since it is the most efficient method used to convert projectile kinetic energy into size separation.

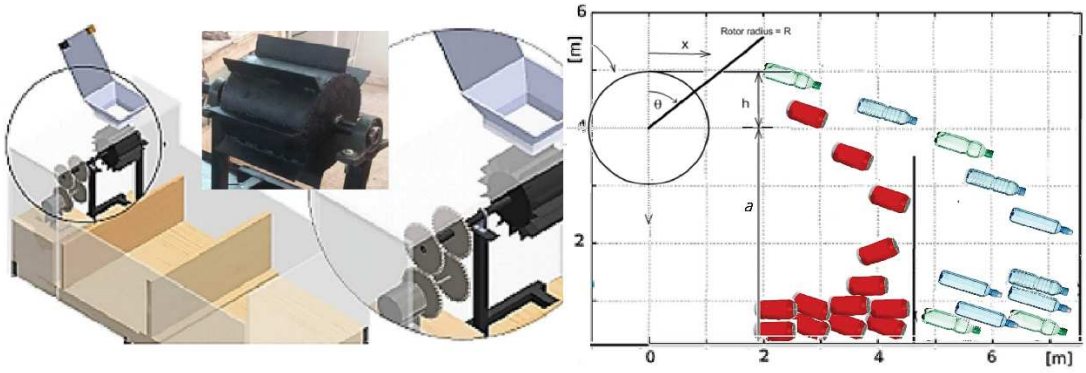

Figure 3: Separation unit

Based on Figure 6, by simple trigonometry, it is:

$$tan(theta) = \frac{x(t)}{h} \quad (13)$$

With x(t) representing the linear position of the sphere along the track.
Substituting theta= w t results in:

$$tan(w\,t) = \frac{x(t)}{h}\,,\ \frac{d}{dt}\,tan(w\,t) = \frac{dx(t)}{dt\ h}$$

using v(t) as time derivative of x(t)

$$w\,sec2(w\,t) = \frac{v(t)}{h}\,;\quad v(t) = h\,w\,sec2(w\,t);\quad v(t) = \frac{h\,w}{cos2(w\,t)};\quad T_0 = \frac{1}{w}\,arcos\ \left(\frac{h}{R}\right)$$

By substituting into equation (16) the velocity of this linear path:

$$Vo = \frac{R2\,w}{h} \quad (14)$$

3. CONCLUSION

This article uses the concept of segregation by vibration and separation by rotation in waste treatment field, with providing a physical and a mathematical description at the mechanical system of separation occurring under vibration and rotational characteristic. The mechanical method in the separation of waste, in this study, was based on the waste components in the study area of Baghdad; this method of treatment has been chose to reduce the value of manual effort in the waste separation process.

References

[1] Low Sheau T., Tee S., Choong W., "*Preferred Attributes of Waste Separation Behaviour: An Empirical Study*", Procedia Engineering 145, 738 – 745, 2016.

[2] Tan, S.T., Ho, W.S., Hashim, H., Lee, C.T., Taib,M.R., & Ho, C.S. Energy, economic, and environmental (3E) analysis of waste-toenergy (WTE) strategies for municipal solid waste (MSW) management in Malaysia. Energy Conversion and Management. 102, 111-120, 2015.

[3] Malaysia Second National Communication to the UNFCCC. ISBN 978-983- 44294-9-2, 2007.

[4] Nadhir A., Roland P., Sven K., "*Suggested landfill sites for hazardous waste in Iraq*", Natural Science, Vol.5, No.4, 463-477, 2013.

[5] Williams J., "*The segregation of powders and granular materials*" Fuel Soc. J. 14 29–34, 1963

[6] Arshad K., "*Size separation in vibrated granular matter*", Reports On Progress in Physics, Institute of Physics Publishing, Rep. Prog. Phys. 67, 2004.

[7] Rosato A., Stranburg K., Prinz F., "*Size segregation of particulate matter by shaking*", Phys. Rev. Lett. 58 1038–41, 1987.

[8] Singiresu S., Mechanical Vibrations, Prentice Hall, ISBN 978-0-13-212819-3 (978-0-13-212819-3), 2011.

[9] Faleh, Nadhim M.; ,Fatigue Life Modification, 2016, scholars-press.

CAD-CAE MODEL FOR THE STRUCTURAL ANALYSIS OF SCARIFIER SCAR-ART MAIN LOAD BEARING STRUCTURE

Gheorghe Gabriel[1], Cardei Petru[1], Vladutoiu Laurentiu[1], Matache Mihai[1], Grigore Ion[1], Bota Marius[2], Marius Marcu[3]
[1]INMA, Ion Ionescu de la Brad Blv. No. 6, Sector 1, Bucharest, 004021-269.32.55, gabrielvalentinghe@yahoo.com
[2] BUILD PR CONSULTING SRL Cluj Napoca 0040747090869, msbota@yahoo.com
[3]SC Artecom SRL, Strada Trandafirilor 195, Localitatea Gologanu, Vrancea, 0040766.631.464, office@artecom-romania.ro

ABSTRACT

This article presents the way to obtain the structural model for elementary linear-elastic static analysis of SCAR-ART scarifier main resistance structure. Also, to prove the functionality of the structural model obtained, structural analysis results for the linear elastic static test are presented. These results are useful for estimating the safety factor and for assessing the behaviour in major overstress situations at the main part of the machine.

Keywords: scarifier, structural model, structural analysis

1. INTRODUCTION

Optimal design or improvement of a complex mechanical structure are activities that are currently carried out in the work of advanced companies working in the field of mechanical and other types structures. Designing an optimal product (at least from some points of view) or optimizing existing products requires complex working tools that are nowadays integrated into CAD-CAE complex programs. The workflow in the CAD - CAE complex is often fragmented, due to the great workload and complex knowledge it requires. For these reasons, in general, the CAD model may come from suppliers who don't have the qualification to do the structural analysis and vice versa, CAE models are used by structuralists who don't have all the engineering knowledge needed to create manufacturing drawings. Moreover, it is known that, in order to make manufacturing drawings, in CAD drawings some gaps are left to be filled by weld seams or other techniques. Such a CAD model is not functional from the point of view of structural analysis. Another problem that generates difficulties in obtaining CAD models is that CAD model providers can work in a drawing program (often older and less performing) while the team performing structural analysis needs the CAD model appropriate to another program.

Considering these obstacles to the direct use of the original designer's CAD model in the structural analysis, a first part of the article is dedicated to transforming the original CAD model into the CAE model undergoing structural analysis in the CAD-CAE SolidWorks program.

The second part of the article presents the elementary results of the structure elastic-static analysis as proof that the transformation was correct. The fact that the results of the structural model are correct, so the results of the structural analysis are correct, can only be found experimentally.

For the time being, as we don't have experimental results, we rely on the fact that the structure has worked in difficult conditions without the occurrence of deficiencies or damages.

Experiments will be done after we have accumulated enough theoretical data to test as many of them within the same experiment.

Global concerns in most of the directions that our research addresses are very common [4], [5], [6], [7], [8].

Converting the provider's CAD model into the SolidWorks CAD model

The analysed structure is a product already made, which can be improved. The real structure can be seen in Figure 1.

Figure 1: Scarifier ARTECOM

The company that designed and built the product made a CAD model in the Inventor Professional 3D CAD program. This model is represented in Figure 2.

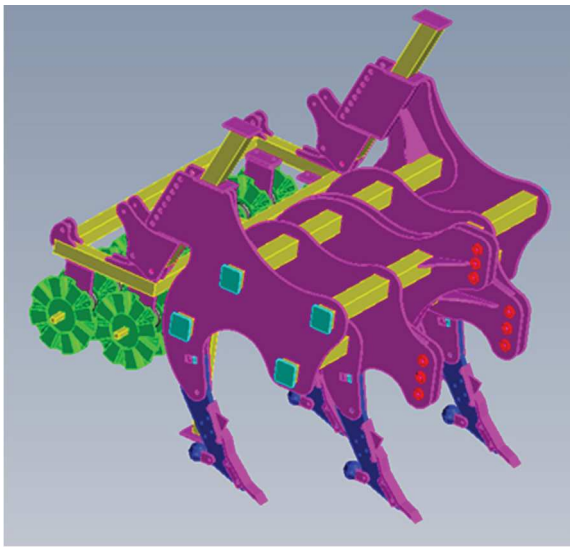

Figure 2: The CAD model of the original structure designer and manufacturer

After the transformations described, we obtained a common CAD model within SolidWorks. This model (Figure 3) is an assembly of 141 components. The mass of the assembly is 1350 kg.

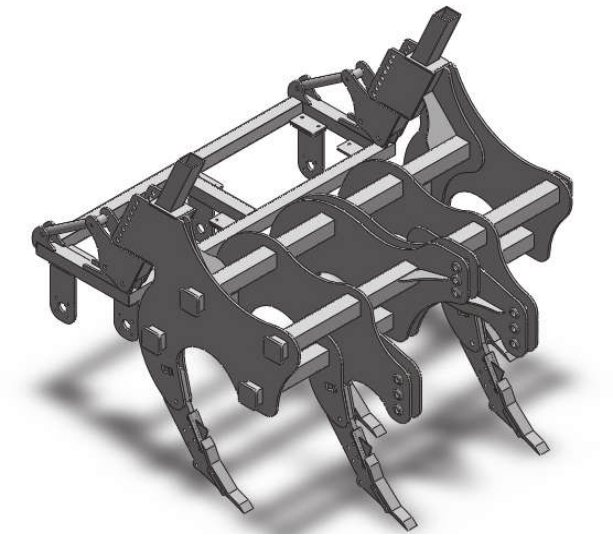

Figure 3: CAD model of the structure in the usual form for SolidWorks program

Converting SolidWorks CAD model into SolidWorks CAE model

Due to the initial model obtained by using Inventor program, CAD conversion to CAE resulted in an assembly that could not be used for structural analysis. To solve this impediment we isolated each benchmark, we revealed each piece and assembled it until it reached its final shape. After making the final assembly, with all its parts, it is necessary to check the existence of interferences in the structure, fig. 4, because the presence of interference (overlap or gap) can prevent the analysis program from running, or, even worse, make it run using wrong results.

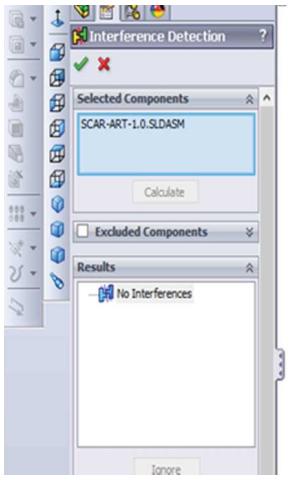

Figure 4: Checking the interferences before starting structural analysis

CAE model structural analysis

The CAD model is simplified. This model introduced in the structural analysis does not contain the rear superstructure of the machine or some small subassemblies. Not all subassemblies are important, but, for example, the safety bolt is an extremely important element for the machine correct functioning. The safety bolt attached to each scarifying part does not appear in this model. Its behaviour in the substructure will be tackled in a separate article, possibly the CAE model developing until the safety screw integration.

Fixing conditions (Structure bearing)

The structure is borne in three points by the tractor attachment system, Figure 5. The attachment to the tractor is (exaggeratedly) made by inserting (cancelling all degrees of freedom on the contact surfaces between the tractor and scarifier attachment elements).

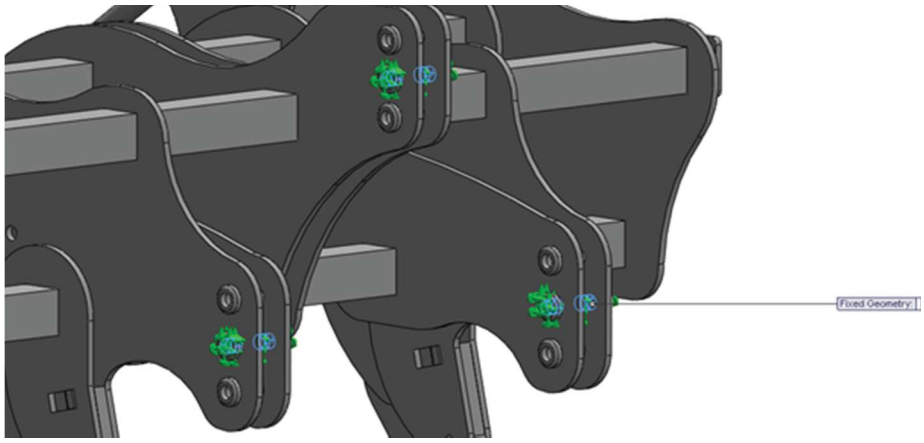

Figure 5: Structure bearing

Structure loading

In this article, we study the response of the structure only for the normal maximum workload. The total force applied to the projection of working parts on the normal plane to the travel direction was calculated using the method of [1], [2], [3].

$$F_0 = ka_0b_0 + \varepsilon a_0b_0v^2, F_1 = ka_1b_1 + \varepsilon a_1b_1v^2, F_2 = ka_2b_2 + \varepsilon a_2b_2v^2$$
$$F_{2o} = F_2 \sin\alpha, F_{2v} = F_2 \cos\alpha \quad (1)$$

where the sizes with index 0 correspond to the chisel type working parts, and those with index 1 correspond to the working parts holders (corresponding to the working depth, up to the working parts level). In (1) F_0 and F_1 are the resistance forces of the soil at the action of the two parts of the working body, a_0, b_0, respectively a_1, b_1 are the working depth and width of the working body's respective parts, while k_0, ε_0, respectively, k_1, ε_1, are soil specific resistances to deformation and soil resistance to deformation coefficients due to the working speed. The working speed has been noted with *v*. In the example considered we used the following values: a_0=0.31 m2, a_1=0.128 m, b_0=0.07 m, b_1=0.07 m, k_0= 100000 Pa, k_1= 20000 Pa. ε_1= ε_2= 2200 kg/m3, v= 10 km/h. We have also considered a traction force, due to the discs, calculated according to the formulas (1), with a_2=0.115, b_2=0.04 m, k_2=20000 Pa, ε_2=1000 k/m3. We have also considered a 9-disc battery with orientation angles α=15°. Forces (2) were applied to the structure according to the graphical representation in Fig. 6.

$$F_0 = 2538N, F_1 = 1048N, F_2 = 127.5N, F_{2o} = 33 \cdot 3 = 99N, F_{2v} = 123 \cdot 3 = 369N \quad (2)$$

Similar estimations of the interaction forces between the working bodies of the machines for soil tillage and the soil, as well as the experimental results, are mentioned in [4], [5] and [6].

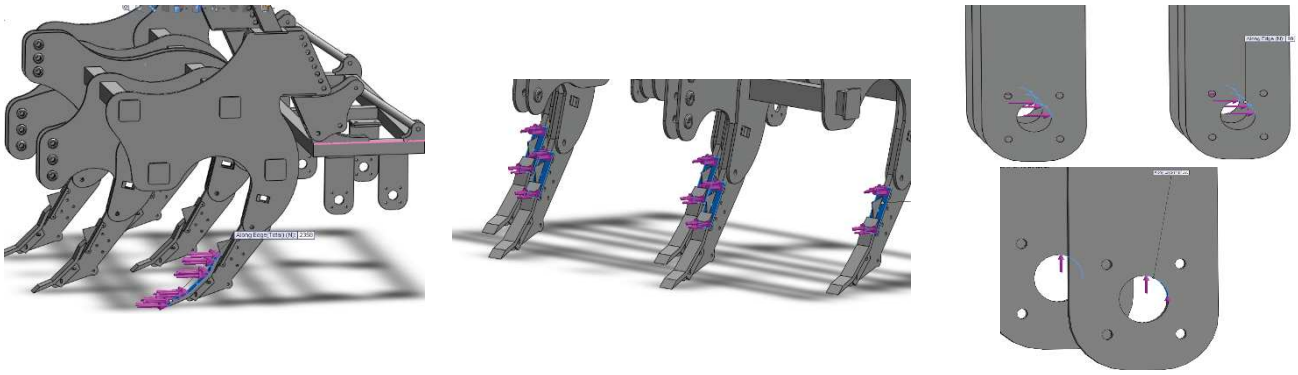

Figure 6: Loads application (forces)

To perform linear-elastic static analysis, the global contact command was applied. This condition applied by the finite element analyser eliminates any kind of clearance, creating stress conditions corresponding to a more rigid structure than the real one. Thus, tensions will be higher than in reality, and relative displacements (deformations) are expected to have lower values than in reality. The discretization of the structure can be seen in Figure 7.

Figure 7: Structure discretization: Projection of finite elements on the structure border

The materials used for the components of the analysed structure are shown in Figure 8 together with the respective properties. For the pipes, S275JR was used, S355 was used for the plate parts and 16MnCr5 was used for the working parts.

Property	Value	Units
Elastic modulus	2.100000031e+011	N/m^2
Poisson's ratio	0.28	N/A
Shear modulus	7.9e+010	N/m^2
Mass density	7800	kg/m^3
Tensile strength	410000000	N/m^2
Compressive Strength in X		N/m^2
Yield strength	275000000	N/m^2
Thermal expansion coefficient	1.1e-005	/K
Thermal conductivity	14	W/(m·K)
Specific heat	440	J/(kg·K)
Material Damping Ratio		N/A

a)

Property	Value	Units
Elastic modulus	2.100000031e+011	N/m^2
Poisson's ratio	0.28	N/A
Shear modulus	7.9e+010	N/m^2
Mass density	7800	kg/m^3
Tensile strength	450000000	N/m^2
Compressive Strength in X		N/m^2
Yield strength	275000000	N/m^2
Thermal expansion coefficient	1.1e-005	/K
Thermal conductivity	14	W/(m·K)
Specific heat	440	J/(kg·K)

b)

Property	Value	Units
Elastic modulus	2.100000031e+011	N/m^2
Poisson's ratio	0.28	N/A
Shear modulus	7.9e+010	N/m^2
Mass density	7800	kg/m^3
Tensile strength	800000000	N/m^2
Compressive Strength in X		N/m^2
Yield strength	590593984	N/m^2
Thermal expansion coefficient	1.1e-005	/K
Thermal conductivity	14	W/(m·K)
Specific heat	440	J/(kg·K)

c)

Figure 8: Material properties: a) S75JR, b) S355 and c) 16MnCr5

2. RESULTS

The main results of the static linear-elastic structural analysis are: the values of the reactions in the holders, vector field distribution of the relative - resultant displacement in the structure, tensor fields' distribution of the specific deformation and the Cauchy stress tensor in

the same structure. Also, an important result for the structure safety is the distribution of the safety factor.

Table 1 shows the values of the resultant forces components, which are also found in the values of the reaction forces (in the three bearing areas).

Table 1: Resultant Forces

Components	X	Y	Z	Resultant
Reaction force(N)	18524.9	-2189.92	0.00846863	18653.9
Reaction Moment(N·m)	0	0	0	0

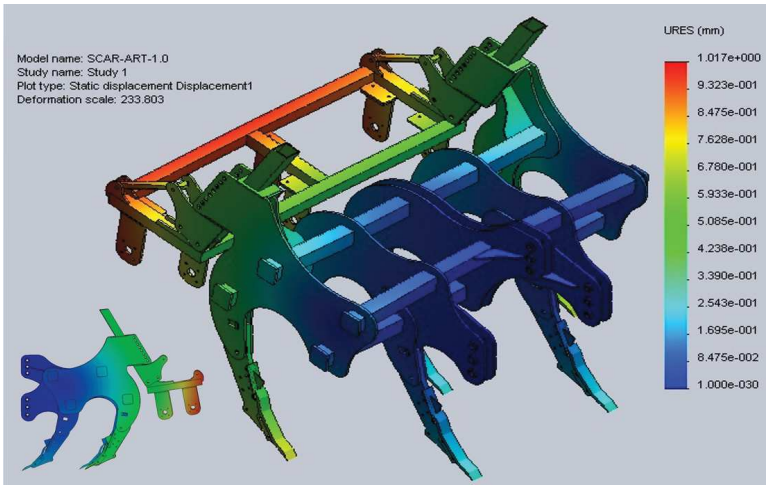

Figure 9: Distribution of the relative displacement field values resulting on the structure border

Figure 9 graphically represents the distribution maps of the relative displacement field values on the structure border. It is noticed that the maximum value (about 1 mm) is located at the back of the structure. This maximum value can be exceeded if we take into account the clearances of the structure and of the connection system between the scarifier and the tractor. Increasing the movement, in the conditions of the considered stress, admitting the clearances, contributes to the relaxation of the structure and consequently to the increase of the safety factor. However, exaggerated clearances generally lead to more or less premature wear.

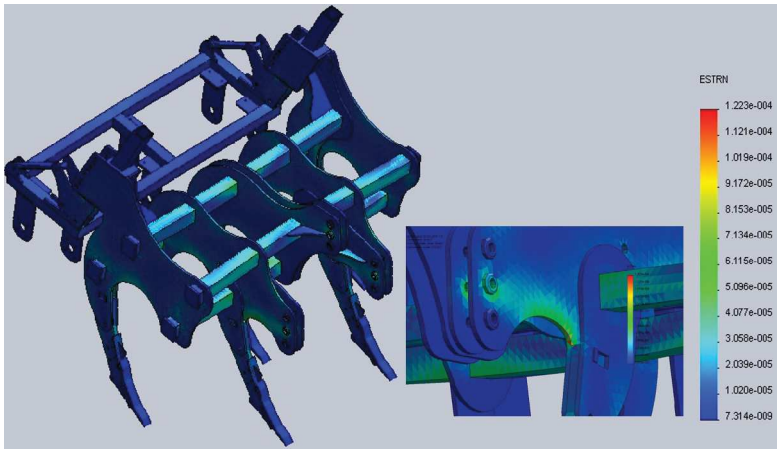

Figure 10: Field values distribution of the total specific deformation on the structure border

In figure 10, the distribution of the total specific deformation values is graphically represented by colour map. The maximum stress area is also indicated in detail. Due to the fact that we are working in the elastic-linear field, the maximum tension will be located in the same area as the maximum specific deformation. The maximum equivalent tension is graphically indicated in the same way in Figure 11.

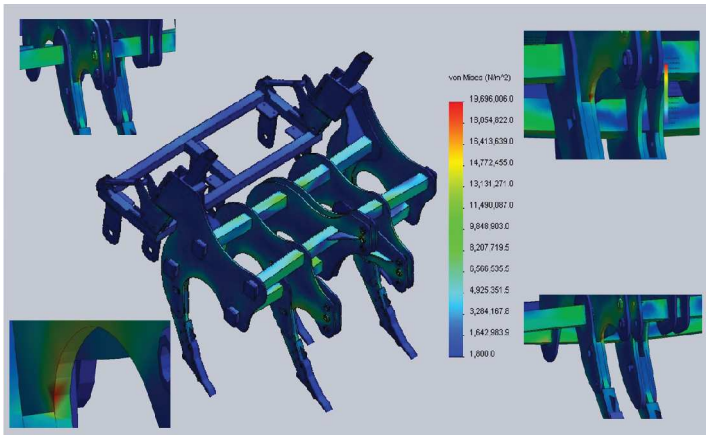

Figure 11: Representation of the equivalent tension distribution on the structure border

Finally, Figure 12 shows the graphical representation of the safety factor distribution in the structure.

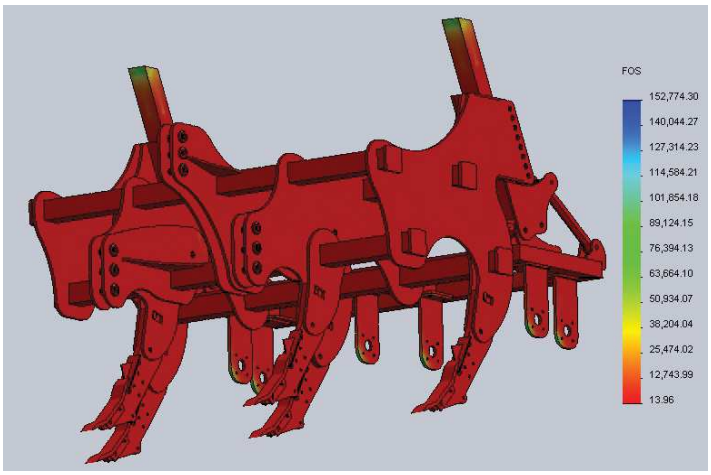

Figure 12: Safety factor distribution in the structure border

The minimum safety coefficient value is 13.936. For agricultural machinery destined to soil works, the usual safety coefficient values are between 1.8 and 2.2. Therefore, this machine is either much oversized, or it works under much tougher conditions. The latter may appear either due to use under improper conditions or due to accidents (impact with hard rocks or roots in soil).

3. CONCLUSIONS

Following this first structural study on the SCAR-ART scarifier, several important conclusions can be drawn for further investigations.

For a normal load, calculated according to the criteria outlined in the paper, the load-bearing structure of the scarifier is overestimated, leaving aside possible accidents in the soil (hard bodies) or the use under improper conditions.

Considering the maximum values of equivalent tension, there are no risks of structure material failure. Also, the maximum relative displacement values guarantee that deviations from working parameters dictated by agrotechnical requirements (working depth, in particular) are negligible, at least regarding the essential part of the scarifier work.

The high value of the safety coefficient (13.96), in relation to its usual values in the practice of designing and manufacturing agricultural machinery for soil works, shows that there is an important potential for optimizing this machine. Obviously, there may be the problem that there have been tests (with working parts of the type used by this scarifier, isolated) that have indicated a maximum value of the resistance coefficient to soil deformation of up to five times the maximum one indicated in [1]. The same values are also indicated by [2] and [3] respectively. Since the scarifier could be used on a land that has not been tilled for five to ten years, there is the possibility of accepting a coefficient of up to 7 - 8; therefore it would be the case for a substantial optimization study.

So far these are the preliminary conclusions on the structure we are dealing with. The following immediate issues will be addressed:

- Study of the effects of the hard bodies in the soil on the bearing structure;
- Study of the own frequencies of the structure, for comparison with the characteristic frequencies of the working regime;
- Stability study of bearing structure plates;
- Study of the structure behaviour considering the completion with the harrow battery, possibly other subassemblies;
- The study of the behaviour and effectiveness of the safety screws the structure is provided with and which, in the model presented in this study, do not appear.

Acknowledgement

This paper has been funded by Ministry of Research and Innovation through the UEFISCDI, within the projects entitled "Conservative tillage technology", contr. 181/2014 and "Enhancing the competitiveness of SC ARTECOM SRL by optimizing an equipment for deep processing of soil", contr. 78BG/2016.

References

[1] M. N. Letosnev, *Agricultural Machines*, Agrosilvica State Publishing House, Bucharest, 1959.
[2] A.V. Krasnicenko, *AGRICULTURAL MACHINERY manufacturer manual*, volume 2, Technical Publishing House, Bucharest, 1964.
[3] A.Sandru, S.Popescu, I.Cristea, V. Neculaiasa, *Agricultural machinery exploitation*, Didactic and Pedagogical Publishing House, Bucharest, 1983.
[4] Cardei Petru A. Meca Georgi Kostadinov, *Working regimes of the agricultural machines designed to soil tillage: From optimization to fundamentals* (1), INMATEH, vol. 37, No. 2/2012, pp.13 – 20.
[5] Cardei Petru, Georgi Kostadinov, *Working regimes of the agricultural machines designed to soil tillage: From optimization to fundamentals (2)*, INMATEH , vol. 37, No. 2/2012, pp. 21 – 28.
[6] Nagy M.Cardei Petru Cota C. Fechete L., *METHOD OF ESTIMATING THE SOIL RESISTANCE FORCE TO SOIL WORKING MACHINE PARTS WITH APPLICATIONS TO THE OPTIMIZATION OF WORKING REGIMES OF MACHINES USED IN HORTICULTURE*, INMATEH , vol. 35, No. 3/2011, pp.27 – 32.
[7] Arjun Kadam, Narendra Chhapkhane, *DESIGN AND ANALYSIS OF SUBSOILER*, International Journal of Modern Trends in Engineering and Science, ISSN: 2348-3221, pp. 11-14.
[8] Gheorghe G, Persu C., Matache M., Mateescu, M., Cujbescu D,.*Finite element method use in the calculation and optimization of the active parts of mulch films applying equipment*, Agricultural and mechanical engineering, ISSN 2537 – 3773, pp.629-634.

CONSIDERATIONS ON VIBRATORY WORKING BODIES USED TO MINIMIZE SOIL COMPACTION

Neluș-Evelin Gheorghiță[1], Sorin-Ștefan Biriș, Nicoleta Ungureanu
University POLITEHNICA of Bucharest, Faculty of Biotehnical Systems Engineering

ABSTRACT

Tillage is a basic in the crop production system. It is a process of mechanical manipulation of the soil by changing bulk density, soil aggregate size distribution and other physical properties of the soil. The problem of soil compaction and soil structure degradation increases with the increased mechanization. Vibration is a very important parameter in operations to minimize soil compaction because it influences the soil properties and draft force.

1. INTRODUCTION

Energy conservation in agriculture operations is becoming increasingly important for the viability of the modern agriculture industry. Moreover, the endless desire for increased productivity from agricultural operations is motivating intensive researches for realizing more efficient methods of soil and earth moving processes. For example, the vibratory tillage operations in the conventional tractive method have been investigated for the potential realization of more effective soil cutting, the potential of the forced vibration as a promising mean for soil pulverization and reducing the draft force and machine weight.[3]

The vibrations of the working tool can be transmitted in the longitudinal, transverse direction or in any direction. Some current assumptions allow evaluating, to some extent, the effect of reducing the traction force necessary in case of longitudinal oscillations, but, in case of transverse oscillations, the effect of reducing the traction force is not yet explained.[4]

High drawbar force of tillage tools is the main causes of soil compaction and wheel slip. So, a reduction in the draught force is one of the most important parameters in the design and application of these implements.[7]

2. METHODOLOGY

Soil compaction reduces rooting, infiltration, water storage, aeration, drainage, and crop growth. To loosen the compact soil however high draft force and energy consumption is needed. It is well-known that tillage-tool vibration will reduce draft force during tillage operation if the maximum velocity of oscillation is higher than the velocity of the implement [1].

In Figure 1 are presented two main actions: prevention of water erosion and undesirable effects of compacted zone.

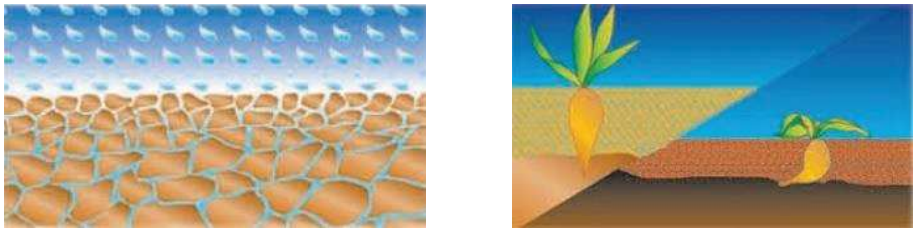

Figure 1: Prevention of water erosion and undesirable effects of compacted zone.

[1] Splaiul Independentei 313, Sector 6, Bucharest, 0726453269, evelin_gheorghita@yahoo.com

Efforts have been made to quantify the effects of soil compaction and to analyze spatial and temporal relationship between extent of compaction and its causes.[1] Key components such as mechanical load, soil physical properties, agronomic operations, and crop rotation can influence soil compaction (Figure 2).

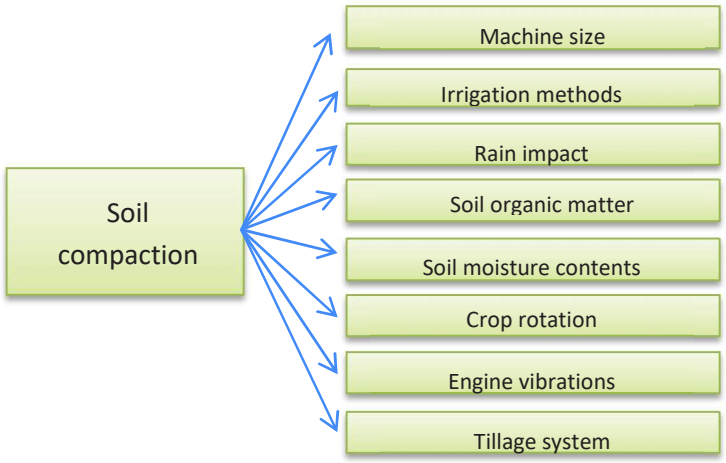

Figure 2 : Summary of causes generating soil compaction

Soil compaction is caused by two factors:

- Natural – conditioned by genetic properties of soil, pressure of roots penetrating the soil, kinetic energy of rain, effects of water logging and successive frost-free winters
- Artificial : – caused by humans
  – field machinery – passes, pressure and drive slip of machines
  –reducing soil strength to compaction by incorrect management practices such as insufficient supply of organic fertilisers, bad choice of fertilisers, mistakes in crop rotations, continuous growing of crops, etc.[2]

3. TYPES OF ACTIVE WORKING BODIES EQUIPPED WITH VIBRATORY SUPPORTS USED TO MINIMISE SOIL COMPACTION

There are working bodies in which the spring is part of the working body shape (Figure 3). These have the advantage that they vibrate and have a lower draught requirement. The vibrating movement also means that material is broken up and graded effectively. Since this type of tine also has a natural stone release force that is limited by the spring, it is most suitable for slightly shallower cultivation up to a working depth of 20 cm. [10]

Figure 3: Vibratory working bodies in which the spring is part of the working body shape[10]

For working depths down to 40 cm, the working bodies are equipped with hydraulic stone release (Figure 4). The advantage of hydraulic release is that it can be adjusted to suit different

conditions and that even at the highest release pressure it gives a natural dampening effect, therefore protecting the frame.

The working body is attached to the frame by a specially designed bolt with conical bushing, which makes it maintenance-free and extends the working life. The spring unit is fitted horizontally, which extends the life of the tine and allows it to rebound back quickly to the right depth.

Figure 4: Vibratory working bodies equipped with hydraulic stone release[10]

For greater working depths, down to 30 cm, there are ridged working bodies with mechanical stone release in the form of a spring(Figure 6). The spring design makes it very reliable in operation and the release force ensures that the correct working depth is maintained.[10]

The stable and gap-free and maintenance-free tine fitting is a solution based around a sleeve with conical ends, against which two concave sleeves are tightened with a bolt(Figure 7). The double springs on the tines give better depth control and extend the life, since the vibrations from the two springs cancel each other out.[10]

Figure 6 : Working bodies with
mechanical stone release in the form of a spring [10]

Based on conventional design methods in ultrasonic technology and common cultivator working body shapes the ultrasonic cultivator tine was designed as a longitudinal oscillator. To achieve a maximized velocity amplitude at the tine's tip, two boosters were positioned between the piezoactuator and the tine. The boosters were also used to bear the ultrasonic cultivator tine.[6]

The most important device to generate the oscillation is the piezoactuator, which is powered by a sine-wave voltage generator in combination with an amplifier [5]. The oscillation mode of the tine is marked red in Figure 7.

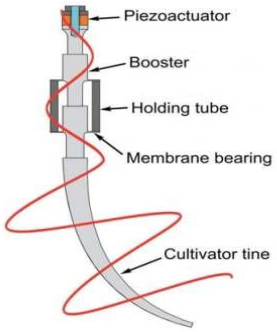

Figure 7: Sketch of the ultrasonic cultivator tine
with its oscillation mode[5]

4. CONCLUSIONS

From the specified ones it results that for the obtaining of the positive effects in the application of the vibrations is conditioned by the knowledge of the physico-mechanical properties of the processed material and their variation depending on various factors, the detailed knowledge of the working process and the negative phenomena that accompany it and of their correct correlation with the applied vibration regime. The lack of these correlations can lead to the opposite of the intended effects.

References

[1]Adnan Noor Sha, Mohsin Tanveer, Babar Shahzad,Guozheng Yang, Shah Fahad,Saif Ali, Muhammad Adnan Bukhari, Shahbaz Atta Tung,Abdul Hafeez,Biangkham Souliyanonh: Soil compaction effects on soil health and crop productivity: an overview, Environmental Science and Pollution Research, January 2017

[2]Athanasios P. Dedousis, Thomas Bartzanas ,Soil Engineering, pp.22, 2010

[3]Awad-Allah, M.A., H.M. Mahgoub, M.E. Abo-Elnor and M.A. Shahin. Experimental investigation of the effect of vibration during tillage process of multi shank plough blade. Proceedings of 13th International Conference on Aerospace Sciences and Aviation Technology, pp: 1-16, Cairo, Egypt, 26-28 May, 2009

[4]Biriș S.Șt, Ungureanu, N., Vlăduț, V., *Study on the influence of mechanical vibrations to the energy required for soil tillage*, 5th International Conference on Thermal Equipment, Renewable Energy and Rural Development TE-RE-RD, pp. 175-180, Golden Sands, Bulgaria, 2-4 June. 2016.

[5]Kattenstroth, R.; Harms, H.-H.; Wurpts, W.; Twiefel, J. (2009): Reducing friction by ultrasound treatment exemplifi ed by tillage. VDI-MEG Tagung Landtechnik, 06.-07.11.2009, Hannover. In: VDI-Berichte 2060, VDIVerlag, Düsseldorf, S. 259-264

[6]Kattenstroth, Ralf; Harms, Hans-Heinrich; Lang, Thorsten; Wurpts, Wiebold; Twiefel, Jens and Wallaschek, Jörg [2010] :Reducing friction in tillage using ultrasonic vibration

[7]Razzaghi, E., Sohrabi, Y., *Vibratory soil cutting a new approach for the mathematical analysis*, Soil and Tillage Research, 159, 33-40, 2016.

[8]Soeharsono, Radite P.A.S. and I Nengah Suastawa, Analytical study of self-excited vibration on two degree of freedom vibratory tillage, Proc. of the 11th International Conference on QiR, paper number: D-S4-2,2009

[9] http://www.minosagri.com/files/pdf/products/vibrating-subsolier

[10] http://www.vaderstad.com/products/cultivators

ASPECTS ON MINT CULTURE TECHNOLOGY

Ion Grigore[1] [1)], Elena Sorică [1)], Cristian Sorică [1)] Carmen Brăcăcescu [1)], Carmen Popescu[2)]

[1)] INMA, Bucharest, Romania; [2)]SC HOFIGAL SA, Romania

ABSTRACT

This paper presents aspects on mint culture technology, which includes all agrotechnical works necessary in the production process for the establishment, maintenance and harvesting of the crop, as well as the importance of cultivating this plant for the pharmaceutical industry, the cosmetic industry as well as the food industry.

It also presents the main production elements of some mint varieties obtained in different cultivation modes, some quality indices achieved in different ways of harvesting mint stolons, as well as the production of plant mass and volatile oil in mint cultivated as annual or biannual plant.

1. INTRODUCTION

Mint (Mentha piperita L.) (picture 1), common name "Good Mint", is one of the oldest medicinal plants and is part, together with other aromatic plants such as thyme, breckland thyme, marjoram, sage or lavender, of the family Lamiaceae.

Mentha piperita is an annual herbaceous plant, considered by many authors to be perennial. [4] Mint culture is of particular importance for the pharmaceutical industry, toothpaste, food, soap, perfume and cigarettes industry. [1]

Mint has its origin in Europe, but it is cultivated on all continents. It was first cultivated in England (1760), where the first quantities of volatile oil were obtained. The largest volatile oil production (3/4 of world production) is provided by the United States. England, France, Italy, Bulgaria, Russia and Japan compete in worldwide production of volatile mint oil.

In Romania, the first experimental culture was founded by Pater in 1908, in Cluj, on an area of 88 m^2, and is cultivated in all areas with a cool climate. As active principles, Herba Menthae and Folium Menthae contain: volatile oil 1.5-3.5%. The oil is rich in menthol 50-60% and menthone 9-12%. They also contain methyl and valerian acetate, tannins, flavonoids, polyphenols and a bitter principle. The pharmacological action consists in the fact that mint leaves have stimulatory, stomachic, antiseptic and antispasmodic, cholagogic and spasmolytic, antiinflammatory, antiemetic, antidiarrheic and antitussive properties. [1]

Figure 1: Mint [5]

[1] INMA, Bucharest, e-mail: ionica_grigore2001@yahoo.com

A lot of varieties are known, among which the most valuable are the varieties: Lubenskaia - 541, Kubanskaia -6, Prilukskaia - 324, Prilukskaia - 6, Maritza-1, Kliment-63, Polymentha, Santocka, etc. while in Romania, the Columna variety is known.

Mint is known for its special qualities, which recommend it especially in the prophylaxis and herbal therapy of digestive, respiratory and circulatory diseases.

Menthol has antispasmodic, antiseptic, carminative effect (calms abdominal pain and favours intestinal gas evacuation) and cholagogic (stimulates bile evacuation into the duodenum), antiinflammatory effect on sinuses and vasodilating effect on the nasal mucosa.

Mint is an adjuvant in hepatic and digestive disorders due to gastric and gallbladder secretion, combats hepatic colic, pyloric and gastrointestinal spasms, spastic and intestinal fermentation colitis, gastrointestinal infections, nausea, vomiting, aerophagia, lazy digestion, abdominal bloating, chronic diarrhea, dysentery and indigestion, cleans the intestines, having beneficial effects in the case of intoxication and pinworm infection.

2. MATERIAL AND METHOD

Mint is a sterile hybrid, which in agricultural practice is multiplied exclusively by vegetative reproduction, using the underground stolons. Sometimes, for scientific purposes, mint is multiplied by aerial stolons, by rooting the stems or even the leaves. [2]

Underground stolons used as propagation material must be white and free from the traces of disease and pest attack. Of particular importance to the quality of the underground stolons is the way of maintaining the culture, its fertilization and exploitation, as well as the age of the plantation. [4]

Perennial species with rhizomes and stolons, in the first year develops a main root that is replaced in autumn by the adventitious roots of the inner part of the stem, which will become the plant rhizome. From the nodules of the rhizome start underground and aerial stolons. The stem is up to 100 cm and has 4 edges; it is green, reddish-violet or violet-brown. The leaves have a short petiole, up to 1 cm long, 3-8 cm long and 1.5-2.5 cm wide limb. Flowers are grouped at the top of the stems and have violet or pink colour (Figure 2) [3] and they bloom in July.

Figure 2: Mint flower [3]

The fruit consists of 4 small nuts, covered with persistent calyx. The weight of 1000 seeds is 0.065 g. [4]

Mint begins to vegetate in the early spring when the average temperature is around 3 to 5^0 C. The optimum temperature for mint growth during summer is 18-20^0 C, maximum 22-25^0 C. The temperature influences the volatile oil content.

Mint special needs for soil humidity are explained by the particular extension of the leaf surface and the presence of a relatively weak and superficial root system.

The lack of humidity is very harmful to mint cultures because it reduces the plant's height by 1.5 times and decreases its weight by about 4 times.

Also, soil humidity is the factor that can decide the optimum planting time. It is very important to know that at soil humidity below 30% the mint must not be planted because most of the stolons dry, regardless of their initial water content.

For normal growth and development, mint needs continuous illumination for at least 12 hours. Volatile oil obtained from shady plants has enhanced menthone content and low menthol content. [4]

Mint culture technology:

*Crop rotation***:** For mint culture, good preplants are: hay maslins, grain legumes, autumn cereals, weeding crops, early vegetable plants, etc. Lucerne, clover, perennial grass crops and grain corn are not indicated. [5]

Fertilization: The effect of organic or mineral fertilizers on increasing the mint production is unanimously recognized. [4]

Phosphorus and potassium are applied annually in the autumn, and nitrogen in spring at the start of vegetation. Recommended doses are: phosphorus: 50-80 kg / ha active substance, nitrogen: 50-70 kg / ha active substance, potassium: 35 - 60 kg / ha active substance.

Well-fermented manure, as a complex fertilizer, applied under the basic tillage, has a particular effect on the production of mint green mass. [4] The manure in doses of 20 - 40 t / ha, is applied well fermented. In this case, mineral fertilizer doses are halved.

Increasing the amount of fertilizer increases production continuously but economically only to a certain level, but the fertilizer quantities do not affect the level of volatile oil content. [4]

Tillage:

Basic soil preparation is based on its humidity at release. When the soil is dry and deep ploughing perfectly ground cannot be performed, after cereals or legumes, first will be performed a coarse mulch work, at 8-10 cm deep, then, when the soil has sufficient humidity, ploughing will be executed at 28-30 cm deep; the preparation of the land for the planting is done by passing the disc harrow in aggregate with the adjustable tooth harrow and the levelling bar at the depth of 15-18 cm by 2 successive passes. Soil preparation does not influence the volatile oil content.

Planting: To obtain large mint crops it is absolutely necessary to execute the planting in autumn and only in exceptional cases in very early spring. The optimum period is set according to soil humidity, generally in October.

Stolons are not planted in dry soil, because they dehydrate very quickly, the planting standard: 1000-1400 pieces / ha, planting distance 70 cm between rows, planting depth 12-15 cm, optimum density 20-26 plants / m2.

Planting on small surfaces is done manually, the stolons being placed on the bottom of the furrow opened by ridge plough, 2-3 pieces in continuous row, taking care to overlap with ¼ of their length.

On large surfaces, the planting is semi-mechanized by opening the furrow using ridge plough, the manual planting, the covering being done with machines adapted to the model of

those used in vegetable gardening or with the stolons planting machine, consisting of: cultivator or SPC-6 + ridge plough + seats for workers + coating pallets. Figure 3 presents the scheme of the mint stolons semi-mechanized planting device: [5]

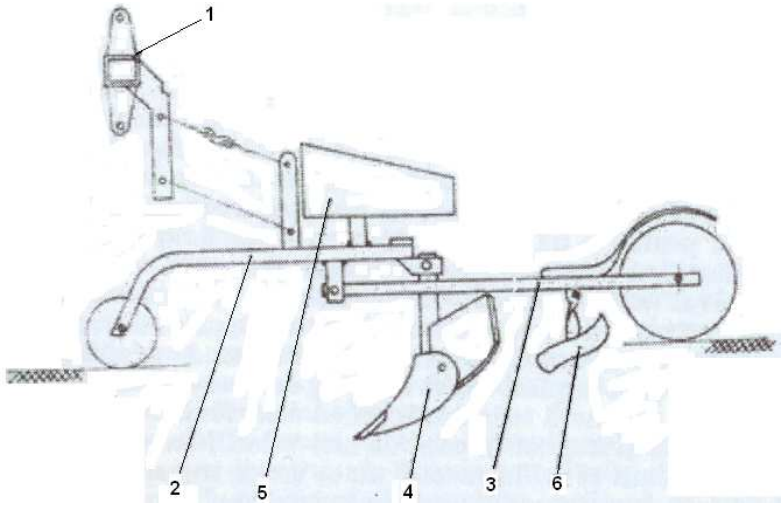

Figure 3: Scheme of the mint stolons semi-mechanized planting device [4]

1 – machine frame (cultivator bar) with attachment triangle; 2 – cultivator section; 3 – carriage with seats for planter; 4 – furrow opening body; 5 – stolon box; 6 – stolon coating pallets

Maintenance works:

In spring, as soon as the conditions allow entry into the field, the mint culture is harrowed perpendicularly to the rows direction, to a depth where the stolons are not removed from the ground.

During the vegetation period, mechanical hoeing is performed 2-3 times, manual hoeing is performed 2-3 times and 1-2 weeding works. In the second year of vegetation, in spring, it will be hoed and rows will be cut with the cultivator at a distance of 50 cm

Chemical weeding:

After planting but before appearing, we can apply Sencor - 1kg / ha or Simadon - 3kg / ha. During vegetation, Basagran can be applied - 3 l / ha, when plants are 6 to 10 cm tall, Fusilade or Furore -2-3l / ha. [5]

Stolons harvesting:

Although the underground stolons are formed in the surface layer of the soil, their harvesting is the most difficult work in the mint cultivation technology. Cutting of underground stolons can be done manually by pitchfork, plough without a breast or by using a potato or onion harvester. In Table 1, some quality indices performed in different ways of harvesting mint stolons are compared:

Table 1 [4]

Indices	**Stolons harvesting methods**		
	by pitchfork, after plough without breast	**by potato harvester without adjustments**	**by potato harvester with adjustments**
Stolons loss, % of which:	9.6	15.2	2.1
- unharvested	9.6	13.8	no
- spread	no	1.4	2.1
Productivity, ha/hour	0.07	0.3	0.4
Labour consumption hours / man/ha	142	35	19

3. RESULTS

In many countries and even in some areas of our country the mint is left in the same place 2-4 years. Researches confirm that mint left in the same place, without any work, for 2 years, can produce green masses that always exceed the yields obtained at the annual mint, but of inferior quality. In the biannual mint, the number of stems is much higher compared to the annual mint. (Table 1)

Table 1

Main production elements of mint varieties obtained by different culture types [4]

Production elements	Banat variety			Prilukskaia - 324		
	Culture type					
	annual	ploughed biannual	Unploughed biannual	annual	ploughed biannual	ploughed biannual
Plants per linear meter (no.)	28	40	181	35	54	244
Plants per linear meter (%)	100	143	646	100	154	697
Ramifications per plant (no.)	27	14	14	23	16	8
Ramifications per plant (%)	100	51	51	100	69	35
Leaves per plant (no.)	169	79	63	195	65	44
Leaves per plant (%)	100	47	57	100	33	22
Leaves fallen from the central stem (no.)	28	37	35	18	41	31
Leaves fallen from the central stem (%)	100	132	125	100	228	172

The data in the table highlights that in the case of the biannual mint, ploughed or unploughed, the number of ramifications and leaves per plant is practically 50% lower in the case of the annual mint. Also, the loss of a large number of leaves from both the central stem and the ramifications contributes to the decrease of the production in general and of the volatile oil in particular (Table 2).

Table 2

Plant mass and volatile oil production for annual or biannual mint [4]

Culture type	Average production of:					
	Fresh herb		Dry leaf		Volatile oil	
	kg/ha	%	kg/ha	%	kg/ha	%
Annual mint	8880	100	1010	100	49.3	100
Ploughed biannual mint	6430	73	7600	75	29.1	59
Unploughed biannual mint	6210	70	7300	72	27.8	56

It is to be noticed that mint maintained for several years on the same land leads to unilateral soil degradation, excessive amount of weeds, especially with perennial plants, as well as increased disease and pest attack.

CONCLUSIONS

Mint culture is of special importance for the pharmaceutical, food and cosmetic industry. As active principles, Herba Menthae and Folium Menthae contain: volatile oil 1.5-3.5%, which is rich in menthol 50-60% and menthone 9-12%, methyl and valerian acetate, tannins, flavonoids, polyphenols and a bitter principle. The pharmacological action consists in the fact that mint leaves have stimulatory, stomachic, antiseptic and antispasmodic, cholagogic and spasmolytic, antiinflammatory, antiemetic, antidiarrheic and antitussive properties.

The optimal temperature for mint growth in summer is $18\text{-}20^0$ C, maximum $22\text{-}25^0$ C. Temperature influences the volatile oil content. Fertilizer quantities and soil preparation do not affect the level of volatile oil content.

The lack of humidity is very harmful to mint cultures because it reduces the plant's height by 1.5 times and decreases their weight by about 4 times.

In the case of biannual mint, the number of stems is much higher compared to the annual mint. In the case of biannual mint, ploughed or unploughed, the number of ramifications and leaves per plant is practically 50% lower than in the case of annual mint.

References

[1] http://www.agrimedia.ro/articole/tehnologia-de-cultura-pentru-mentha-piperita-lhuds-izma-buna;

[2] http://plantemedicinale.crestere-melci.ro/27/menta-cultivarea-prelucrarea-si-utilizarea-mentei;

[3] Daniela Trifan – *Medicinal Plants Recognition Guide / Ghid de recunoaştere a plantelor medicinale*;

[4] Emil, P., Aurel, M., Anela, D., Maria, V., Oltea, C., *Treaty of medicinal and aromatic plants,* vol. II, Publishing House of the Socialist Republic of Romania, Bucharest, 1988 / *Tratat de plante medicinale şi aromatice*, vol II, Editura Academiei Republicii Socialiste, Bucureşti, 1988.

[5] Course - *Technologies for cultivation of medicinal and aromatic plants in Calarasi - Silistra area* / *Tehnologii de cultivare a plantelor medicinale şi aromatice în zona Călăraşi - Silistra*.

NUMERICAL SIMULATION OF DYNAMIC BEHAVIOR OF A MULTIFUNCTION MOTOR VEHICLE EQUIPPED WITH A PRIMARY ADJUSTMENT HYDROSTATIC TRANSMISSION

Ioan LEPĂDATU [1], Corneliu CRISTESCU[1],
Liliana DUMITRESCU[1], Polifron – Alexandru CHIRIȚĂ[1]
[1]INOE 2000 - IHP

ABSTRACT

The present paper analyses the solution of implementing a hydrostatic transmission in the kinematic chain of a mechanical transmission of a multifunction motor vehicle.

In this regard, a request came from a company in the field of road maintenance to develop a special transmission that allows achieving low speeds during working operations with increased torque and minimal wear of mechanical transmission.

The product is developed under a research project between a company and INOE 2000-IHP, which is a research institute, specialized in hydraulic and pneumatic drives.

Hereinafter, we present: the construction and operation of the transmission, the diagram and the structure of the hydrostatic transmission, and also the numerical simulation of the main functional parameters of the multifunction motor vehicle.

1. INTRODUCTION

Multifunction motor vehicles are trucks on which technological equipment is implemented to carry out road-related works such as snow removal, scrapping, sweeping and sprinkling of streets, mowing of public roads, or tree trimming.

Multifunction motor vehicles have two working modes.

● *Marching mode* - the motor vehicles move quickly, from one location to another. Engine torque is small and the travel speed is high.

● *Technological mode* - the motor vehicle moves at a low speed (maximum 5 km/h), imposed by the technology of the equipment attached to the truck. The torque on the motor wheels is high and the travel speed is small. The traditional mechanical transmission [1] (gearbox, cardan coupling, differential) is effective in fast-moving (high speed) but cannot achieve and maintain low travel speeds, and to achieve and maintain a low travel speed with an increased torque on the wheel on uses the hydrostatic transmission, which, besides high power density, also offers increased flexibility in motor vehicle travelling. Practically the motor vehicle has two independent types of transmission: mechanical and hydrostatic. Switching from one transmission to the other is done by simply switching a button. Mechanical transmission is used in marching mode, i.e. travelling on a high-speed road, and hydrostatic transmission - in "technological mode". Electronic control of the hydrostatic transmission ensures a smooth start with a continuous speed control and safe braking.

2. CONSTRUCTION AND OPERATION OF HYDROSTATIC TRANSMISSION

The constructive and functional scheme of the hydrostatic transmission is shown in figure 1. In figure 1.a one can notice that in the case of the mechanical transmission, the torque

[1]14 Cutitul de Argint, 040558, Bucharest, Romania, +40213363991, lepadatu.ihp@fluidas.ro

supplied by the MT motor is transmitted to the RM drive wheels via the CV gearbox, the AC cardan shaft and the DF differential.

Implementation of hydrostatic transmission is achieved by introducing the MH hydraulic motor into the kinematic chain of the mechanical transmission, as shown in figure 1.b, the PH pump being driven from the power outlet of the MT heat motor.

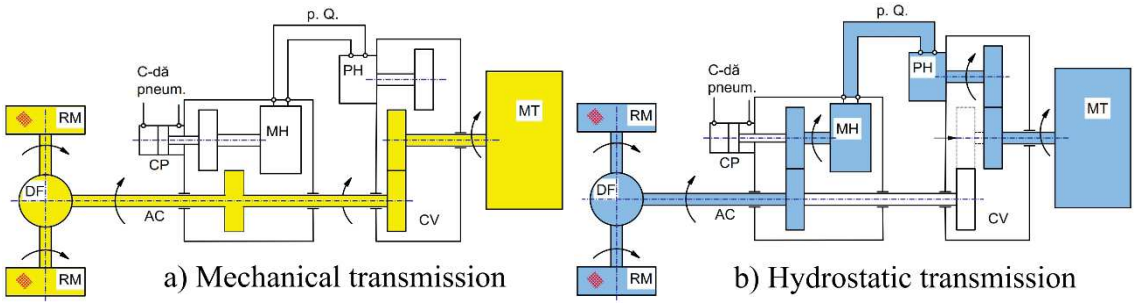

Figure 1. Constructive and functional scheme of hydrostatic transmission

Connecting or disconnecting the MH hydraulic motor from the AC cardan shaft is carried out with the pneumatic cylinder CP powered by the compressed air network of the motor vehicle. The hydraulic PH pump is driven from the power outlet of the truck directly or via a cardan shaft.

Activating the hydrostatic transmission is thus [2] (figure 1b): change the CV gearbox to neutral to deactivate the mechanical transmission. This disengages the MT heat motor from the AC cardan shaft; couple the power outlet for the PH pump drive; engage the MH hydraulic motor with the AC cardan shaft by using the CP pneumatic cylinder.

The kinematic chain of hydrostatic drive has two branches: • Hydraulic power generation kinematic chain: MT-CV-PH; • Hydraulic power use kinematic chain: MH-AC-DF-RM. The energy flow of the hydrostatic transmission [3] undergoes two energy conversions: a) The PH hydraulic pump converts the mechanical power (torque x speed), received from the MT heat motor, via the CV gearbox, into hydraulic power (pressure x flow), which it transfers to the MH hydraulic motor; B) The MH hydrostatic motor converts the hydraulic power received from the PH pump into mechanical power (torque x speed), which it transfers to the drive wheels, via the AC cardan shaft and the DF differential.

3. DIAGRAM AND STRUCTURE OF HYDROSTATIC TRANSMISSION

The hydrostatic transmission shown in figure 2 consists mainly of: hydrostatic pump 1, hydrostatic motor 2 and conditioning valve 3. These components together form a closed loop hydraulic circuit. [4]

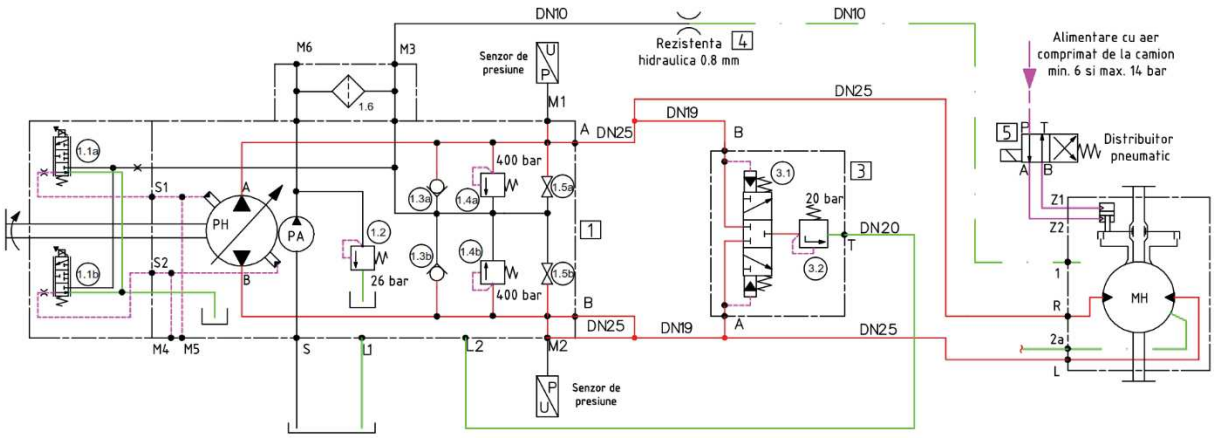

Figure 2. Diagram of hydrostatic transmission

The main PH pump provides hydraulic power to the MH motor. The PA auxiliary pump compensates for the internal losses of the two hydraulic machines and introduces cooled and filtered oil into the closed loop hydraulic circuit. Reversing the discharge direction and changing the flow rate of the PH pump is achieved by proportional electric valves 1.1.a and 1.1.b. The safety valve 1.2 protects the PA pump against overpressure. The check valves 1.3.a and 1.3.b lead the flow rate of the PA pump into the low pressure branch of the closed loop circuit. The pressure valves 1.4.a and 1.4.b protect against overpressure the two branches A and B of the closed loop circuit. The 1.5.a and 1.5.b tap valves open when the truck is towed and the MH hydro motor becomes a pump. The filter 1.6 ensures filtering of oil pumped into the system. The valve 3.1 removes an oil amount (about 10% of the PH pump flow) from the low-pressure branch of the closed loop circuit, oil that comes from the hydro motor. The extracted oil is replaced with "fresh" oil supplied by the PA pump through the filter 1.6 and the check valves 1.3.a or 1.3.b. The pressure valve 3.2 maintains a pressure of approx. 20 bar on the closed loop circuit low-pressure branch [5]. Part of the flow rate of the PA pump is routed through the resistor 4 to the MH hydro motor in order to lubricate and cool it in the fast travel phase. The pressure sensors transmit information to the electronic controller of the transmission. The pneumatic valve 5 connects/ disconnects the MH hydro motor to/from the cardan shaft.

4. ENERGY EFFICIENCY IN THE TECHNOLOGICAL MODE

The thermal motors fitted to multifunction motor vehicles operate at maximum efficiency in the speed range of 1200 to 1800 rpm, as shown in figure 3.

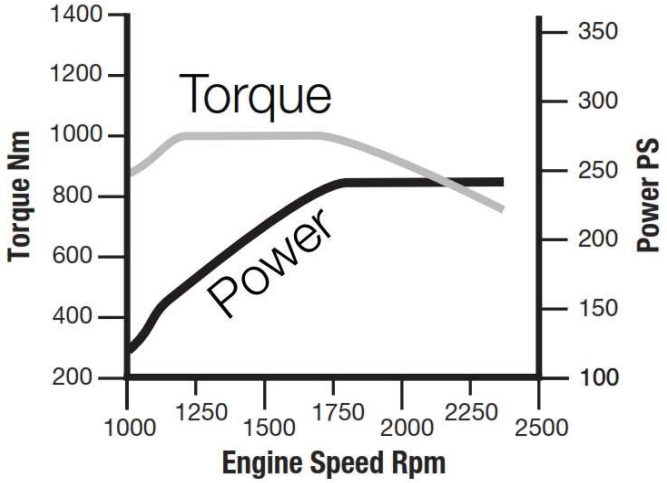

Figure 3. Torque, power and speed diagram of the thermal motor [6].

In the maximum efficiency range the torque developed by the engine is constant. Also, the ratio of power/torque supplied and the fuel consumption is maximum, i.e. its energy efficiency is maximum. Using the heat motor at speeds below 1200 rpm, in order to achieve the very low travel speeds required by the technological needs of multifunction equipment, removes the heat motor from the working range with maximum efficiency.

Hydrostatic transmission offers that which the mechanical transmission can not accomplish: low travel speeds with the heat motor operating in the maximum efficiency range. This can be seen from the diagrams shown in figure 4.

It results from this figure that the hydrostatic transmission ensures that the vehicle is driven at very low speeds (0.5 ÷ 5 km/h), at a motor speed of 1250 rpm, located in the maximum efficiency range. The mechanical transmission can not achieve low travel speeds in the efficient working range of the heat motor.

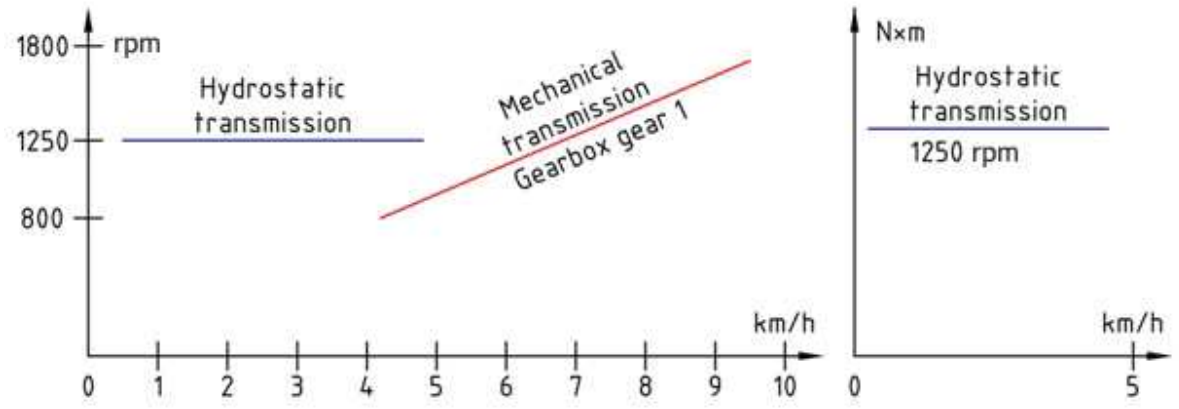

a) Velocity and speed diagram b) Speed and torque diagram

Figure 4. Comparative diagrams: mechanical transmission - hydrostatic transmission

5. NUMERICAL SIMULATION OF THE MAIN PARAMETERS OF HYDROSTATIC TRANSMISSION

The numerical simulation of the main parameters of the hydrostatic transmission has been performed using the AMESIM simulation environment. [7] [8]

The simulation diagram is shown in figure 5.

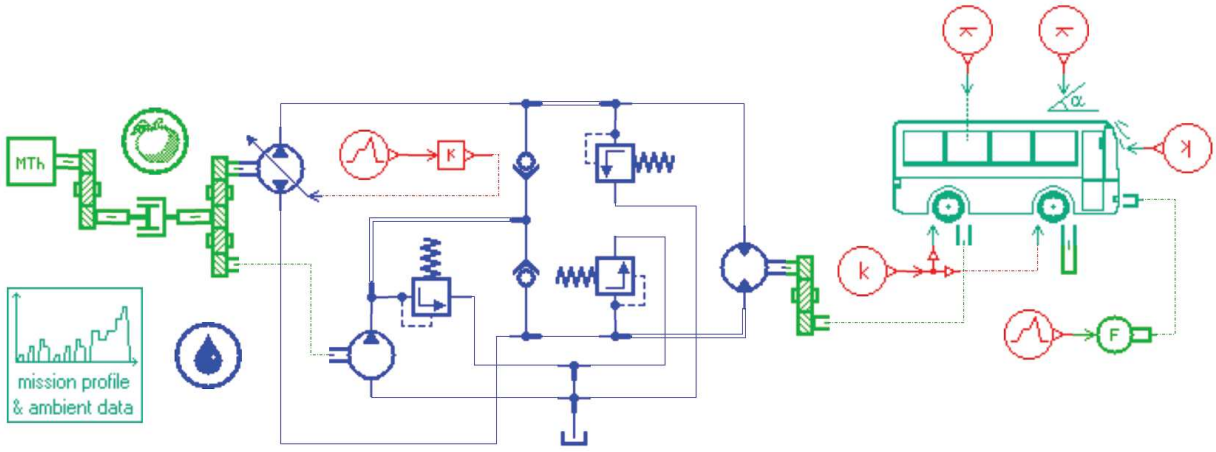

Figure 5. Simulation diagram

Table 1: The main parameters of the simulation:

Heat motor - 1250 rpm and 1000 Nm	PTO - 1524 rpm and max. 600 Nm
Variable flow pump - 75 cc/rev	Compensation pump - 1 cc/rev
Hydrostatic motor – 1000 cc/rev	The weight of the loaded vehicle - 18 t

The goal of hydrostatic transmission implementation is to achieve travel speeds of 0.5 to 5 km/h.

The charts resulting from numerical simulation are shown in figure 6. They show the evolution of the main parameters and the dynamic behavior of the multifunction vehicle.

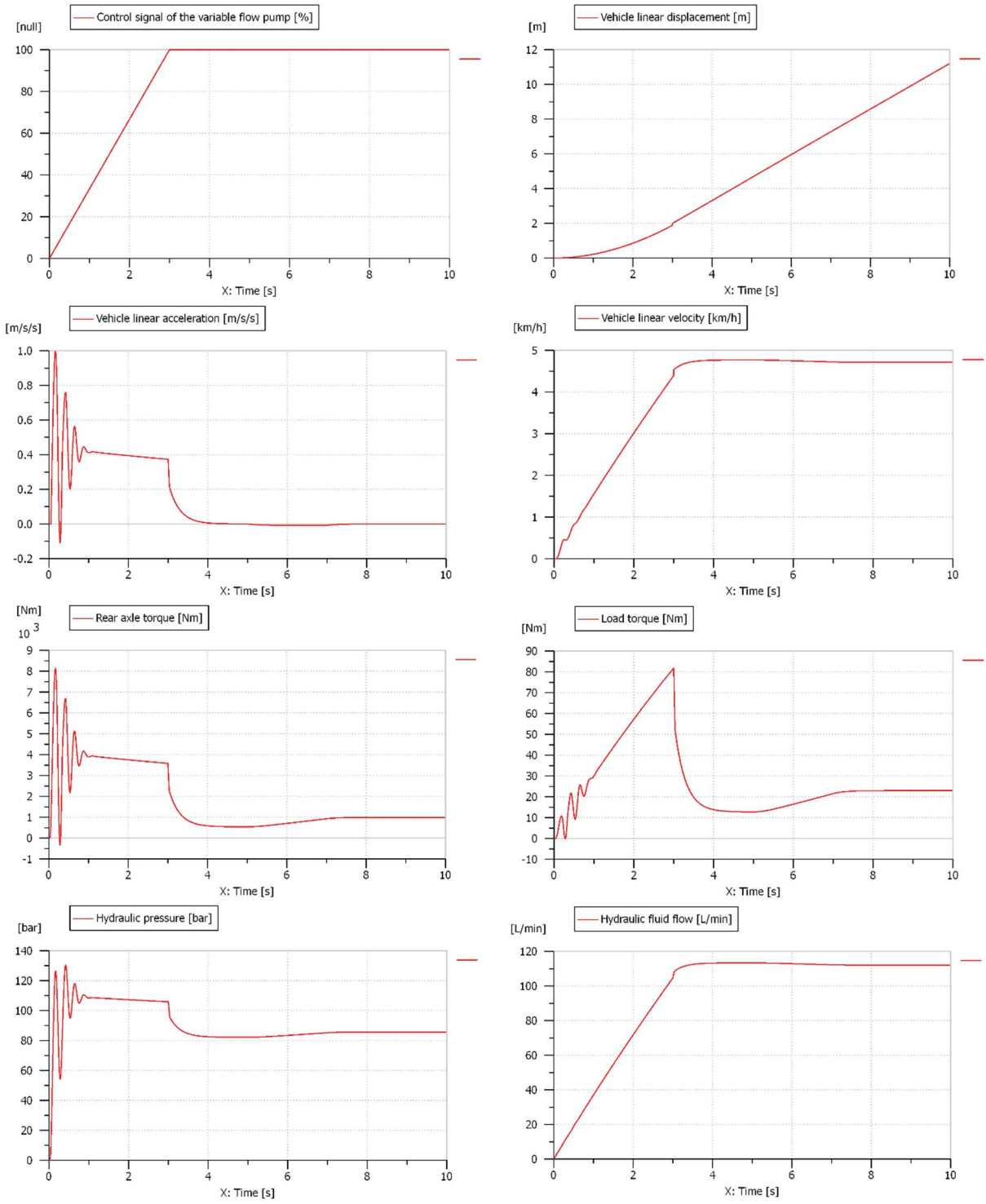

Figure 6. Variation of the main parameters of the simulated system

Figure 6 shows the response of the system to the ramp signal; for the start the displacement occurs slowly, and for the rest – linearly, at a constant speed of 4.8 km/h. In the first phase, there is a variation of the acceleration which is rapidly attenuated, as it has small amplitude relative to the mean value. The other parameters do not exceed the limit values.

After obtaining the physical model and testing it, the results obtained by the simulation will be compared with the experimental ones, which will lead to the validation of the simulation model.

6. CONCLUSIONS

Following the analysis of the proposed solution it can be concluded that the use of hydraulic transmission in the technological travel regime has the following advantages:

- The truck can achieve lower travel speeds than those it can achieve with mechanical transmission;
- The heat motor operates in the maximum efficiency range even at these very low speeds.

The hydrostatic transmission ensures for the multifunction vehicle operation performances which the mechanical transmission cannot achieve: very low travel speeds at the maximum energy efficiency of the heat motor.

Confirmation of these conclusions and the results obtained by numerical simulation will be done after the physical development and testing of the hydrostatic transmission model.

Acknowledgements

This paper has been developed in INOE 2000-IHP, with financial support of Executive Unit for Financing Higher Education, Research, Development and Innovation - UEFISCDI, under PNCDI III - Programme 2, Subprogram 2.1 – Transfer project to the economic operator (PTE-2016), Submission code PN-III-P2-2.1-PTE-2016-0077, Financial agreement no. 11PTE/2016, project title: *High energy efficiency (HEE) electro hydraulic equipment (EHE) for multifunction vehicles (MFV)*, project acronym ECHIPEFEN, Project main domain: 3. Energy, Environment and Climate Change, Subdomain: 3.1. Energy.

References

[1] Oprean, I. M., Andreescu, C., *Transmisii automate pentru autovehicule*. Vol.1 - *Transmisii hidraulice*. Universitatea POLITEHNICA Bucureşti, Romania, 1997.

[2] Vasiliu, N., Vasiliu, D., *Acţionări hidraulice şi pneumatice*, Vol. I, Editura Tehnică, Bucureşti, ISBN 973-31-2248-3, (820 p.), 2005.

[3] Drumea, P., Dumitrescu C., Hristea, Al., Popescu A. M., E*nergy Use in Hydraulic Drive Systems Equipped with Fixed Displacement Pumps*, HIDRAULICA Magazine, Romania, issue 2, pp 48 – 57, 2016.

[4] Popescu, T. C., Guta D. I., Marin, Al., *Adjustment of hydrostatic transmission through virtual instrumentation technique*, ENERG_02, Proceedings of ISC 2010, June 7-9, 2010, Budapest, Hungary, ISBN: 978-90-77381-5-57, pp 248-253.

[5] Drumea, P., Dumitrescu, C., et al., *Energy loss reduction in hydraulic systems with fixed pump in agricultural machinery*, Proceeding of the 5th International Conference of Thermal Equipment, Renewable Energy and Rural Development TE-RE-RD 2016, Golden Sands – Bulgaria, 2-4 June 2016, ISSN 2359-7941, ISSN-L 2359-7941, pp 221-226.

[6]*** MAN TGM BL15R250/06 Issue Date: April 2011, http://www.truck.man.eu/de/en/building-site-and-heavy-duty/tgm/technology/Technology.html.

[7]*** LMS Imagine.Lab AMESim Help.

[8]*** MAN guide to fitting body TGL/TGM Edition 2017 v 0.1, http://www.truck.man.eu.

EXPERIMENTAL RESEARCHES ON SOIL TEMPERATURE OPTIMIZATION IN ROOTS AREA

Manea Dragoș, Gheorghe Gabriel, Marin Eugen, Mateescu Marinela, Pop Florin, Ph.D. Eng. Brăcăcescu C.
INMA, 6 Ion Ionescu de la Brad Blv., Sector 1, Bucharest, 004021-269.32.55,
manea_dragos_05@yahoo.com

ABSTRACT

This paper presents the results of the experimental researches of a temperature optimization installation in the area of the plant roots, which was carried out at INMA Bucharest. The experimental researches aimed to compare the temperature regime registered in the root zone with the use of the optimization installation and that recorded on the control plot located in the immediate vicinity. The soil temperature was monitored in the root zone and at a depth of 2 meters using temperature sensors Pt100. Comparison of the soil temperature variation in the plant root area, both systems (experimental and control plot), as well as the variation of the solar air temperature. Conclusions from experimental research have highlighted that the temperature optimization installation in the root zone is capable of maintaining the temperature within an optimal range for plant growth.

1. INTRODUCTION

Deep soil temperature variation

The heat stored at the surface of the soil, due to solar radiation, is propagated to the deep layers by the caloric conductivity specific to each type of soil. The propagation of the heat in depth, for a homogeneously assumed ground, occurs in accordance with several laws established experimentally by J. Fourier [3]:

- Thermal oscillation periods are the same at all depths (one day and one year);
- When the depth increases in arithmetic progression, the amplitude of thermal oscillations decreases in geometric progression; so, in the soil there are layers with diurnal and annual invariable (constant) layers at certain depths;
- Moments of maximum and minimum temperature delays in proportion to depth;
- The depths at which temperature oscillations with different periods are amortized are proportional to the square roots of the respective oscillations; therefore, the depth at which the annual thermal oscillations are exacerbated is much higher than the depth at which the diurnal ones are depreciated; therefore, the annual thermal oscillations propagate at much greater depths than diurnal ones.

In real conditions, deviations from Fourier's laws are due to the inhomogeneity of the composition and soil structure. In this regard, Ciulache [1], in 1985, described the four laws, and Dragomirescu and Enache [3], in 1998, developed the law regarding the delay of producing the maximum and the minimum temperature for thermal oscillations with different periods (ex. one year) that occurs in the same ratio at depths directly proportional to the square root of that period. After these last authors, the first law refers to the temperature oscillation period, the next two to the thermal amplitude variation, and the last two to the delays in producing the temperature maxima and minima. From these laws, it must be borne in mind that the propagation of surface-to-deep heat requires a certain amount of time, so that the thermal extremes occur with a time difference compared to the surface, the value of which depends on the depth at which the observation is made .

The amplitude of the daily and annual variations in soil temperature decreases proportionally to depth, and the moment of peak and minimum occurrence is greatly delayed

as the depth increases. Soil temperature undergoes changes (thermal oscillations) to a certain depth, after which it remains constant (the isotherm layer), where the magnitude of the annual variations is canceled. The layer of isotherm is also known as the layer of constant annual temperature or invariant layer [2].

The isothermal layer is at varying depths on the surface of the Globe, but also regionally and locally, depending on a number of factors that determine the propagation of heat in the soil. In the tropical areas this is about 6-8 m, in the temperate 20 m and in the polar areas at 25 m. After this layer of isotherm, the soil temperature in the deep layers increases with the depth due to the internal heat of the Earth, according to Geothermal gradient. It has an average value of 3.3°C/100 m. The depth for which the temperature rises by 1°C represents the geothermal stage, whose average value is 33 m / degree. The variation limits are between 20 and 40 m, depending on local particularities [4].

Vertical distribution of soil temperature

During one year there are two types of heat propagation in the soil: the type of sunstroke and the type of radiation.The type of sunstroke is characterized by a gradual decrease in temperature to the isothermal layer and is specific to tropical lands where it is observed throughout the year. In temperate and cold areas it only occurs in the summer season, in the sunny days with strong sunlight. Local factors (vegetation, precipitation, etc.) can disrupt this type of soil temperature distribution [6].The type of radiation belongs to the high latitudes and the winter period in the temperate zones and is characterized by the increase of the surface temperature to the interior of the soil [7]. In the transition seasons, in the spring, a cold layer is located between two warmer layers, and in the autumn, a warm layer is placed between two cooler layers [5].

2. METHODOLOGY

Concept description and working hypotheses

The principle underlying the temperature optimizing system in the plants roots area is that the temperature gradient betweeen the soil surface and a certain depth is maintaining approximately constant throughout the year. In other words, the temperature of the soil to a certain depth is greater than the temperature of the surface of the soil during the cold season and less than that in the hot season. Within the context of current climate change, this temperature difference became significant, reaching and even exceeding 10ºC [8].

Due to the cooling effect of the root area during the summer, is maintained soil moisture and evaporation rate is reduced. System energy requirements are minimal and are assured of unconventional energy sources, such as solar. It is a simple and reliable system that requires a low initial investment and low maintenance costs (fig. 1).

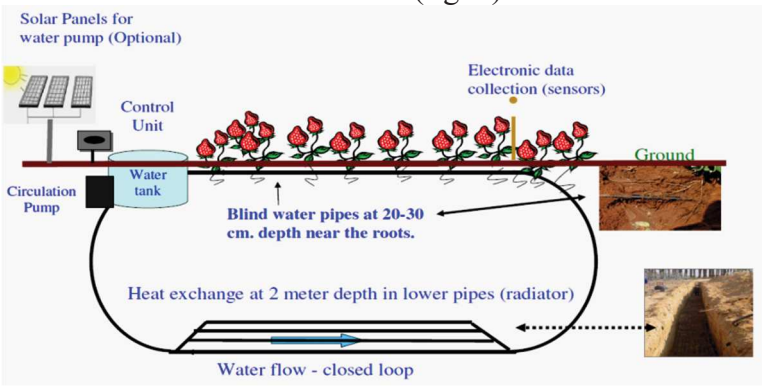

Figure 1: The scheme of temperature optimization system in the area of plant roots [8]

Description of the experimental installation

The temperature optimization installation in the area of plant roots (figure 2), designed and manufactured at INMA Bucharest, consists of a network of copper pipes in variant I or PHD pipes in version II, mounted in a closed loop, through which water is recirculated. The pipe network is arranged on two levels, the first level at a depth of 2 meters and the other one in the root zone, at 0,2 meters (figure 2, *a, b, c*).

The water filling of the installation is made only once, from the water tank (figure 2, *d*), after which it is necessary only filling in the eventual loss. Selecting the Cu / PHD working variant is done by using the three-way valve. The water recirculation is carried out with the circulation pump UPS 15-50 CIL 130 (figure 2, *e*).

The soil temperature was monitored using the Pt100 heat-resistance sensors (Figure 2, *f*), located in the ground at the root of the plants and at a depth of 2 meters in the immediate vicinity of the pipe network. The solar air temperature was monitored by means of a sensor for measuring the relative humidity and the temperature type 0-10 Vcc (Figure 2, *g*). The information taken from the temperature sensors is transmitted to a programmable logic controller model AL2-12MR-D (fig 2, *h*), in which the preset temperature limit values were entered.

a. *b.* *c.* *d.* *e.* *f.* *g.* *h.*

Figure 2: The temperature optimization installation in the area of plant roots

The scheme of the control algorithm for managing the temperature optimization installation in the plant root area, is presented in figure 3. If the soil temperature reaches the upper limit value, the programmable controller controls the starting of the circulation pump and keeps it running until the ground temperature reaches the lower limit value.

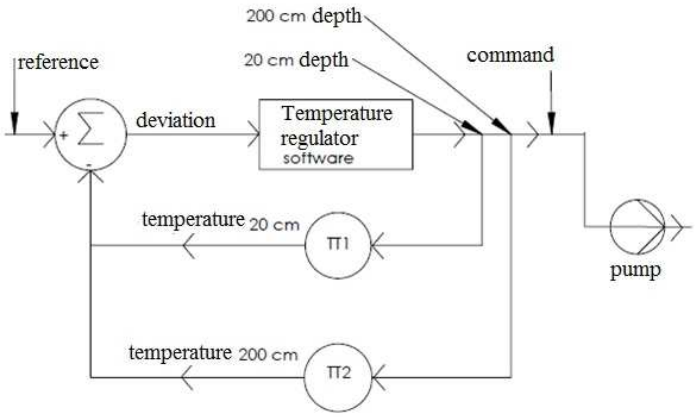

Figure 3: Scheme of the control algorithm for managing the temperature optimization installation in the plant root area

The temperature optimization installation in the area of plant roots was placed inside a solar with vertical gothic walls, 10 m wide and 30 m long, covered with double-folded foil (figure 4).

Figure 4: Solar with vertical gothic walls

The experimental researches aimed to compare the temperature regime registered in the root zone with the use of the optimization installation and that recorded on the control plot located in the immediate vicinity.

The data recorded by the programmable logic controller was exported into the Excel spreadsheet and processed, resulting the variation diagrams in time.

3. RESULTS

In the first phase, the initial working assumptions in the first paragraph were verified, according to which the soil temperature undergoes changes (thermal oscillations) to a certain depth, after which it remains constant (the isothermal layer), where the amplitude of the annual variations is canceled, and the temperature difference between the root zone and the isotherm layer reaches and even exceeds 10°C.

For this purpose, over a period of 30 days, the soil temperature in the root zone and at the depth of 2 meters was monitored by Pt100 heat-resistant temperature sensors. The results obtained are presented graphically comparatively in figure 5.

Analyzing the diagram in figure 5, it is noted that:

- the temperature evolution over time at 2 meters depth is approximately linear;
- the average temperature recorded at 2 meters depth was 11.9°C;

– the maximum temperature difference between the two levels is 12.96°C, and the minimum difference is 3.72°C.

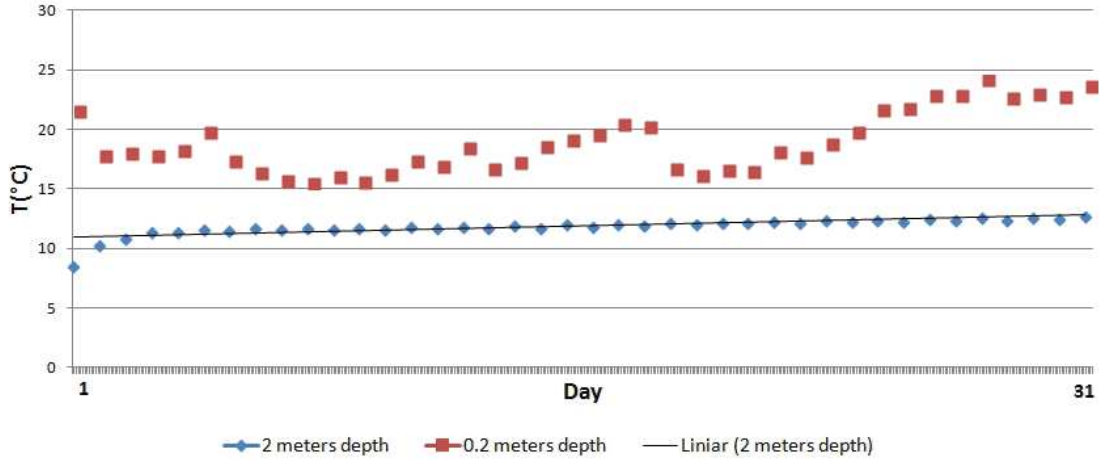

Figure 5: Comparative chart of the time variation of the temperature at the depth of 2 m and in the root zone

Thus, the initial work assumptions were validated.

Subsequently, the following working parameters were determined:

- time variation of temperature in the plant root area, both for the experimental model and for the control plot;
- the maximum temperature difference in the plant root area between the experimental model and the control plot.

The results presented in this paper were obtained using the working variant I, with the copper pipe network.

If the air temperature inside the solar increases greatly, as happens during very hot days, the temperature optimization installation in the root area keeps the temperature at an optimum level. This can be seen in the diagram in Figure 6, which compares the variation of soil temperature in the plant root area for both systems (experimental and control) as well as variation of solar air temperature.

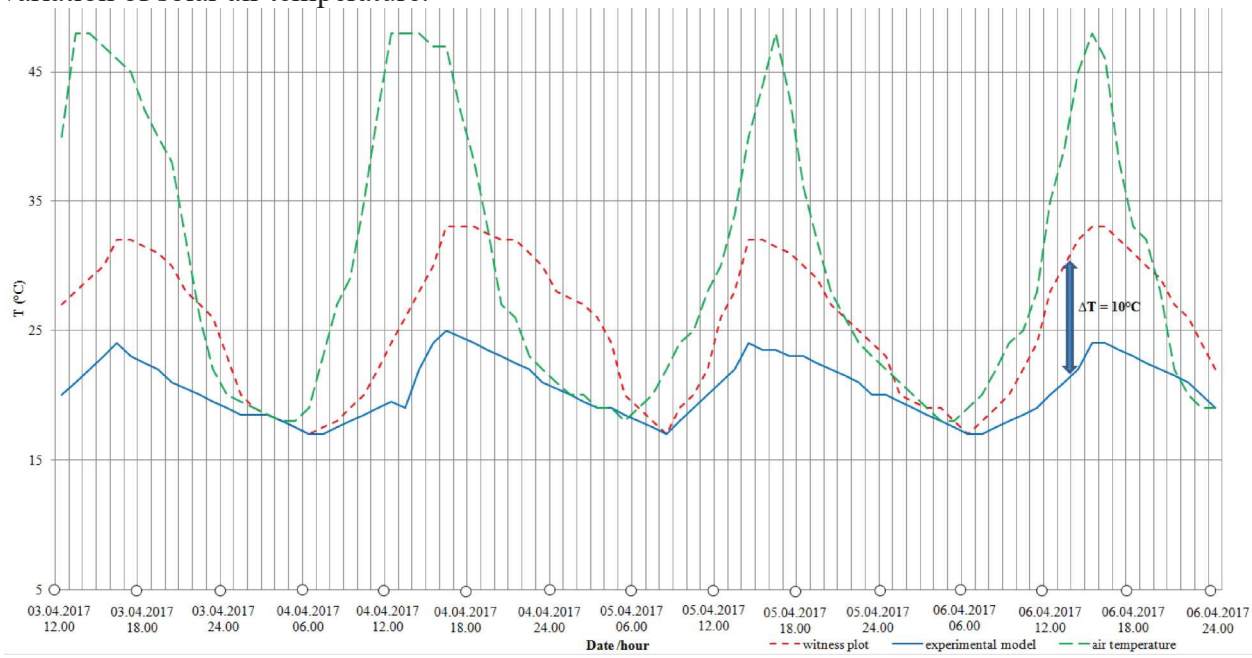

Figure 6: Comparative chart of time variation of temperature in plant root area for experimental model, control plot and air temperature, during the hot days

We can see a temperature stabilization around 25°C during the day for the experimental model, while the daylight temperature reaches 33°C, as the solar air temperature reaches 48°C. There is a significant difference of 8°C between the two systems. The maximum temperature difference between the experimental model and the control over the monitored period was 10°C. Thanks to the cooling effect of the root zone, during very hot days, soil moisture is maintained and the evaporation rate is reduced.

4. CONCLUSIONS

The experimental research presented in this paper highlights the fact that the temperature optimization installation in the root zone is able to maintain the temperature within an optimal range for plant growth.

This is particularly useful especially on hot summer days when plants in solariums are affected by heat stress.

Acknowledgement

This work was funded by the The Ministry of Research and Innovation, within the project PN 16 24 01 01 - *Intelligent system for condensation irrigation in greenhouses and solariums*, Ctr. 8N / 09.03.2016, Ad. no. 1/2017.

References

[1] Ciulache S., *Meteorologie şi Climatologie*, Editura Universitară, Bucureşti, 2002.
[2] Dissescu C.A., Luca I., Tudor M., Dăbuleanu M.L., Şoltuz V., *Fizică şi Climatologie agricolă*, Editura Didactică şi Pedagogică, Bucureşti, 1971.
[3] Dragomirescu E., Enache L., *Agrometeorologie*, Editura Didactică şi Pedagogică, Bucureşti, 1998.
[4] Hakansson I., Lipiec J., *A review of the usefulness of relative bulk density values in studies of soil structure and compaction*, Soil & Tillage Research, Incorporating Soil Technology, ELSEVIER , ian. 2000, vol. 53, no.2;
[5] Horn R., H. van den Akker J.J.,Arvidson J., *Subsoil compaction Advances in geology*, Reiskirchen, p. 258-268.
[6] Mohan Gh., *Ecologia şi protecţia mediului*, Ed. Scaiul, Bucureşti,1993.
[7] Stănescu R., Bobirica L., Orbulet O., *Remedierea solurilor contaminate*, Ed. Agir, Bucureşti, 2006.
[8] *** http://rootssat.com.

CUSTOMER SERVICE MANAGEMENT IN A BOARDING HOUSE

Petruţa Mihai [1], Oana Vlăduţ[2], Mihaela-Florentina Duţu[3],
Daniel-Ion Vlăduţ[4], Iulian-Claudiu Duţu[5]
University Politehnica of Bucharest

ABSTRACT

This paper serves as documentation for designing an application of customer service management (CSM). The goal here is to introduce the topic and give a summary of several issues that the accommodation units are generally challenged with. We will therefore present the benefits of the applications pertinent to the customer service management (CSM). Similarly, we are going to follow up on the problems of such boarding house in Sinaia and the advantages derived from the implementation of the CSM application in dealing with them and how this application actually operates.

1. INTRODUCTION

The customer service management systems generally intend to study the behavior of the customers, in order to provide them with full satisfaction. These systems collect information about the customers, organize is after certain criteria and examine them, so as to create market segments that the company is able to cover, depending on the requirements and expectations of those specific customers.

The first leverage of the CSM technology- relying system is the ability of using and building customized databases and, also, the reduction in the costs of consumables (paper, pens) that are traditionally used in abundance.[1]

A CSM system mainly improves the performance in business by increasing the satisfaction of the customers and building the customer loyalty.

Figure 1. Chain of customer satisfaction
(from Francis Buttle, 2009, p.43)

The list of the benefits in the CSM systems includes:

- sales maximization;
- costs reduction;
- acquisition and retention of the profitable customers.

[1] Splaiul Independentei nr.313, sector 6, Bucharest and mihaipetruta@yahoo.com
[2] Splaiul Independentei nr.313, sector 6, Bucharest and oanavladut2016@gmail.com
[3] Splaiul Independentei nr.313, sector 6, Bucharest and dutumihaelaflorentina@gmail.com
[4] Splaiul Independentei nr.313, sector 6, Bucharest and v_vladuta@yahoo.com
[5] Splaiul Independentei nr.313, sector 6, Bucharest and iulian_claudiu.dutu@upb.ro

2. PAPER CONTAIN

The idea of designing a CSM application in a Sinaia boarding house has come about after identifying this particular need. This establishment, almost one year old in this industry, does not have such system implemented and it is facing other issues that relate to this line of business.

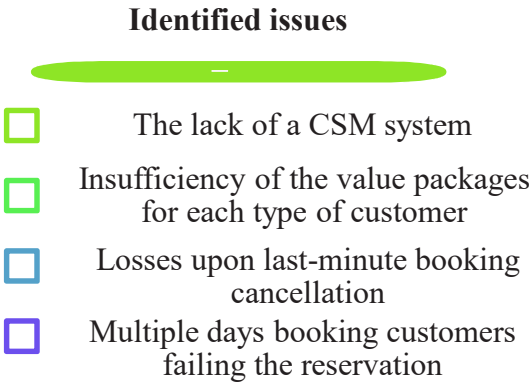

Figure 2: Issues to be identified at the "Anotimpuri' boarding house in Sinaia

The application aims to find solutions in this case. Moreover, the application will be able to generate certain reports on the up-to-date activity of the boarding house, based on the data introduced by the user, and also certain prognoses.

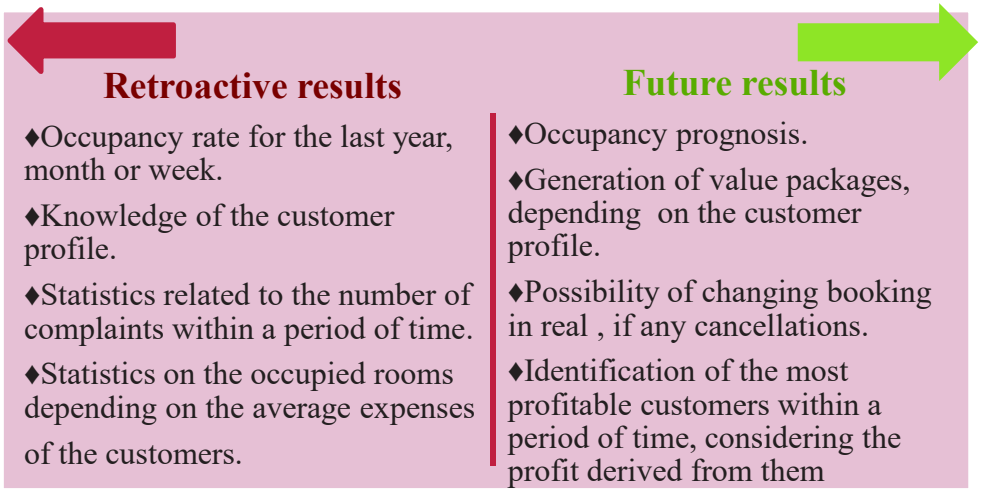

Figure 3: Results of the CSM application

The objectives of the application can be as follows:

1. *Profit increase* by attracting customers and building their loyalty - The possibility of customized value packages, depending on their preferences (for instance, seasonal packages).
2. *Reduction of costs* regarding the administration of the information in the databases, lowering the marketing costs (by sending the value packages to the customers via internet or mobile phones).
3. *Determination of the occupancy rate of the boarding house* for a certain period of time by identifying certain pertinent variables to help calculating this indicator.

The benefits of this application are listed below:

a. the existence of a database, completed with information on customers;

b. establishing better relations with customers and keeping them posted about the value packages, depending on their needs (for instance, the boarding house will have a value package for the month of June if a customer wishes to have a holiday time during that month)
c. knowledge and fulfilling the requests of the customers, thus increasing their satisfaction level;
d. solving the complaints made by the customers;
e. attracting and retaining the profitable customers, i.e. those customers who have the possibility of re-acquisition of the service and state their desire of doing so;
f. profit maximization by meeting all the above criteria..

The occupancy prognosis is probably the most important function of this application. This prognosis provides the boarding house management with information about the:

- future earnings;
- what value packages should be applied so as to increase the demand, if needed;
- seasonal employment of cleaning staff, on condition that a busy time is foreseen ahead.

The prognosis of the occupancy rate can be done for any month in the next year, depending on the capacity of the boarding house in regards to the number of rooms..

The occupancy rate will be an indicator that will encompass more variables, such as;

A. the number of rooms already booked for the month X under discussion;
B. the coefficient of the booking cancellations;
C. the occupancy rate of the boarding house in the same month of the previous year;
D. the occupancy rate of the city in the same month of the previous year;
E. the number of customers who expressed their desire to come back but they have not yet made the reservation;
F. the time when these customers take their vacation time;
G. the average time spent on vacation by such customers;
H. the predominant weather forecast for the month being examined.

We should consider that the case study is about a boarding house with 8 rooms to be booked during a month could be *240 bookings/room/night* (8 bookable rooms/night * 30 days/month).

Starting from the above, we calculate the number of reservations/room/night (R) that will be surely honored:

$$R = A * (1 - B) \quad (1)$$

where A = number of booked nights for the month X;

B = coefficient of the booking cancellations.

All these lead to the fact that the possible number of reservations/room/night ca be equal with:

$$\text{Nr.nop.}_{\text{left}} = 240 - R \quad (2)$$

$$\text{Nr.nop.}_{\text{left}} = 240 - A * (1 - B) \quad (3)$$

This number R of reservations/room/night corresponds to an initial occupancy number (Go'):

$$Go' = \frac{R}{240} \quad (4)$$

$$Go' = \frac{A*(1-B)}{240} \quad (5)$$

From now on, the other variables will join the calculations. They will be given scores with a maximum of 50 points; depending on the final score, Go'' will be calculated (intermediary occupancy rate) that will be added with Go' (the initial occupancy rate), thus resulting the forecast occupancy rate (Gop) for the boarding during the month of X being examined.

For the variables **C** and D, the scores will be given, as seen in table 1.

Table 1. Setting the C and D variable points

The occupancy rate of the pension (C) in the same month of the previous year (%)	City occupancy (D) in the same month of the previous year (%)	Scoring offered
0-10	0-10	0
10-20	10-20	1
20-30	20-30	2
30-40	30-40	3
40-50	40-50	4
50-60	50-60	5
60-70	60-70	6
70-80	70-80	7
80-90	80-90	8
90-100	90-100	9
100	100	10

The variables **E** (number of customers who expressed their desire to come back but they have not yet made the reservation), **F** (the time when these customers take their vacation time) and **G** (the average time spent on vacation by such customers) will be looked at, jointly.

The initial number of reservations/room/night that customers might make who said they might come back to the boarding house:

$$Nr._{nop} = E * G \quad (6)$$

Based on the variable F, the percentage of the customers taking their vacation in the month X out of the total number of customers who expressed their desire to come back but they have not yet made the reservation will be calculated and a value Pcl_x will be calculated and then we will have a value depending on the other 2 ($Nr._{nop}$ and Pcl_x), therefore giving scores, as in table 2.

Table 2. Determining the E, F and G variable scores

	Pcl_x	Scoring offered
If $Nr.nop \leq Nr.nop._{left}$	0-10	0
	10-20	1
	20-30	2
	30-40	3
	40-50	4
	50-60	5
	60-70	6
	70-80	7
	80-90	8
	90-100	9
	100	10
If $Nr.nop > Nr.nop._{left}$	0-10	1
	10-20	2
	20-30	4
	30-40	6
	40-50	8
	50-60	10
	60-70	12
	70-80	14
	80-90	16
	90-100	18
	100	20

In case the number of reservations/room/night that can be made by the customers who expressed their desire to come back is higher than the number of the reservations/room/night being left, scores from 1 to 20 will be given, in order to increase the occupancy rate to a realistic value.

Since the number of customers is larger than necessary and they wish to come back to the boarding house during the interval being examined, this will lead to a 100% occupancy rate, even if only a part of them will be able to be accommodated until the maximum capacity of the establishment has been reached.

The scores for the variable **H** (weather forecast) are divided into 2 categories:

1. The interval under consideration coincides with one of the following months: November, December, January, February and March.

Table 3. Determination of variable scores H - case 1

Weather Forecast (H)	***Scoring offered***
Snow	10
Sun	8
Cloudy	6
Rain	4
Blizzard	1

2. The interval under consideration coincides with one of the following months: April, May, June, July, August, September, October.

Table 4: Determination of variable scores H - case 2

Weather Forecast (H)	***Scoring offered***
Sun	10
Cloudy	7
Rain	4
Heavy rain	1

When taking into account the items above, α is calculated.

Table 5: Calculation of α

Final Score (Amount of points offered)	**α (%)**
0	0
0-5	10
5-10	20
10-15	30
15-20	40
20-25	50
25-30	60
30-35	70
35-40	80
40-45	90
45-50	100

After the application has generated all the results, the forecast occupancy rate (Gop) is obtained:

$$Go'' = \alpha * (1 - Go') \quad (7)$$

$$Gop = Go' + Go''(\%) \quad (8)$$

When analyzing the activity at the boarding house, it can be noticed to have had good results in less than one year since its opening (the anniversary is for this June), as follows:

Table 6: Statistics Pension "Anotimpuri" Sinaia

Month	Number of tourists	Overnight stays	Number of bookings/ room/night	Income	Costs
June 2016	11	11	5	1480	2022.45
July 2016	115	190	93	5200	1557.32
August 2016	136	323	154	11024	2837.93
September 2016	79	144	71	6834	2544.12
October 2016	96	188	94	7712	2233.82
November 2016	67	134	65	8184	1801.24
December 2016	54	134	67	9830	2318.94
January 2017	49	96	41	6207	2847.88
February 2017	97	215	105	7461	3069.88
March 2017	89	145	68	6194	3423.95
April 2017 (up to 20 April 2017)	105	229	112	9824	2247.77
Total	*898*	*1809*	*875*	*79950*	*26905.3*

3. CONCLUSIONS

In terms of the future actions of the boarding house, this establishment is on its way of being given the 3-star distinction.

Similarly, there is an ongoing process for the improvement of the services provided, thanks to being receptive to the suggestions of the customers on both the online sites where the boarding house is advertised (booking.com, turistinfo.ro) and also via the surveys being handed at its location.

Another potential action is to implement this CSM application so as to solve all the issues, since there is an estimation of profit increase as a result of the generation of value packages, depending on the foreseen occupancy rate.

References

[1] Buttle F., *Customer Relationship Management - Concepts and Technologies*, Ed. Butterworth-Heinemann, 2009.

[2] http://www.money.ro/care-sunt-principalele-probleme-ale-industriei-turistice-din-romania_1222440.html

[3] http://managementstudyguide.com/importance-of-crm.html

[4] https://statistici.insse.ro/shop

CORRELATION BETWEEN THE IMPULSE AND PERFORMANCE OF THE EMPLOYEES WITHIN THE "APELE ROMANE" NATIONAL ADMINISTRATION

Petruţa Mihai [1], Oana Vlăduţ[2], Mihaela-Florentina Duţu[3],
Daniel-Ion Vlăduţ[4], Iulian-Claudiu Duţu[5]
University Politehnica of Bucharest

ABSTRACT

The present paper features a case study conducted within the "Apele Romane" National Administration concerning the correlation between the impulse and the performance of the employees. One of the goals of this establishment is to achieve a pleasant work environment, since the company development relies on the staff inner impulse.

In order to come to the Performance Management System, we have implemented the following stages: increasing the expectations towards the performance between the manager and the employees and the monitoring of the performance evolution. This process of performance monitoring needs to be approached from two angles, such as the performance of the team members, as well as the performance of the entire department. Similarly, the monitoring has been done by including five basic fields: results, efficiency, progress, methods and procedures and practices.

1. INTRODUCTION

The impulse is an intricate phenomenon, close to a trigger, by means of the strategies implemented and by how it is really perceived. ***Motivation is thus seen as the impulse area***, where the latter is the practice for the former, since an efficient impulse activates the motivation.[3]

The impulse starts with the highlight of the demands and needs, where they are a primary source of the actions, since any deficiency leads to a need. The demands/needs are considered as physiological or psychological states, hypothetical constructions that can be deduced from the behaviors manifested by a person.

This is the reason why the demands represent conditions of a biological or psychological nature, whose satisfaction is aimed at maintaining a balance. The impulse starts from the lack coming from the non-satisfaction of a need and ends with the effort made to satisfy that need, via a motivated and focused behavior towards the desired goal.

2. PAPER CONTAIN

The first stage in the Performance Management System is to increase the expectations towards the performance along with the employee. The agreement between the manager and employees in terms of their future duties is fundamental for an efficient management.

This agreement needs to include the description of the duties to be performed, of the results to be reached and the priorities in scheduling the work timetable. Such an agreement becomes the ground of the performance management and provides the employees with the direct motivation and the direction they should adopt in doing their duties. Similarly, this gives a means of control and a basis of evaluation of the employees and their efficiency.

[1] Splaiul Independentei nr.313, sector 6, Bucharest and mihaipetruta@yahoo.com
[2] Splaiul Independentei nr.313, sector 6, Bucharest and oanavladut2016@gmail.com
[3] Splaiul Independentei nr.313, sector 6, Bucharest and dutumihaelaflorentina@gmail.com
[4] Splaiul Independentei nr.313, sector 6, Bucharest and v_vladuta@yahoo.com
[5] Splaiul Independentei nr.313, sector 6, Bucharest and iulian.dutu23@gmail.com

In a nutshell, the increasing of the expectations towards the performance is mainly an issue pertinent to definition and clarification.

The principal components of the performance standards can be: the title (to identify the employee who will be subjected to those standards), the field of results, the performance indicators and the standards set up for each of the indicators.

The performance requirements cover a wide range of duties and responsibilities assigned to an employee. These employees need to get involved in the increase of the performance expectations that are work implemented for two reasons:

1. The employees hold valuable information that can contribute to building the corresponding expectations.
2. The employees will have an easier time to accept the imposed conditions, since they have helped with their creation.

The monitoring of the performance evolution is the second stage in the Performance Management System. This process of monitoring is usually overlooked by the managers over other issues deeming more important; the bottom line is that the lack of a systematic method to monitor the evolution is less likely to lead to the desired outcome.

This process of performance monitoring needs to be approached from two angles, such as the performance of the team members, as well as the performance of the entire department. Similarly, the monitoring has been done by including five basic fields: results, efficiency, progress, methods and procedures and practices.

The monitoring of the results will contemplate the following elements – the quantity of results, the quality of results, the compliance with the deadlines, the profit and costs. The performance monitoring can be done via the personal inspection, contact with the customers, bookkeeping, midway progress verifications, audit.

To be functional and viable in a competitive world, the companies need to motivate their people into doing the ensuing actions:

- to join the company and keep working for it;
- to fulfill the duties in their job descriptions;
- to adopt a creative, spontaneous and innovative behavior.

The “Apele Romane” National Administration is a public institution of a national interest, with legal personality that operates on a basis of administration and economic autonomy.

This Administration is a single operator for the natural or upgraded surface water resources, irrespective of the acquisition title of the development holder and for the underground water resources, regardless of their nature and related facilities, to which purpose it will allot the right of use of the water resources with their natural potential, within the law, save for the ones explicitly stated in the current specific regulations.

The resources are elements of the organization and they are featured as tangible or intangible. To examine the different categories of resources, their classification upon content (financial, human, physical, etc) is frequently used, along with the manner of their functional use within the company (production, marketing, personnel etc).

The conclusion from the value chain analysis VRIO was that the human resource holds a crucial role in the institution is a true pillar.

The company in this case study is well known at the national level, which means that has a large number of employees and is in need for a good management of its human resources. Hence, more motivational theories are implemented so that the personnel are able to fulfill its duties in a convenient manner.

An increasing importance is assigned to the need for comfort and satisfaction of the employee at the work place, which has turned into a trend for the large companies. One of the

objectives of the “Apele Romane" National Administration is to achieve a pleasant work environment, since the company development relies on the staff inner impulse.

According to Maslow Pyramid of Needs, the employees wish to have their needs taken care of, by fulfilling their duties with no limitation and with a corresponding effort for that purpose. It is an obvious fact that this institution favors the participatory, hands-on style, and the research shows that the outcome is positive, based on trust and cooperation.

When using the 5-managerial style grill, this company is associated with a balanced style, i.e. a concern for both people and economic activity. For the employees, the management organizes holidays, teambuilding and economic incentives for Christmas and Easter. The style of this Administration is, hence, close to the team-based model.

To design an efficient management style, the managers have to take into account the nature of the activity, of the group, the position of the leader and his/her qualities, the organizational norms, etc.

A survey has been sent to circa 40 employees, which aim to forefront the motivational factors acting upon the behavior of the employees. The survey includes 16 items of different types:

- close questions with ranked answers, which request the surveyed people to order their answers as suitable to their preferences;
- close questions with multiple choice, which allow the respondent to select the option that defines him best.

For the validity of the sample, the following criteria had to be met:

- the respondents come from all the existent age groups;
- the respondents are both male and female;
- the respondents come from different age categories.

The first part of the survey intended to identify the needs of each employee and how to satisfy them, while considering the below:

- balanced relations with the co-workers;
- working conditions;
- need for an intellectual development;
- the need for a superior responsibility;
- the job stability;
- the need for having a status and recognition from the others.

According to the analysis of the survey, we have the percentage distribution of the motivational factors and the conclusion is that they are crucial for the employees and that these people are satisfied by the company at an average level. While the satisfaction of these needs is essential for the subjects, the activity conducted for this purpose is satisfactory.

The highest percentage is held by the wages (21%), followed by the working conditions (18%) and the job stability (17%).

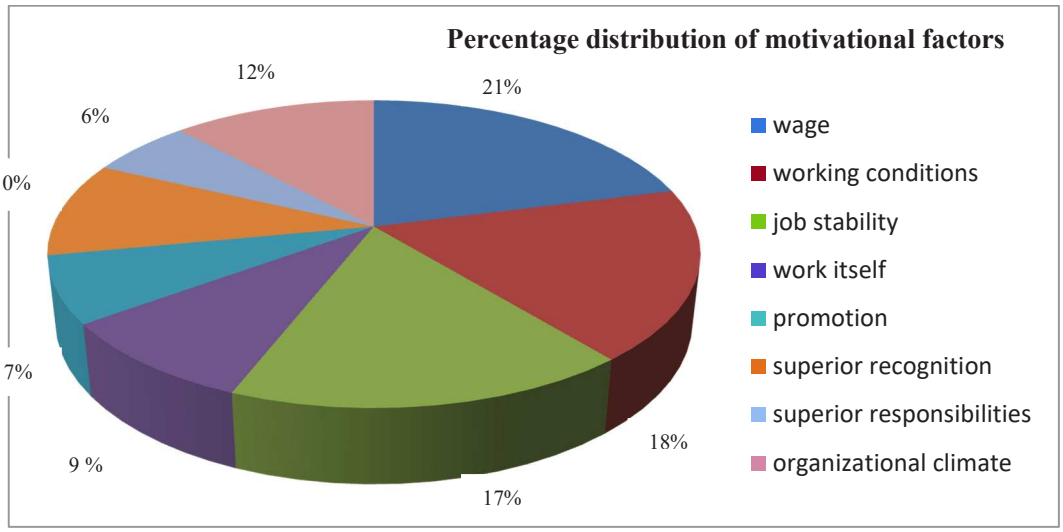

In line with Maslow theory upon the needs for assurance, labor security and safety, job stability, these must be satisfied before the social needs of esteem and personal fulfillment. As ERG Alderfer's theory says, the needs related to existence are the ones that provide basic requirements of the material life and the wages, working conditions and the job stability are all pointing to these needs.

For this company, these results confirm that the employees are more interested in financial rewards, relations with the co-workers and opportunities for promotion. This is why the company management needs to pay a higher attention to the needs of the employees related to the wages and the organizational climate, in order to have them concerned about the quality standards and a more lucrative labor. This outcome can be also explained by the fact that most respondents conduct a routine activity that does not require superior managerial abilities and creativity.

A survey for 40 people has therefore been suggested in this context. According to the analysis of the survey, we have the percentage distribution of the motivational factors and the conclusion is that they are crucial for the employees and that these people are satisfied by the company at an average level.

The answers to the survey also reveal that the employees are satisfied with the company management, the working conditions and with the manner in which their leaders motivate them for favorable results.

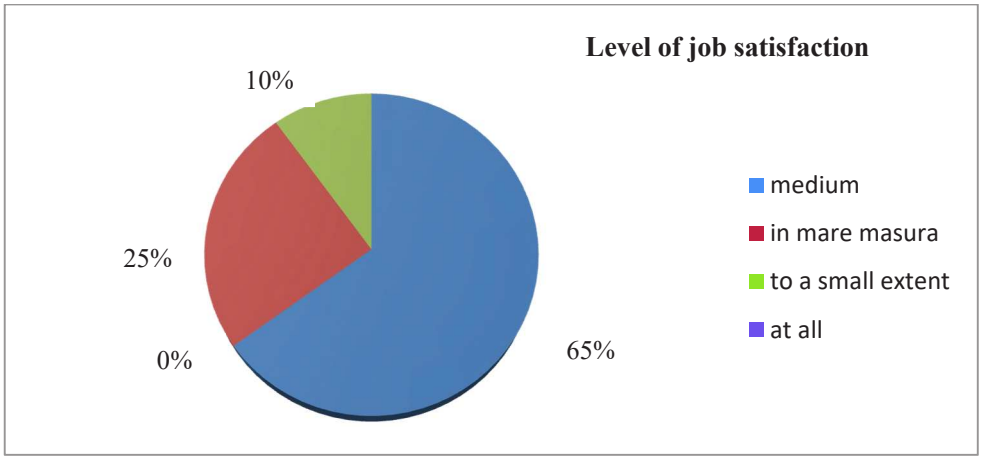

Another reason for this survey was to find out about the factors generating feelings of dissatisfaction, where the employees had the possibility to select from items such as wages, working conditions, vacation leaves, and the managerial behavior.

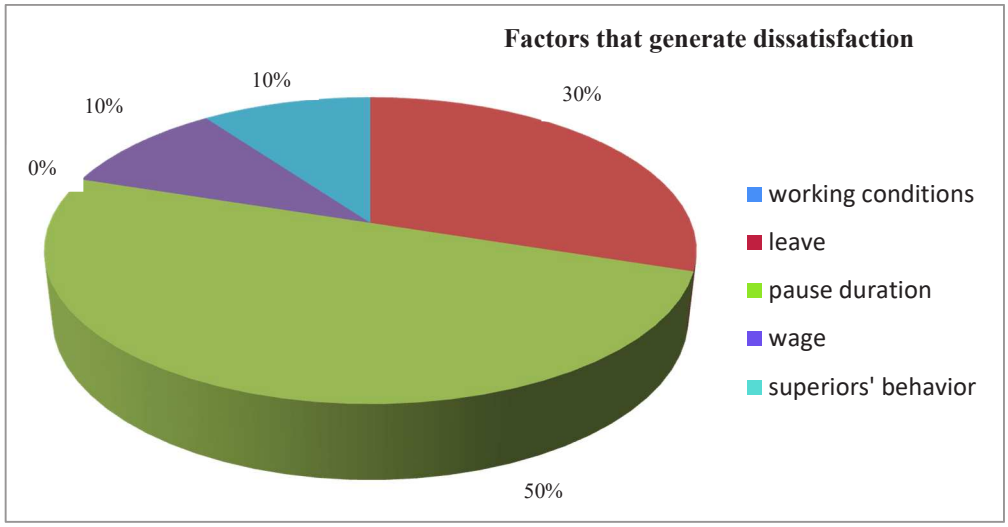

The results state that half of the respondents are not content with the duration of the breaks at their employment place. For 8 to 9 nine hours of work, they have a 20-minute break, a 10-minute lunch break and two more 5-minute breaks.

With this information available, an explanation can be found for the above complaint. Since most of the employees work in a sitting position, the company management must consider their need for moving during breaks.

There is no preplanned schedule for the vacation leaves, as the employees are able to take them in dependence on the work demands and the ongoing projects.

The same interval can vary from one year to another and, hence, the employees can be taken aback by the busy or less busy times at the work place.

The survey also targets the effects that these factors have upon the employees and the answer options are: an increased stress level, frustration, intent to quit, intent to call in sick, lower involvement in work. The results are visible in the below graph:

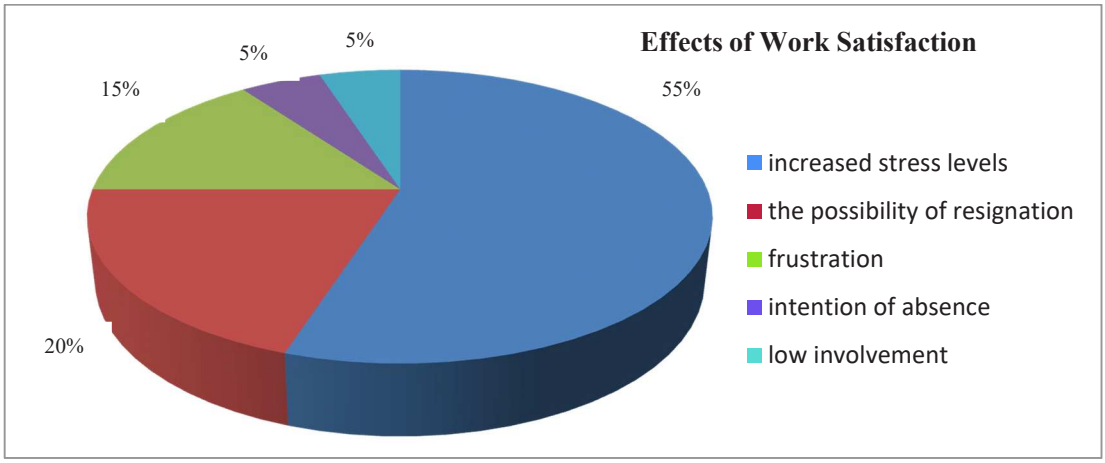

An examination of this graph says that 55% of the respondents feel the in satisfaction at work due to a surging level of stress, followed by 20% with the intent of quitting.

Since this research has proven that most employees are happy with the work environment, it would be easier to pinpoint the ones that are slightly dissatisfied through an

analysis of the behavior and performance or, better yet, via another similar survey so as their state of mind does not turn contagious for the others. In other words, the management should consider hiring a person to conduct activities pertinent to the Human Resources department, along with the other employees, to identify their needs.

3. CONCLUSIONS

Following the quantity evaluation of the results and data interpretation, several conclusions can be made:

- the institution meets the needs of its employees in a satisfactory manner, not as much as desired, while 10% do not perceive it at all.
- the working conditions are satisfactory.
- the need of having a status and recognition from other others is acceptable.
- the main motivational factor is the wages.
- there is a possibility that a large number of employees be unaware of all the benefits of the institution, which is the result of a defective communication between the employees and the company system.

Several recommendations are derived here from to benefit the company management, such as:

- designing a motivational politics with long-term objectives for the employees and the organization.
- taking into account the complex series of needs that people have in reference to the work place.
- accepting the fact that the contractual relation with the employees requires involvement and commitment from both parties.

It would be extremely useful to adopt a democratic and participatory management style, where the employees should be given the opportunity to have an active part in the management process and communicate to their managers their ideas for stimulating the innovation and creativity at the work place.

References

[1] Zlate M., *Psihologia muncii - relatii interumane*, “Didactica si Pedagogica” Publishng,Bucharest, 2011

[2] Stoica-Constantin A., Constantin T.. *Managementul resurselor umane*, “Institutul European” Publishng, Iasi, 2015

[3] Druta F., *Motivatia economica*, Economica Publishing, Bucharest, 2009

[4] Zorletan T., Burdus E., Caprarescu G., *Managementul organizatiei*, Holding Reporter Publishing, Bucharest, 2016

[5] www.anar.ro

COLORADO BEETLE BIOLOGICAL CONTROL

PhD. stud. eng Mircea C.[1], PhD. eng Covaliu C.I. [2], PhD. stud. eng Zaica A.[1], eng. Anghetet A.[1], eng. Turcan M.O.[1], PhD. stud. eng Sorica E.[1], PhD. eng Caba I.L. [1]
[1]INMA
[2] University Politehnica of Bucharest

ABSTRACT

The Colorado beetle *(Leptinotarsa decemlineata)* is an insect with origin in North America, described for the first time in 1824. It feeds on plant tissue, making holes and grazing leaves surface. Colorado beetle biological control is made by repeated spraying of chilli pepper infusion, concentrated solution of onion peels or by sowing plants such as chrysanthemum, tagetes, coriander, marigold, etc. in the damaged crop.

1. INTRODUCTION

The insect world depends to a large extent on the nature of the flora that provides them with food, shelter and safety. If we consider that some insects are harmful, it implies that others are useful. According to this idea, insect pests would be extra in nature, which would involve neutralizing them. But the truth is completely different. Absolutely everything that exists in nature is not extra. There is a trophic chain that makes the ecosystem we are all part of to function the best way possible. Most of the time, when we talk about harmful insects and useful insects, we take into account only the "human economy". Taking into account the "nature economy," all insects on Earth are useful. Nature is organized in such a way that everything depends on everything.

In Romania, the "ae" logo, fig.1, is used for certification-identification purposes and is applied to the labels and packaging of organic food products.

National logo for certified organic products

National logo for promoting organic products

EU organic farming logo

Figure 1: Examples of “ae” logos [9].

Profitable potato production continues to be threatened by Colorado potato beetle, *Leptinotarsa decemlineata*, the most destructive insect defoliator of potato in the world. Having developed resistance to virtually all insecticides used against it, the beetle is considered one of

[1]INMA Bucharest, +40766420952, costinmircea@yahoo.com

the most severe agricultural pests in terms of insecticide resistance. Unfortunately, limited commercial utility of biological, cultural and biotechnological control options means that growers remain heavily reliant on insecticides [2].

This insect has a diverse and flexible life history that is well-suited to a variety of environmental conditions. It is also extremely adaptable to adverse conditions, including those created by humans in an attempt to control the pest. The beetles integrate diapause, dispersal, feeding, and reproduction into an ecological "bet-hedging" strategy, distributing their offspring in both space (within and between host habitats) and time (within and between seasons). As a result, they are a very challenging pest to manage [1].

Originally from the North American continent, the high plateaus of Colorado, this beetle was first reported in Europe in 1876, in Germany, with the first potato imports. It was later reported in 1922 in France and in 1952 in Romania in Sapanta, in Maramures County. In our country, its development area extends everywhere, especially where spontaneous solanaceous species emerge.

Leptinotarsa decemlineata (Say.) (fig.1, 2) has 2-3 generations per year. It spends the winter as a larva in the soil at 10-90 cm deep. In spring, they transform into a pupa, and adults emerge from the end of March to the end of May. Then, there is a feeding period, when sexual maturity occurs and afterwards takes place the mating. The eggs are deposited gradually on the lower part of the leaves, in groups of 10-100. A female can deposit up to 2500-3000 eggs. Incubation lasts 4-5 days and larval development 15-30 days, depending on temperature. Pupa transformation takes place in the soil and lasts for 12-20 days. Adults emerge in early August. In the steppe areas, a third generation may emerge [5]

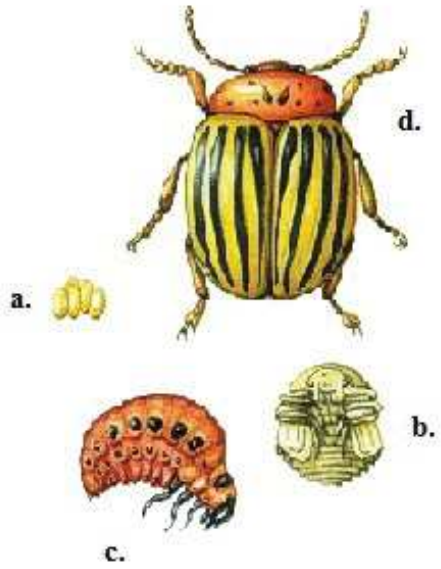

Fig.2 – *Leptinotarsa decemlineata* (Say.) a – eggs; b – nymph; c – larvae; d – adult [6]

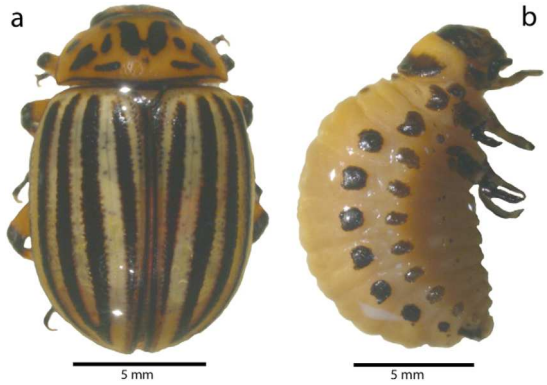

Fig.3 – General body shape of Colorado potato beetle (a – adult, b – larvae) [4]

Adults eat leaves, producing irregular perforations on the surface of the limb, and eventually turning the leaves into skeletons. An adult can consume, in only two or three days, the entire leaf surface of an eggplant, immediately after crop establishment. Young larvae perforate the leaves in the form of small holes, and as they age, they eat leaves completely, sometimes even the shoots. In the course of evolution, a single larva can consume a leaf tissue area equivalent to 30-40 cm² [7].

2. METHODOLOGY

According to their purpose, the methods used to combat pests that act on cultivated plants are classified as preventive methods and curative methods.

Preventive, prophylactic or indirect methods apply either to prevent or to stop the action of a pest attack.

Curative methods (neutralizing) or direct methods are designed to directly combat the pest in a particular attack phase.

According to the means used, the preventive and curative methods of pest control are grouped into the following categories: agrophytotechnical methods, phytosanitary quarantine measures, use of resistant plant varieties and hybrids, physical methods, mechanical methods, biological methods and chemical methods.

Colorado beetle attacks especially plants of the Solanaceae family (Figures 4, 5, 6). It is associated with the potato storages and crop places where it acts as a pest, causing important damage.

Not only crop plants are attacked by Colorado beetle. They attack some spontaneous plants such as jimsonweed, black nightshade, laurel, henbane, belladonna, etc. Other plant species like salad, garden orache, lucerne, etc. can also be attacked by chance. Tomatoes (*Solanum lycopersicum*) are not only attacked by hibernating adults but also by larvae, nevertheless, in very few cases they are found on bushes. Also, pepper is very little attacked by this pest. Numerous eggs have been found on the weeds in potato crops, namely: foxtail millet (*Setaria sp*), wheatgrass (*Agropyrum sp*), field bindweed (*Convolvurus arvensis*) and Johnson grass (Sorghum Helapense), but larvae have never been found on these plants [17].

Fig.4 – Colorado potato beetle destroying a crop [3]

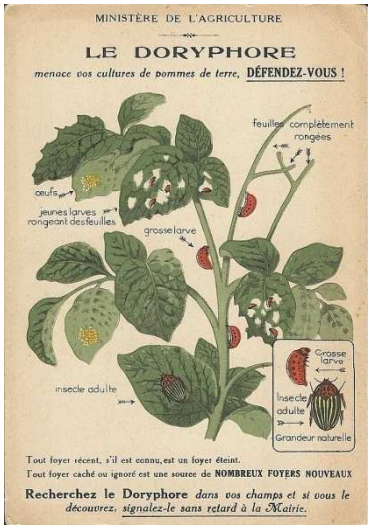

Fig.5 – "Ministry of Agriculture. Potato beetle threatens crops, Fight!". Old postcards [12]

Fig.6 – Potato plant defoliated by beetle larvae [12]

Over the years, researchers have conducted numerous studies on the predators, parasites and pathogens that reduce the population of this pest, with a favourable impact on the development of potato culture. These natural enemies of Colorado beetle are shown in Table 1.

Table 1: Main natural enemies of the Colorado beetle [11]

Type	Species	Classification	Stage attack	Geographical area
Parasitoid	*Chrysomelobia labidomerae*	mite	adults	U.S., Mexico
	Edovum puttleri	hymenoptera	eggs	Colombia, Mexico, U.S.
	Anaphes flavipes	hymenoptera	eggs	U.S.
	Myiopharus aberrans	diptera	adults	U.S.
	Myiopharus doryphorae	diptera	larvae	Canada, U.S.
	Meigenia mutabilis	diptera	larvae	Russia
	Megaselia rufipes	diptera	adults, nymphs	Germany
	Heterorhabditis bacteriophora	nematode	adults	cosmopolitan
	Heterorhabditis heliothidis	nematode	adults	cosmopolitan
Predators	*Lebia grandis* (fig.6)	coleoptera	eggs, larvae, nymphs	U.S.
	Hippodamia convergens (fig.7)	coleoptera	eggs, larvae	U.S., Mexico
	Euthyrhynchus floridanus	hemiptera	larvae	U.S.
	Oplomus dichrous	hemiptera	eggs, larvae	Mexico
	Perillus bioculatus (fig.8)	hemiptera	adults, eggs, larvae	Canada, U.S., Mexico
	Podisus maculiventris (fig.9)	hemiptera	larvae	U.S.
	Pselliopus cinctus	hemiptera	larvae	U.S.
	Sinea diadema	hemiptera	larvae	U.S.
	Stiretrus anchorago	hemiptera	larvae	Mexico
Pathogens	*Bacillus thuringiensis subsp. tenebrionis*	bacterium	larvae	U.S., Canada, Europe
	Photorhabdus luminescens	bacterium	adults, larvae	cosmopolitan
	Spiroplasma	bacterium	adults, larvae	North America, Europe
	Beauveria bassiana (fig.10)	ascomycete	adults, larvae	U.S.

A method to attract insects feeding on Colorado beetle larvae is to put, between the potato rows, plants that attract these insects such as tansy, marigold, caraway, garlic, costmary, beet, horseradish, coriander, catnip etc. Tagetes stops the invasion of nematodes and other pests.

Fig.7 - *Lebia grandis* [16]

Fig.8 - *Hippodamia convergens* [14]

Fig.9 – *Perillus bioculatus F.* [10]

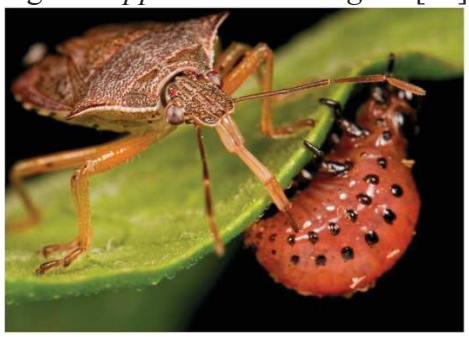

Fig.10 - *Podisus maculiventris* [15]

Fig.11 – *Beauveria bassian* [13]

Another ecological method to combat Colorado beetle is spraying a solution obtained by infusing chili peppers. To prepare this solution, we need 10-20 pieces of chili pepper, we add boiling water and leave to infuse for 12-24 hours. Then dilute with water, add soap (40 g to 10 litres) or liquid soap to adhere better to the leaves. When the plant has grown enough (about 10-15 cm), we powder poultry manure on pre-moistened plants, but even better, concentrated solution of onion skins. This procedure should be done approximately 3-4 times a summer [8].

Another non-toxic method to prevent Colorado beetles from attacking crops is to sprinkle diatomaceous earth on the soil around the plants and on the leaves. This procedure must be repeated after each rain.

In Teleorman County, within a private farm, chrysanthemums were planted among the potato rows to avoid potato crop chemicalization in order to fight against Colorado beetle.

On the experimental plot four potato rows were planted at regular distances, next to them being planted a single row of chrysanthemums (a mixture of varieties and species), at a distance of 35 cm between plants on the row, with the seedling material obtained by separating the bush. For the potato crop, Desire and Ostara varieties have been selected, which are usually susceptible to Colorado beetle attack.

Although during vegetation the potato plants didn't receive any treatment against the pests, no beetle was observed in the crop.

To verify the correctness of the conclusions reached after the first year of testing, the experiment was repeated in the same place. Meanwhile, chrysanthemum bush grew more

vigorous. The probability of a possible Colorado beetle attack was greater as the potato crop rotation did not take place. Even this time, the Colorado beetle adults did not lay eggs on chrysanthemum-protected plants. It is to be mentioned that outside the experiment area, the Colorado beetle was present even in the crops treated with chemicals [18].

Researchers have shown that pyrethrin (the chrysanthemum insecticide) removes pests that are dangerous for potato cultivation, such as the Colorado beetle. Pyrethrin-based synthesis insecticides have been created for this purpose but they do not meet the requirements of organic farming. Cultivation of chrysanthemums on rows intercalated in potato crops in rotation proved to be an effective solution to fight this pest.

3. CONCLUSIONS

Organic farming is the most important source of healthy food for the individual.

To achieve this goal, researchers have tried to create efficient farming technologies based on environment-friendly norms.

In the case of Colorado beetle, the use of mushrooms, insects and certain plants containing repellents can be a good environmental practice in combating it.

References

[1] A. Alyokhin, M. Udalov, G. Benkovskaya, *Chapter 2 – The Colorado Potato Beetle*, Insect Pests of Potato 2013, Pages 11–29

[2] G.C. Cutler, C.D. Scott-Dupree, J.H. Tolman, C.R. Harris, *Field efficacy of novaluron for control of Colorado potato beetle (Coleoptera: Chrysomelidae) on potato*, Crop Protection Volume 26, Issue 5, May 2007, Pages 760–767

[3] D. Denkenberger, J. M. Pearce - *Chapter 2 – Worldwide Crop Death: The Five Crop-Killing Scenarios* - Feeding Everyone No Matter What Managing Food Security After Global Catastrophe 2015, Pages 5–16

[4] M. Kaya, T. Baran, S. Erdoğan, A. Mente^{o}, M.A. Özüsağlam, Y. S. Çakmak - *Physicochemical comparison of chitin and chitosan obtained from larvae and adult Colorado potato beetle (Leptinotarsa decemlineata)*, Materials Science and Engineering C 45 (2014) 72–81

[5] M. Mustata, I Andriescu, – *Biology of animal pests*, Iasi: Junimea 2006

[6] http://0219662.ro/daunatori/gandaci/gandacul-de-colorado-85

[7] http://www.botanistii.ro/blog/insecte-daunatoare-plante-gandacul-de-colorado/

[8] http://agrointel.ro/35629/solutii-bio-pentru-combaterea-gandacului-de-colorado/

[9]https://www.paradisverde.ro/daunator/cand-e-momentul-optim-pentru-tratamente-chimice-impotriva-gandacului-de-colorado

[10] http://macroid.ru/

[11] https://fr.wikipedia.org/wiki/Doryphore

[12] http://www.wikiwand.com/fr/Doryphore

[13] http://www.ipmsupportethiopia.org/index.php/articles/latest-articles/biological/micro/9-beauveria

[14] https://www.natgeocreative.com/photography/1153264

[15] https://figshare.com/

[16] http://fineartamerica.com/

[17] https://ro.wikipedia.org/wiki/G%C3%A2ndac_de_Colorado

[18] http://www.agriculturae.ro/index.php/agricultura-ecologica/tehnologii-ecologice/271-combatere-ecologica-a-gandacului-de-colorado.html

[19] http://www.onpterbv.ro/index.php?option=com_content&view=article&id=9&Ite

INFLUENCE OF KNEADING RATE ON KINETICS OF WHEAT DOUGH STRUCTURE

M.G. Munteanu[1], Gh. Voicu[1], M. Dincă[1], G.A. Constantin[1], M. E. Stefan[1], B.Șt. Zăbavă[1]
[1] Politehnica University of Bucharest, Faculty of Biotechnical Systems Engineering, Romania

ABSTRACT

In recent years, the manufacturing processes of products based on wheat cereals, have been in progress regarding the endowment with performant machines, equipment and installations. The quality of the bakery products can be influenced by a number of parameters such as: the physical characteristics of the bakery flour, the production process, the kneading rate, the kneading and the baking time.

This paper presents the influence of the kneading rate on the structure of the wheat flour dough through the results obtained during of some experimental researches.

1. INTRODUCTION

Bread is a basic food, prepared by baking dough containig flour and water. It is popular all over the world and is one of the oldest food in the world. One of the most important operations in the bread making process is the kneading of the dough. The main purpose of the kneading operation is to obtain a homogeneous mixture of the raw and auxiliary materials and at the same time to obtain a dough with structure and vasco-elastic properties. Moreover, during kneading, an amount of air is included in the dough, which is very important for the rheological properties of the dough and for the quality of the final product [6].

Today, the study of rheological properties, with their implications in the bakery process, has gained a great deal. With the help of the methods and equipment used, researches are being carried out to establish the essential principles that contribute to the mechanical behavior of the dough, in correlation with the physical structure of the dough, with the molecular structure of the continuous protein phase in the dough and with the chemical reactions of the functional groups [2].

The rheological attributes of the dough influence the volume and shape of the bread, the elasticity of the core and shell, and also the maintenance of freshness. When the dough has elasticity and extensibility large enough, the resulting bread is loose, with developed volume and core with thin wall pores. If the dough is too strong (tenacious), the bread is undeveloped with a dense core, and when the dough is excessively extensible, the bread flattens, has low volume and coarse porosity [5].

2. METHODOLOGY

Christoph Verheyen and al. [1] studied the impact of different kneading speed on kinetics of wheat dough structure, and in order to show the effects of different kneading velocities on dough development, the power input for 80 rpm, 320 rpm, as well as for the standard speed of 200 rpm was plotted against the kneading time (figure 1).

The kneading time (20 min), the temperature of ingredients (20 °C), the water addition (60 %) and dough mass (5,000 g) were kept at constant levels.

It could be proven that with decreasing kneading speed the time required to reach the kneading optimum increases.

[1]University Politehnica of Bucharest, Faculty of Biotechnical Systems Engineering, phone no: 0767236522, email: munteanumaya@yahoo.com

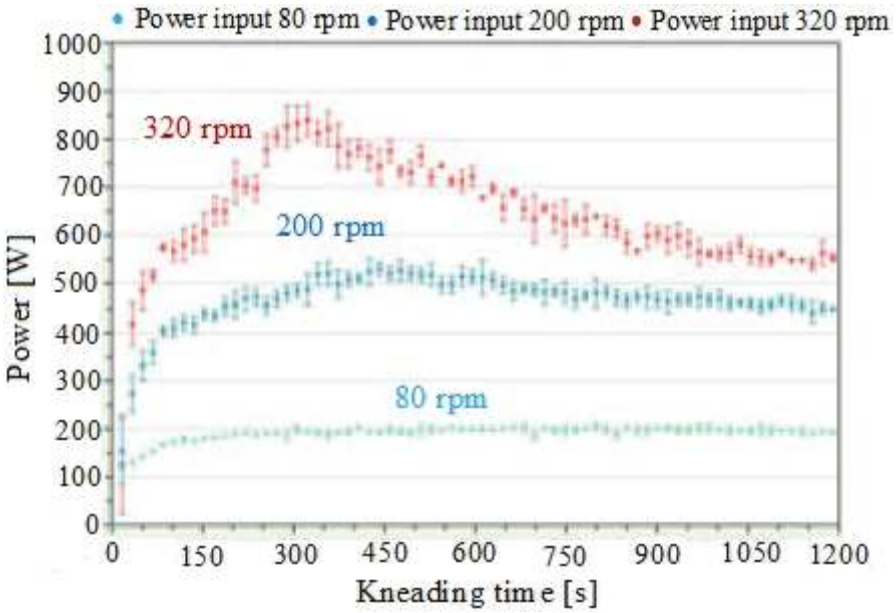

Figure1: Power curve of a 20 min kneading process performed with different velocities [1]

Despite the energy input being almost the same, the dough temperature varies from 30.3 °C at 80 rpm, 31.3 °C at 200 rpm to 32.3 °C at 320 rpm. There might be a change of apparent viscosities responsible for elevating the temperature.

Despite an almost constant volume of the bread loaf, the bread crumb becomes significantly softer with higher kneading velocities. A possible explanation could be a finer and more uniform structure due to higher shear forces and a related elongation of gluten strands. Microscopic images made with confocal laser scanning microscopy, presented in the following illustration this hypothesis (figura 2) [1].

Wheat dough produced with slowkneading velocities features a coarser protein structure with wide gluten filaments, while increasing velocities cause a much thinner and disrupted network [1].

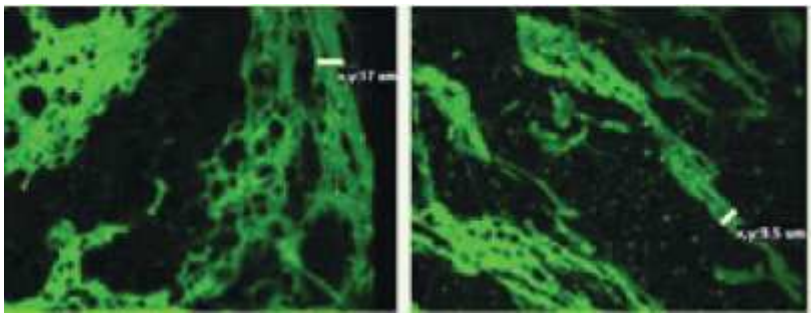
Figure 2: Slow –kneading speed High – kneading speed [1]

Another study made by G.G. Codina and S. Mironeasa [3] showed that the mixing rate has a great influence on the dough microstructure. The wheat flour dough network has been studied using light microscopy (LM), atomic force microscopy (AFM), scanning electron microscopy (SEM), transmission electron microscopy (TEM), confocal scanning laser microscopy (CSLM) and epifluorescence light microscopy (EFLM) [3].

The research was carried out on 10 samples of different commercial wheat flour. The chemical composition of the flour was determined according to the Romanian or international standard methods: moisture (ICC Standard Method No. 110/1, 1982), protein content (ICC Standard Method No. 202), wet gluten content (ICC Standard Method No. 106/1, 1984), gluten

deformation index (SR Romanian Standard Method No. 90, 2007), ash content (ICC Standard Method No. 104/1, 1990) and falling number index (ICC Standard Method No. 107/1, 1995) [3].

The effect of mixing speed on the EFLM analysis of dough mixed for 3 and 5 min at different speeds is shown figure 3. It can clearly seen from the obtained images how the amount of the protein matrix increased with energy addition and therefore with mixing time and speed. At low time and rate of mixing, the proteins are swelling and just begin to become interconnected. At lower mixing are stretched into a continuous network and surround most of the starch granules. Images show that the mixing of wheat flour dough at 80 (Figs. 3a and b) and 160 rpm (Fig. 3c) leads to the formation of distinct areas of starch granules which are the most visible, demonstrating structural inhomogeneity of the dough [10].

Mixing dough at higher speed, 250 rpm, led to the formation of a very finely homogenous gluten structure with starch granules highly embedded in the protein matrix. The formed gluten fibres completely surrounded starch particles and other dough components, having extremely fine gluten strands and high resistance to breakage [3].

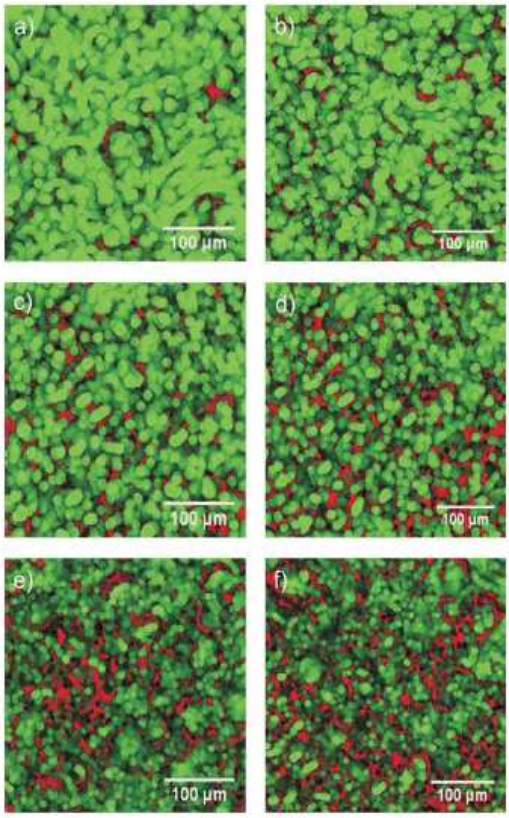

Figure 3: Images of dough microstructure taken by EFLM: a) at 80 rpm for 3 min (5.01 (W·h)/kg), b) at 80 rpm for 5 min (8.70 (W·h)/kg), c) at 160 rpm for 3 min (10.78 (W·h)/kg), d) at 160 rpm for 5 min (18.73 (W·h)/kg), e) at 250 rpm for 3 min (19.96 (W·h)/kg), and f) at 250 rpm for 5 min (34.81 (W·h)/kg). Green are starch granules, while red is protein [3]
Green - Starch granules; Red – protein

The obtained results for all samples recorded by the Mixolab device at different mixing speeds (80, 160 and 250 rpm) is shown in Fig. 4. The patterns obtained during mixing, pasting and gelling greatly varied with the mixing speeds used. Therefore, the variation in mixing speed

modifies all the parameters registered on the curve by the Mixolab. It must be mentioned that the first stage of the Mixolab curve is the only one that provides information about the wheat flour dough rheological behaviour during the kneading stage comparable with those determined by other rheological devices like Brabender farinograph. The rest of the curve shows dough behaviour during heating and offers information about protein weakening, starch properties and flour enzyme activity, simulating its behaviour during baking process [3].

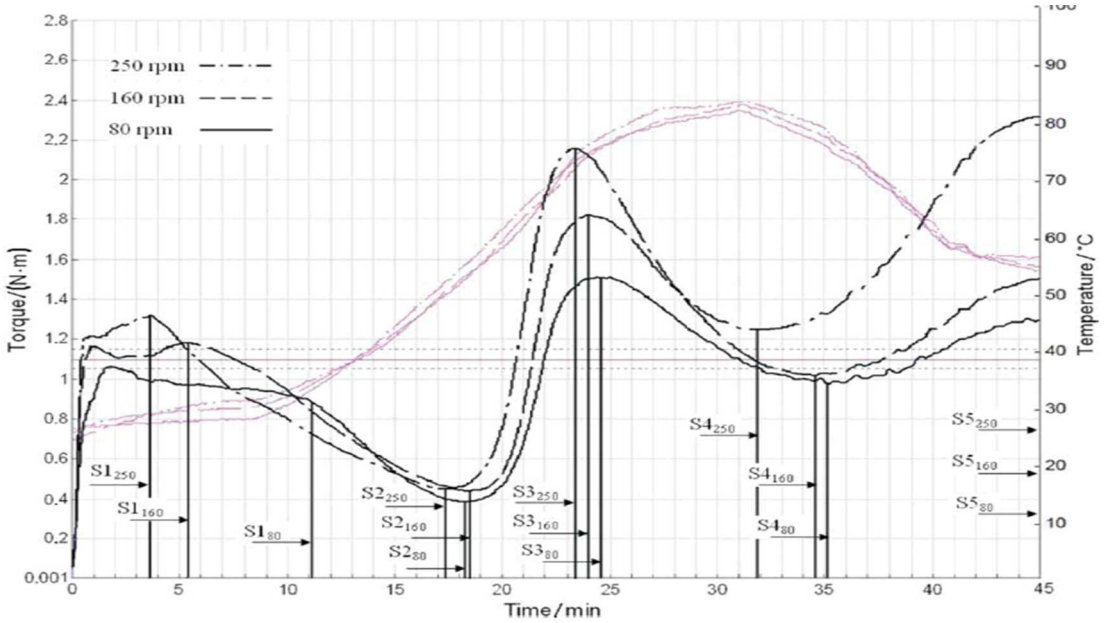

Figure 4: Mixolab curves recorded at different mixing speeds (80, 160 and 250 rpm) for good quality baking flour; S1=initial mixing, S2=protein weakening, S3=starch gelatinization, S4=stability during baking, and S5=retrogradation are the stages of Mixolab curves; pink curves indicate dough temperature [3]

L. Ruska and al., [4] conducted researches on doughs made up of four different types of flour and mixing at different speeds (slow kneading, rapid kneading).

The operational program for obtaining the products was the following:

- *with slow kneading*, it was kneaded with a mixer with spiral at low speed for 18 minutes, then it was left to rest for 20 minutes, it was modeled, put in the form, left to leaven (final fermentation) for 50 minutes, then the baking was done at 230^{0}C for 35 minutes, cooling in the form 2 hours, it was taken out of the form and cooled 2 more hours;

- *with fast kneading* it was kneaded with a mixer with spiral at low speed for 2 minutes, then it was mixed at high speed for 8 minutes, it was left to rest for 20 minutes then it was modeled, put in the form, then the final fermentation was done for 50 minutes, it was baked at 230^{0}C for 35 minutes, it was left to cool in the form for 2 hours, it was taken out of the form and cooled 2 more hours.

In tables 1, 2, 3, 4 are shown the influences of the kneading arm revolution on the bread quality obtained from the sorts of flour F1, F2, F3, F4 at slow and fast kneading of bread.

Table 1: The influence of the kneading arm revolution on the bread quality at slow and fast kneading from flour F1 [4]

Test		Slow kneading	Fast kneading
Volume	$m^3/100g$	305	315
Porosity	%	74	76

Elasticity	%	94	94
Acidity	0	2.6	2.6
Organoleptic estimation		Taste and smell specific to the product, golden yellowish peel, crumb with a uniform porosity	Taste and smell specific to the product, golden yellowish peel, crumb with a uniform porosity

Table 2: The influence of the kneading arm revolution on the bread quality at slow and fast kneading from flour F2 [4]

Test		Slow kneading	Fast kneading
Volume	$m^3/100g$	315	330
Porosity	%	75	78
Elasticity	%	94	94
Acidity	0	2.6	2.6
Organoleptic estimation		Taste and smell specific to the product, golden yellowish peel, crumb with a uniform porosity	Taste and smell specific to the product, golden yellowish peel, crumb with a uniform porosity

Table 3: The influence of the kneading arm revolution on the bread quality at slow and fast kneading from flour F3 [4]

Test		Slow kneading	Fast kneading
Volume	$m^3/100g$	310	330
Porosity	%	78	78
Elasticity	%	94	94
Acidity	0	2.5	2.5
Organoleptic estimation		Taste and smell specific to the product, golden yellowish peel with a darker shade, crumb with a uniform porosity	Taste and smell specific to the product, golden yellowish peel with a darker shade, crumb with a uniform porosity

The influence of the kneading arm revolution on the bread quality at slow and fast kneading from flour F4. Tabelul 4[4]

Test		Slow kneading	Fast kneading
Volume	$m^3/100g$	325	280
Porosity	%	78	74
Elasticity	%	94	88
Acidity	0	2.6	2.6
Organoleptic estimation		Taste and smell specific to the product, brown yellowish peel, crumb with a uniform porosity, slightly breakable	Taste and smell specific to the product, brown yellowish peel, crumb with a uniform porosity

After the analysis of the results, it is found that the changing of the mixer's arm revolution, with which the dough kneading takes place, influences the physico-chemical

characteristics of the finished product. By comparing the products obtained through higher revolution of the mixer's arm with the ones obtained through a slower kneading (low revolution of the mixing arm), it has been noticed that the changes are influenced by the amount of gluten and its qualities. Thus, at the products obtained from flour F1, F2, F3 through mixing at a higher revolution, it is noticed an improvement of the characteristics, like volume and porosity, while at the products obtained from flour F4 it can be noticed a significant decrease of these qualitative parameters [4].

The growth in volume and porosity of the tests obtained from flour F1, G2, F3 through mixing at a higher revolution is due to the higher content of gluten. Characteristic of the mechanical development of the dough is the quantity of energy and the speed with which it is transmitted to the dough. The specific energy consumption for the sorts of flour with a higher content of proteins is bigger (25-35 kJ/kg dough). The most significant growth could be noticed at the products obtained from flour F1 and F2. This can be explained through the fact that these sorts of flour, besides the higher content of gluten, they have a lower deformation value, which denotes a tighter connection between gluten proteins, which, when more intensely kneaded, they were in a small extent fragmented, in this way increasing the dough's elasticity [4].

3. CONCLUSIONS

As a results of the presented experiments, it was concluded that at 250 rpm the protein network is more compact and continuous than at 160 and 80 rpm. The amount of starch granules is low as the mixing speed increases [3].

The dough preparation method influences a lot the organoleptic characteristics of the finished product, therefore those obtained by slow kneading are much more superior from this point of view (taste, aroma) but in the case in which some technological qualities of the flour are inferior (gluten's quantity and quality), the finished products obtained through this method are much more reduced qualitatively (volume, porosity) [4].

References

[1] Verheyen, C., Jekle, M., Becker, T., Technische Universität München, Institute of Brewing and Beverage Technology, Workgroup Cereal Process Engineering, Freising, Germany, 2012.

[2] Codină, G.G., *The rheological properties of the wheat flour dough*, Series Food Engineering, Publishing house Agir, 2010.

[3] Codină, G.G., Mironeasa, S., *Influence of mixing speed on dough microstructure and rheology*, Food Technol. Biotechnol., 51 (4), p. 509–519, Suceava, 2013.

[4] Ruska, L., Timar, A., Chereji, R., *The influence of the kneading arm revolution on the bread quality*, Annals of University of Oradea, Fascicula: Ecotoxicology, Zootechnics and Food Industry Technologies, Vol. VII, Oradea, 2008.

[5] Luchian, M., I., *Contribution on the energetic optimization of bread dough mixing process* ,PhD thesis, Brasov/ Romania, 2012

[6] Sabovics, M., Straumite, E., Galoburda, R., *The influence of baking temperature on the quality of triticale bread*, FOODBALT, 2014.

STUDY ON THE PROCESS OF SOWING MEDICINAL AND AROMATIC PLANTS

PhD. Stud. Eng. Muscalu Adriana[1,2)], Eng. Bolintineanu Gheorghe[1)],
PhD. Stud. Eng. Cujbescu Dan [1,2)], Phd. Eng. Marin Eugen[1)]
[1)]INMA Bucharest
[2)]University Politehnica of Bucharest - Faculty of Biotechnical Systems Engineering

ABSTRACT

Nowadays, according to the data from WHO, more than 80% of the total world population uses medicinal and aromatic plants in phyto-therapeutic purposes or as food supplements. The need to satisfy consumer demands has determined: the increase of surfaces cultivated with these species, the modernization of growth technologies to obtain high yields of plant raw materials, with a high content of active principles. The paper presents the study on the capability of the experimental model of a technical equipment called SPM-0 (equipment for sowing medicinal and aromatic plants) to fulfil one of the conditions determining an optimum sowing process. This refers to achieving the sowing norms provided in the crop technologies. The assessment was conducted by analysing and interpreting the results obtained from the verification performed on the test stand, for a sowing station with mechanical distribution, belonging to the SPM-0 equipment, using various medicinal and aromatic plant seeds.

1. INTRODUCTION

For thousands of years, medicinal and aromatics plants have been recognized and they are widely used as an important source for the treatment and prevention of various diseases [1]. The therapeutic action of these species is determined by the presence of some bioactive chemical components, also called active principles, which have effects on the entire metabolism. Also, these substances do not accumulate in the human body, do not generate adverse secondary effects, but can have multiple effects on human body, simultaneously acting on the different processes or physiological states. [2]

For medicinal and aromatic plant crops, the quality of the plant material is given by the content of active principles. It is conditioned by ecological factors, species zoning, crop technology, biological value of the reproduction material (population, variety, hybrid, etc.) [3]. The sowing process occupies an important place in the crop technology of these species, its optimization implying a seed distribution at parcel level as even as possible, complying with the demands of each species. The sowing depth also represents an important parameter, influencing the optimum germination, reason for which it needs to be maintained precise and constant at the prescribed dimension by each specific technology. [4, 5]

Sowing precision, materialized by obtaining constant distances between seeds on the row is influenced by the interaction between seeds and different working bodies, by the way the seeds reach the devices for soil distribution, the soil type as well as its degree of grinding. However, it is accepted that the distribution device represents the essential body of a sowing machine participating at achieving the sowing precision.

The quality of the seeding process in the case of medicinal and aromatic plants is strongly influenced by the germination characteristics of seeds [6], by their purity, the mass of 1000 grains, the texture of seed surfaces, etc., which differ very much from one species to another.

[1]6, Ion Ionescu de la Brad Bd., tel: 0726234242, e-mail:adrianamuscali@gmail.com

For this reason, in the case of using conventional precision sowing machines or of those for small seeds, the results were not satisfactory [5].

The strong hereditary conservativism of some medicinal and aromatic plant species, as well as the tendency to maintain the attributes characteristic for weeds (staggered germination and low germination coefficient) make it necessary to adopt high sowing norms per hectare, in the case of direct sowing in the field. Being part of crops with special destination, in general, the seeds of these species are expensive. Thus, in order to avoid losses, many times it is preferred to obtain the multiplication material in greenhouses and solariums, in the view of replanting it in the field, at well-established times. A good quality uniform seedling ensures an adequate crop in terms of uniform plant growing and developing [7].

In Romania, the growth of medicinal and aromatic plants is done mainly by profile economic agents, together with small farmers, which dispose of relatively reduced land surfaces. For the latter, INMA designed and built an Experimental Model for an Equipment for seeding medicinal and aromatic plants, called SPM-0.

The paper presents a study on the capability of the SPM-0 experimental model to achieve the seeding norms provided by specific crop technologies [7]. Also, implicitly, from the experiments conducted were established the types of distributors adequate for sowing certain species of medicinal and aromatic plants.

2. METHODOLOGY

The experimental model for the Equipment for sowing medicinal and aromatic plants (SPM-0) is destined for incorporating the seeds of medicinal and aromatic plants in the soil, greenhouses/solariums, as well as directly in the field, on medium and small parcels. SPM-0 (fig. 1) has in its componence the following subassemblies: 1.–sowing station; 2.–station support frame; 3.–left handlebar tube; right handlebar tube; 5–handlebar; 6.–track marker; 7.–support cable.

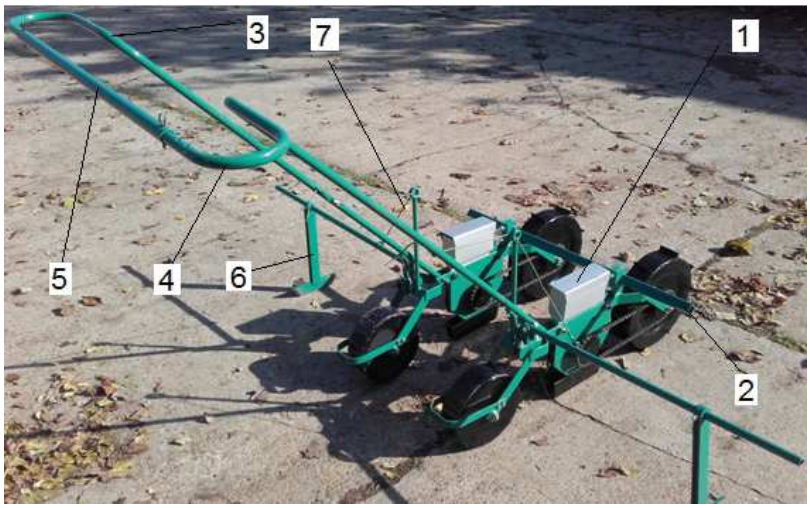

Figure 1: Equipment for sowing medicinal and aromatic plants, SPM-0

Through the left-right movement, the position of the two identical sowing stations on the frame can change, depending on the distance between the rows. Adequate handlebar adjustment can be achieved using the left and right handlebars, made of steel tubes with high resistance. The row marker (pos. 6) was achieved in the shape of a metallic construction, which can be sustained or lowered by the metallic cables (pos. 7). As in the case of sowing stations, its position can be adjusted depending on the distance between the rows.

In figure 2 is shown the main element of the equipment, represented by the sowing station with mechanical distribution, fitted on the equipment's frame. The sowing station is made of the following subassemblies: frame (1), distribution device (2), drive wheel (3), compaction wheel (4), scrapper for the compaction wheel (5).

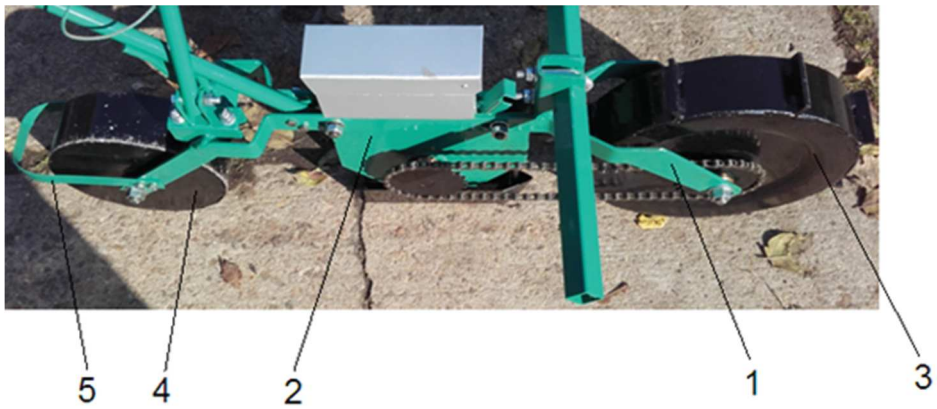

Figure 2: Sowing station fitted on the frame of the sowing machine

The device for seed distribution (fig. 3) is made of the following main elements: 1 – assembled housing; 2 – ploughshare; 3 – distribution disk; 4 – chain wheel; 5 – seed box; 6 – axle; 7 – fixing piece; 8 – brush; 9 – scrapper.

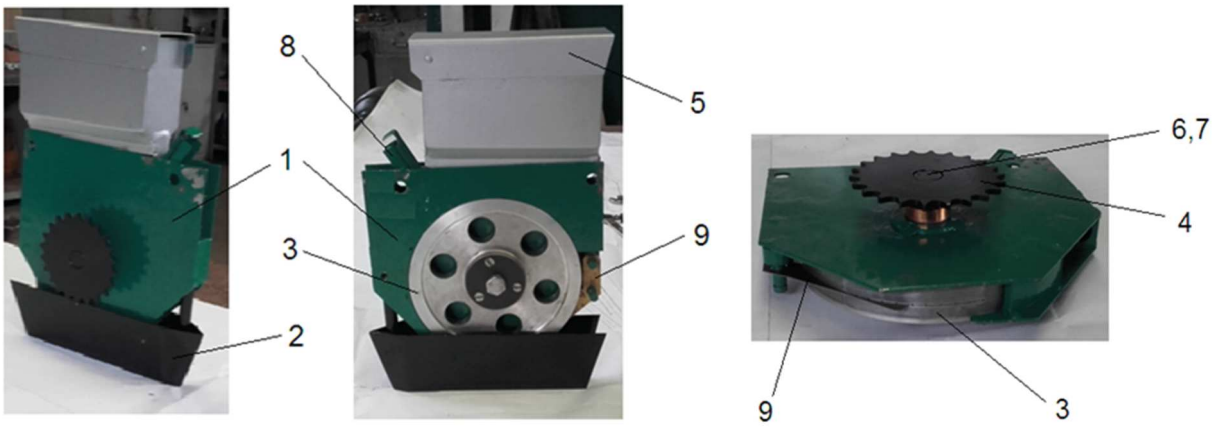

Figure 3: Device for mechanical seed distribution (without cover)

The assembled housing was achieved as a welded metallic construction, on which and in which the rest of the components are fitted. The distribution disk is fitted inside the housing and is built in the shape of a cylinder, made of aluminium alloy, in order to avoid the electrostatic charging of seeds. The orifices for seeds are placed equidistantly on the median circumference of the lateral surface of the respective cylinder. The distance between orifices determines the distance between seeds on the row. The disk with orifices (3) has the same rotation frequency as the chain wheel (4), due to the common axle (6) and to the fixing piece (7). The chain wheel is fitted in the exterior of the case, and through it, due to the chain transmission, taking the movement from the drive wheel. The brush (8) together with the scrapper (9) are fitted inside the housing. The brush has the role of taking out the seeds remaining in the orifices, while the scrapper removes the excess seeds from the orifices. The housing is closed by a cover that conceals the distribution disk. The area towards the ploughshare (2) is open, in order to allow seeds to drop in the channel opened by it. The ploughshare can operate at various working depths.

To study the process of sowing medicinal and aromatic plants, the stand for determining the sowing precision was used. The frame represents a main component, on which the sowing machine's stations can be fitted with the possibility to simulate the slope of the field between 0-12º. To this is added the electric motor with variable rotation frequency, thus allowing to simulate working speeds between 0-12 km/h for driving the distribution devices of the sowing stations.

The sowing station of the SPM-0 equipment was fitted on the frame, as shown in figure 4. The movement speed of the sowing machine's operator (2 km/h) was considered as the equipment's working speed. The rotation frequency of the motor was adjusted, so that with the help of chain transmissions to achieve the speed considered previously.

Figure 4: The sowing station of SMP-0 equipment fitted on stand

Keeping in mind that the distance between stations is 0.5 m, the circumference of the drive wheel is approximately 1 m, the working speed *v=2 km/h*, it results that a 1 m^2 surface is achieved after 2 complete rotations (of the drive wheel). Tests were conducted simulating equipment movement on a 20m length, in order to achieve the cover of a 10 m^2 surface by the 2 sowing stations. The seeds resulted from the distribution of the seeding station were collected in special capsules and then weighed using the analytical balance.

For samples were used seeds from the following species of medicinal and aromatic plants: Valerian *(Valeriana officinalis L.)*, Lemon balm *(Melissa officinalis L.)*, chamomile *(Matricaria chamomilla L.)*, St John's wort *(Hypericum perforatum L.)*, Hyssop *(Hyssopus officinalis L.)*, Anise *(Pimpinella anisum L.)*, Common yarrow *(Achillea millefolium L)*. Their physical characteristics are shown in table 1.

Table1: Physical characteristics of medicinal and aromatic plants

Species	**Hectolitre weight [kg/hl]**	**WTG [g]**
Valerian *(Valeriana officinalis L*	34.236	2.0272
Lemon balm *(Melissa officinalis -L.)*	68.602	0.5717
Chamomile *(Matricaria chamomilla L.)*	14.930	0.055
St John's wort *(Hypericum perforatum L.*)	42.414	0.3615
Hyssop *(Hyssopus officinalis L.)*	51.206	0.9696
Anise *(Pimpinella anisum L.)*	46.167	2.0272
Common yarrow *(Achillea millefolium L)*	8.825	-

For the three versions of distribution disks used for tests, the differentiation element is represented by orifice size. They were achieved at a diameter of: 2.2 mm, 2.7 mm and

respectively 3 mm. Also, no matter the size, the orifices have an inclined position compared to the vertical plane, thus their loading/unloading is performed easily, avoiding seed crushing.

For each species, the tests were performed with three repetitions, with the three versions of the distribution disk. The results from the experiments are presented synthetically in table 2.

Table 2: Correlation between the distribution disk version and the sowing norm

Species	Recommended sowing norm [kg/ha] [7]	Disk orifice sizes [mm]	Seed norm achieved experimentally [kg/ha]
Valerian	3-6	Φ 2.7	6.5
Lemon balm	8-10	Φ 2.2	13.5
Chamomile	3-4	Φ 2.7	5.4
St John's wort	3-4	Φ 2.2	10.2
Hyssop	5-10	Φ 2.2	7.7
Anise	8-12	Φ 2.7	8.5
Common yarrow	3-4	Φ 3	3.4

3. CONCLUSIONS

After conducting the tests in the laboratory, a correlation was established between the size of orifices in the distribution disk and the seeding norm [kg/ha] for each sample tested. For some species, the seeding norm is a little higher. Taking into consideration the relatively decreased germination degree of medicinal and aromatic plant seeds, this exceeding can be permitted.

In the absence of specialized equipment, in the crop technologies of medicinal and aromatic plants, is particularly recommended to use SUP21/29 sowing machines, equipped with distributors for small seeds. This is the way large norms are usually distributed. To be easier distributed using this type of equipment, due to their physical characteristics, depending on the species, the seeds of medicinal and aromatic plants are distributed together with indicator plant seeds of with inert materials (ex.: sand, corn flower, sawdust, etc.).

Compared to these, we consider as encouraging the results obtained in laboratory conditions from testing the experimental model of SPM-0. Also, these results constitute an important premise for experimenting SPM-0 equipment in exploiting conditions. Thus, it will be equipped with the adequate distribution disk, depending on the species of medicinal and aromatic plant.

The continuation of experiments on SPM-0 experimental model is indispensable, in the view of achieving a specialized, efficient equipment, having a low cost price, being destined for sowing medicinal and aromatic plants, on medium and small surfaces.

Acknowledgement

The work has been funded by the Ministry of Research and Innovation, within the project entitled „Innovative technology and equipment for increasing the quality of plant raw material obtained from medicinal and aromatic plants, in the view of elaborating competitive organic products", PN 16 24 03 03.

References

[1] Silva, N., Jounior F, *Biological properties of medicinal plants: a review of their antimicrobial activity*, The Journal of Venomous Animals and Toxins including Tropical Diseases. 16(3): 402-413, 2010;

[2] Grigore A , Pirvu L. , Bubueanu C , Colceru-Mihul S., Ionita C., Ionita L. *Medicinal plant crops - important source of high value-added products,* Scientific Papers. Series A. Agronomy, Vol. LIX, 2016;
[3] GUIDE of July 11, 2011 of good practice for the cultivation and harvesting of medicinal and aromatic plants Published in the Official Journal of Romania, Part I no. 527 of July 26, 2011;
[4.] Ziegler K., Göbel E., Schmittmann 0., Schulze Lammers P. *Precision seed drill tests in Germany 2009-2011*. International sugar journal 114/1367, 795-803 , 2012;
[5.] Meinhold T., Blum H., Budde M., Damerow L., Schulze Lammers P. *Partial Process-Analysis of the Sowing Process for Fine Seeds*. Conference proceedings Land. TechnikAgEng 2013, 8.9. Nov. 2013 Hannover, 189-195;
[6] Jafarinia M, Yazdanbakhsh Z. *An Investigation of Seed Germination Characteristics of Twenty Medicinal Plants* Journal of Applied Environmental and Biological Sciences, 6(2)94-100, 2016;
[7] Verzea Maria et al.- *Crop technologies for medicinal and aromatic plants*, Horizons Publishing House, Bucharest, 2001.

SOYBEAN SEEDS DRY EXTRUSION PROCESSING TO OBTAIN HIGH NUTRITIONAL VALUE FORAGE FOR ANIMAL FEED

Păun Anişoara[1)], Brăcăcescu Carmen[1)], Caba Ioan[1], Ciobanu Valeria[1)], Milea Dumitru[1)], Zaica Alexandru[1)]

[1)]National Institute of Research-Development for Machines and Installations designed to Agriculture and Food Industry – INMA / Bucharest, Romania

ABSTRACT

The need to modernize agriculture and its related areas, namely livestock sector, finding new technologies and advanced, intelligent technical equipment solutions that would cope with beneficiaries' demands, increasing transformation efficiency; optimizing food products, reducing losses of raw materials processing in the food chain as well as quality and safety requirements, are more and more intense preoccupations of research in livestock field. Taking into account the importance of knowing extrusion processing of soybean seeds, this paper presents some concentrated fodder processing methods, the extrusion technology to obtain feed ingredients, the installation for soybean seeds superior capitalization – IVSS and the advantages of using it.

1. INTRODUCTION

The quality of mixed fodder significantly influences the quality of animal products obtained. From this point of view, fodder producers and farmers worldwide are facing serious problems with food security, ensuring comfort for animals and the environment protection.

By its amino acid content, soybean completes together with cereals the ration of these animals, which leads to the production of mixed fodder, balanced in terms of essential amino acids and makes possible to achieve performance and economic potential of the respective animals [1,2, 3, 4].

Taking into account that raw materials to satisfy nutritional needs are necessary, one must consider the processing method used to obtain these ingredients, which can influence the animal's performances [6].

Progresses in livestock field have shown that fodder rations containing soybean may be supplemented with vitamins eliminating the need for adding animal protein in the ration and soy grit is an important protein component in animals fodder ration, in particular pigs. For our country, soy grit is also a key source of protein, being a basic component, along with cereals, in mixed fodder structure.

Most commonly used is the heat treatment of soybeans. Taking into consideration that the anti-nutritional factors, in most cases, are proteins, the processing method can adversely affect soybean proteins. Therefore, it is important to obtain a product rich in nutrients (energy and usable proteins) and free of anti-nutritional factors [5, 7].

Improving extruders has been a permanent concern of manufacturers and users. For the superior capitalization of feed resources in livestock farms, INMA Bucharest elaborated a technology and an installation that can be used to obtain a wide range of mixed fodder directly in the farm, in terms of efficiency and quality as required at world level.

2. METHODOLOGY

By processing the seeds, physical (shape, structure, grain size) and chemical changes are obtained, which raise the nutritional value of the fodder, increase the degree of digestibility, improve the taste, allow obtaining wide and complete ranges of fodder recipes and create the premises for mechanization and automation of feed distribution to animals.

Figure 1: Installation for soybean seeds superior capitalization – IVSS / INMA Bucharest
Productive capacity 150÷200 kg/h
1-Inclined screw conveyor; 2- Supply system; 3- Extruder; 4- Cooling system; 5- Mobile belt conveyor; 6- Command and control system

The installation for soybean seeds superior capitalization – IVSS will be a support in the interest of farmers who want to approach a strategy on: choosing fodder recipes depending on the animals in the farm, using own fodder and not only, the technical base necessary to the farm, and in the same time they will meet the requirements according to which agriculture no longer serves only to produce wheat, corn, milk and other agricultural products, but it also provides environment conservation and product consumers food safety

Dry extrusion of soybean seeds is a process that occurs due to the high oil content of seeds. During the extrusion process, the product can reach temperatures of approx. 140-150°C. As a result of the combination of temperature and pressure is ensured the distortion of anti-nutritional factors, oxidative enzymes and the release of oil from the cells by breaking the cell walls [2]. In the case of wet extrusion soybean seeds are conditioned with superheated steam before the extrusion process.

Extrusion is a process based on processing soy beans under pressure, under high temperature and humidity conditions [5, 6].

The product obtained by roasting and extruding, known as full fat soybean, is a valuable raw material because, in addition to high quality protein in a proportion of 30-42%, it has a high energy value, of 4180 kcal / kg EM in the case of pigs due to rich oil content (18-22%) which has not been extracted by processing.

One of the main functions of the extruder, beside the transport (and sometimes boiling) one, is to create a certain pressure necessary for the processed material to pass through the die orifice. The basic components that contribute to achieving these functions are: the screw, the extrusion barrel and the die (Fig. 2).

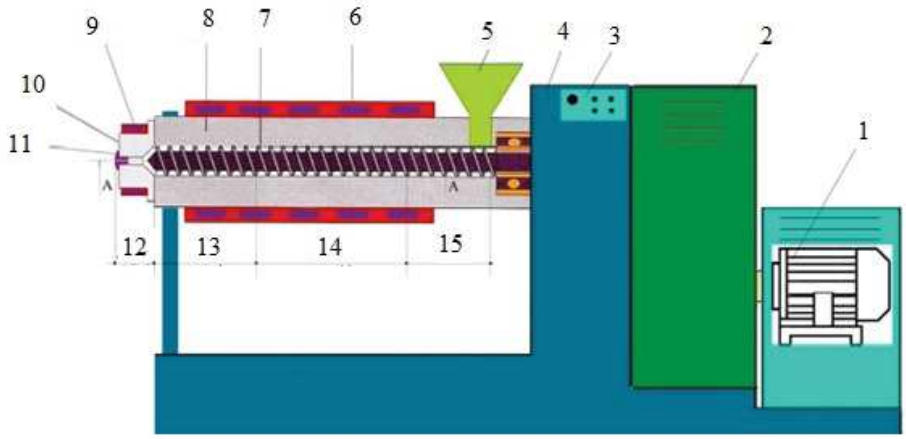

Figure 2: Extruder scheme**:** 1 - electric motor; 2- mechanical transmission; 3 - control panel; 4- frame; 5- supply hopper; 6- heating-cooling system for barrel; 7- screw; 8- barrel; 9- heating-cooling system for die; 10- die; 11- nozzle; 12- die section; 13- pressure section; 14- transition section; 15- feed section

The screw, beside the function of conveying the material from the supply hopper to the die entrance, influences, by its geometry, the mixing, shearing, the amount of mechanical energy dissipated in the heat and the pressure developed before the die.

Figure 3 shows the main geometric parameters of the screw, as well as the action directions of speeds and flows inside the extruder.

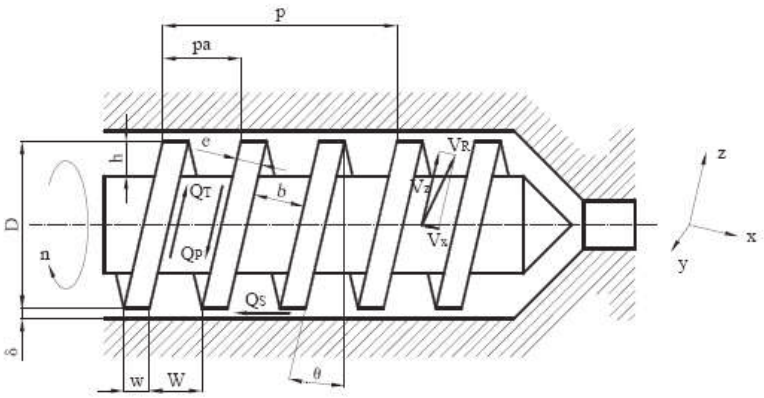

Figure 3: Screw geometric parameters, speeds and flows inside the extruder [2]

To determine the extruder flow rate, we consider only the flow in direction z.

Once v_z is determined, the extruder volumetric flow rate Q can be calculated according to the formula:

$$Q = i \int_0^h \int_0^b v_z \, dydx \tag{1}$$

where: Q is the extruder volumetric flow rate

i is the number of screw parallel channels.

According to the literature, the total volumetric flow rate Q depends on the size of the screw (D, h, L), the operating conditions (n, P) and the mass viscosity μ_m.

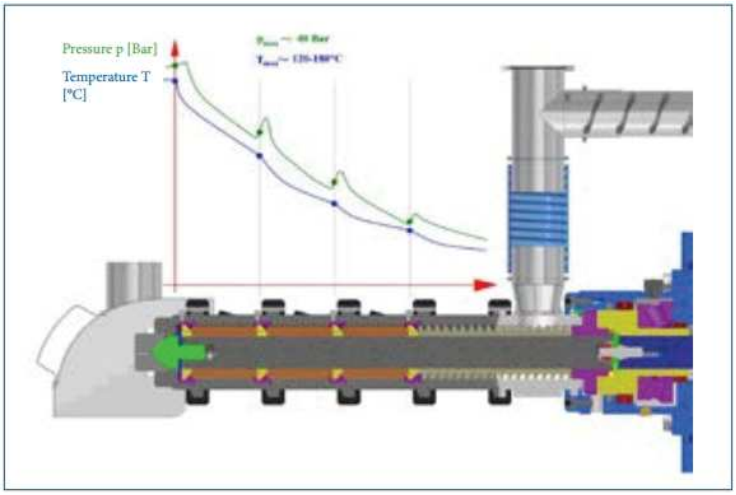

Figure 4: Extruder operating scheme and working parameters variation diagram

To analyse the flow rate and energy consumption of the extruder, take into account the pressure section (dosing) of the screw, because it controls the extrusion flow, explains energy consumption and generates uniform pressure behind the die.

The operating point of a food extruder screw results by combining screw and die characteristics (Fig.4).

In order to determine the flow passing through the die, in the case of processing a material with Newtonian behaviour in a fluid state, Hagen-Poiseuille equation can be applied. If we neglect the effects of material input and output from the die, we can write:

$$Q = k\,\Delta P/\,\mu_m \tag{2}$$

where: ΔP is the pressure difference

The maximum total flow rate of the extruder is obtained when the flow created by the counter-pressure is zero, thus leaving the extruder exit completely open, and is equal to the transport flow rate.

The issue is to determine that value of the total flow rate that still allows ensuring the desired quality of the finished product, in terms of acceptable energy consumption. This value will be called hereinafter the extruder flow rate Q. There are: a mass flow rate Q_m, which is measured in kg / h, and a volumetric flow rate Q_v, measured in m3 / h, that are in the relation:

$$Q_m = \rho_e \cdot Q_v \tag{3}$$

where ρe is the density of the expanded product.

The extruder flow rate is considered to be equal to the mass flow rate up to which the expanded product corresponds in terms of quality and there are no interruptions at the exit from the die.

For calculating the power absorbed, the studied are is the screw pressure section, where there is the highest power consumption.

Power consumption of the extruder shaft may be expressed as:

$$dN = dN_h + dN_p + dN_c + dN_j \tag{4}$$

where:

-dN – total power consumption;

-dN_h – power consumed for viscous dissipation in the channel;

-dN_p – power consumed for increasing fluid's pressure;

-dN_c – power required for increasing kinetic energy;

-dN_j – viscous power dissipated in the clearance between the barrel and the screw.

The operating point of a food extruder screw results by combining screw and die characteristics.

Figure 5 shows screw and die characteristics for two different temperatures of the processed material in the screw pressure section, respectively at die input.

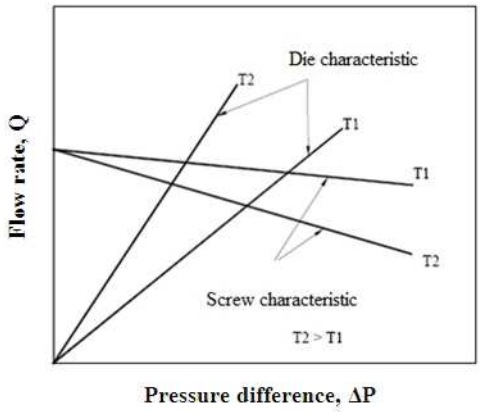

Figure 5: Screw and die characteristics for two different temperatures of extrusion

It is noted that the slope of the die characteristic when processing a material with a higher temperature is bigger than when processing a material with a lower temperature. Consequently, the extruder operating point moves to the left when the temperature of the processed material increases.

3. CONCLUSIONS

The main advantages of the extrusion technology compared to traditional methods are:

– Reducing production costs (consumption of heat, electricity, raw materials, labour costs and capital investments)

– Intensification of production process - high productivity and automation - extruders ensure continuous processing of raw materials and can be partially or completely automated;

– Adaptability: the process can be very easily modified to make new products, according to consumers' demand;

– High quality products - extrusion is a process that takes place at high temperature in a short time, and because of this, degradation of nutrients in raw materials is minimal;

– Minimum waste: the process of extrusion does not generate or generates only an insignificant volume of by-products as waste, thus with zero ecological impact;

– Increasing the use of raw material;

– Getting food products ready for consumption or creating components for them;

– Reducing the microbiological contamination of products;

Acknowledgement

This paper was financed with the support of National Agency for Scientific Research and Innovation, Programme NUCLEU, no. 8N/09.03.2016, Addendum No. 1/2016, Project PN 16 24 03 01 – "Innovative technology and installation for soybean seeds superior capitalisation in animal feeding".

References

[1] Ciobanu V., Vişan A. L., Păun A., Bunduchi G. Economic importance of feedig the wet flattened corn. Proceeding of International Symposium ISB-INMA TEH' 2016, Agricultural and mechanical engineering, 27-29 oct.2016, Bucharest, Romania,2016.

[2] Cioica N., Balc G., Ionut V. Thermal transitions by directly expanded extruded maize grits. Food processes and technologies, Vol.XI, No.2, Agroprint PublishingTimisoara, 2005 [3] Halga P. & col. Animal nutrition and feeding. Alfa Publishing House, Iasi , Romania, 2005.

[3] Koleva A.Zh. Dry pet food. Part 2. Hydrothermal processes for production. Scientific Works of the University of Food Technologies-Plovdin, Bulgaria, 2012.

[4] Nagalakshmi D., Reddy D.N. On farm evaluation of expander-extruder processed complete diet containing maize cobs in Murrah buffaloes. Indian Journal of Veterinary Research, Bareilly, India, 2008 .

[5] Nedelcu A., Găgeanu P., Popa L., Ciupercă R., Zaica A., Bunduchi Gh. Mechanical processing of camelina seeds for assuring the required conditions at superior capitalization of byproducts. Proceeding of International Symposium ISB-INMA TEH' 2016, Agricultural and mechanical engineering, 27-29 oct.2016, Bucharest, Romania, 2016.

[6] Păun A., Găgeanu P., Danciu A . Impact of Technologies of Obtaining Concentrated Fodder Upon Animal Nourishment and Environment. Bulletin of University of Agricultural Sciences and Veterinary Medicine Cluj-Napoca, Vol.66 No.1, 2009.

[7] Păun A., Pirnă I., Cojocaru I., Găgeanu P., Brăcăcescu C. Optimization and implementation of technologies for concentrated fodder to improve the quality and chemical safety of products derived from livestock by providing the facility of obtaining concentrated fodder– IONC, Journal of INMATEH-Agricultural Engineering, Vol.18, No.3, 2006.

EVALUATION HONEY YIELD OF SUNFLOWER (*HELIANTHUS ANNUUS L.*) CROP UNDER CLIMATIC CONDITIONS FOR RUSE REGION IN BULGARIA

Milen Petrov[1], Atanas Atanasov[1], Ivailo Hristakov[1], Hristo Beloev[1] Sorin-Stefan Biris[2], Valentin Vladut[3]
University of Ruse „A.Kanchev"[1], University of Politehnica[2], INMA Bucharest[3]

ABSTRACT

Honey yield of sunflower crop under climatic conditions for Ruse region in Bulgaria was evaluated. The study was conducted in 2016 year in the Northeast part of Bulgaria in village Brestovica. Geographical location of experimental apiary in Brestovica is 43°32'4.02"C N, 25°45'14.10" E and at an altitudinal range of 222 m above sea level. The influence of weather conditions in the weight of the hive due to the nectar secretion Y_{12} for the period of the blooming of the sunflower hybrid was analysed by regression analysis. Results of the investigation show that regression analysis for the linear model make obvious, that the coefficient of the distinctness $R^2 = 0,71$ or, that 71% from the alteration of the Y_{12} is due to the factors temperature of the air X_1, humidity of the air X_3 and atmospheric pressure X_4.

1. INTRODUCTION

For the Ruse region, sunflower (*Helianthus annuus L.*) is one of the four major pastures of great importance for the development of the bee colonies. Sunflower honey is quite popular, as sunflower is a number of fields, and during the sunflower blooming period, honey bee colonies are active, taking full advantage of the forage, which leads to much higher yields per a bee hive. On the other hand, honey bees are the main pollinators of many agricultural crops including sunflower. Studies on the pollination efficiency of honey bees in sunflower investigated of [2], [4]. The study of the climatic factors affecting the foraging activity during the sunflower blooming period is of great importance for the pollination of crops and for the obtaining of higher honey yield.

Individual researchers propose monitoring of foraging activity other parameters related to foraging activity and the visiting of plants include, the number of foragers per flower [5]; the number of visited flowers per forager [3]; and time spent per flower [5]; Interesting observations are made by [6] about determine influence of weather conditions on activity of honey bees for different sunflower hybrids.

The climatic diversity, the zonal character and the phenological features in the different geographic regions make it difficult comprehensible to obtain the data of the Ruse region in Bulgaria.

The aim of this study was to determine honey bee yield of sunflower crops under climatic conditions for Ruse region in Bulgaria.

2. METHODOLOGY

The study was conducted in 2016 year in the Northeast part of Bulgaria in village Brestovica. Geographical location of experimental apiary in Brestovica is 43°32'4.02"C N, 25°45'14.10" E and at an altitudinal range of 222 m above sea level. In the region of great importance honey source plant for honeybee is Sunflower (Helianthus annuus L).

There are many factors that can impact foraging activity of honeybee. These factors can be divided into two major groups: in-colony factors and out-colony factors. With regard to out-

[1]University of Ruse, Studentska Str.8, e-mail aatanasov@uni-ruse.bg

colony factors, the availability of suitable plant resources has a great impact on foraging activity [1]. In our study we took into account the influence of external factors such as outside temperature and air humidity, atmospheric pressure and the amount of precipitated rainfall on the weight change of the hive due to the flow of nectar secretion during the various hours of the day. To achieve the aim of the present work, a prototype of a meteorological station for the measurement of the microclimate in the bee colonies and outside Fig.1. Consisting of: 1) a hardware configuration including an electrical module, a LAN module, a temperature sensor - DS18B20, a combined temperature / humidity sensor DHT22 and others. 2) software configuration using common applications, such as CarterLake.org и PHP conversion by Saratoga-Weather.org, TNET Weather [Kevin Reed], Long Beach WA [Mike Challis], Saratoga-Weather.org, AJAX TNET Weather common PHP site design. [Ken True].

The recording of the change in the weight of the hive was carried out with an electronic beekeeping scales of TEHTRON-VAGA. Reporting was done three times a day over the period of 15 days at 9 a.m. to 12 am in the afternoon from 3 pm 21 pm The received data was stored on the web-based applications and then downloaded as numeric values in Excel spreadsheets. For the statistical processing of the data obtained, the software STATISTICA 10 was used. Regression analysis were used to evaluate and compare the results obtained.

Fig.1. Meteorological station for measuring the microclimate in the bee colony and beyond

During the investigation period the weather was sunny with air temperature fluctuated from 26, 2 ^{0}C to 36, 4 ^{0}C and humidity from 25 % to 48 %. The atmospheric pressure fluctuated from 931 to 934 hPa. The data obtained are shown in Table 1.

Table 1. The change of the temperature of the air $\mathbf{X_1}$, rainfalls $\mathbf{X_2}$, the humidity of the air $\mathbf{X_3}$, the atmospheric pressure $\mathbf{X_4}$ and changes in the weight of the hive due to the nectar secretion $\mathbf{Y_{12}}$ for the period of the blooming of the sunflower in the region in the village of Brestovitsa.

	1 x1	2 x2	3 x3	4 x4	5 Y12
1	26,8	0	48	931	68,08
2	29,6	0	39	932	70,66
3	27,8	0	37	933	71,68
4	30,6	0	39	934	72,32
5	33	0	34	931	73,36
6	33,3	0	47	935	74,22
7	36,4	0	32	932	74,35
8	33,8	0	47	993	74,86
9	34,5	0	32	991	74,78
10	27	0	37	993	75,08
11	27	0	37	994	75,36
12	28,4	0	33	994	75,72
13	26,2	0	32	991	75,76
14	27,4	0	47	993	75,76
15	31,4	0	25	992	75,64
16					

The results of the regressional analysis for the linear model make obvoius , that the coefficient of the distinctness $\mathbf{R^2 = 0,71}$ or, that **71%** from the alteration of the $\mathbf{Y_{12}}$ is due to the factors $\mathbf{X_1}$, $\mathbf{X_3}$ and $\mathbf{X_4}$ and is described from the linear model which certainly looks like this:

$$Y_{12}=13,35 + 0,021.X_1 - 0,05.X_3 +0,058.X_4 \quad (1)$$

The factor $\mathbf{X_2}$ is not included as it is a **constant**=0 there is no rainfalls. It is substantial the influence of $\mathbf{X_4}$ and $\mathbf{X_1}$ at the standard of importance 0,1 due to which for then **p-value** = 0,1 is less than 0,1.

Regarding to that the p-value is smaller than the standard level of 0,1.

It is insignificant the influence of the factor $\mathbf{X_3}$ because for it the value **p-value** = 0,36 greater than 0,1.

Table 2 is an expansion of the Table 1 with the addition of two more columns i.e. these are $X_{14}= X_1.X_4$ and $X_{11}= X_1.X_1=X_1^2$

	1 x1	2 x2	3 x3	4 x4	5 Y12	6 x14	7 x11	8 NewVar3
1	26,8	0	48	931	68,08	24950,8	718,24	
2	29,6	0	39	932	70,66	27587,2	876,16	
3	27,8	0	37	933	71,68	25937,4	772,84	
4	30,6	0	39	934	72,32	28580,4	936,36	
5	33	0	34	931	73,36	30723	1089	
6	33,3	0	47	935	74,22	31135,5	1108,89	
7	36,4	0	32	932	74,35	33924,8	1324,96	
8	33,8	0	47	993	74,86	33563,4	1142,44	
9	34,5	0	32	991	74,78	34189,5	1190,25	
10	27	0	37	993	75,08	26811	729	
11	27	0	37	994	75,36	26838	729	
12	28,4	0	33	994	75,72	28229,6	806,56	
13	26,2	0	32	991	75,76	25964,2	686,44	
14	27,4	0	47	993	75,76	27208,2	750,76	
15	31,4	0	25	992	75,64	31148,8	985,96	
16								

After the so done regression analysis has been ascertained, that the coefficient of definition $\mathbf{R^2}$ is receiving significantly a bigger value 0,93 which means that 93 % of $\mathbf{Y_{12}}$ is being owed to the factors $\mathbf{X_1}$, $\mathbf{X_3}$ and $\mathbf{X_4}$. Not a significant influence is seen with the factor $\mathbf{X_3}$ and $\mathbf{X_1^2}$.

There is noticed strong interaction between the factors $\mathbf{X_1}$ and $\mathbf{X_4}$ which is confirmed by the coefficient $\mathbf{b_{14}}$ = **-0,012** for the which probability **p-value =0,000499** is much less in size than 0,05 counting only the most significant coefficients of the model his final looking view will be :

$$Y_{12} = -385,64+14,55.X_1+0,428.X_4 – 0,012.X_1.X_2 \quad (2)$$

Reporting, the main factors are $\mathbf{X_1}$ and $\mathbf{X_4}$ there will be presented graphically the surface of the echo.

$$Y_{12}= f(X_1 ,X_4)$$

And the lines of similar echo

$$f(X_1 ,X_4)=constant$$

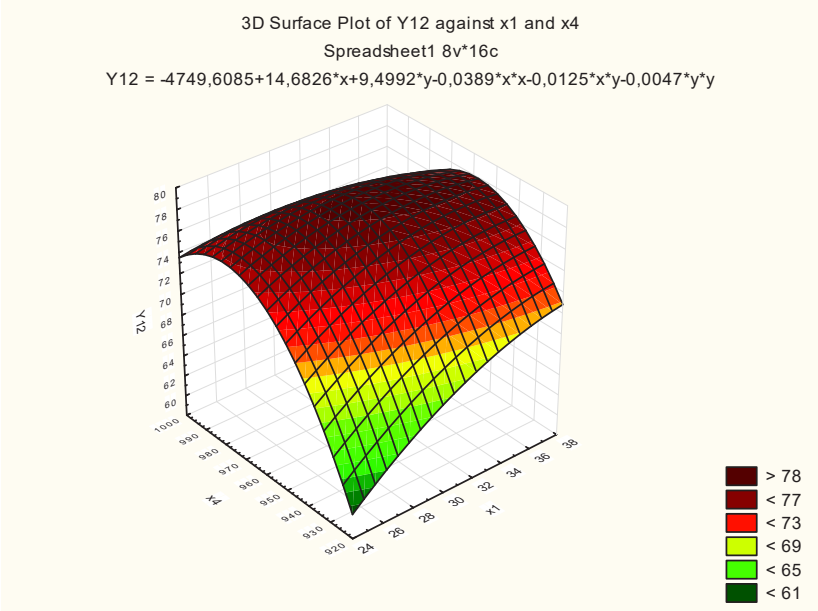

Fig.2. The surface of the echo $Y_{12}= f(X_1, X_4)$

From Fig.2 is seen, that the surface of the echo has a parabolic character and from it there could be difficultly defined the favorable values of $\mathbf{X_1}$ and $\mathbf{X_4}$ into which the changes in the weight of the hive due to the nectar secretion $\mathbf{Y_{12}}$ has greater values. This question is better cleared out by means of the lines of the same echo, which are thus shown on Fig.3.

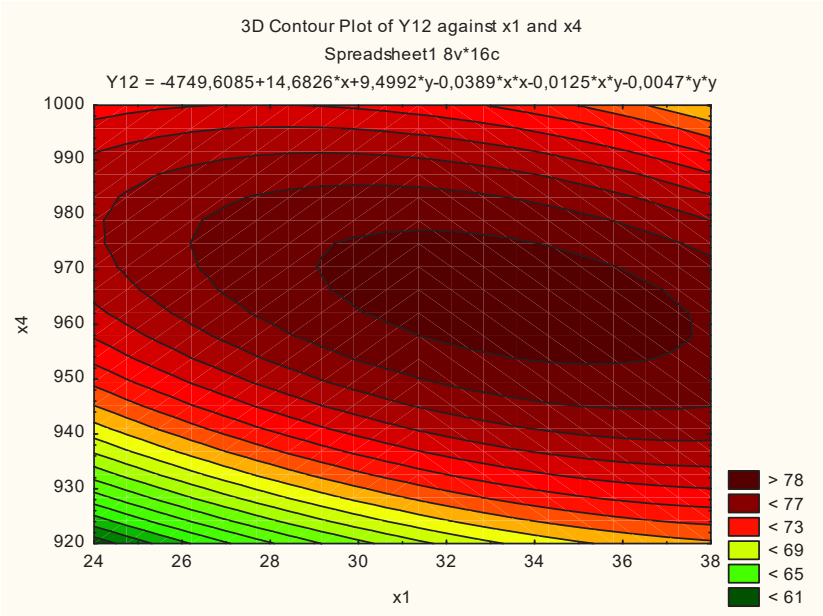

Fig.3 A line of the same echo f (X_1, X_4)=constant

The lines of similar echo have an ellipse character and in the center of the most inner ellipse we will have the most favorable conditions we receive the $\mathbf{Y_{12}}$ greater than 78 kg.

These conditions are defined from $\mathbf{X_1}$ approximately 33 C^0 и Pa (atmospheric pressure) $\mathbf{X_4}$=965 hPa.

The degree of the influence of the certain factors we can define as we exclude from the model the correspondent factor. The largest influence this factor is having at the threshold of its exclusion the coefficient of distinctness is smallest. Consequently by each other we excluded the factors $\mathbf{X_1}$, $\mathbf{X_3}$, $\mathbf{X_4}$ in this case we could come at the accretion that $\mathbf{R^2}$ has the smallest value at the exclusion of the factor $\mathbf{X_4}$, that is the factor $\mathbf{X_4}$ has the strongest influence on the changes in the weight of the hive due to the nectar secretion. Strongest influence on the factor $\mathbf{X_1}$ and a less weakly it is expressed the influence of the factor $\mathbf{X_3}$ with which exclusion there we have R^2= 0,868 this meaning that with the exclusion of X_3 the model is getting worse in the smallest degree.

3. CONCLUSIONS

Regression analysis for the linear model make obvious, that the coefficient of the distinctness R^2= 0,71 or, that 71% from the alteration of the Y_{12} is due to the factors temperature of the air X_1, humidity of the air X_3 and atmospheric pressure X_4 .and is described from the linear model Y_{12}=13,35 + 0,021.X_1 - 0,05.X_3 +0,058.X_4

Changes in the weight of the hive due to the nectar secretion Y_{12} is highest at the temperature of the air X_1=33 ^{0}C and atmospheric pressure X_4=965 hPa

References

[1] Abou-Shaara, H. F. (2014):The foraging behaviour of honey bees, Apis mellifera: a review. Academic Journal Veterinarni Medicina, 59: 1–10

[2] Kumar, M., Singh, R. (2003): Pollination efficiency of Apis mellifera in seed production of sunflower (Helianthus annuus L.). Journal of Entomological Research, 27 (2): 131-134.

[3] Mattu VK, Raj H, Thakur ML (2012): Foraging behavior of honeybees on apple crop and its variation with altitude in Shimla hills of western Himalaya. International Journal of Science and Nature 3, 296–301.
[4] Mehmet Oz and all. Effects of honeybee (Apis mellifera) pollination on seed set in hybrid sunflower (Helianthus annuus L.) African Journal of Biotechnology Vol. 8 (6), pp. 1037-1043, 20 March, 2009
[5] Sushil SN, Stanley J, Hedau NK, Bhatt JC (2013): Enhancing seed production of three Brassica vegetables by honey bee pollination in north-western Himalayas of India. Universal Journal of Agricultural Research 1, 49–53.
[6] Z. Puškadija and all. Influence of weather conditions on honey bee visits (Apis mellifera carnica) during sunflower (Helianthus annuus l.) blooming period, Agriculture, Vol.13 No.1 June 2007.

SEPARATION OF CHOPPED CHICORY MATERIAL ON FLAT SIEVE LENGTH

Pruteanu A.[1], Matache M.[1)], David L.[2)], Muscalu A.[1)], Nițu M.[1)], Rădulescu E. L.[3)], Bota M.S.O.[4)]
[1)]INMA Bucharest; [2)] UPB Bucharest; [3)] USAMV Bucharest, [4)] Build PR Consulting SRL Cluj-Napoca

ABSTRACT

The separating process of granular and vegetal materials is a complex technological process influenced by a series of factors from which we remind: mechanical oscillatory motion, inclination of the sieve, the intensity of shaking and technological factors. Based on correlations between the presented elements one can establish the technological parameters of the separating process so that to realize a quality separation.

This paper presents experimental data on the separation process of chicory herb (*Cichorium intybus*) on the flat sieve length depending on the material flow rate, sieve angle of inclination and oscillations sieve frequency. Mixture of dried and chopped chicory fragments was separated on a dimensional separator of medicinal plants, equipped with oscillating flat sieve.

For characterization of separation process of chicory herb on length of oscillating flat sieve it shows: separation intensity on the length of the sieve and cumulative separation on the length of the sieve. The experimental results have been tested by Rosin-Rammler distribution law.

The results may be used for designing and optimizing separating process of of medicinal plants.

1. INTRODUCTION

The medicinal plants species owe their phyto-therapeutic action to some bioactive components, also called active principles, influencing the metabolism of the whole body of human beings or animals. Depending on the presence of some active principles, the plants have specific effects, increased by their synergic action, having nourishing, therapeutic and also preventive qualities. The useful substances from medicinal and aromatic plants can generally be extracted either by means of water (usually hot water), or a solvent,(e.g. the alcohol). The plant parts are broken in small fragments (leaves, flowers, herbs up to 5 mm, the skinny leaves up to 1mm and the stems, bark and underground parts, under 3 mm, the fruits and seeds, under 0.5 mm) [3].

Medicinal plant primary and advanced processing suppose volatile oils obtaining, macerated tea, vegetable extracts, tinctures, syrups, tablets, food colourings, cosmetics, natural fertilizers, bio-insecticides etc. [9].

The technological process of primary manufacturing the medicinal plants represents that part of manufacturing process which comprises the totality of operations and interrelated stages necessary to prepare, respectively store, pack and subsequently process the matter harvested or purchased [8]. A compulsory condition for current herb trades is presenting them on the internal or external market as uniform batches which must meet certain quality requirements. Preparing medicinal plants according to their use and imposed quality standards is done through a sequence of technological operations (harvesting, conditioning, chopping, separation, extraction) whose complexity and specificity depend on the raw plant material, the product's destination and the level of technical equipment [4].

The separating operation can be performed with technical equipment meant for separating one or more components from a solid-solid heterogeneous mixture. Separation by the nature of the constituents can be made based on the differences of physical and chemical constants:

[1] INMA Bucharest, *E-mail:* pruteanu_augustina@yahoo.com

density, color, superficial properties of the surface, magnetic susceptibility, solubility, chemical affinities etc, [4].

In terms of obtaining the vibrations, vibrating separators can be: with a shaft mechanism with eccentric masses; with an autooscillant mechanism; with an eccentric shaft mechanism; with a connecting rod mechanism elastically linked to the mobile or resonating frame; with an electromagnetic mechanism.The following parameters can be adjusted: separation surface inclination; the direction of the vibration propagation; the vibration amplitude [5].

Recent studies have found some of the important constituents in chicory such as: flavonoids sesquiterpene lactones, caffeic acid derivatives, inulin, sugars, proteins, hydroxycoumarins, alkaloids, steroids, terpenoids, oils, volatile compounds, coumarins, vitamins, saponins, tannins. Leaves of the plant contain salts such as sulphates and phosphates of sodium, magnesium and potassium as well as potassium nitrate [1,7].

Many studies investigated the biochemical, phytochemical and antioxidant composition of root, stem, leaves and seeds of *Cichorium intybus* L., [11]. In many parts of the world *Cichorium intybus* has been used as vegetable [6].

This paper presents vegetal process separation of chicory on oscillating flat sieve length, varying different parameters.

2. METHODOLOGY

At experimental determinations were used chicory plants, identified and harvested within spontaneous flora, in respect to their morphological characteristics and according to specialty guides [2]. Chicory was dried naturally in the shade, until it reached the storage humidity (maximum 13%), cleaned of foreign bodies (inorganic materials or other plants, injured parties) under the provisions of Romanian Pharmacopoeia [12], and then was chopped in bulk using the TIMATIC grinder for medicinal plants, adjusted to the size of 10 mm.

The experimental researches were conducted on a dimensional sortator of cut plants (figure 1), existing in working within INMA Bucharest, equipped with 9 sieve frames with bore sizes ranging from 1.15 to 13.2 mm, used in sets of three as needed.

The bedframe construction allows access to sieves for cleaning in case of warping. The sieves bedframe rests on a support made of welded rolled profiles by means of rubber shock absorbers.

Vibrating motors are mounted on symmetrically welded plates outside of which construction enables their rotation and changing inclined position to the horizontal in order to adjust the amplitude and frequency of oscillation.

Sieve tilting the can vary between 12-15^0 depending on the type of the culture, but also by other unwanted plants parties.

Figure 1: Sorter of cut plants

Figure 2: Collection box

The supply of the sorter material was carried out by means of an inclined conveyor belt, which carry on plant material in the centre of the sorter feed hopper and from there on its upper sieve where the separation process takes place.

The experiments were performed on a sieve with squares measuring 10 mm, sieve having a length of 1.395 m and a width of 0.6 m. Under chosen sieve, a sheet collection box was fitted (figure 2) delineated into seven equal compartments, each compartment having 0,195 m.

During experiments were used three sieve inclination angles of inclination ($12{,}08^0$, $13{,}33^0$, $14{,}7^0$), for each angle ware varied two feed debits (60 kg/h, 45 kg/h) and two vibration frequency (50 Hz, 40 Hz).

Interpretation of results was done by separating cumulative correlation experimental data on sieve along with theoretical data obtained using the Rosin-Rammler equation [10], represented by the relation (1):

$$R = e^{-\left(\frac{D}{D_n}\right)^n} \tag{1}$$

where:

R is the cumulative retained at a size D (%);

D is the compartments size of collection box (m);

D_n and n are fitting parameters.

3. RESULTS

Primary experimental data on separate plant fragments along sieve separate for different feed rates, oscillation frequencies and angles of inclination of the grid were reported in Table 1.

Table 1: Experimental data on separation intensity along sieve

Frequency [Hz]	Flow rate adjusted, [kg/h]	*Sieve length from which chicory fragments are collected, m*						
		0.195	*0.395*	*0.595*	*0.795*	*0.995*	*1.195*	*1.395*
		Separated fragments percentage (*intensity separation*), [%]						
		1	**2**	**3**	**4**	**5**	**6**	**7**
Slope angle, $12{,}08^0$								
50	60	62,23	24,12	6,64	3,32	2,36	0,86	0,48
	45	54,11	27,73	8,89	4,05	3,20	1,16	0,86
40	60	84,95	8,69	1,51	0,85	1,86	1,02	1,13
	45	82,7	11,63	1,55	0,91	1,36	0,71	1,15
Slope angle, $13{,}33^0$								
50	60	41,5	29,9	12,39	6,51	4,92	3,06	1,72
	45	44,28	30,66	10,85	6,12	4,33	2,43	1,33
40	60	72,71	20,83	3,4	1,07	0,98	0,53	0,5
	45	69,71	21,82	3,53	1,78	1,25	0,84	1,07
Slope angle, $14{,}7^0$								
50	60	47,05	28,66	9,89	5,63	4,06	2,37	2,34
	45	54,38	26,54	8,05	4,12	2,94	1,40	2,56
40	60	63,87	26,73	3,78	1,76	1,9	1,1	0,85
	45	61,62	26,6	3,98	2,34	2,36	1,39	1,71

Results obtained after chicory fragments separation were graphic represented in figure 3, by representing variation curves of separation intensity.

Chicory fragments separation efficiency along sieve is shown by the degree of separation and separation cumulative. The separation intensity on sieve length of is defined by the percent (%) of fragments separated in each box compartment from the total amount of fragments that are in the collection box.

Cumulative separation is defined as percentage of separated fragments (%) gathered in compartments (united) from total amount of fragments in the collection box.

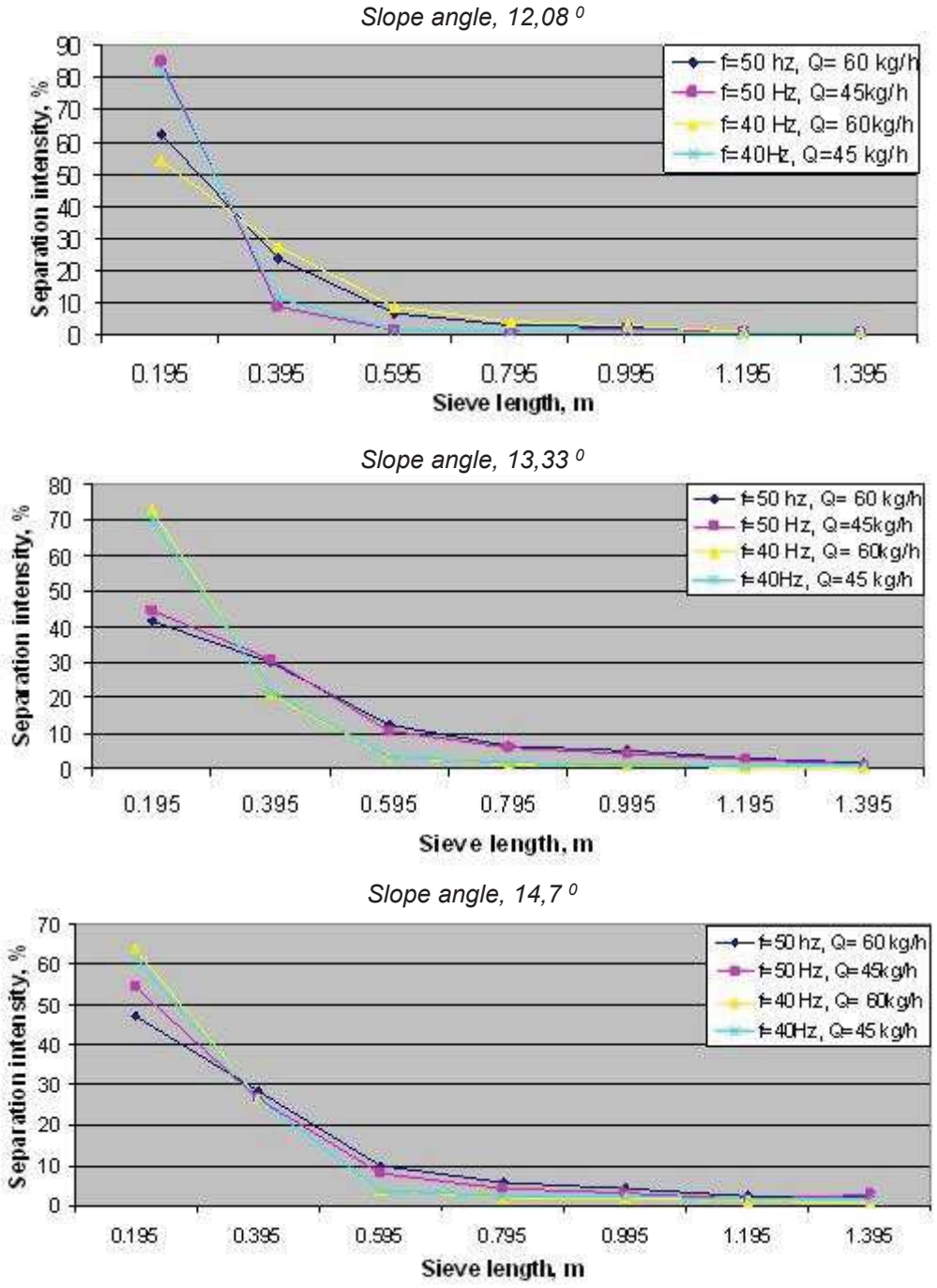

Figure 3: Intensity variation of chicory fragments separation, on sieve length

In figure 3 is observed that separation intensity decreases on the sieve length. The intensity of separation is maximum for all frequencies in feeding zone, regardless of angle of inclination.

The intensity of separation is evident in the first part of the screen and it becomes insignificant at the end of the sieve, resulting that the length of the screen is sufficient to achieve the separation process.

Results obtained after cumulative separation process of chicory fragments, were mathematic al modelling using Rosin Rammler function. Both experimental results and theoretical ones were graphically represented in figure 4.

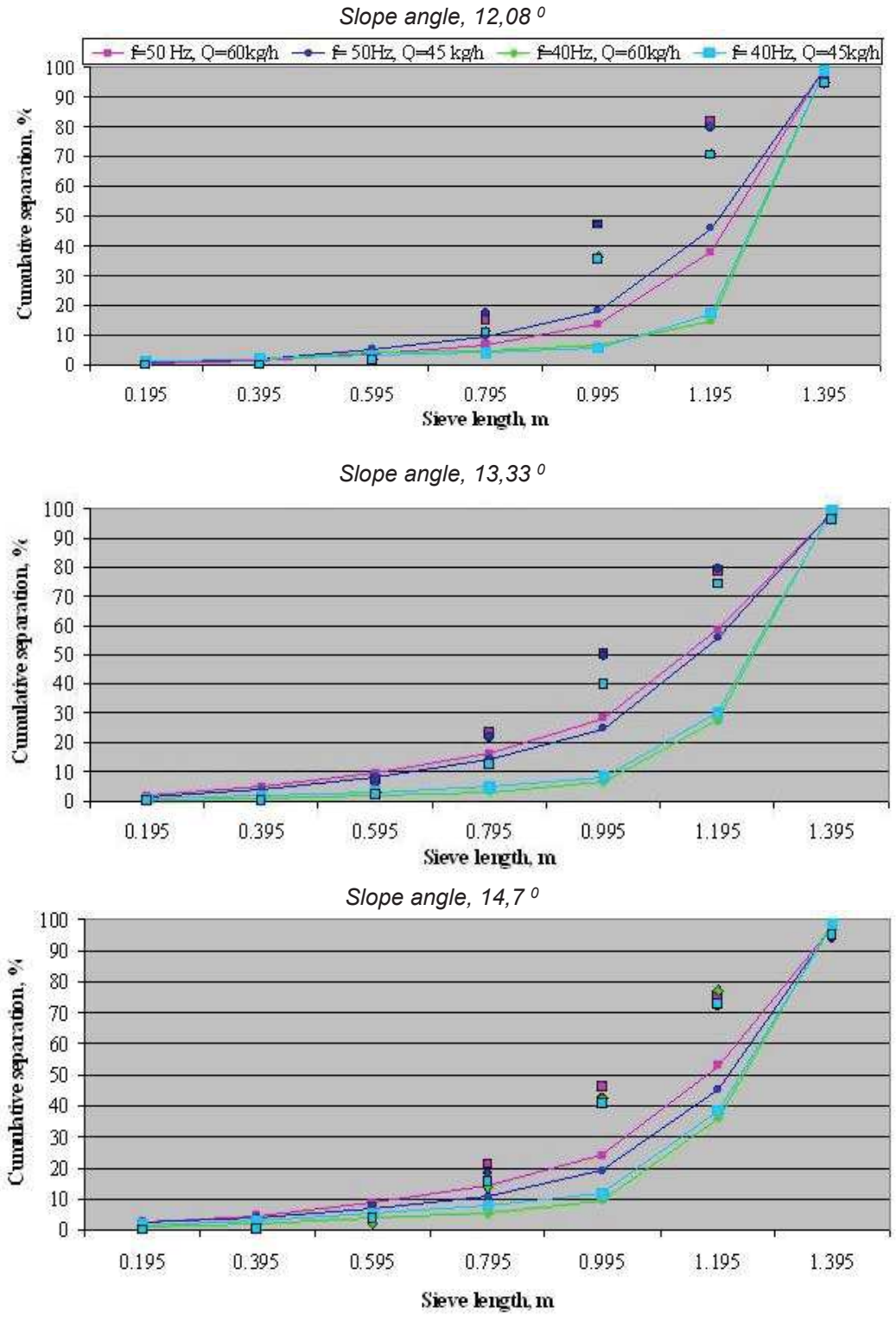

Figure 4: Cumulative variation of chicory fragments separation, on length of flat sieves, for three slope angle, for experimental values (represented by cu lines) and for Rosin-Rammler mathematical model values (represented without lines)

Coefficients values D_n and n for experimental data correlated with Rosin-Rammler equation (ec. 1), and R^2 correlation coefficient are presented in table 2.

Table 2: Coefficient values for experimental data correlated with Rosin-Rammler law type (ec. 1), D_n and n, and the R^2 coefficient of correlation for chicory

Experimental parameters	Coefficients								
	D_n	**n**	**R^2**	**D_n**	**n**	**R^2**	**D_n**	**n**	**R^2**
	Slope angle 12,08^0			***Slope angle 13,33^0***			***Slope angle 14,7^0***		
	Frequency 50 Hz								
Q_{alim} =60 kg/h	1.536	3.211	0.819	1.453	2.580	0.906	1.506	2.399	0.892
Q_{alim} =45 kg/h	1.523	2.936	0.851	1.471	2.716	0.890	1.573	2.341	0.866
	Frequency 40 Hz								
Q_{alim} =60 kg/h	1.690	2.643	0.734	1.617	3.177	0.781	1.591	2.899	0.809
Q_{alim} =45 kg/h	1.701	2.667	0.744	1.636	2.775	0.794	1.608	2.531	0.824

4. CONCLUSIONS

In the paper was presented the mode in which it is used distribution length low (Rosin-Rammler equation) of vegetable fragments in chicory fragments repartition on oscillating in function of plane sieve length in function of sieves hole dimensions. The chosen equation it is correlated well enough with experimental data values, being obtained high correlation coefficients $R^2 \geq 0{,}906$ for frequency 50 Hz, slope angle 13.33^0 , feed rates 60 kg/h but for frequency 40 Hz, slope angle 12.08, feed rates 60 kg/h being obtained low correlation coefficients $R^2 \geq 0{,}734$. Optimal separation efficiency is obtained when the vibrations parameters and slope angles have values high, for both feed rates, the thing that has been proven by many researches and by practical applications.

Acknoledgement

This paper was financed by support of National Agency for Scientific Research and Innovation, NUCLEU Programme, no. 8N/09.03.2016, Ad. Act nr.1/2016, Project PN 16 24 03 03 - „*Innovative technology and equipment for increasing the quality of plant raw material obtained from medicinal and aromatic plants, in the view of elaborating competitive organic products”.*

References

[1] Al-Snafi A. E., *Medical importance of Cichorium intybus – A review*, Volume 6, Issue 3, pp.41-56, 2016.
[2] Ardelean A., Mohan Gh., *Medicinal flora of Romania*, All Publishing House, Bucharest, pp. 285-286, 2008.
[3] Danciu A., Postelnicu E., Vlădut V., Voicea I., Matache M., Ludig M., Martinov M., Atanasov A., Florea C., *Experimentation of technology and equipments for primary processing of medicinal and aromatic plants. Obtaining of extractive solutions from medicinal and aromatic plants*, Magazine INMATEH - Agricultural Engineering, Vol. 34, No.2, 2011.
[4] Florea C.C., Bratucu Gh., *Study regarding the conditioning operation of medicinal plants and specific separation equipment*, Bulletin of the *Transilvania* University of Braşov, Series II: Forestry • Wood Industry • Agricultural Food Engineering • Vol. 6 (55) No. 1, 2013.
[5] Ioancea L., Kathrein, I., *Conditioning and Superior Capitalization of Vegetables Products in Food Purposes. Technologies and Installations*, Bucharest, Ceres Publishing House, 1998.
[6] Munteanu N., Sîrbu C., *Wild species of Compositae (Asteraceae) - vegetable potential in Iasi County*, Scientific Papers - vol. 51, series Agronomy, Iaşi, 2008.
[7] Neha M., Deepshikha P. K., Vidhu A., Amitesh K., Vidushi J., Alka M., Ritu V., *Determination of antioxidant and hepatoprotective ability of flavonoids of Cichorium intybus*, International Journal of Toxicological and Pharmacological Research; *6*(4): 107-11, 2014.
[8] Oztekin S., Martinov M., *Medicinal and aromatic crops: harvesting, drying and processing*, Haworth Press Publishing House, United States and Canada, 2007.
[9] Păun G., Gheorghe O., Diaconu M., *Guide of medicinal plants processing*, MedPlaNet Project, pp. 5,11, 2012.
[10] Rosin, P., Rammler, E., *The laws governing the fineness of powdered coal*, J. Inst. Fuel 7 (31), 29–36, 1933.
[11] Shad M. A., Nawaz H., Rehman T., Ikram N., *Determination of some biochemicals, phytochemicals and antioxidant properties of different parts of Cichorium intybus L.: A comparative study*, The Journal of Animal & Plant Sciences, 23(4): 1060-1066, 2013.
[12] *** – *Romanian Pharmacopoeia*, The Xth Medical Edition, Bucharest, 1993.

COOLING SYSTEMS FOR HYDRAULIC FLUID USED IN ELECTRO HYDRAULIC OPERATED INDUSTRIAL MACHINERY

Radoi Radu[1], Hristea Alexandru[1], Tudor Bogdan[1], Iulian C. Duțu[2]
[1]INOE 2000 – IHP Bucharest
[2]UPB - Faculty of Biotechnical Systems Engineering – Department of Biotechnical Systems;

ABSTRACT

Machinery which works long time (e.g endurance test stands) or in heavy conditions (e.g metallurgical industry), require cooling systems for hydraulic fluid used in actuation installations. Oil heating occurs because of power loss in the actuation system. Power losses occur at the oil circulation through pipelines or in hydraulic control devices (pressure relief valves, directional valves, proportional valves, etc.). Hydraulic fluid cooling can be achieved with water or air, via heat exchangers. The article shows the description of some components for cooling systems and theoretical elements on a cooling system sizing.

1. INTRODUCTION

A very important issue for the proper operation of a hydraulic installation is the provision of an optimal thermal regime for the working fluid, especially in the case of installations working continuously in automatic mode. Oil heating occurs because of power loss in the actuation system. Power losses occur at the oil circulation through pipelines or in hydraulic control devices (pressure relief valves, directional valves, proportional valves, etc.). Hydraulic fluid cooling can be achieved with water or air, via heat exchangers. Each system has advantages and disadvantages related to the gauge, installation and maintenance costs, corrosion and operating noise.

2. OIL HEATING IN HYDRAULIC ACTUATION SYSTEMS

Oil heating in hydraulic drives is caused by pressure drop [1] on elements of the installation such as relief valves, drosels, undersized directional valves, servo proportional directional valves, undersized pipes and contaminated oil, which cause increased differential pressures.

For laminar flowing regime that do not cause heating of the oil, the pipes dimensioning should be according to the values in Table 1.

Pressure drops that lead to oil heating may also occur when charging or discharging accumulators, hydraulic motor braking, and pump and valve leaks. Other causes of heating may be of a mechanical nature such as bearings friction or dynamic seals [2, 3] and heat produced by the solenoid valves.

The transfer and dissipation of the heat in the hydraulic installations is produced by the following ways:

- by conduction into solid bodies;
- by convection inside the hydraulic fluid;

[1]Cutitul de Argint street, No. 14, Bucharest, Romania, Tel. +4021 336 39 91, radoi.ihp@fluidas.ro
[2]313 Splaiul Independentei, Bucharest, Romania

- by radiation from a heat source.

Table1 : Regime of laminar flow rate in the pipeline

Type of pipeline	Fluid speed rate	
Suction and drainage	v = 0,5 … 1,5 m/s	
Return pipes	v = 2 … 3 m/s	
Pressure pipes	v = 3 m/s	for p < 25 bar
	v = 4 m/s	for p < 50 bar
	v = 4 … 5 m/s	for p = 50…100 bar
	v = 5 … 6 m/s	for p = 100…200 bar
	v = 6 … 7 m/s	for p > 200 bar

Components in the hydraulic drive system that have high pressure drops heat up and dissipate heat through conduction and radiation to nearby elements. Figure 1 shows a diagram for oil heating in a hydraulic installation containing proportional valves, obtained using a data acquisition system. The temperature of the oil is increased by 40 °C within ~ 30 min, the installation not being equipped with forced oil cooling system.

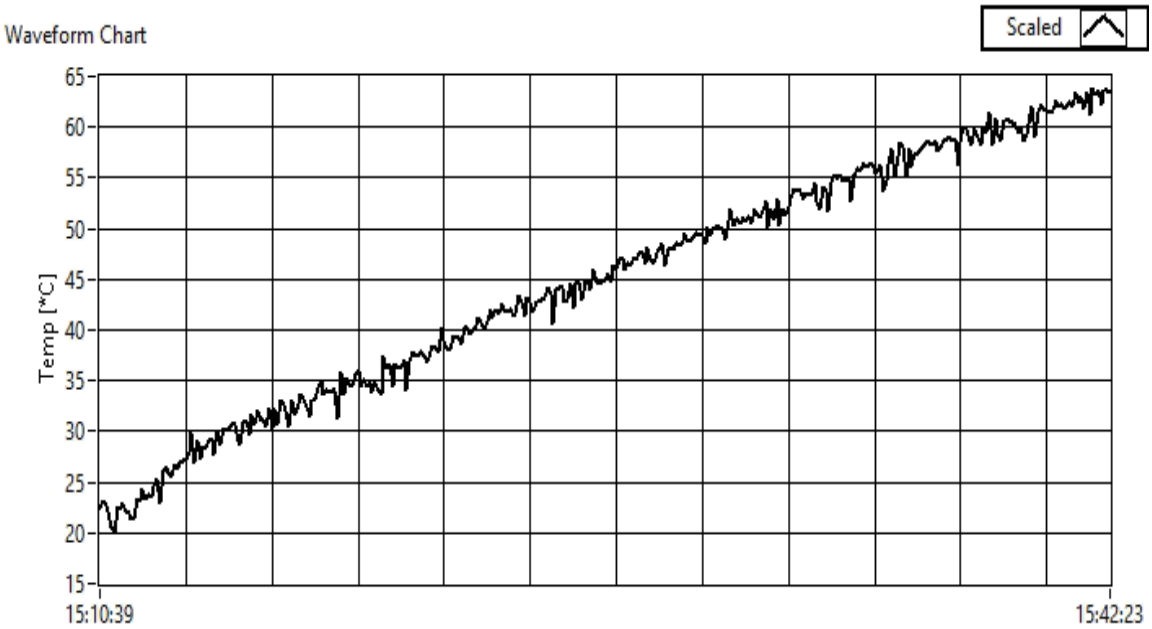

Fig. 1 Diagram of temperature increase of the oil in the installation

The heat stored in the hydraulic fluid naturally dissipates through pipelines through the walls of the tank or through components in which are no pressure drops and are colder.

The volume of the oil tank must be dimensioned as 2-3 times the flow rate of the pump for intermittent operation and 4-6 times for the continuous operation of the hydraulic installation. For example at a flow rate of 20 l / min the oil tank should have ~ 100 liters for a continuous operation.

Forced cooling of the hydraulic fluid can be done with heat exchangers. Figure 2 shows the location of a heat exchanger in the scheme of a continuous casting system that uses the proportional hydraulics. The installation includes a thermostat (10) which controls an electrovalve (8) which opens a cooling water circuit.

Hydraulic installations that work under heavy conditions and over long periods require mandatory refrigeration equipment. Hydraulic drives that operates intermittent or occasionally can also be built without forced cooling systems and can optionally be equipped with an

thermostat for warning when a certain temperature threshold is reached. The heat exchanger can be located on the return circuit to the tank or on an oil recirculation circuit from the tank.

Components

1	Hydraulic cylinder for product fastening
2	Hydraulic cylinder for product advance
3.1; 3.2	Proportional directional valve
4	Double pump
5.1; 5.2	Pressure valve
6.1; 6.2	Pressure filter
7	Tap
8	Water electrovalve
9	Heat exchanger
10	Thermostat
11.1; 11.2	Pressure transducer
12	Force transducer
13	LVDT

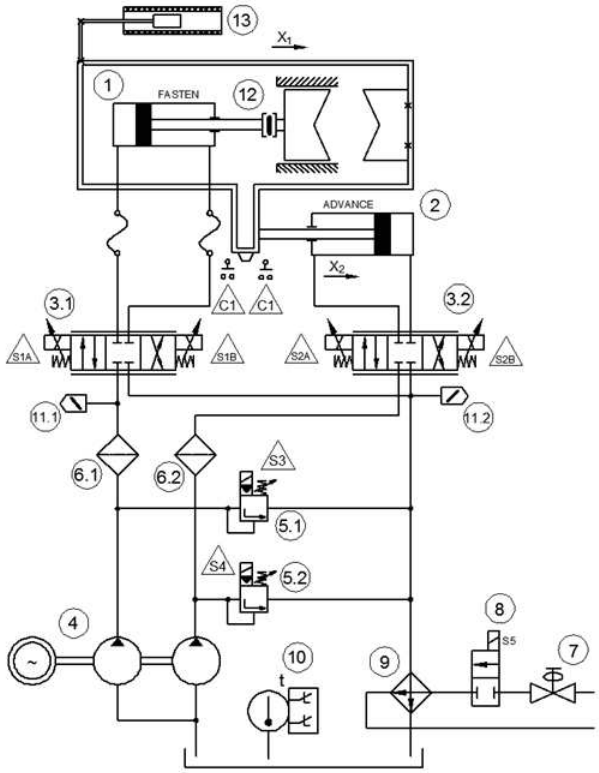

Fig. 2 Scheme of continuous casting installation provided with heat exchanger

3. DESIGN AND CHARACTERISTICS OF HEAT EXCHANGERS

Heat exchanger used in hydraulic actuation installations can be with heat exchange between oil and air or between oil and water.

Figure 3 shows the construction of an oil / air heat exchanger [4]. It consists of a radiator with fins and a casing on which a fan is mounted. The fan drive motor can be a compact electric motor, a normal electric motor or a hydraulic motor.

Fig. 3 Heat exchanger air oil with compact electric motor

The OILAIR 2020K model from Hansa Flex has a 230/400 V 50 Hz electric motor with a speed of 2600 rpm and an air flow of 645 m^3/h.

Oil / air heat exchangers can have built-in thermostat useful for the cooling automation system.

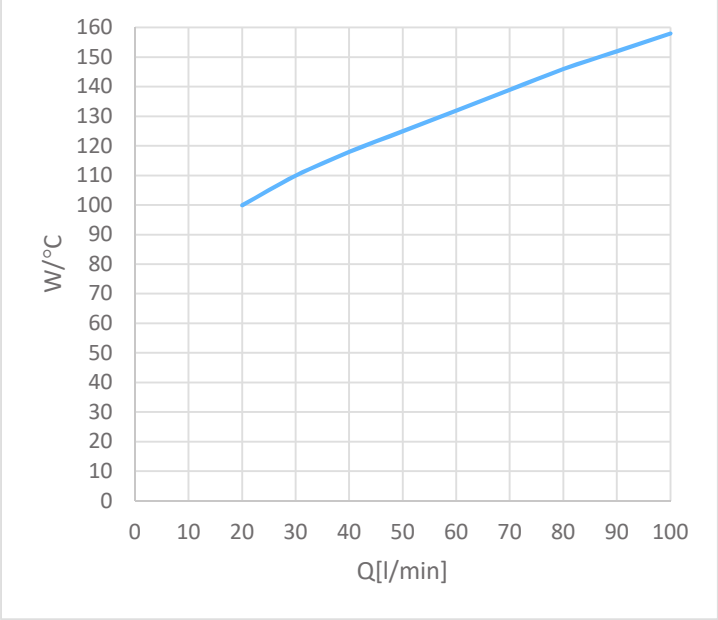

Fig. 4 Cooling capacity chart for OILAIR 2020K

Chiller charts are based on the inlet oil temperature and ambient air temperature. For example, if the oil temperature is 60°C and air temperature is 20 °C temperature difference is 40 °C and multiplying with 140 W/°C (figure 4) at a oil flow of 70 l/min results in a total cooling capacity of 5.6 kW. In figure 5 is the pressure drop chart for this model of heat exchanger.

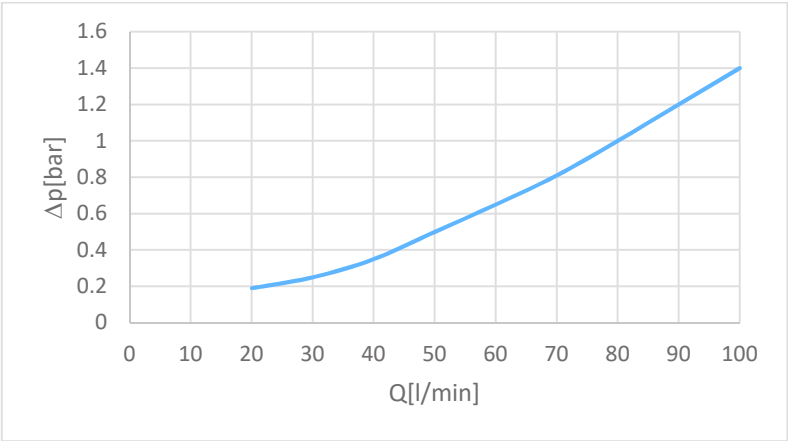

Fig. 5 Pressure drop chart for OILAIR 2020K

The second type of heat exchanger is the plate oil /water heat echanger [5]. They are designed to deliver high efficiency with the lowest pressure drop for hydraulic drive applications.

Figure 6 shows the construction of a plate heat exchanger. These coolers are manufactured by overlaying multiple layers of stainless steel plates with embossed patterns reversed on each layer, creating a network of contact points. The edges of the plates are glued by the brazing process in vacuum ovens. Oil and water circulate turbulently between plates and in opposite directions. By adjusting the flow rates, the oil temperature can be lowered to

close to that of the water. If the flow between the plates is turbulent, it prevents deposits of impurities that obstruct heat transfer.

The assembly should not be rigid in order to prevent the vibrations in the system from being transmitted to the cooler which can be damaged. Flexible hoses must be used for this purpose.

Fig. 6 PWO oil/water heat echanger from OLAER

Charts from figure 7 are given for ISO VG68 oil, inlet temperature of 60°C, water inlet temperature of 20°C and oil / water flow ratio 2:1.

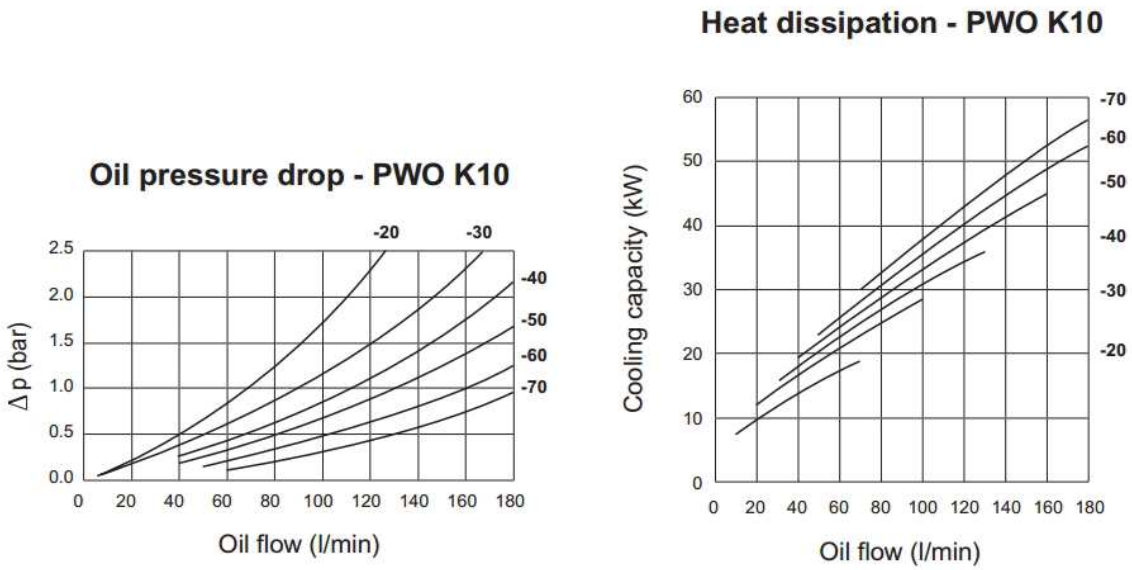

Fig. 7 Pressure drop and cooling capacity for a K10 heat exchanger produced by OLAER

Sizing of an oil / water heat exchanger

Sizing consists of calculating the area of heat exchange and water flow [6].
The area of the exchange surface is calculated with:

$$S = \frac{Q}{K \cdot \Delta T_m} \quad (1)$$

Q – heat to transfer (kcal/h)
For a hydraulic power unit of 7,5 kW → 50 % Q = 3,75 kW = 3224 kcal/h
K – coefficient of exchange (600 kcal/h°cm^2 for oil viscosity v = 46 mm^2/s)
ΔT_m - difference between oil and water average temperature
$\Delta T_m = T_{mo} - T_{ma}$
T_{mo} - average temperature of the oil (°C)

$$T_{mo} = T_o - \frac{\Delta T_o}{2} \quad (2)$$

T_o – max temperature of oil (°C)

$$\Delta T_o = \frac{Q}{q_o C_{so} 60} \quad (3)$$

q_o- oil flow in the heat exchanger (l/min)
C_{so} – oil specific heat (0,44 kcal/kg °C)
T_{ma} - average temperature of cooling water (°C)

$$T_{ma} = T_a + \frac{\Delta T_a}{2} \quad (4)$$

T_a – temperature of cooling water (°C)
ΔT_a – water temperature difference (for T_a = 20 °C → ΔT_a = 10°C)
q_w - cooling water flow (l/min)

$$q_w = \frac{Q}{\Delta T_a C_{sw} 60} \quad (5)$$

C_{sw}- water specific heat (1 kcal/kg °C)

3. CONCLUSIONS

A very important issue for the proper operation of a hydraulic installation is the provision of an optimal thermal regime for the working fluid.

Oil heating in hydraulic actuation systems is caused by the pressure drop on elements in the installation.

Some of the heat stored in the hydraulic fluid dissipates during the operation of the installation through the pipes, the walls of the tank or through some colder components.

It has been experimentally demonstrated that in a proportionally controlled hydraulic system without cooling system the oil temperature increases significantly over a short period of time.

References

[1] C. Cristescu, C. Dumitrescu, G. Vranceanu, L. Dumitrescu, "Considerations on Energy Loses in Hydraulic Drive Systems", In: Hidraulica Magazine, no. 1/2016, pp. 36-46, ISSN 1453 – 7303;
[2] P. Drumea, C. Cristescu, O. Heipl, "Experimental researches for determining the friction forces in the piston seals of the hydraulic cylinders / Experimentelle untersuchungen zur bestimmung der reibkräfte in kolbendichtungen von hydraulikzylindern", in: Proc. of the 17-th International Sealing Conference ISC-2012, pp. 473-48, Sept. 13-14, 2012, Stuttgart, Germany;
[3] G. Matache, St. Alexandrescu, A. G. Pantiru, Gh. Sovaiala, M. Petrache, "The analysis of flow losses through dynamic seals of hydraulic cylinders", HIDRAULICA no. 1, pp. 52-60, ISSN 1453 – 7303, 2013;
[4]Hansa-Flex, http://cat.hansa-flex.com/en/Hydraulic_components/Heat_exchangers/Oilair_coolers
[5] Olaer, http://www.olaer.com.au/pdf/cooler/catalogue/PWOinstallation.pdf, 2017.
[6] "Hydraulics in Industrial and Mobile Applications" (Assofluid), Publishing House: Grafiche Parole Nuove s.r.l., Brugherio (Milano), Italy, September 2007, pp.562-576.

RESEARCHES REGARDING THE DRIFT PHENOMENON IN THE FIELD CROPS SPRAYING MACHINES

PhD. Stud. Eng. Rosu (Nitu) M. [1)], Emeritus. Prof. PhD. Eng. Casandroiu T. [2)],
PhD. Eng. Matache M. [1)], PhD. Stud. Eng. Cujbescu D. [1)],
PhD. Stud. Biologist Pruteanu A.[1)], PhD. Eng. Rădulescu D.L.[3)], Eng. Bota M. S. O.[4)]
1)INMA Bucharest, 2) University Politehnica of Bucharest, 3) USAMV Bucharest,
4) BUILD PR Consulting SRL Cluj Napoca
E-mail: rosumihaelan@yahoo.com

ABSTRACT

Quality of agricultural products is closely related to the soil and plants state of health. Through application of phytosanitary treatments, it's intended to reduce the substance quantity at the same time with increasing the treatment efficiency. Quality of phytosanitary is determined in a great measure by the crop covering degree with phytosanitary substances and the reducing of drift phenomenon.

In this review we give a systematic report on the relevant physical properties of agricultural spray liquids, how these influence spray characteristics, and influence of spray characteristics on potential spray drift of field crop sprayers.

1. INTRODUCTION

In the modern agriculture, in addition to mechanization and irrigation, plant protection contributes to the continuous growth of production and labor productivity [6].

Growing social concern about the impact of pesticide applications on the environment and human health is promoting legislation to limit exposure to potentially dangerous plant protection products. Drift is recognized as being the most important source of diffuse environmental contamination caused by pesticide applications. According to ISO Standard 22866, spray drift is the quantity of plant protection product that is carried out of the treated area by the action of air currents. Drifting material may take the form of droplets, dry particles or vapor, and has potential negative effects on living organisms in areas adjacent to treatment. Currently it is not possible to avoid spray drift completely, but great efforts are carried out worldwide in order to minimize it. Impressive engineering advances have been achieved in creating increasingly accurate methodologies for assessing drift, new physical and mathematical models are improving our knowledge about all the phenomena associated to pesticide fate and deposition and novel technology and management practices are continuously emerging to reduce drift [11].

Pesticide exposure via spray drift can have a negative impact on bystanders, residents, livestock, terrestrial and aquatic ecosystems. Awareness of drift risks when operating with agricultural chemicals is therefore essential in order to minimize off-target contamination and at the same time fully benefit from product efficacy. Pesticides are typically applied as sprays which are formed when the liquid is atomized through a hydraulic nozzle [9].

Pesticide spray drift is the movement of pesticide from the target area to areas where the pesticide application was not intended. Pesticide drift is caused by the movement of spray droplets. Several factors contribute to the potential for the drift of pesticide spray droplets. Drift management strategies often focus on weather conditions as the primary culprit in pesticide movement. However, the influence of weather conditions, such as wind, temperature, and humidity, is based on spray droplet size. The larger the spray droplet, the lower the risk of pesticide drift [5].

The paper is a review which presented the spray components contributing to drift potential, the relevant physical properties of spray liquids, type of spraying according to the droplet diameter and pesticide type and coverage according droplet size.

2. METHODOLOGY

Considering data present in the paper [1], was investigated how some measurable characteristics can be linked with spray drift as measured in a wind tunnel.

A systemic representation of drift physical factors was adopted in this study as given in Fig. 1. In this figure three main systems are identified: droplets, the spray pattern and external conditions. Drift potential can be attributed to a combination of these systems. It is obvious that the system "droplets" is a sub-system of the system "spray" but this representation was chosen to evidence that external conditions can interact both with individual droplets and their characteristics but also with the spray in its globality. The measurable characteristics of each system are indicated in boxes [1].

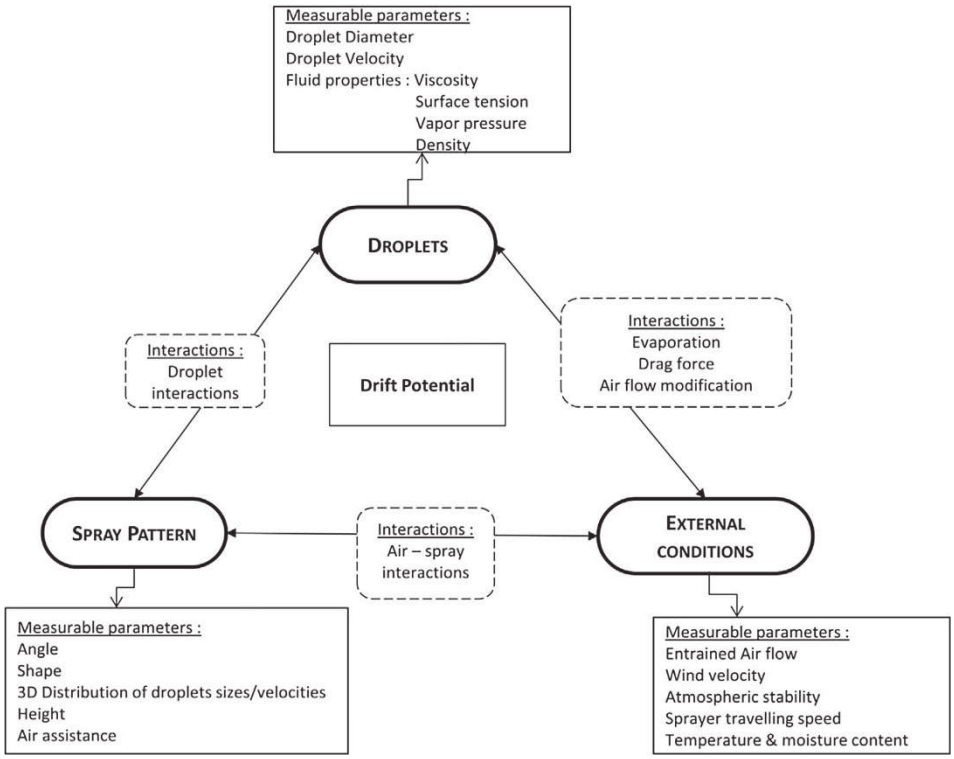

Figure 1: Systemic representation of spray components contributing to drift potential. Interactions between components and components measurable parameters are indicated in dash and solid rectangles respectively [1]

Spray drift is influenced by environmental and meteorological conditions, the spray technique and the crop. Wind speed and wind direction are meteorological factors that influence spray deposition. Relative humidity and high air temperature can reinforce evaporation by decreasing the droplet size of particularly small spray droplets subsequently decreasing their sedimentation velocity and making the more drift-prone. The fate of spray droplets is influenced by operating conditions such as application height, driving speed of sprayer, nozzle spacing . Air-assisted spraying and use of shielded sprayers in general reduce spray drift . The use of an end nozzle at the edge of the field prevents overspray of pesticides [9].

The researches on agricultural sprays shows that there are essentially three relevant physical properties of spray liquids that influence the mechanism of spray formation. These

properties are: shear and extensional viscosity; surface tension; the presence of inhomogeneities in the spray liquid such as emulsion droplets or solid particles [9].

The extensional **viscosity** is the resistance of a fluid to stretching forces in an extensional flow that determines the resistance of a fluid to form a new interface [3].

Polymer-based drift control additives are commonly used in US and Australia to decrease spray drift. The general mode of action of polymeric material is based on the increase of the liquid viscosity which induces the formation of coarse sprays by shifting the droplet size distribution to a larger size. Polymer liquids that show elongational thickening increase most efficiently the spray droplet size. Three parameters have been outlined that influence the elongational viscosity of polymer solutions: rigidity of the polymer chain, its molecular weight and concentration [9].

Dyes that are used to trace spray droplets in drift experiments can decrease the **surface tension** of the spray liquid . Polymers have little effect on the surface tension of spray solutions. Additives such as spreader and wetting agents contain surfactants that promote the wetting and the coverage of the target surface. This effect was correlated with a decrease in the dynamic surface tension of the spray liquid at the moment of droplet impact on the leaf surface. The dynamic surface tension at much shorter times is relevant for the spray formation process. This implies that additives that decrease the dynamic surface tension sufficiently to improve the retention and the wetting properties of spray droplets will not necessarily influence spray formation. The surface tension of water decreases with increasing temperature. This effect has to be considered because water is mostly the carrier liquid in agricultural spray applications [9].

Agricultural sprays that contain solid particles such as crystalline active ingredient, emulsion droplets, or both are liquid systems with **inhomogeneities**. Many pesticide formulations contain a crystalline active ingredient of a few microns in size. These crystals are homogeneously distributed throughout the bulk liquid by means of dispersing additives. In several experiments reported in literature, solid dispersions were shown not to influence either the spray droplet size spectra or the spray disruption patterns. However, some experiments have been performed where spray liquids with solid particles coarsen the spray droplet size [9].

3. RESULTS

In theory, depending on the average size, respectively, of the average volumetric diameter of the droplets used in the spraying work, spraying is classified according to the table 1 [12]. Agricultural sprays [2] are often characterized by a mean droplet diameter, according to the table 1.

Table 1: Tipul de pulverizare în funcţie de diametrul volumetric al picăturilor[12, 2]

Type of spraying	Droplet diameter [μm]	
	Reference [12]	Reference [2]
Extremely coarse	-	> 450
Very coarse atomisation	> 500	375 – 450
Coarse atomisation	300 – 500	250 – 375
Medium atomisation	200- 300	175 - 250
Fine atomisation	100-200	100 - 175
Very fine atomisation	< 100	< 100

The desired spray droplet size is dependent on the type of pesticide (Table 2) [5].

Table2: Droplet size classification [5]

Classification	Size [µm]	Pesticide type
Very fine	< 119	Insecticide
Fine	119 - 126	Fungicide
Medium	217 - 353	Contact herbicides
Coarse	354 - 464	Translocated herbicides
Very coarse	> 464	Soil-applied herbicides

In practice, depending on the droplet size, different degrees of coverage have emerged, using different nozzle types (table 3) [7].

Table 3: Droplet deposition results for each nozzle type listed by the collector position for each model [7]

Nozzle	Pressure [kPa]	$D_{v0,5}$ [µm]	Ground	Lower	Middle	Top
			Coverage [%]			
XR 11003 (reference)	350	213	35.1	34.4	36.4	37.7
AI 11002	350	499	20.2	24.5	22.9	25.2
AIXR 11002	350	381	30.9	31.7	30.7	34.2
Mini Drift 11002	350	375	29.3	28.4	30.5	30.9
TDADF 11002	350	365	28.5	31.9	34.2	32.1
Turbo Teejet 11002	350	279	26.8	26.9	29.0	30.1
TTI 11002	350	722	21.0	23.5	21.5	26.0
XR 11002	350	157	36.6	37.4	37.5	38.3

The results in table 3 shows that the coverage was not as strongly correlated to droplet size, though the nozzles that resulted in the highest and lowest coverage across collector placement were the Finest and Coarsest spray quality nozzles respectively.

Table 4 presents the characterization of the physicochemical properties of the applied pesticides. The tracer did not cause major changes to the spray due to the similarity between the properties of the water and the spray to be applied [4].

Table 4: Characterization of the physicochemical properties of the water and spray liquid [4]

Physicochemical properties	Water		Spray liquid	
	Mean	Standard deviation	Mean	Deviation
pH	7.50	±0.02	7.42	±0.03
Electrical Conductivity (µS cm^{-1})	18.0	±2.38	18.8	±5.14
Density (kg l^{-1})	997.5	±1.7	993.7	±2.1
Viscosity (mPa s)	1.05	±0.02	1.04	±0.02
Surface tension (mN m^{-1})	80.0	±0.41	74.04	±1.34

The risk of spray drift is closely related to the spray droplet size. At the same time droplet velocities, trajectories and porosity of the spray plume influence droplet deposition. Nozzle design, orifice size, operating pressure and entrained air currents influence the size and the velocity of spray droplets. Coarser sprays with a smaller fraction of fine droplets are produced by low-drift and air-induction nozzles. Drift reduction for low-drift nozzles can be defined as the reduction in the airborne portion as compared to a reference nozzle [9].

Air - induction nozzles produce larger droplets that contain air bubbles and that move with lower velocities as compared to droplets of equivalent size produced by conventional flat

fan nozzles. Several methods exist to estimate the quantity of the air intake for air - induction nozzles [9].

In the paper [8], the authors tested the drift reduction at DISAFA (Italy) and DEAB (Spain) laboratories in the different environmental conditions:

- For the DEAB field trials, the average wind velocity during all the tests was 0.20 m s^{-1}, with a maximum value of 0.45 m s^{-1}. The temperature ranged from 10 to 25°C, and the relative humidity was between 70% and 90%.
- For the DISAFA trials, the average wind velocity measured during the tests was 0.45 m s^{-1}, with a maximum value of 0.69 m s^{-1}. The air temperature ranged between 18° C and 20^0C, and the relative humidity was between 65% and 75%.

The table 5 presented drift reduction values obtained for conventional and air induction nozzles.

Table 5: Drift reduction values (%) obtained for conventional and air induction nozzles [8]

Nozzle size	DISAFA		DEAB	
	Conventional nozzle	Air induction nozzle	Conventional nozzle	Air induction nozzle
ISO 02	- 69.4	70.9	-37.6	89.4
ISO 03	0	81.5	0	58.6
ISO 04	33.6	80.2	52.7	75.9

These drift reduction values were obtained considering the conventional ISO 03 nozzle as the reference nozzle. Negative values imply an increase in drift [8].

In the Netherlands was introduction of unsprayed buffer zones for reducing pesticide impacts on linear landscape elements adjacent to cropland. A model was constructed for the relationship between distance from treated fields and deposition of pesticides. To this end was used a power model of the form

$$y = a(x + c)^{-b} \quad (1)$$

where y is the deposition as a percentage of maximum field dose, x is the distance from the last sprayer nozzle, c is the distance between the last nozzle and the field edge, and a and b are constants (see Fig. 1). For these two constants a best-fit method was adopted. With this equation, at the field edge x =0 m and c =the buffer zone width [10].

In the table 6 are presented the main characteristics of the nozzles used in both test trials [1, 8].

Table 6: Drift estimated according to nozzle type and working parameters

Nr. Crt.	Nozzle type	Nozzle angle	Distance [mm]	Pressure [bar]	Drift [%]	Reference
1	Hardi LD F110 02	110	500	3	4,21	[1]
2	Hardi LD F110 03	110	500	3	2,94	[1]
3	Hardi LD F110 04	110	500	3	3,28	[1]
4	Hardi Injet 110 02	110	500	3	1,31	[1]
5	Hardi Injet 110 03	110	500	3	1,16	[1]
6	Hardi Injet 110 04	110	500	3	0,97	[1]
7	XR 110 02	110	500	3	35,71	[8]
8	XR 110 03	110	500	3	24,32	[8]
9	XR 110 04	110	500	3	20,31	[8]
10	AIXR 110 02	110	500	3	2,78	[8]
11	AIXR 110 03	110	500	3	2,11	[8]
12	AIXR 110 04	110	500	3	1,74	[8]

3. CONCLUSIONS

– The application of pesticides in field crops with a conventional nozzle depend on the ejecting velocity, the design of the nozzle, the size of the orifice, and physical properties of the spray liquid and the ambient gas.

– The important factors which affect drift behavior during application of pesticide products, are the environmental and meteorological conditions (temperature, humidity and wind speed).

– According to the data reported in literature, it can be concluded that not only spray-mix additives but also certain formulation types can be used to reduce spray drift.

– Spray drift has been studied extensively in a series of field trials and crops, the results from these studies are currently used in quality growth spraying.

– Drift risk is often correlated with spray droplet size, in particular with the percentage of fine spray droplets.

– Coverage varies depending on the nozzle type, droplets size and pesticide type.

– For adequate coverage and good pest control, but large enough that the risk of drift is reduced, the particles must haven't less a mass small, because are more prone to travel long distances.

References

[1] Al Heidary M., Douzals J.P., Sinfort C., Vallet A., *Influence of spray characteristics on potential spray drift of field crop sprayers: A literature review*, Crop Protection 63, pp.120÷130, 2014

[2] ASAE., *S-572 Spray Tip Classification by Droplet Size. Developed by the Pest Control and Fertilizer Application Committee*; Approved by the Power and Machinery Division Standards Committee; Adopted by ASAE PM41, 2009.

[3] ASTM International,. *Designation: E2408 - 04. Standard Test Method for Relative Extensional Viscosity of Agricultural Spray Tank Mixes*, 2006.

[4] Bueno M. R. , Paulo J., Cunha A. R., Santana D. G., *Assessment of spray drift from pesticide applications in soybean crops* , Biosystems engineering 154, pp. 35 -45, 2017

[5] Colquhoun J., *Drift management: practical methods to increase spray particle size*, www.mssoy.org/uploads/files/colquhoun-osu-ext-serv.pdf

[6] Costache N, Luca E., *Mechanization of Chemistry Works in Agriculture,* Publishing House CERES, Bucharest, 1982

[7] Ferguson J. C., Chechetto R. G., Hewitt A. J., Chauhan B. S., Adkins S. W., Kruger G. R., O'Donnell C. C., *Assessing the deposition and canopy penetration of nozzles with different spray qualities in an oat (Avena sativa L.) canopy*, Crop Protection 81, pp.14-19, 2016

[8] Gil E., Balsari P., Gallart M., Llorens J., Marucco P., Andersen P. G., Fàbregas X., Llop J., *Determination of drift potential of different flat fan nozzles on a boom sprayer using a test bench*, Crop Protection 56, pp. 58÷68, 2014

[9] Hilz E., Vermeer A. W.P., *Spray drift review: The extent to which a formulation can contribute to spray drift reduction*, Crop Protection 44, pp.75÷83, 2013

[10] Jonga F. M.W.,. Snoob G. R, Zandec J. C., *Estimated nationwide effects of pesticide spray drift on terrestrial habitats in the Netherlands*, Journal of Environmental Management 86, pp. 721÷730, 2008

[11] Moltó E., Chueca P., *Engineering approaches for reducing spray drift*, Biosystems Engineering, Volume 154, February 2017, pp 1–2

[12] Stahli W., Bungescu S. T., *Apparatus, equipment and machinery for plant protection,* Publishing House AGROPRINT, Timişoara, 2006

VIBRATORY PHENOMENONS IN CLEANING EQUIPMENTS OF AGRICULTURAL PRODUCTS WITH OSCILLATING PLANE SIEVES AND VIBRATORY CONICAL SIEVES

Stoica D. [1], Voicu Gh.[1], Duțu I.C.[1], Constantin G.A.[1]
[1] University Politehnica Bucharest, Biotechnical Faculty of Engineering, dorelstc@yahoo.com

ABSTRACT

Within this paper are presented the results of some experimental researches on the workflow and on its efficiency of a sieve having conical exterior surface and alternative periodic movement. The sieve is suspended at the upper and bottom part, by means of three elastic cables (made of silk), having the diameter ϕ1.5 mm. The diameter of the circular holes of the sieve is ϕ4.2 mm. The sieve is centrally feed, at the upper part, through a tube with diameter ϕ50 mm having adjustable position towards the sieve, to obtain different work flows. The separated material is collected at the bottom part of the sieve, in a container consisting of various circular segments, of different diameters. The oscillatory movement was obtained by means of an eccentric drive, placed in horizontal plane, and acting on tangential direction to the sieve, at adjustable distances. The sieve was used to sort rapeseeds with dimensions varying between 1.6 mm and 2.5 mm, in percentage of 90%.
Keywords: conical sieve, oscillating movement, sieving, rapeseeds, sorting degree, unseparated seeds

1. INTRODUCTION

Dynamic development of the highest achievements of science and technology, of all industrial branches, has posed problems with ample dimensions to design, machinery and equipment construction and their exploitation.

Performance enhancement can be achieved by applying new concepts, new calculation methods, new technologies and materials, being justified concerns oriented to a more reliable operation, more efficient.

Of the many parameters that, by measurement, give a picture of the state of operation, vibrations and noise produced by machinery and equipment have attracted, in recent years, the attention of researchers, designers, builders and exploiters. Together with other parameters, vibration and noise provide great sensitivity to the analysis, but also individuality to concrete situations, apparently repeated.

Development of vibration and noise measurement technique, as well as the development of signal processing techniques, have enabled important improvements in the control, monitoring and diagnostic systems.

Prior to the capitalization of agricultural products in various fields, they are subjected to a conditioning process involving preparatory operations as: cleaning of foreign bodies, drying, wetting, depending on the purpose in which it is intended to be used.

In the first operation of processing agricultural products, in order to obtain finished products, of superior quality, there is also the removal of foreign bodies, in particular from seed mixtures of different agricultural crops.

Also, using seeds for sowing, both the removal of foreign bodies is necessary, which is different from the seeds of agricultural crops in general, by their physical characteristics, and the removal of seed with low germination capacity, of the poorly developed or crushed seed.

[1] University Politehnica Bucharest, Biotechnical Faculty of Engineering, Splaiul Independentei, 313, District 6, Bucharest, Romania, 0724917143, dorelstc@yahoo.com

The vibratory movement is used, in practice, in many areas of activity, both for the transport of granular and powdered products or even in the form of pieces, and to complete the separation processes.

Also, vibratory movement is used to feed uniformly with material the various separation or processing machines, as is the case of harvesting and processing agricultural products field.

Agricultural machines performing these operations, often inseparable, perform one or more of these concurrently, the name of the equipment being determined by the main operation (e.g. seed cleaner equipment, seed cleaning and sorting machine, selector).

Machines for cleaning and sorting seeds must meet certain requirements for the smooth running of the work process, namely:

- To ensure the production of a good quality product that meets the requirements of the standards in force;
- Not to cause seed loss through breakage or mechanical injury;
- Be as universal as possible (can be used in seed of as many crops);
- Not to be sources of dust, as most work in closed rooms;
- Be as simple as constructive and have high safety in operation;
- Ensure that adjustments and supervision are as easy as possible during operation;
- To allow wide-ranging adjustment of the main functional parameters related to the machine specific working process;
- To require as little energy as possible;
- To meet the requirements of labor protection laws.

Production and quality of any agricultural crop is determined by factors that influence from the time of sowing to harvesting, as well as those who directly influence seed prior to sowing.

Following the harvesting process, is obtained a mixture formed from seeds, chaff, dust, seeds from other crops, including weeds, mechanical impurities.

Seed preparation for seeding or consumption, to respond to increasingly demanding modern technologies, comprises a complex of operations to remove all impurities and non-valuable seeds.

In order to achieve great and high quality productions, an important role is to provide a seed fund of hybrids with the highest genetic attributes appropriate for each pedoclimatic area. Taking into account these conditions, the cleaning and sorting operations must be performed on specific and performing machines. At cleaning, from the initial mixture the seeds of the basic culture are separated from the rest of the mixture, and in sorting these are separated into fractions that differ according to one or more of the criteria: Dimensions, density, shape, aerodynamic properties, color, electromagnetic properties et al.

Sorting can be done separately or concurrently with the base or extra cleaning. Seeds sorted (uniform as size) is sowing with greater precision, grow uniformly and produce more vigorous plants.

Also agricultural products for consumption (vegetables, fruits, seeds), must be as uniform as possible, of the appropriate quality, and their cleaning and sorting imply among others, in the majority of cases, working organs with vibratory movement.

Therefore, developing and continuing research on study of technology that imply vibratory phenomena in machinery and equipments for the processing of agricultural products, aims to improve mechanized cleaning and sorting of seeds.

Because researches conducted nationally and globally concerning the equipment used for seed conditioning have not exhausted all the aspects to be taken into account, it is necessary to continue these researches, on the study of modern technologies that involve

vibrational phenomena, in equipments and machinery for the processing of agricultural products, in general, and seed conditioning in particular.

At the same time, are equipments for agricultural products processing which have been proposed by various specialists in the field whose work process has remained unstudied, both as a whole, as well as the influence of the various parameters of the working regime and on the process and on the process quality indices.

Experimental research on the separation process on sieves with oscillating motion has been carried out by numerous researchers around the world.

So, separation of material on sieves is influenced by the amplitude and frequency of the oscillations, which ensures the relative movement of the material on the separation surfaces. Other parameters that affect separation are: sieve slope, the internal and external friction angles of the material, sieve aperture size, average particle size, [1].

Clogging of the sieve aperture depends on the particle size, phenomenon investigated by R.Feller in papers [2,3].

Mechanical grading of seeds by sieves is not a complete classification, every time in a fraction being found 10-20% from particles of another fraction, [4].

In these paper, are presented the results of some experimental research on a sieve from perforated sheet with outer conical separation surface, with the angle of inclination of 8°, provided with circular apertures of diameter ϕ4.2 mm, used to separate large impurities from rape seeds, but which, by the oscillation motion made can also be used for sorting seeds with dimensions smaller than the diameter of the apertures of the sieve.

2. METHODOLOGY

The simplified scheme of the machine used for the experimentation is presented in fig.1. [5]

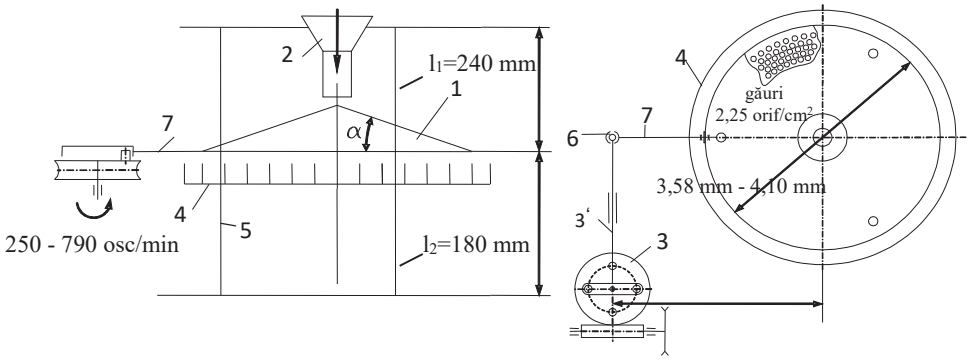

1.conical sieve with circular aperture; 2.feeding funnel; 3. actuating mechanism with worm gear and oscillating slide; 3'.oscillating slider arm; 4.collecting box for separated material; 5.metallic suspension cables; 6. spherical joint; 7. Radial connection arm of the sieve actuator

The actuation mechanism is composed of an electric motor with alternating current of 710 W electric power and a system of worm gear and oscillating slide type, with the actuator button eccentrically arranged on the worm gear of the transmission of mechanism.

No. sample	Sieve interval on which the seeds are collected x, (m)		0	0.04	0.07	0.1	0.13	0.16	0.205	Over sieve
1	Working regime parameters		A_2 = 3.74 mm; F_1= 250 osc/min; Q_1 =0.020 kg/s							
	Seeds collected under the sieve	g	0	147	200	140	12	1	0	0
		%	0	29.4	40	28	2.4	0.2	0	0
2	Working regime parameters		A_2 = 3.74 mm; F_1= 250 osc/min; Q_2 =0.033 kg/s							
	Seeds collected under the sieve	g	0	141	159	105	52	28	15	0
		%	0	28.2	31.8	21	10.4	5.6	3	0
3	Working regime parameters		A_2 = 3.74 mm; F_1= 250 osc/min; Q_3 =0.042 kg/s							
	Seeds collected under the sieve	g	0	115	141	92	59	42	21	30
		%	0	23	28.2	18.4	11.8	8.4	4.2	6

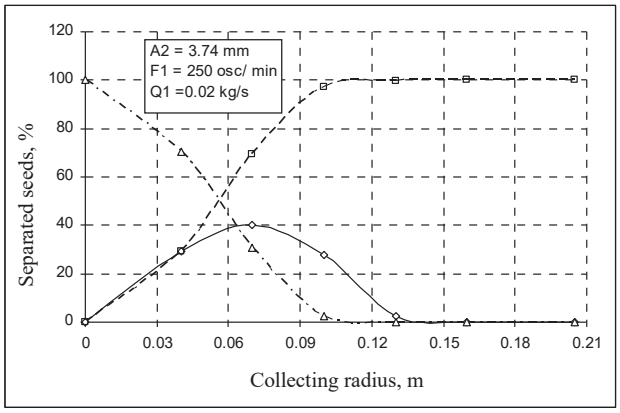

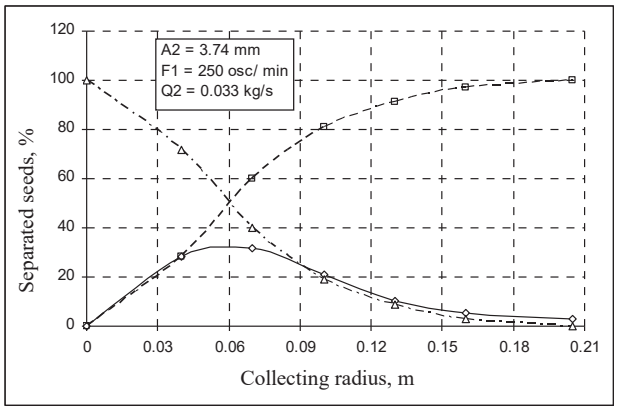

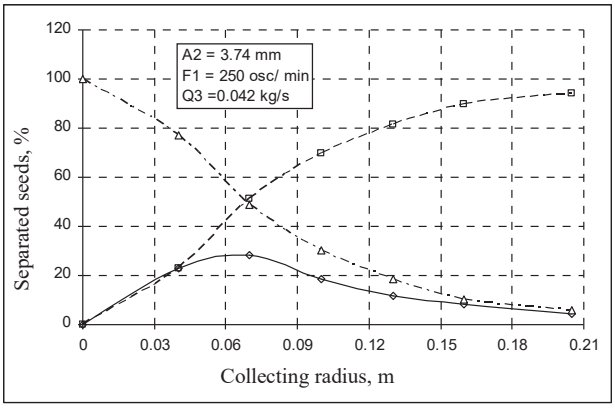

Separation curves of material on the conical sieve generatrix for motion amplitude A_2=3.74 mm, oscillation frequency F_1 = 250 osc/min and three workflow feed Q_1=0.020 kg/s, Q_2=0.033 kg/s and Q_3=0.042 kg/s

—◇— material distribution curve -□- cumulative curve of sifted material on sieve
-·△·- cumulative curve of refused material by sieve

Were recorded the sample mass and high impurity content were recorded, length of sieve arm measured from vertical axis of conical sieve to arm joint with the actuator stem, the distance between the bottom edge of the feed funnel to the sieve surface, position of the actuator button (oscillation frequency), experiment time.

After performing the experimental determinations, the material in each compartment of the collecting box, was collected, weighted and recorded in data tables correlated with the position of the compartment on the sieve generatrix.

Was calculated the feeding workflow, reporting the seed mass of the sample at the drainage time of material from the funnel.

During experimental determinations it was found that starch impurities in the seed mass have completely exceeded the bottom edge of the sieve, to all the samples performed.

For ease of data processing And plotting representative experimental curves of the working process, the mass of material collected in each box under the sieve was reported on the seed mass of the sample, results being shown as a percentage of this.

The centralized table has been compiled with measured and calculated data for experimentation in which the following data was recorded: feeding workflow (in kg/s), oscillation frequency (osc/min), oscillation amplitude A_i .

At the same time, were recorded quantities of material collected on sieve radius both in grams and in percentages, as well as the quantities of material that passed beyond the edge of the sieve.

Based on percentages of seeds separated on collecting radius of sieve were plotted the separation intensity curves, i.e. the relative distribution of the material separated within the radius of the base of the cone.

The course of the oscillating slide of actuating system is of 16 mm, slide arm being articulated through a spherical joint to the reinforced arm with the sieve arranged radially to the cone base circle.

Oscillation frequency can change from the electric motor by varying the electrical current parameters, and oscillation amplitude Can be changed by changing the position of the actuating mechanism relative to the radial arm of the sieve, Articulated to each other by the spherical joint 6.

Density of circular apertures on the separation surface was of 2.25 orif/cm^2, Which led to an active area of about 31%, the length of the suspension cables of the sieve being l_1 =240 mm, l_2 = 180 mm.

Reduced dimensions of the separation surface were chosen so that the experimental determinations do not require a large amount of material, but by geometric similarity its dimensions can be increased in such a way that the working capacity of the sieve under exploitation conditions, can grow either.

Starting from the distribution curve that presents the amount of material collected over a given sieve range, one of the other two curves can be obtained, which presents either the cumulative amount of material separated through the apertures of the sieve, or the cumulative amount of material not separated and carried by the sieve to the outlet end.

Curves can be plotted based on the amount of material separated, expressed both in mass units and in percentages, but it is preferable to estimate in percent for a more suggestive presentation of experimental data.

Our analyzes, have used normal distribution laws in regression analysis, and from studying the obtained graphs it was found that these curves have a maximum positioned at a certain distance by the feeding point of the sieve, which leads to the conclusion that the material movement on the separation surface can be appreciated by the position of this maximum towards the end of the sieve (to us its center where the material is being fed).

As a result, the curves may show a certain asymmetry over the sieve collection center, Either of left or of right, Which shows the rapidity or delay with which the material has been separated, as can be seen from fig.2.

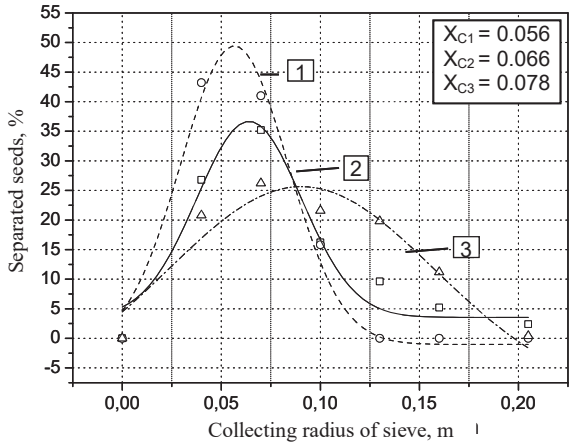

Fig.2. Types of distribution curves with different asymmetry
1. curves with left asymmetry; 2. curves without asymmetry; 3. curves with right asymmetry

If the graph shows a left asymmetry, respectively, the maximum of curve is closer to the feed end of the sieve, It means it has separated faster, while if the graph shows a right asymmetry, respectively, the position of the maximum of distribution curve is further from the feed end, it means that the separation was done somewhat later.

3. CONCLUSIONS

The process of separating the material on the sieves with oscillating motion, Can be represented by two curves (or three), which represents:

- the intensity of material separation along the length (radius) of sieve
- the distribution curve and one of the total separation curves (cumulative) of the material that has passed through apertures on a given sieve length or of the material that has not been separated on the same length or separation zone.

The findings resulting from the analyzes performed are specified in each subchapter. Thus, an efficient separation of seeds through the apertures of the sieve Takes place at a frequency of oscillation between 250 – 520 osc/min and at the average amplitude of the sieve movement in the direction of the actuating arm.

The sieve can also be successfully used for sorting by sizes seeds of the same crop If the working regime parameters are appropriately selected.

References

[1]. H. P. Harrison, A. Blecha, 1983. Screen oscillation and aperture size – Sliding only, *Transactions of the ASAE*, pp.343-348.
[2]. R. Feller. 1977. Clogging rate of screens as affected by particle size, *Transactions of the ASAE*, pp.758-761.
[3]. R. Feller. 1980. Screening analysis considering both passage and clogging. *Transactions of the ASAE*, pp.1054-1056.
[4]. C. Elfverson, S. Regnér. 2000. Comparative precision of grain sieving and pneumatic classification on a single kernel level, Applied Engineering in Agriculture, VOL. 16(5): 537-541.
[5]. Stoica D. Contributions to the study of vibrational phenomena in the field of processing of agricultural products (PhD Thesis)
[6]. D. Stoica, G Voicu, GA Constantin, C Carp-Ciocardia, V Moise - Kinematic study of a vibrating conical sieve for separating impurities from seed of agricultural crops- Proceedings of the 41 International Symposium on Agricultural Engineering – Actual Tasks on Agricultural Engineering, ISSN 1333–2651, Opatija, Croatia 19-22. february 2013

INFLUENCE OF THE NUMBER OF PASSES ON SOIL COMPACTION – A REVIEW

Nicoleta UNGUREANU[1], Valentin VLĂDUŢ[2], Sorin-Ștefan BIRIȘ[1], Dan CUJBESCU[2], Daniel Ion VLĂDUŢ[1], Neluș-Evelin GHEORGHIȚĂ[1], Ioan CABA[2]
[1]Politehnica University of Bucharest, Faculty of Biotechnical Systems Engineering, Romania;
[2]INMA Bucharest, Romania

ABSTRACT

Compaction is the most difficult type of soil degradation and it can be regarded as a mechanical pollution arising as a consequence of poor management of agricultural practices. In mechanized agriculture, soil tillage is often carried out by heavy agricultural machinery, with repeated passes, most often on soils with high moisture content. These machines apply mechanical stresses to the soil, which are further transmitted to different depths, resulting in the artificial compaction of soil, a phenomenon that affects the capacity of plant development and hence the agricultural production. The paper presents a summary of results reported in the literature regarding the influence of the number of passes of agricultural machinery on the artificial compaction, under various conditions, in terms of the variation of cone index and of stresses transmitted into the soil.

1. INTRODUCTION

In the actual context of continuously increasing world population, to cope with the demand for more food it became necessary the intensification of farming and cropping systems. As a result, more and heavier farm machinery and animals per soil area have become common all over the world. Soil compaction is a form of physical degradation resulting in densification and distortion of the soil where biological activity, porosity and permeability are reduced, strength is increased and soil structure partially destroyed [20].

Soil compaction is not a recent phenomenon. It existed in form of hardpans long before the advent of intense agriculture [4]. Nowadays, the risk of soil compaction increased due to the dramatic increase of weight of agricultural machinery, necessary in modern agriculture, that compact the soil with each passage and reduce its production capacity. All tillage operations, starting with seedbed preparation, fertilizer and chemical applications and finally harvesting, increase the risk of degradation of agricultural soil through artificial compaction.

The potential of any soil to compact depends on its physical properties, water content and the nature of forces applied on soil surface. There can be small forces by the size of raindrops, or large forces such as those produced by tractors and agricultural machinery.

In developed countries, all agricultural soils show some degree of compaction. Recent research has shown that compaction is the most widespread type of soil physical degradation in Central and Eastern Europe. It has been estimated that nearly 40% of European soils suffer from compaction, but no precise data are available. More than a third of the soils in Europe are highly susceptible to compaction in the subsurface layers [18].

Concerns related to the environmental effects of soil compaction are increasing worldwide. Many studies have shown that compaction reduces the ability of soil to hold water and air, it prevents water from infiltrating properly in the soil, increases the risk of surface runoff, erosion and leakage of pesticides and nutrients into groundwater, increases the

[1]Splaiul Independenţei 313, sector 6, Bucharest, 0724086492, nicoletaung@yahoo.com

emanations of exhaust gases which ultimately contribute to the global warming [9, 14]. In terms of agronomic consequences, soil compaction is a common and constant problem on most farms that till the soil, mainly because it impedes root growth, restricts root penetration into the subsoil, decreases the ability of crops to take up nutrients and water efficiently from soil, reduces crop yield potential, increases plowing resistance and fuel consumption [11, 12].

2. METHODOLOGY

Stresses applied by the agricultural machinery are transmitted to different soil depths, through the footprint between the soil and tire, resulting in artificial topsoil and /or subsoil compaction (Figure 1).

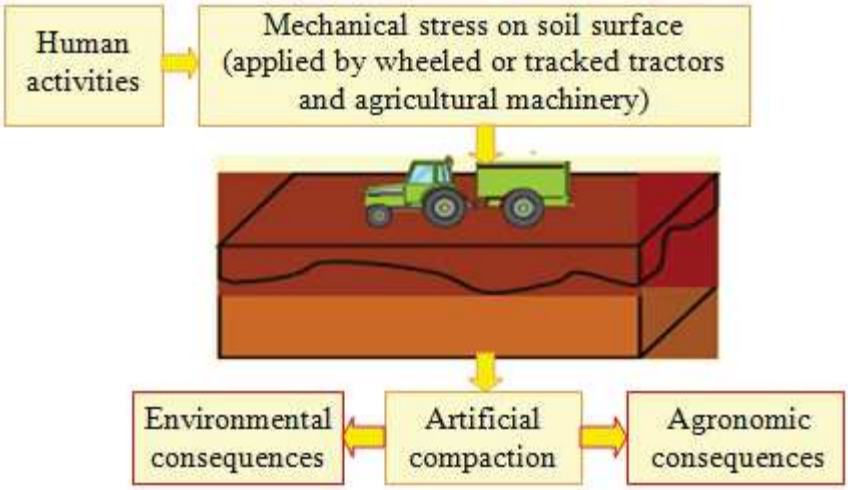

Figure 1: Basic mechanism of artificial compaction of soil

Topsoil compaction has a significant effect on crop yield and may last for some years, but it may be alleviated by tillage, drying-wetting and freeze-thaw cycles, and by the action of soil biota. Subsoil compaction (occurring below 25 cm depth) is particularly persistent and the compacted layer cannot be removed by conventional tillage [17].

Figure 2 presents some important factors that have a large influence on the artificial compaction of soil. Literature also mentions other factors, which are related to the agricultural machinery: contact pressure, tire size, speed of machinery, tire slippage and vibrations.

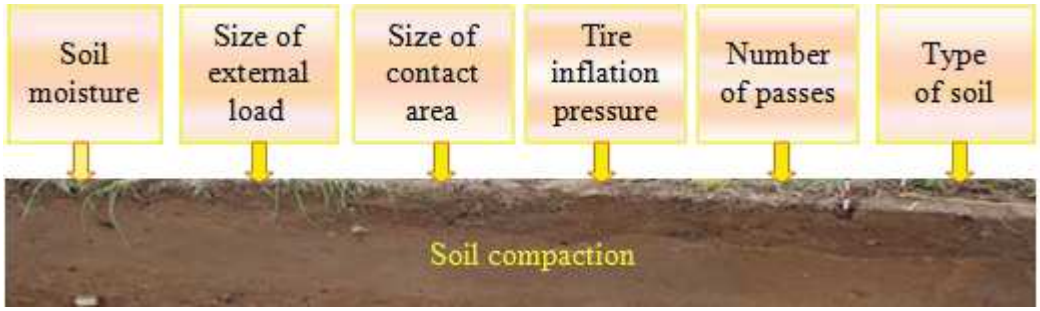

Figure 2: Main factors that influence the artificial compaction of soil

Moreover, the repeated treading by livestock around gateways and watering points also leads to artificial soil compaction. The stress applied by animals trampling can be great, but since the gross mass of the animals is smaller than that of the vehicles, compaction by animals is restricted only to soil surface [15].

The intensity of trafficking, also referred to as the number of passes of agricultural machinery on the soil, plays an important role in soil compaction because the deformation of soil increases with the number of passes. The first pass of a wheel does the most compaction. Research in tilled soils has shown that approximately 75% of the increase in soil density and 90% of wheel sinking is caused during the first pass [6]. However, the effects of repeated wheeling can still be measured after several passes. Experiments conducted on mineral soils have shown that, for the same vehicle, increasing the number of passes on the same track increases the depth of stress distribution and the volume of soil affected by compaction.

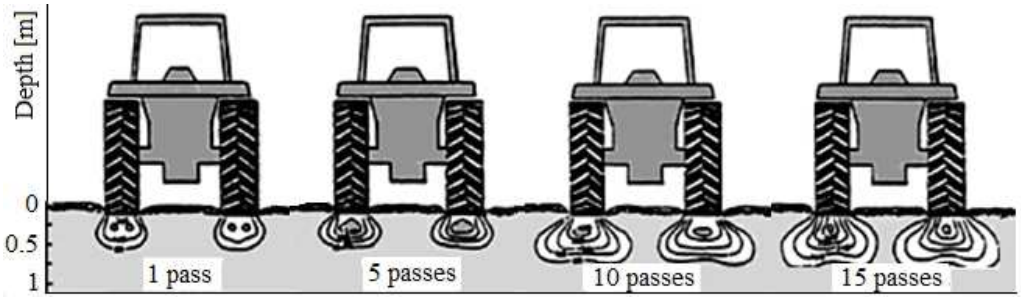

Figure 3: Stress distribution in soil depth depending on the number of passes [19]

Using light tractors involves an increased number of passes on the soil, thus enhancing compaction of topsoil [7]. By using heavy agricultural machinery, the number of passes / soil area / agricultural work is reduced, due to a larger working width, which means that compacted layers of soil occur at lower depth and the degree of subsoil compaction is reduced [1]. The repeated number of wheel passes may also increase the risk of subsoil compaction. Machinery traffic, repeated annually, may cause cumulative effects if the effects of earlier subsoil compaction have not disappeared before new trafficking [2].

3.RESULTS

Pytka (2005) showed that the most obvious deformation of the soil is caused by the first two passes of the wheeled tractor and soil deformation decreases in the following passages [6]. The findings in [3] showed that 10 passes significantly affected soil properties of the surface layer to 50 cm depth compared to the first pass and no-traffic control treatments.

Jorajuria and Draghi (2000) have determined the influence of the number of passes and the size of external load on subsoil compaction. Two tractors were used, one light and one heavy, and for each of them, the traffic intensity was varied (1, 5 and 10 passes). Tests have shown that 10 repeated passes of a light tractor, on the same track, are needed to produce the same degree of subsoil compaction as a heavy tractor in a single pass [8]. Studies conducted on clayey and organic soils have shown that penetration resistance was 22– 26% greater, the soil water contents were lower, and the soil structure more massive, in plots compacted with four passes than in the control plots [6].

Sakai et. al. (2008) investigated the effects on soil compaction of 1, 8 and 24 passes of an 8-WD forwarder, unloaded and loaded with 9520 kg of timber, equipped with low and high pressure tires, respectively with tracks. They found that compaction occurred during the first passes, and heavy compaction occurred after 8 passes. An increase in contact pressure of 100 kPa caused a decrease in soil porosity of 5.7% at 10-15 cm depth after 24 passes. Maximum increment of cone index of 85 kPa, at depths between 14 and 28 cm, meant a decrease of 1% in soil porosity at 10-15 cm deep. Increasing the number of passes of the agricultural machinery over the soil increased its porosity and cone index, resulting in topsoil compaction and unsuitable physical soil conditions for seed emergence [16].

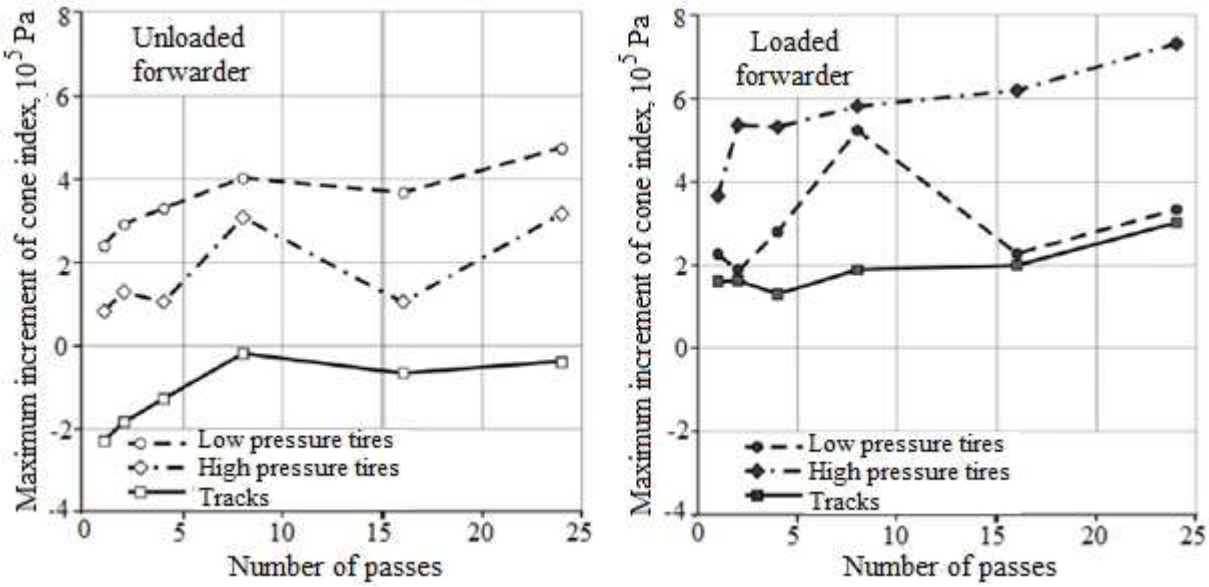

Figure 4: Maximum increment of cone index with the number of passes [16]

Botta et. al. (2009) investigated the interaction of cone index and rut depth induced by traffic of two different weight tractors in two tillage regimes: soil with 10 years under direct sowing system and soil worked in conventional tillage system. Treatments included five different traffic frequencies (0, 1, 3, 5 and 10 passes on the same track).

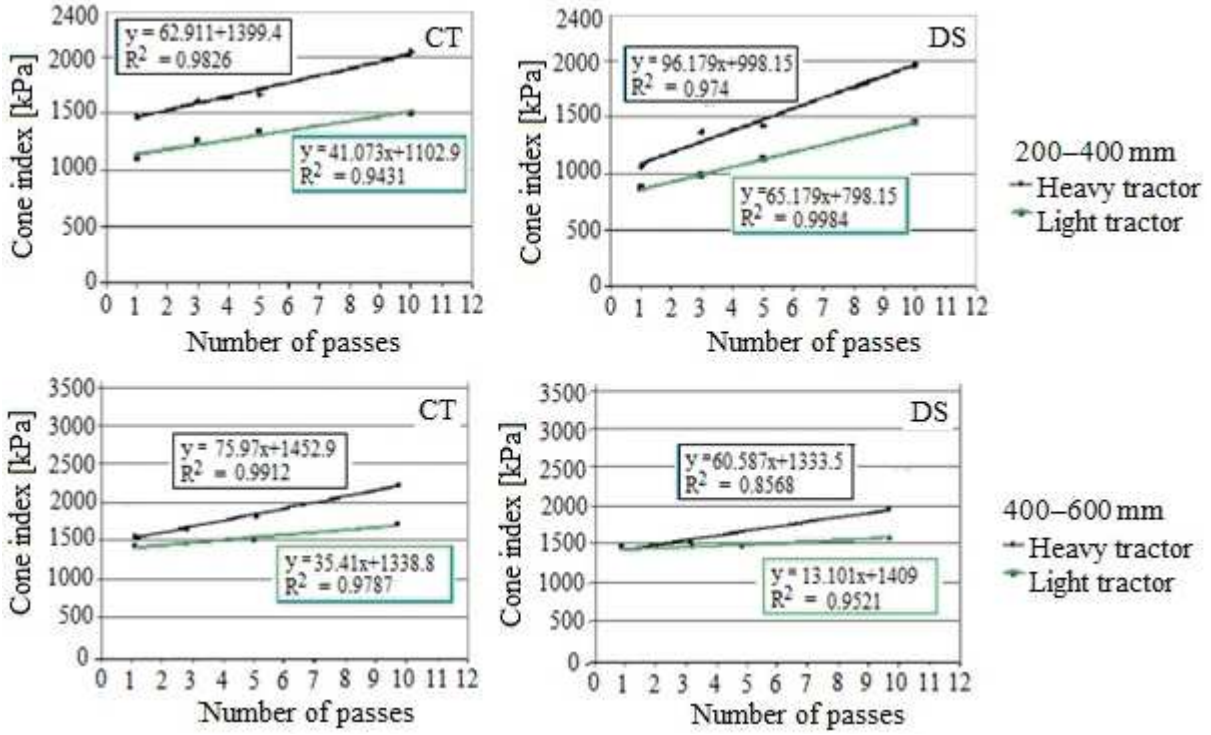

Figure 5: Variation of cone index with the number of passes, in conventional tillage (CT) and direct sowing (DS) [5]

In the topsoil, up to 5 passes of the heavy and light tractors, as in 1 and 3 passes, the cone index responded to the ground pressure being higher for the light tractor. Until the 5th pass, the light tractor caused in both soils higher values in cone index than the heavy tractor. Between 200–600 mm, compaction increased with the number of passes. For 200–400 mm and 400–600 mm depth, there is a good correlation between tractor passes and cone index in

both tillage regimes. The heavy tractor produced higher cone index than the light tractor. From 200 mm depth, the higher values for cone index were for the heavy tractor. Highest values of cone index were measured between 400–600 mm for all treatments in both soils conditions. So, below 200 mm depth, tractor load was responsible for subsoil compaction [5].

Over 30% of soil area is trafficked by heavy machinery with tires, even in no-till system (one pass at sowing). Under minimum tillage (2-3 passes) the percentage exceeds 60% and in conventional cropping (multiple passes) it exceeds 100% during one cropping cycle [10].

In another research study [13], stress state transducers were installed in the soil to depths of 15 and 30 cm, to determine the distribution of stress in the soil at the multiple passes of an agricultural tractor of 29 kW. The total mass of the tractor was 2480 kg, with 850 kg load on the front wheel and 1630 kg load on the rear wheel. Two soils were tested: a sandy soil with bulk density of 1.70 g/cm^3 and a loess soil with bulk density of 1.63 g/cm^3. Figure 6 shows the effect of multiple passes on the same track, on stress distribution in the soil.

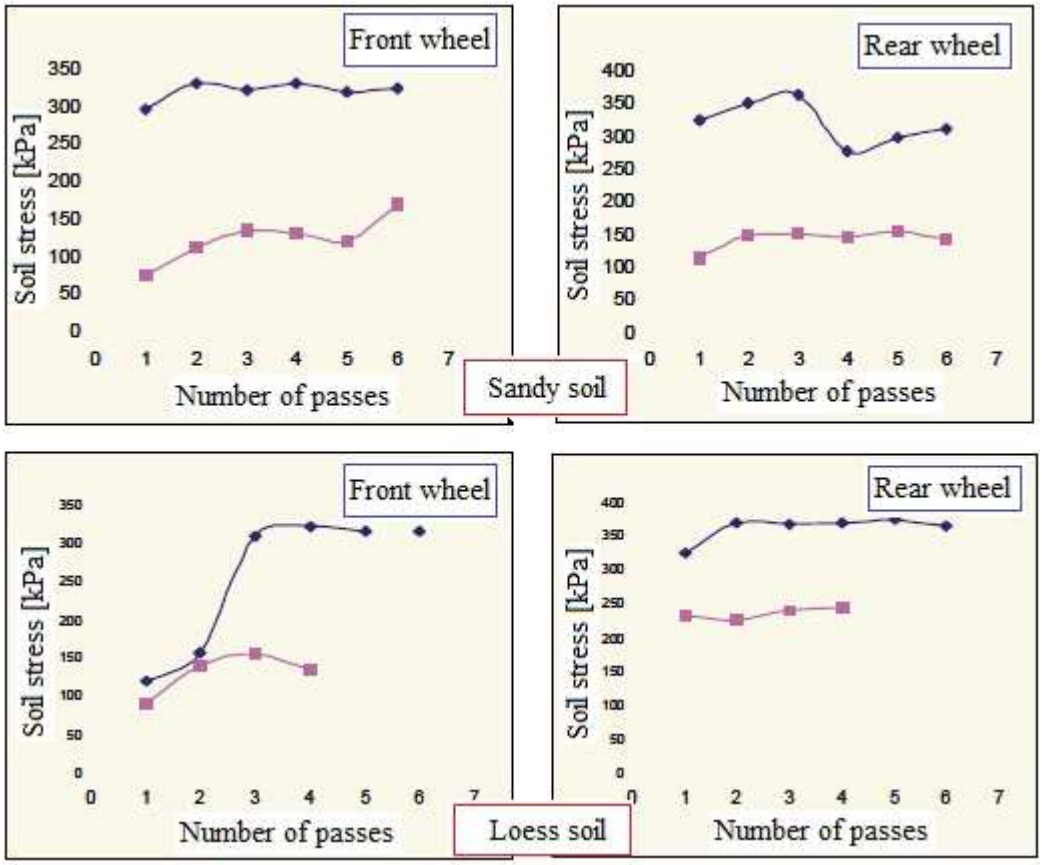

Figure 6: The effect of the number of passes over stresses in the soil [13]

The first 2-3 passes had the greatest importance and the increase in peak stress was significantly higher between the first and second pass, than between the second and third pass. On subsequent passes, the stress increased very slightly. Stresses recorded after the fourth and fifth passes were lower than those measured in the second and third pass, and this may be due to soil consolidation after several passes on the same track [13].

4. CONCLUSIONS

The artificial compaction of soil is due to the technological errors in agriculture, such as excessive traffic on wet soils during the agricultural works. Compaction increases with increasing mass of agricultural machinery, tire inflation pressure, intensity and frequency of soil tillage.

Soil compaction can lead to various undesirable changes in soil properties (cone index, bulk density, porosity, etc.), with significant environmental and agronomic consequences. Those changes are greatly intensified by the repeated passes during agricultural works.

Most compaction occurs after the first pass of wheeled machinery, and this is obvious both by the changes in soil physical properties and the distribution of stresses in soil depth, but the effects of repeated wheeling can still be measured after several passes.

Acknowledgement

This work has been funded by the Ministry of National Education and Research, through the UEFISCDI, within the project entitled *„Conservative tillage technology*", contr. 181/2014.

References

[1] Alakukku, L., *Subsoil compaction due to wheel traffic*, Agricultural and Food Science in Finland, vol. 8, pp. 333-351, 1999.
[2] Alakukku, L., *Soil compaction*, Combatting soil degradation, pp. 217-221, University of Helsinky, 1999.
[3] Balbuena, R.,H., Terminiello, A.,M., Claverie, J.,A., Casado, J.,P., Marlats, R., *Soil compaction by forestry harvester operation. Evolution of physical properties*, Revista Brasileira de Engenharia Agricola e Ambiental, vol. 4, pp. 453–459, 2000.
[4] Batey, T., *Soil compaction and soil management – a review*, Soil Use and Management, vol. 25, pp. 335–345, 2009.
[5] Botta, G.F., Tolon Becerra, A., Bellora Tourn, F., *Effect of the number of tractor passes on soil rut depth and compaction in two tillage regimes*, Soil & Tillage Research, vol. 103, pp. 381-386, 2009.
[6] Duiker, S.,W., *Avoiding soil compaction*, Conservation Tillage Series, Penn State University, Department of Crop and Soil Sciences, 1-8, 2004.
[7] Hamza, M.,A., Anderson, W.,K., *Soil compaction in cropping systems. A review of the nature, causes and possible solutions*. Soil&Tillage Research, vol. 82, pp. 121-145, 2005.
[8] Jorajuria, D., Draghi, L., *Sobre compactación del suelo agricola parte I: influencia diferencial del peso y del número de pasadas*, Revista Brasileira de Engenharia Agrícola e Ambiental, vol. 4(3), pp. 445-452, 2000.
[9] Keller, T., Lamandé, M., *Challenges in the development of analytical soil compaction models*, Soil & Tillage Research, vol. 111, pp. 54-64, 2010.
[10] Kroulik, M., Kumhala, F., Hula, J., Honzik, I., *The evaluation of agricultural machines field trafficking intensity for different soil tillage technologies*, Soil and Tillage Research, vol. 105, pp. 171-175, 2009.
[11] Mari, G., R., Changying, Ji., *Influence of agricultural machinery traffic on soil compaction patterns, root development, and plant growth, overview*, American-Eurasian J. Agric. & Environ. Sci., vol. 3(1), pp. 49-62, 2008.
[12] Nawaz, M.,F., Bourrié, G., Trolard, F., *Soil compaction impact and modelling. A Review*, Agron. Sustain. Dev. Springerlink, 2012.
[13] Pytka, J., Szymaniak, G., *Investigations of stress state in soil under tractor tyres*, Polish Academy of Sciences Branch in Lublin, 2004.
[14] Quraishi, M., Mouazen, A.,M., *Calibration of an on-line sensor for measurement of topsoil bulk density in all soil textures*, Soil & Tillage Research, vol. 126, pp. 219-228, 2013.
[15] Raper, R.,L., Kirby, J.,M., *Soil compaction: how to do it, undo it, or avoid doing it*. ASAE Distinguished Lecture 30, pp. 1-14, Agricultural equipment technology conference, ASABE Publication no. 913C0106, 2006.
[16] Sakai, H, Nordfjell, T, Suadicani, K, Talbot, B, Bøllehuus, E., *Soil compaction on forest soils from different kinds of tires and tracks and possibility of accurate estimate*, Croat J For Eng., vol. 29, pp. 15–27, 2008.
[17] Schjønning, P., van den Akker, J.,J.,H., Keller, T., Greve, M.,H., Lamandé, M., Simojoki, A., Stettler, M., Arvidsson, J., Breuning-Madsen., H., *Soil compaction*, Chapter 6, pp. 69-78, Soil Threats in Europe - Status, methods, drivers and effects on ecosystem services, Publisher: EU Joint Research Centre, 2016.
[18] Stolte, J., Tesfai, M., Øygarden, L., Kværnø, S., Keizer, J., Verheijen, F., Panagos, P., Ballabio, C., Hessel, R., *JCR Technical Reports – Soil threats in Europe. Status, methods, drivers and effects on ecosystem services*. A review report, deliverable 2.1 of the RECARE project, 2016.
[19] *Le compactage des sols et les pneumatiques*, Instructions complètes, Ministère de l'Agriculture, des Pêcheries et de l'Alimentation, Quebec, 2002.
[20] http://eusoils.jrc.ec.europa.eu/projects/Soil_Atlas/Pages/115.html.

METHOD DEVELOPED FOR DETERMINATION OF UNCERTAINTY OF THE TRANSIENT RESISTANCE OF PROTECTIVE EARTH CONNECTIONS

Vyara Vasileva, Rosen Vasilev[1], Ivaylo Nedelchev
Technical University of Varna

ABSTRACT

This paper focuses on the method developed for determination of uncertainty of the transient resistance of protective earth connections according to p.27.2 of EN 60335-1:2001. To assess the uncertainty mathematical model of measurement is given, as well as how to evaluate the input variables, the determination of the uncertainties of the input variables and output evaluation. The budget of uncertainty and an example is attached.

1. INTRODUCTION

The paper presents the methodology developed by the authors for evaluating the uncertainty in the quantitative tests related to the measurement of transient resistances of protective earth connections in the tests under item 27.2 of EN60335-1: 2001 [1].

Current obtained from a source with an idle voltage of not more than 12V and equal to 25A (or 1.5 times the rated electrical appliance, whichever is greater) is passed between the protective earth terminal or the protective earth pin and each of exposed conductive part of the appliance successively.

The drop of a voltage between the protective earth terminal of the appliance or the protective pin of the appliance's plug and the exposed conductive part is measured. From the current and the measured voltage drop, the resistance is calculated.

Measurement uncertainty assessment is based on publication EA-4/02 "Measurement uncertainty of calibration" [2].

2. EVALUATION OF UNCERTAINTY IN MEASURING TRANSIENT RESISTANCE WITH VOLTMETER AND AMMETER

The value of the measured transient resistance is derived from dependence:

$$R = \frac{U}{I}, \tag{1}$$

където: U - drop of a voltage between the protective earth terminal and exposed conductive part [V]; I - current through the protective earth terminal [A].

2.1. Mathematical model of measurement.

The mathematical model of the dependence of the output magnitude (transient resistance) on the input variable on which the measurement result is evaluated:

$$R_x = \frac{\overline{U}_s + \delta U_c + \delta U_r}{\bar{I}_s + \delta I_c + \delta I_r}, \tag{2}$$

[1]Varna, Bulgaria Technical Univercity 1 Studentska str., phone number +35952 383 249 email: rsnvasilev@abv.bg

where: $\overline{U}_s$ - the value of the voltage drop recorded by the voltmeter; δU_c - voltmeter correction from its last calibration; δU_r - a correction of a difference between the voltage drop recorded on the voltmeter and its reading due to the ultimate resolution of the voltmeter; $\bar{I}_s$ - current value through the protective earth terminal accounted for by the ammeter; δI_c - correction of the ammeter readout obtained since its last calibration; δI_r - a correction of a difference between the current measured on the ammeter and its reading due to the ultimate resolution of the ammeter.

2.2. Estimation of input variables.

Estimates $\overline{U}_s$ (3) and $\bar{I}_s$ (4) are defined as the arithmetic mean of *n* repeatable measurements with limits defined by the mean square deviation of the arithmetic mean:

$$\overline{U}_s = \frac{1}{n}\sum_{j=1}^{n} U_j \,, \tag{3}$$

$$\bar{I}_s = \frac{1}{n}\sum_{j=1}^{n} I_j \,, \tag{4}$$

In a single measurement, the measured value of the voltage or current is the one measured at the single measurement with the limits defined by the absolute error of the voltmeter or the ammeter.

Estimates δU_c (5) and δI_c (6) shall be defined as the difference between the measured and actual values indicated in the calibration certificate of the voltmeter / ammeter, with the limits defined by the uncertainty specified therein:

$$\delta U_c = -\left(U_{изм} - U_{действ}\right), \tag{5}$$

$$\delta I_c = -\left(I_{изм} - I_{действ}\right), \tag{6}$$

Where there is no calibration in the calibration certificate at the point corresponding to the measured value, the correction shall be calculated by linear interpolation of the nearest two adjacent calibration points between which the measured value is located.

Estimates δU_r and δI_r are assumed to be zero with limits defined by the voltmeter / ammeter resolution.

2.3. Weighted average uncertainty calculation of the input variables.

Uncertainty of the estimate of the arithmetic mean value of the voltage $\overline{U}_s$ and respectively of the current $\bar{I}_s$ of the measurement values (mean square uncertainty) is calculated by formula (7) and corresponding formula (8):

$$u\left(\overline{U}_s\right) = \sqrt{\frac{1}{n(n-1)}\sum_{j=1}^{n}\left(U_j - \overline{U}\right)^2} \,, \tag{7}$$

$$u\left(\bar{I}_s\right) = \sqrt{\frac{1}{n(n-1)}\sum_{j=1}^{n}\left(I_j - \bar{I}\right)^2} \,, \tag{8}$$

In a single measurement, the mean square uncertainty is calculated by the formula (9) respectively (10):

$$u(U_s) = b.a_v, \tag{9}$$

$$u(I_s) = b.a_A, \tag{10}$$

where: b - a coefficient for normal distribution and confidence probability p=0,95 is equal to 0,5; a_v - limit value of the corresponding voltage distribution (absolute error of the voltmeter); a_A - limit value of the respective current distribution (absolute error of the ammeter).

Uncertainty of the calibration correction evaluation of the voltmeter δU_c respectively of the ammeter δI_c for the actual value of the voltage / current are calculated by (11) and (12):

$$u(\delta U_c) = \frac{U_v}{k}, \tag{11}$$

$$u(\delta I_c) = \frac{U_A}{k}, \tag{12}$$

where: U_v - the extended uncertainty specified in the calibration certificate of the voltmeter; U_A - the extended uncertainty specified in the calibration certificate of a ammeter; k - the security factor indicated in the calibration certificate of the voltmeter / ammeter.

When there is no calibration in the calibration certificate at the point corresponding to the measured value, the uncertainty is calculated from the expanded uncertainty with a higher value at two adjacent calibration points between which the measured value.

Uncertainty of the evaluation of the repair of the final resolution of the voltmeter δU_r, respectively of the ammeter δI_r are calculated using (13) and (14):

$$u(\delta U_r) = \frac{d_v}{2\sqrt{3}}, \tag{13}$$

$$u(\delta I_r) = \frac{d_A}{2\sqrt{3}}, \tag{14}$$

where: d_v is the value of a scale interval / the smallest significant digit / of the voltmeter; d_A is the value of a scale interval of the ammeter.

2.4. Calculate the sensitivity coefficients for each of the input variables.

The sensitivity coefficients are calculated as private derivatives of the function of the model from (2) with respect to each of the input variables with the formula:

$$c_i = \frac{\partial R}{\partial x_i} = \frac{\partial R}{\partial X_i}, \tag{15}$$

$$c(\overline{U}_s) = \frac{\partial R}{\partial \overline{U}_s} = \frac{1}{\overline{I}_s + \delta I_c + \delta I_r}, \qquad c(\delta U_c) = \frac{\partial R}{\partial \delta U_c} = \frac{1}{\overline{I}_s + \delta I_c + \delta I_r}$$

$$c(\delta U_r) = \frac{\partial R}{\partial \delta U_r} = \frac{1}{\bar{I}_s + \delta I_c + \delta I_r}, \qquad c(\bar{I}_s) = \frac{\partial R}{\partial \bar{I}_s} = -\frac{\bar{U}_s + \delta U_c + \delta U_r}{(\bar{I}_s + \delta I_c + \delta I_r)^2}$$

$$c(\delta I_c) = \frac{\partial R}{\partial \delta I_c} = -\frac{\bar{U}_s + \delta U_c + \delta U_r}{(\bar{I}_s + \delta I_c + \delta I_r)^2}, \quad c(\delta I_r) = \frac{\partial R}{\partial \delta I_r} = -\frac{\bar{U}_s + \delta U_c + \delta U_r}{(\bar{I}_s + \delta I_c + \delta I_r)^2}$$

2.5. Calculating the contributions $u_i(y)$ of the mean quadratic uncertainty of each of the inputs for the quadratic uncertainty of the output quantity.

The contributions of the rhythmic uncertainty of each input parameter to the uncertainty of the measured transient resistance are calculated by the formula:

$$u_i(y) = c_i . u(x_i), \tag{16}$$

$$u_{u_s}(R) = c(\bar{U}_s) u(\bar{U}_s), \quad u_{\delta u_c}(R) = c(\delta U_c) u(\delta U_c), \quad u_{\delta u_r}(R) = c(\delta U_r) u(\delta U_r)$$

$$u_{I_s}(R) = c(\bar{I}_s) u(\bar{I}_s), \quad u_{\delta I_c}(R) = c(\delta I_c) u(\delta I_c), \quad u_{\delta I_r}(R) = c(\delta I_r) u(\delta I_r)$$

2.6. Calculation of the weighted average uncertainty of the output quantity assessment $u(R)$.

The quadratic uncertainty of the measured transient resistance is calculated using:

$$u(R) = \sqrt{u_{u_s}^2(R) + u_{\delta u_c}^2(R) + u_{\delta u_r}^2(R) + u_{I_s}^2(R) + u_{\delta I_c}^2(R) + u_{\delta I_r}^2(R)}, \tag{17}$$

2.7. The expanded uncertainty of the transient resistance measurement result is calculated using:

$$U = k . u(R), \tag{18}$$

2.8. Measurement result.

The final result for the measured transient resistance together with the expanded uncertainty is given as:

$$R = R_x \pm U, \tag{19}$$

The specified expanded measurement uncertainty is expressed as a quadratic measurement uncertainty multiplied by the confidence interval k = 2, which under normal distribution law corresponds to a 95% probability of the confidence interval. The standard measurement uncertainty is determined in accordance with publication EA-4/02.

3. APPLICATION OF THE METHOD OF ASSESSING THE UNCERTAINTY OF THE RESULT OF MEASURING TRANSITIONAL PROTECTION OF PROTECTIVE CONNECTIONS

3.1. Processing of measurement results.

Measurement of transient resistivity of protective connections with measurement uncertainty (Table 1) in the measurement as a calibrated measuring instrument is analogue ammeter "METRA" with id. № 404803, range /0÷50/A, class 0,5, division value 0,5A and

digital voltmeter D 1216, id. № 41660 with range /0÷20/V, error ± 0,5%, division value 0,01V, using measuring method - BDS EN 60335-1: 2001 (item 27.5).

3.2. Evaluate the input parameters:

- $\overline{U}_s = \frac{1}{n}\sum_{1}^{10} U_j = 2{,}502\ V$ (in a single measurement $U_s = 2{,}502V$)
- $\delta U_c = -(U_{изм} - U_д) = -(2{,}500 - 2{,}485) = -0{,}015\ V$, $\delta U_r = 0V$
- $c(\bar{I}_s) = -\frac{\overline{U}_s + \delta U_c + \delta U_r}{(\bar{I}_s + \delta I_c + \delta I_r)^2} = -0{,}004\frac{V}{A^2}$, $c(\delta I_c) = -\frac{\overline{U}_s + \delta U_c + \delta U_r}{(\bar{I}_s + \delta I_c + \delta I_r)^2} = -0{,}004\frac{V}{A^2}$

$$c(\delta I_r) = -\frac{\overline{U}_s + \delta U_c + \delta U_r}{(\bar{I}_s + \delta I_c + \delta I_r)^2} = -0{,}004\frac{V}{A^2}$$

Table 1: Measurement result processing

№	U_j [V]	$U_j - \overline{U}$ [V]	$(U_j - \overline{U})^2$ [V^2]	I_j [A]	$I_j - \bar{I}$ [A]	$(I_j - \bar{I})^2$ [A^2]
1	2,50	-0,002	0,004.10^{-3}	25,0	0,1	0,01
2	2,52	0,018	0,324.10^{-3}	25,0	0,1	0,01
3	2,51	0,008	0,640.10^{-3}	25,0	0,1	0,01
4	2,50	-0,002	0,004.10^{-3}	24,5	-0,4	0,16
5	2,49	-0,012	0,144.10^{-3}	24,5	-0,4	0,16
6	2,50	-0,002	0,004.10^{-3}	25,0	0,1	0,01
7	2,50	-0,002	0,004.10^{-3}	25,0	0,1	0,01
8	2,48	-0,022	0,484.10^{-3}	24,5	-0,4	0,16
9	2,52	0,018	0,324.10^{-3}	25,5	0,6	0.36
10	2,50	-0,002	0,004.10^{-3}	25,0	0,1	0,01
	$\overline{U}$ =2,502		1,936.10^{-3}	$\bar{I}$ = 24,9		0,9

3.3. Contributions to the baseline uncertainty of the baseline assessment:

- $u_{U_s}(R) = c(\overline{U}_s).u(\overline{U}_s) = 0{,}04\frac{1}{A}.0{,}2.10^{-3}V = 0{,}008.10^{-3}\Omega$
- $u_{\delta U_c}(R) = c(\delta U_c).u(\delta U_c) = 0{,}04\frac{1}{A}\cdot 0{,}004V = 0{,}16.10^{-3}\Omega$
- $u_{\delta U_r}(R) = c(\delta U_r).u(\delta U_r) = 0{,}04\frac{1}{A}\cdot 0{,}0029V = 1{,}16.10^{-3}\Omega$
- $u_{I_s}(R) = c(\bar{I}_s).u(\bar{I}_s) = -0{,}004\frac{V}{A^2}\cdot 0{,}1A = -0{,}4.10^{-3}\Omega$
- $u_{\delta I_s}(R) = c(\delta I_c).u(\gamma I_c) = -0{,}004\frac{V}{A^2}\cdot 0{,}145A = -0{,}58.10^{-3}\Omega$
- $u_{\delta I_r}(R) = c(\delta I_r).u(\gamma I_r) = -0{,}004\frac{V}{A^2}\cdot 0{,}14A = -0{,}56.10^{-3}\Omega$

3.4. Weighted average uncertainty of the output assessment:

$$u(R) = \sqrt{(0{,}008.10^{-3})^2 + (0{,}16.10^{-3})^2 + (0{,}116.10^{-3})^2 + (0{,}4.10^{-3})^2 + (0{,}58.10^{-3})^2 + (0{,}56.10^{-3})^2} = 1{,}94.10^{-3}\,\Omega$$

3.5. Extended uncertainty of the result of the transient resistance measurement:

$$U = k.u(R) = 2.1{,}94.10^{-3} = 3{,}9.10^{-3}\,\Omega$$

3.6. Uncertainty budget for the specific test (Table 2).

Table 2: Uncertainty budget

i	X_i	x_i	$u(x_i)$	Distribution	C_i	$u_i(R) = c_i.u(x_i)$ [Ω]
1	$\overline{U}_s$ [V]	2,502	0,2.10^{-3}	normal	0,04 [1/A]	0,008.10^{-3}
2	δU_c [V]	-0,015	0,004	normal	0,04 [1/A]	0,160.10^{-3}
3	δU_r [V]	0	0,029	rectangular	0,04 [1/A]	1,16.10^{-3}
1	$\bar{I}_s$ [A]	24,9	0,100	normal	-0,004 [V/A^2]	-0,400.10^{-3}
2	δI_c [A]	-0,01	0,145	normal	-0,004 [V/A^2]	-0,580.10^{-3}
3	δI_r [A]	0	0,140	rectangular	-0,004 [V/A^2]	-0,560.10^{-3}
Y	R_x [Ω]	0,0999	1,94.10^{-3}	normal		

3.7. Measurement result:

$$R = (0{,}0999 \pm 0{,}0039)\,\Omega$$

The specified expanded measurement uncertainty is expressed as a quadratic measurement uncertainty multiplied by the confidence interval k = 2, which under normal distribution law corresponds to a 95% probability of the confidence interval. The standard measurement uncertainty is determined in accordance with publication EA-4/02.

4. CONCLUSIONS

A methodology has been developed to allow estimation of uncertainty in the transient resistance of protective earth connection measurement. The method is approbated for the calibration of a measuring instrument complying with BDS EN 60335-1:2001. The method is applicable to laboratory measuring transient resistance of protective earth connections according to BDS EN 60335-1: 2001.

References

[1] BDS EN 60335-1:2001.
[2]. EA-4/02 „Expression of measurement calibration uncertainty ”.
[3]. Vasilev, R., Electrical measurements, TU-Varna, Varna, 2010.

TRENDS OF THE ROMANIAN RURAL POLICY IN THE CURRENT EUROPEAN CONTEXT

Oana Vlăduţ[1], Petruţa Mihai[2], Sanda Maiduc (Osiceanu)[3]
University Politehnica of Bucharest

ABSTRACT

The rural development requires a major attention coming from the management institutions in the European Union, thus achieving a policy to cover all the adjacent sub-domains to this purpose. The paper aims to introduce only a part of this complex field, which we consider imperative for Romania. Hence, the focus will be falling on the rural agriculture and tourism in our country, since it is our opinion that they can be better capitalized and brings additional profit to the state budget, while providing new employment places for both young and middle-aged people.

1. INTRODUCTION

The rural space represents an important place in the policy in any country, both at the national level and within the European Union. This space is an inexhaustible provider of resources, considering that it is most benefitted from.

The Common Agricultural Policy yields decent living standards for the farmers and agricultural products that are in line with the standards of the European Union and the quality requested by the Union citizens. It intends to reach a competitive and sustainable agriculture in the EU via direct payments made to the farmers, market measures taken and the development programs for the rural areas financed in the Union.

Europe places first among the top tourist destinations and this is the reason why the European policy wishes to maintain that ranking by promoting sustainable and high quality tourism and by competitiveness stimulation in the European tourism sector.

The rural tourism stands as another trend in the rural policy, thanks to which Romania can derive important income. Since the oldest times, our country has been doing rural tourism –under a rather disorganized form in the beginning that has turned nowadays into a more systematized activity covering a larger and larger surface in the Romanian rural space.

In terms of this space, Romania confronts itself with a significant loss of the human resource, which makes it difficult to capitalize on the natural wealth that is abundant in our country.

2. PAPER CONTAIN

The essential priorities of the policy, defined within the European Union and also decisive for Romania, include employment places, sustainability, innovation and quality. [3]

As far as we are concerned, all these things can be achieved for our country by means of a more efficient agriculture, based on up-to-date and clean technologies and of a rural tourism, efficiently coordinated.

Romania's rural development policy has long-term objectives:

[1] Splaiul Independentei nr.313, sector 6, Bucharest and oanavladut2016@gmail.com
[2] Splaiul Independentei nr.313, sector 6, Bucharest and mihaipetruta@yahoo.com
[3] Splaiul Independentei nr.313, sector 6, Bucharest and s_maiduc@rectorat.pub.ro

- stimulating the agriculture competitiveness,
- guaranteeing the durable management of the natural resources,
- refute of the changes in the climate conditions,
- encouraging the balanced territorial development of the rural communities,
- creating and maintaining the employment places.

Unlike other European Union member country, Romania enjoys the advantage of a varied landscape, rich in vast fields, hills and mountains that have an extraordinary tourism potential. It would be crucial for these two activities in the rural space – agriculture and tourism – be taken the maximum advantage from.

The Common Agricultural Policy can be defined as a bridge between the expectations of the EU citizens regarding the agriculture and of the farmers in the member states who are facing economic and environment issues and it is extremely important from the perspective of the food safety, economic growth in the rural areas and of the environment.

The main pillars of the Common Agricultural Policy for the 2014 – 2020 intervals are as below:

- ecology and efficiency in agriculture,
- provision of a healthy food at affordable prices,
- revitalization of the rural areas and communities.[6]

Both the Common Agricultural Policy defined until 2013 and the version for the 2014-2020 feature a series of measures to help the farmers with conducting as efficient as possible economic activities in order to overcome the unanticipated conditions that are emerging, independently from their will. This series includes the system of direct payments, the support schemes, single payments per surface, etc.

At the European Union level, the Common Agricultural Policy intends for 2014-2020 more reasonable and ecological direct payments, the implementation of certain market measures so that the farmers be ranked in a better place in the food supply chain and provide support in the key priorities that are particular to each EU member state.

Should we refer to the previous times of the Common Agricultural Policy (2007 – 2013), it is a sure thing to state that the Romanian agriculture has had some leverage that has not been capitalized on to the maximum value. In other words, the Romanian farmers had access to the system of direct payments that made employment possible in the primary sector, representing around 30% of the total of the number of jobs.

Towards the end of this time window, market measures were adopted for the vine-bearing industry, as well as for the fruits and vegetables. The idea was that Romania grows a wide variety of grapes that are highly valued abroad, thanks to their outstanding qualities. The Romanian wines are appreciated in other countries but the main setback has been the poor promotion, both in and outside of Romania.

According to the Eurostat statistics in the European Union, there were 2.4 million plantations in 2015 that were cultivating 3.2 hectares of vines. The average surface per plantation was 1.3 hectar, greatly varying from one member state to another.

In spite of the fact that Romania had 855,000 vine plantations in 2015 – 36% of the total in the EU – thus exceeding Spain (518,000 plantations or 22%), Italy (299,000 plantations in 2010 or 12%), Portugal (212,000 plantations or 9%) and Greece (189,000 plantations or 8%), our local vines are not known as well or best sellers as in the other member states.[4]

Additional evidence is that the area in Romania meant for the high quality wines was of 50,968 hectares in 2015, which equals 27.7% for the superior wines/total surface ratio. This type of wines is given by either the grapes under the protection of the brand names 64.2% or of the geographical indications 35.8%.

Similarly, the sector of fruits and vegetables is represented by extended areas that are cultivated with a large variety of them, along with fruit-bearing trees. The issue is that these

areas belong to family-based associations that do not have significant income to allow them face unforeseen weather conditions or other phenomena that are affecting their production volume.

Another important activity has been the preservation of the natural landscape in Romania, so that tourism benefits to the maximum from this natural ‚upper hand'. Creating employment places in the rural space and the attempt to attract or retain the young people in the rural area has been a paramount objective to reach in our country.

Thanks to the Romanian landscape and landforms, the rural tourism has always drawn a huge interest from the national tourists. Following the opening of the borders in 1990, foreign tourists came to Romania looking for a natural oasis that had kept its authenticity and presented a quiet life similar with the rural areas.

The emergence of the legislative regulations and their correlation with the community ones has led to the necessity of accessing the European funds by the small entrepreneurs in the rural tourism, in their intent to comply with the law. New accommodation spaces were needed to be registered and classified, besides the camping sites and log cabins already in place. The range of services has widened and improved and more and more villagers welcomed the tourists.

In time, the accommodation capacity in the rural tourism has witnessed a yearly increase, thus proving the level of interest and degree of attractiveness of different geographical areas. Another factor to influence the rural tourism in Romania is the seasonality, which means a lower or a higher number of tourists.

The rural tourism has also a series of strong points, among which we can mention the capitalization on the local customs and traditions, the cultural and architectural patrimony of a specific area, creation of employment places and the infrastructure improvement. The companies in this space are also facing new and high accreditation costs, due to the lack of assurance of the warranties needed to grant credits, since the real estate in the rural space is lowly evaluated.

Romania holds a unique spot in Europe. The Danube Delta is an ecosystem with a rich flora and fauna but where the living conditions are not the best for the inhabitants. To preserve the ecosystem and provide the locals with a decent life, the Romanian government has drafted a strategy of durable development, which aims to capitalize on the natural and cultural heritage and build better economic opportunities.

The tourism potential in the Delta Danube area is large but poorly exploited due to the urban services (running water, sewage, waste collection) and to the insufficient tourism infrastructure. Nevertheless, the economic development of this area cannot and should not have a negative impact upon the environment.

The Article 3 in the Lisbon Treaty underlines the fact that the European Union promotes the economic, social and territorial cohesion, as a response to the challenges targeting the globalization, weather and demographic changes, safety and energy.[5]

The development of the Danube Delta area is possible by a tourism relying on the exploiting of the natural and cultural heritage and creating employment in the fishing industry and agriculture.

3. CONCLUSIONS

A solution to the current situation of the Romanian rural space is the access to the funds so as to build smart eco-social villages. This concept addresses the villages hosting a high number of unemployed people, of deserted houses following the demise of the aged and the youth migration to the urban space. In Romania, only 7.3% of the farmers are under 35 (7.5%

in the EU) while 37.9% are over 64 (30% in the EU). A striking reality in those areas is the lack of basic services, such as sanitary, banking, education, etc.

At the same time, a fund for emergency situations can be established, which could help the farmers overcome such moments, considering that agriculture is an activity involving a high amount of unexpected situations.

The rural tourism presents many opportunities of economic and social nature, as it means a real future for the rural communities. This type of tourism has had a quick development, as it has expanded its spectrum of services and brought an economic development to the rural territories.

The Danube Delta retains a great tourism potential, from which the local communities can benefit as these conduct priority economic activities for the present times: fishing and agriculture. This area has, though, a disadvantage given by its remote location and the low density of population, which is instead a favored position for the evolution of the nature-based tourism.

References

[1] Dragoi A.E., *Dezvoltarea rurala pe principiile sustenabilitatii economice si sociale*, Romanian Academy, 2013.
[2] Glăvan V., *Turism rural, Agroturism, Turism durabil, Ecoturism*, Editura Economica, 2003.
[3] http://ec.europa.eu/agriculture/index_ro
[4] http://ec.europa.eu/eurostat
[5] Tratatul de la Lisabona, 2009
[6] http://www.mdrap.gov.ro

ANALYSIS OF THE HOME DESIGN MARKET IN ROMANIA AND ITS CURRENT TRENDS

Oana Vlăduţ[1], Sanda Maiduc (Osiceanu)[2], Petruţa Mihai[3], Daniel-Ion Vlăduţ[4]
University Politehnica of Bucharest

ABSTRACT

On average, people spend 340 days at home per year, which makes our home a very important place. As a result, the concept of ‚homing' is gaining more and more ground, as strongly focusing on the ambience. Romanians are open to novelty, which is why they welcomed the imported furniture very well, mainly thanks to its innovation. This paper aims to follow up on the furniture companies in Romania in conducting an analysis of what exactly the customers of this industry in Romania are looking for.

1. INTRODUCTION

Romanians used to change their furniture only once in 10-15 years but now they are in the habit of redecorating their houses at every few years. The differences between Romania and other EU member states are immense, in the fact that the former consumers spend ten time less than the EU average to purchase furniture and ornamental decorations.

The furniture retailers feel optimistic about the development of the local market, both in the volume of sales and in the emergence of new international players. The fact that Romanians started discarding old and used furniture from their homes is reflected in the significant annual increase on this market.

The local furniture market is around two billion euros, with Bucharest reaching 600 million euros. According to the Romanian Furniture Manufacturers Association (APMR), the local market is valued at 1.193 million euros, out of which 36.6% is covered by imports.

In 2013, the furniture production was estimated at 1.75 billion euros, with the exports 58.5% in the amount of 998 million euros, whereas the sales on the local market cumulated 752 million euros.

The local furniture market is around two billion euros, with Bucharest reaching 600 million euros. According to the Romanian Furniture Manufacturers Association (APMR), the local market is valued at 1.193 million euros, out of which 36.6% is covered by imports.

In 2013, the furniture production was estimated at 1.75 billion euros, with the exports 58.5% in the amount of 998 million euros, whereas the sales on the local market cumulated 752 million euros.

2. PAPER CONTAIN

The companies in the furniture and home design retailing start occupying strategic positions on the local market, banking on the not yet prospected potential of the market and the furniture consumption that is four times lower than in the developed countries.

[1] Splaiul Independentei nr.313, sector 6, Bucharest and oanavladut2016@gmail.com
[2] Splaiul Independentei nr.313, sector 6, Bucharest and s_maiduc@rectorat.pub.ro
[3] Splaiul Independentei nr.313, sector 6, Bucharest and mihaipetruta@yahoo.com
[4] Splaiul Independentei nr.313, sector 6, Bucharest and v_vladuta@yahoo.com

After IKEA's timid start with the Baneasa store that ran out of its stocks immediately and generated sales of almost double size than expected, Austrian retailer Kika invested 31 million euros in a first store in Bucharest.

The furniture market has witnessed a different development on the three value segments, such as low, middle and top.[1]

For the 2014-2016, the premium segment (top price) registered an yearly increase of 28% for the house furniture and of 18% for the business segment.

The supply in Romania is dominated by the furniture in the middle segment but the market will polarize itself, in the near future, on the premium and economic segments, which translates as good opportunities for the companies.

The positive influence factors on the furniture market are:

- ✓ Construction of houses: In order to meet the demand, a number of 670,000 new buildings should be erected. Currenly, only 20,000 of houses are being under construction.
- ✓ A surging interest in spatious houses: According to INS data, only 61% of Romanians are now living in private houses, compared to 39% in collective housing. As for the domestic premises, 83% of the population live in houses of less than 3 rooms and 79% in homes of less 50 sqm in surface area.
- ✓ The trend is to have a house with spatious rooms or individual residences on the outskirt of the cities.
- ✓ The internal migration of the population: between 2014 and 2016, the internal migration rate rose from 14.7% to 20.5%; 6.2% to 6.9% from the rural to the urban area and 9.5 % to 18.6 % from the urban to the rural area.
- ✓ The number of marriages: the number of marriages went up from 165,000 in 2015 to 184,600 in 2016.

The main competitors on the home design market in Romania are NEOSET, KIKA, MOBEXPERT, IKEA.

NEOSET joined the Romanian market in 1991with one store; ever since, the attractive NEOSET furniture has had an excellent impact upon the customers and become a prestigious brand. The second NEOSET factory was opened in 1999 and it has a 10,000 sqm in surface area.

One of the strengths of this company is its intent to develop a loyalty-based relation with the customers and that this team will always assist its customers with impeccable services, advice and relevant aid.

NEOSET suggests home design solutions that will bring comfort and functionality in the customer's lifestyle, since it has high quality and modern products available, with a pleasant and aesthetic design, along with exceptional services.

Thanks to its efficient management of the resources, NEOSET is a top company on the Romanian furniture market, with no major weakness.

KIKA opened the first store in Romania after an investment of more than 30 million euros, thus lifting higher the standard in the furniture retailing. Its market has exceeded one billion euros.

Kika comes with a new concept for Romania, represented by an offer addressed to the entire price range, and with plans for other ten stores in the next few years.

Kika focuses on services, advice for the customers in planning their choices. In all its countries where it operates, Kika is the owner of both the land and the stores erected on it.

Established 15 years ago, ***MOBEXPERT*** Group is the leader of the furniture market in Romania. With a turnover of 168 million euros in 2007, Mobexpert places among the first 12 European companies in the furniture industry.

All the activities and investments of the latest years have aimed at a more polished offer made to the customer: integrated solutions that are just ‚to die for', at a high standard in the quality sector and affordable price – all these confirm the idea that ‚The best ideas are not necessarily the most expensive ones.'

Besides the fact that is it the most renowned Romanian brand, Mobexpert also boasts with other strengths, such as the expertise in this field and a good local and international reputation, coming from a developed commercial infrastructure and a multitude of services.

In terms of weaknesses, Mobexpert has been slammed many times for its poor customer service and its not very well inspired placement on the premium segment of the market.

The store ***IKEA*** in Romania corresponds to the ‚all in one store' concept. There are over 7,000 items in the store, from furniture for living rooms, kitchens, bedrooms, baby rooms, bathrooms, office, to home textiles, curtains, carpets and bathroom rugs, bed linen, bathroom fabrics, lighting devices, kitchen ustensils, organizers and, last but not least, decorations.

The strengths at IKEA are the functionality and accessibility, with a multitude of products that are stylish and provide complete solutions for all the house areas. Some of its weaknesses are the finishing of the products, the materials they are made of, the fact that they do not last as long as lifetime; there are complaints that their policy is one of consumerism – after you buy some decorations this year, they will break and you will have to go next year and get some new ones from their store, again!

The trends for the 2017 home design are as below:

1. Outdoor lounges in the living room

This piece of furniture will bring a slice of the living nature to the indoors. They will have to be, of course, more refined and manufactured in such a way they should fit the space. The only thing that remains the same is the material they are made of.

2. Vintage furniture – this has been a staple among the accessories in the last years. If refurbished and accompanied by modern elements, it will help turn your room into a chic and mysterious space.

3. Buy furniture made to order – this is the most practical method, which will finally bring your ideas to life. The specialized stores will make some special pieces for you, even for the remotest corner in the room. This is an increasing trend for the people remodelling their house.

4. Metallic furniture – included among the trends of the year 2014. This is how the lockers in the movies will have a perfect fit in the teen room in the house. At the same time, you can use chairs that have metallic parts, either in silver or gold colour.

5. Minimalistic furniture – it is ideal for the small spaces. This furniture will help create the sensation of a larger and more airy room.

6. Technologized furniture – we are living in a digital era and of smartphones, hence the furniture should be controlled by them. There are, therefore, kitchen counters with an integrated tablet PC, sink faucets with an integrated smart system so you can turn the water on from any corner in the house.

A string of innovations has emerged on the furniture market, such as the tile-decorated wardrobe, squaring, etc.

The tile-decorated wardrobe is a furniture item created by the Field Day designers who used a tile called Western Red Cedar. The wardrobe impresses by its height – circa 1.82 meters – a property that makes it very versatile since you can fit it anywhere in the house. It is the perfect storage space for clothing and footwear in the hall; it will give a classical and rustic look to the kitchen, compared to a so-much desired warm and modern atmosphere in the bedroom. The tile is a resistant material and the wooden tile is quite useful for the thermal insulation.

This item called Squaring, truly special and innovative, was created by Korean designer Sehoon Lee. It is represented by an apparently simple set of wooden boxes, which can do something unexpected thus being included in a new trend, that of the flexible furniture.

The boxes are actually connected to one another via an ingenious system and, when spun, they will have the shape of your choice as they move around in their hinges. Squaring is a perfect example of a flexible furniture that adjusts to the desire of its owners.

3. CONCLUSIONS

The Romanian home design customer makes between 2001 and 3000 RON per month and purchases furniture at least once in 7 years, when he desires to redecorate or bring some fresh air into the house. The pieces of the purchased/changed furniture are usually meant for the bathroom, kitchen and living room.

When it comes to the furniture material, Romanians will usually opt for the fibreboard (PAL). As for the information sources on the latest in home design, they will use the promotional materials and the internet. For the real purchase, the customers in Romania prefer the great retailers in this industry.

Generally speaking, they are willing to spend an amount ranging between 501 and 1000 RON to buy furniture, after asking for advice from family and specialists before doing a purchase.

References

[1] Druta F. *Motivatia economica*, Economica Publishing, 2009
[2] http://www.insse.ro/cms/
[3] http://www.apmob.ro/industria.htm
[4] http://www.apmob.ro/industria.htm

ASPECTS REGARDING THE CONSTRUCTION AND WORKING PROCESS OF SEWER VACUUM TRUCKS FOR SEWAGE UNCLOGGING

Gh. Voicu[1], I.C. Duțu, P. Tudor, G. Ipate
University POLITEHNICA of Bucharest

ABSTRACT

Mainly, in this paper are presented some aspects regarding the construction and working process of vacuum trucks for sewer channels unclogging. There are presented general component parts of these machines, the cleaning diagram with working process describing, calculus of the centrifugal pump flow rate for cleaning pressure and driving power, pressure regulator of the cleaning equipment and a few types of nozzles used for cleaning and washing sewers and pipes.

1. INTRODUCTION

Motor vehicles used for sanitation comprise the ones designed for collecting and transporting garbage (container trucks, garbage trucks), sewer vacuum truck, sewer cleaning trucks, auto-sprinklers (with or without brooms), collecting auto-sweeps, snow removal tucks and so on, [4,5,6,7].

Sewer vacuum truck are used in operation, maintenance and interventions activities on the sewerage network, extraction and transport of waste waters, fecal materials, liquids and non-flammable sludge. These utility vehicles have usually capacities of 3-10 m3 or even more. Towed vacuum trucks are often used in the livestock sector for emptying, transporting and spreading at the soil surface both the decayed manure and the coarse material collected in the tanks (fosses) from the animal stables, but can be used in other sectors of activity, [1,3,6,7].

Among the technical and functional requirements of these special machines are to be noted: dislocation and disposal of deposits (coarse suspensions, sludge, sand deposits) from the sewage and septic tanks; sewer cleaning for waste water transport; high maneuverability; operation conditions in winter down to –20°C and in summer up to +40°C, [2,3].

2. METHODOLOGY

The combined sewer vacuum truck ACV-1 (fig.1), manufactured by Automecanica Medias, Romania, has an engine power of 170 kW, having two concentric tanks, one for liquids with a volume of 4 m3 and the other one for vacuum having a volume of 5 m3. The vacuum pump has a flow rate of 216 m3/h and can maintain a depression of 0.8·105 Pa, while the pressure pump has a flow rate of 0.23 m3/min and can work at maximum 13·106 Pa, [7].

The inner vacuum tank, used for collecting liquid residues and waste water, has two visor, washing and emptying caps, while the outer tank is used to store clean water.

Working installation of the machine comprises a suction system made of a supporting arm for the suction tube, vacuum pump, protection and suction hoses pneumatic system and a pressure system made of a high-pressure pump, filters and two hose pressure drums, hydraulic driven. The pumps and hydraulic installation are powered from the power coupling on the auto chassis gearbox.

[1]Splaiul Independentei 313, Sector 6, Bucharest, 0724715585, ghvoicu_2005@yahoo.com

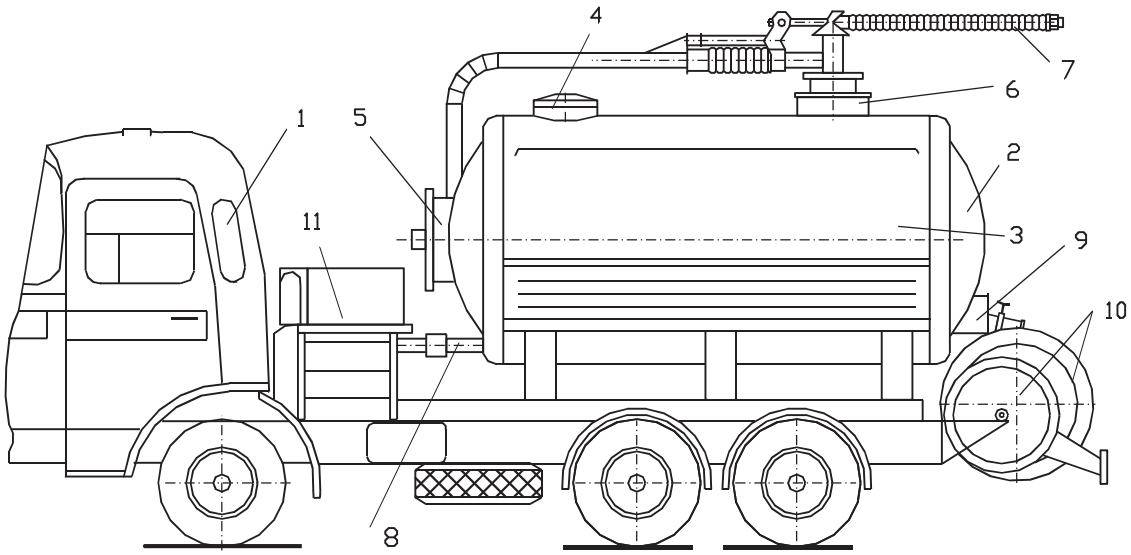

Fig.1. Combined sewer vacuum truck, model ACV–1, [3,7]
1.auto-chassis; 2.collecting tank; 3.clean water tank; 4,5,6.doms with visiting caps;
7.remote sprinkler lance; 8,9.emptying pipes; 10.pressure hose drum;
11.gearbox with power coupling

When cleaning sewers or suctioning sludge (residues) there can be used sewer vacuum trucks of various construction types that combine in a single structure the cleaning and suction functions. The cylindrical reservoir can have two compartments: one chamber for sludge and another one for water. In some constructive models emptying of the combined reservoir it made by swinging back, while other models have a pneumatic emptying piston as a movable partition between clean water chamber and sludge chamber. This two-chamber separation of the tank allow an optimum adjustment for various needs (tank can be used entirely for water or sludge).

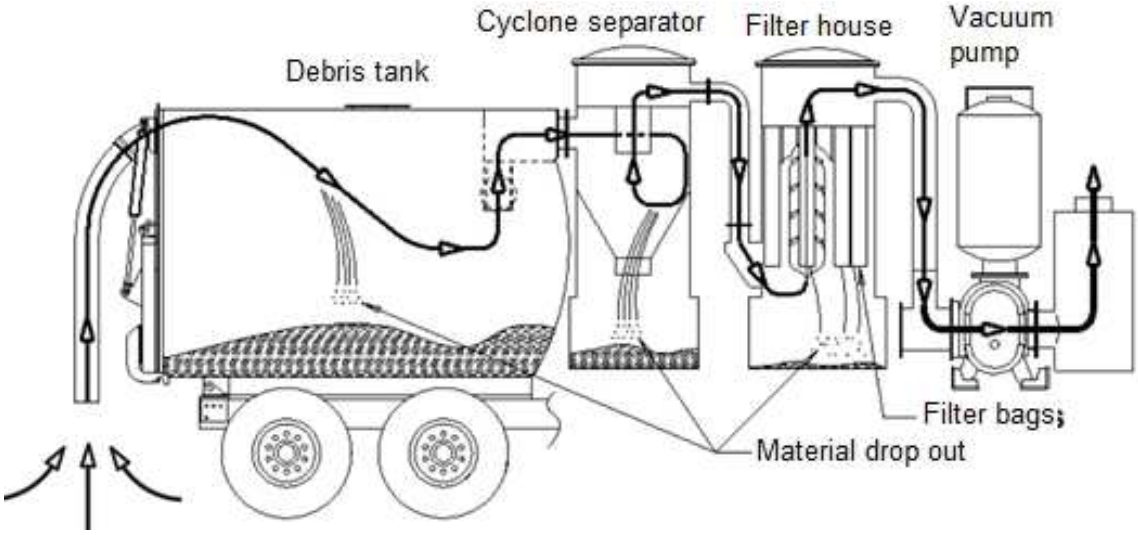

Fig.2. Functional principle of sewer vacuum truck, [8,9]

There are constructive variants having a double concentric tank with the possibility of swinging back and washing with high pressure water. The inner cylindrical tank is used for sludge, while the outer one (between inner and outer cylinder) is used as a water tank.

In frontal part of the inner tank, dirty water is collected and can be emptied through a purging tube or through pushing. Sludge is emptied by swinging back. Dense sludge that tend to adhere to inner walls of the tank can be evacuated by using high pressure water nozzles located inside the tank.

The construction with two concentric tanks allows a maximum use of the available volume and at the same time a good distribution of the load on the axle. A high-pressure water jet system can be used to clean the sewage channels (fig.3). Once the high pressure hose reaches the bottom of the shaft, the pump is in operation, the nozzle at the head of the hose seeks to move alone through the channel due to its special construction.

In the cleaning nozzle the water jet is directed to the back which causes a strong kickback force, causing the hose and the nozzle to advance forward through the network pipe.

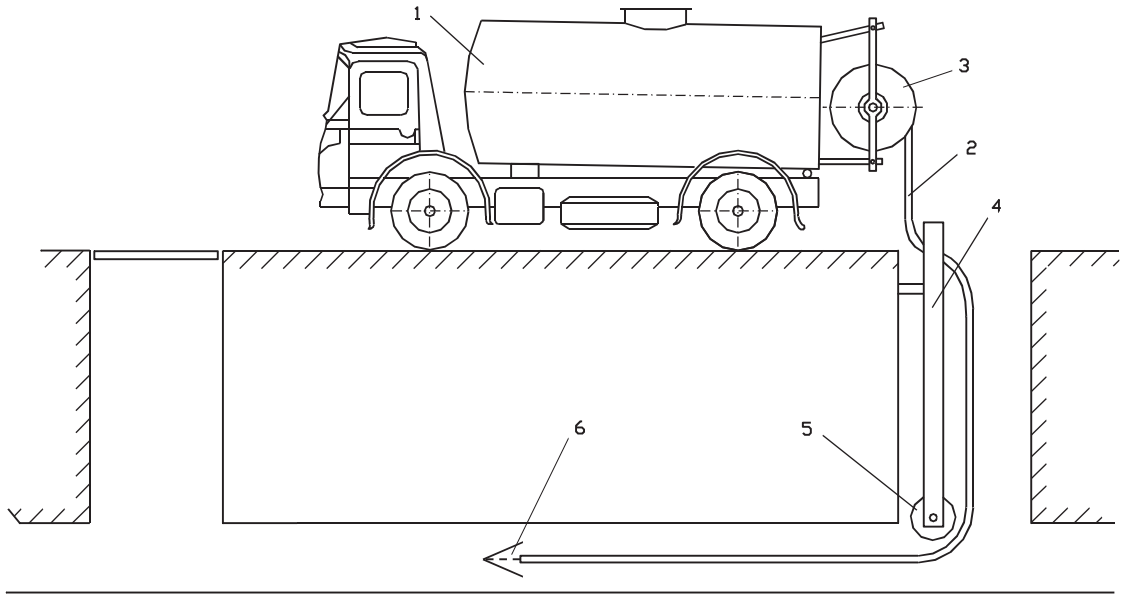

Fig.3. Diagram for sewer cleaning using water under pressure, [3,7]
1. vacuum truck; 2.rolling drum; 3.high pressure hose; 4,5.hose guidance equipment;
6. pressure nozzle

Strong water jet penetrates sediment deposits by dislodging sludge and residues in swirls, while aerating sewers.

All the while, the hose drum is free to allow it to unfold and advance. Upon returning the tube to the hydraulic driven drum, the umbrella-shaped water jet drives the detached particles, sludge and other matter into the drainage shaft from where they can be suctioned.

In Fig. 4 there is shown a pressure regulator of the cleaning and washing system for sewers used in some sewer vacuum truck, having a double valve system and safety valve.

For filling and transport of flammable liquids, vehicles are equipped according the international prescriptions for hazardous materials.

Technical characteristics of these sewer vacuum truck are: tank volume: 2-14 m3; steel tank diameter 1100-1800 mm; service pressure 0,5 bar; vacuum pump flow rate 425-3640 m^3/h; power consumption: 15-120 kW.

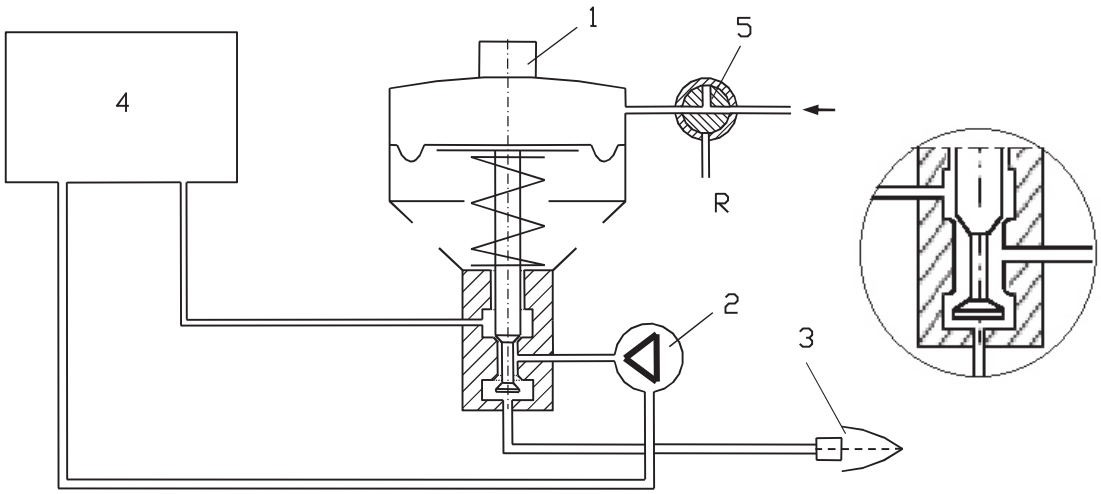

Fig.4. Pressure regulator of some sewer unclogging machines, [3,7]
1.safety valve; 2.high-pressure pump; 3.high-pressure hose with nozzle;
4.water tank; 5.two-way maneuvering valve

The cleaning system itself is working using the effects given by the cleaning head's nozzle that can engage the water jet into a helicoidally movement for a better washing of the sewer walls, as well as a kickback effect for a free movement of the equipment into the sewer. The front pressured water jet erodes the deposits inside the channel, while the side jets push the device forward.

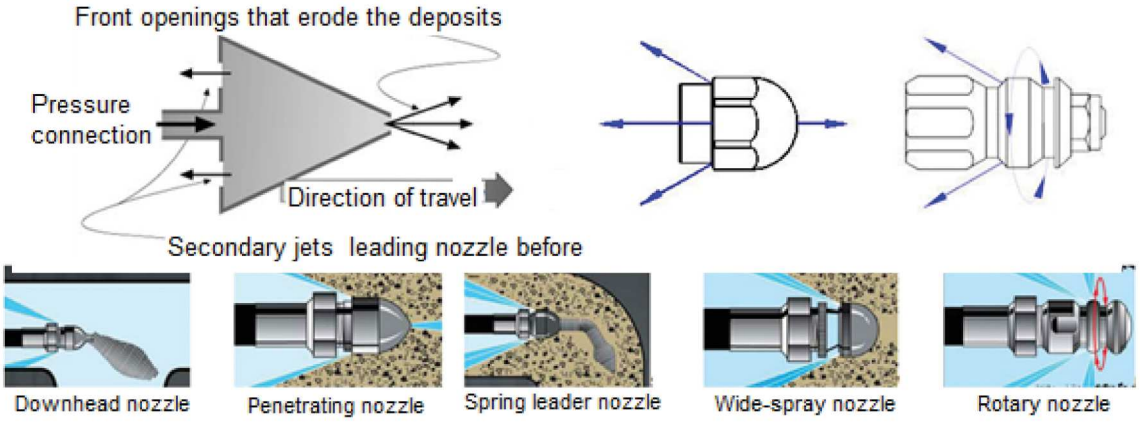

Fig.5. Nozzle modes for sewer unclogging, [10]

The nozzles of the unclogging equipment are designed in such a way that can perform both cleaning sewage pipes and penetrating agglomerations, eliminating grease deposits, cutting off roots that have entered the sewer, etc. The nozzles are chosen so that they can both clean the inner walls of the sewer and forward movement of the cleaning equipment. Thus, the narrow inclination angles of secondary jets can lead to an easier movement of the equipment in the sewer to the detriment of the cleaning capacity. On the contrary, wider angles of the secondary jets develop larger cleaning forces, but the forward pushing force decreases significantly. Therefore, nozzles with angles of 40-50^{o} of secondary jets will have greater cleaning efficiency than nozzles with angles of 8-10^{o}, but forward pushing forces will be smaller.

Fig.6. Various types of cleaning devices for sewers and waste water channels, [10]: general cleaning and obstacle penetration device; frontal and six side nozzles that can be replaced, used for greases; rotary head device (6 nozzles at 30^o and 3 nozzles at 60^o) for greases; rotary head device with forward nozzles in the rear body; device with nozzles and impact chains for strong agglomerations and roots; saw blade device for cutting roots.

The human operator on the vacuum truck must be aware of the type and condition of the pipes so he can choose the appropriate device. It should be known, for example, that saw blades are not suitable for universal cleaning and penetrating nozzles are not suitable for removing grease.

3. RESULTS

Flow rate of the liquid centrifugal pumps, of the sewer vacuum trucks, can be calculated using:

$$Q_{pc} = \frac{\pi}{4} \cdot \left(D^2 - d^2\right) \cdot v_m \tag{1}$$

in which: v_m is the average speed of the liquid at the pump inlet (2 – 4 m/s).

$$v_m = \sqrt{2g\,k\,H} \tag{2}$$

where: k is a coefficient depending on the specific rotational speed (k = 0.22-0.36), and H is the pumping height.

$$H = k' \cdot D_2^2 \cdot n^2 \tag{3}$$

k' – coefficient depending on stator's type (k'= $(1.3–1.5)\cdot 10^{-4}$ for a stator with blades; k' = $(1.0–1.4)\cdot 10^{-4}$ – for a simple stator; n – rotational speed of the rotor (rot/min).

Power required at the centrifugal pump shat is given by:

$$P = \rho \cdot g \cdot Q \cdot \frac{H}{\eta} \qquad [W] \tag{4}$$

Reacting force of the water jet is:

$$F_c = Q_{jet}\,\rho v = 2\,\mu s\,p \tag{5}$$

where: p – output pressure of the fluid (Pa); μ – flow coefficient (depending on the fluid viscosity); s – fluid outlet section (m^2); v – flow speed of the fluid (m/s); Q_{jet} – flow rate of the fluid jet (m^3/s); ρ - density of the fluid (kg/m^3).

If the fluid jet is directed at an angle θ, then the reaction force of the jet will have the following relation:

$$F_c = Q_{jet} \cdot \rho v \sin\theta = \rho s v^2 \sin\theta \quad (6)$$

For a nozzle with 2mm diameter, the reaction force of the water jet at a pressure of 20 bar will be about 8.8N, if the nozzle diameter will double (4 mm), then the reacting force will be about 35.2N.

4. CONCLUSIONS

Unclogging sewers and waste water drainage pipes requires special equipment provided with specific systems and devices built in conjunction with the logs and pipes geometry, but also with the type of agglomerations that obstruct the passage. Movement of the unclogging and cleaning device through the clogged pipes is due to the special way of building it.

At the same time, the human operator should be trained both in the general use of sewage cleaning and unclogging, but also in the choice of the optimal device for practical cases.

The special construction of the devices and equipment for unclogging and cleaning sewers presents solutions for forward movement inside sewers and pipes, but also regarding the breaking of the material clumps or appropriate washing of the pipe walls.

Data presented in the paper may be particularly useful for those using such equipment, but also for engineers for the calculation of reaction forces of main and secondary water jets.

Acknowledgement

This work was supported by a grant of the Romanian National Authority for Scientific Research and Innovation, CNCS/CCCDI – UEFISCDI, project number PN-III-P2-2.1-PTE-2016-0077, contract no.11-PTE/06.10.2016, title "*High energy efficiency (HEE) electrohydraulic equipment (EHE) for multipurpose motor vehicles (MPMV)*", acronym *ECHIPEFEN*, within PNCDI III - Program 2, Subprogram 2.1, Domain Energy.

References

[1] Hazem Elzarka, Ce Gao, Evaluation of trench and slotted drain maintenance and cleaning – Phase 1, The Ohio Department of Transportation, Office of Statewide Planning & Research, 2017.
[2] Pisano W.C., O'Riordan O.C., Ayotte F.J., Barsanti J.R., Carr D.L., Automated Sewer and Drainage Flushing Systems in Cambridge, Massachusetts, Journal of Hydraulic Engineering, 2003, 260-266.
[3] Gh.Voicu, Equipment for municipal and sanitation communities (Utilaje pentru gospodarie comunala si ecologizarea localitatilor), MatrixRom Publishing House, 2007, 255 pages, ISBN 978-973-755-253.
[4] * * * – Vacuum truck solids handling apparatus, US Patent 7523570 B2, 2009.
[5] * * * – Vacuum cleaners with self-cleaning filtration, and other self-cleaning filters, US Patent 8211216 B2, 2012.
[6] * * * – Vacuum Tank Maintenance and Operations Manual, Amthor International, www.amthorinternational.com, 2013.
[7] * * * – Prospects: Automecanica Medias, Romania. TOLLENSE GmbH, FAUN – Germania.
[8] * * * – An Introduction To Air-Mover Vacuum Trucks, Jet News, Water Jet Technology Association, February 2007.
[9] * * * – Guzzler Classic – 4 Stage Filtration Process, https://vac2go.com/guzzler-classic-4-stage-filtration-process/.
[10]* * * – Nozzle Spray Patterns, www.cleaner.com/editorial/2013/12/chemical_and_mechanical_root, & http://www.aquamole.com/sewer-nozzle-kit.

THEORETICAL ASPECTS REGARDING THE DRYING OF FODDER PLANTS BY VENTILATION FOR PRESERVATION AND STORAGE UNDER OPTIMUM CONDITIONS

**PhD. Stud. Eng. Zaica A., Ph.D. Eng. Nedelcu A., PhD. Stud. Eng. Zaica Al.
Ph.D. Eng. Ciupercă R., Ph.D. Eng. Popa L., PhD. Stud. Eng. Mircea C.,
Ph.D. Eng. Brăcăcescu C.**

ABSTRACT

Conservation fodder plants in order to assure animal feed throughout the year, is a core activity for livestock farmers. This paper addresses some theoretical aspects of the technological process of ventilation drying fodder plants in conservation, storing and maintaining nutritional qualities.

As a result, some parameters that influencing the drying process were analyzed: the required air flow rate, the air pressure ventilation, the amount of water to be removed from the feed. Also, the parameters involved in the dimensioning of a feed ventilation installation have been identified.

1. INTRODUCTION

On livestock farmers in hilly and mountainous area of meadows interest them as it operates to provide the necessary fodder for the entire calendar year. The problem occurs with increasing altitude due to bad weather conditions increase the number of days required for the maintenance of animals indoors during the winter, so at altitudes above 900 m, indoors during the winter period is equal to the suburbs.

The main objective of the technology of preparation and conservation forage as hay meadows and forage crops is to provide a final product with nutritional value as close to the original (harvesting) of green fodder, here is based from latter satisfies the conditions premise that a feed of high quality, both in terms of its botanical composition (balanced mix of perennial grasses with legumes), and in the epoch of harvest on.

Green fodder can be preserved and stored as silage or hay. Forage production is dominant in countries with intensive production systems and high productions of milk. In 2010 in Romania the production of hay still prevails over that of silage [2].

The main purpose within the technology is to reduce the drying time and therefore the loss of nutrients, so have developed several methods for obtaining hay, such as: natural drying stubble; drying racks; drying fodder with cold air through the ventilation; fodder drying by ventilating hot air; drying green fodder dehydration thermal drying and briquetting special stations.

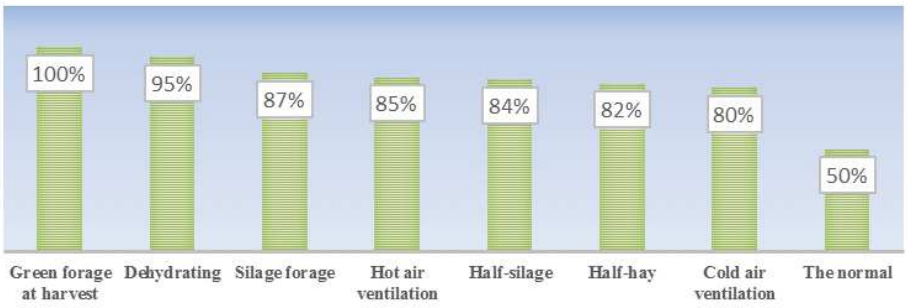

Figure 1: Nutrient content forage through different processes, [3]

[1] PhD. Stud. Eng. Zaica Ana from National Institute of Research – Development for Machines and Installations Designed to Agriculture and Food Industry – INMA, Bucharest, ROMANIA, 6 Ion Ionescu de la Brad, Blv, sector 1, Bucharest 71592, OP 18, Phone: 004021-269.32.55, e-mail: acanpeanu@yahoo.com.

High nutrient losses have occurring from natural drying of fodder. These losses reach, in case of bad weather or even 50 ... 60%, the drying time increased to over 6 ... 8 days. The smallest losses, 4 ... 5% dehydration achieved with green fodder in special drying stations and briquetting, figure 1.

Hay quality depends on botanical composition, chemical composition and digestibility of organic matter expendability, all of which are subject to the natural environment they grew up plants, stage and method of harvesting, drying and storage technique.

2. METHODOLOGY

In the first stage the drying of the green fodder in order to obtain hay, stubble evaporate most of the water (from about 80% to 35%), the step proceeds in about 2 days in the case of favourable time, because favourable gradient of humidity. After this step, are gathered fodders in the field, transported and stored on platforms or hay barn provided with facilities that use ventilation air. Fodder gathered on the soil, moisture between 35…45%, completely eliminate qualitative and quantitative forage losses.

In the second stage drying is aimed at eliminating the feed venting of relatively small amounts of water from 35% to 17%, but requires more time because the gradient of moisture is continuously smaller.

The conditions for drying the feed vary from species to species, depending on their further destination. These terms refer to the temperature of the drying humidity and duration of the drying process. There is a correlation between the size of a complex form, which depends on a number of constructive and functional parameters of dryers for drying feed; architecture drying chamber, the speed of the drying agent, the drying agent humidity.

As the temperature of the feed and the drying time (required for the extraction of moisture) can be adjusted by changing the value of the temperature of the drying, this means finding the best mode of the drying process.

Identifying the factors, Figure 2, which are decisive parameters of the drying process is a particularly important given that material subject to the drying process thermolabile products with a certain moisture content (U), on which both the temperature level (T_a) and the humidity of the drying agent is of special importance [1].

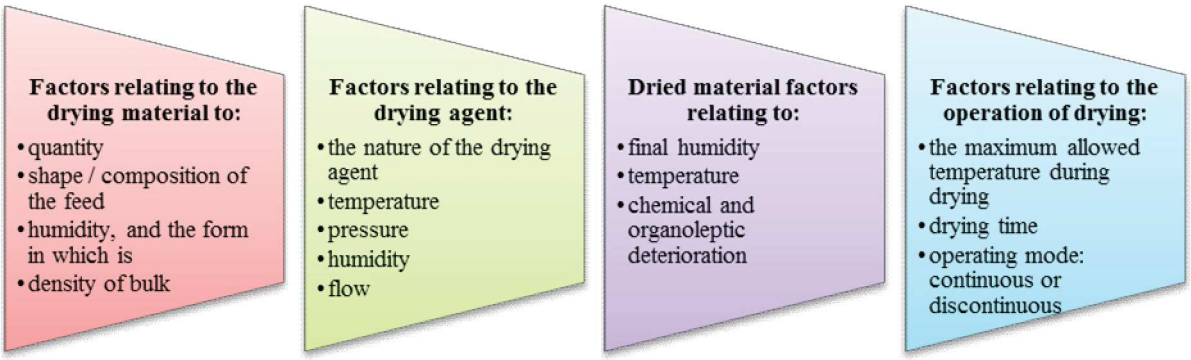

Figure 2: The main factors that intervene and influence the processes of drying, [6]

There are numerous storage systems feed, keeping dry is now the system most widely used, regardless of destination, in these circumstances physiological processes resulting with the intensity very small microorganisms not exceed the terms of development and is therefore economically effective, [4].

The objective is to reduce humidity drying the feed mass to the balance, which may be keeping long time without loss [6]. The mechanism drying operation is represented by a diffusion process, the passage of moisture from the material into the environment which is

based on the evaporation of moisture from the surface of the material and the diffusion of moisture from the interior layers to the surface of the material.

The condition of the drying operation, namely, the drying takes place only when the pressure of the vapour on the material is higher than the partial pressure of their environment. Drying is a process of mass transfer and heat simultaneously being influenced by factors related to material subjected to drying, the drying agent, and factors affecting the operation of drying mentioned above.

Drying agents most commonly used are: air, gases, superheated steam and mixtures thereof, and ways of drying: the most common are natural drying, performed outdoors and artificial drying, performed with a drying agent heated [1]. Essentially, three factors determine the success of drying: air circulation, temperature control, humidity control.

3. RESULTS

Conditions of using active ventilation with cold air

The data presented in Figure 3 on the moisture content of the atmospheric air grams of water per 1 kg of dry air in function of temperature and relative humidity give us a clear view about the effectiveness of drying under ventilation with atmospheric air, unheated.

For example, Figure 3, where atmospheric air ventilation with a moisture content of 40% and a temperature of 30°C to a moisture content equal to 10.32 g/kg. In these conditions when air passes through a layer of moisture fodder subjected to drying up because it adds humidity and temperature taken from material decreases because part of the heat to the evaporation of water.

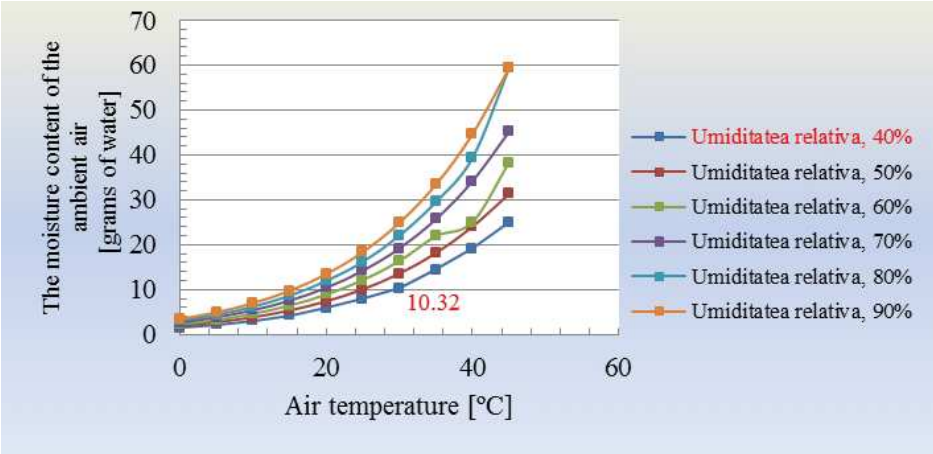

Figure 3: The moisture content of the air in grams of water depending on the temperature and relative humidity, the source data [7]

Evidently drying time, Δt, is inversely proportional to the amount of evaporated water per kg air to be admitted when a constant amount of air per hour. Therefore, drying time under adverse conditions will be approximately 5...20 times longer than favourable weather conditions, increase energy consumption for drying and productivity will decrease in inverse proportion dryers.

An accurate assessment of the amount of water extracted from an m^3 of air is possible using diagrams that as the basis of the air temperature and relative humidity on entry and exit. It resulted from experimental data that can count on an evaporation of about 1...2 g water/m^3 air and favourable weather conditions for about 3...4 g water/m^3 ventilated air.

Capacity of the water by air can rise when the incoming air is preheated. It is necessary to preheat 5...8 °C, to increase as much as the amount of water extracted during drying should be reduced to one-third to one-half of the total time necessary for drying with cold air.

The conditions and the hot-air drying technology

The technology of drying by ventilation hot-air feed are generally the same steps as in the case of drying with cold air, but with some differences as follows: moisture gathering in the field of animal feed is increased to 40…45%, and if the heat source is continuous when charging is continuous feed to complete filling of the dryer or the installation.

The need to reduce consumption of conventional energy have been developed a lot fodder dryers venting hot air produced in solar [5] or geothermal installations. Also, biogas can be used for livestock farms which operate its production facilities.

Regardless of the heat source used to heat the air, it is necessary when working continuously to control the temperature of forage mass, which must not rise above 30°C. Drying is terminated when the internal temperature stabilizes at 20°C and when after a break of 12...24 hours no longer produce heating feed [3].

Warm air drying in solar product is successfully applied to dry feeding stuffs, especially since the harvest period coincides with the period of maximum isolation.

The drying in this case is made in layers, the first layer being 40% of the total amount of feed. During the brief rain will cool ventilation air.

The size of the drying system for fodder by ventilation with hot or cold air is calculated needs hay of the farm. It is calculated based on the daily consumption of hay feeding in winter the number of days and number of animals that must be fed. The size of the storage area of a plant usually lies between 100...150 m^2 to 200 m^2 less.

The large area is divided singular installation surfaces and more fans using related areas. Knowing the actual dimensions of the platform and maximum height of feed can be placed on that platform can calculate the number of drying plants, N, using the relationship 1:

$$N = \frac{F}{B \cdot L \cdot h \cdot \rho} \text{ [kg]}, \quad (1)$$

Where:

F - the demand for hay of the farm, kg;

B - usable width of the platform driers, m;

L - the length dryer's useful platform, m;

h - the maximum height of the forage that can be placed on the drying platform in question, m;

ρ - density of the feed mass, kg/m^3.

Table 1 shows some volumetric mass values hay in bulk from different plant species and of various qualities or hay moisture retention strapping 17%.

Table 1

Table volumetric hay moisture of 17% [3]

Specification and types of hay	Volumetric weight [kg/m^3]
Hay bulk	
Lucerne or clover hay	57...75
Hay of vetch, Lucerne or clover mixtures of different herbs, natural hay with high proportion of legumes	55...70
Small natural grass hay (hill and mountain) of superior quality	50...65
The hay grasses grown waist high	45...62
Hay natural (hill and mountain) medium quality	42...55
Strapping hay	
Strapping hay bales small rectangular	130...170
Strapping hay bales big round or rectangular	80...130

Ventilation air pressure amounts to 30 mmH_2O recommended for a total height of the hay 5 ... 6 m at a volumetric forage table, ρ, of up to 100 kg / m^3. If the mass density is higher, and the short chopped grass hay usually applied wet, then the required air pressure of up to 50 mm H_2O. Ventilation air pressure is greater in the case of the dried forage in the form of bales; it reaches up to 80 mm H_2O. It is recommended to install a U-shaped tube for measuring the air pressure in the groove behind the fan.

The flow rate of air required usually for the ventilation of the feed is expressed in m^3/s per m^2 of base area. It is recommended that the ventilator forage flow to the average level of 0.1 m^3 air per m^2/s. This means you will ventilate 0.1 m^3 per square meter of surface storage of forage within one second. This level of flow ensures the proper drying, [2]. In dry climates it is recommended that a specific air flow of 0.06 m^3/s per m^2 (200 ... 250 m^3/h per m^2) of surface drying. In most humid climates, for example in the hills or mountains, it is recommended that a specific air flow rate of 0.08 ... 0.12 m^3 / s per m^2 (300 ... 450 m^3 / h per m^2) of surface drying. The figures are for surface installation to a layer height of 2 m as the feed volume weight of 60 to 100 kg / m^3 final moisture of 20%.More air debits are required when the facility has no or insufficient sidewalls and bulkheads that works with air leaks, [3].

The actual quantity of water to be removed from the forage by ventilation [7] to obtain a fan with the moisture retention of 18% is calculated from the relation 2:

$$Q_a = P_i \frac{U_i - U_f}{100 - U_f} \tag{2}$$

Where:

Q_a – represents the quantity of water to be removed from the forage, kg;

U_i – represents the initial moisture (from mowing) to feed, %;

U_f – final moisture content of the hay storage (less than 18%), %;

P_i – initial mass of green fodder at harvest, kg.

If known dry weight (P_f) amount of water extracted is:

$$Q_a = P_f \frac{U_i - U_f}{100 - U_i} \tag{3}$$

To calculate the weight that should be dry hay based on the moisture content at harvest and reaching the recommended moisture content can be used for the preservation of formula 3 or formula 4:

$$P_f = P_i \frac{100 - U_i}{100 - U_i} \tag{4}$$

The resistance of the hay layer which the fan airflow encounters depends on the thickness of the layer, the type and structure of the feed [2]

The specialty literature recommends that the air velocity in the aeration channels should not exceed 5 m/s [2]. It has also been pointed out that when air streams are fed to the mass of feed the air pressure decreases depending on the air velocity and the distance between the individual feed particles

4. CONCLUSIONS

Addressing the needs of livestock breeders in the hilly and / or mountainous area that they are interested in as the grassland area they exploit to provide their feed needs for the entire calendar year to feed animals on farms, have been presented a number of factors

influencing the quality of the feed and parameters of the drying process for conservation and preservation:

- the natural environment in which the plants grew, the harvesting phase and the method of harvesting, the drying and storage technique contributes to the botanical composition, chemical composition, digestibility of organic substances and consumables;

- to shorten the time from harvesting to preserving hay fodder, the drying technology has been introduced by hot or cold air ventilation, which reduces the feed humidity from about 40% to below 18%, recommended for storage and preservation;

- the main factors affecting the parameters of the drying process are those related to the material to be dried (quantity, composition, humidity, etc.), the drying agent, the technical characteristics of the drying plant;

- studying the process of the feed drying by ventilation involves the determining and analyzing the following parameters: the temperature and humidity of the ventilator, the required air flow, the ventilation air pressure, the amount of water to be removed from the feed, the humidity required for preserving and maintaining the organoleptic qualities.

Because high nutrient losses occur when the feed is naturally dried, we recommend the use of the technology for drying fodder plants by hot / cold air ventilation.

References

[1] Cioabla A., Jădăneanţ M., Popescu F., „*Study on the influence of air-gas mixture on the quality of cereals in the drying process"*, Buletin AGIR nr. 2-3/2010.

[2] Frederiksen H., Dănuţ D., Maşinistru M., Greculescu A., „*Fodder Storage Systems - Farm Standards, Manual"*, Project: Modernization of the Information and Knowledge System in Agriculture, MAKIS – MADR 04/QCBS/2008 – No.3166, 2010.

[3] Hermenean I., Mocanu V., „*Technologies, machinery and plants for harvesting and preserving hay forage from meadows"*, Editura Universităţii Transilvania din Braşov, 2008.

[4] Traşcă T.I. „*Unitary operations in the food industry"*, Ed. Eurostampa Timișoara, 2005.

[5]. Nedelcu A., Ciuperca R., Popa L, Voicu E., Zaica A., „*Researches Regarding the Solar Radiation Use as Heating Source in Hay Ventilating Installations*", INMATEH - Agricultural Engineering, , Vol. 43, No.2 / 2014, pp. 81-86, p-ISSN 2068-4215, e-ISSN 2068-2239.

[6] Available at: http://cadredidactice.ub.ro/gavrilalucian/files/2013/12/Uscarea.pdf.

[7] Available at: http://www.creeaza.com/tehnologie/tehnica-mecanica/USCAREA519.php.

LABORATORY EQUIPMENT FOR R&D

With an experience of more than 25 years, SARTOROM offers complete solutions for all industrial laboratories (R&D, production, quality control), being the first provider for laboratory instruments in Romania certified ISO 9001.

Headquarter:

- Bucharest: Sales office, Service and Calibration Laboratory

Regional ofices:

- Timișoara: Sales office and Calibration Laboratory;
- Cluj: Sales office;
- Craiova: Sales office;
- Brașov: Sales office;
- Iași: Sales office and Service.

Certification:

- ISO 17025:2005 Calibration laboratory for balances and weighing platforms
- ISO 17025:2005 Calibration Laboratory for pipettes
- ISO 17025:2005 Calibration laboratory for testing machines and extensometers
- ISO 17025:2005 Calibration laboratory for calorimeters
- Integrated Management System ISO 9001/ISO 14001/ISO 18001 TÜV Hessen

SARTOROM is an exclusive partner:

NETZSCH - Thermal Analysis Division, part of the NETZSCH Group, develops and manufactures the complete line of equipment for high-precision thermal analysis and measurement of thermophysical properties: Thermogravimetry (TG), Differential Scanning Calorimetry (DSC), Simultaneous thermogravimetric - differential scanning calorimetry, dilatometer, thermo-mechanical analysis, dynamo-mechanical analysis, dielectric analysis, different couplings (QMS, FTIR, GC-MS) for analyzing the gases emitted by combustion, reactive calorimetry (ARC), thermal diffusivity and conductivity analyzer, etc.

NETZSCH instrumentation is successfully used both in research and quality control (eg. polymers), environmental analysis, chemical, pharmaceutical and construction materials.

ACREDITARE RENAR:
Laborator Etalonare LE – 016/2010
Laborator Analize Cereale LI – 1094/2016
AUTORIZARE BRML:
Verificări Metrologice 040/2015

SARTOROM
Garantează. Inovează. Excelează

Differential Scanning Calorimetry DSC

Thermogravimetric Analysis (TGA) / (TG)

STA coupled to various gas analyzers

Simultaneous Thermogravimetry STA-DSC

Accelerating Rate Calorimetry ARC

ACS, ATT's ambient tests division is known worldwide since 1952 for the design and implementation of a variety of room types to test climate, based on room climate for the automotive industry, electronics, plastics, including testing equipment high-tech, such as vacuum chambers for aerospace applications, thermal shock chambers and calorimeters.

Fritsch Laborgeräte GmbH is the market leader at devices for sample preparation and particle size analyzers. Mills laboratory Fritsch, shaker, particle size analyzers, laser, sample dividers are tools already established in Romania, being appreciated in research, mining and energy, construction materials, etc.

IKA is a German company of tradition, producer of adiabatic calorimeters - calorimeter C5000, izoperibole calorimeters - calorimeter C2000, magnetic stirrers, shakers paddle stirrers orbital appliances sample preparation laboratory, and industrial installations such as mixers, lenses and colloid mills for production.

SARTOROM IMPEX S.R.L

Tel: 021.255.31.32
Fax: 021.255.30.66
info@sartorom.ro
http: www.sartorom.ro

Şos. Bucureşti-Măgurele nr. 232
051434 Bucureşti 5
J40/15959/1991
RO378562

Cont: RO05 BACX 0000 0045 1629 2000
deschis la UNICREDIT TIRIAC
Cont: RO37 TREZ 7005 069X XX00 3185
deschis la ATCPMB

ENACHE MORĂRIT SRL

A SUCCESS OF AGRICULTURE, ENERGY AND ENVIRONMENT

In 1993 a business with milling and bakery products was set up, Enache Morărit SRL. From 1993 to 1998, the company has mainly engaged in the production of crude and refined oils as well as milling and bakery products. Subsequently, the company also developed cereal crops, mechanized services, agricultural chemistry and phytosanitary protection. It leased, year after year, nearly 2,500 hectares of land, which were cultivated with wheat, corn or sunflower. The turning point in the company's activity is the year 2003, when it comes to the first energy-related works by biomass briquetting - it is the straw resulting from the harvesting of wheat, a residue that Moldova, in general, and Vaslui, especially as agricultural county, is abundant.

After the first calculations, it turned out that the idea was applicable and it started the steps for drawing up the project. However, the obstacles were not absent. From SAPARD, 140.000 euros were received - non-reimbursable funds. The second project followed, amounting to 420.000 euros. Then the purchase of silos, grain storage facilities, modern machines and a corn mill was imposed. In order to produce, with maximum efficiency, straw briquettes, two plants were purchased: one of German production and one of Polish origin. While the German plant has a productivity of 500 kg straw/hour, the Polish works with 50 kg straw / hour. The installation of briquettes from the vegetal biomass belonging to SC Enache Morarit Husi is unique in Romania. In 24 hours, the plant produces 14-15 tons of briquettes. The price of a ton of straw briquettes reaches 250 lei, a competitive amount on the fuel market. In addition, two kilos of briquettes equate to about one cubic meter of natural gas. At this time, Enache Morarit sells around 500 tons of straw briquettes per year, both in Vaslui County and other counties in Moldova. A new project is related to changing kilns from the bread factory by changing the burners to work with the new unconventional fuel. The second project involved changing burners from grain drying silos and switching them from LPG fuel. It is mentioned that a local community in northern Moldavia chose the heating solution for public buildings with straw briquettes.

Starting in 2016, the company has developed pelleting of wheat straws, making it in original technological lines.

Among the energy successes highlights:

- construction of boilers producing hot water of 80 kW, 150 kW and 450 kW thermal power;
- development of a boiler construction suitable for burning straw with a flame tube, a construction that ensures a strong cooling in the furnace, avoiding the adhering deposits of ash;
- development of a fully automated boiler control system;
- development of original burners with horizontal burning variant for straw pellets.

Flame of pellet combustion

Hot water boiler of 450 kW